KIMBERLITES

Mineralogy, Geochemistry, and Petrology

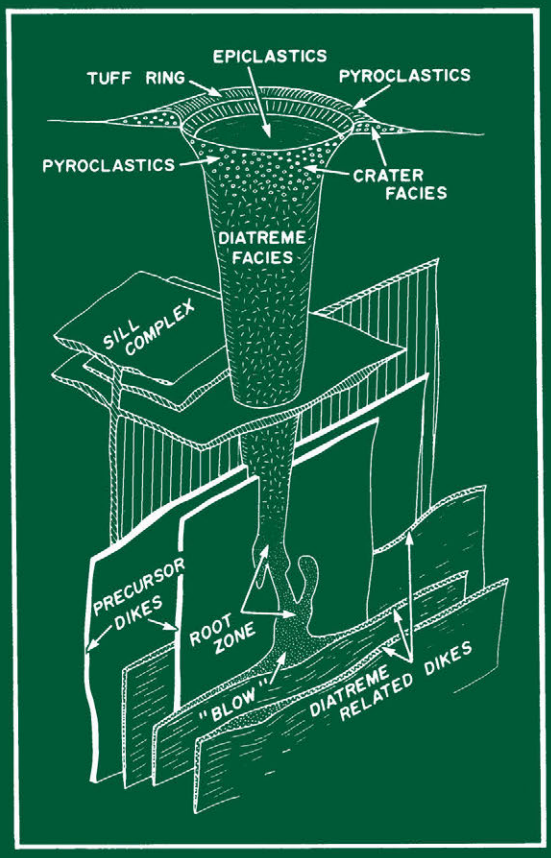

Roger H. Mitchell

KIMBERLITES

Mineralogy, Geochemistry, and Petrology

KIMBERLITES

Mineralogy, Geochemistry, and Petrology

Roger H. Mitchell
Lakehead University
Thunder Bay, Ontario, Canada

SPRINGER SCIENCE+BUSINESS MEDIA, LLC

Library of Congress Cataloging in Publication Data

Mitchell, Roger H.
Kimberlites: mineralogy, geochemistry, and petrology.

Bibliography: p.
Includes index.
1. Kimberlite. I. Title.
QE462.K5M58 1986 552'.3 86-3295
ISBN 978-1-4899-0570-3 ISBN 978-1-4899-0568-0 (eBook)
DOI 10.1007/978-1-4899-0568-0

First Printing—April 1986
Second Printing—March 1989

This work is dedicated to

JOHN BARRY HAWTHORNE

in recognition of his foresight and
assistance in supporting and
encouraging petrological studies of
kimberlites and the upper mantle.

PREFACE

This is a book about the petrology of kimberlites. It is not about upper mantle xenoliths, diamonds, or prospecting for kimberlites. The object of the book is to provide a comprehensive survey and critique of the advances which have been made in kimberlite studies over the last twenty-five years.

Kimberlites are rare rock types; however, their relative obscurity is overriden by their economic and petrological importance to a degree which is not shared with the commoner varieties of igneous rocks. Kimberlites are consequently of interest to a diverse group of earth scientists, ranging from isotope geochemists concerned with the evolution of the mantle, to volcanologists pondering the origins of diatremes, to exploration geologists seeking new occurrences of the diamondiferous varieties. A common factor essential to all of these activities is a thorough understanding of the characteristics of kimberlites.

For the petrologist, kimberlites are exciting and challenging objects for study. Their petrographic diversity, complex mineralogy and geochemistry, and unusual style of intrusion provide endless opportunities for stimulating hypothesis and conjecture concerning their origin and evolution. Kimberlites are a part of a wide spectrum of continental intra-cratonic magmatism. Only by understanding all of the parts of this activity in detail may we make progress in our understanding of the whole.

This book is intended to be informative to the neophyte while being of lasting value to the specialist. I believe that this work will satisfy the needs of such apparently incompatible groups while providing a thorough and comprehensive review of the topic.

It is hoped that the ideas and concepts advanced in this book will serve to stimulate further kimberlite studies. Some of the hypotheses discussed will undoubtedly suffer the inevitable fate of being proven incorrect—yet they and the book will have then served their purpose, that of continuing the quest for a greater understanding of the natural world about us.

This monograph was not conceived in isolation and I wish to acknowledge the contributions made over many years by the following colleagues and friends who share a deep interest in all things concerned with kimberlites: Roger Clement, Howard Coopersmith, Barry Dawson, John Gittins, Steve Haggerty, Barry Hawthorne, Bram Janse, Mal McCallum, Barbara Scott Smith, Simon Shee, Mike Skinner, Bruce Wyatt, and Peter Wyllie. They are all thanked for critical comments, much discussion, samples, preprints, and unpublished and/or difficult to obtain information. Works of this character are not possible without such interaction.

Special thanks go to Henry O. A. Meyer for providing many hours of microprobe time at Purdue University and for his help in the continuance of my kimberlite research.

This book would not have been possible without the continued and enthusiastic support of my wife, Valerie, who provided the environment suitable for its conception, gestation, and birth.

Those who helped materially during the production of the work include Sam Spivak, who drafted all of the original figures; Wendy Bons, who typed the manuscript; Ron Bennett, who has made hundreds of thin sections of these "difficult" rocks; and Maureen Downey, who edited the bibliography. John Scott and Simon Shee are thanked for the photographic work.

Particular gratitude is expressed to Henry Meyer, Iain Downie, and Valerie Dennison for reviewing and proofreading various drafts of the whole work. Howard Coopersmith, Bram Janse, Barrie Clarke, and Dave Eggler are thanked for useful comments on and reviews of Chapters 3, 6, 7, and 8, respectively, although I bear the responsibility for all errors and sins of omission or commission which may be found in the text.

The Natural Sciences and Engineering Research Council of Canada; Lakehead University; the Polar Continental Shelf Project of Energy, Mines, and Resources, Canada; and De Beers Consolidated Mines are acknowledged for financial and logistical assistance in connection with my research on kimberlites and alkaline rocks, which has led to this monograph.

Roger H. Mitchell
Thunder Bay

CONTENTS

KIMBERLITES

Ex Africa semper aliquid novi.
Pliny The Elder, Natural History Book 8

1

HISTORICAL ASPECTS OF KIMBERLITE PETROLOGY

1.1. ORIGINAL DISCOVERY, DESCRIPTION, AND ETYMOLOGY

The history of the discovery of the rock type now known as kimberlite is intricately interwoven with events following the discovery of alluvial diamonds in the vicinity of the confluence of the Vaal, Orange, and Riet Rivers of South Africa in 1866–1867. The ebb and flow of prospecting activity between these alluvial deposits and those which were eventually recognized as kimberlite is described in detail by Roberts (1976), Lenzen (1980), and Wilson (1982).

The first find of diamonds derived from kimberlite appears to have been purely serendipitous and occurred on the farms of Bultfontein and Dorstfontein, locally known as Dutoitspan, in 1869. The diamonds were found in mud excavated from small quarries located adjacent to shallow water-filled depressions known in South Africa as "pans." The mud was used in the construction of farmhouses. These discoveries precipitated a "diamond rush" to the farms. In October 1869, one Frederick Phillipson Stow, a Cape Town attorney visiting the area, remarked that "people were crawling about like so many ants looking for gems on the surface of the ground" (Roberts 1976, p. 17). Times have not changed! Similar scenes can be witnessed whenever present day mineralogists descend upon a kimberlite pipe, although the object of the search is likely to be megacrysts and xenoliths rather than diamonds. (Knee-pads are more useful than hammers to such aficionados.)

Unfortunately, no large-scale mining activity initially occurred at Bultfontein and Dutoitspan as the nature of the mud and the significance of the pans were not recognized. The deposits were effectively abandoned early in 1870 by most prospectors because of the inhospitable climate, lack of water, and the lure of easily obtained alluvial diamonds at Pniel and Klipdrift on the Vaal River. The lack of association with rivers, in fact, led to these diamond occurrences

becoming known as the "dry diggings" in contrast to the "wet diggings" along the Vaal and Orange Rivers. At this time the dry diggings were regarded as being alluvial deposits formed when the Vaal River had overflowed its banks in some earlier time. Reports of the occurrence of diamonds in a similar environment, from Koffiefontein and Jagersfontein to the southeast of Bultfontein, in July 1870 did not stem the rush to the alluvial fields.

Local farmers and a few die-hard prospectors retained an interest in the dry diggings. Their perseverance was rewarded in May 1871 with the discovery of plentiful, easily extracted diamonds on the farm Vooruitzigt. This farm, the home of Johannes Nicolaas de Beer, became the site of a diamond rush, these dry diggings being termed the "De Beer's Rush." Two months later diamonds were discovered at Colesberg Kopje, a low hill 3.5 km west of the De Beer's Rush site. As this new locality was also located on De Beer's farm it became known as the "De Beer's New Rush."

These discoveries heralded the boom in diamond mining that resulted in the development of four major diamond mines around the hamlet of Colesberg—the Kimberley Mine (De Beer's New Rush), the De Beers Mine (De Beer's Old Rush), and the Bultfontein and Dutoitspan Mines.

The earliest workings were developed in highly altered decomposed rock termed "yellow ground," which gave way with increasing depth to a more compact rock termed "blue ground." The latter material, now known to be diatreme facies kimberlite, was soon recognizable as the primary source of diamond. By 1872 it was clear that the deposits were not alluvial in origin and occurred in cylindrical pipe-like structures. Credit for introduction of the term "pipe" into geological literature is usually given to E.J. Dunn (1873). However, Janse (1985) notes that the first scientist to state in print that the dry diggings were steep-sided cylindrical columns representing volcanic conduits was Professor Ernst Cohen. He maintained that the deposits were pipes of eruptive tuff and the diamonds were brought up from below by volcanic action (Cohen 1872).

Despite the economic importance of the deposits there was a significant lack of interest in the host rock and it was not until 1886, at a meeting of the British Association for the Advancement of Science in Birmingham, that Henry Carvill Lewis described the rock as a porphyritic mica-bearing peridotite, and recognized that it was a type of volcanic breccia (Lewis 1887). It was not until 1887, at a meeting of the same association in Manchester, that Lewis stressed the unique character of the rock (Lewis 1888). Following the type locality nomenclature rules of the day, this was named, from its occurrence at Kimberley, South Africa, as *kimberlite*.

As an historical aside it should be noted that had petrologists taken a keener interest in these rocks following their discovery in 1871 a different name would have been used; it was only in 1873 that the Colesberg–New Rush–Vooruitzigt area became known as Kimberley. This arose because Lord Kimberley, the Secretary of State for the Colonies, insisted that before electoral divisions in Griqualand West could be defined they must receive "decent and intelligible

names" (Roberts 1976, p. 115). His Lordship, it appears, "declined to be in any way connected with such a vulgarism as New Rush and as for Vooruitzigt . . . he could neither spell nor pronounce it." (Roberts 1976, p. 115). John Blades Currey, a government secretary to Richard Southey, the Lt. Governor of Griqualand West, made quite sure that Lord Kimberley would be able both to spell and pronounce the name of the main electoral district by calling it after his Lordship. The names "New Rush," "Colesberg," and "Vooruitzigt" all were abandoned when the new name was proclaimed in July 1873. Interestingly, had the renaming taken place only a few months later, geologists might now be studying "carnarvonite," given the continued political pandering of Curry, as Lord Kimberley was replaced by Lord Carnarvon as Colonial Secretary in February 1874.

Further, Lewis might have lost his chance to introduce kimberlite as a new rock type had similar rocks discovered in the United States contained diamonds. As early as 1837 mica peridotites had been found at Ithaca and Syracuse in New York (Vanuxem 1837, Williams 1887), and at Ison Creek, Kentucky (Crandall 1885). These latter rocks were described as peridotites (Diller 1885, 1886, 1887). Subsequent investigations have shown that they are in fact *bona fide* kimberlites.

Other names proposed for the new type of diamond-bearing rock included "adamasite" (Meunier 1882) and "orangite" (Wagner 1914). The latter was proposed for the micaceous kimberlites of the Orange Free State. Given their distinctive mineralogical and isotopic characteristics relative to other kimberlites, this name might be usefully revived.

1.2. INFLUENTIAL STUDIES: 1887–1950

Summaries of the earliest papers dealing with kimberlite are given by Wagner (1914), Williams (1932), Nixon (1973c), and Janse (1985). The majority of these works, which have not survived the test of time, were concerned with the emplacement of kimberlite, or the origin of diamonds and the rounded ultramafic inclusions. Significantly, with regard to the latter, even in these early days, opinion was divided between cognate and xenocrystal schools of thought.

Apart from Lewis' (1887, 1888, 1897) pioneering studies, the petrography of kimberlite was largely ignored. Diller's (1885, 1886, 1887) and Crandall's (1910) observations on the Ison Creek "peridotite" did not receive the attention they deserved as the rocks lacked diamond and thus were not considered to be kimberlites. Harger (1905) appears to have been the first to suggest that many of the crystals found in kimberlites are derived from the fragmentation of ultramafic inclusions.

These early investigations culminated in, and were eclipsed by, Percy Wagner's monograph *The Diamond Fields of South Africa* published in 1914. This important text summarized the information obtained during the initial exploration and development of the South African kimberlite province. The work provided

the first comprehensive petrographic descriptions of many varieties of kimberlites, and presents the first information regarding the deep structure of the pipes. The influence of Wagner's book on all subsequent kimberlite studies was immense. In particular, the division of kimberlites into "basaltic" and "lamprophyric" (micaceous) varieties remained unchallenged until the 1970s and to this day forms the basis of most Soviet classifications of kimberlite.

Wagner's text was such a milestone that interest in kimberlites apparently died and it was not until 18 years later that a comparable work was published. This was Alpheus Williams' two-volume book *The Genesis of Diamond*. This text summarized and updated Wagner's observations. Its major contribution is the presentation of detailed petrographic descriptions of kimberlite and ultramafic xenoliths illustrated by excellent color photographs. Unfortunately Williams' hypotheses regarding the origin and emplacement of kimberlite did not meet with the same approval as his petrographic work and were quickly forgotten. The book however remains an outstanding contribution and original editions are much sought after by petrologists and bibliophiles alike.

During the 1930s petrologists were concerned primarily with the origins of granites and intermediate rocks and few were interested in such rare exotica as kimberlites. Williams' text however appears to have stimulated the interest of Arthur Holmes and S.J. Shand, the two giants of petrology at that time. Shand (1934) and Holmes (1936) concluded that kimberlites were either merely altered melilite basalts (melilitites) or equivalent to melilite basalts plus "emanations" (e.g., H_2O, CO_2) and fragmented lherzolites. Taljaard (1936), a student of Shand's, in a much quoted but commonly uncritically accepted paper gave further credence to this viewpoint. The ideas stemmed from the geographic overlap of kimberlite and melilitite provinces in southern Africa and from the belief that all calcite in kimberlites was secondary and derived from the breakdown of melilite. It should be remembered that during the 1930s petrologists were acrimoniously debating the origin of carbonatites and nepheline-bearing rocks and that Shand was one of the chief opponents of the magmatic theory. Hence Shand and Taljaard were unable to admit to the possibility that the carbonates found in kimberlite might be of primary magmatic origin. Because of the eminence of Holmes and Shand, their claims were widely accepted and have colored many subsequent ideas concerning the nature of kimberlite. In particular they have led to the Soviet view that the groundmass of kimberlite is an olivine melilitite, and ultimately to Von Eckermann's and Dawson's ideas that kimberlites occur in alkaline rock–carbonatite complexes (see Chapter 2).

1.3. MAJOR DEVELOPMENTS: 1950–1970

Subsequent to 1950, a cherished dogma was dispelled when it became clear that kimberlites, including diamondiferous varieties, were not confined to South

Africa. Major kimberlite provinces were discovered in Tanzania, Lesotho, Colorado–Wyoming (U.S.A.), and Yakutia (U.S.S.R.). Summaries of the locations of these and other occurrences can be found in Dawson (1967a, 1980), Davidson (1967), Bardet (1973, 1974, 1977), and Janse (1985).

The discovery of the Siberian province in 1954 resulted in a flood of information describing aspects of the geology, petrography, and geochemistry of these kimberlites. Much of this original Russian literature is difficult to obtain, being published in isolated regional centers. Several monographs, e.g., Bobreivich (1959b, 1964), Kovalski (1963), Milashev (1965), and Frantsesson (1968), and hundreds of short papers, were produced. Unfortunately most of this literature has not appeared in English (the 1970 translation of Frantsesson's book being a notable exception). Most of the early studies were undertaken before modern mineralogical techniques and concepts were applied to the study of kimberlites. Consequently, much of the compositional data presented is, at best, semiquantitative, and the descriptive work, parochial.

Soviet petrologists in their initial studies relied entirely upon the works of Wagner, Williams, Shand, and Holmes; thus the study of the Yakutian province did not produce any significant advances in kimberlite petrology but merely extended the Lewis–Wagner mineralogical-textural classification to overly complex derivatives and affirmed a genetic relationship between kimberlite and melilitite.

It is regrettable that many Soviet papers consider mineralogical, petrographic, or geochemical data in complete isolation from other data and promote hypotheses and conjecture as if they were fact. Western petrologists accustomed to a more comprehensive and rigorous approach to science consequently find many of these publications trivial and/or unrewarding. It should be recognized that Soviet scientists have a different working philosophy than that of Western geologists. Moreover, there are difficulties related to the translation of petrological terms from Russian to English. Further confusion stems from factionalism which results in different groups of Soviet petrologists using their own preferred terminology to the exclusion of that of others (Frantsesson 1970).

The Soviet approach however has the merit that unconventional ideas are regularly published. These may stimulate discussion of the type that enlivened the pages of *Economic Geology* in 1964 and 1965, subsequent to Davidson's (1964) enthusiastic, but uncritical, endorsement of Mikhayenko and Nenashev's (1962) hypothesis that kimberlites are emplaced as cold mixtures of gases and solids. This concept was one of the few ideas emanating from Yakutia which caught the imagination of other petrologists and which exerted a significant influence on models of kimberlite emplacement in the late 1960s. The hypothesis was adopted by Edwards and Howkins (1966), Kennedy and Nordlie (1968), and McGetchin (1968) and survives to this day in various guises in some fluidization models of emplacement (Wyllie 1980).

The only other major concept stemming from the Yakutian province work

was that of epeirogenic magmatism as espoused by Staritski (1963), Kirillov (1961), and Arsenyev (1962). The ideas were extensively promoted by Bardet (1964, 1973), but have not been widely accepted.

The major advances of the period were derived from studies of southern African kimberlites. Tremblay (1956), Mannard (1962, 1968), and Edwards and Howkins (1966), as a result of their studies of the Tanzanian province, presented the first descriptions of epiclastic/pyroclastic kimberlites and laid the foundations of modern concepts of kimberlite magmatism. Mannard's (1962) work on what are now termed crater facies kimberlites deserves to be more widely known (see Section 3.2.).

The Institute of African Geology at Leeds University proved to be a major force with respect to stimulating studies of kimberlite. Theses presented by Dawson (1960), Nixon (1960), and Janse (1964) broke new ground with descriptions of kimberlite fields in Lesotho and Namibia which were unknown to Wagner and Williams.

The influence of Dawson's (1962, 1966, 1967a,b, 1970) papers cannot be overestimated. Two concepts introduced by him proved to be particularly persistent and widely accepted; i.e., the fluidized intrusion and the central complex kimberlite models.

The hypothesis of fluidized intrusion, derived from Reynold's (1954) work on granites, appeared to answer many of the questions concerning kimberlite emplacement. This idea has dominated Western and Soviet ideas of kimberlite intrusion since its introduction and it is only recently that the concept has been seriously challenged by the "hydrovolcanologists" (see Section 4.4.3.).

The hypothesis that kimberlites of the central complex variety (Dawson 1966) occur in association with alkaline rocks and carbonatites was stimulating but ultimately unrewarding, as it also ushered in the kimberlite–carbonatite debate. An unfortunate result of the concept was that usage of the term *kimberlite* was broadened to include any micaceous ultramafic lamprophyre, thus opening a Pandora's box of petrological confusion that was only resolved at the end of the 1970s.

The "Upper Mantle Project" of the 1960s heralded an upsurge of interest in kimberlites. Unfortunately this was not because of their intrinsic petrological value as igneous rocks, but for the ultramafic xenoliths that they have transported from the inaccessible upper mantle; depths that never would have been attained by the ill-fated "Project Mohole." This interest set the stage for the dichotomy that developed in the following decade, which still exists, between those who study kimberlites and those who are merely concerned with its xenolith suite.

1.4. CONTEMPORARY ADVANCES: 1970–1985

The early 1970s saw a quantum leap in our understanding of kimberlites. This resulted from detailed studies of kimberlites and megacrysts from the U.S.A.,

Canada, Lesotho, and South Africa by modern mineralogical and geochemical techniques. Kimberlite petrologists benefitted even more than other petrologists from the rise of electron microprobe analysis as a routine analytical technique, as at last it became possible to study the minerals found in the previously intractable groundmass. Neutron activation analysis and mass spectrometric techniques enabled geochemists to apply the concepts developed from the study of other mantle-derived magmas to kimberlites, and to place constraints upon their evolution and origin.

Particular impetus was provided by the First International Kimberlite Conference held in Cape Town, South Africa in 1973. Field excursions to the Kimberley area and Lesotho enabled earth scientists having diverse interests to assemble a comprehensive collection of kimberlites, megacrysts, and xenoliths, the study of which formed the basis of many of the major advances in kimberlite petrology later in the decade. The Conference proceedings (*Physics and Chemistry of the Earth,* Volume 9, 1975), and a collection of papers edited by P.H. Nixon published as *Lesotho Kimberlites* (1973) mark the dawn of modern kimberlite and upper mantle xenolith studies. Interest in these topics remained so high that the Second International Kimberlite Conference held in Santa Fe, New Mexico in 1977 proved to be equally successful. Field excursions enabled petrologists to visit the Colorado–Wyoming kimberlites and the diamond-bearing lamproites (then termed kimberlites) in Arkansas, and to obtain material for further detailed studies. The Conference proceedings, published in two volumes by the American Geophysical Union, illustrated the increasing sophistication of kimberlite studies as compared with those presented at the 1973 conference, especially in the fields of experimental petrology and detailed mineralogical–petrographic studies.

The principal advances of the 1970–1980 period resulting directly and indirectly from these conferences and the increased availability of kimberlite samples were recognition of the following:

1. Different facies of kimberlite exist.
2. Kimberlites are formed from high-temperature magmas.
3. Kimberlite magmas undergo differentiation and this process can result in the formation of a spectrum of rock types forming a kimberlite clan.
4. The lherzolite xenolith suite contains information in their equilibration parameters regarding the depth of origin of kimberlite magmas.

Significant advances were made with respect to the definition and classification of kimberlites, resulting in the final overthrow of the Lewis–Wagner classifications. These new mineralogical-textural genetic classifications of kimberlites, coupled with detailed mineralogical studies, led to the realization that kimberlites are complex hybrid rocks and to a clarification of their relationships with other alkaline ultramafic rock types.

The object of much of the work undertaken during the 1970–1980 period was the petrographic, mineralogical, and geochemical characterization of kimberlite. Few syntheses of these data into integrated models of kimberlite mag-

matism were attempted, although subsequent to 1980 attempts were made to place kimberlite magmatism in the framework of plate tectonics.

The Third International Kimberlite Conference held in Clermont-Ferrand, France in 1982 did not result in any major advances in kimberlite petrology, although there was a realization that diamonds are xenocrysts in kimberlites. The Conference re-kindled an interest in ultrapotassic rocks with the presentation of the first descriptions of diamond-bearing olivine lamproites from Australia and the reclassification of some kimberlites, e.g., those found at Prairie Creek, Arkansas as lamproites. Consequently, many kimberlite petrologists have now turned their attention to studies of lamproites and other ultrapotassic rocks in a desire to determine the relationships between these diverse groups of mantle-derived magmas.

The advances of 1970–1985 are the subject of this book. It is hoped that the synthesis presented will clarify concepts and stimulate further work. Kimberlites have attracted the attention of many petrologists over the past two decades; their study is no longer the preserve of a handful of dedicated enthusiasts. Importantly, despite the vast amount of information now available, there is no consensus regarding the origin and evolution of kimberlite magma. This diversity of opinion is instructive in that it indicates that we do not yet know enough about kimberlites to allow the formulation of a general magmatic model. Kimberlite studies are thus not destined to stagnate but will continue to evolve rapidly as long as there is an interest in the petrogenesis of alkaline rocks and the nature of the upper mantle.

Don't take action because of a name! A name is an uncertain thing, you can't count on it!
Bertolt Brecht

2

KIMBERLITE AND RELATED ROCKS

2.1. THE NATURE OF KIMBERLITE

Kimberlites are petrographically complex rocks. In addition to exhibiting modal mineralogical variation arising from magmatic differentiation processes, they are hybrid rocks consisting of crystals originating from three distinct sources: mantle-derived xenoliths, the discrete nodule suite, and primary phases crystallizing from the kimberlite magma.

The relative contributions to individual kimberlites from each of these sources vary widely. In some instances it is not possible to assign, unambiguously, a given mineral to a particular source. Failure, until recently, to recognize the hybrid nature of kimberlite is in part responsible for the confusion that has arisen with regard to the exact nature of kimberlite and its relationship to other rocks. Many earlier definitions of kimberlite included minerals which are currently considered to be xenocrysts.

2.1.1. Mantle-Derived Xenoliths and Xenocrysts

Many kimberlites contain rounded-to-subangular blocks of rocks whose mineralogy indicates derivation from the upper mantle. Geothermobarometric studies support such an origin and provide information regarding the depths of origin of kimberlite magmas (see Section 9.10). The major groups of xenoliths recognized by Dawson (1980) are: the peridotite–pyroxenite suite, eclogites and grosspydites, metasomatized peridotites containing potassic richterite and/or phlogopite, and glimmerites and the MARID (*M*ica-*A*mphibole-*R*utile-*I*lmenite-*D*iopside) suite of rocks.

Lherzolites and harzburgites of the peridotite–pyroxenite suite typically are predominant and usually comprise less than 2% of the host rock, although some

kimberlites are notably enriched in these xenoliths, e.g., Matsoku (Lesotho) and the sills of the Pyramidefjeld area (Greenland). In other kimberlites, e.g., Roberts Victor (South Africa) and Zagodochnaya (Yakutia), eclogites and grosspydites predominate or occur to the exclusion of lherzolites. MARID suite xenoliths are rare and known primarily from South Africa (Dawson and Smith 1977). Dawson's (1980) group of metasomatized xenoliths probably represents a transitional group formed by the addition of MARID-suite minerals to lherzolites. Detailed discussion of the mineralogy of these mantle-derived xenoliths is beyond the scope of this work but can be found in Sobolev (1977), Dawson (1980), and Nixon (in press).

Fragmentation of these mantle-derived xenoliths during transportation in kimberlite results in the addition of xenocrysts to the magma. In some instances such xenocrysts are easy to recognize on the basis of their compositional equivalence with minerals in the xenoliths, e.g., chrome diopside and chrome pyrope derived from lherzolites or jadeitic pyroxenes and grossular-rich garnets from eclogites. In other cases such a distinction is not possible because of compositional overlap with minerals crystallizing from the magma, e.g., olivine and phlogopite, or with minerals belonging to the discrete nodule suite, e.g., chrome-poor garnets and magnesian ilmenite.

2.1.2. Discrete Nodule or Megacryst Suite

The discrete nodule suite (Nixon and Boyd 1973b) consists principally of large (1–20 cm) single crystals of magnesian ilmenite, Cr-poor titanian pyrope, diopside (commonly subcalcic), enstatite, phlogopite, and zircon. Coarse-grained lamellar intergrowths of pyroxene and ilmenite are common, as are small inclusions of one phase within larger crystals of another. The compositional variations and relationships exhibited by coexisting members of the discrete nodule suite (see Chapter 6) suggest that they represent a series of crystals precipitating from a single differentiating magma. Opinion differs as to the nature of this magma. Boyd and Nixon (1975) believe that it is unrelated to kimberlite and that the discrete nodules are xenocrysts derived from "crystal mush magmas" sampled by kimberlites during their ascent. Gurney *et al.* (1979) and Harte and Gurney (1981) believe that they are products of isobaric crystallization of "protokimberlitic" magmas in the mantle. Mitchell (1977, 1979a) advocates a cognate high-pressure origin.

In view of the diverse hypotheses regarding the origin of the suite, Dawson (1980) recommends that they be termed *megacrysts*. This term has no genetic connotation and is merely descriptive of the large size of the crystals. Fragments of megacrysts are common in many kimberlites and are referred to as macrocrysts (see Section 2.2).

Whether the macrocrysts and their parental megacrysts should be considered cognate or xenocrystal is one of the major unresolved problems of kimberlite

petrology. Similar megacrysts are common in alkali basalts, nephelinites, and alnöites (see Chapter 6), and in these parageneses the megacrysts are commonly considered to be high-pressure phenocrysts. Regardless of their origin, the megacrysts, as found in kimberlite, have distinctive compositions and the discovery of these typomorphic minerals is commonly regarded as a definitive indicator of kimberlitic magmatism.

2.1.3. Primary Phases

Primary liquidus phases are considered to be phenocrysts and microphenocrysts of subhedral to euhedral habit, and minerals which can be shown to have crystallized *in situ* to form the kimberlite groundmass. The former may include olivine, phlogopite, and chromite; the latter olivine, phlogopite, Ti-bearing spinels, perovskite, ilmenite, diopside, monticellite, apatite, calcite and serpentine. All of these minerals may not be found together in any given kimberlite as a consequence of differentiation processes and/or variations in the bulk composition of the magma.

2.2. MACROCRYSTAL AND APHANITIC KIMBERLITES— THE OLIVINE MACROCRYST PROBLEM

Kimberlites exhibit a distinctive inequigranular texture due to the presence of relatively large (0.5–10-mm) rounded-to-anhedral crystals (primarily olivine) set in a finer-grained matrix. Some petrologists have considered these large crystals to be cognate and thus phenocrysts. Kimberlites are therefore described as porphyritic rocks (Milashev 1963, Kovalsky 1963, Mitchell 1970). Others (e.g., Dawson 1971, Boyd and Clement 1977, Skinner and Clement 1979, Clement *et al.* 1984) regard the minerals as xenocrysts derived from lherzolites, harzburgites, or the discrete nodule suite. Description of kimberlites as porphyritic rocks is clearly not appropriate if these minerals are not cognate. Clement *et al.* (1984) have recommended that such cryptogenic pseudophenocrystal phases be referred to as *macrocrysts,* a term devoid of genetic inferences.

Macrocrysts of magnesian ilmenite and Cr-poor titanian pyrope are compositionally equivalent to the ilmenites and garnets of the discrete nodule suite and undoubtedly represent fragments of such megacrysts. The origins of the olivine and phlogopite macrocrysts are less easily determined and the olivine macrocryst problem, in particular, remains one of the more controversial aspects of kimberlite petrology.

Figure 2.1 illustrates a typical macrocrystal texture in which large rounded olivines are set in a fine-grained matrix. In Figure 2.2 olivines of similar size form euhedral to subhedral single crystals set in a fine-grained groundmass. The texture is undeniably porphyritic, and as such crystals have no morphological

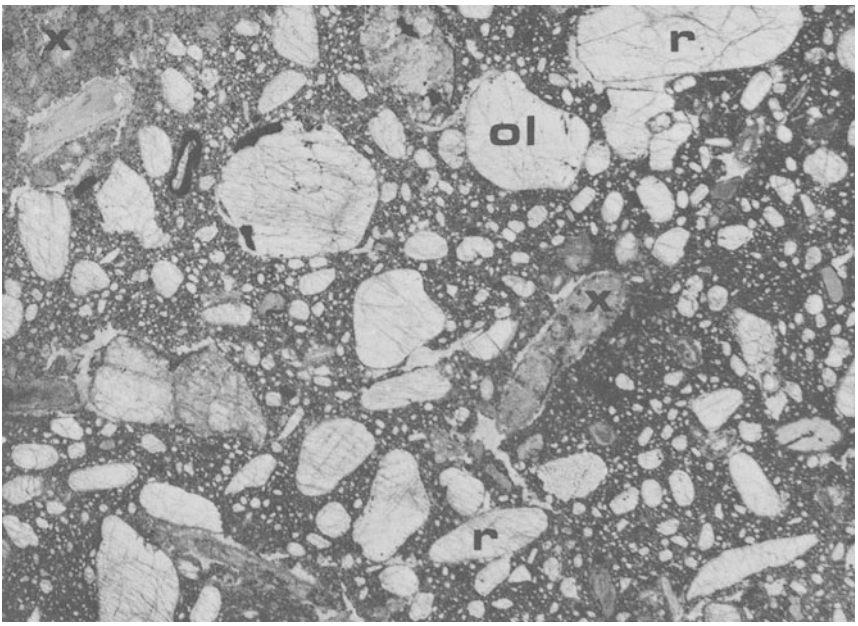

Figure 2.1. Macrocrystal hypabyssal kimberlite, Wesselton Mine, South Africa. Note the characteristic inequigranular texture formed by the large rounded and resorbed olivine macrocrysts (ol) in conjunction with the smaller subhedral microphenocrystal (groundmass olivines). Some of the macrocrysts (r) appear to have been originally euhedral crystals. The olivines are fresh except within the vicinity of "dewatered" sedimentary xenoliths (x), where they are completely serpentinized. (Field of view 25 mm.)

counterparts in lherzolites, these must have formed as phenocrysts in the kimberlite magma. The crux of the olivine macrocryst problem lies in whether the rounded olivines seen in Figure 2.1 are derived from euhedral phenocrystal precursors, are simply rounded lherzolite-derived xenocrysts, or are a mixture of olivines derived from both sources. In some kimberlites, mixed assemblages of rounded and subhedral olivines are present, indicating that more than one type of olivine is indeed present. Compositional data demonstrate that the macrocrystal olivine population is made up of several components, and that both xenocrystal and phenocrystal olivines are present (see Section 6.5). So far it has proven impossible to determine their relative proportions as there is compositional overlap between the more magnesian ($>Fo_{90}$) phenocrystal and lherzolitic olivines. These latter olivines may, in some instances, be recognizable by textural features (kink banding, and undulose extinction) or by the presence of small inclusions of lherzolitic minerals such as Cr-rich pyrope or enstatite.

The rounded aspect of the olivine macrocrysts has been attributed to mechanical attrition during fluidized emplacement of kimberlite (Dawson 1962, Mitchell 1973a). The recognition of olivines of identical morphology in hypa-

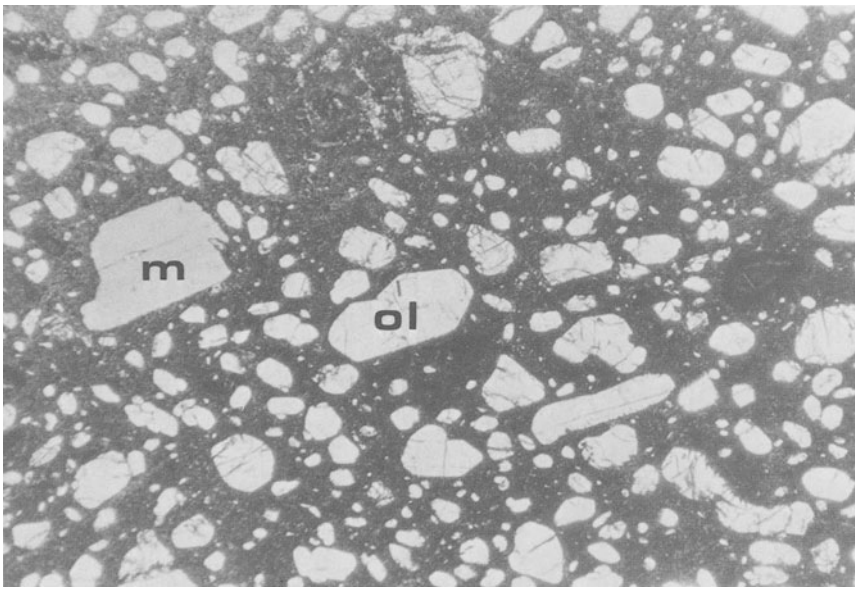

Figure 2.2. Macrocrystal hypabyssal kimberlite, De Beers Mine, South Africa. This kimberlite contains an unusually high proportion of euhedral to subhedral olivine (ol) macrocrysts, which, in this example, may be considered to be phenocrysts. Some anhedral and irregularly shaped macrocrysts, presumed to be xenocrysts, are also present. Phlogopite (m) is present as a broken and corroded macrocryst. (Field of view 25 mm.)

byssal kimberlites which could not have experienced this process mitigates against such an origin. The occurrence of re-entrant concave margins and the highly irregular shapes of some macrocrysts suggests that they have undergone resorption. It is therefore recommended that the terms "pre- and post-fluidization olivine" introduced by Mitchell (1973a, 1978a) be abandoned.

In rare instances olivine and other macrocrysts may be entirely or locally absent. This may be a consequence of near-surface flow differentiation or crystal fractionation at depth. Fine-grained microporphyritic kimberlites (Figure 2.3), from which macrocrysts are absent or present in small (<5%) quantities, are termed *aphanitic* kimberlites (Apter *et al.* 1984). Mineralogically aphanitic kimberlites are equivalent to the matrix or macrocryst-free portions of macrocrystal kimberlites.

2.3. KIMBERLITE DEFINED

Although early definitions of kimberlite (Kovalski 1963, Milashev 1963) included minerals derived from mantle xenoliths, e.g., Cr-rich pyrope, most

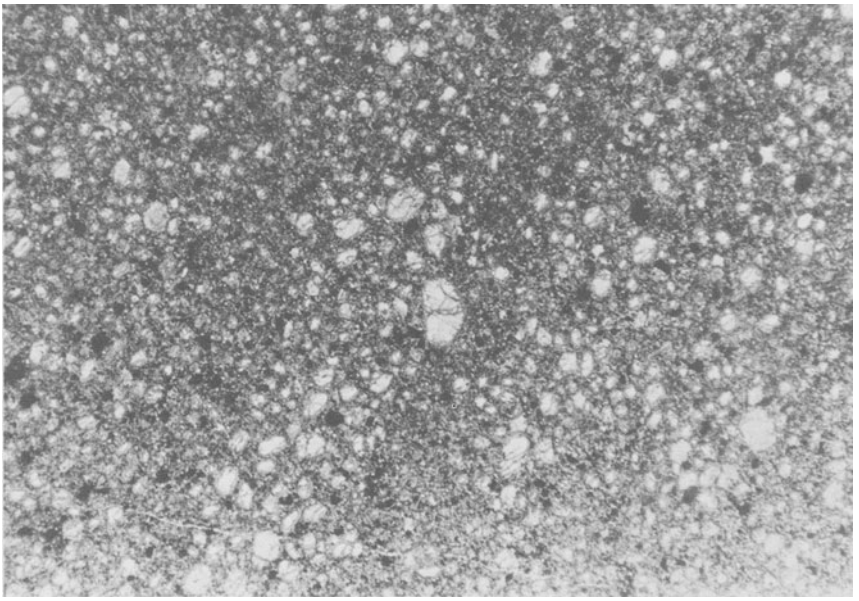

Figure 2.3. Aphanitic hypabyssal kimberlite, Wesselton Mine. This kimberlite lacks olivine macrocrysts and consists of microphenocrystal (groundmass) olivines (colorless crystals) set in a uniform matrix of spinel, perovskite, serpentine, and calcite. (Field of view 8.8 mm.)

petrologists now agree that such xenocrysts should not be included in kimberlite definitions.

Some Soviet petrologists, however, require the presence of such minerals in a rock in order that it be termed a kimberlite. Artsybasheva *et al.* (1964, p. 1773) state, "where fragments of pyrope-bearing peridotite and associated minerals are absent from a rock it cannot be called kimberlite." This concept has colored much of the Russian petrological thought; thus Frantsesson (1970) considers that kimberlites are mixtures of pyrope hyperbasites (garnet lherzolites), glimmerites, and ore pyroxenites (discrete nodule suite) within a picrite porphyry host. Marakushev (1982) believes that kimberlites form only as a result of the replacement of garnet lherzolites by carbonatitic magmas.

Such definitions of kimberlite have profound petrological ramifications as they do not allow the existence of kimberlite magmas in their own right; a conclusion at variance with most recent geological and mineralogical studies of kimberlite.

If the discrete nodule or megacryst suite is related to kimberlite then definitions must include this mineral assemblage. This approach has been taken in part by Milashev (1963), Kovalski (1963), and Mitchell (1970, 1979a). Thus Mitchell (1979a, p. 571) defines kimberlites as follows:

> Inequigranular alkalic peridotites containing rounded and corroded megacrysts of olivine, phlogopite, magnesian ilmenite and pyrope set in a fine-grained groundmass of second generation euhedral olivine and phlogopite, together with primary and secondary (after olivine) serpentine, perovskite, carbonate (calcite and/or dolomite) and spinels. The spinels range in composition from titaniferous magnesian chromite to magnesian ulvöspinel-ulvöspinel-magnetite. Accessory minerals include diopside, monticellite, apatite, rutile, and nickeliferous sulphides. Some kimberlites may contain major modal amounts of diopside or monticellite.

Mitchell (1979a) also introduced the concept of a *kimberlite clan* in recognition of the spectrum of rocks produced by the differentiation of kimberlitic magmas. Three main members of this clan are the following:

1. Kimberlites as defined above, which contain the characteristic suite of megacryst/macrocryst minerals, e.g., Monastery, Thaba Putsoa, Wesselton, and Tunraq.

2. Kimberlite as defined above, but poor in, or lacking, the heavy mineral and megacryst/macrocryst assemblages, these minerals having been lost during differentiation, e.g., Peuyuk, Jos, Benfontein and many aphanitic kimberlites, e.g., Mayeng.

3. Carbonate-rich residua, poor in silicates and oxides and the minerals of the megacryst/macrocryst suite, e.g., the Premier carbonate dikes, the Wesselton sills, and carbonate-rich ocellular dikes. These rocks would be termed *carbonatites* using the petrographic classification of Heinrich (1966). They have, however, very different mineralogies, antecedents, and comagmatic rocks to the carbonatites of alkaline rock complexes, and are better termed *calcite-kimberlites* to reflect this petrogenetic difference (Mitchell 1979a).

If the megacryst suite is unrelated to kimberlite, then it follows that definitions and classifications of kimberlite must be based solely upon minerals which are definitely known to have crystallized from the kimberlite magma. This approach has been advocated by Skinner and Clement (1979) and Clement *et al.* (1984), who define kimberlite as follows:

> . . . a volatile-rich potassic ultrabasic igneous rock which occurs as small volcanic pipes, dykes and sills. It has a distinctive inequigranular texture resulting from the presence of macrocrysts set in a fine grained matrix. This matrix contains as prominent primary phenocrystal and/or groundmass constituents, olivine and several of the following minerals: phlogopite, carbonate (commonly calcite), serpentine, clinopyroxene (commonly diopside), monticellite, apatite, spinels, perovskite, and ilmenite. The macrocrysts are anhedral, mantle-derived, ferromagnesian minerals which include olivine, phlogopite, picroilmenite, chromian spinel, magnesian garnet, clinopyroxene (commonly chromian diopside) and orthopyroxene (commonly enstatite). Olivine is extremely abundant relative to the other macrocrysts, all of which are not necessarily present. The macrocrysts and relatively early-formed matrix minerals are commonly altered by deuteric processes, mainly serpentinization and carbonatization. Kimberlite commonly contains inclusions of upper mantle-derived ultramafic rocks. Variable quantities of crustal xenoliths and xenocrysts may also be present. Kimberlite may contain diamond but only as a very rare constituent.

Both Mitchell's (1979a) and Clement *et al.*'s (1984) definitions have inadequacies, but serve to indicate the general character of kimberlite. Mitchell (1979a) fails to emphasize the macrocryst problem and refers to kimberlites as peridotites. Most kimberlites do not contain sufficient pyroxene to warrant such an appellation. Clement *et al.*'s (1984) definition does not emphasize the characteristic compositions of the kimberlitic mineral assemblage and introduces extraneous geological information (e.g., intrusion style, presence of xenoliths) to a petrological definition.

A revised definition incorporating aspects of both of the above definitions is as follows:

Kimberlites are a clan of volatile-rich (dominantly CO_2) potassic ultrabasic rocks. Commonly, they exhibit a distinctive inequigranular texture resulting from the presence of macrocrysts (and in some instances megacrysts) set in a fine-grained matrix. The megacryst/macrocryst assemblage consists of rounded anhedral crystals of magnesian ilmenite, Cr-poor titanian pyrope, olivine, Cr-poor clinopyroxene, phlogopite, enstatite and Ti-poor chromite. Olivine is the dominant member of the macrocryst assemblage. The matrix minerals include: second generation euhedral primary olivine and/or phlogopite, together with perovskite, spinel (titaniferous magnesian aluminous chromite titanian chromite, members of the magnesian ulvöspinel-ulvöspinel-magnetite series), diopside (Al- and Ti-poor), monticellite, apatite, calcite, and primary late-stage serpentine (commonly Fe rich). Some kimberlites contain late-stage poikilitic eastonitic phlogopites. Nickeliferous sulphides and rutile are common accessory minerals. The replacement of early-formed olivine, phlogopite, monticellite, and apatite by deuteric serpentine and calcite is common. Evolved members of the clan may be devoid of, or poor in, macrocrysts, and composed essentially of calcite, serpentine, and magnetite, together with minor phlogopite, apatite, and perovskite.

2.4. MINERALOGICAL CLASSIFICATIONS OF KIMBERLITE

Kimberlites exhibit extensive mineralogical variation coupled with considerable textural diversity. Unfortunately, these features have been combined in classifications of kimberlites which are of a geological nature rather than being based solely upon the mineralogical character of the rocks. Only recently have mineralogical classifications been divorced from morphological classifications.

Lewis (1887, 1888) originally noted that some varieties of kimberlite were particularly rich in mica. This observation was substantiated by Wagner (1914), who divided kimberlites into *basaltic* (i.e., olivine-rich rocks with less than 5% phenocrystal mica) and *lamprophyric* (i.e., mica phenocrysts in a groundmass containing more than 50% mica) varieties. The terminology was apparently introduced to describe the macroscopic appearance of the rock and has no genetic significance. Lamprophyric kimberlites were subdivided according to the pres-

ence or absence of clinopyroxene. Russian petrologists accepted Wagner's (1914) classification and incorporated it within several mineralogical-morphological classifications of Yakutian kimberlites (Bobrievich *et al.* 1959b, 1964, Kovalski, 1963, Milashev 1963, Artsybasheva *et al.* 1964, Frantsesson 1970). Further subdivisions were based upon the presence or absence of olivine, pyroxene, monticellite, or melilite. The latter mineral is included in these classifications because of the wider latitude allowed in the mineralogy of kimberlite in some of the Russian definitions.

Wagner's (1914) terminology has been widely accepted (Williams 1932, Dawson 1962, 1967a) and is still utilized uncritically by many geologists. This is unfortunate, in that the term *basaltic kimberlite* is particularly inappropriate, incorrect, and misleading, as feldspar is absent and the rocks are not mineralogically or genetically related to basalts (Mitchell 1970, Skinner and Clement 1979).

Mitchell (1970) proposed that three mineralogical varieties of kimberlite are recognizable, based upon the amounts of olivine, phlogopite, and calcite present: kimberlite (equivalent to basaltic kimberlite), micaceous kimberlite (equivalent to lamprophyric kimberlite), calcite or calcareous kimberlite. The latter category was introduced in recognition of the occurrence of primary magmatic calcite in kimberlite. Previously (Shand 1934, Milashev 1963, Frantsesson 1970) calcite was considered to be a secondary mineral.

Skinner and Clement (1979) and Clement *et al.* (1984) adopted the novel approach of classifying kimberlites solely on the basis of their groundmass modal mineralogy. This method is predicated upon the premise that it is not possible to distinguish the relative amounts of primary phenocrystal and xenocrystal olivines of the macrocryst population, and that all other macrocrysts are not related to kimberlite. Primary microphenocrystal or euhedral groundmass olivine is considered to be common to all kimberlites, and subdivisions are not made upon the basis of olivine content.

Five varieties of kimberlite, based upon the predominance of diopside, monticellite, phlogopite, calcite, and serpentine, are proposed by Skinner and Clement (1979). Further subdivisions are made by the use of an appropriate prefix to the basic name if sufficient quantities of one or more of these minerals are present, e.g., monticellite serpentine kimberlite. In some differentiated kimberlites, apatite, perovskite, or spinel are present in more than accessory amounts and in such cases can be included in the descriptive name. Illustrative examples of the use of this classification are given in Table 2.1.

Skinner and Clement's (1979) classification has proven useful in providing a rational terminology which allows comparison of kimberlites on a worldwide basis. Drawbacks of this system are that the modal variations of phenocrystal olivine shown by kimberlites are not reflected in the terminology, and that phlogopite textural relationships are ignored. For example, it is important to distinguish between kimberlites which are mica rich as a consequence of either

Table 2.1. Representative Modal Analyses and Classifications (Skinner and Clement 1979) of Kimberlites

	1		2		3		4		5		6		7		8	
	A	B	A	B	A	B	A	B	A	B	A	B	A	B	A	B
Phlogopite	44	67	28	38	1	1	22	34	20	34	1	1	1	2	9	15
Calcite	8	12	1	1	29	50	—	—	4	7	29	50	5	10	19	32
Serpentine	4	6	25	35	11	19	16	25	5	9	11	19	14	28	6	10
Diopside	—	—	18	25	—	—	26	40	—	—	—	—	27	54	—	—
Monticellite	—	—	—	—	—	—	—	—	18	31	—	—	—	—	—	—
Apatite	1	1	—	—	5	9	—	—	—	—	5	9	—	—	—	—
Opaques	6	9	1	1	11	19	1	1	5	9	11	19	1	2	20	33
Perovskite	3	5	—	—	1	2	—	—	5	9	1	2	2	4	6	10
Olivine	34	—	28	—	42	—	34	—	42	—	42	—	50	—	40	—

A, Volume percentages including cryptogenic olivine.
B, Volume percentages of A recalculated to exclude olivine.

1, Phlogopite kimberlite, Sydney-on-Vaal; 2, serpentine-phlogopite kimberlite, Finsch; 3, serpentine phlogopite calcite kimberlite, Wesselton; 4, phlogopite-diopside kimberlite, Bellsbank; 5, monticellite-phlogopite kimberlite, Matsoku; 6, calcite kimberlite, De Beer's dike; 7, diopside kimberlite, Letlhakane DKl; 8, opaque mineral-rich calcite kimberlite, Wesselton.

the concentration of macrocrystal/phenocrystal mica or the presence of groundmass poikilitic phlogopite. Consequently the classification should not be used in such cases without accompanying textural information or comment with regard to the macrocryst assemblage.

Skinner and Clement (1979) also drew attention to the common alteration of kimberlite by deuteric, metasomatic, and weathering processes. In the case of deuteric alteration the changes are a direct consequence of the crystallization of the magma, and the resulting alteration products are, for the purposes of classification, considered to be primary. Weathering and metasomatic processes will also obscure the original mineralogy of the kimberlite by the formation of secondary serpentine, calcite, dolomite, chlorite, and clay minerals. Skinner and Clement's (1979) classification is not applicable to such altered rocks. They can, however, be described as carbonatized, dolomitized, or serpentinized varieties of kimberlite.

2.5. THE RECOGNITION OF KIMBERLITE

It is important to realize that Skinner and Clement's (1979) classification is purely petrographic and can be used only when it has been determined by some other means that a particular rock is a kimberlite. For example, in terms

of the petrographic mode, the classification is applicable to a wide variety of alkaline ultrabasic rocks including mica peridotite, lamprophyres, picrite porphyry, and olivine lamproite. These rocks are similar in being characterized by the assemblage olivine, phlogopite, serpentine, calcite, opaque oxides, perovskite, diopside, and/or melilite. With the exception of the melilite-bearing varieties, these rocks are petrographically very similar to the matrix of the macrocrystal kimberlites or to differentiated aphanitic calcite serpentine kimberlites. Such rocks and their apparent relationship to kimberlite are described in Section 2.6.

Clement *et al.*'s (1984) definition of kimberlite does not provide the means of discrimination between it and other alkaline ultramafic rocks, unless the macrocrystal assemblage and some of the geochemical features of the rocks are taken into consideration. A curious aspect of Clement *et al.*'s (1984) definition, therefore, is that the presence of minerals considered to be unrelated to kimberlite is required for the recognition of the rock. This paradox is eliminated if some of the macrocrystal phases are considered to be cognate.

Mitchell (1979a, 1983), Clement *et al.* (1984), and Scott Smith and Skinner (1984a) have discussed the problem of identifying kimberlite and shown that kimberlites can be recognized by consideration of the mode in conjunction with the composition and paragenesis of the phases present. Mitchell (1979a) has stressed also that, in the case of calcite kimberlites, study of the nature of antecedent comagmatic rocks is especially important if these rocks are not to be classified on a purely petrographic basis as carbonatites.

The following petrographic and mineralogical criteria are presented as a guide for the recognition of kimberlites in conjunction with the definition given above (Section 2.4). Not all of these features may be present in any given kimberlite and macrocrysts in particular may be absent in differentiated kimberlites. An individual criterion taken in isolation is not necessarily diagnostic; the mineral assemblage and its compositional variation as a whole must be considered before deciding upon the nature of the samples studied. *Kimberlites cannot be identified solely on a petrographic basis.*

1. The presence of megacrysts and macrocrysts of Cr-rich (>1000 ppm), Nb-rich (>100 ppm) magnesium (3–23% MgO) ilmenite, low Cr_2O_3 (0%–3%) titanian (0%–1.5% TiO_2) pyrope [Mg/(Mg + Fe) = 0.90–0.65] and calcic to subcalcic [Ca/(Ca + Mg) = 0.25–0.50] low TiO_2 (<1%), Al_2O_3 (<3%), Na_2O (<2%), Cr_2O_3 (<1%) diopside.

2. The occurrence of two generations of olivine of different morphology which give the rock an inequigranular appearance. These consist of an earlier generation of round macrocrystal olivines and a later suite of microphenocrystal or groundmass euhedral to subhedral olivines. The macrocrysts are typically single crystals and comprise a mixed population of resorbed xenocrysts and phenocrysts. Euhedral phenocrysts of equivalent size are rare in kimberlites but are common in lamprophyres, mica peridotites, and lamproites. In these latter

rocks the phenocrysts also occur as complex multiple parallel growth aggregates (Figure 2.8), or as single crystals with skeletal or hopper morphologies. Scott Smith and Skinner (1983, 1984a) have stressed that such olivines are not characteristic of kimberlites.

Kimberlite groundmass olivines have a relatively restricted composition and are not richer in iron than Fo_{85}. Overgrowths of this limiting composition are common on macrocrystal olivines. The presence of iron-rich olivines ($<Fo_{85}$) indicates the presence of xenocrysts or primary olivines which have formed from magmas unrelated to kimberlite.

3. Mica occurs in two generations: macrocrystal titanian ($<6\%$ TiO_2) phlogopite; and microphenocrystal and groundmass Ti-poor ($<3\%$ TiO_2) phlogopite, eastonitic phlogopite, or Ti-poor ($<1\%$ TiO_2) tetraferriphlogopite. Highly titaniferous ($>6\%$ TiO_2) phlogopites, titanian tetraferriphlogopites, sodian tetraferriphlogopites and BaO-rich ($>3\%$) phlogopites, as found in lamproites, alnöites, and minettes are absent in kimberlites.

4. Groundmass diopsides are poor in TiO_2, Al_2O_3, Na_2O, and Cr_2O_3 (all usually less than 1%), demonstrating that solid solution toward calcium tschermak's pyroxene, titanpyroxene, and acmite does not occur. This is in contrast to pyroxenes from monchiquites, camptonites, and alnöitic rocks.

5. Groundmass spinels are, typically, Ti- and Cr-rich and Al-poor relative to lamprophyre spinels. Two compositional trends are evident: evolution from titaniferous magnesian aluminous chromite through members of the magnesian ulvöspinel-ulvöspinel series to magnetite; and evolution from titaniferous magnesian chromite to titanian chromite to ulvöspinel-magnetite. Compositional trends are distinctly different from those of spinels in lamprophyres and alnöitic rocks (see Section 6.10). Spinels are particularly useful aids in the identification of kimberlites as they are commonly unaffected by deuteric or weathering alteration processes.

6. Perovskites are poor in rare earths, Na_2O, FeO, Nb_2O_5, and Ta_2O_5, relative to perovskites from carbonatites, i.e., knopite, latrappite, dysanalyte, leushite, and loparite are absent in kimberlites.

7. Calcites are all low MgO ($<1.0\%$) and FeO-poor ($<0.5\%$) varieties relative to carbonatite calcites. Exsolution intergrowths of dolomite and calcite are absent in kimberlites.

8. Calcite kimberlites are lacking in the characteristic minerals of carbonatites, e.g., pyrochlore, bastnaesite, synschisite, monazite, alkali amphiboles, and pyroxenes.

9. Primary serpentine, commonly Fe rich, occurs within the groundmass or as discrete segregations. (see Section 3.7.2.1.)

10. Feldspars and feldspathoids are absent in kimberlites.

11. Primary and secondary (after melilite) andradite-schorlomite garnets are absent in kimberlites.

2.6. PSEUDOKIMBERLITES

The diversity of opinion regarding the nature of kimberlite has had some unfortunate consequences in that many rocks, which should be placed within other petrological associations, have been labeled kimberlites. Such interpretations have resulted in unwarranted speculation regarding the relationships between kimberlites and other magma types.

2.6.1. Mica Peridotites and "Kimberlitic Rocks"

Mica peridotites, originally described from west Kentucky by Diller (1892), consist of phenocrysts of serpentinized olivine set in a matrix of phlogopite, serpentine, opaque oxides, calcite, chlorite, and minor amounts of pyroxene, apatite, perovskite, and andraditic garnet (Koenig 1956). The similarity of this mineral assemblage to that of kimberlite, coupled with Wagner's (1914) description of lamprophyric kimberlite as a variety of mica peridotite, has led to the terms becoming virtually synonymous. Thus, any rock containing the assemblage phlogopite-spinel-olivine-calcite and/or pyroxene is commonly termed *kimberlite*. This usage is especially prevalent in North America where calcite-rich ultrabasic dikes of small size and limited exposure are referred to as "kimberlitic dikes" (Brown *et al.* 1967, Gittins *et al.* 1975, Watson 1955, Watson *et al.* 1978), with the implication that the sample sizes are too limited to find any of the characteristic minerals (e.g., magnesian ilmenite, etc.) of kimberlite. Dikes with significant calcite contents have been termed "kimberlitic-carbonatitic" (Gittins *et al.* 1975) or "carbonatite-kimberlite" (Zhabin 1967). It should be noted that the latter term is applied to ultramafic dike rocks associated with the Arbarastakh carbonatite complex and is *not* synonymous with the same term as used by Malkov (1975) to describe calcite-rich kimberlites (*caveat lector*).

It is difficult to discuss many of these rocks in terms of the kimberlite recognition criteria listed in Section 2.5, as few modern mineralogical studies of them have been undertaken.

Figure 2.4 illustrates a mica peridotite and show that such rocks are petrographically different from macrocrystal kimberlites and can be described as porphyritic rocks. Mitchell (1979a) has shown that such rocks do not have affinities with kimberlite, by virtue of their containing biotitic phlogopites (6%–9% FeO), aluminous titanian pyroxenes (Al_2O_3 = 4%–8%; TiO_2 = 1.5%–2.8%), late-stage MgO-poor (<0.2%) manganoan (1-3% MnO) ilmenites together with spinels which are distinctly more aluminous and magnesium poor, relative to kimberlite spinels. Spinel compositional trends in the Claylick Creek and View mica peridotites (Figure 6.46) and the Keith Township "kimberlitic dike" (Figure 6.47) are different from those established for kimberlites (see Section 6.9.10).

Ferguson and Sheraton (1979), Ferguson *et al.* (1979), Stracke *et al.* (1979),

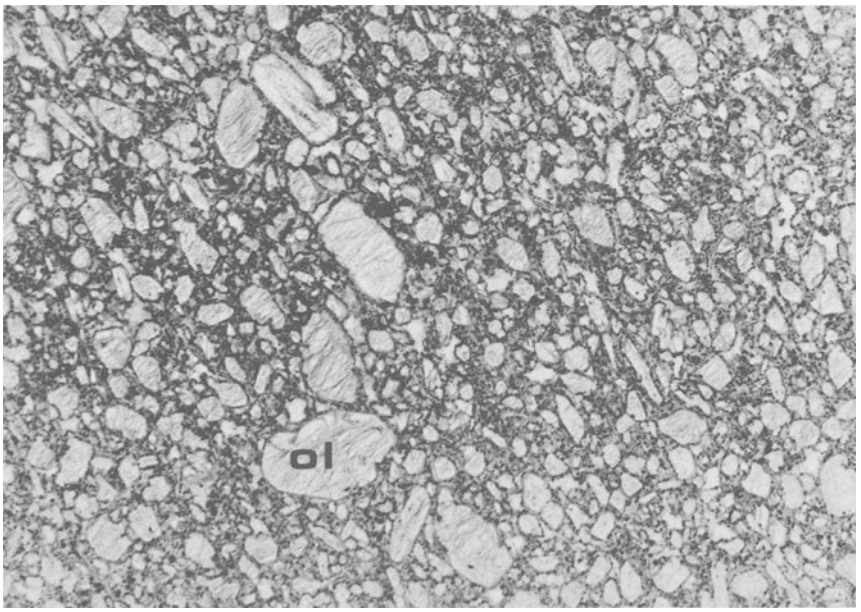

Figure 2.4. "Mica peridotite," Claylick Creek, west Kentucky. A pseudokimberlite consisting of anhedral to subhedral serpentinized olivine (ol) phenocrysts set in a matrix of spinel, aluminous pyroxene, phlogopite, calcite and chlorite. (Field of view 10 mm.)

and Jaques *et al.* (1984a,b) have used the term "kimberlitic" to refer to a variety of undersaturated basic rocks occurring in New South Wales and Victoria, Australia. The rationale for this terminology lies in Ferguson and Sharaton's (1979) apparent belief that these rocks cannot be identified unequivocally. Consequently any rocks that have been emplaced as diatremes and which contain mantle-derived xenoliths are termed "kimberlitic rocks." It seems unnecessary to introduce the terminology, as Ferguson and Sheraton (1979) state clearly that none of the rocks in question are at all like kimberlites and, in fact, have nephelinitic or alkali basaltic affinities. Ferguson and Sheraton (1979) ignore the contemporaneous volcanism and their own mineralogical data which clearly demonstrate the nature of the parental magmas. It is unsatisfactory to define a rock as kimberlitic, the implication being that the rock is a kimberlite, on the basis of the mode of emplacement of the magma and the presence of mantle-derived xenoliths. Many rocks derived from diverse and unrelated magmas would fit this description. The continued promotion of the terminology by Jaques *et al.* (1984a,b) is inexplicable on a scientific basis, but is understandable on proprietary grounds, and is all the more confusing in that *bona fide* kimberlites are present in the adjacent Terowie region of South Australia. Further comments on pseudokimberlitic volcanism can be found in Section 3.2.5.

In summary, it is concluded that the term "mica peridotite" is not synonymous with kimberlite and that such rocks are unrelated to kimberlite. The terms "kimberlitic dike" and "kimberlitic" used as *nouns* by North American and Australian geologists respectively, should be abandoned as the rocks referred to are not kimberlites.

N.B. *"Kimberlitic" is used in this work strictly as an adjective unless otherwise explicitly stated.*

2.6.2 Picrite Porphyry

Picrite porphyries are magnesium-rich, olivine-phyric, effusive (Egorov 1970), and hypabyssal (Frantsesson 1970) rocks. The olivine phenocrysts (commonly serpentinized and carbonatized) are set in groundmass containing pyroxenes, mica, monticellite, nepheline, titanomagnetite, perovskite, serpentine, chlorite, calcite, and/or melilite (Figure 2.5). Soviet petrologists (summarized by Frantsesson 1970, Malkov 1972) believe that picrite porphyries form the matrix of kimberlites. This hypothesis denies a magmatic origin for calcite and

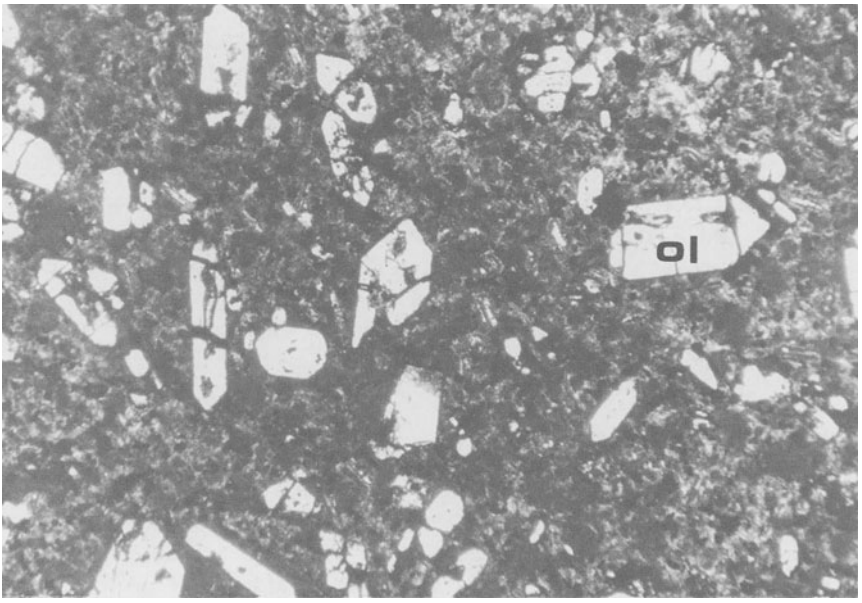

Figure 2.5. Olivine melilitite, Coral Rapids Sill, northern Ontario. This ultramafic sill would be described as a picrite porphyry by Soviet petrologists. Note the characteristic resorbed, "hopper-type" euhedral olivine (ol) phenocrysts; olivines of this type have not been described from kimberlites. The unresolved groundmass consists of melilite laths, spinels, perovskite, and calcite.(Field of view 4.0 mm.)

assumes that the serpentine-calcite-rich matrix of kimberlite has formed as a result of alteration of pre-existing pyroxene, melilite, and monticellite. Consequently, descriptions of rocks termed picrite porphyries may refer to hypabyssal macrocryst-poor facies of genuine kimberlites, or to porphyritic ultramafic dikes and lavas associated with alkaline ultrabasic complexes such as the Gulinskaya intrusion in the Maimecha-Kotui region of northern Siberia (Egorov *et al.* 1961).

Application of the same term to magmas of diverse origins is unacceptable and has resulted in the erroneous concept that kimberlites are hybrid rocks (see Section 2.3) and can contain melilite or nepheline as a primary groundmass phase.

Conversely, picrite porphyries and similar rocks associated with alkaline rock–carbonatite complexes are termed kimberlites and account for the concept advocated by many Soviet petrologists (e.g., Vaganov 1978), that there exist two different types of "kimberlite fields": kimberlites equivalent to those as defined by Mitchell (1979a) or Clement *et al.* (1984), e.g., the Daldyn-Alakit and Muna fields; and kimberlites accompanied by picrite porphyries, pyroxene-sövite, and carbonatites, e.g., the Maimecha-Kotui, Luchakan, and Kuonapka fields. These latter rocks are named kimberlites, despite the great differences in petrography, mineralogy, and geochemistry of the two groups.

As a consequence of this synonymity, not all kimberlites referred to in the Russian literature are kimberlites, e.g., kimberlites of the Maimecha-Kotui region (Makhlaev and Surina 1966) or the Bargydamalakh kimberlite-olivine melilitite composite intrusion (Ukhanov 1963). Each reported occurrence of kimberlite must therefore be carefully evaluated in the context of the above comments.

A further consequence of this Soviet approach to the nature of kimberlite is that the effusive rocks termed *meimechites* (Moore and Sheinmann 1946, Butakova and Egorov 1962) are the extrusive equivalents of kimberlite. The rocks are related to the picrite porphyries, but are mineralogically and petrographically unlike kimberlites (Malkov 1972, Dawson 1971, Bagdasarov *et al.* 1981). Dawson (1980) and Egorov (1970) have discredited any relationship to kimberlites and noted that the rocks are simply olivine-phyric picrites.

2.6.3. Central Complex Kimberlites—Alnöitic Rocks

Dawson (1966, 1967a) introduced the term *central complex kimberlite* to describe the micaceous basic to ultrabasic dikes and plugs found in or near some alkaline rock–carbonatite complexes, e.g., Ngualla (Tanzana), Rangwa (Kenya), Arbarastakh (Yakutia), Fen (Norway), and Ile Bizard (Quebec). The term is equivalent to the rock name *damkjernite* (Brögger 1921, Kapustin 1981).

Designation of such rocks as kimberlites also stems from Von Eckermann's (1967) study of dikes associated with the Alnö carbonatite complex, Sweden. In defining kimberlite, Von Eckermann relies upon Shand's (1934) definition,

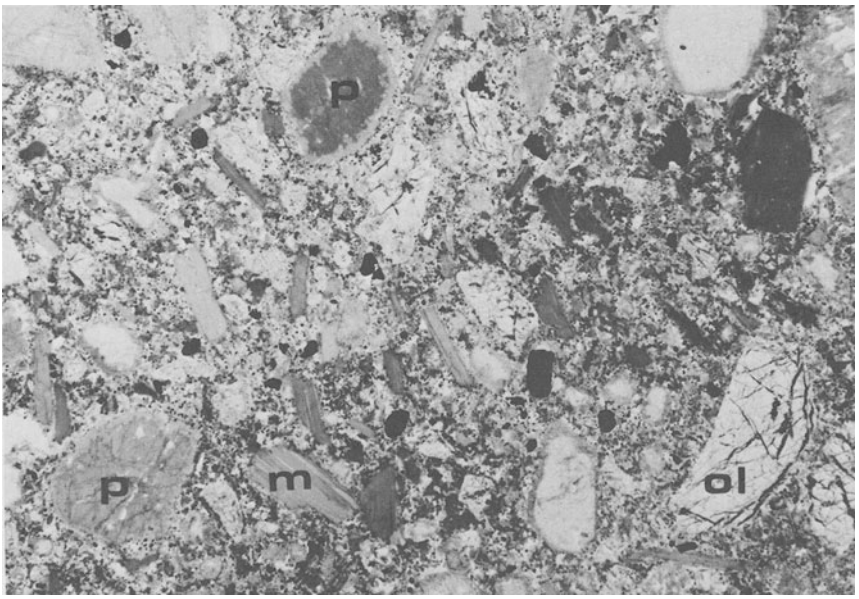

Figure 2.6. Damtjernite (= damkjernite = alnöite), Fen Complex, southern Norway. This rock is an example of a "central complex kimberlite" (Dawson 1966, 1967a), and consists of phenocrysts of zoned and mantled aluminous salite (p), titanian phlogopite (m), and macrocrysts of anhedral olivine (ol), set in a matrix of Mg-rich biotite, Ti-Al salite, ferropargasite spinel, and calcite. (Field of view 25 mm.)

which implies that melilite, now replaced by calcite, is an essential mineral of kimberlite.

Kresten (1979) has shown that all of the dikes at Alnö are modal variants of *alnöitic rocks;* i.e., "Lamprophyric rocks with phenocrysts of phlogopitic mica, titanomagnetite, olivine, diopside, or calcic amphibole, set in a matrix of phlogopite, titanomagnetite, perovskite, and apatite; some varieties contain melilite, andraditic garnet, picotite or chromite" (Kresten 1979, p.4).

This definition embraces damkjernite. Kresten (1979) considers that modal variations in olivine, melilite or calcite content result in gradations into kimberlitic rocks, melilitolites (okaites, bergalites etc.) and alvikites (sövites), respectively.

Figures 2.6 and 2.7 illustrate a central complex kimberlite (Fen), and an Alnö kimberlitic rock, respectively. Petrographically they are unlike kimberlites as defined in this work. Mitchell (1970, 1979a, 1983) has shown that the mineralogy and the compositional trends exhibited by the pyroxenes (Ti and Al enrichment) and spinels (Figure 6.46) are unlike those of kimberlite. The presence of titanian pargasite, melilite, nepheline, and andraditic-schorlomitic garnet,

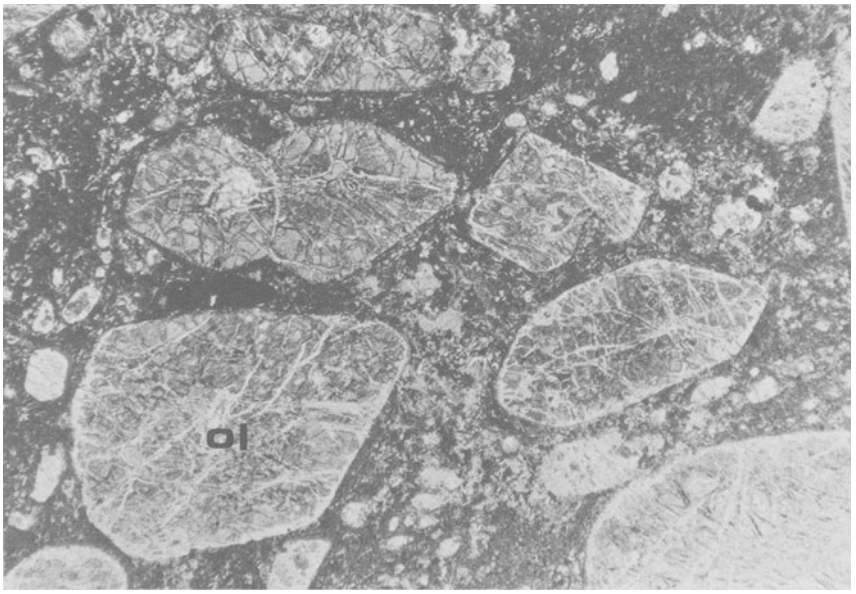

Figure 2.7. Alnöite, Nederkorsta, Alnö, Sweden. This rock consists of euhedral serpentinized olivine (ol) phenocrysts set in an unresolved groundmass of altered melilite laths, spinel, perovskite and calcite. This is an example of Kresten's (1979) "kimberlitic alnöites." (Field of view 8.8 mm.)

further emphasizes their lack of affinity with kimberlite. Alnö kimberlitic rocks are incorrectly named being actually alnöites (i.e., Von Eckermann's kimberlites), or ultramafic (olivine-rich) members of a consanguineous suite of alnöitic-carbonatite magmas (i.e., Kresten's 1979, kimberlitic rocks).

Alnöitic rocks are related to nephelinite-melilitite volcanism (Nixon *et al.* 1980, Mitchell 1979a) and represent the products of crystallization of such magmas under plutonic conditions over a wide range of CO_2 and H_2O pressures. Such magmas are mantle-derived and can contain xenoliths of spinel and garnet lherzolites, e.g., Fen, Ile Bizard, and Malaita. The presence of these xenoliths, or of xenocrysts derived from them, is indicative only of the deep origin of the magmas and not of any relationship to kimberlite.

2.6.4. Olivine Lamproites

Diamond-bearing rocks in the West Kimberley region of west Australia have been classified as kimberlites, kimberlitoids, or ultrapotassic kimberlites (Atkinson *et al.* 1982, Jaques *et al.* 1982, Madigan 1983, McCulloch *et al.* 1983, Nixon *et al.* 1982). In naming the rocks these authors appear to have been unduly influenced by the presence of diamond, rather than by the obvious min-

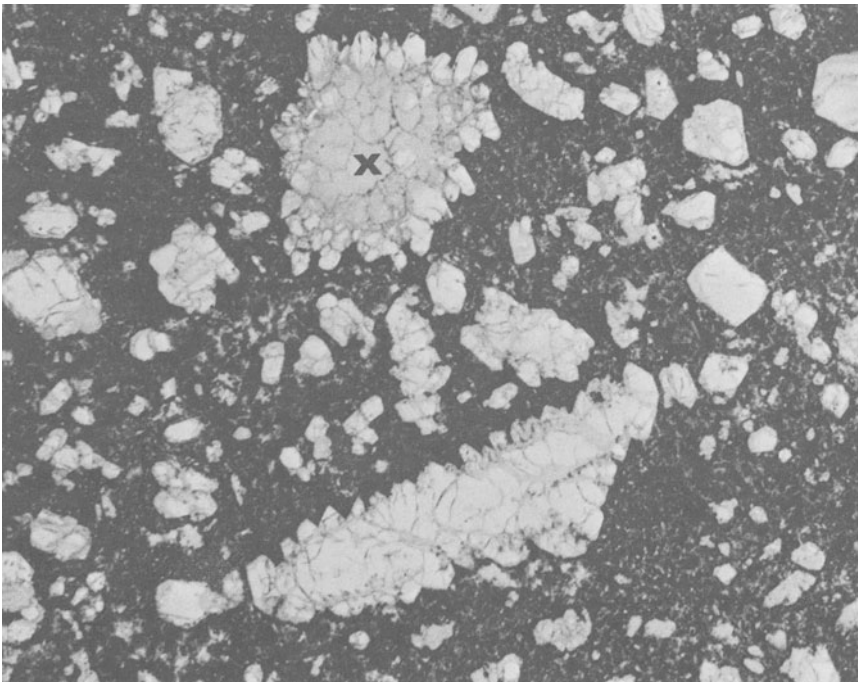

Figure 2.8. Olivine lamproite, Kimberlite Mine, Arkansas. This lamproite is characterized by microphenocrysts of corroded euhedral olivine and by anhedral megacrysts (x) mantled by parallel multiple growth aggregates of olivine. Such growth features are not found in kimberlites. The unresolved groundmass contains perovskite, phlogopite, K-Ti-richterite and altered glass and/or potassium feldspar. (Field of view 6.0 mm.)

eralogical and geochemical affinities with contemporaneous lamproites. In subsequent studies, Jaques *et al.* (1984a,b,) have modified the terminology, and the diamondiferous ultramafic rocks are described as olivine lamproite or "kimberlitic rocks." Some examples are said to resemble micaceous kimberlites.

Olivine lamproites consist of large olivine phenocrysts of complex morphology set in a fine grained to glassy matrix containing smaller olivines, phlogopite, diopside, apatite, perovskite, spinels, and glass (Figure 2.8). Coarser grained varieties contain groundmass poikilitic plates of titanian phlogopite, titanian potassian richterite and wadeite. In the West Kimberley area there is complete mineralogical gradation to leucite lamproites with decreasing amounts of olivine (Jaques *et al.* 1984a).

Scott Smith and Skinner (1983, 1984a,b), Mitchell and Lewis (1983), and Mitchell (1985) have demonstrated that the diamond-bearing rocks previously described as kimberlites from West Kimberley and Arkansas (Meyer 1976) are, in fact, lamproites on the basis of the criteria outlined in Section 2.5. Olivine-

rich rocks are merely ultramafic components of a differentiated lamproite magma. None of the rocks have any petrogenetic relationship to kimberlite.

2.6.5. Metakimberlites

Diamondiferous dikes found in the Mitzic and Seguela regions of Gabon and the Ivory Coast respectively have been termed meta-kimberlites by Bardet (1973). The rocks are highly altered, sheared, and have the appearance of talc schists. They lack the typical kimberlite megacryst suite but contain chromite and anatase. In the less-altered varieties it is possible to recognize pseudomorphs after olivine. The presence of relatively fresh, corroded, and zonation-free phlogopite phenocrysts has been noted by Mitchell (1985) in the Bobi dike, Seguela. These phenocrysts have the optical and chemical characteristics of lamproitic phlogopite. The close spatial association with fitzroyite dikes has led Mitchell (1985) to the conclusion that the so-called meta-kimberlites are, in reality, merely highly altered olivine phlogopite lamproites. Metamorphosed *bona fide* kimberlites, to which Bardet's (1973) term might be applied, have not yet been recognized.

Extinct volcanoes brood in silence
Ash scatters down into their keep
Reposing from their evil deeds
The giants are now sunk in sleep.
Bella Akhnatovna Akhmadulina

3

KIMBERLITE MAGMATISM AND TEXTURAL GENETIC CLASSIFICATIONS OF KIMBERLITE

3.1. MODELS OF KIMBERLITE MAGMATISM

Initial studies of kimberlites (Wagner 1914) demonstrated that they occur as carrot-shaped vertical intrusions termed pipes or diatremes and as tabular dikes (fissure kimberlites).

The diatremes, because of their economic importance, attracted far more attention than the dike rocks. As a consequence of this bias, kimberlites came to be regarded as fragmental rocks (e.g., Fozzard 1956) and the existence of kimberlitic magma was doubted. The absence of thermal metamorphic effects associated with diatreme emplacement led to hypotheses that kimberlites were intruded from the mantle as cold crystal mushes (Mikheyenko and Nenashev 1962) or cold gas–solid fluidized systems (Davidson 1964, Edwards and Howkins 1966, Kennedy and Nordlie 1968). This restricted view of kimberlite was not shared by many Soviet petrologists who recognized the existence of kimberlitic (albeit hybrid) magmas in the development of the Yakutian kimberlite provinces (Milashev 1963, Artsybasheva *et al.* 1964, Lebedev 1964, Frantsesson 1970).

The studies of Dawson and Hawthorne (1970, 1973), Dawson (1971), and Hawthorne (1975) established the basis for modern concepts of kimberlite magmatism by recognizing (1) the existence of hot mobile kimberlite magmas, (2) that such magmas could undergo differentiation, (3) the occurrence of pyroclastic and epiclastic kimberlites, (4) that diatremes with increasing depth are gradational into nonbrecciated hypabyssal kimberlites, (5) the existence of kimberlite sills.

Diatremes were thus seen to be only a particular manifestation of a more general magmatic style and not some unique cryoclastic pseudomagmatic system.

Kimberlites are now recognized as volatile-rich ultrabasic magmas whose evolution and emplacement can be described in terms of standard differentiation, intrusion, and extrusion processes.

Figure 3.1 illustrates an idealized kimberlite magmatic system showing the relationships between effusive rocks, diatremes, and hypabyssal rocks. Cur-

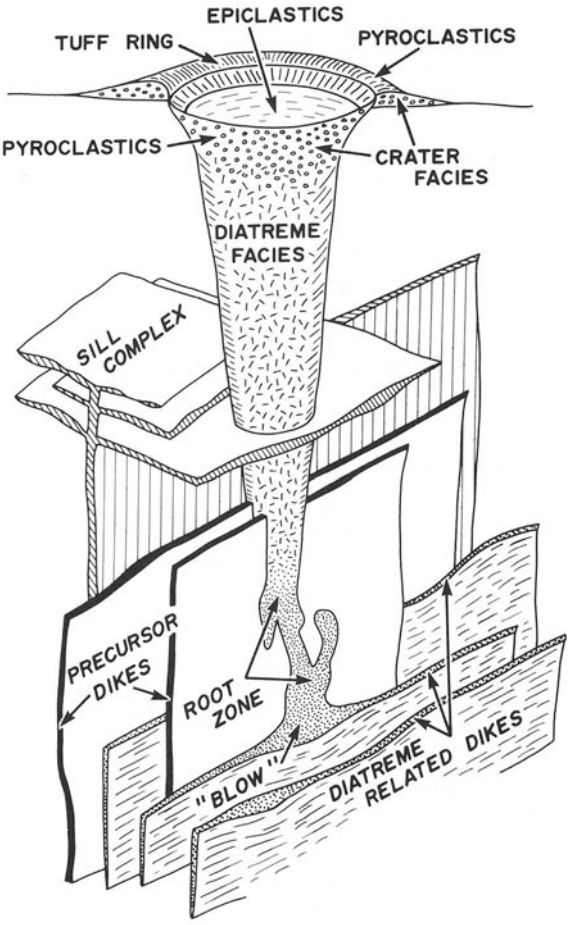

Figure 3.1. Model of an idealized kimberlite magmatic system, illustrating the relationships between crater, diatreme, and hypabyssal facies rocks (not to scale). Hypabyssal facies rocks include sills, dikes, root zone and "blow."

rently, three textural genetic groups of rocks, each associated with a particular style of magmatic activity, are recognized: (1) crater facies, (2) diatreme facies, and (3) hypabyssal facies (Dawson 1971, Hawthorne 1975, Clement and Skinner 1979, Scott Smith and Skinner 1984b). Hypabyssal rocks occur in the root zones of diatremes and as sill complexes and dike swarms.

The basic features of each facies are described below, with further details of diatreme facies kimberlites being given in Chapters 4 and 5.

3.2. CRATER FACIES KIMBERLITES

A record of subaerial effusive activity has only been preserved in a few areas where erosion has been minor. Most of the deposits occurring in these regions have not been adequately investigated or subjected to modern volcanological study. The eruption of a kimberlitic volcano has not yet been witnessed.

Crater facies rocks can be divided into (1) lavas, (2) pyroclastic rocks, and (3) epiclastic rocks.

3.2.1. Lavas

Bona fide uncontaminated glassy or aphyric kimberlite lavas have not yet been recognized. The only lava which *might* be considered to be effusive kimberlite occurs as a small flow emitted from one of the Igwisi Hills (Tanzania) tuff cones (Sampson 1953, Bassett 1954, Fozzard 1956). This vesiculated lava consists of rounded olivine crystals commonly mantled by chromite, set in a fine-grained matrix of carbonate, serpentine, complexly zoned titanian spinels, perovskite, and apatite (Fozzard 1956, Reid *et al.* 1975). Some examples exhibit a flow texture defined by laths of calcite aligned in parallel. This lava is petrographically similar to some macrocrystal kimberlites, and to the kimberlites of the Benfontein sills (Reid *et al.* 1975). The groundmass spinels belong to the magnesian ulvöspinel-ulvöspinel-magnetite series and are similar to Ti-rich spinels in evolved kimberlitic magmas.

Reid *et al.* (1975) consider that all of the spheroidal olivine macrocrysts are derived from a garnet lherzolite precursor and that the lava is hybrid, formed by the mixing of these xenocrysts with a volatile-rich kimberlitic magma. This magma, lacking in other megacrysts, rich in calcite and containing evolved spinels, represents a differentiatè of a kimberlitic magma and cannot be regarded as being representative of primary kimberlitic liquids.

Meimechite (see Section 2.6.2) has been discredited as a possible extrusive equivalent of kimberlite.

3.2.2. Pyroclastic Rocks

The only known examples of kimberlite pipes surrounded by the remnants of tuff rings or tuff cones are found at Kasami, Mali (Hawthorne 1975), and the Igwisi Hills, Tanzania (Reid *et al.* 1975).

At Kasami a 250 m-diameter pipe is surrounded by a ring (125 m in width) of laterized kimberlitic tuffs. The tuff is 1–4 m in thickness and rests upon a level land surface. Unfortunately no information is available regarding the petrography or stratigraphy of this tuff.

Tuff cones forming the Igwisi Hills have crater diameters of approx. 400, 250, and 200 m, with the rims standing only 15–50 m above the surrounding peneplain. The tuffs are vesicular, highly altered, and carbonatized. They are petrographically similar to the Igwisi lava as they contain many olivine macrocrysts set in a fine-grained serpentine and calcite-rich groundmass.

The Igwisi and Kasami occurrences have the characteristics of maar volcanoes, i.e., low volcanic cones with bowl-shaped craters that are wide relative to rim height (Fisher and Schminke 1984).

At other localities tuffs are preserved only within craters. They are particularly common in the Singida (Tanzania) kimberlite province where differences in erosional levels have enabled Mannard (1962) to distinguish four types of bedded pyroclastics. From the deepest (oldest) parts of the craters to the shallowest (youngest) these are (1) basal breccias, (2) poorly stratified coarse pyroclastics, (3) well-stratified tuffs, and (4) epiclastic lacustrine deposits (see Section 3.2.3).

The well-stratified tuffs consist of alternating layers of coarse lapilli-sized (2–64 mm) tuffs and laminae of finer ash sized (<2 mm) tuffs. Coarse and fine layers are of identical composition and consist of serpentine pseudomorphs after olivine, together with phlogopite, garnet, and ilmenite macrocrysts set in a matrix of serpentine, clays, calcite, and chlorite. These crystal tuffs grade into lithic tuffs by increasing contents of quartz, feldspar, and biotite derived from the country rock. Graded beds and depositional features appear to be absent. Mannard (1962) believes that these tuffs are primarily airfall deposits which, in some cases, may have been deposited in water.

Underlying these well-stratified tuffs are poorly stratified tuffs and tuff breccias containing fragments of kimberlite, country rock, and mantle-derived xenoliths cemented by pyroclastic material similar to that of the overlying tuffs. Complex folds, attributed by Mannard (1962) to slumping, are common.

Shards of glass, cauliflower bombs, scoriaceous materials, and pelletal lapilli were not observed by Mannard (1962).

Bedded pyroclastics occur at the Winkler Crater, Kansas (Brookins 1970) but detailed descriptions have not been published. Figure 3.2 illustrates that one well-bedded "tuff" consists of pelletal lapilli within a clay mineral matrix and is very similar in petrographic character to some diatreme facies kimberlites (Figure 3.6).

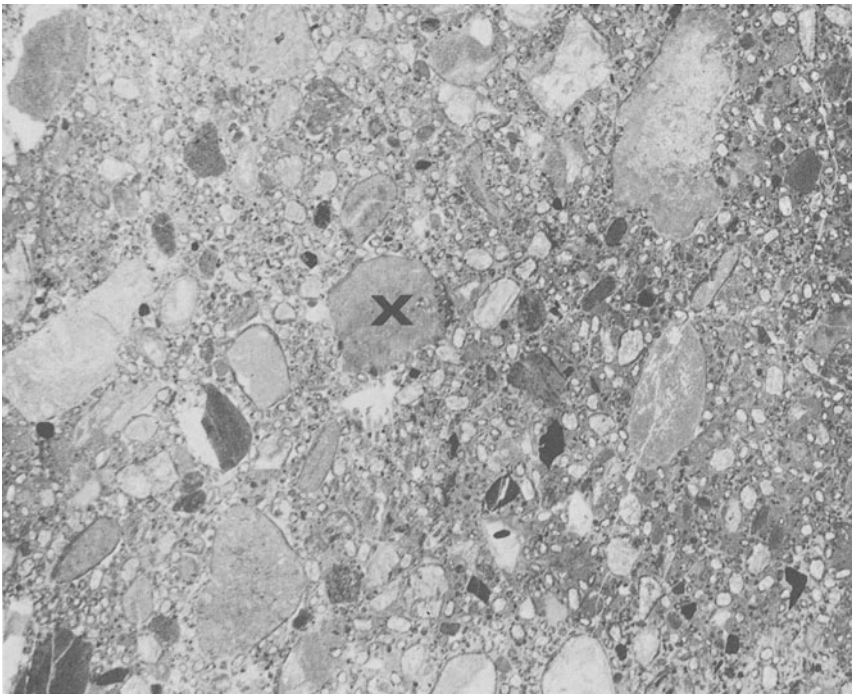

Figure 3.2. Pyroclastic(?) kimberlite, Winkler Crater, Kansas. Large clasts of country rock (x), serpentinized olivine macrocrysts and much smaller rounded and angular autoliths and pelletal lapilli of kimberlite are set in a matrix of clay minerals and zeolites. (Field of view 25 mm.)

3.2.3. Epiclastic Kimberlites

Epiclastic kimberlites are produced by the fluviatile re-working and re-deposition of kimberlite tuffs in crater lakes (maars) formed above diatremes. Commonly, the deposits include fragments of in-washed country rocks. The deposits are named according to standard sedimentological particle size terminology (e.g., kimberlitic shales, kimberlitic sands, etc.).

Epiclastic rocks are preserved in areas which have undergone little erosion since the emplacement of the diatreme, or as down-faulted or slumped blocks in crater and diatreme facies kimberlites. Examples of the former occur at Mwadui, Tanzania (Edwards and Howkins 1966), Kolonge, Magoba, and Mahenga in the Singida region, Tanzania (Mannard 1962), Orapa, Botswana (Hawthorne 1975), and Mbuji-Mayi, Zaire (Fieremanns 1966), and the latter at Kao, Lesotho (Rolfe 1973), the Kimberley area diatremes, South Africa (Clement 1982), and Winkler Crater, Kansas (Coopersmith, personal communication).

Hawthorne (1975) notes that epiclastic rocks are usually found in oval or elliptical bowl-shaped, basin-like structures 50–1500 m in diameter. The margins of the basins dip inwards at angles of 25°–70°. The basins may extend to depths of over 300 m below the present land surface but commonly are less than 150 m deep. The epiclastic succession is complex and resembles a series of overlapping alluvial fans together with lake-bottom deposits. The epiclastic rocks overlie "tuffaceous" kimberlites.

Detailed modern sedimentological–volcanological studies of epiclastic kimberlites have not yet been published, and brief geological descriptions are available for only a few localities.

At the Mwadui pipe, Edwards and Howkins (1966) have noted that epiclastic kimberlites overlie unsorted kimberlite breccias consisting of boulders of granite set in a matrix of altered kimberlite. This breccia is believed to be related to the breakthrough stages of eruption and to represent shattered and permeated country rock. Coarse and fine grained sedimentary rocks overlie this breccia. Near the crater walls the kimberlite sediments are very poorly sorted and consist of an aggregate of granite and kimberlite boulders set in a matrix of coarse detritus. Further away from the crater walls the sediments become progressively finer grained and are well sorted and well-bedded. Fossil plants are common in these grey and yellow shales and mudstones that were deposited in the central parts of the crater lake. Slumping of poorly bedded deltaic deposits from the margins of the crater over these shales has occurred. The presence of magnesian ilmenite and pyrope in the heavy mineral fraction of the shales indicates that they were derived in part from the erosion of kimberlite.

Similar shales and mudstones, in some cases containing fossil fish, have been described from the Singida field, Tanzania by Mannard (1962). The particles in the sediments range from clay to sand size and include detritus from the granitic country rocks and the kimberlite crater walls. The coarser fractions form beds up to several centimeters in thickness, with the finer material occurring as thin laminae. Graded bedding is common. Some of the epiclastic rocks have been replaced by chalcedony as a result of late-stage volcanic hot spring activity.

3.2.4. Surface Expression of Kimberlitic Volcanism

Studies of crater facies kimberlites indicate that kimberlitic magmas rarely form lavas, but typically produce pyroclastic deposits. The volume of pyroclastics is small and they are confined to craters and to thinly bedded tuff rings or small cones; large, steep-sided tuff cones and complex stratovolcanoes are not formed. Pyroclastic volcanism is not followed by the upwelling of magma to form crater lava lakes, and the establishment of a conduit filled with magmatic kimberlite does not occur.

Figure 3.3.A illustrates a cross section of a kimberlite volcano as described by Mannard (1962) with the addition of a Kasami-type tuff ring and a maar

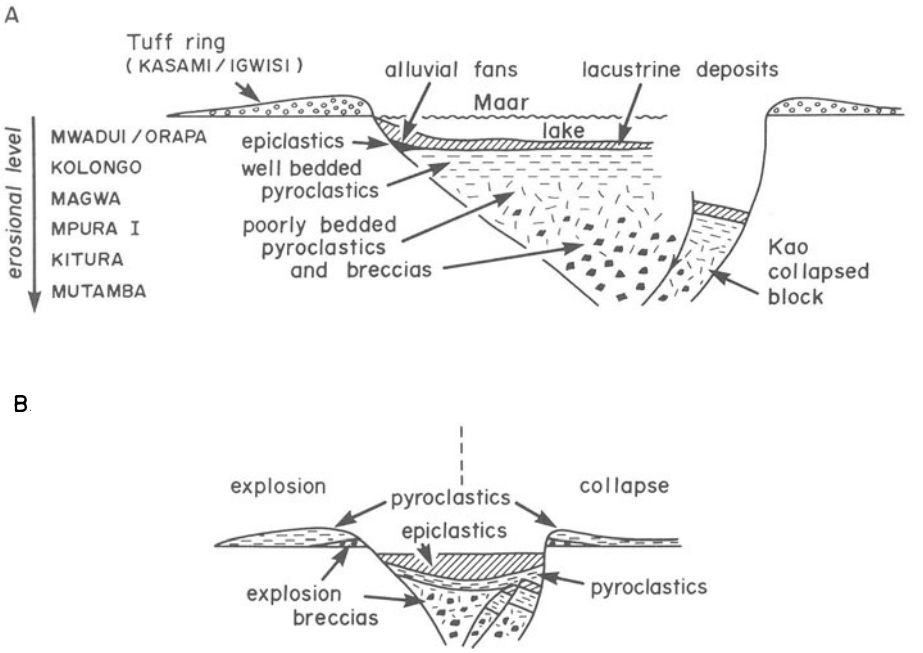

Figure 3.3. A. Idealized cross section of the surface expression of a kimberlite volcano based upon crater facies kimberlites from Tanzania and Orapa (Botswana) and the Kasami (Mali) and Igwisi (Tanzania) tuff rings. B. Model of a tuff ring formed by hydrovolcanism (Wohletz and Sheridan 1983).

crater lake. Eruption of such a kimberlitic volcano would result in the initial formation of a breccia, followed by the deposition of bedded pyroclasts. These overlie the breccia, fill the crater, and form tuff rings with low bedding angles. Ultimately activity ceases, the tuff rings are eroded, and the detritus is deposited upon the crater-filling pyroclastics as epiclastic kimberlites. Contemporaneous downfaulting along the margins of the crater may preserve the crater facies deposits at depth as inclusions in diatreme facies kimberlites.

This model of kimberlite subaerial volcanism is directly comparable with Wohletz and Sheridan's (1983) model of a tuff ring formed by hydrovolcanism (Figure 3.3.B.). The similar stratigraphy and morphology *may* indicate that crater facies kimberlites are the result of hydrovolcanic eruptions caused by the interaction of groundwater with magma.

According to Wohletz and Sheridan (1983), tuff rings evolve through a stage of explosion breccia emplacement to a stage dominated by highly inflated (high water/melt ratio) base surges which deposit thinly bedded layers of pyroclastics. Activity may continue to a third stage characterized by rocks emplaced by poorly inflated (low water/melt ratios) base surges and ballistic fallout. This

latter activity results in the growth of cones above tuff rings and, if a sufficient supply of magma is available, will produce high steep-sided tuff cones. In the case of kimberlite magmatism, activity appears to cease relatively soon after the initial breakthrough and low water/melt ratios result in the formation of explosion breccias containing abundant cognate and accidental clasts.

Modern volcanological studies are required of kimberlite pyroclastic deposits in order that this hydrovolcanic model of volcanism be verified or rejected.

It is important to note that the processes described above are *not* necessarily relevant to the emplacement of the diatremes which presumably lie beneath the craters. These aspects of kimberlite emplacement are discussed in Chapter 4.

3.2.5. Pseudokimberlitic Volcanism

Tuffaceous rocks found at the Moroto (Uganda), Lesorogoi (Kenya), and Lashaine (Tanzania) volcanoes have been considered by Nixon (1973c) to have kimberlitic affinities because they contain mantle-derived pyropes and garnet lherzolite xenoliths. The rocks have been shown to be nephelinitic, ankaramitic or carbonatitic tuffs (Dawson 1980, Dawson *et al.* 1970) and to be merely pyroclastic components of the carbonatite-nephelinite volcanism associated with the East African Rift; they are thus unrelated to kimberlite.

The Gross Brukkaros volcano, Namibia, has been stated to have kimberlitic affinities (Janse 1969, Ferguson *et al.* 1975). This edifice is constructed of a thick sequence of bedded microbreccias which exhibit graded bedding, cross bedding, and other sedimentary depositional features. The microbreccias are derived entirely from the country rocks and are cemented by carbonate or potassium feldspar. Pyroclastic material is not present. Associated with the main cryptovolcanic structure are subsidary vents containing breccias of fenitized sandstones and shales in a matrix of carbonatite, radial carbonatite dikes, and sills of a monticellite-melilite-phlogopite-bearing rock of alnöitic character (Mitchell, unpublished data); the scale and character of the activity is clearly non-kimberlitic. The microbreccias were probably deposited by highly inflated surges produced during the breakthrough stages of eruption of a carbonatite-melilitite-nephelinite volcano.

Diatremes, plugs, and dikes occurring on the Colorado Plateau, previously considered to be kimberlites, e.g., Buell Park, Mule Ear, Moses Rock, and Cane Valley (Schmitt *et al.* 1974, McGetchin and Silver 1970, McGetchin *et al.* 1973), are now known to be related to minettes (Ehrenberg 1978, 1982).

3.3. DIATREME FACIES KIMBERLITES

Diatremes are long (1–2-km) carrot-shaped bodies that underlie crater facies kimberlites (Figure 3.1). They have vertical axes and steeply dipping (80°–85°)

margins. Their elliptical or roughly circular cross-sectional areas decrease regularly with depth until they terminate in a region known as the *root zone* (Hawthorne 1975, Clement 1979, Clement and Skinner 1979). This zone is marked by the expansion, contraction, or splitting up of the diatreme into an irregularly shaped multiphase intrusion of hypabyssal kimberlite. The structure of diatremes and their relationships to root zones are described in detail in Chapter 4.

Diatreme facies rocks are currently classified as *tuffisitic kimberlites* and *tuffisitic kimberlite breccias* (Clement 1979, Clement and Skinner 1979). They are named tuffisites because they are considered to consist of intrusive pyroclastic fragments. Use of the term *tuffisite* (Cloos 1941) has definite genetic connotations and implies that the fragments were emplaced by a rising-gas stream, during formation of the diatreme by a gas–solid fluidization (Reynolds 1954) process. While such a process may have played some role in the formation of the diatreme facies rock it may not have been the principal diatreme-forming process (Clement 1979, 1982, and Chapter 4). As the nature of the volcanic processes which produce diatremes is still the subject of much debate, diatreme facies rocks might better be termed *volcaniclastic kimberlites* until these processes are adequately understood. The general term "volcaniclastic" was introduced by Fisher (1961) to include all clastic volcanic materials formed by any process of fragmentation, dispersed by any kind of transporting agent, and deposited in any kind of environment.

Tuffisitic kimberlite breccias are the commonest rocks of the diatreme zones. They contain abundant angular to rounded country rock inclusions, the bulk of which are small, ranging from a few centimeters down to microscopic particles. Present in lesser quantities are clasts (autoliths) representing earlier generations of hypabyssal kimberlites which have been fragmented and carried up into the diatreme. Discrete and fractured grains of olivine, garnet, and ilmenite megacrysts and macrocrysts, are common. These clasts and mineral fragments are set in a fine grained matrix which, when fresh, consists of microcrystalline diopside and serpentine. Importantly, primary calcite is very rare as an interclast cementing medium. The groundmass is unfortunately extremely susceptible to alteration and in the near-surface weathering environment is typically replaced by clay minerals and secondary calcite. Although tuffisitic kimberlite breccias contain a heterogeneous assemblage of clasts, they present an overall well-mixed homogeneous appearance.

Tuffisitic kimberlites are not as common as tuffisitic kimberlite breccias and differ petrographically only in the content of clasts. They occur as lenslike bodies intruding earlier breccias or as screens at the margins of the pipe (Clement 1982).

Diatreme zones usually contain one to three texturally distinctive varieties of tuffisitic kimberlite breccias, e.g., Letseng-la-terae (Bloomer and Nixon 1973).

Diatreme facies kimberlites are recognized by their fragmental nature. Their characteristics are described in Section 3.6.

3.4. HYPABYSSAL FACIES KIMBERLITES

Hypabyssal kimberlites are rocks which have formed by the crystallization of a volatile-rich kimberlite magma. They exhibit igneous textures and show the effects of magmatic differentiation; pyroclastic fragments and textures are absent. The rocks commonly contain sufficient quantities of country rock xenoliths that they may be termed *kimberlite breccias*. The term *kimberlite* used without modification refers in this work to these magmatic rocks; their mineralogy is defined in Section 2.3.

Hypabyssal facies kimberlites form the root zones of diatremes and occur as dikes and sills. Root zone kimberlites comprise the bulk of the occurrences in many kimberlite provinces as a consequence of the removal of the upper portions of the diatremes by erosion. Petrographically they are similar to the kimberlites occurring as dikes and sills, and appear to be gradational with depth into dike-like bodies. Root zone kimberlites commonly intrude tuffisitic kimberlite breccias in the lower-to-mid portions of diatremes. Diatreme–root-zone–dike relations are described in Section 4.3.4.

3.4.1. Dikes

Kimberlite dikes typically are vertically dipping tabular bodies 1–3 m in width. Rarely, examples are found up to 10 m in width. Many can be traced for several kilometers along strike as continuous bodies or isolated dike segments. Commonly they form swarms of parallel or *en enchelon* dikes, e.g., Orroroo, South Australia (Scott Smith *et al.* 1984), Koidu, Sierra Leone (Tompkins and Haggerty 1984); Liberia (Haggerty 1982); Swartruggens, South Africa (Fourie 1958); Barkly West, South Africa (Bosch 1971); Butha Buthe, Sekameng and Malibamatso, Lesotho (Nixon and Kresten 1973a, Dempster and Tucker 1973, Kresten and Dempster 1973).

Typically, the dikes occupy vertical to sub-vertical parallel fractures or joints, their emplacement being controlled by the regional fracture pattern. Dikes pinch out and swell along parallel fracture systems or form *en echelon* segments. Commonly, they bifurcate or split into sub-parallel anastomozing stringers and veins. Lateral pinch-outs are continued by fracture zones. Dikes encountered at depth in mines commonly pinch out toward the surface (Fourie 1958) and thicken with depth. Rarely, downward terminations are observed (Dempster and Tucker 1973). Most of the dikes are single intrusions, although some composite dikes do occur. Many have a heterogeneous appearance due to the effects of flow differentiation. Glassy selvedges are absent. Contact metamorphic effects are slight and include minor baking and metasomatism resulting in the bleaching of the host rocks together with the introduction of carbonate or mica (Ferguson *et al.* 1973a). Dikes can be traced along strike by the occurrence of such alteration

zones, by the presence of fractures, by distinctive vegetation above the dike, or by lines of springs.

Some dikes expand along strike into lenticular enlargements termed "blows." These may be up to 10–20 times the average dike width and up to 100 m long. They may contain kimberlites identical to those of the contiguous dikes and/or petrographically distinct varieties of kimberlites. In many cases the blows have acted as a focus for subsequent kimberlite intrusions, e.g., Pipe 200, Lesotho (Kresten and Dempster 1973). Blows may represent the lowermost portions of root zone intrusions (see Section 4.3.4).

Where erosion has been limited, or where deep mining has been undertaken, the relationships between diatremes and dikes can be discerned. Several groups of dikes named with respect to their time of emplacement relative to associated diatremes are now recognized. These are (1) antecedent (Wagner 1914) or precursor (Clement 1982) dikes, (2) contemporaneous dikes, (3) consequent (Wagner 1914) or internal (Clement 1982) dikes, and (4) subsequent or cross-cutting dikes.

Antecedent or precursor dikes (Figure 3.1.) were emplaced prior to diatremes and their root zones as evidenced by the cross-cutting relationships that these intrusions display with respect to the dikes. Examples from South Africa are described by Wagner (1914), Williams (1932) and Clement (1982), and from Lesotho by Kresten (1973a) and Kresten and Dempster (1973).

The dikes form swarms which have similar characteristics to the regional dike swarms described above. The dikes are apparently concentrated in the vicinity of pipes (Clement 1982). They are observed to extend to levels well above the points at which diatremes expand upwards, but not to their uppermost levels or to the original land surface. The antecedent dikes represent an early pre-pipe episode of dike formation that penetrated to higher levels than the dikes which are postulated to have participated in diatreme and root zone formation. These latter dikes undoubtedly utilized the same fracture system but for some reason did not penetrate to the same levels as the antecedent dikes. The emplacement of the earlier dikes may play an important role in diatreme localization and formation by providing zones of weakness and access points for groundwater into the magmatic system.

Dike swarms in deeply eroded terrains, e.g., the Sekameng swarm (Dempster and Tucker 1973) which contain embryonic pipes or blows, may thus consist of antecedent dikes *and* pipe feeder dikes. The time interval between antecedent dike and pipe emplacement is unknown. The magmatism is likely to be contemporaneous and not resolvable even by the most precise current geochronological techniques.

Contemporaneous dikes represent off-shoots from the main pipe into the adjacent country rock. Curiously such dikes are very rare and most diatremes apparently lack such features. When present they occur as short ($\approx$ 1 m) injection

dikes along joints or bedding planes. At Wesselton and Dutoitspan contemporaneous dikes extend up to 50 m from the pipe (Clement 1982).

Internal dikes are common in most diatremes and root zones. They cross-cut the intrusions within the pipes but do not extend into the adjacent country rocks. Commonly, the dikes are small, rootless, sinuous, or arcuate in shape and pinch out laterally and vertically. They may be localized at the diatreme-wall rock contact or at the contacts between discrete intrusions within the diatreme. Most dikes have no preferred orientation. Some internal dikes occur only in one phase of the pipe and are truncated by subsequent intrusions. Several periods of internal dike formation, coincident with waxing and waning episodes of diatreme and root zone formation, account for the varied petrological character of the dikes. They thus may be unevolved macrocrystal hypabyssal kimberlite, aphanitic kimberlites, mica-rich varieties, or calcite-rich late differentiates, as seen in the De Beers (Donaldson and Reid 1982) or the Premier (Daly 1925) kimberlites.

Subsequent or cross-cutting dikes are extremely rare (Clement 1982). Their absence indicates that the diatreme-forming event marks the closing stages of kimberlite magmatism.

3.4.2. Sills

Kimberlite sills are relatively rare. In South Africa major sill complexes are found at the Wesselton Floors (Hawthorne 1968), the Wesselton Water Tunnels (Hill 1977, Clement 1982, Mitchell 1984a), Benfontein (Dawson and Hawthorne 1973) and Mayeng (Apter *et al.* 1984). Other sills have been found at Kamfersdam (Wagner 1914), Trentham, Saltpetrepan, and Karolusdrift (Hawthorne 1968). An extensive but poorly known sill complex is found in the Iramba Plateau area of Tanzania (Williams 1939, Mannard 1962). Other localities include the Wessels Sill, Rhodesia (Hawthorne 1968), Pyramidefjeld, Greenland (Andrews and Emeleus 1975), the Iron Mountain field, Wyoming (Coopersmith, personal communication), and possibly Bakwanga, Zaire (Mayer de Stadelhofen 1963). At this latter locality flat-lying tabular bodies up to several hundred meters thick extend several hundred meters beyond the rims of pipes. The rocks are emplaced at the contact between Mesozoic sediments and Precambrian rocks. Meyer de Stadelhofen regards the rocks as effusive rather than intrusive kimberlites.

In the Kimberley area, sill emplacement is controlled by the presence of a Karroo dolerite sill emplaced in Carboniferous Dwyka shales. This dolerite has acted as an impermeable barrier to upwelling kimberlitic magma which, upon encountering this unit, has spread out laterally to form a stockwork of sills within the well-bedded Dwyka shales. In the Mayeng area a similar sill complex has developed in well-jointed Ventersdorpf lavas located below a massive porphyritic

lava. In the Iramba and Pyramidefjeld examples, sills are developed along horizontal joints in granitic rocks.

The emplacement of kimberlite sills is thus governed by local structural controls and is in no manner different to the emplacement of sills of other magma types.

Kimberlite sills within shales or lavas vary in thickness from fractions of a centimeter to doubly convex lensoid bodies up to 45 m in thickness. Most sills are from 1–2 m in thickness. These commonly pinch and swell along strike and taper out along bedding or joint planes. Apparently isolated lensoid bodies are common. In the more competent granitic rocks the sills are relatively uniform tabular bodies from 1–10 m in thickness. Contact effects include silicification and minor thermal metamorphism.

Sills vary in composition from macrocrystal kimberlites, containing pyrope, ilmenite, and xenoliths (Mayeng, Kisiriri, Pyramidefjeld) to highly evolved carbonate-rich kimberlites (Benfontein, Wesselton Water Tunnels). Many of the sills are composite (Figure 3.4) and show the effects of flow differentiation. Carbonate-rich sills exhibit some of the more spectacular examples of magmatic sedimentation and differentiation features observed in kimberlitic rocks.

Dawson and Hawthorne's (1973) description of the Benfontein sill complex is the best-documented example of these features. Each sill results from several injections of kimberlite that have consolidated to give the sill a macroscopically well-defined layering. Many of the layers show magmatic sedimentation features and cumulus textures. Cross bedding is conspicuous. While some of the layering is the result of *in situ* differentiation, other layers have resulted from pre-injection differentiation. Isomodal layers, in which the proportions of cumulus phases remain constant with respect to each other and to intercumulus calcite, consist of olivine, olivine-spinel-perovskite, or spinel-perovskite cumulates. Mineral graded layers exhibit systematic changes in the ratio of olivine to spinel plus perovskite and to the amount of intercumulus calcite. Commonly, the tops of the layers consist entirely of calcite. Size grading is not common and the degree of sorting of the cumulus phases is, in general, poor. In some cases, intercumulus liquids have been mobilized by density contrasts and have risen through overlying denser spinel-perovskite cumulates as diapir-like bodies. These segregated intercumulus liquids have crystallized to rhombohedral or prismatic crystals of calcite. Acicular apatite and dendritic calcite (Figure 3.21), presumably representing rapidly quenched liquids, are common.

Similar layered sills have been described from the Wesselton Water Tunnels sill complex (Hill 1977, Mitchell 1984a). These differ from the Benfontein sills in being richer in mica and in containing calcite segregations that have been mobilized in response to a thermal gradient.

The feeder dikes to most sill complexes have not been located; exceptions include the Mayeng sills, which Apter (et al. 1984) consider to have been fed

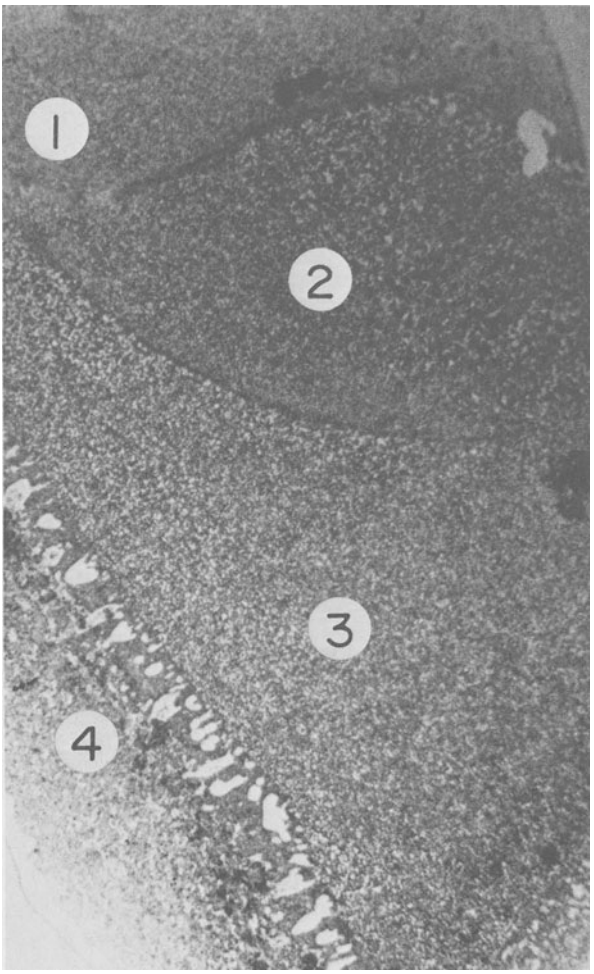

Figure 3.4. Hypabyssal spinel perovskite phlogopite kimberlite, Skinner's Sill, Wesselton Water Tunnels sill complex, South Africa. Four cross-cutting separate injections of kimberlite are present in this complex multiple sill. Note the branching calcite segregations orientated normally to the contact between unit 3 and 4. (Field of view, top to bottom, 45 mm.)

by a single micaceous kimberlite dike, and the Wesselton Water Tunnels sills. These latter sills are directly related to, and fed by the precursor dikes and cross-cut by the Wesselton diatreme (Hill 1977, Clement 1982). Hawthorne (1968) also noted that sills in the Kimberley area were emplaced about 500 m below the original land surface and thus must have penetrated to much higher levels than the bases of the diatremes.

Sill emplacement thus apparently precedes diatreme formation and is a part of the precursor or antecedent dike magmatism.

3.4.3. Cumulate or Plutonic Kimberlites

The existence of highly differentiated sills and dikes, and the evidence that repeated intrusion and mixing of kimberlite magmas (Chapter 6) of slightly different composition occurs at a single location, suggests that pooling or ponding of magma should occur at depth.

Differentiation should lead to the formation of cumulates of phenocrystal olivine, spinel, perovskite, and the megacrystal/macrocrystal phases perhaps associated with coarsely crystalline carbonate-rich rocks derived from residual fractions of the magma. Such plutonic kimberlite complexes are as yet unknown. This is surprising, in that the plutonic equivalents of other magmas of relatively small volume and limited distribution, such as carbonatites, alnöites, and lamproites, are known. It may be that such complexes either do not form, have not been recognized, occur at levels deeper than currently exposed by erosion, or have been continuously disrupted by subsequent batches of magma.

3.5. TEXTURAL GENETIC CLASSIFICATIONS OF KIMBERLITES

Lewis (1887) recognized three textural varieties of kimberlite: (1) kimberlite, a massive rock of porphyritic texture, (2) kimberlite breccia and (3) kimberlite tuff. These original divisions were supported by Wagner (1914) and Williams (1932) and by most other South African and European petrologists until the 1970s.

The discovery of kimberlites in Siberia resulted in several classification schemes for kimberlitic rocks. Frantsesson (1970) comments that these schemes were independently devised by different groups of Soviet petrologists, with the consequences that the same variety of kimberlite is described by different authors under different names. Comparison and correlation of rocks from individual kimberlite fields is thus extremely difficult.

Most of the Russian classifications (Kovalski 1963, Milashev 1963, Bobrievich *et al.* 1959b, 1964, Rabhkin *et al.* 1962) are extensions of the original Lewis–Wagner classification, involving the recognition of the three basic genetic types with further subdivision, according to the amount of mica present, into basaltoid and lamprophyric varieties. An undesirable feature of these classifications is the combination of mineralogical subdivisions with morphological characteristics.

In the Soviet classifications, *massive kimberlites* containing few or no inclusions of country rock, occurring predominantly in veins and dikes, are referred to as *hypabyssal* or *subvolcanic* rocks. *Kimberlite breccias* contain 20%–60%

fragments of diverse rock types set in a matrix of massive kimberlite. Two types of breccia are recognized, *autolithic breccias* in which fragments of kimberlite comprise the bulk of the clasts, and *heterolithic* or *xenolithic breccias* in which fragments of country rock predominate (Milashev 1963, Rabhkin *et al.* 1962). Kimberlite breccias have been variously described as eruptive (Milashev 1963, Bobrievich *et al.* 1964), explosive (Kovalski 1963), or intrusive (Kovalski 1963, Dawson 1967a). Usage of these terms, which have genetic implications, has been criticized by Frantsesson (1970) and Clement (1982) on the basis that they are incorrectly applied. Thus Clement (1982) notes that not all breccias observed in kimberlite intrusions are intrusive and that many are better described as intrusion breccias. Most of the breccias are not eruptive as they form at depth within the diatreme and not at the Earth's surface (Frantsesson 1970).

Kimberlite tuffs consist of fine grained kimberlite or kimberlite mineral fragments cemented by hydrothermal-type minerals (serpentine, calcite). With increasing amounts of country rock fragments they are transitional into *tuff breccias* or *xeno-tuff breccias* (Milashev 1963, Rabhkin *et al.* 1962).

Both kimberlite breccias and tuff breccias can be described as fine, medium, or coarse grained where the average size of the fragments is less than 1 cm, 1–5 cm, or greater than 5 cm, respectively (Milashev 1963).

Other Soviet petrologists (Frantsesson 1970, Artsybasheva *et al.* 1964, Krivoshlyk 1980) dispute the existence of a separate class of kimberlite tuffs and regard such rocks as being a special class of autolithic kimberlite breccia, as they differ from airfall tuffs in their texture and mode of formation.

Frantsesson (1970) thus recognizes only massive kimberlite, a hypabyssal rock with a porphyritic texture and kimberlite breccia, i.e., a rock of brecciated texture, composed of kimberlite fragments of an earlier generation, cognate inclusions, and country rocks, cemented either by kimberlitic material or by the products of its alteration.

Artsybasheva *et al.* (1964) divide kimberlites into (1) massive (<25% fragmental material), (2) breccia-form (25%–50% fragments), and (3) breccias (>50% fragments). Further subdivisions are based upon the nature of the clasts, these being (1) peridotites, (2) cognate fragments of kimberlite, and (3) fragments of mixed composition including country rock xenoliths. Cognate clasts include material currently described as pelletal lapilli (see Section 3.6.2). Artsybasheva *et al.*'s (1964) classification is not as comprehensive as that of Milashev (1963) and the introduction of breccia-form kimberlites as a separate class for rocks which are breccias is of dubious value.

Elimination of tuffisitic kimberlite in the above classifications is in part responsible for the difficulties involved in comparing Russian with other descriptions of kimberlites. A tuffisitic kimberlite breccia with 30% cognate and xenolith clasts might thus be termed a kimberlite xeno-tuff breccia (Milashev 1963), a Type 3 breccia-form kimberlite (Artsybasheva *et al.* 1964), a kimberlite breccia (Frantsesson 1970), or an autolithic kimberlite breccia (Krivoshlyk 1980).

All early classifications focused upon the macroscopic appearance of the rocks and little attention was given to their microscopic petrographic textural features. An exception was Milashev's (1963) introduction of the term *microlitic* to describe the appearance of flow-aligned small prismatic crystals of diopside or calcite in the groundmass of some kimberlites.

Further, these earlier studies, although recognizing that different textural varieties of kimberlite occurred in dikes and pipes, made little attempt to correlate specific textural features with emplacement conditions or to relate these to a model of kimberlite magmatism.

The concept that different *kimberlite facies* could be recognized was introduced by Dawson (1971) who, synthesizing Russian and South African observations, proposed the existence of *diatreme facies* and *hypabyssal facies kimberlites*. The former consist of fragmental tuffs and agglomeritic rocks cemented by massive magmatic kimberlite and occur predominantly in diatremes. The latter facies consist of massive rocks with magmatic textures (flow textures, etc.) and are found in dikes, sills, and the deeper parts of diatremes. The facies were related to a specific model of kimberlite magmatism in which diatremes originate from hypabyssal feeder dikes.

Clement and Skinner (1979) and Clement (1982) have incorporated Dawson's (1971) facies concept and Hawthorne's (1975) model of a kimberlite pipe with petrographic studies of the texture of the kimberlite groundmass. The resulting textural-genetic classification (Figure 3.5) recognizes *crater facies, diatreme facies,* and *hypabyssal facies kimberlites*. These three groups reflect the formation of the rocks under differing magmatic or volcanic conditions according to the model of a kimberlite magmatic system as described in Sections 3.2–3.5.

Crater facies kimberlites are divided into *epiclastic* and *pyroclastic* types, with further subdivision being made according to standard sedimentological or volcanological particle size terminology.

Diatreme facies kimberlites are subdivided into *tuffisitic kimberlites* and *tuffisitic kimberlite breccias*. These differ only in the abundance of clasts. An arbitrary limit of greater than 15 vol % of clasts larger than 4 mm, marks the transition to the breccia variety. Further subdivisions are based upon textural features of the clasts and the groundmass. Crystallinoclastic varieties are rocks with minor amounts of groundmass or matrix minerals; they grade into varieties containing abundant groundmass material, these being divided into *uniform* or *segregationary* textured types depending upon whether or not groundmass phases form a uniform aggregate or have crystallized in discrete patches of differing mineralogy. *Pelletal*-textured rocks are characteristic of diatreme facies kimberlites and contain ellipsoidal to spherical lapilli-sized (2–64-mm) bodies of kimberlite in addition to other angular clasts. Examples of these textural varieties of diatreme facies kimberlite are described in Section 3.6.

Hypabyssal kimberlites are divisable into kimberlites and kimberlite breccias, differing only in their clast content: rocks containing more than 15 vol %

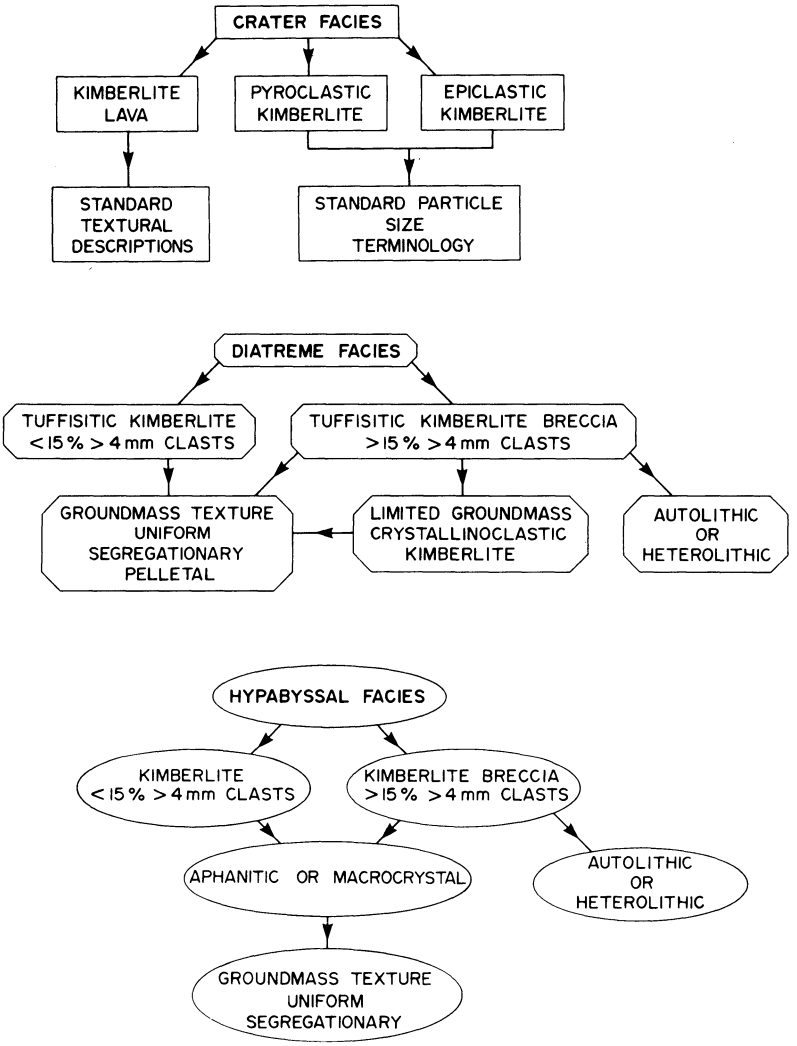

Figure 3.5. Textural genetic classification of kimberlite. Modified from Clement and Skinner (1979) and Clement (1982).

of clasts larger than 4 mm are termed breccias. Clement (1982) subdivides each group into *macroporphyritic* and *aphanitic varieties*, depending upon the presence or absence of macrocrystal olivine. Groundmass textures are described as *uniform* or *segregationary*. Standard descriptive petrographic terms can be applied to the uniform groundmass rocks which have crystallized directly from a magma. The separation of early- or late-crystallizing constituents of the groundmass into globular or patchy emulsion-like (Clement 1975) features results in

segregation-textured rocks. Examples of the textures of some hypabyssal kimberlites are described in Section 3.7.

Clement and Skinner's (1979) classification has proven to be the most useful classification scheme developed to date, in that it facilitates comparative studies of kimberlites. Modifications to the scheme have been proposed in recognition of the diverse origins of the olivine macrocryst suite. Consequently, macroporphyritic hypabyssal kimberlites are now termed *macrocrystal hypabyssal kimberlites* (Clement *et al.* 1984). Further refinements might include recognition of lavas as a third group of crater facies rocks and description of the breccias as *autolithic* or *heterolithic* according to the nature of the clasts. Autolithic is used here in the original sense of referring to fragments of an earlier generation of kimberlite found within a younger kimberlite (Rabhkin *et al.* 1962). Such igneous clasts might also be described as non-vesiculated juvenile fragments or cognate lithics (Wright *et al.* 1980).

3.6. TEXTURAL FEATURES OF DIATREME FACIES KIMBERLITES

Diatreme facies kimberlites, macroscopically, are rocks with a fragmental appearance. They are grey to grey-black or grey-green in color and have a relatively well-mixed homogeneous aspect despite being composed of a variety of clasts. In thin section most tuffisitic kimberlites and tuffisitic kimberlite breccias are unsuitable for petrographic study as a consequence of secondary alteration, which is facilitated by their high permeability. Gross textural features are commonly preserved but the interclast matrix is typically replaced by secondary minerals. The clast content of tuffisitic kimberlite breccias varies widely in character and content. Country rock clasts are typically angular, cognate clasts may be rounded or angular. Figure 3.6 illustrates representaive examples of diatreme facies kimberlites, including a *crystallinoclastic kimberlite,* an extreme variant of tuffisitic kimberlite breccia recognized by Clement and Skinner (1979).

3.6.1. Pelletal Lapilli and Nucleated Autoliths

Spherical to elliptical lapilli-sized clasts of kimberlite, termed "kimberlite pellets," were initially described by Clement (1973) from the Kao diatreme. Subsequently, these objects have been recognized as a characteristic component of many diatreme facies kimberlites. Kimberlite pellets are now termed *pelletal lapilli* by Clement and Skinner (1979). Representative examples of pelletal lapilli-textured kimberlites are shown in Figure 3.7.

Pelletal lapilli vary considerably in size (1–10 mm) and commonly have a pronounced sphericity. Many contain at their centers a single relatively large euhedral crystal or crystal fragment. These kernels are predominantly pseudo-

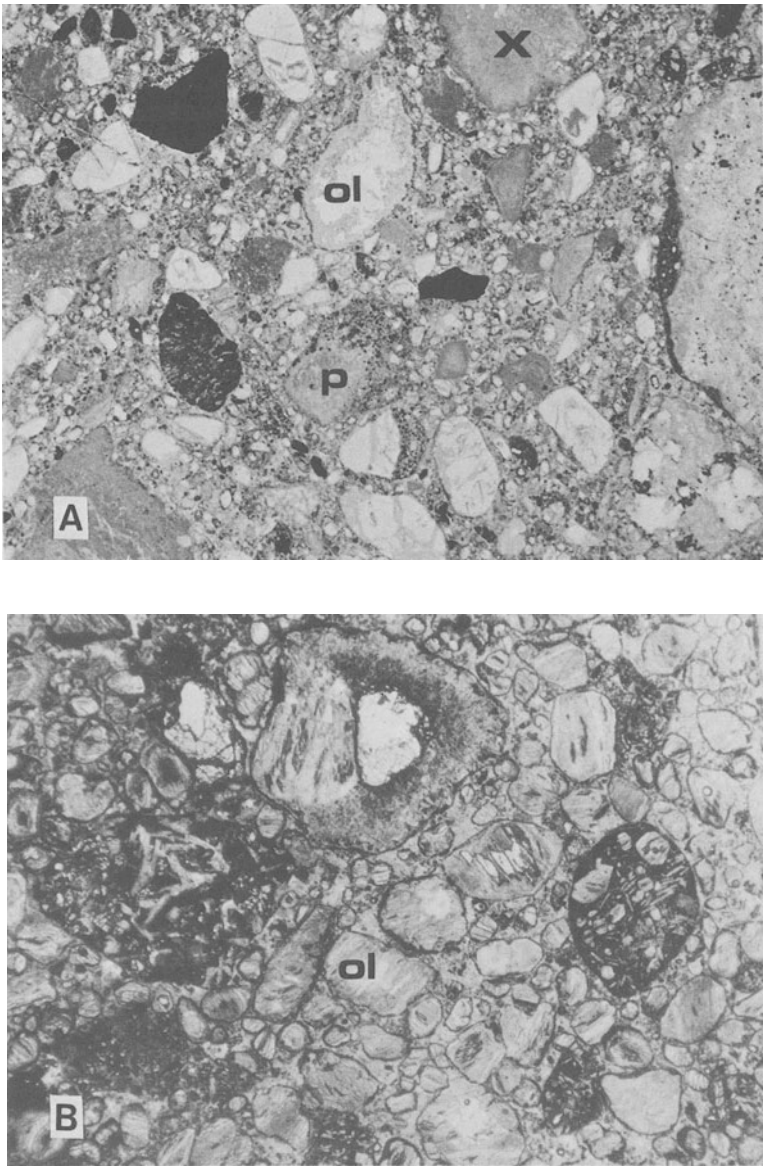

Figure 3.6. Representative tuffisitic kimberlite breccias. A. Lennardville Kansas (field of view 25 mm); B. Letseng-la-terae, Main Pipe, Lesotho (field of view 8.8 mm); C. Finsch, South Africa (field of view: 8.8 mm); D. Crystallinoclastic kimberlite, Dokolwayo, Swaziland (field of view 8.8 mm), characterized by angular quartz (q) crystals and xenoliths (x). Note in particular the abundance of angular xenolithic clasts (x) and serpentinized olivine (ol) macrocrysts. Pelletal lapilli (p), that in some instances contain eccentric cores of olivine or country rock, are diagnostic textural features of this facies. A well-defined uniform interclast matrix is visible in B.

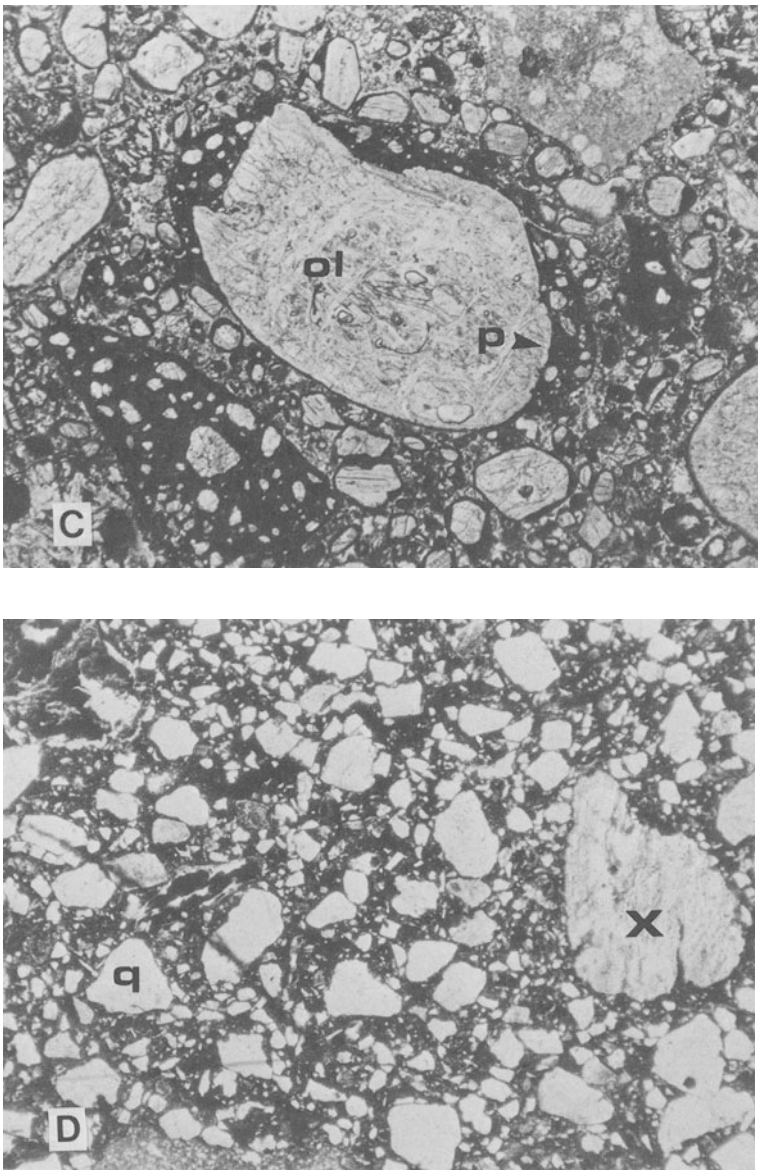

Figure 3.6. (Continued)

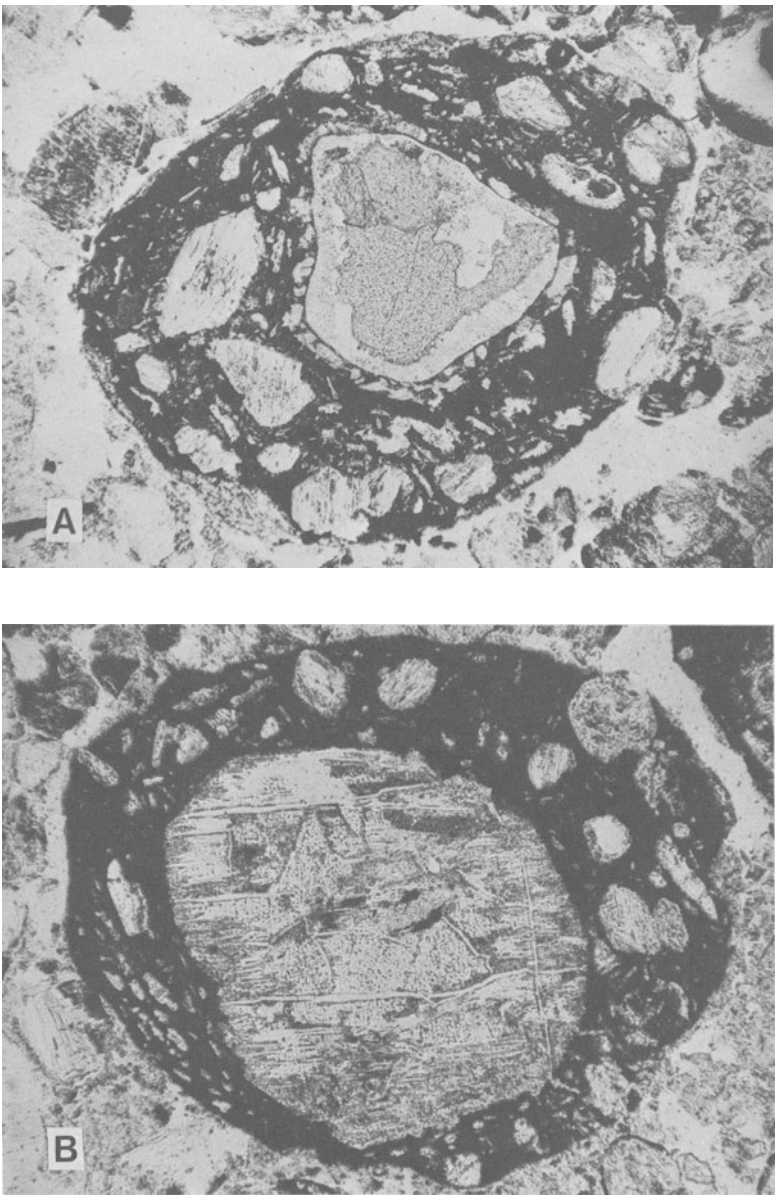

Figure 3.7. A. and B., Pelletal lapilli, Koffiefontein, South Africa (field of view 3 mm). Note the tangential arrangement of the lath-shaped minerals and the euhedral habit of the microphenocrysts of pseudomorphed olivine.

morphed olivines and less commonly phlogopite or other macrocrysts. Only rarely do country rock fragments form the kernel. Associated country rock clasts are typically devoid of kimberlite mantles (Figure 3.7). The kimberlite forming the lapilli is a very fine-grained microphenocrystal variety containing euhedral olivine and phlogopite phenocrysts. Found less commonly are pseudomorphs after a prismatic mineral (Figure 3.7) considered by Clement (1982) to be melilite (see Section 8.3). The groundmass is commonly optically unresolvable and appears as an amorphous dark brown material. Spinels and perovskite can be recognized as components of the matrix, and phlogopite and diopside can be observed in relatively coarse-grained and unaltered examples. Calcite is rarely found as a primary phase. The margins of the lapilli are commonly altered and replaced by secondary minerals or by serpentine and/or diopside derived from the interclast matrix.

Prismatic minerals are commonly concentrically orientated about the nucleus of the lapilli and a poorly defined concentric structure is discernable in many of the mantles as a whole. Phlogopites in some examples may be tangentially orientated only at the margins of the lapilli (Dawson 1980). Phenocrysts in some otherwise identical lapilli, lack any preferred orientation. There are complete gradations between lapilli containing nucleii and orientated phenocrysts, to lapilli lacking kernels and with randomly oriented phenocrysts. Kernels may be centrally or eccentrically disposed. The occurrence of the nucleii at lapilli margins is due in some cases to the breakage of larger lapilli. Vesicles and composite lapilli are absent.

The lapilli have the textural characteristics of having formed by the rapid crystallization of a volatile-poor magma containing phenocrysts, and are best described as lapilli of microphenocrystal hypabyssal kimberlite. The pelletal lapilli are not, on the basis of their textures, examples of accretionary lapilli. These latter lapilli are formed by the aggregation of platy glass shards in eruption clouds (Fisher and Schminke 1984).

Occurring in association with pelletal lapilli are angular-to-sub-angular fragments of kimberlites that may be similar or different in texture and mineralogy to the pelletal lapilli, but lacking phenocrysts with preferred orientation or central kernels. Such clasts are undoubtedly derived from the fragmentation of bodies of consolidated kimberlite and are best described as autoliths (see Section 3.5).

Similar nucleated spheroids of a much larger size (up to 8 cm), termed autoliths or *nucleated autoliths* have been described by Ferguson *et al.* (1973b) and Danchin *et al.* (1975). They differ from the pelletal lapilli in that they are relatively coarser grained and commonly have large fragments of country rock as their nucleii. In these latter examples the kimberlite coating may be relatively thin with respect to the size of the nucleus.

Importantly, Clement (1973) and Danchin *et al.* (1975) postulated different origins for each type of spherical clast. Clement (1973) proposed that the lapilli were quenched magma droplets formed by the rapid cooling of a spray of magma

(see below). Danchin *et al.* (1975) believed that "nucleated autoliths" grew by magmatic crystallization about nucleating centers.

These genetic distinctions have been essentially ignored in subsequent studies and any kimberlite containing spherical clasts of kimberlite is referred to as an *autolithic kimberlite* (Dawson 1980). This practice is unsound in that (1) no distinctions are made between genetically different types of clast and it is assumed that they merely represent a size continuum of clasts having a single origin, and (2) the term autolith is best reserved for fragments derived from the disruption of consolidated kimberlite.

Relationships between "nucleated autoliths" and pelletal lapilli have not yet been satisfactorily resolved. Some "nucleated autoliths" are petrographically similar to the coarser varieties of the pelletal lapilli and to globular segregations (Section 3.7.2) occurring in hypabyssal kimberlites. Others seem more akin to cored bombs or armored lapilli than to pelletal lapilli. Cored bombs have rinds of lava enclosing cores of country rock and armored lapilli form when wet ash becomes plastered around a solid nucleus during hydroclastic eruptions (Fisher and Schminke 1984). Clearly these spherical bodies may have several modes of formation and require further study. The relationship between pelletal lapilli and globular segregations is discussed further in Section 3.7.2.

Pelletal lapilli similar to those occurring in kimberlites have been described from olivine melilitite (Cloos 1941, Lorenz 1979), alnöitic (Singewald and Milton 1930, Raeside and Helmstaedt 1982), and alkali basalt (Kaminskii 1977) diatremes. In many examples (Figure 3.8) the lapilli are unaltered and contain fresh melilite and/or glass. The presence of glass is consistent with an origin by the rapid quenching of magma droplets. The amorphous brown material occurring in some kimberlitic pelletal lapilli may thus represent devitrified glass.

Magma droplets are thought to form by the fragmentation of magma caused by either rapid expulsion of dissolved volatiles (Clement 1973, 1982, Dawson 1980), or by interaction with groundwater (Lorenz 1979). In the latter case, water flashes into steam and the magma is explosively disrupted as droplets. The shapes and textures of the lapilli are considered to be due to surface tension effects combined with the rotation of the drops as they are propelled into open spaces above the magma (Dawson 1980) or within a fluidized gas–liquid system, i.e., an aerosol model of transport.

Formation of the lapilli by volatile expulsion is discounted by Lorenz (1979) on the grounds that kimberlitic and melilitic magmas have very low viscosities and may have been devolatilized prior to the lapilli-forming event. The absence of vesicles and the paucity of carbonate in the clasts is evidence in favor of this hypothesis.

Regardless of the mechanism of disruption of the magma, the presence of olivine nucleii indicates that, prior to disruption, some crystallization had occurred. Surface tension effects would result in magma adhering to such crystals and other clasts after disruption.

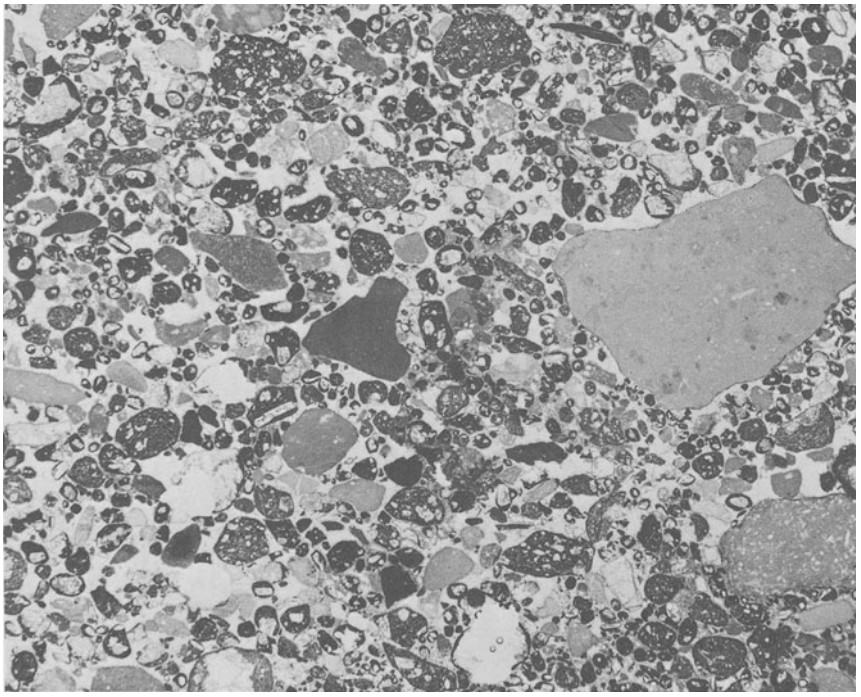

Figure 3.8. Pelletal-textured olivine melilitite, Calverbuhl, Swabia, West Germany. Note the similarity of this very fresh diatreme facies melilitite to the tuffisitic kimberlite breccia illustrated in Figure 3.6A. (Field of view 25 mm.)

The wide range in degree of crystallization shown by the lapilli is not consistent with the view that all magma droplets were rapidly quenched. This implies that considerable crystallization occurred prior to lapilli formation or that the rates of crystallization within individual droplets varied as they were transported. Clement (1982) believes that some of the coarser grained lapilli grew as globular segregations in a volatile-rich system and were subsequently mixed with spray lapilli (see Section 3.7.2.2). Concentric layering within lapilli has been ascribed to successive liquid accretion around a core prior to magma disruption (Lorenz 1979) or subsequently within a gas-magma droplet fluidized system (Clement 1982).

3.6.2. Interclast Matrices

The matrix supporting the pelletal lapilli, autolithic and xenolithic clasts, when fresh, consists essentially of diopside and serpentine, and less commonly includes phlogopite. The outstanding petrographic feature of this matrix is that

all of the crystals are extremely fine grained or cryptocrystalline and normal igneous granular or poikilitic textures are absent. Diopside occurs as extremely fine grained aggregates disseminated in a serpentine base (Figure 3.9), as needle-like crystals forming fringes upon altered pelletal lapilli (Figure 3.10), and as tiny prisms projecting into pool-like segregations of serpentine (Clement and Skinner 1979, Scott and Skinner 1979). Depending upon the degree of development of the fringes or discrete segregations of diopside and serpentine, the matrix can be described as *uniform* or *segregationary* (Clement and Skinner 1979). Secondary alteration may produce a groundmass which is uniform with respect to the distribution of clay minerals (Figure 3.2), recrystallized serpentine, or secondary calcite. Such matrices are *not* uniform in the sense in which the term is employed by Clement and Skinner (1979) and should be described by the use of a prefix indicating the nature of the alteration, e.g., clay-mineralized pelletal tuffisitic kimberlite. Because of the common destruction of the primary mineralogy by secondary alteration few descriptions of fresh interclast matrices

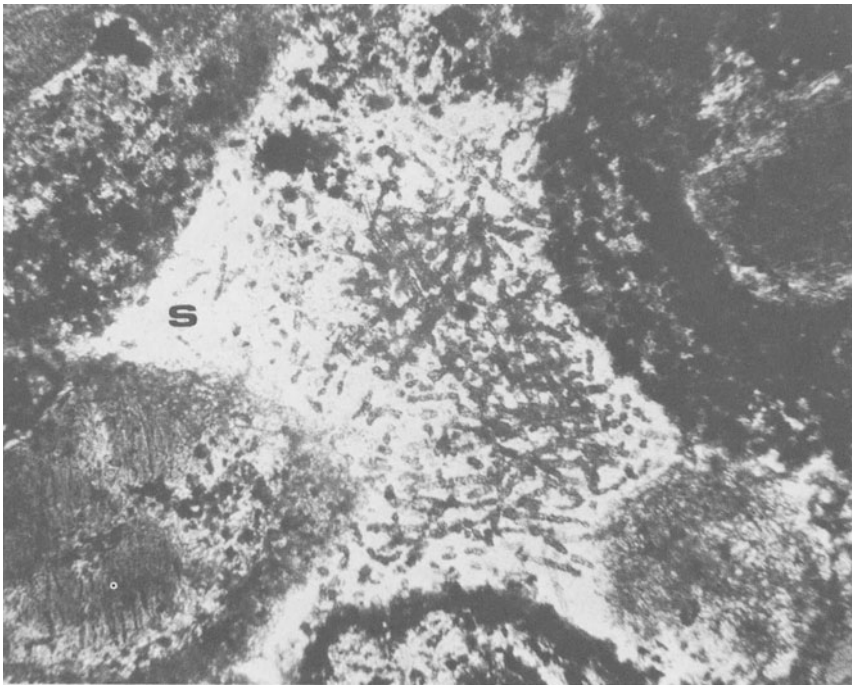

Figure 3.9. Interclast matrix, tuffisitic kimberlite breccia, Finsch, South Africa. The matrix consists of chain-like arrangements of microcrystalline diopside set in a serpentine matrix (s). The margins of the lapilli and xenolithic clasts exhibit fringes of microcrystalline diopside (d). (Field of view 2 mm.)

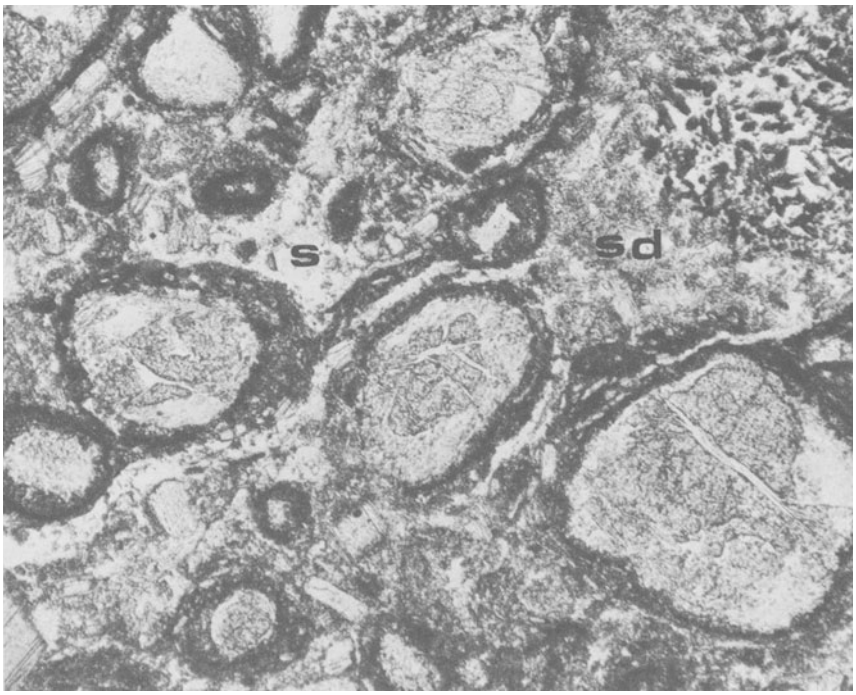

Figure 3.10. Segregation-textured interclast matrix, tuffisitic kimberlite breccia, Finsch, South Africa. Light-colored areas are serpentine-rich (s), grey areas are mixtures of serpentine and diopside (sd). The dark fringes around the serpentinized macrocrysts are primarily microcrystalline diopside. (Field of view 8.0 mm.)

have been published. Examples similar to Figures 3.9 and 3.10 have been described from the Letlhakane Dkl pipe (Skinner and Clement 1979), the Premier (Scott and Skinner 1979), and Kimberley area pipes (Clement 1982).

The paucity of primary calcite, especially in the serpentine segregations, is notable (serpentine-rich segregations in hypabyssal kimberlites are commonly associated with calcite: see Section 3.7), and has been attributed by Clement (1979) to the loss of CO_2 from the system prior to formation of the matrix.

Textural features of the matrix are commensurate with rapid non-equilibrium deposition from a hydrothermal fluid or the condensate derived from a vapor–solid fluidized system (Clement 1979). Variations in the temperature, composition, and rate of crystallization of such fluids can account for gradations between the uniform and segregationary-textured groundmasses. Crystallization of the fluid, in some cases, commences with nucleation of diopside upon the substrate provided by the clasts, the residue subsequently crystallizing as ser-

pentine. In other cases crystallization of both phases occurs more or less contemporaneously and uniformly throughout the pore spaces.

The abundance of diopside and the absence of monticellite and/or melilite in diatreme facies rocks can be explained by contamination of the matrix-forming fluids with silica. Diopside is not a common constituent of many hypabyssal kimberlites, with the exception of isotopic group-II phlogopite kimberlites, e.g., Finsch, New Elands (see Section 7.5.2), and is absent, or present in very small quantities, in hypabyssal root zone kimberlites. Such rocks commonly contain monticellite, and Mitchell (1979a) has noted that there appears to be an antipathetic relationship between monticellite and diopside. When diopside is present it commonly appears to have formed by reactions between the magma and country rock xenoliths or has crystallized from residua in association with serpentine, such segregations being very similar to those of the diatreme facies matrix (Clement 1982). It is noted in Sections 4.4.3 and 4.4.5 that groundwater may play an important role in diatreme development. Such heated waters will react with xenoliths and country rocks and extract silica. The silica activity of the fluids which form the interclast matrix may thus be raised to levels that prevent the formation of monticellite or melilite (see Section 9.9). Evidence in support of this type of contamination is seen in the diopsidized xenoliths referred to above.

These fluid-phase transport and cementation processes result in a decrease in the porosity of the diatreme facies rocks by binding clasts together. Although taking place at low temperatures, as shown by the absence of thermal effects upon limestone and shale clasts or fragments of wood (see Section 4.2.3) the processes are in some respects akin to those occurring during the cooling of pyroclastic flows and may be regarded as a form of welding or sintering.

3.7. TEXTURAL FEATURES OF HYPABYSSAL FACIES KIMBERLITES

Macroscopically, hypabyssal facies kimberlites are massive black to brown rocks of igneous aspect in which macrocrystal olivines and lesser amounts of other macrocrysts (phlogopite, ilmenite, garnet) are commonly visible. The macrocrysts impart a "pseudoporphyritic" texture to the rocks (Section 2.2). Flow differentiation may in some cases produce alternating regions of macrocrystal and aphanitic kimberlite. A wide variety of igneous sedimentation features, e.g., cross bedding, scour and fill structures, graded bedding, modal layering etc., similar in appearance to those described from layered basic intrusions, are common in calcite-kimberlite sills (Dawson and Hawthorne 1973, Hill 1977, Mitchell 1984a). Globular or irregularly shaped calcite-rich segregations are typical of many hypabyssal kimberlites (Section 3.7.2).

Hypabyssal kimberlite breccias differ from diatreme facies breccias in that included rock fragments have commonly reacted with their host magma. Xenoliths may contain, or be rimmed by, monticellite and/or phlogopite (Mitchell 1978a) or diopside and phlogopite (Clement 1982). Shale and limestone xenoliths are commonly recrystallized and bleached at their margins and appear concentrically zoned. Similar effects have been noted in the country rocks adjacent to dikes by Dawson and Hawthorne (1970). Shale xenoliths may be "de-watered" and surrounded by an aureole of serpentinized olivines (Figure 2.1). Wagner (1914), Kharkiv (1967a), and Dawson (1980) have described concentrically zoned garnet-, cuspidine-, and diopside-bearing dolomites and marls in diatreme facies rocks. Dawson (1980) suggests that the metamorphism occurred in hypabyssal facies rocks, the xenoliths having been subsequently transported to their current positions.

All of the macroscopic features of hypabyssal kimberlites are indicative of the existence of hot, mobile, volatile-rich magmas, a conclusion initially emphasized by Dawson and Hawthorne (1970).

In thin section, hypabyssal kimberlites exhibit a wide variety of igneous crystallization textures together with some unusual segregation textures. The textural relationships allow deduction of the approximate paragenetic sequence of crystallization as depicted in Figure 3.11. The entire paragenetic sequence may be observable in some kimberlites, but in others differentiation processes may remove earlier crystallizing phases. The mineralogy of any kimberlite de-

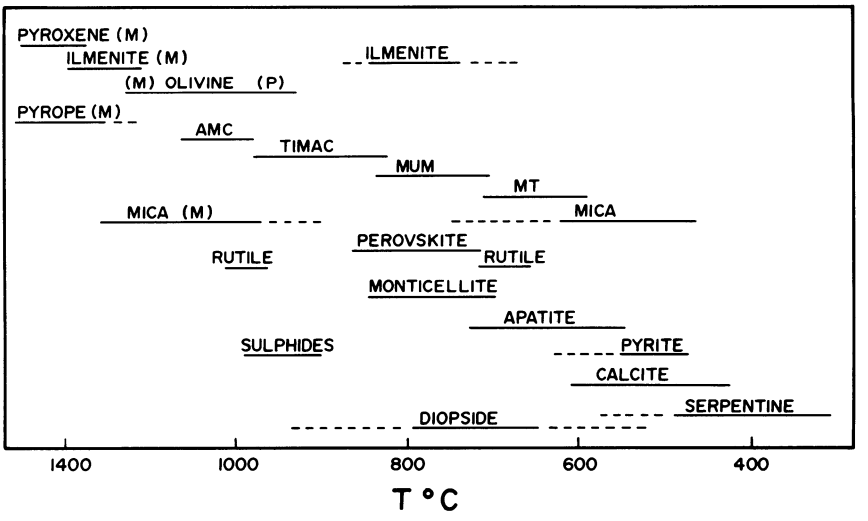

Figure 3.11. Paragenetic sequence of crystallization of the principal megacryst, macrocryst, and groundmass minerals of kimberlite.

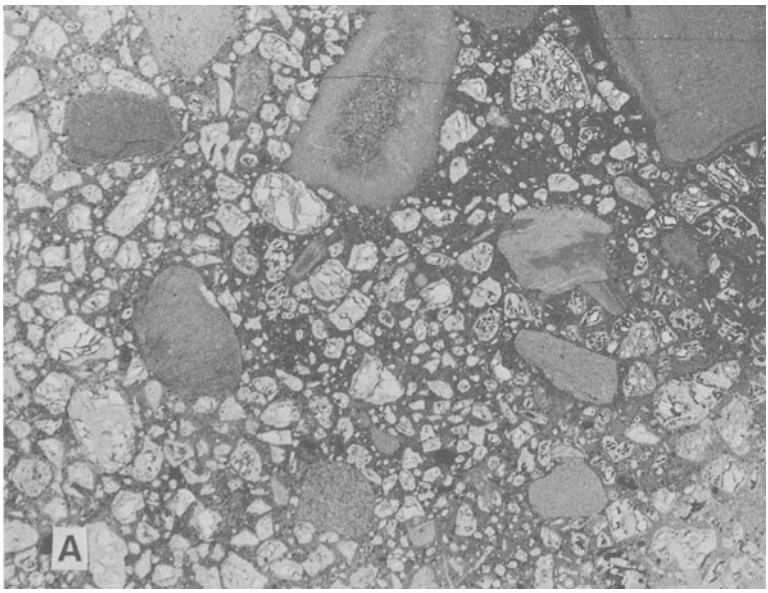

A. Tunraq kimberlite breccia, Somerset Island, Canada

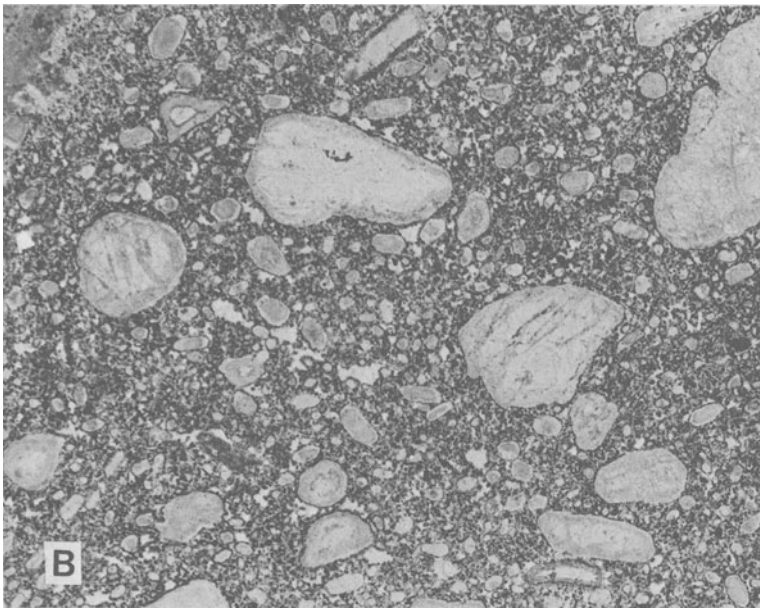

B. Frank Smith Mine, South Africa

Figure 3.12. Representative hypabyssal facies kimberlites. Note the characteristic inequigranular texture. (Fields of view ≈ 25mm.)

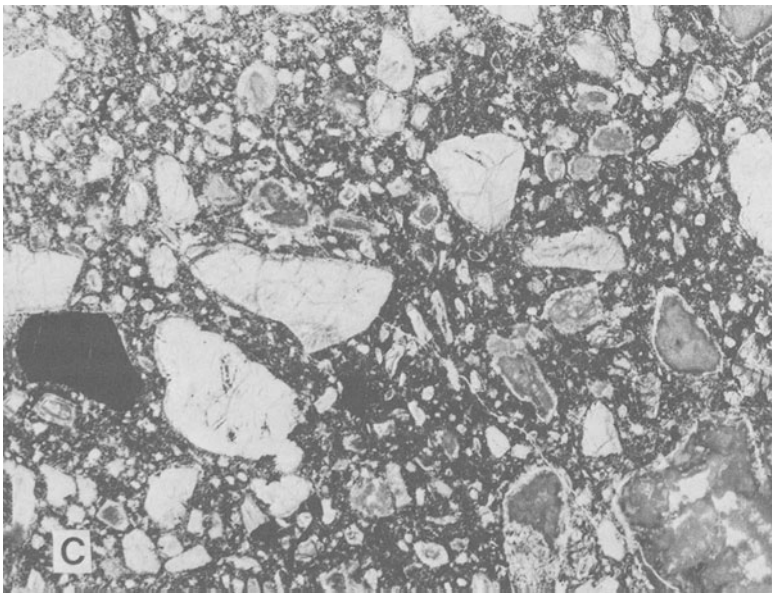

C. Lavarattam 1, India

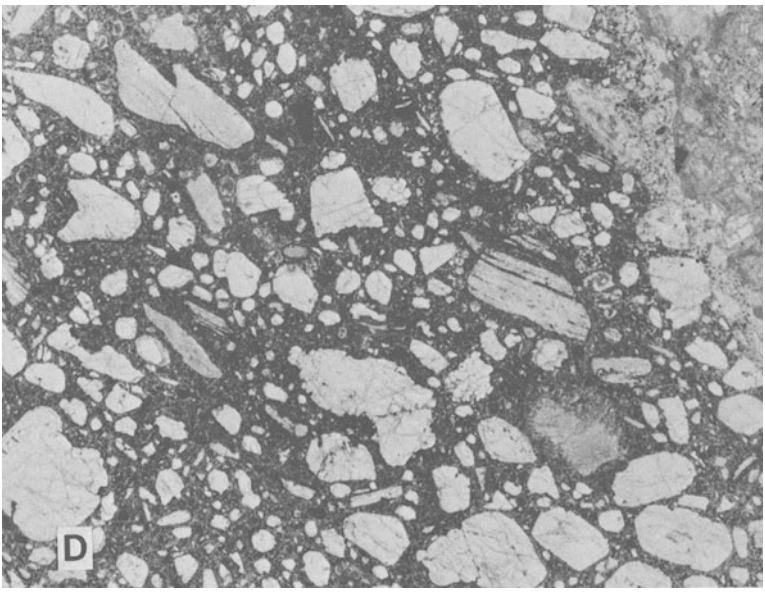

D. Mukorob 2, Namibia

Figure 3.12. (Continued)

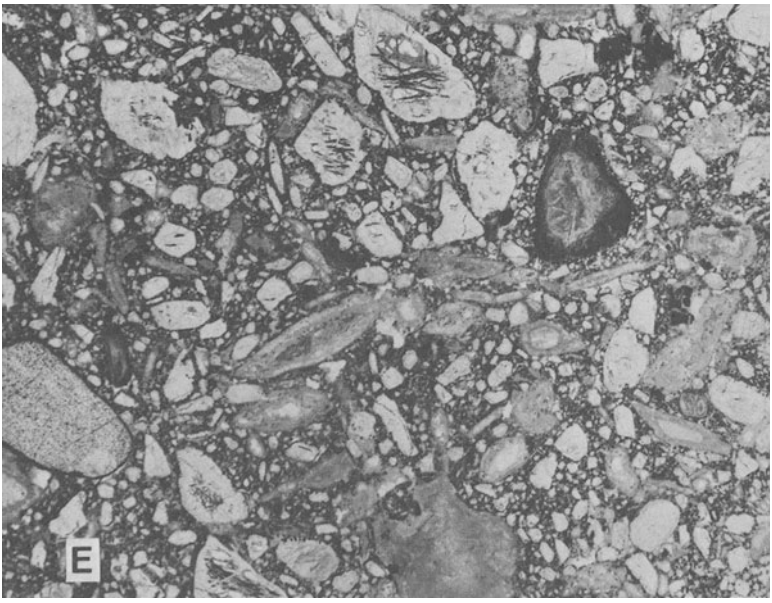

E. Nix, Colorado

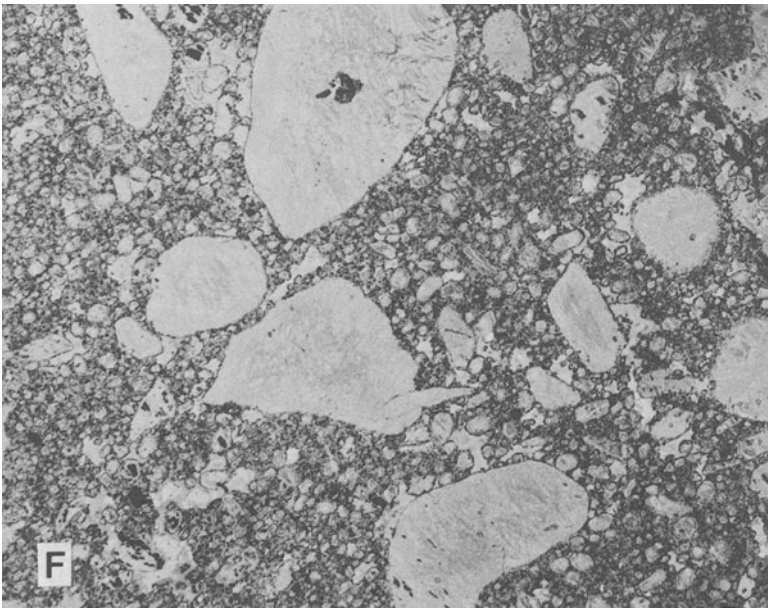

F. Qengli, Shadong, China

Figure 3.12. (Continued)

pends upon the bulk composition and stage of differentiation of the particular batch of magma sampled. Differentiation can occur prior to, during, or subsequent to intrusion. Wide variations exist therefore in the habits and modal proportions of the principal groundmass phases and macrocrystal olivine or phlogopite.

3.7.1. Petrographic Features of Uniformly Textured Kimberlites

The principal textural and mineralogical varieties of hypabyssal kimberlite likely to be encountered in any kimberlite province are illustrated in Figures 2.1–2.3 and 3.12–3.21. Space restrictions do not permit illustration of the entire spectrum of modal and textural variations. Detailed discussion of the paragenesis (and composition) of individual minerals is presented in Chapter 6. The basic features of kimberlite petrography, as outlined in Chapter 2, have been derived primarily from study of hypabyssal kimberlites, as a consequence of their freshness and predominance in most kimberlite fields relative to diatreme facies kimberlites.

Figures 2.1, 2.3, and 3.12 illustrate the general appearance of several typical fresh and altered hypabyssal kimberlites in thin section. Especially notable is the characteristic inequigranular texture which imparts a pseudoporphyritic tex-

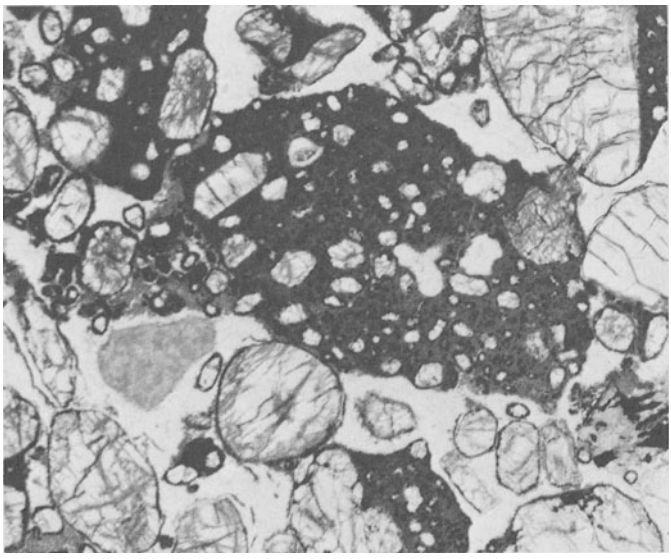

Figure 3.13. Autolithic clast containing euhedral second generation groundmass olivine, Peuyuk, Somerset Island, Canada. Note the calcite segregation (clear) and fresh olivine macrocrysts. (Field of view $\approx$ 10 mm.)

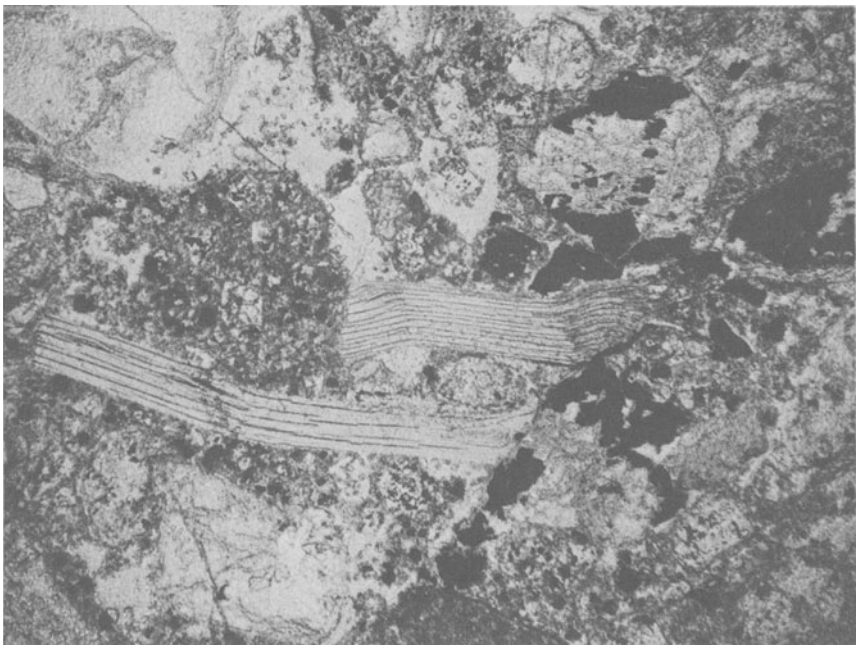

Figure 3.14. Phlogopite macrocrystal kimberlite, Tunraq, Somerset Island, Canada. The large distorted phlogopite macrocrysts are flow-aligned and impart a distinct foliation to this rock. (Field of view 10 mm.)

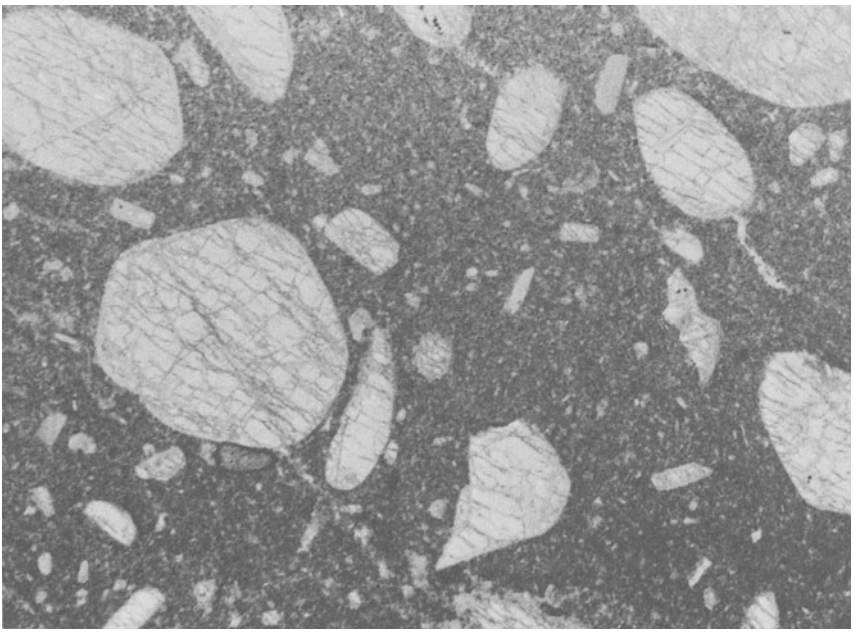

Figure 3.15. Macrocrystal micaceous kimberlite, Bellsbank, South Africa. Large subhedral olivine macrocrysts set in dark matrix composed essentially of tabular phlogopite (see Figure 3.16), perovskite and calcite. (Field of view 20 mm.)

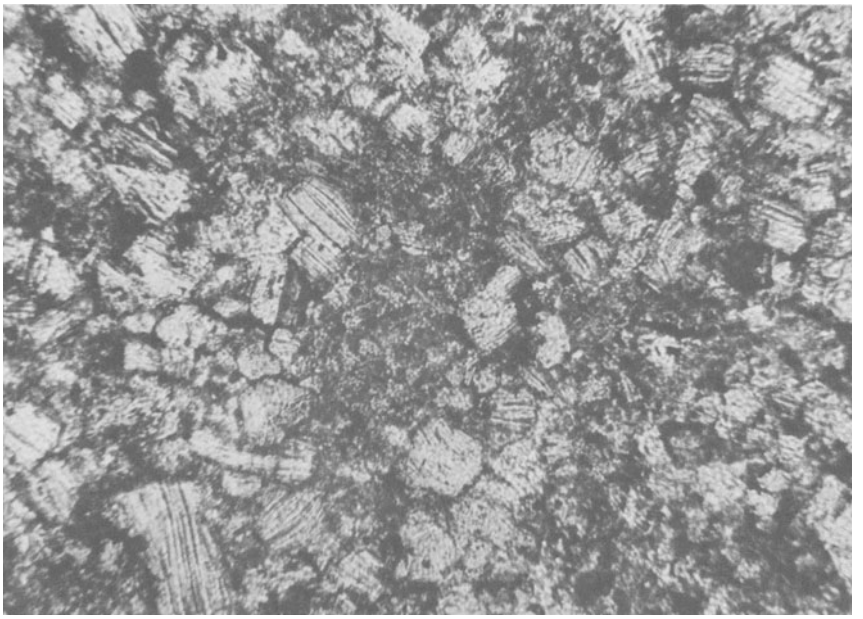

Figure 3.16. Micaceous kimberlite, New Elands, South Africa, illustrating the typical appearance of the groundmass of micaceous kimberlites and consisting of closely packed tabular crystals of phlogopite. (Field of view ≈1.5 mm.)

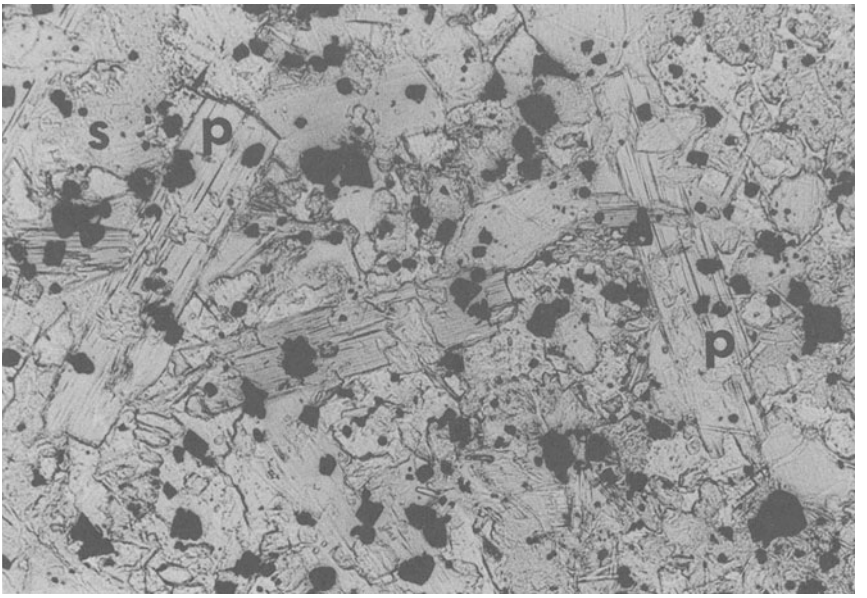

Figure 3.17. Late-stage groundmass phlogopite (p) laths poikilitically enclosing spinel and perovskite (opaque), Orroroo, South Australia. S = serpentine matrix. (Field of view 0.4 mm.)

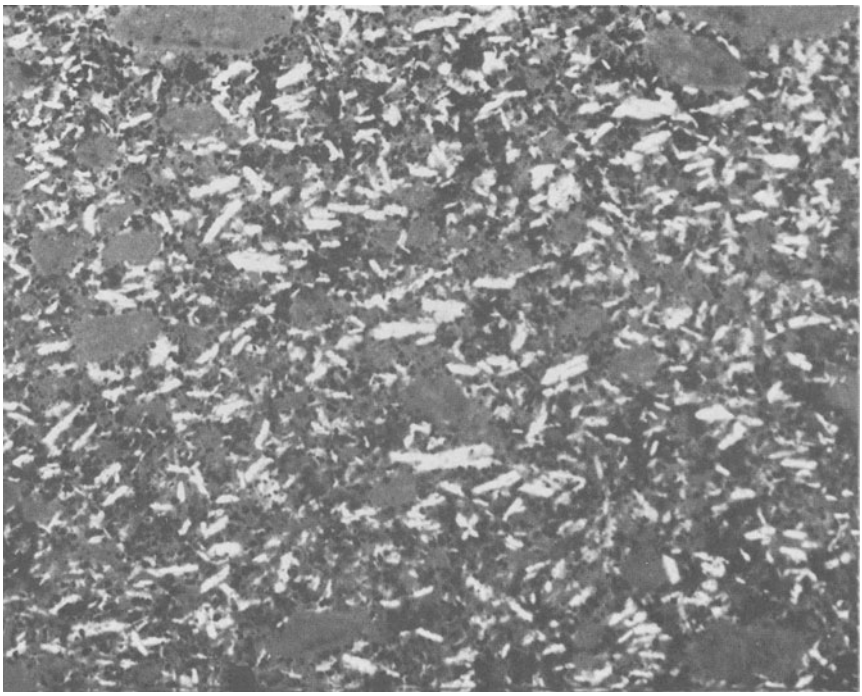

Figure 3.18. Calcite kimberlite, Mukorob dike, Namibia. Flow-aligned prisms of microphenocrystalline calcite. Grey areas are carbonatized olivine. (Field of view ≈10 mm.)

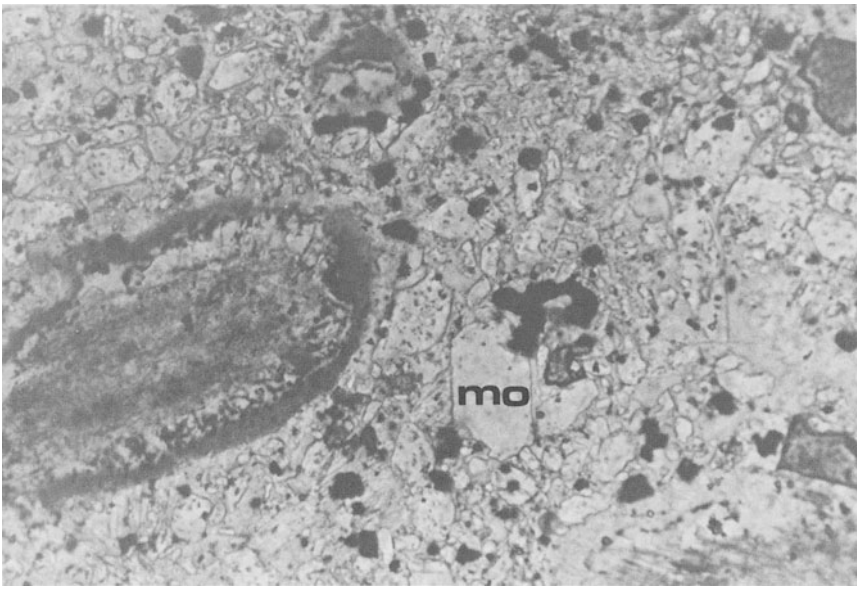

Figure 3.19. Monticellite kimberlite, Elwin Bay, Somerset Island, Canada. Euhedral to subhedral crystals of monticellite (mo) set in a matrix of calcite, serpentine and late-stage phlogopite. (Field of view 0.6 mm.)

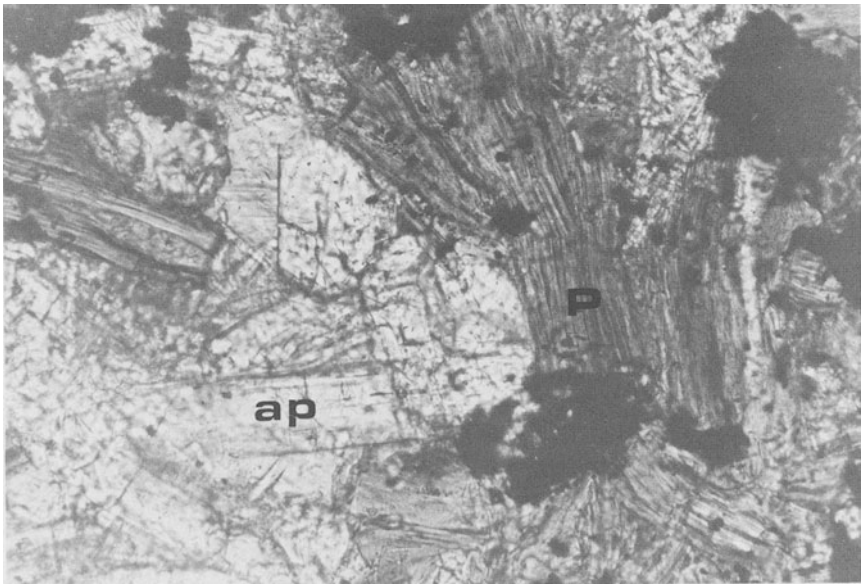

Figure 3.20. Apatite-phlogopite kimberlite, Frank Smith, South Africa. Euhedral prisms of apatite (ap) and phlogopite (p). (Field of view 0.6 mm.)

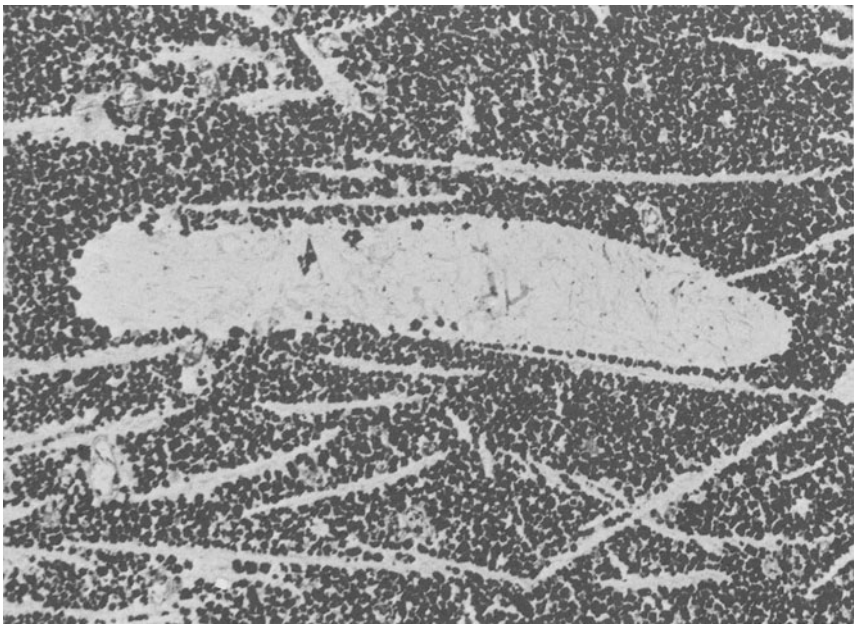

Figure 3.21. Spinel perovskite kimberlite, Benfontein Sill, South Africa. A cumulate consisting of spinel and perovskite crystals (opaque) set in a serpentine-calcite matrix. Also present are dendritic crystals of calcite (clear) and a calcite segregation. Opaque phases in the latter are rare and consist of magnetite. (Field of view 10 mm.)

ture to the rock. Note however, that the macrocrysts are typically rounded and embayed. A second generation of microporphyritic olivine of euhedral to subhedral habit can be seen in Figures 2.1, 3.12, and 3.13. The groundmass of the kimberlites illustrated in Figure 3.12 is essentially uniform. Minor segregations of serpentine and calcite are visible in Figures 3.12B and 3.12F. Figures 2.1 and 2.3 depict typical phlogopite-poor hypabyssal kimberlites: both varieties possess uniformly textured groundmasses which consist primarily of spinels and perovskite set in a calcite-serpentine matrix. Using the combined mineralogical-textural genetic classification of Skinner and Clement (1979) and Clement and Skinner (1979), these rocks would be termed macrocrystal and aphanitic calcite-serpentine kimberlites, respectively.

Mica can occur as (1) macrocrysts/phenocrysts (Figures 3.12B, 3.14), (2) microphenocrysts and groundmass micas (Figures 3.15, 3.16, 3.20), or (3) late-stage crystals poikilitically enclosing earlier apatite, monticellite, and spinels (Figure 3.17). It is important to note that *only* rocks containing groundmass phlogopite can be described as phlogopite kimberlite by the terminology of Skinner and Clement (1979). Concentration of phlogopite macrocrysts may also produce highly micaceous kimberlites and such rocks as illustrated in Figure 3.14 should be termed phlogopite macrocrystal hypabyssal calcite-serpentine kimberlites to emphasize this petrographic difference.

Calcite in uniformly textured kimberlites is typically intimately intergrown with groundmass serpentine (Figures 2.3, 3.13) as tiny anhedral crystals. Coarse aggregates are found only in segregations or as pseudomorphs of other phases (olivine, monticellite, mica, apatite). In some kimberlites tabular or prismatic crystals occur. These may be randomly oriented, form a decussate texture, or be flow-aligned (Figure 3.18), thus imparting a microlitic (Milashev 1963) or trachytic texture (Dawson 1980) to the rocks. Such calcite laths were originally interpreted to be pseudomorphs after melilite, but are now considered to be primary liquidus phases (see Section 8.3). Dendritic crystals of calcite (Figure 3.21), apparently formed by rapid quenching, are common in the Benfontein sill.

Figures 3.19, 3.20, and 3.21 illustrate the appearance of monticellite, apatite-phlogopite, and spinel-perovskite kimberlites, respectively.

3.7.2. Segregation Textures

3.7.2.1. Calcite-Serpentine Segregations

Scattered throughout the groundmass of many hypabyssal kimberlites are discontinuous irregular veins and amoeboid patches of calcite and serpentine (Figure 3.22). These have in some examples coalesced into larger, irregular pod-like segregations that characteristically have curvilinear or lobate margins. The segregations (Figures 3.22–3.24) consist of widely varying proportions of calcite and serpentine. The calcite is of a much coarser grain size than that occurring

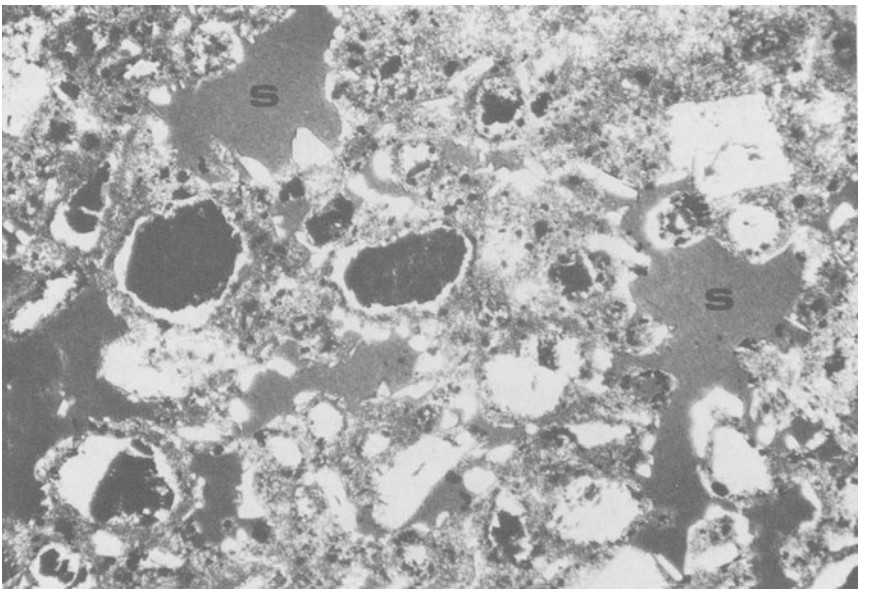

Figure 3.22. Segregation-textured serpentine calcite kimberlite, Ham, Somerset Island, Canada. The segregations (s) consist primarily of isotropic serpentine (serpophite). (Field of view 0.8 mm.)

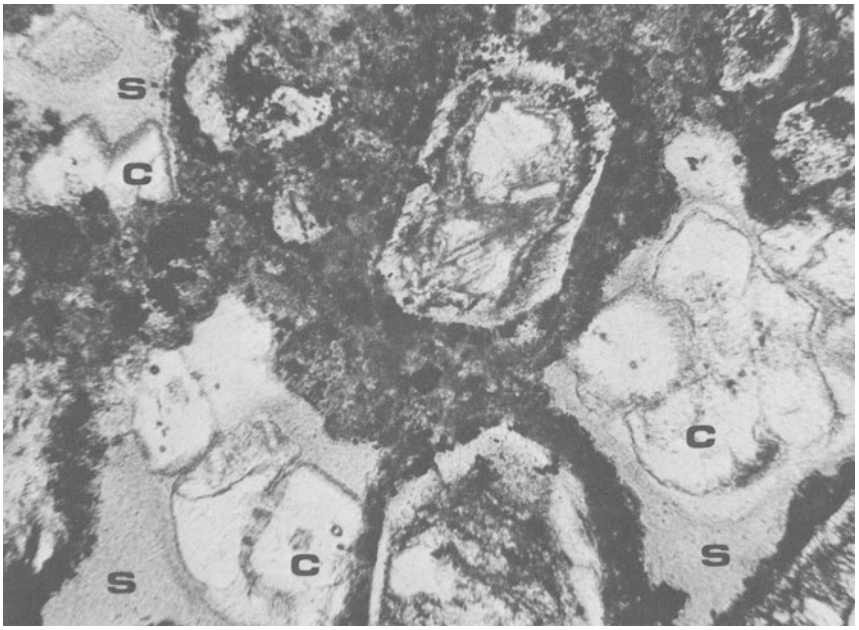

Figure 3.23. Segregation-textured serpentine-calcite kimberlite, Elwin Bay, Somerset Island, Canada. The segregations consist of resorbed calcite rhombs (c) and primary isotropic serpentine (s). (Field of view 0.5 mm.)

in the adjacent uniform groundmass and has commonly been replaced by serpentine. Rounded and embayed crystals are common (Figure 3.23). The serpentine is usually isotropic and consists of the fine grained cryptocrystalline aggregate of 1-T lizardite, termed serpophite (Section 6.11.4). The segregations may contain apatite, as stout euhedral prisms or radiating sprays of slender crystals. The apatite may be pseudomorphed by calcite and this in turn by serpentine. Notably absent from the segregations are spinels, perovskite, monticellite, and other earlier crystallizing phases. The margins of most segregations are not sharply defined and are gradational over a distance of 20–100μm into the adjacent silicate-oxide groundmass. Commonly, euhedral crystals of phlogopite, apatite, diopside, and calcite project from this matrix into the segregations.

Textures of the type described above have been referred to as emulsion (Clement 1975), amoeboid (Clarke and Mitchell 1975), or segregationary (Clement and Skinner 1979). They clearly result from the separation of the late-crystallizing components of the magma into discrete masses. These either crystallize as isolated pools interstitial to previously crystallized material, or coalesce, migrate and invade the possibly incompletely solidified parent material.

Dawson and Hawthorne (1973), Donaldson and Reid (1982), and Mitchell (1984a) have reported from calcite-rich kimberlites segregations which are mineralogically similar to those described above but which differ in exhibiting a sharp well-defined boundary toward their host groundmass. These segregations are globular, oval, or diapirlike cylindrical bodies. The latter variety commonly bifurcate or branch at one extremity and have a preferred orientation with respect to the margins of the intrusion (Figure 3.24). The segregations appear to have existed as physically distinct bodies of either liquid or fluid at the time of their formation. The walls of the segregations have, in many instances, acted as a substrate for the growth of inward-projecting mica, apatite, and calcite crystals. Some segregations are mineralogically zoned, with calcite rhombs lining the walls and serpentine filling the remainder of the body. Others are entirely filled with calcite-laths or interlocking anhedral plates of calcite. Dawson and Hawthorne (1973) were able to demonstrate that segregations in the Benfontein sill had migrated from the region of their formation and invaded other partially consolidated layers of the sill. It is assumed by Donaldson and Reid (1982) and Mitchell (1984a) that similar branched segregations in other sills have also migrated, but under the influence of thermal gradients rather than by density contrast induced mobilization.

The origin of these *migration* or *bounded segregations* is still in dispute. They have been considered to be immiscible liquids (Clement 1975, Clarke and Mitchell 1975, Mitchell 1984a), gas condensates in vesicles, i.e., true migration amygdales (Clement 1982), or vesicles which have been breached and filled with residual carbonate-rich fluid (Donaldson and Reid 1982, Clement 1982). Several origins may be possible and each example must be considered on its own merits with respect to any proposed genetic mechanism. It is particularly important to

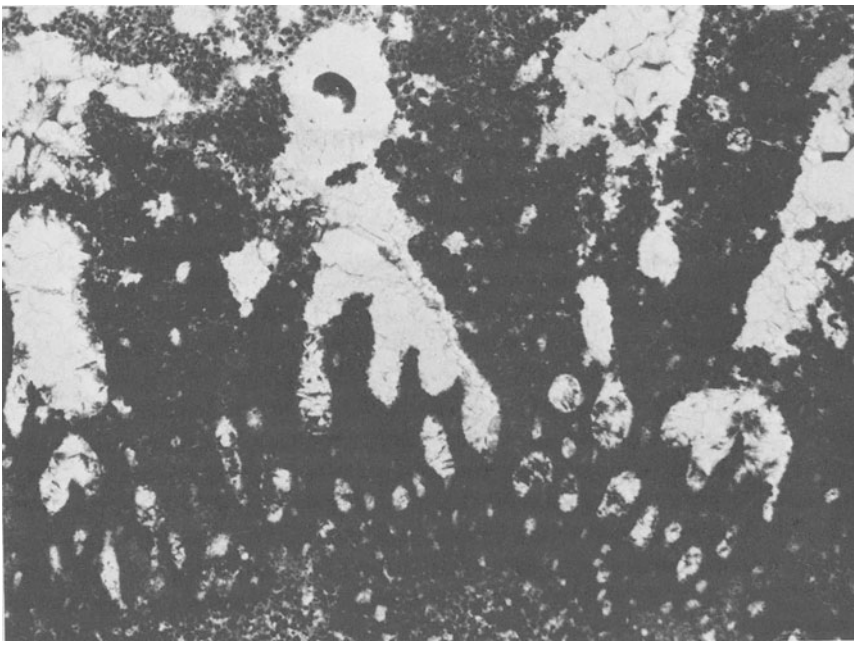

Figure 3.24. Segregation-textured calcite perovskite phlogopite kimberlite, Skinner's Sill, Wesselton, South Africa. (Field of view 8 mm.)

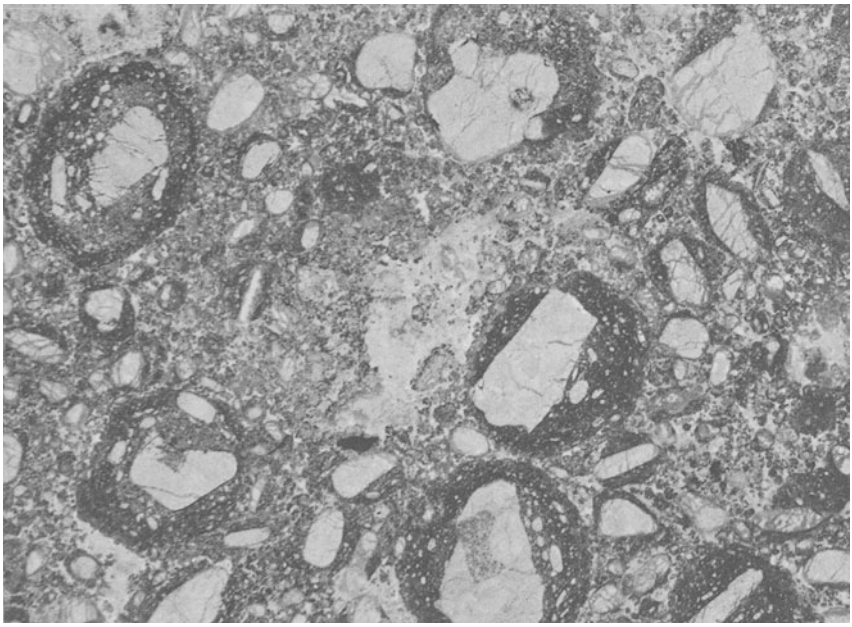

Figure 3.25. Globular segregations or nucleated autoliths (*sensu* Danchin *et al.* 1975) Finsch, South Africa. (Field of view 25 mm.)

note that the bounded segregations are mineralogically identical to the irregular merging segregations of the groundmass. Coalescence of the latter into discrete globular masses, and separated by surface tension effects from their higher viscosity parent crystal-rich matrix, can easily be envisaged and might be the ultimate step in the segregation process. Dawson and Hawthorne (1973) note that such processes, while not the result of immiscibility in a strict thermodynamic sense, do give rise to textures which are identical to those produced by that process.

3.7.2.2. Globular Segregations

Some hypabyssal kimberlites, e.g., Kimberley Mine (Wagner 1914), Dutoitspan (Clement 1982), Finsch (Clement 1975), Korvik-Selatiavak (Mitchell 1975a), and Mukorob Dike (Frankel 1956), contain globular masses of kimberlite up to several centimeters in diameter giving the rock a pseudoconglomeratic (Wagner 1914) appearance. *These segregations consist of the earlier crystallizing minerals of kimberlite and are thus quite different in character to bounded globular calcite-serpentine segregations.* They are found only locally in otherwise uniformly textured hypabyssal kimberlite. At Mukorob (this work), the

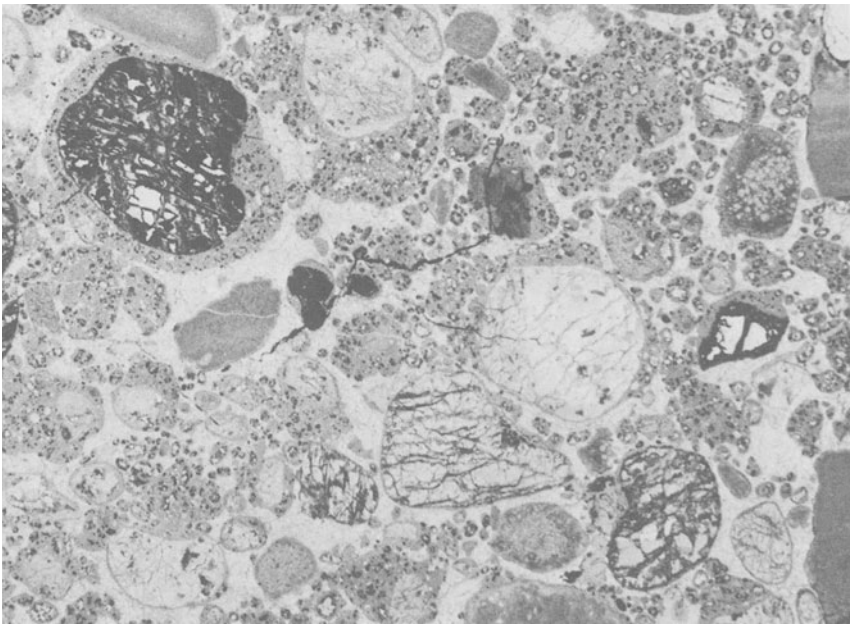

Figure 3.26. Globular segregations in a calcite matrix, Korvik-Selatiavak, Somerset Island, Canada. (Field of view 25 mm.)

globular segregations occur in a 10 m section of an otherwise uniform dike, and in a dike at Dutoitspan are concentrated into pockets aligned along one side of the dike (Clement 1982). Contact, coalescence, and distortion of the globules in the Finsch F2 kimberlite have been attributed by Clement (1975, 1982) to transport and compaction of plastic segregations.

The globular segregations (Figures 3.25, 3.26) have some petrographic similarities to pelletal lapilli (Section 3.6.1) in containing phenocrysts concentrically orientated about an olivine or country nucleus. They have however much coarser matrices and are essentially relatively fine grained hypabyssal uniformly textured kimberlites. They differ also in containing calcite, and are commonly set in a primary calcite inter-segregation matrix.

Globular segregations have been insufficiently studied and their origins and relationships to "nucleated autoliths" (Section 3.6.1) remains enigmatic. They are found in volatile-rich kimberlites which have not been involved in diatreme formation. Clement (1982) believes the segregations are formed during the local devolatization, or boiling, of kimberlite magma in closed systems in near-surface environments. In such a situation semi-solidified plastic masses of magma might be molded by surface tension effects into spherical masses. Rotation could generate concentric structures. Mitchell (1975a) ascribes globular segregations (Figure 3.26) in the Korvik–Selatiavak dike to liquid immiscibility, on the basis of the occurrence of globules of silicate-oxide-rich kimberlite in a calcite matrix and vice versa. Such structures could also result from viscosity differences between early and late fractions of the magma.

Clement (1982) considers that globular segregations develop primarily in environments which are transitional between diatreme and hypabyssal facies, and that "nucleated autoliths" represent globular segregations that have been transported from the site of their formation and incorporated into diatreme facies rocks. A similar process has been advocated by Kharkiv (1967b) to account for ball-shaped inclusions of hypabyssal kimberlite found in crystallinoclastic breccias at the Legkaya pipe.

Have you found a secret door
to let you down to the earth's deep core?
You'll be back in time for tea
With a diamond to show me, Silly!
Skip-along-Sam (Leitch) . . . preferably
as sung by Cleo Laine

4

DIATREMES AND ROOT ZONES

4.1. DIATREMES

Models of the structure of kimberlite pipe systems are based upon evidence obtained by the deep mining of kimberlites in South Africa and the recognition of epiclastic kimberlites as the near-surface and subaerial expression of kimberlitic volcanism. Combination of these observations has resulted in a model of a kimberlite pipe system (Figure 3.1) in which crater, diatreme, and root zones can be recognized (Hawthorne 1975, Clement 1979, 1982, Clement and Skinner 1979). Each zone is characterized by specific geological features and contains kimberlites of a distinct petrographic type.

Crater zones represent a near-surface flaring of the pipe and are unlikely to have been formed by the same processes that are responsible for the emplacement of diatremes and root zones. The nature and origins of crater zones are described in Section 3.2.

Some discussion of the term *diatreme* is necessary before descriptions of the features of kimberlite diatremes are presented, as current usage of the term has definite genetic overtones.

Pipelike bodies filled with igneous material and country rock xenoliths are referred to as *breccia pipes* or *diatremes*. The names have become synonymous, although the mineralized bodies associated with porphyry copper deposits are more commonly termed breccia pipes. Diatreme is used as "a general term for a volcanic vent or pipe emplaced in rocks by the explosive energy of gas-charged magmas" (AGI Dictionary of Geological Terms 1976). The genetic implications of this usage are undesirable in that it is difficult to evaluate the mechanisms leading to the formation of many diatremes. Consequently Williams and McBirney (1979, p. 53) have proposed that diatremes are: "steep sided, more or less

cylindrical or funnel-shaped breccia pipes that have penetrated the crust, apparently as moderately low temperature gas-rich intrusions."

Unfortunately this definition also has genetic implications and the purely descriptive definition of Bryner (1961) may be considered preferable: "breccia pipes are crudely cylindrical (often tapering downwards) inclined or vertical structural units composed wholly or in part of angular or rounded rock fragments with or without a matrix."

To reflect the association of diatremes with volatile-rich magmas such as kimberlite, minette, or melilitite and to distinguish them from the breccia pipes associated with acidic plutonism and volcanism, diatremes are defined in this work as: "Cone-shaped, downward-tapering, inclined or vertical structural units, composed wholly, or partly, of angular or rounded clasts of cognate or xenolithic origin, with or without a matrix. Xenolithic clasts may be derived from the walls or the roof of the body. They are commonly well-mixed and some xenoliths have apparently sunk within the diatreme. Diatremes are volcanic features associated with volatile-rich magmatism, commonly of an ultrabasic composition."

4.2. KIMBERLITE DIATREMES

4.2.1. Morphology

Kimberlite diatremes are vertical (Hawthorne 1975), or steeply inclined (Williams 1932, Novikov and Slobodskoy 1979), cone-shaped bodies consisting primarily of tuffisitic kimberlite breccia and lesser amounts of tuffisitic kimberlite. Their marginal dips are steep, ranging from 75°–85° (average 82°) and are largely independent of the mechanical properties of the rocks penetrated (Hawthorne 1975, Bloomer and Nixon, 1973, Clement 1982). Diatremes with vertical margins are rare, but have been noted from Kao (Rolfe 1973) and some Yakutian diatremes (Nikitin 1982). The typically constant dip and downward-tapering of the diatreme results in the cross-sectional area of the body decreasing regularly with depth. Representative outcrop plan views of some diatremes are illustrated in Figure 4.1. Approximately circular (e.g., Zarnitsa) or elliptical (e.g., Premier) diatremes are common and have led Nikitin (1982) to propose that the shapes of diatremes can be represented as hyperboloids of rotation with various degrees of curvature. Diatremes such as Udachnaya and Frank Smith-Weltevreden appear to have formed by the coalescence of two diatremes. Many closely related diatremes may have been composite intrusions at higher structural levels. Extremely irregular outcrop patterns are exhibited by some intrusions considered to be diatremes, e.g., Dalnayaya, Hanaus 1. Care must be exercised in referring to these as diatremes, as irregular shapes are characteristic of root zones (Section 4.3). Such bodies can be assigned to the correct facies by study of the type of kimberlite present within them.

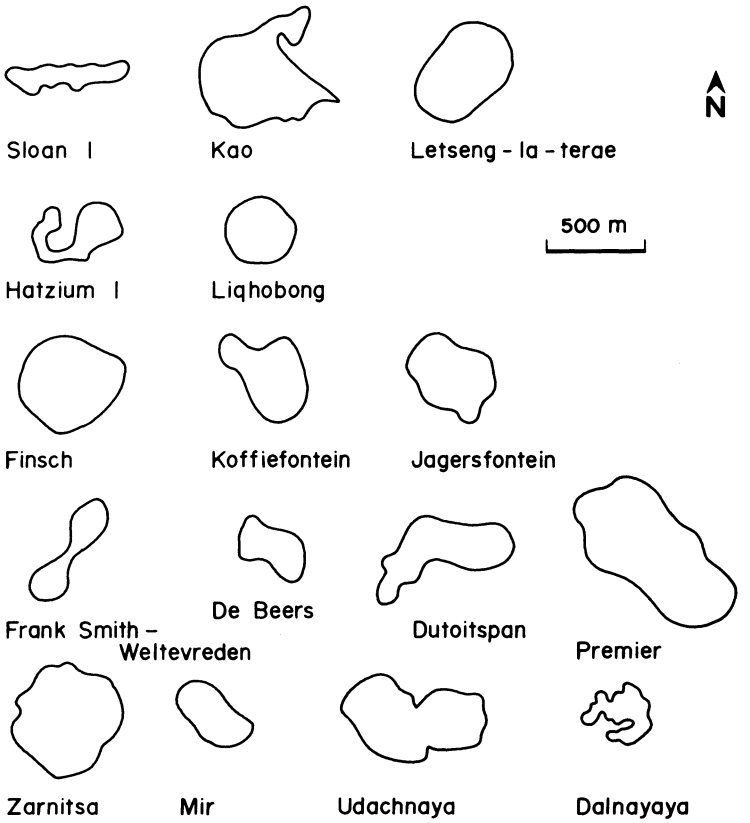

Figure 4.1. Outcrop plan views of some kimberlite intrusions. Data from Dawson (1962), Janse (1975), Lebedev (1964), McCallum (1976), and Wagner (1914).

Outcrop areas depend upon the extent of erosion of the diatreme. Axial lengths are estimated to range from 300 to 2000 m (Hawthorne 1975, Frantsesson and Boris 1983). Short and long axis diatremes can occur in close proximity to each other, e.g., the St. Augustine and Kimberley diatremes (Williams 1932). Depending upon the axial length, hypabyssal and diatreme facies, kimberlites can outcrop at the same erosional level of geographically closely related kimberlites. Hawthorne (1975) has therefore stressed that there is no direct relationship between the area of a diatreme at the present day surface and the depth to which it has been eroded. Hawthorne (1975), however, states that, regardless of axial length, all kimberlitic diatremes have similar structures. Thus by careful study of the morphology and internal features it may be possible to determine the extent of erosion.

The maximum dimensions of kimberlitic diatremes are difficult to determine. In the Kimberley area it has been estimated that the upper 1400 m of the

pipe (including the crater zone) have been removed by erosion (Hawthorne 1975). Upward projection of the diatreme contacts indicates that just below the crater zone, a diatreme of ≈2000-m axial length could be ≈700 m in diameter. As this is probably close to the maximum axial length it is unlikely that diatremes with diameters greater than 1000 m will exist. The much greater diameters (≈1500 m) quoted for kimberlite pipes such as Orapa or Mwadui (Dawson 1980) refer to the diameter of the crater zone and *not* to the diatreme zone. Crater zones will always be larger than diatreme zones as a consequence of their outward flaring and shallower contact angles.

Diatremes occur in clusters, the diameter of these being on the order of 40 km (Janse 1985). Several clusters define a kimberlite field. Diatreme locations are related to local structural features (Chapter 5).

Kimberlitic diatremes do not form positive topographic features, regardless of depth of erosion, even in regions where little chemical weathering occurs. They do not contain lava ponds or massive rocks formed by the consolidation of magma in a volcanic conduit. Dissected volcanic necks with accompanying radial dike swarms of the Hopi type (McBirney 1959) are not characteristic of kimberlitic volcanism.

4.2.2. Contact and Emplacement-Related Features

Structural and contact metasomatic/metamorphic effects associated with diatreme formation are remarkably few. Emplacement has apparently been non-dilational and the host rocks are rarely deformed or upwarped. Particularly notable is the typical absence of updoming or concentric and radial fracturing of the rocks overlying and adjacent to the upper levels of the diatremes (Mannard 1962, 1968; Hawthorne 1975). Minor structural disturbances extend only a few meters from the contacts and consist of brecciation and upturning of the enclosing rocks. Some of the upturning may result from the expansion of kimberlite during post-intrusion serpentinization (Williams 1932).

The margins of the diatremes have, typically, sharply defined cross-cutting contacts. The pipe wall rocks may be grooved, striated, and slickensided in some cases. Commonly these features are vertically oriented but other attitudes can be found (du Toit 1906, Williams 1932). Kimberlite adjacent to the contact may be highly sheared with mylonitic zones, mud seams, and calcite veins (Williams 1932, Bloomer and Nixon 1973).

Two types of breccia can be found at the pipe margins. One is an intrusion breccia resulting from the detachment of blocks and fragments of the wall rock with subsequent *in situ* incorporation of the clasts in a tuffisitic kimberlite matrix (Clement 1982, Novikov and Slobodskoy 1979, Mikheyenko and Nenashev 1962). The second consists of shattered masses of country rock lacking any apparent igneous matrix (Clement 1982, Bloomer and Nixon 1973, Nixon 1973a,

Kresten 1973a). Both types of breccia do not extend laterally or vertically more than a few tens of meters. They form thin screens with respect to the wall rock and the diatreme proper, and contacts with the kimberlite may be sharp or gradational.

Diatreme emplacement does not impose a new joint pattern on the enclosing rocks (Dawson 1962, Edwards and Howkins 1966). The shape of some diatremes, e.g., Kao (Rolfe 1973) and the State Line Field diatremes (C.B. Smith *et al.* 1979), may be influenced by pre-existing structures. Sheeted contacts, i.e., systems of closely spaced parallel joints, of the type found adjacent to mineralized breccia pipes (Sillitoe and Sawkins 1971), are absent.

Penetration of contemporaneous dikes (Section 3.4.1) or apophyses of the diatreme-filling material into the country rock is rare. Complex bedding plane or joint controlled "intrusive breccia" veins and dikes of a tuffisitic character (Section 4.4.2) are absent.

Exceptions to the above generalizations are rarely found, but Kobets and Komarov (1958) and Nitikin (1982) have noted the occurrence of concentric fracture systems surrounding some unspecified Russian diatremes. Nitikin (1982) has shown these to be crescent-shaped faults along which blocks of country rock have subsided. These collapse structures are a consequence of updoming of the country rocks above the pipe. Such domes are considered to have a positive topographic expression of up to four times the pipe diameter. Short folds (brachyfolds) and small thrusts associated with these structures, are ascribed to kimberlite intrusion (Nitikin 1982), or post-intrusion regional folding (Popov and Asatkin 1978).

These structures, indicative of forceful intrusion, are not characteristic of kimberlites in general. No information concerning the nature of the magmatism in these pipes is given by Nitikin (1982). Given the wider latitude allowed by Soviet geologists as to what rocks may be termed kimberlite, some care must be exercised before stating that the structures are due to kimberlitic magmatism and not to melilitite or nephelinite volcanism.

4.2.3. Internal Features: Xenoliths

The tuffisitic kimberlite breccias filling the diatremes contain principally angular xenoliths, derived from the local sedimentary and volcanic rocks, together with lesser quantities of rounded lower crustal (granulite, gneiss, etc.) and mantle-derived (lherzolite, harzburgite, eclogite) xenoliths. The proportions and variety of inclusions vary widely from diatreme to diatreme.

One of the most important aspects of the xenolith suite is that fragments of formations which existed at the time of diatreme emplacement, but since removed by erosion, are preserved in the diatreme. In many instances it can be demonstrated that such inclusions have descended distances of as much as 1000 m

within the diatreme (Williams 1932, Hawthorne 1975, Novikov and Slobodskoy 1979). In some diatremes, e.g., Wesselton and Kao, sunken blocks of epiclastic kimberlite can also be found (Clement 1982, Rolfe 1973).

Most clasts are *angular*, small (4 mm–5 cm) and show no evidence of being thermally metamorphosed. The presence of bituminous shale and carbonized wood indicate that high temperatures did not occur during diatreme emplacement (Wagner 1914, Williams 1932, Novikov and Slobodskoy 1979).

Extremely large blocks (50–300 m) of country rocks, termed "floating reefs" in South Africa, are common in many kimberlites. The largest of these detached and *sunken* mega-xenoliths are mainly, but not entirely (e.g., Premier), peripherally located in the upper portions of pipes (du Toit 1906, Williams 1932, Hawthorne 1975). Smaller blocks persist to considerable depth in some diatremes, e.g., Finsch (Clement 1982), Kimberley (Wagner 1914), but are *absent* from the root zone hypabyssal kimberlites. The mega-xenoliths show all gradations, from massive unbrecciated rocks to extensively brecciated types with no kimberlite matrix, to varieties veined and disrupted by kimberlite (Clement 1982). Complete disruption produces small fragments in a kimberlite host, similar to those observed in parts of the diatreme lacking mega-xenoliths, and to the wall rock contact breccias. This similarity suggests that the mega-xenoliths are simply resistant rocks which have not succumbed to the processes leading to the formation of tuffisitic kimberlite breccias. Supporting this hypothesis is the evidence that the largest mega-xenoliths are composed of competent quartzite (Premier) or basalt (Voorspoed).

Clement (1982) has suggested that the original stratigraphy of the formations in which the diatreme is emplaced is crudely preserved in the distribution of the "floating reefs" in the Kimberley area pipes.

Novikov and Slobodskoy (1979) and Dawson (1962) state that in some Siberian and Lesothan kimberlites, the number of locally derived xenoliths decreases with depth and that they are concentrated at the diatreme margins, while lower crustal and mantle-derived xenoliths occur in the central zones. This distribution has not been confirmed in all kimberlites (see Section 4.4.3). A characteristic feature of kimberlite diatremes is that xenoliths derived from a variety of crustal levels are juxtaposed with mantle-derived xenoliths. These latter xenoliths have been transported upwards from great depth and, in contrast to the crustal xenoliths, may be altered and metamorphosed.

4.2.4. Internal Features: Kimberlites

The petrographic character of diatreme facies kimberlite has been described in Section 3.6. Unfortunately few studies of the relationships between kimberlites occurring in diatremes have been published. Evidence from Letseng-la-terae (Bloomer and Nixon 1973), Kao (Rolfe 1973), Premier and the Kimberley area

(Wagner 1914, Williams 1932, Clement 1982) demonstrates that diatremes are filled by several petrographically distinct, tuffisitic kimberlite breccias. These may differ with respect to the size, shape, and type of xenoliths or cognate clasts and ultramafic inclusion content. Sharp contacts are found between the different varieties of kimberlite. These may have acted as a focus for later dike intrusion or alteration processes (Clement 1982, Bloomer and Nixon 1973). Relationships between the intrusions are complex and no consistent pattern with respect to the conduit geometry is recognizable. Central intrusions are absent. Diatremes contain relatively fewer distinct varieties of kimberlite than root zones (see Section 4.3).

In summary, diatremes present a picture of low-temperature, non-violent emplacement. Particularly striking is the extensive mixing of xenoliths and the lack of magmatic rocks, except as clasts in juxtaposition with angular unmetamorphosed country rock fragments.

Diatremes taper downward until they are about 100–200 m in diameter. With increasing depth they are gradational into the irregularly-shaped bodies of hypabyssal kimberlites which comprise the root zone.

4.3. ROOT ZONES

4.3.1. Morphology

Information regarding diatreme–root-zone relationships has been obtained principally from the Kimberley area group of pipes, as mining of most other kimberlites has rarely reached the root zone.

In the Kimberley area the depth to the diatreme–root-zone transition is dependant upon the axial length of the diatreme and the extent of erosion. The transition can always be recognized, however, by an abrupt change in the morphology of the pipe and the replacement of diatreme facies kimberlites by hypabyssal kimberlites (Hawthorne 1975, Clement 1979, 1982).

At the root zone the regular contraction of the diatreme walls ceases and the pipe may rapidly or gradually expand or contract. These changes are accompanied by a change in orientation and root zones are commonly found to be inclined structures (Figure 4.2.). Unlike diatremes, the shape and attitude of root zones is strongly influenced by the joint and fracture systems present in the country rocks. Consequently, sections of the pipe may be linear or elongated and accompanied by abrupt changes in orientation where fractures intersect. Elongation of root zones may parallel the strike of precursor dikes (Clement 1979, 1982).

In cross section, root zones are highly irregular bodies (Figure 4.2.). In some instances, e.g., De Beers, the main pipe splits up with increasing depth

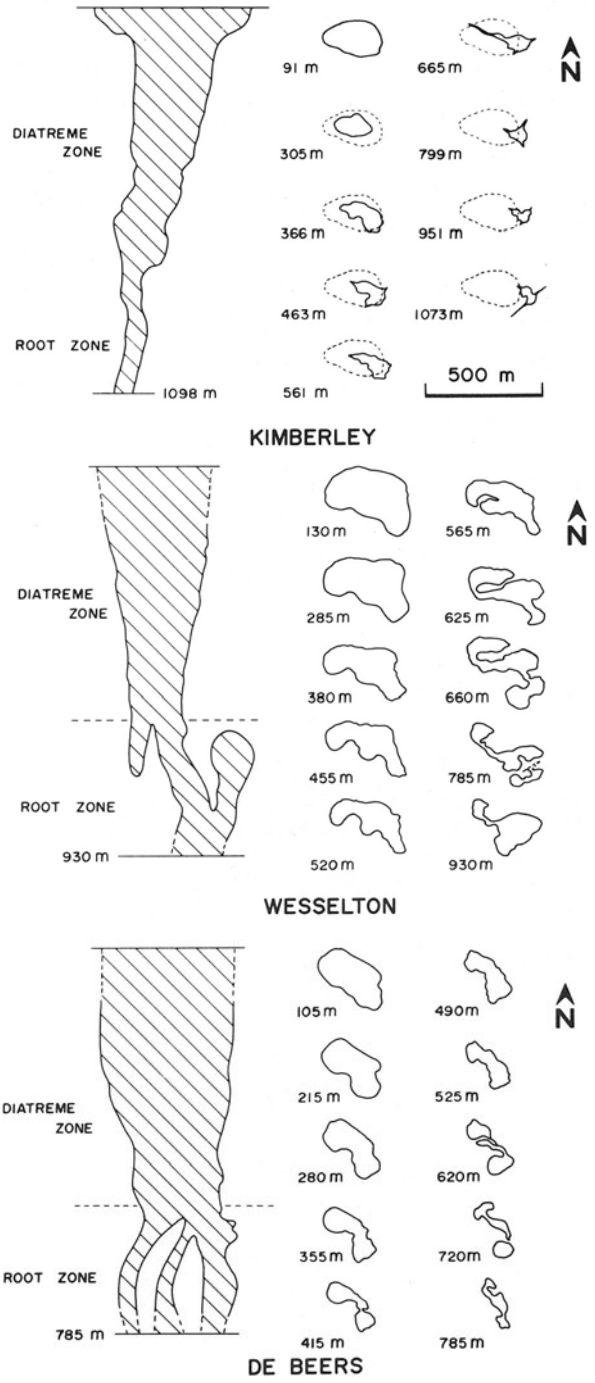

Figure 4.2. Vertical and horizontal cross sections of the Kimberley (Williams 1932), Wesselton (Clement 1982), and De Beers (Clement 1982) diatremes.

into distinct segments. The cross-sectional appearance changes rapidly over short vertical distances (Figure 4.2.). Separate irregular pipe-like sections may be linked by dike-like bodies.

The short axis diatreme of the St. Augustine Mine was found by Wagner (1914) and Williams (1932) to contract from a circular diatreme at the surface to a narrow fissure over a distance of about 250 m. The root zone is encountered 100 m below the present surface. Root zones of the larger pipes in the Kimberley area persist for distances up to 500 m. Only the Kimberley and Bultfontein pipes have been mined to depths which allow the transition to a dike to be observed. The Kimberley pipe is found to expand above the intersection of two dikes (Williams 1932), one tending NW–SE, the other NE–SW. The Bultfontein pipe is located upon a single NW–SE feeder dike (Clement 1982).

These occurrences demonstrate that root zones apparently originate as enlargements of dikes (see Section 4.3.3).

4.3.2. Contact Breccias and "Blind" Extensions

Intrusion of root zone kimberlites has been accompanied by the detachment of blocks of country rock along joints, to form simple intrusion breccias, and by the formation of other breccias, termed *contact breccias* by Clement (1979, 1982). These latter breccias are characteristic features of the root zones and may be up to 50 m in width and vertically continuous for many tens of meters. The breccias are typically located under overhanging areas of wall rock (Figure 4.3) or at the top of dome-like offshoots of the main pipe. The breccias contain locally derived clasts *only*. These have not been greatly displaced from their adjacent unbrecciated parent wall rock and the original stratigraphy is retained. The clasts are extremely angular and densely packed giving the appearance that the breccia was produced by intense shattering. Clast sizes range from a few millimeters to 50 cm. Commonly the largest clasts are found adjacent to the country rock, with the fragment size decreasing toward the kimberlite. Many breccias are devoid of kimberlite, others appear to have been permeated by kimberlite subsequent to their formation. Contacts with the wall rocks and/or kimberlite are commonly sharply defined and irregular. Contact breccias have been recognized in the root zones of the De Beers, Wesselton, Dutoitspan, New Elands, and Loxtondal pipes (Clement 1982), in the IM9 intrusion of the Iron Mountain field (Coopersmith, personal communication) and adjacent to the Amayersuk pipe, Somerset Island (this work).

Offshoots of the main pipes which are roofed by country rocks (Figures 4.2., 4.3.) are termed "blind" extensions (Clement 1979, 1982) and "blind" pipes or "roofed" dikes (McCallum 1976). They are filled with hypabyssal kimberlite and have contact breccias at their upper margins. Whitelock (1973) has described the blind extension of the Monastery pipe and noted that the core is composed of xenolith-free hypabyssal kimberlite. This core is surrounded by a

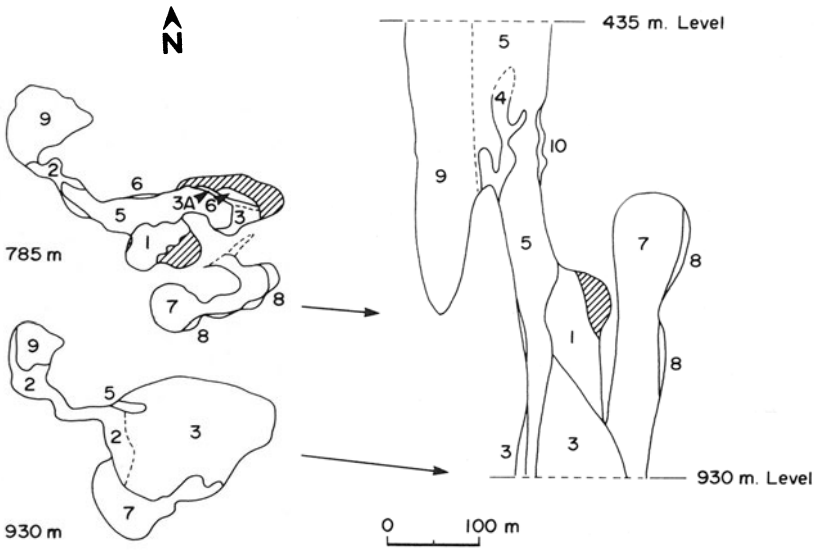

Figure 4.3. Vertical and horizontal cross sections of the root zone of the Wesselton diatreme (Clement 1982, Shee 1984). Numbers signify petrographically distinct varieties of kimberlite (not in sequence of intrusion). Diagonal shading indicates contact breccias. Note the blind diatreme represented by units 7 and 8.

dome-shaped zone of kimberlite containing sedimentary xenoliths which increase in quantity upward until only locally disturbed sedimentary rocks are found. Outside this region the sediments have been injected by a stockwork of kimberlite veins. Similar features can be observed at Mothae where a neck connecting two pipes is overlain by *in situ* lavas which have been fractured and which are gradually replaced downward by kimberlite (Nixon 1973).

These roof breccias are similar to the contact breccias described by Clement (1982) and it may be summarized that these latter breccias in some cases are remnants of former roof breccias.

Blind pipes are considered by McCallum (1976) and Clement (1979, 1982) to represent incipient diatremes which have become isolated from the main pipe due to surface breakthrough of other portions of the system.

4.3.3. Root Zone Kimberlites

Root zones are occupied exclusively by hypabyssal kimberlite and kimberlite breccia. Country rock xenoliths in the latter may be strongly serpentinized, carbonatized, or metamorphosed. Detailed mapping by Clement (1982) of the root zone of the Kimberley area intrusions has established that they are complex multiple intrusions (Figure 4.3). Individual kimberlites can be recognized on the

basis of their petrography, megacryst, and inclusion content. Mineralogical distinctions between individual root zone kimberlites from De Beers and Wesselton have been described by Pasteris (1983) and Shee (1979, 1984). The number of intrusions in a root zone varies widely; e.g., in the Wesselton root zone, ten intrusions have been recognized (Shee 1984). Some of these occur only as selvedges upon the pipe walls (Figure 4.3) or as blocks enclosed by later intrusions. The youngest intrusions are irregular pipelike bodies which intrude and replace earlier intrusions. The deepest parts of the root zone appear to be occupied by the youngest intrusions.

The root zones demonstrate that repeated injections of different batches of kimberlite magma have occurred and that sufficient time was available for each batch to crystallize completely prior to emplacement of younger magmas.

Diatreme zones contain fewer recognizable distinctive units of kimberlite than root zones. So far it has not been possible to establish temporal or genetic relationships between kimberlites occurring in the two zones. Shee (1984) notes that macrocrystal kimberlite breccia is gradational to tuffisitic kimberlite breccia within the "blind" extension of the Wesselton pipe. In the Dokolwayo diatreme, hypabyssal kimberlites are intruded by later tuffisitic kimberlites (Hawthorne *et al.* 1979).

4.3.4. Root-Zone–Feeder-Dike Relationships

Root zone complexes are similar in many respects to the enlarged fissures or "blows" associated with dike swarms that are exposed in deeply eroded terrains (Section 3.4.1). These intrusions are structurally controlled by the local joint and fracture system and contain a number of petrographically distinct varieties of hypabyssal kimberlite. The similarities are unlikely to be fortuitous and support Dawson's (1962, 1971, 1980) contention that incipient diatremes (blind pipes) or fully developed diatremes (including crater zones) originally existed above the blows. The hypothesis is further supported by the root-zone–feeder-dike relationships observed at the St. Augustine, Kimberley, and Bultfontein pipes (Section 4.3.1).

Accordingly, any irregularly shaped or elongate multiple intrusion of hypabyssal kimberlite can be regarded as being a part of a root zone complex. The Peuyuk, Pipe 200, and Blow 144 kimberlites illustrated in Figure 4.4 are thus interpreted to illustrate the transition from the deeper parts of the root zone to the feeder dike system with increasing depth.

Kimberlite fields such as the Lesotho Lowlands (Nixon 1973b) or Somerset Island (Mitchell 1976) can thus be regarded as the erosional remnants of formerly more extensive diatreme-bearing provinces.

Establishment of root-zone–feeder-dike relationships may allow recognition of the factors that control diatreme location (see Chapter 5).

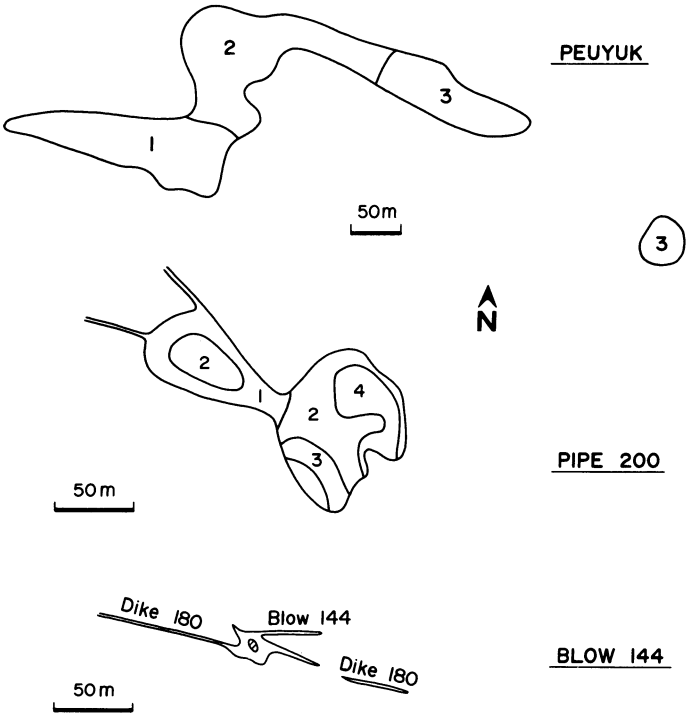

Figure 4.4. Horizontal cross sections through the Peuyuk (Mitchell 1975a), Pipe 200 (Kresten and Dempster 1973), and Blow 144 (Kresten 1973a) kimberlites. Numbers signify petrographically distinct varieties of kimberlite.

4.4. DIATREME–ROOT-ZONE EMPLACEMENT

4.4.1. Explosive Volcanism

The volcanic nature of kimberlite was soon recognized (Lewis 1887, Bonney 1899) and under the influence of ideas advanced by Geikie (1902) to explain the origins of similar diatremes in Scotland, it was proposed that kimberlites were emplaced by explosive-boring (Wagner 1914). Kimberlitic diatremes were thus regarded as volcanic vents erupting explosively from depths of up to 2 km. The eruption was considered to have originated from the violent explosive liberation of highly compressed vapors and gases of magmatic origin (Wagner 1914). The level at which this occurred is now marked by the transition from feeder dike to diatreme.

Subsequent to the discovery of the Siberian kimberlites, Russian petrologists did not seriously question this plutonist viewpoint and merely modified the explosive-boring hypothesis to account for the complex structure and the presence

of multiple intrusions in some pipes. Following an initial proposal by Leontyev and Kadenskii (1957), and re-iterated in various forms by Erlikh (1959), Vasilyev *et al.* (1961, 1968), Lebedev (1964) and Trofimov (1971, 1980), it is suggested that kimberlitic diatremes form by a continuous process in which a number of stages are recognizable.

Kimberlite magma is considered to rise from the deep mantle along cracks and fissures. The magma is believed to contain insufficient volatiles to allow direct explosive eruption, and its ascent is therefore halted when some impermeable level is reached. Pooling produces magma chambers, at relatively shallow depths, termed *intermediate chambers* (Trofimov 1971, 1980). Crystallization in these chambers results in volatile build up. Sufficient pressures are eventually generated to cause upwarping and fracturing of the roof. Explosive eruption of kimberlite with concomitant brecciation of the conduit then follows until the excess pressure is reduced. Repetition of the process can account for multiple intrusion at a single vent, or the occurrence of closely spaced diatremes if the roof fracture occurs at slightly different points above the magma chamber.

Kostrovitsky and Vladimirov (1971) and Kostrovitsky (1976) have opposed the intermediate chamber concept on the grounds that kimberlitic diatremes are far too deep, relative to their surface radii, to have originated from a single episode of explosive degassing of a magma chamber at 1–2 km's depth. Instead, it is suggested that repeated upwardly migrating small sub-surface explosions take place. The process is believed to commence at depths on the order of 5 km with final breaching taking place from 150 m or less. Intermediate chambers and paroxysmal single eruptions do not occur. Each small explosion is considered to produce a breccia zone and a series of concentric vertical fractures above the explosion focus. The spaces created provide a site for a subsequent explosion at a higher level. Repetition of the process results in self-perpetuating upward migration of the activity as the magma degasses and confining pressures fall.

The explosive-boring hypothesis has been found by most petrologists to be untenable as a means of explaining the emplacement of kimberlites, although a measure of popularity remains among some Soviet petrologists, e.g., Trofimov (1980). The principal arguments against the hypothesis, either in its original form (Wagner 1914) or in modified versions (Leontyev and Kadenskii 1957, Kostrovitsky and Vladimirov (1971), are the following:

1. No evidence for forceful intrusion exists. There is an absence of updoming concentric fracturing, imposition of new joint systems, etc. (Dawson 1962, 1967a, Mannard 1968, Clement 1982).
2. There are no explosion centers at depth, either at the base of the diatremes or the root zones (Hawthorne 1975, Clement 1979, 1982, Novikov and Slobodskoy 1979, Portnov 1979).
3. Deep mining has not revealed intermediate chambers either in Yakutian (Novikov and Slobodskoy 1979) or South African (Wagner 1914, Clement 1979, 1982) kimberlites.

4. Deep-seated explosions will not generate upwardly expanding cone-shaped conduits up to 2 km in length (Novikov and Slobodskoy 1979, Portnov 1979, Kostrovitsky and Vladimirov 1979, Williams and McBirney 1979).
5. Explosive boring is not consistent with the restriction of breccias to the interior of conduits, some of which have never reached the surface (McBirney 1959).
6. The zonal arrangement of xenoliths; the sinking of xenoliths; and the preservation of the pre-existing country rock stratigraphy in the mega-xenolith assemblage, are not consistent with explosive vent clearing (Dawson 1962, Clement 1979, 1982).
7. Projections of country rock into the diatreme are found which could not survive explosive activity (Dawson 1962, 1967a).
8. Diatreme–root-zone relationships are not explained (Clement 1979).
9. The hypothesis provides no explanation as to why volatile-rich dikes and sills could penetrate to higher crustal levels than the diatreme base and not undergo explosive eruption.

4.4.2. Fluidization

Fluidization is a name given to an industrial process in which gas or liquids are passed upward through a bed of particles in order to promote combustion or chemical reactions. A similar natural process, gas-tuff fluxion, was proposed by Cloos (1941) to explain the formation of the Swabian melilitite diatremes. In these examples, high-velocity gases of deep-seated origin were thought to have bored through the crust and opened channelways by abrasion of the wall rocks. Citing Cloos' (1941) study and the other apparent gas–solid intrusions, Reynolds (1954) introduced the term *fluidization* to describe a geological process characterized by the circulation and transportation of solids by a high-velocity gas flow. The process was readily seized upon by volcanologists, e.g., Shoemaker *et al.* (1962), Barrington and Kerr (1961), Francis (1960, 1962), Dawson (1962), as a means of explaining the characteristics of diatremes, associated with a wide variety of magmas, which did not fit the explosive-boring model.

Fluidization is the condition attained when, at a certain fluid velocity, the minimum fluidization velocity (U_{mf}), the drag force exerted across the bed by the fluid flow is equal to the buoyant weight of the bed. At this velocity particles are no longer in contact and are held in suspension in the fluid stream. In the industrial process the particulate phase is a solid; however, geological usage has extended the term beyond Reynolds' (1954) original concept to include liquid–liquid and gas–liquid systems (Wohletz and Sheridan 1979).

To understand the relevance of fluidization in diatreme formation it is necessary to describe the behavior of fluidized beds with respect to the fluid flow rate (U) and the density contrast between the suspended phase and the fluidizing

medium. When the density contrast is high (gas–solid) the excess fluid is passed through the bed as bubbles (if $U > U_{mf}$) forming an *aggregative fluidized system.* If the density contrast is low (liquid–solid), the bed expands to accommodate the extra flow without bubbling, forming a *particulate fluidized system* (Zenz 1971).

In gas–solid systems, flow velocities less than U_{mf} result in a packed-bed condition and the gas flows around the particles. When the flow velocity exceeds U_{mf} the bed expands and becomes fluidized. In cylindrical systems this will occur at the top of a pipe before it occurs at the bottom because of expansion and hence higher velocities at the top. Further increases in velocity cause further separation of the particles and the excess fluid forms bubbles. The passage of the bubbles causes the bed to become turbulent and leads to mixing of the solids. Without bubbling, gas–solid systems are very poorly mixed because inter-particle contact prevents movement of the material. If large particles are dropped into the bubbling fluidized bed they will sink or float depending upon their density relative to the apparent density of the system. (Kunii and Levenspiel 1969, Gelperin and Einstein 1971). It is these characteristics of aggregative fluidized systems that have proven to be particularly attractive to volcanologists as a means of explaining the mixing and attrition of xenoliths derived from many sources and the sinking of mega-xenoliths into diatremes.

At high gas velocities, bubbles coalesce into bands extending across the bed (a phenomenon known as slugging) which are capable of transporting plugs of solids. Further increases in velocity result in transportation of all particles in a dilute fluidized system, which is equivalent to Cloos' (1941) gas-tuff fluxion process.

Dawson (1962, 1967a, 1971, 1980) has been the principal advocate of the fluidized emplacement of kimberlite diatremes. He believes that the distribution, rounding, and striation of inclusions, the juxtaposition of xenoliths derived from various depths, the surrounding and partial detachment of blocks of country rock, the absence of updoming, and lack of thermal metamorphic effects can only be explained by this process.

Dawson (1971) thus envisions a gas-charged kimberlite magma rising from the upper mantle through a fracture system. At suitable points of crustal weakness, breakthrough to the surface occurs from depths of 2–3 km. Adiabatic expansion of magmatic gases (dominantly CO_2) occurs and the explosion vent is enlarged and infilled by fluidized fragmental kimberlite, drilling upward with a sandblasting effect and following major joint systems. In some diatremes later gas surges emplace distinctive tuff columns, while cavities in the vent may be infilled with magma which consolidates as massive kimberlite or incorporates clasts to form kimberlite breccia.

It is important to note that the initial contact with the surface is considered to be of an explosive nature. Only the shaping and filling of the pipes is the result of subsequent gas streaming.

A similar process has been advocated by Novikov and Slobodskoy (1979) to explain Siberian kimberlite diatreme formation. Their hypothesis differs in that the initial eruptions are believed to be fissure eruptions. These transform at suitable points into diatremes by gas-streaming erosion processes. The model is basically an adaptation of basaltic Icelandic fissure-type eruptions to kimberlite magmatism. The hypothesis is untenable as there is no evidence for fissure eruptions associated with either the precursor dikes or with crater facies kimberlites.

Woolsey *et al.*'s (1975) experimental studies of diatreme formation are commonly cited in support of fluidized emplacement models. In these studies a stream of compressed air was passed through unconsolidated beds of sand, silt, clay, and marble dust in cylindrical, parallel plate, and box-like containers. The structures produced (Figure 4.5) are similar to those observed in many actual diatremes, but may not be relevant to kimberlite diatreme formation for reasons noted below. Woolsey *et al.*'s (1975) work is, however, particularly important in showing that accretionary lapilli can form at depth in bubbling fluidized systems. These lapilli are not equivalent to the pelletal lapilli of diatreme facies kimberlites in that liquids were not involved in their formation.

These experimental studies form the basis of McCallum's (1976) development of the fluidization hypothesis to explain the formation of blind diatremes and the contrasting xenolith assemblages in spatially closely related pipes. In this model, a volatile-rich kimberlite magma ascends from the upper mantle along fractures and is channeled into pre-existing fractures in the upper crust. As load pressure is decreased, the gas-rich magma begins to fluidize and two or more pipe-shaped intrusions are developed above a feeder dike. Upward migration of these adjacent conduits then occurs. It is considered unlikely that each conduit will be identical in size and activity, and therefore that one conduit will be larger and more active than others. This conduit may ascend more rapidly and breach the surface sooner than others which are advancing more slowly at depth. Breakthrough of this column will disturb the pressure balance of the system and all activity in the sub-surface columns will cease. Continued activity at this primary conduit is accompanied by crater formation, sinking of country rock xenoliths, and development of a collar of inwardly dipping country rocks around the crater (Figure 4.5). Columns which fail to break through to the surface remain inactive and represent blind or incipient diatremes. After activity has ceased, erosion of the active vent to stratigraphic levels at which blind diatremes can be exposed results in the outcrop of pipes containing different country rock xenolith assemblages. The blind diatreme will lack high-level xenoliths and may be petrologically simpler, owing to the absence of the repeated intrusive activity that will have characterized the primary conduit.

Dawson's (1962, 1971) original concept of upper crustal fluidization has been extended by Davidson (1967), Kennedy and Nordlie (1968), McGetchin (1968), McGetchin and Ulrich (1973), McGetchin *et al.* (1973), Ellis and Wyllie

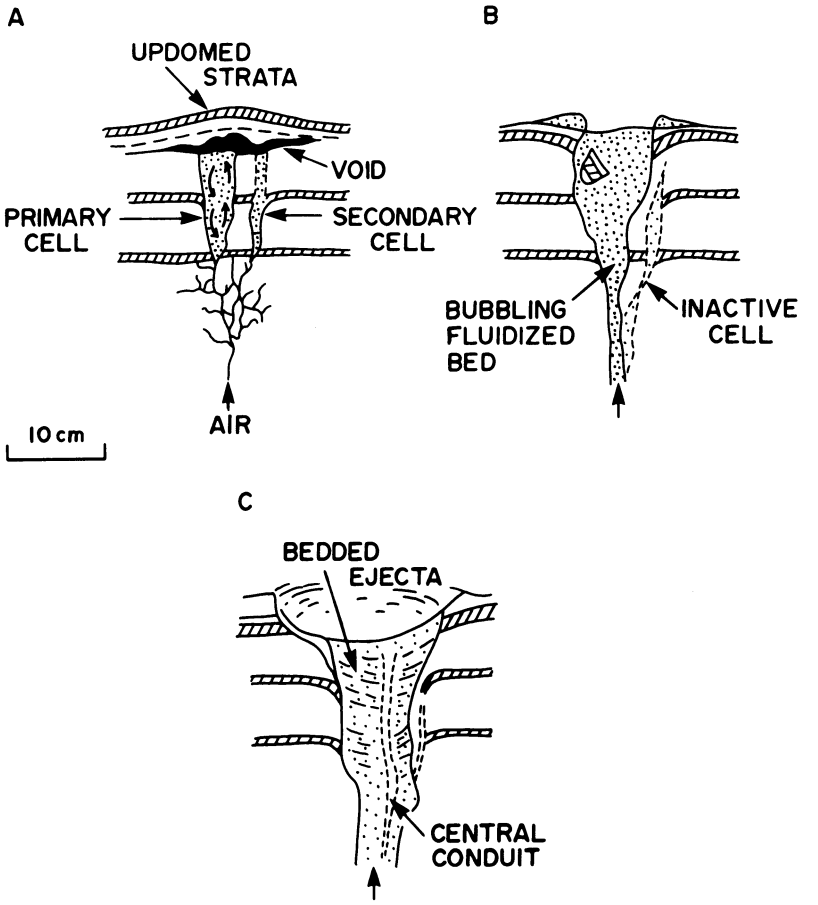

Figure 4.5. Stages in the development of a diatreme by fluidization as modeled by Woolsey *et al.* (1975). A. Initial conduit formation and doming of overlying strata; B. formation of a blind diatreme (inactive cell); C. development of the central conduit, downturning of adjacent strata and of bedded ejecta in the crater.

(1980), and Wyllie (1980) to lower crustal and upper mantle depths. Most of these works are based upon McGetchin's (1968) study of the Moses Rock Dike. McGetchin (1968) formulated his ideas on the basis of the occurrence in this diatreme/dike of a tuffisite composed of fragments of pulverized mantle-derived rocks. This comprises the "igneous" component of the diatreme and was termed kimberlite by McGetchin (1968). To explain this rock McGetchin proposed that breakdown of dense, hydrous phases in the mantle leads to the fragmentation of garnet and spinel lherzolite and incorporation of the pulverized rock into the ascending gas stream. Wyllie's (1980) model differs only in the nature of the volatile phase and he proposes that a decarbonation reaction (see Section 8.1.4)

initiates the ascent. These authors envision that the mixture of gas and crystals then rises from depth with ever-increasing velocity until it breaks through to the surface at supersonic velocities. Diatreme formation is a consequence of this high-velocity gas streaming.

The basic flaws in the McGetchin (1968) model are that (1) the igneous component of the diatreme is inadequately characterized; the tuffisite is petrographically and mineralogically totally unlike any diatreme facies kimberlite and is probably related to the regional minette magmatism; (2) the model ignores the hypabyssal infrastructure present in either minette or kimberlite provinces; this indicates that diatremes are high-level features developed above magmatic feeder dikes; (3) the extremely high emplacement velocities predicted are a consequence of an inappropriate application of equations describing pressure drop during flow of liquids in pipes to heterogeneous systems ascending uninterruptedly from depths of 150 km.

Diatreme formation by fluidization has not been accepted by all volcanologists and has been rejected in particular by those who believe that diatremes form by hydrovolcanic processes (Section 4.4.3). The principal arguments advanced against fluidization are the following:

1. It is very unlikely that high vapor pressures and large volumes of gases will be exsolved from slowly cooling magmas deep in the crust. Rapid vesiculation can occur only at shallow depths (Williams and McBirney 1979). With regard to kimberlites, it is clear that volatiles are retained in hypabyssal facies rocks at and above levels at which diatremes are formed and not released rapidly. Moreover these intrusions are of such small volume that it is doubtful whether they could produce sufficient quantities of volatiles to support a 2-km-long fluidized bed.
2. Dawson (1962, 1971) advocates enlargement of a channel after surface breakthrough (mechanism unspecified). McBirney (1963) believes that this will not occur as analysis of gas flow in pipes indicates that the relatively high velocities required for wall erosion would be achieved only in the upper 10% of the conduit. Further, Lorenz (1975) notes that widening of the pipe by gas-tuff fluxing is unlikely as increases in diameter will be accompanied by a decrease in velocity and hence erosional capacity of the gas stream.
3. Magma is believed not to be involved in the fluidization process. It is not specified why the gas phase should exsolve all at once and disrupt the magma into pyroclasts, or why other batches of kimberlite do not exsolve gases in the same manner. Autholithic clasts in diatreme facies kimberlites are not vesicular or shardlike; commonly they are angular and fractured and show no signs of the abrasion features expected as a consequence of involvement in gas-tuff streaming.
4. Most of the xenolith clasts are angular and have not therefore been subjected to extended periods of aggregative bubbling fluidization.

5. The concentration of xenoliths at specific horizons and the preservation of a crude stratigraphy in the mega-xenolith suite (Clement 1982) is not consistent with long periods of bubbling fluidization. The presence of the xenoliths is not compatible with the required earlier period of erosional widening of the pipe by high velocity gas-tuff streaming. Advocates of fluidized emplacement do not specify the spatial and temporal relationships of the different types of fluidized bed behavior required either to mix xenoliths or to erode pipe wall rocks.
6. Cloos (1941), Reynolds (1954), and Coe (1966) have described, in detail, the characteristic features of tuffisitic intrusions. Important among these are the pronounced structural control of intrusion by preexisting joints and bedding planes or by fractures created during tuffisitization, the occurrence of partially detached, commonly irregular protruberances of wall rock, irregular and serrated contacts, and fluid-like penetration of the tuffisite into all available joints, fractures, and cracks. This latter feature leads to the development of a complex network of tuffisitic veins within, and adjacent to, the intrusion. Xenoliths may be eroded and exhibit a fretted surface on one side only or, if rotation in the gas stream has occurred, become rounded, polished, and striated by attrition.

The above features are not characteristic of kimberlitic diatremes. In particular the lack of tuffisitization and veining of the wall rock adjacent to the diatreme and the root zone is convincing evidence that fluidization did not occur. Figure 4.6 illustrates the differences between a tuffisitic diatreme and kimberlitic diatremes at similar levels of erosion. The complex veining and detachment of country rock blocks seen in the Moses Rock dike is at variance with the apparent simple perforation and replacement of the country rock by kimberlitic diatremes.

Tuffisitized and fretted xenoliths of the type described by Coe (1966) have not been found in kimberlites. Such features should be common, particularly on the underside of mega-xenoliths supported in a high-velocity gas stream.

7. Recent studies (Wilson 1980, 1984) have cast doubt upon the applicability of industrial models of fluidization to geological systems as most of these models are based upon the behavior of well-sorted particles. Experiments using poorly sorted beds indicate that there is no single flow velocity at which fluidization occurs and the behavior of the system is complex and varies with the size distribution and density of the particles involved. In experiments using moderately-to-poorly-sorted pyroclastic materials, Wilson (1980, 1984) observed that an initial stage of bubbling fluidization evolves rapidly by bubble coalescence into a non-bubbling segregation column that propagates upward. Bubbles form at the top of this column and initiate circulation in the overlying material. Eventually breakthrough to the surface occurs and

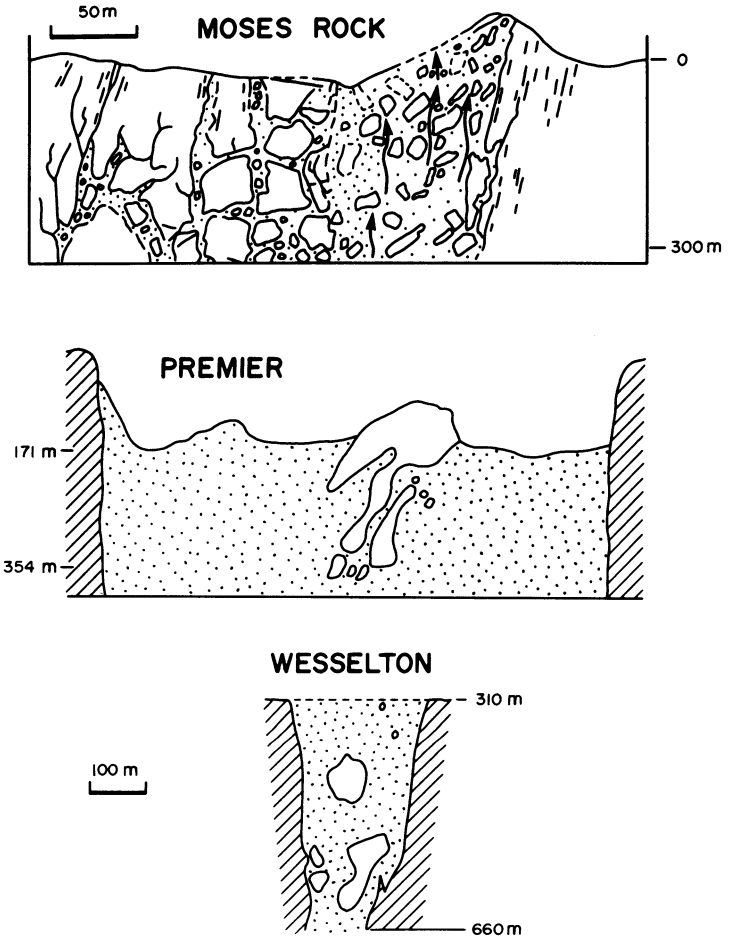

Figure 4.6. Vertical cross sections of the Moses Rock (McGetchin 1968), Premier, and Wesselton diatremes (Clement 1982) showing the distribution of mega-xenoliths. The Moses Rock diatreme illustrates the characteristic features of a tuffisitic intrusion with extensive marginal veining and brecciation, features not associated with kimberlite diatremes.

the column collapses into a packed bed and bubbling circulation ceases. Fine material may form a bubbling layer at the top of the channel. Increasing flow velocity to restore the fluidized condition results in break up of the channel into crescentic pods which are carried downward or remixed into the bed, and the eventual formation of a new segregation channel. This cycle is repeated with each attempt to restore a fluidized condition. The ultimate result is the formation of size and density graded layered beds. Only when the fluid flow rate is equivalent to U_{mf} for

the coarsest bottom beds will fluidization of the whole system occur. Decreasing velocity causes the process to operate in reverse. The principal conclusions of Wilson's (1980, 1984) work are that fluidization of poorly sorted beds results in size and compositional layering and grading, and that once generated, these features cannot be destroyed. Although flow velocities may be increased to remix layered beds, the layering reappears as the flow rate is decreased.

Clearly, none of the features described in these experiments matches the internal structures of kimberlite diatremes.

8. Kimberlite diatremes do not exhibit features predicted by Woolsey *et al.'s* (1975) experimental modeling of diatreme emplacement. The most important of these are the typical absence of updoming and associated subsurface voids above fluidized beds, the absence of features indicating prolonged tuffisitization, the lack of inwardly dipping beds of country rock around the crater, and the general absence of central conduits (see below).

Evidence apparently in favor of fluidization is limited and open to other interpretations. Tuffisitic intrusions, e.g., Mule Ear (Shoemaker and Moore 1956, Shoemaker *et al.* 1962) and the Missouri River Breaks diatremes (Hearn 1968), are reported to consist of an outer zone, containing fragments which have descended along the margins of the conduit, and an inner zone, containing inclusions that have risen from lower stratigraphic levels. A central core of magmatic rock may also be present. Woolsey *et al.'s* (1975) fluidization experiments have reproduced these features by demonstrating that the descent of material along the walls of the conduit may be accompanied by simultaneous rise of xenoliths within the central zone.

In apparent concurrence with these observations, Dawson (1962) has noted the occurrence of three kimberlites from Lesotho which are zoned with respect to their xenolith content. Novikov and Slobodskoy (1979) have reported similar zonation in unspecified (number and location) Yakutian kimberlites.

One of Dawson's (1962) examples, Kao, has subsequently been shown not to contain a central conduit. The kimberlite outcropping in the center of the intrusion, although rich in mantle-derived material, is merely a large remnant block of an earlier kimberlite surrounded and underlain by later intrusions. It is unknown whether other apparently zoned kimberlites can be similarily explained.

Although the general absence of central conduits and xenolith zoning is not supportive of fluidized intrusion, it is undeniable that some xenoliths appear to have descended considerable distances within the diatreme in a manner suggestive of sinking in a fluid medium.

It is commonly suggested that rapid adiabatic expansion of gases during fluidization is responsible for the lack of thermal effects associated with diatreme

formation (Dawson 1971). Lorenz (1975), however, interprets the evidence to be indicative of low-temperature hydrovolcanism and suggests that gas-tuff mixtures will not cool during expansion as the solids will act as a heat sink for heat lost by the expanding gas.

In summary, while the fluidization hypothesis has been widely accepted as a mechanism of diatreme emplacement, it has been subjected to little critical assessment. The observations and criticisms given above, together with those presented by Lorenz (1975, 1979) and Clement (1979, 1982), indicate that the process does not play a significant role in the formation of kimberlitic diatremes.

4.4.3. Hydrovolcanism

Hydrovolcanism refers to volcanic phenomena produced by the interaction of magma or magmatic heat with an external source of water, such as a surface body or aquifer (Sheridan and Wohletz 1983). Deposits produced by this process are termed hydroclastic (Fisher and Schminke 1984). Phreatomagmatism (Stearns and MacDonald 1946) is a particular type of terrestrial hydrovolcanism and refers to explosions resulting from the conversion of groundwater to steam by ascending magma. Products of phreatomagmatism include water, steam, brecciated country rock, and autolithic clasts. In discussions of maar and diatreme formation the terms "hydrovolcanic" (Sheridan and Wohletz 1983), "hydroclastic" (Fisher and Schminke 1984), and "phreatomagmatic" (Lorenz 1975, Wolfe 1980) are used synonymously.

Until recently the role of non-magmatic water in volcanism was either ignored, underestimated, or poorly understood, and maars and diatremes were thought to have originated by the discharge of only mantle-derived volatiles. Since about 1970, volcanologists have recognized that many volcanic phenomena can be interpreted only in terms of hydrovolcanic eruptions. These eruptions are particular examples of a class of physical processes termed fuel–coolant interactions. These violent interactions involve the contact of two fluids. One, termed the fuel, has a temperature well above the boiling point of a second, termed the coolant. On mixing, transfer of excess heat in the fuel to the coolant causes explosive fragmentation of both. The fuel is chilled and the coolant vaporized within a fraction of a second (Sheridan and Wohletz 1983, Fisher and Schminke 1984).

Wohletz and Sheridan (1983) and Sheridan and Wohletz (1983) have concluded that different types of hydrovolcanic activity form a continuum dependant upon water/melt ratios, and range from maars, tuff rings, and tuff cones formed at low ratios (<0.3), to subaqueous volcanoes formed at high ratios (>10).

Most maars and tuff cones are now interpreted to be the products of hydrovolcanic eruptions, on the basis of geological and experimental evidence (Wohletz and Sheridan 1981, 1982, 1983) and direct observation of their formation, e.g., Nilahue maar, Chile (Muller and Vehl 1957), Ukinrek maar, Alaska

(Kienle *et al.* 1980), and maars associated with the Taal Volcano, Philippines (Moore *et al.* 1966). As the surface expressions of diatremes are interpreted to be similar to maar or tuff cone it can be assumed that the hydrovolcanic processes leading to the formation of the crater may have also played a role in the development of the underlying diatreme.

Hydrovolcanic diatreme formation, initially suggested by McBirney (1963), has been strongly advocated by Lorenz (1973, 1975, 1979, 1984) and supported by Wolfe (1980).

Lorenz proposes that diatremes and maars form at hydraulically active zones of structural weakness such as faults or lineaments. Magma rising as a dike enters the fracture and contacts circulating groundwater (Figure 4.7); the resulting hydrovolcanic explosion fragments and chills the magma and brecciates the country rock. Hydroclastic debris may be ejected as a tuff ring surrounding a maar. Continued activity results in the enlargement of the fissure by further wall rock brecciation and spalling of the rock into the fracture as a consequence of pressure differences between the wall rocks and the explosion chamber formed where the water and magma interact. Eventually a hydrovolcanically active conduit surrounded by a zone of brecciated and spalled rock is developed. A ring fault is then formed at the outer margins of the brecciated zone. The diameter of the fault system depends upon the mechanical properties of the country rock. This fault extends from the surface to the level at which water–magma interaction occurs (Figure 4.7). The enclosed wall rocks and overlying bedded crater deposits then subside into the vent; because of drag along the ring fault the subsidence structures are saucer-shaped (Figure 4.7). During subsidence further fracturing and faulting may occur, and at high structural levels large blocks of country rock may become detached and even rotated during subsidence until their bedding parallels the ring fault planes. At lower levels only smaller xenoliths are found owing to the increased load and greater tendency toward spalling and brecciation. The margins of the vent thus become regions characterized by the gradual downward transport of country rock fragments. The central region of the vent remains hydrovolcanically active and transports country rock and autolithic clasts upward to be ejected as pyroclastic (hydroclastic) and epiclastic deposits in the subsiding crater. Material carried down the margins of the vent may eventually enter the central conduit and be re-cycled.

The process produces diatremes with a well-developed internal structure (Figure 4.7) as seen in the Black Butte (Montana) diatreme (Hearn 1968). Similar structures are common in melilitite- and alkali basalt-related diatremes but not kimberlites. Recognizing this, Lorenz (1975) believes that fluidization may occur in the central conduit, the resulting tuffisites being able to penetrate the adjacent collapse structure. Continued circulation of all of the material within the ring fault, together with tuffisitization, is considered to destroy, ultimately, the bedding of the crater facies rocks and the saucer-shaped subsidence structures. Eventually a well-mixed diatreme is formed and all evidence of subsidence along

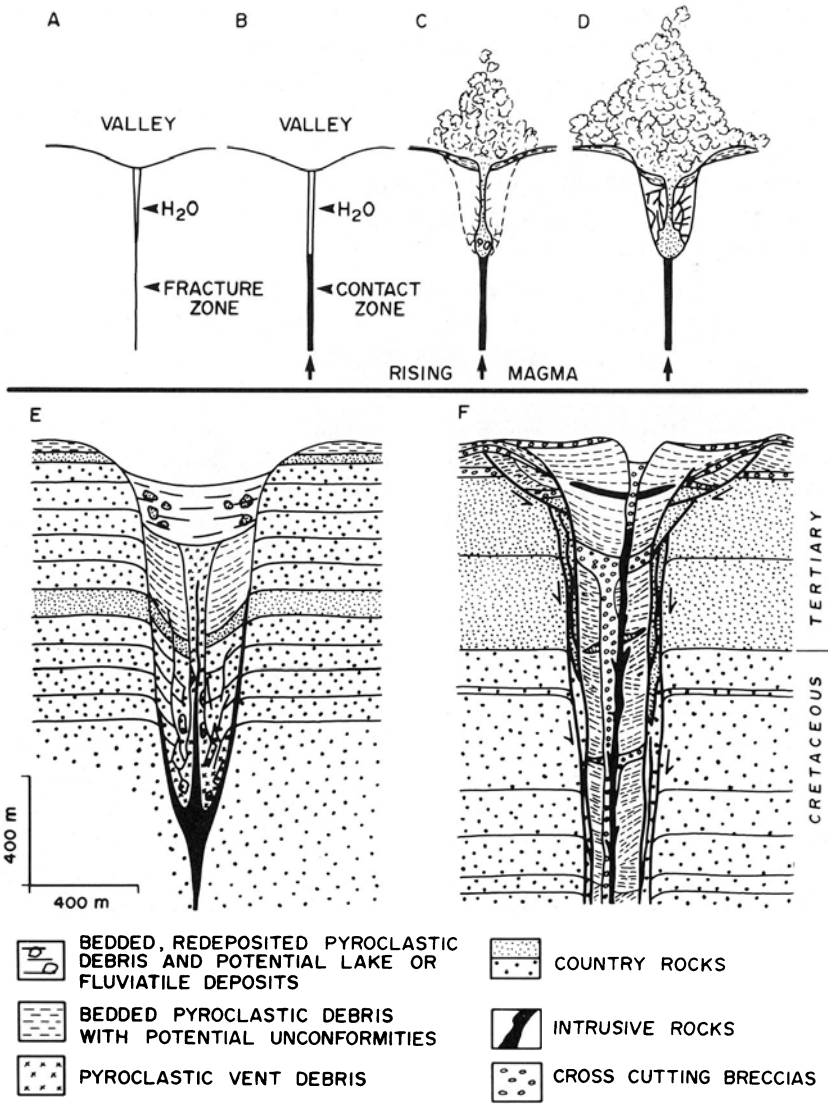

Figure 4.7. A. to E., Stages in the development of a hydrovolcanic diatreme as envisioned by Lorenz (1975, 1984); F., vertical cross section of the Black Butte diatreme, Montana (Hearn 1968).

ring faults is lost. Migration of the central conduit is proposed to account for the distinct varieties of kimberlite found in the diatremes. In this scenario, the absence of lava ponds and conduit-filling plugs of magmatic rocks is considered to be due to cessation of magmatic activity before access of water to the system is restricted.

A key aspect of Lorenz's hypothesis is that the axial length of any diatreme is determined by the level of the initial water–melt interaction. All subsequent processes serve only to widen and develop the structure. Contrary view points have been expressed by Williams and McBirney (1979) and Wolfe (1980), who believe that diatremes develop by the *downward* migration of hydrovolcanic explosions. This process is considered further in Section 4.4.4.

Lorenz's hypothesis of diatreme formation is attractive in that the following features of kimberlitic diatremes may be explained:

1. The absence of thermal metamorphism within and adjacent to the diatreme.
2. Diatremes (and maars), in general, are clearly related to linear features. Many kimberlite diatremes at their lower levels are seen to be located at the intersection of dikes and fractures. Feeder dikes appear to have risen into pre-existing fracture systems. All of these zones of weakness may be hydraulically active.
3. Diatremes are commonly developed in thick sequences of sedimentary and volcanic rocks of high porosity and permeability. Diatremes are less commonly found in rocks of low permeability such as granite-gneiss terrains, e.g., the Tanzanian and Colorado–Wyoming provinces. A well-developed joint system in such provinces provides suitable aquifers, despite the impermeability of the host rocks.
4. Kimberlite diatremes occur in groups. Modern maars and Tertiary diatremes also occur in clusters and their close geographical association is apparently related to the local hydrological regime (Lorenz 1975, 1984).
5. Pelletal lapilli could be products of fuel–coolant interactions as advocated by Lorenz (1979) and discussed in Section 3.6.1. This process can account for the association of unmetamorphosed angular country rock clasts with spherical autolithic clasts.
6. Marginal subsidence can account for the downward transport of xenoliths and crater deposits.
7. Mega-xenoliths (floating reefs) are interpreted as down-faulted and/or subsidence features.
8. Isotopic evidence (Section 7.6) indicates that groundwater has been involved in the serpentinization of diatreme facies rocks.
9. The occurrence of epiclastic kimberlites indicates that the crater above the diatreme was at times filled with water. The presence of blocks of these kimberlites at depth in the diatreme indicates that the crater lake can be disturbed by later eruptions. Drainage will obviously promote hydrovolcanic eruptions in the underlying diatreme.

Other features of kimberlitic diatremes not consistent with Lorenz's hypothesis include the following:

1. The absence of internal structures, especially saucer-shaped subsidence structures and central conduits. It is unreasonable to assume that all of these features in all kimberlite diatremes will be destroyed by circulatory re-cycling processes and tuffisitization.
2. No evidence exists for marginal ring faulting. The slickensides and mylonitization observed at the diatreme-wall rock contacts are probably the result of post-consolidation subsidence.
3. There is no evidence for tuffisitization (see Section 4.4.2).
4. Country rocks at the upper levels of diatremes are not downwarped and slumped. There is no rotation of detached mega-xenoliths as observed in some melilitite diatremes (Lorenz 1979).
5. Lorenz (1984) believes that diatremes form only in valleys, which mark the easily eroded traces of hydraulically active faults or lineaments. In contrast, fractures at higher topographic levels are poor in groundwater, and dikes emplaced along these fissures do not have the opportunity to interact with groundwater, hence only scoria cones and fissure eruptions of lava take place. This topographic–hydrological control of style of eruption has not been found in kimberlite provinces which have undergone little erosion, e.g., Singida (Mannard 1962).
6. The hypothesis does not consider the development of the diatreme root zones.

In summary, the hydrovolcanic explanation of diatreme formation as proposed by Lorenz (1971, 1973, 1979, 1984) cannot explain adequately all the features of kimberlitic diatremes. A major drawback is that diatreme–root-zone relationships are not considered, and the development of kimberlite pipes is believed to be a consequence of the action of a single volcanic process.

4.4.4. Embryonic Pipe Modification (Fluidization)

Recognizing the complexity of kimberlite pipes, Clement (1979, 1982) believes that no single process can account for their diverse geological and petrographic characteristics. In his model, root zones are interpreted as embryonic pipes which are modified by post-surface breakthrough fluidization into diatremes.

Clement's (1979, 1982) interpretation of root zone emplacement places great emphasis upon the occurrence of contact, permeation, and intrusion breccias, blind extensions roofed by breccias, and the demonstrable structural control of intrusion. Root zones are believed to develop by a variety of subsurface processes including hydraulic fracturing and wedging, magmatic stoping, intermittent explosive and/or implosive brecciation, spalling, slumping, and rock bursting. The emplacement process is based in part upon models of intrusion

breccia and breccia pipe emplacement proposed by Hunt (1938), McBirney (1959), Wright and Bowes (1968), and Norton and Cathles (1973).

Dikes rising from depth are believed to develop a precursor volatile phase due to exsolution of CO_2 liberated as a consequence of pressure decrease. This volatile phase, being under high pressure, penetrates fractures and joints in the wall rocks (hydraulic ramming) above and at the margins of the intrusion. Fluctuations in the rate of magma flow lead to pressure reduction and implosion and shattering of the country rocks as gas within them expands. Wall rock spalling and bursting may also occur. The advancing front of contact brecciation is followed by magma which penetrates the breccias and any joints or fractures present. Intrusion breccias are formed and wall rocks are wedged into the conduit. The path of the advancing magma is controlled by pre-existing structures. The change from fissure filling to root zone development may be due to increasing volatile exsolution as pressure falls upon ascent, intersection of the dike with a fracture that can be exploited or which contains groundwater. Once formed the initial root zone "bud" will be self-propagating as it will act as a focus for subsequent activity. During root zone development the magma, in effect, gnaws its way through the country rock by repeated cycles of shattering and erosion caused by the surging and churning of the magma within the conduit.

To produce complex root zones and embryonic pipes, several batches of magma are required. Earlier buds (incipient diatremes) are cut off as blind extensions or cored out by later intrusions (Figure 4.8). This process is envisioned to continue until the magma reaches a level where explosive breakthrough to the surface is possible. Clement (1979, 1982) believes that this occurs at 300–400 m and may be promoted by groundwater–magma interactions. Diatremes are then formed by the post-surface breakthrough modifications of the basal portions of the crater zone and the upper levels of the root zone (Figure 4.8). As a consequence of breakthrough and pressure release, the magma in the root zone is believed to de-gas rapidly and to form a vapor–liquid–solid fluidized system. The vapor exsolution surface is considered to migrate rapidly downward as a consequence of expansion and further pressure release. During this period of fluidization, pre-existing root zone hypabyssal kimberlites, high level contact breccias, and degassing magma are thoroughly mixed. Lack of rounding of country rock clasts indicates that the fluidized system existed only briefly. During this stage of diatreme development some pipe enlargement by the plucking of joint bounded blocks may occur, but no widening by gas-tuff fluxion is envisaged. Following degassing, activity ceases, and during the waning stages of pipe evolution activity may be confined to the emplacement of root zone intrusions. Repetition of the whole process will produce diatremes containing several distinct varieties of diatreme facies kimberlites and very complex root zones.

Clement's (1979, 1982) hypothesis accounts for most features of kimberlite pipes and in particular the complex root zone systems which are not explicable

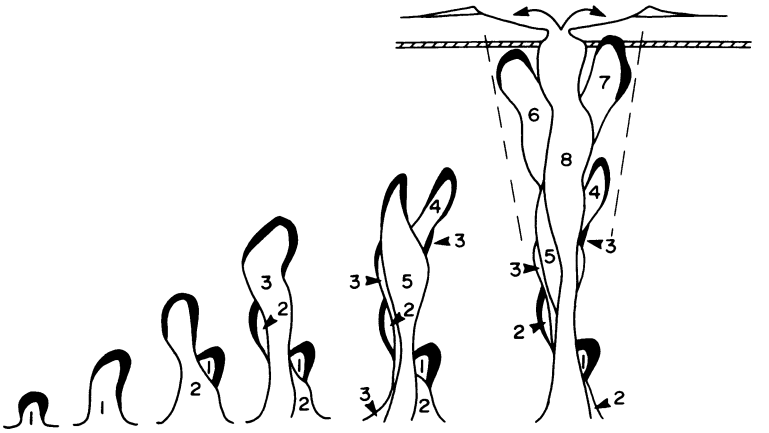

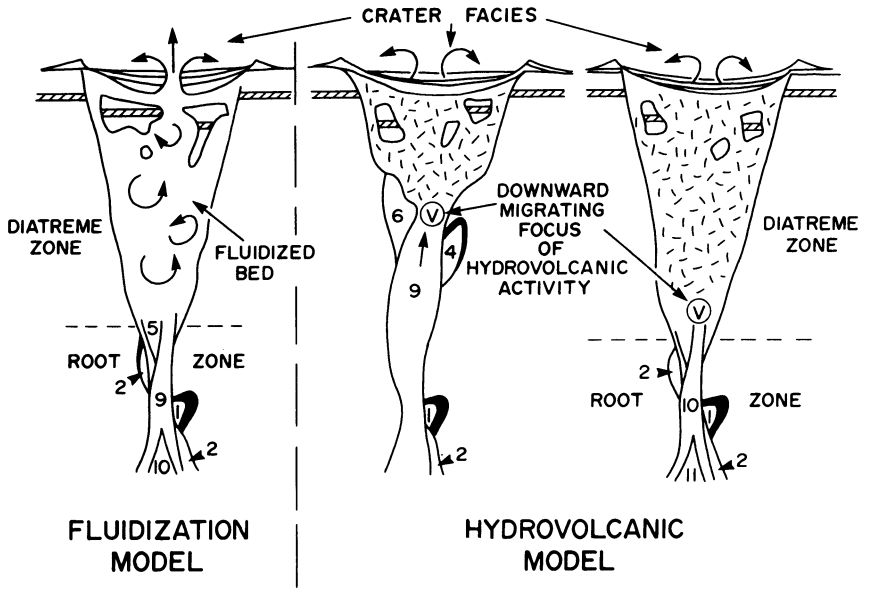

Figure 4.8. Stages in the development of a diatreme as envisioned by Clement (1982). The period of embryonic pipe development is followed by either fluidization (Clement 1982) or hydrovolcanism (this work).

by fluidization or hydrovolcanic processes. Although diatreme formation results in the destruction of the upper level root zone, evidence for its former existence is preserved in the occurrence of high-level contact breccias and in brecciated mega-xenoliths. These latter bodies are interpreted to be downslumped masses of embryonic side-wall materials. The presence of root zones is reflected also in the admixture of fragments of hypabyssal kimberlite with breccia-derived country rock clasts in the diatreme.

In support of Clement's contention that sub-surface brecciation processes are precursors to diatreme formation, are Delaney and Pollard's (1981) descriptions of contact breccias adjacent to minette dikes. These breccias are identical to those described from kimberlite root zones and have formed at dike margins and enlargements termed buds and plugs (incipient diatremes). Transport and erosion of breccias by flowing magma has occurred. Delaney and Pollard (1981) believe that pressurization of pore fluids in the wall rocks due to heating is a major cause of brecciation. The dikes are interpreted to be illustrative of the infrastructures of the Navajo–Hopi plugs and diatremes.

The most serious drawback to Clement's (1979, 1982) hypothesis is the proposition that fluidization plays a major role in the final stages of diatreme formation. The process is introduced to explain the mixing of xenolithic and autholithic clasts, the occurrence of pelletal lapilli and the sinking of xenoliths within the diatreme.

Especially cogent arguments against fluidization are the absence of tuffisitization features and the problems of generating sufficient volumes of volatiles to support a 1–2-km-long fluidized system (Section 4.4.2). Moreover it is unlikely that decompression and explosive degassing of the magma will result in the formation of a bubbling fluidized bed within the diatreme. Ejection of the diatreme contents and central conduit formation would seem more probable. Alternatively, the low viscosity of the magma may inhibit explosive devolatization (Lorenz 1979). Clement (1979, 1982) recognizes the arguments against fluidization and stipulates that the process occurs for only a short period of time in order that the angularity of xenoliths be preserved. This assertion is however in conflict with transport of material down into the diatreme, as long-term fluidization would be required to account for such transport.

In summary, Clement's (1979, 1982) hypothesis can account for the root zones of diatremes and the development of embryonic pipes. Reliance upon fluidization processes for their subsequent modification is not, however, totally supported by the available evidence.

4.4.5. Embryonic Pipe Modification (Hydrovolcanism)

The occurrence of epiclastic kimberlite indicates that substantial quantities of groundwater were present at the time of kimberlite eruption. Convincing evidence has been presented by Lorenz and others that maars and diatremes are

hydrovolcanic phenomena (see Section 4.4.3). The geology and morphology of crater zone kimberlites is consistent with such an origin. It is therefore appropriate to assign some role to hydrovolcanic processes in diatreme formation (Figure 4.8). These processes can account for such features as pelletal lapilli, mixing of xenoliths, and lack of thermal metamorphism without recourse to fluidization processes, for which there is little supportive evidence.

Accordingly, kimberlite pipe formation is considered to begin with root zone development above a dike as described by Clement (1979, 1982). Hydrovolcanic processes will play only a minor role at depth, but undoubtedly will become more important as the embryonic pipe advances towards the surface and encounters increasing amounts of groundwater. At high levels activity may be of a mixed character with episodes of hydrovolcanism interspersed with subsurface brecciation. At shallow levels load pressures will decrease sufficiently to allow formation of hydrovolcanic explosion craters or maars, with continuing activity leading to the development of tuff rings or cones. High-velocity gas-tuff fluxion or rapid decompression of underlying magma does not occur. The maar will act as a focus for groundwater accumulation. This water will seep into the underlying embryonic pipe and encounter new batches of ascending magma. Explosive interactions will lead to the formation of new breccias, and disruption of preexisting ones. Pelletal lapilli are considered to be produced by fuel–coolant interactions wherever magma and water come into contact.

Residual coolant will condense as the interclast matrix. Mega-xenoliths are interpreted to be remnants of the roofs of root zone buds, slices of country rock incorporated into the embryonic pipe during ascent or down-slumped wall rocks.

Subsequent to breakthrough the embryonic pipe will be modified by repeated hydrovolcanic explosions. The process will not lead to the development of internal structures and the resulting breccias will be well mixed. The lack of lava pools and central conduit plugs indicates that the magma supply declined while water was still available. Declining magmatic activity can therefore be expected to result in the downward migration (Figure 4.8) of the focus of hydrovolcanic explosions (Wolfe 1980, Williams and McBirney 1979). This process would result in the destruction of the precursor upper levels of the root zone and incorporation of clasts of hypabyssal kimberlite into the diatreme breccias. Slumping and mixing may result in the downward creep of high-level xenoliths.

The axial lengths of diatremes will depend upon the balance between the water and magma supply; diatreme formation may cease once relatively impermeable zones are reached. Each diatreme can be expected to be unique with respect to its internal structure and development. Repetition of the magmatic cycle will generate complex diatremes and root zones. After activity ceases, diatremes will consist of highly porous breccias. They will be subject to slumping and to the circulation of groundwater throughout the body. The latter process may result in extensive secondary alteration.

The above hypothesis is presented as an attempt to reconcile the conflicting

hydrovolcanic and magmatic viewpoints of Lorenz (1975) and Clement (1979, 1982), respectively, and to provoke further discussions about diatreme genesis.

4.4.6. Other Emplacement Processes

Mikheyenko and Nenashev (1962) suggested that kimberlites were intruded as cold, but fluid, diapiric intrusions of mantle peridotite that had been mobilized by crustal subsidence. The basis for this assertion was the lack of thermal effects associated with diatremes and the discovery that the K–Ar ages of phlogopite macrocrysts were much greater than the stratigraphic age of the intrusion.

Mikheyenko and Nenashev's (1962) hypothesis was modified, embellished, and promoted enthusiastically by Davidson (1964, 1967), who concluded that kimberlites are genetically related to carbonatite–alkali rock complexes and that pipes and dikes of kimberlite breccia are derived from pre-existing solid kimberlite and are emplaced as a cold mush or slurry of rock, highly charged with volatiles. The kimberlite breccias were thought to be derived from alkaline complexes emplaced in the lower crust which were subjected to reactivation several hundreds of millions of years after their initial crystallization. Davidson's (1964, 1967) hypothesis of cold, fluid intrusion of fragmented periodotite or kimberlite was supported by Edwards and Howkins (1966) and Kennedy and Nordlie (1968) and clearly influenced McGetchin's (1968) views on diatreme formation. The hypothesis has never won general acceptance by most petrologists in view of the observation that hot mobile kimberlite magmas can exist in the upper crust and by the recognition that the anomalous K–Ar ages are a consequence of the presence of excess ^{40}Ar in phlogopite macrocrysts (Zartman *et al.* 1967).

Williams (1932) believed that kimberlites never existed as volcanoes and that kimberlite magmas simply invaded a network of fissures formed during some earlier and totally unrelated tectonic event. The fissures were considered to have been filled with rock fragments derived from their walls. Upon kimberlite emplacement these fragments were either pushed upward or incorporated into the quietly advancing magma. Pipes were formed where fissures intersected. Pipe development consisted of a single, continuous intrusive event. Petrographic variations within pipes were ascribed to the mixing of batches of partially solidified magma with later influxes of fresh magma. Diatremes were believed to be filled with turbulent magma within which xenoliths could rise or fall depending upon their size.

Perry (1961) has suggested that kimberlite pipes are cauldron subsidence structures. The hypothesis is based upon an interpretation of the mega-xenoliths found in the Premier kimberlite as a down-faulted cupola roof.

Neither Williams' (1932) nor Perry's (1961) hypotheses are viable in terms of the structure and petrology of kimberlite pipes as outlined above and in Chapter 3.

4.4.7. Summary

The complex structure of kimberlite pipes indicates that no single process is responsible for their formation. Pipe development is initiated by sub-surface brecciation processes (Clement 1979, 1982) which lead to the formation of a complex root zone above a feeder dike. Surface breakthrough is not the result of explosive-boring but the gradual ascent of the root zone complex to levels where crater formation by hydrovolcanic explosion can occur. Diatremes appear to be secondary structures formed by the subsequent modification of the underlying root zone or embryonic pipe, by fluidization (Clement 1979, 1982) or downward migrating hydrovolcanism (this work). Diatremes are not produced by gas-tuff fluxing (Cloos 1941) fluidization (Dawson 1971, 1980), or circulatory hydrovolcanism (Lorenz 1975, 1984). High velocity intrusions of crystal mushes or gas–crystal mixtures directly from the upper mantle (Wyllie 1980), are highly unlikely to occur.

I made a very lengthy examination of the districts where diamonds are said to be found but saw no indication that would suggest the finding of diamonds or diamond-bearing deposits in any of these localities. The geological character of that part of the country renders it impossible, with the knowledge in our present possession of diamond bearing rocks, that any could have been discovered there.

James R. Gregory (1869), from a report assessing the occurrence of diamonds in the Griqualand West (Kimberley) area.

5

KIMBERLITE FIELDS AND PROVINCES: THEIR TECTONIC SETTING

5.1 KIMBERLITE FIELDS AND PROVINCES

5.1.1. Introduction

Kimberlites are products of continental intra-plate magmatism. Occurrences have not been described from oceanic environments or young fold belts. Clifford (1966) initially recognized that areas of kimberlite magmatism are confined to regions of the continental crust that are underlain by old cratons. Commonly these regions consist of a core of very old (>2.4 gigayear) rocks to which have been fused younger (>1.0 Ga) belts of deformed rocks. This process of accretion of mobile belts to the older cores is termed cratonization. The resulting structures subsequently act as rigid blocks with respect to younger tectonic events. Cratons are typically covered with Phanerozoic platform sediments and associated continental volcanics. In response to epeirogenic uplift and downwarping these rocks are faulted and/or deformed into broad basins and swells (syneclises and anteclises). It is within these platform rocks that kimberlite magmatism, especially diatreme formation, finds its greatest expression. Relatively few important kimberlite provinces are known from the exposed cores of cratons, the principal examples being the Colorado–Wyoming (McCallum *et al.* 1975) and the Tanzanian (Mannard 1962) kimberlite provinces.

Clifford (1966) and Dawson (1970) have noted that kimberlites occurring within the younger accreted belts of cratonized regions are not economic with respect to their diamond content, e.g., the Namibian, Somerset Island, and

Kundelungu provinces. Economically important kimberlites are found in regions underlain by portions of the cratons which are older than 2.4 Ga.

Cratonized regions of the lithosphere which have acted as a focus for kimberlite magmatism are defined here as *kimberlite provinces*. These provinces consist of one or more *kimberlite fields*. A kimberlite field is defined as a geographically and genetically closely related group of kimberlites of similar age. All of the kimberlites within a given field were probably derived from a single source in the mantle. Petrographic and textural variations evident within fields are the result of diverse styles of intrusion, and differentiation of different batches of magma. Janse (1985) believes that most kimberlite fields have a diameter on the order of 40 km. In this work an arbitrary diameter of 50 km is assumed as a useful working limit.

Three types of kimberlite provinces can be recognized: (1) provinces consisting of a single kimberlite field, e.g., Somerset Island (Mitchell 1976), Kundelungu (Verhoogen 1938), and Riley County, Kansas (Meyer 1976); (2) provinces consisting of several kimberlite fields of similar age, e.g., Colorado–Wyoming (McCallum *et al.* 1975, Smith *et al.* 1979), Tanzania (Mannard 1962, Dawson 1970); and (3) provinces containing several kimberlite fields of differing age and petrological character, e.g., the Yakutian province of the East Siberian platform (Bobrievich *et al.* 1964, Lebedev 1964, Davidson 1967), the Southern African province overlying the Transvaal–Rhodesian craton (Clifford 1966, Dawson 1970).

Type-1 and type-2 provinces may evolve into type-3 provinces if these regions remain sites of kimberlite magmatism.

5.1.2. Kimberlite Fields (Type-1 and -2 Provinces)

Kimberlite fields may consist of up to one hundred individual kimberlite intrusions. Each field may exhibit considerable inter-kimberlite diversity with respect to the petrology of the intrusions and their diamond, megacryst, and mantle-derived xenolith content.

The distribution of intrusions within a field depends mainly upon the level of erosion with respect to the diatreme–root zone–feeder-dike system (Figure 3.1). Within fields composed principally of high-level diatreme facies rocks, the distribution of intrusions is commonly, apparently random. A distinctive feature of such fields however is the occurrence of *kimberlite clusters*. Each cluster is composed of 1–20 distinct intrusions in close proximity (<1 km) to each other and separated by distances of 2 km or more from other similar clusters.

Clustering appears to be a characteristic feature of diatremes associated with many different types of magmatic activity and can be observed in the Bushmanland (Cornelissen and Verwoerd 1975), West Eifel, and Swabian (Lorenz 1979, 1984) melilitite fields. If the location of diatremes is controlled by hydrological factors, as proposed by Lorenz (1984), it follows that the clustering

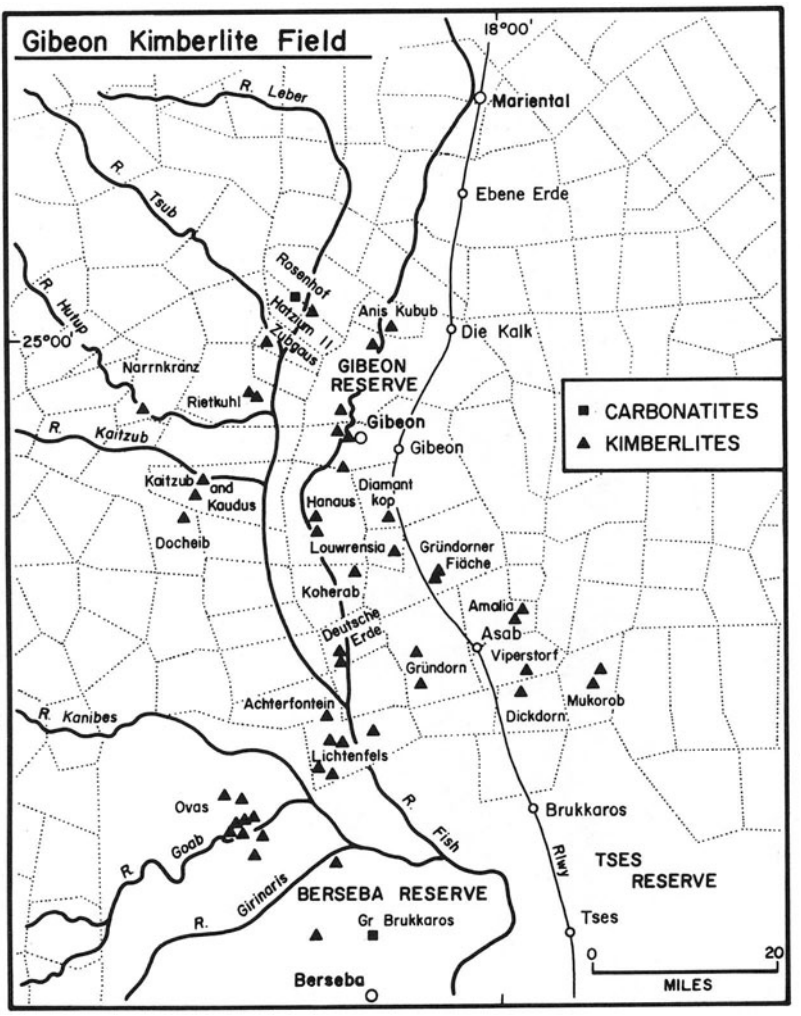

Figure 5.1. Distribution of kimberlites in the Gibeon field, after Janse (1975).

of kimberlite diatremes reflects the local hydrological environment and topography at the time of their emplacement. This conclusion will not apply to more deeply eroded fields in which root zone and feeder dike systems are exposed.

Figures 5.1–5.6 and the following discussion illustrate the changing characters of kimberlite fields with respect to their level of erosion.

Figure 5.1 illustrates the distribution of kimberlites in the Gibeon field (Janse 1975) of the southern African province. Clusters of kimberlites are defined by groups of 2–9 kimberlites, e.g., Ovas (9), Achterfontein–Lichtenfels (6), Gibeon

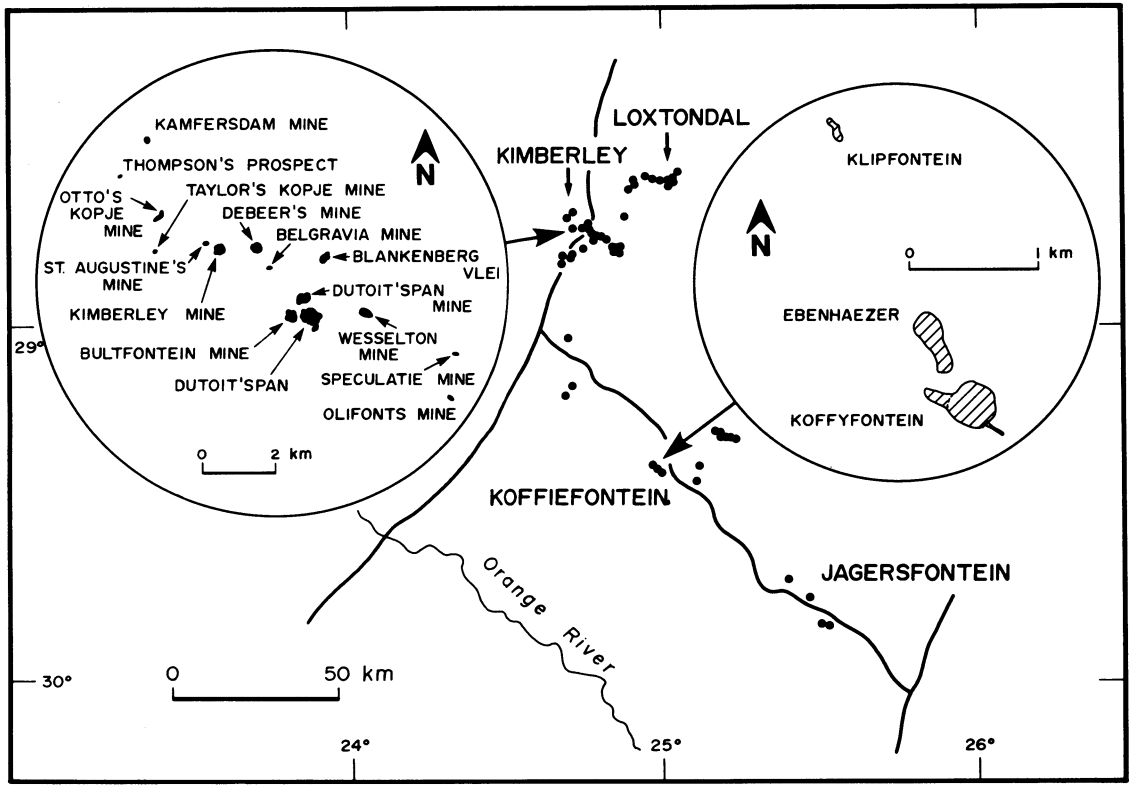

Figure 5.2. Distribution of kimberlites in the Kimberley field of the southern African kimberlite province, after Wagner (1914), Williams (1932), and *Guide to the First Field Excursion of the First International Conference on Kimberlites* (1973).

Townlands (4). Numerous isolated occurrences also are present. Local structural control of individual intrusions with respect to the fracture pattern in the country rocks can be recognized in some cases. The field as a whole, however, has no organization and the distribution of intrusions is apparently random.

Figure 5.2 illustrates occurrences of kimberlite in the 80–90 Ma Kimberley field of the southern African province. Important clusters of kimberlites occur in the vicinity of Kimberley, Loxtondal, Koffiefontein, and Jagersfontein. The northwestern portion of the field overlaps the approx. 120 Ma Barkly West field of micaceous kimberlites. Particularly striking is the linear distribution of kimberlites forming the Kimberley cluster. This trend is a result of the development of diatremes above a system of northwest–southeast trending feeder dikes; examples of these dikes being found at depth in the Kimberley, Kamfersdam, and Bultfontein pipes (see Section 4.3.4). The Koffiefontein cluster is similarly aligned and both Wagner (1914) and Williams (1932) have suggested that the Koffiefontein, Eberhaezer, and Klipfontein kimberlites are linked at depth to a northwest–southeast trending dike. A chain of diatremes of similar orientation defines a cluster to the northeast of Koffiefontein. The distribution of kimberlites in this field clearly reflects the orientation of the feeder dike system and it is not fortuitous that the Kimberley, Koffiefontein, and Jagersfontein clusters define a northwest–southeast trending line. The feeder dikes cut across the east–west foliation of the basement gneisses (Dawson 1970) and lie parallel to a major system of northwest–southeast fractures (Pretorius 1973).

Other kimberlite fields have been eroded to levels at which the transition from diatreme to root zone kimberlites is revealed. Two such fields occur within the Devonian Colorado–Wyoming type-2 province (Figure 5.3).

The State Line field (McCallum *et al.* 1975, C. B. Smith *et al.* 1979) contains 13 clusters and 12 isolated occurrences of kimberlites (Figure 5.4). The number of intrusions per cluster varies from as few as 2, at Sloan, to as many as 19, at Schaffer. The shapes and locations of individual intrusions reflect local structural controls. Typically kimberlites are elongated parallel to northwest–southeast trending fractures in the Precambrian granite and metamorphic country rocks. Diatremes, e.g., Sloan 1, may be located at the intersection of the main fracture system and east–west fractures (McCallum 1976).

In contrast to these local structural controls, the general trend defined by the clusters is north–south. This is in keeping with the trend outlined by the province as a whole (Figure 5.3). This trend is parallel to the eastern mountain front of the Front and Laramie Ranges and may reflect kimberlite localization at some deep seated lineament or fault zone. In this field it is apparent that the structural controls in the emplacement of diatremes are not the same as those which allow access of kimberlite magma to the upper crust. The distribution of diatremes does not therefore reflect the attitude of the feeder systems as observed in the Kimberley area.

In the Iron Mountain field (C. B. Smith *et al.* 1979, Smith 1977) denudation

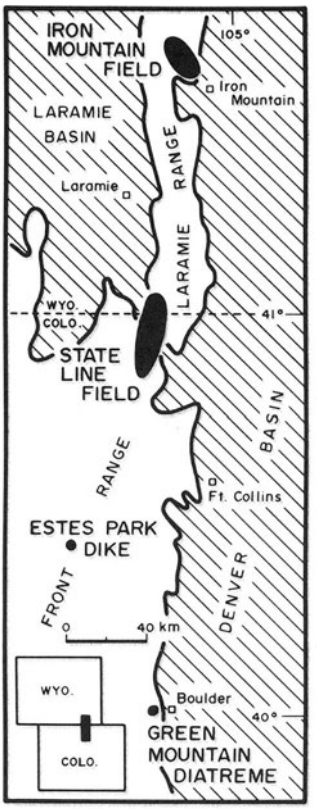

Figure 5.3. Distribution of kimberlite fields in the Colorado–Wyoming kimberlite province, after McCallum *et al.* (1975), and Coopersmith (personal communication 1985).

has been more extensive than in the State Line field and the erosional level lies just above the point at which root zones bud from feeder dikes. Consequently the outcrop patterns of the kimberlites (Figure 5.5) are very complex, but do illustrate the orientation of the feeder dikes and sills. The dikes trend northwest and northeast, the former trend being followed also by Precambrian diabase dikes. Erosional levels of the Iron Mountain field are similar to those of the Somerset Island province (Mitchell 1976).

Figure 5.6 illustrates the distribution of kimberlites in two portions of the North Lesotho field (Dawson 1962, Nixon 1973b) of the southern African province. In the Highlands (eastern) region of the field, erosion has not been sufficiently extensive so as to remove all of the diatreme facies rocks. The deeply incised plateau reveals the presence of kimberlite as dikes, root zones (blows), and diatremes. In the Lowlands (western) region of the field, erosion has been more extensive and diatremes are absent. Root zones are present but relatively rare and the hypabyssal infrastructure of the field is revealed as a swarm of subparallel dikes.

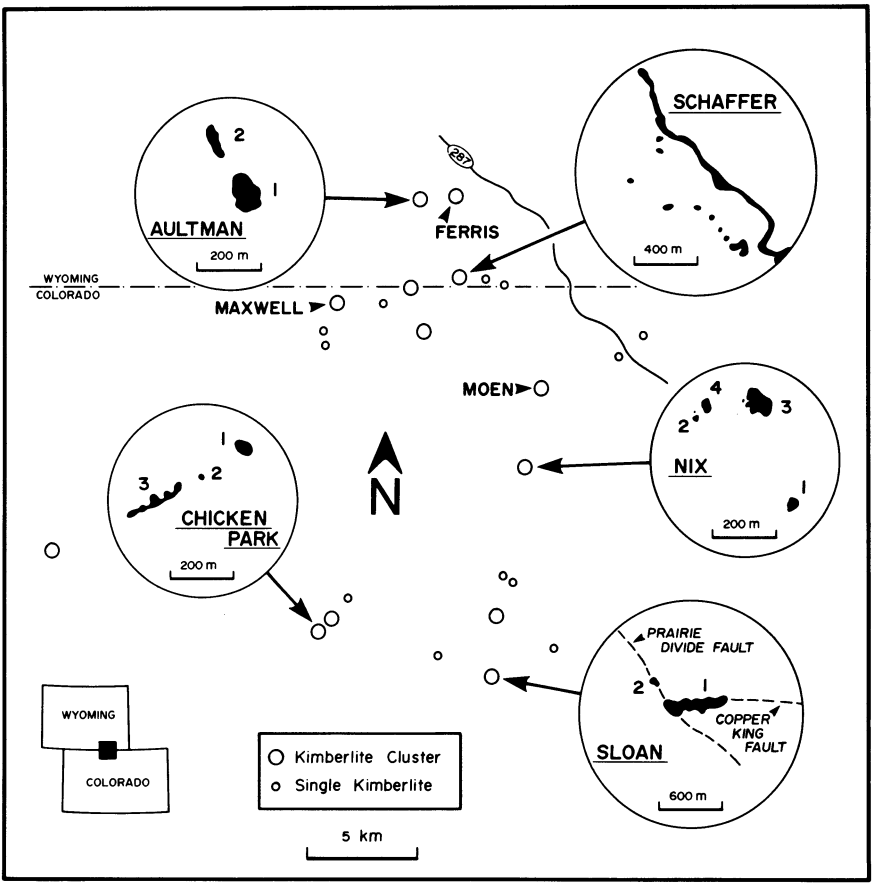

Figure 5.4. Distribution of kimberlites in the State Line field of the Colorado–Wyoming kimberlite province, after McCallum (1976), *State Line Kimberlite Guide of the Second International Conference on Kimberlites*, and Coopersmith (personal communication 1985).

The principal and secondary strike directions of the dikes are west–northwest and east–southeast, respectively. The kimberlites have the same strike as an earlier swarm of basaltic dikes and the main fracture direction in the Karoo sedimentary and volcanic country rocks. Pipes originate where west–northwest trending dikes are cross-cut by east–southeast striking dikes or fractures, and where they intersect basaltic dikes. The Letseng-la-terae pipe is located at the intersection of fractures which are devoid of kimberlites at this level of erosion. It is apparent in this field that the disposition of diatremes and their root zones reflects the attitude of the underlying feeder systems.

The distribution and emplacement of kimberlites is controlled by the regional west–northwest striking fracture pattern. Norman *et al.* (1977) have determined

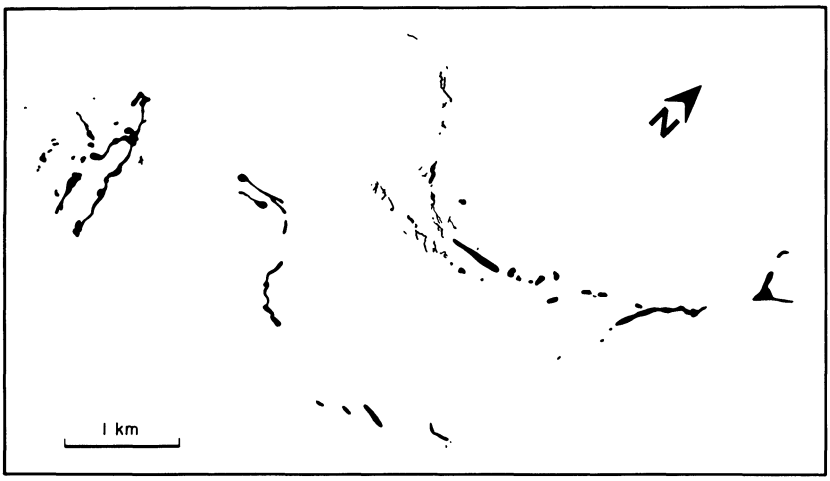

Figure 5.5. Outcrop patterns of sills and diatreme root zones in the Iron Mountain field of the Colorado–Wyoming kimberlite province, after Smith (1977).

that the stress field responsible for these fractures persisted over an extended time and was characterized by several periods of movement, consequently basaltic and kimberlite dikes have similar orientations. Importantly, most of the available fractures have not been filled by kimberlite, therefore clusters of dikes are found. Development of diatremes above these dike clusters would lead to the formation of diatreme clusters which could not be related entirely to near-surface hydrogeologic factors. The North Lesotho field demonstrates the regional structural controls on the emplacement of the hypabyssal infrastructure of kimberlite fields. The fractures which control the location of the feeder dikes do not coincide with the strike of the accreted Orange River Belt (Dawson 1970) and are related to Mesozoic epeirogenic fracturing.

Other fields in which erosion has been sufficiently extensive to expose a sub-parallel swarm of feeder dikes include West Greenland (Scott 1981), Swartruggens (Fourie 1958), Barkly West (Bosch 1971), and Orroroo (Scott Smith *et al.* 1984).

A final word of caution must be added to any discussion of the distribution of kimberlites within a given field. It is entirely possible that as a consequence of insufficient investigation and/or poor exposure, not all kimberlites occurring within the field have been discovered. The following examples illustrate this point:

1. The Somerset Island kimberlites are found only upon plateau areas where the bedrock is exposed; none are known from the intervening valleys or lowlands which are filled with solifluction flows and glacial debris.

2. In the Kundelungu region (Verhoogen 1938) kimberlites are exposed only at the margins of the plateau where stream erosion has occurred; none have

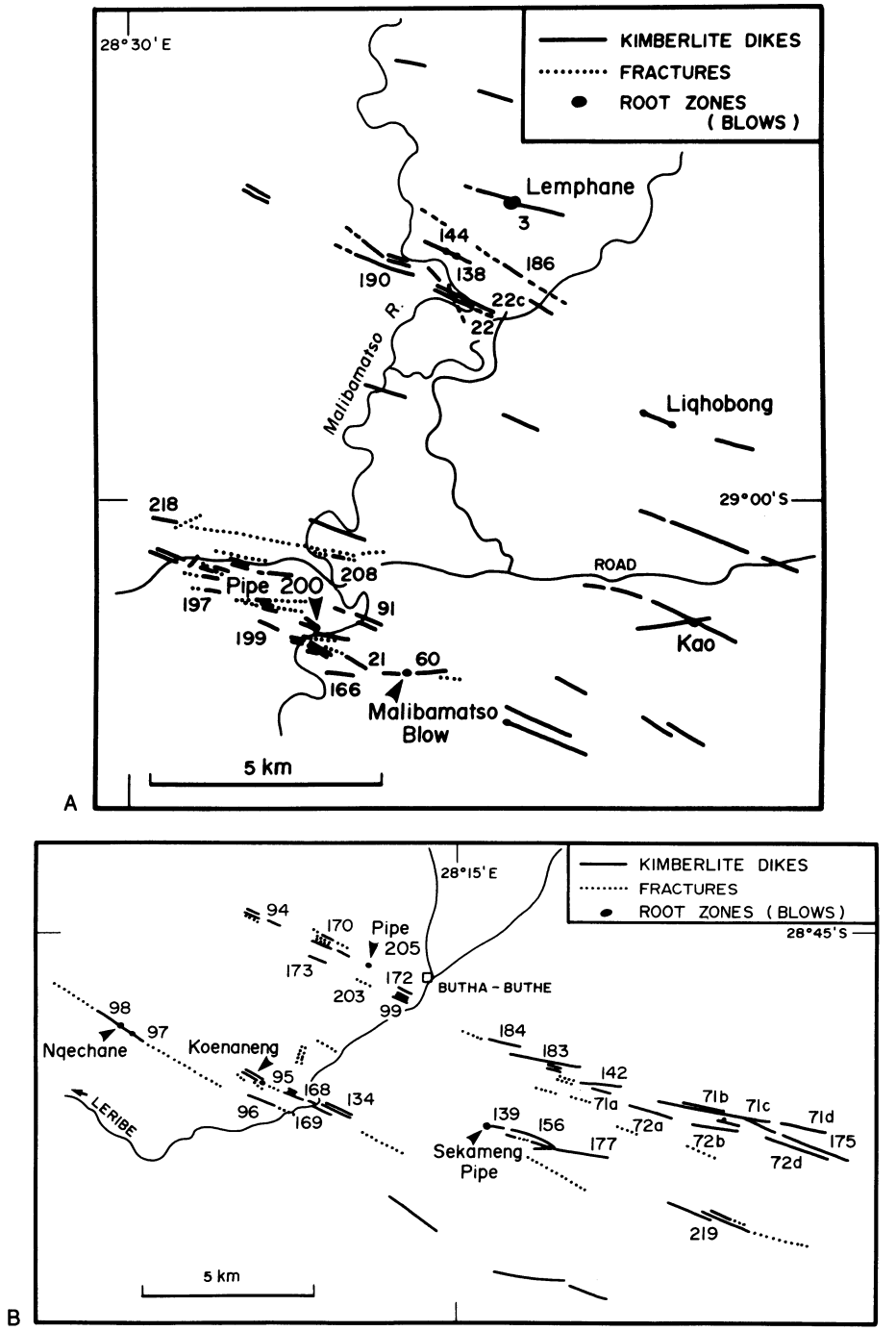

Figure 5.6. Distribution of kimberlite dikes and blows in A., the Malibamatso River region of the Lesotho Highlands, and B., the Butha–Buthe region of the Lesotho Lowlands. Compiled from Kresten (1973a), Dempster and Tucker (1973), Kresten and Dempster (1973) and Nixon and Kresten (1973).

yet been reported from the plateau interior where outcrop is not present. This poor exposure undoubtedly imparts a false bimodal distribution to the kimberlite distribution.

3. Most of the kimberlites in Botswana are buried under tens of meters of unconsolidated sand (Janse 1985) and the actual distribution is correspondingly difficult to determine.

4. In the case of type-3 kimberlite provinces, older fields may be covered by younger platform sediments and the actual extent of the field cannot be determined.

5.1.3. Type-3 Kimberlite Provinces

Provinces exhibiting multiple episodes of magmatism are important with respect to the elucidation of the tectonic controls on the emplacement of kimberlite magmas and the location of their source regions. The most important and extensively investigated provinces to date are the southern African and Yakutian provinces. Information pertaining to provinces related to other cratons is scant and cannot readily be synthesized into a coherent picture of the province. This is a consequence of the limited geological and geochronological investigations of such provinces.

5.1.3.1. Southern African Province

In the southern African province kimberlites occur in rocks of the Transvaal–Rhodesian craton, the accreted Orange River Belt and the overlying Phanerozoic platform sedimentary and volcanic rocks. Details concerning the distribution of individual kimberlites can be found in Wagner (1914), Williams (1932), Bardet (1974), and Dawson (1970, 1980).

At least eight periods of magmatism have been recognized (Figure 5.7). The presence of diamonds in the Witwatersrand conglomerates indicates a further primary source of diamond older than 2.0 Ga. The oldest kimberlites are exposed in the northwestern regions of the province where erosion has stripped away the Phanerozoic platform rocks. Ages in the province range from Precambrian (ca. 1200 Ma) Premier field to the Late Cretaceous (ca. 70 Ma) Gibeon field. The maximum period of activity appears to have been in the Mid- to Late Cretaceous and coincides with a period of pronounced regional uplift (Dawson 1970, 1980). The extent of the buried Precambrian and Paleozoic fields is, however, unknown.

Several fields were formed during each episode of magmatism. The principle examples of such type-2 sub-provinces include the Mid-Cretaceous (ca. 80–90 Ma) Kimberley, Orapa, and North Lesotho fields and the Late Cretaceous (ca. 70 Ma) Gibeon and Central Cape fields.

Younger fields overlap, or occur in close proximity to, older fields; thus the Late Jurassic (ca. 150 Ma) Swartruggens field is found only 200 km from

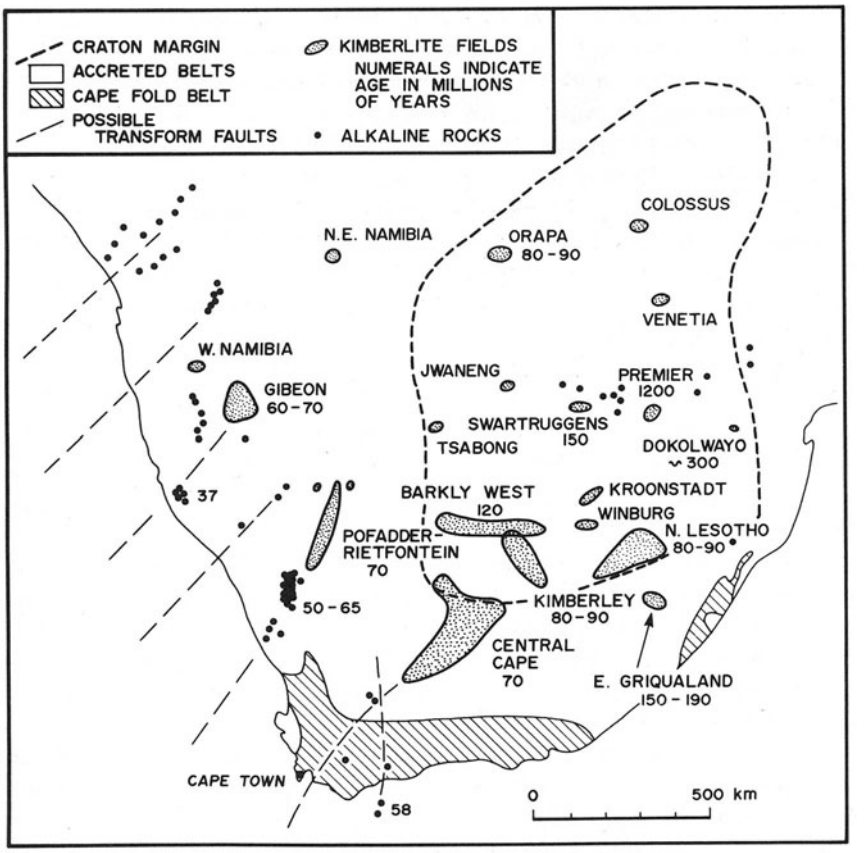

Figure 5.7. Distribution of kimberlite fields in the southern African kimberlite province.

the Precambrian Premier field. The Mid-Cretaceous northwesterly trending Kimberley field overlaps the east–west trending Early Cretaceous (ca. 120 Ma) Barkly West field. This latter field consists of the Postmastburg, Barkly West, and Boshof clusters and may extend eastward to include the Winburg field (cluster) (Figure 5.7). The Barkly West field consists of a swarm of east–west trending subparallel feeder dikes. Pipes and root zones, e.g., Finsch, Roberts Victor, and New Elands, are relatively rare. In constrast the Kimberley field occurring at the same erosional surface consists of diatreme facies kimberlites whose distribution is controlled by northwest–southeast oriented feeder dikes.

In the province as a whole the high-level controls in the emplacement of kimberlites can be related to regional fracture systems. Why the region should have acted as a focus for kimberlite magmatism is less clear and the distribution of fields cannot be related simply to any tectonic features.

Crockett and Mason (1968) termed the 600-km-long and 200-km-wide zone of kimberlites stretching from Postmastburg to Northern Lesotho the "Lesotho Trend." They suggested that the concentration of kimberlites in this region is related to structural controls imposed by northwest–east southeast striking faults in the Precambrian basement rocks. Although the region does exhibit seismic activity (Dawson 1970) there is scant basis for the existence of this trend as Crockett and Mason have ignored all the other kimberlites in the southern African province in drawing their arbitrary structural zone. Bardet (1964) originally believed tht the province occurred at the margins of the Okavango basin (syneclise) but has since rejected this hypothesis with the discovery of the Botswana kimberlite fields (Bardet 1974).

Figure 5.7 indicates that the relatively older and economically important kimberlites occur entirely within regions underlain by the oldest portions of the craton. The youngest, non-economic kimberlites are found only within the accreted belt at the southwestern and southern margins of the province. These kimberlites can be related to linear tectonic features, unlike the older kimberlite fields which have no simple linear alignment.

In the Cape Province of South Africa, and Namibia these kimberlites lie at one extremity of northeasterly-trending zones of alkaline magmatism. These zones can be correlated with the landward extension of transform faults in the eastern Atlantic ocean (Figure 5.7). The oceanic extremity of these zones is characterized by younger (ca. 35–60 Ma) melilititic, nephelinitic, phonolitic, and carbonatitic activity.

Such a simple distribution of magma types is not evident at the northern and eastern borders of the craton. Here no young kimberlites have been located. Alkaline undersaturated rocks of a wide variety of types and ages are present but elucidation of their tectonic setting is complicated by the presence of the southern extremity of the African Rift system. Intrusions in these regions previously reported to be kimberlites are either alnöitic (e.g., the Ruhuru Valley intrusions, Dawson 1970) or lamproitic (e.g., Luangwa graben diatremes).

5.1.3.2. Yakutian Province

The Yakutian Province is located entirely within the Eastern Siberian Platform. This consists of an Archean basement overlain by Paleozoic and Mesozoic sedimentary and volcanic rocks. These latter rocks have been deformed by epeirogenic movements into broad anticlinal and synclinal structures termed anteclises and syneclises by Russian geologists. The crystalline basements emerge through the anteclises as the Anabar and Aldan shields (Figure 5.8).

The geology of the platform and of the kimberlite fields has been described by Bobrievich *et al.* (1959a,b, 1964), Kovalski (1963), Milashev (1965), Krasnov *et al.* (1966), and Frantsesson and Prokopchuk (1968). Summaries in English

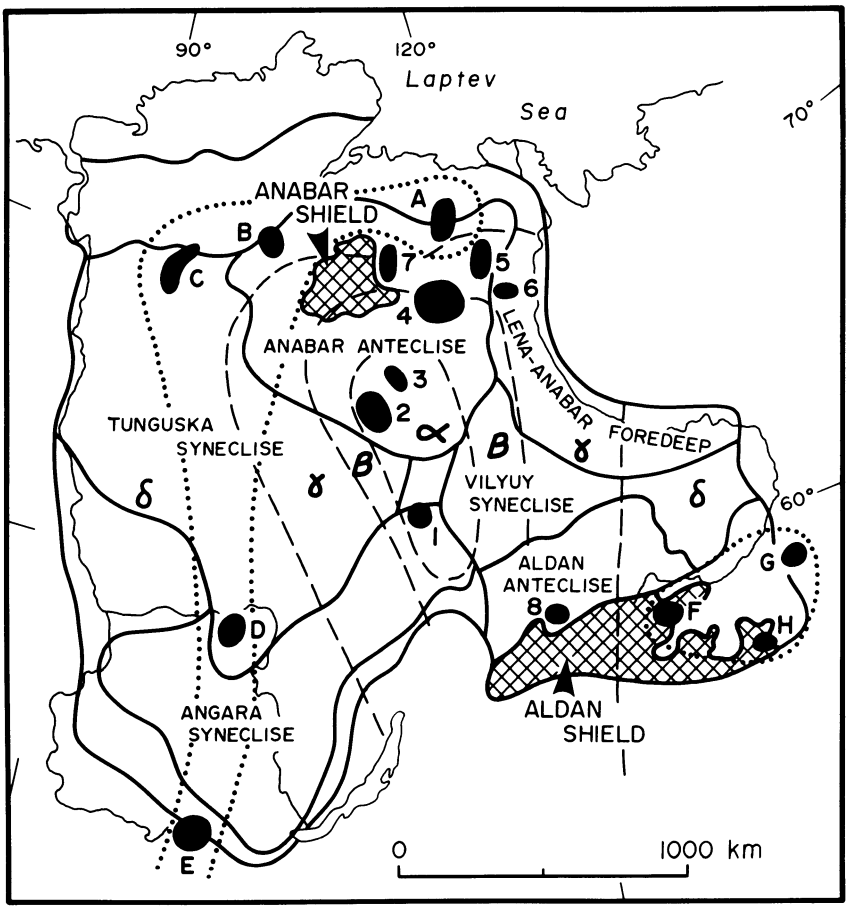

Figure 5.8. Distribution of kimberlite fields and alkaline rocks in the Yakutian province of eastern Siberia. Kimberlite fields: 1, Malo Butuobinsk; 2, Daldyn-Alakit; 3, Muna; 4, Middle Olenek; 5, Lower Olenek; 6, Pri-Lena; 7, Kuonapsk (Upper Anabar); 8, Upper Aldan. (Frantsesson 1970). Alkaline rock-carbonatite provinces; A, Udschinski (Udzha); B, Maimecha-Kotui; C, Kamenski; D, Chadobets; E, Pri-Sayan; F, Tobukski; G, Ingili; H, Arbarastakh. Dashed lines define the mineral subfacies of kimberlites as proposed by Kaminski (1972); α, diamond; β, diamond-pyrope; γ, pyrope; δ, rocks of "kimberlitic" aspect and alkaline complexes. Dotted lines outline the two major provinces of alkaline complexes (this work).

and French are provided by Lebedev (1964), Bardet (1965), Davidson (1967), Frantsesson (1970), and Dawson (1980).

Kimberlites occur in seven major fields which define a north–south trending zone from the Malo-Botuobinsk field in the south, to the Lower Olenek field in the north (Figure 5.8). Within each field the emplacement of individual pipes

and dikes is controlled by local high-level fracture systems. Milashev (1983) thus notes that most of the intrusions in the Daldyn-Alakit field occur at the intersection of fractures. The shapes of the intrusions are also controlled by these fractures. Similar conclusions were presented by Brakhfogel and Kovalskii (1979) for the Middle Olenek field.

Regional structural controls allowing the ascent of kimberlite magma in this province are subject to some debate. All of the fields are located within the Anabar anteclise and Milashev (1974) believes that this type of structure controls their location within the craton. Malkov (1974) and Trofimov (1967) however, believe that kimberlites are emplaced near flexures between upwarped and depressed portions of the platform. These hinge lines are presumed to be the sites of hidden deep-seated fractures which are subject to repeated movement. Kimberlites are then located on, or at, intersections of these major fracture zones (Arsenyev 1962). In these hypotheses kimberlites are emplaced at the margins of syneclises and their occurrence now within anteclises is due to post-intrusion epeirogenic uplift (Malkov 1974).

Recent U–Pb age determinations on kimberlite zircons summarized by Davis *et al.* (1980) and Sobolev (1985), have shown that there were five periods of kimberlite magmatism in this province: I, Late Ordovician; II, Late Silurian; III, Late Devonian; IV, Permo-Triassic; and V, Late Jurassic. Some fields are characterized by several episodes of activity; thus, in the Malo-Botuobinsk field, episodes I, II, and III can be recognized. In the Middle Olenek and Daldyn-Alakit fields, kimberlites belonging to episodes II and III are present.

The distribution of the fields with respect to their age, indicates that the focus of kimberlite magmatism migrated northward during the development of this province. As in the southern African province it appears that the youngest kimberlites are not economic and are emplaced toward the margins of the craton. The distribution of such barren kimberlites cannot be related to the occurrence of an accreted belt in this province. (N.B. It is not stated by Soviet geologists what they consider to be a barren or non-economic kimberlite in terms of its diamond tenor.)

Milashev (1965, 1974) and Kaminskii (1972) believe that the presence or absence of diamond and pyrope in kimberlites can be used to define four subfacies of kimberlites which outline a regional zoning pattern (Figure 5.8). From the periphery of the craton toward its center, rocks "related to kimberlite" are succeeded first by kimberlites of the pyrope subfacies (diamond-free), then by kimberlites of the diamond-pyrope subfacies, and finally by the diamond subfacies. The latter rocks contain the highest content of diamond and include the Malo-Botuobinsk, Daldyn-Alakit, and Muna fields. Subcalcic chrome pyropes appear to be confined to the diamond subfacies, the pyrope subfacies being characterized by xenocrystal chrome pyrope and megacrystal Cr-poor titanian pyrope (Sarsadskikh 1970). Kaminskii (1972) also notes that kimberlitic minerals such as ilmenite become poorer in iron and richer in magnesium toward the

center of the craton. Ilupin *et al.* (1974) have proposed that major compositional differences exist between the subfacies (see Section 7.2.2.2).

Although there is a well-documented change in the character of the kimberlites from the center toward the margins of the craton, the concept of a concentric zonation of subfacies as proposed by Kaminskii (1972) is not supported by the actual distribution of kimberlites. Kaminskii's (1972) subfacies boundaries are highly speculative and not based upon the presence of kimberlites to the east, west, or south of the main linear zone of fields. The outer zone of "kimberlites and related rocks lacking high pressure minerals" are not kimberlites as defined in this work but are alnöites, nephelinites, melilitites, etc., and include the picrite porphyries and meimechites of the Maimecha-Kotui region (Section 2.6.2). These alkaline rocks actually define two distinct provinces of differing age: a Precambrian province which includes the Ingili and Arbarastakh carbonatite–alnöite–ijolite complexes (Frantsesson 1970, Zhabin 1967) and the Paleozoic–Mesozoic province of alkaline ultrabasic rocks and carbonatites including the Maimecha-Kotui, Chadobets, and Pri-Sayan complexes (Frantsesson, 1970) lying in a zone parallel and perpendicular to the kimberlite province (Figure 5.8).

The Yakutian province is similar to the southern African province in that multiple episodes of magmatism result in the juxtaposition of older and younger fields and in the formation of type-2 subprovinces during each magmatic episode. Further similarities are evident in the distribution of diamond-bearing kimberlites, barren kimberlites, and marginal alkaline undersaturated magmatism. The latter appears to be contemporaneous with kimberlite magmatism in the Yakutian province. The provinces differ in that the kimberlite fields of Yakutia can be related to linear features (faults, disjunctive zones) within the craton but not to the continental extensions of transform faults. Isotopic group-II micaceous kimberlites such as comprise the Barkly West field are absent from the Yakutian province.

5.2. KIMBERLITES AND RIFT VALLEYS

It is commonly suggested that kimberlites are associated with continental rifting (Brummer 1978, A. H. G. Mitchell and Garson 1981). This belief arises from the description of alnöitic and other ultrabasic rocks occurring in carbonatite complexes as kimberlites, e.g., the central complex kimberlites of Dawson (1966) or Von Eckermann (1967), and the supposed association of kimberlites with rift structures, e.g., the Tanzanian and Somerset Island provinces. As some carbonatites appear to be spatially and temporally associated with rifts it follows (*reductio ad absurdum*) that all kimberlites must be related to such active, incipient, or paleo rifts (Brummer 1978).

The initial premise has been shown by Mitchell (1970, 1979a) and in Section

2.6 to be incorrect, thus eliminating one of the arguments for the hypothesis. The second premise can be challenged by consideration of the actual distribution of kimberlites with respect to rift systems.

There is no evidence to support the contention that bona fide kimberlites occur in association with such major continental rifts as the Rio Grande, Gardar, East African, Rhine-Oslo, or Baikal rift systems (Sorenson 1974). These structures are devoid of kimberlites. Significantly, King (1970) and Bailey (1974) in their descriptions of volcanism associated with the Eastern African Rift make no mention of kimberlites. Dawson (1970), Verwoerd (1966, 1970), and Bailey (1974) all remark that kimberlites occur in non-rifted or inter-rift regions. Figure 5.9 shows clearly that the kimberlites of the Southern African province are not associated with the East African Rift Zone. Although many carbonatites and alkaline volcanics are associated with this rift, Verwoerd (1966) and Le Bas (1977) note that many others show no such relationship. According to Bailey (1964, 1974), rifts merely represent the broken crests of crustal arches. Alkaline magmatism and rifts are thus both the expression of a more fundamental process, e.g., crustal uplift due to mantle metasomatism. Rifts are thus not a pre-requisite for the emplacement of carbonatite and alkaline volcanics (or kimberlites). Any deep lineament or fracture zone is capable of channeling mantle-derived magma into the crust (see Section 5.3). McConnell (1972) has shown that rifts form at zones of weakness in the accreted belts and rarely traverse the old cores of cratons. Consequently, rift zones encircle these older resistant blocks (Figure 5.9). Interestingly, if the East African Rift Zone eventually extends westward and southward by the development of fractures in the accreted Orange River Belt, then these fractures will superimpose themselves upon pre-existing kimberlite fields.

The Tanzania province has been suggested by A. H. G. Mitchell and Garson (1981) as an example of the association of kimberlites with rifting. In this province the Singida, Iramba, Nzega, Shinyanga, and Kimali fields define a broad NNW–SSE trending zone which Dawson (1970) interprets to be the expression of a deep-seated fracture zone. Kimberlites are emplaced where this zone cross-cuts metasedimentary roof pendants in the basment gneisses or northeasterly trending fractures. The majority of the kimberlites are located far from the rift faults which surround the Tanzanian shield, and Dawson (1970) and Verwoerd (1966) envisage no association with these structures. In the eastern regions of the shield a series of subparallel normal splay faults, representing an extension of the Gregory Rift Valley, penetrate the margins of the shield. These faults do not transect the Singida or Kimali kimberlite fields. The faults represent an unsuccessful attempt by Tertiary rifting to penetrate the Tanzanian shield (McConnell 1972). They have no control on the emplacement of the kimberlites even though their orientation may have been influenced by the pre-existing fractures in the shield. Kimberlite in the Nzega field has a U–Pb age of 53 Ma (Davis 1977); therefore, as most of the motion of the rift fractures probably post-dates the time

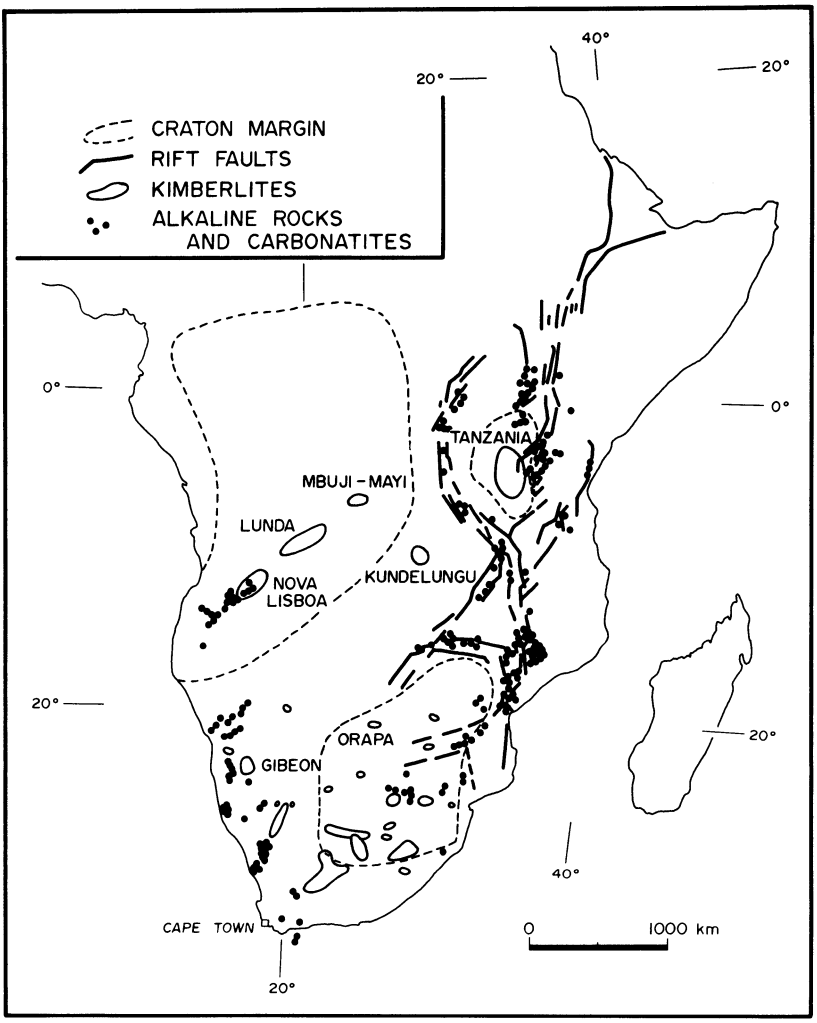

Figure 5.9. Distribution of kimberlite fields and alkaline rocks in southern Africa with respect to the African Rift system. Compiled from Dawson (1970), McConnell (1972), A. H. G. Mitchell and Garson (1981), and Janse (1985).

of kimberlite emplacement and most of the kimberlites are in no manner related to these faults, it is concluded that the Tanzanian province has no association with rifting. Further development of the rift might result in encroachment into the Singida field.

Brummer (1978) has suggested that kimberlites of the Somerset Island province are associated with Tertiary Eurekan rifting and cites the parallelism of trends, defined by some of the intrusion centers with the rift faults surrounding

Somerset Island, in support of this hypothesis. However, the locations of these rift faults are determined by pre-existing features. The north–south trending Boothia-Cornwallis Arch has been an active tectonic feature in this region from the Precambrian to the present day and has controlled the attitudes of all faults and folds in the overlying platform sediments (Kerr 1980). High-level controls on the emplacement of the kimberlites are related to structures produced during the Paleozoic Cornwallis folding of the Ordorvician and Silurian country rocks. These may or may not act as a focus for later Tertiary rifts but are all related to basement structural features with respect to their orientation. The north–south Boothia-Cornwallis arch is the location of a major fault zone and this deep seated lineament undoubtedly controlled the ascent of the kimberlite magma from the mantle. The age of the kimberlites is unknown, but is estimated on geological evidence to be Mesozoic. The rift structures are thus believed to have been superimposed upon a pre-existing kimberlite province. Magmatism associated with the rifting is nephelinitic in character and not kimberlitic (Mitchell and Platt 1984).

In summary, there is little evidence to support the contention that kimberlites are related to rift structures. In all cases where this association has been proposed it can be demonstrated that the rocks in question are not kimberlites, e.g., the Ile Bizard alnöite of the St. Lawrence Rift (Brummer 1978, Mitchell, 1979a, 1983) or that rifts have been superimposed upon pre-existing provinces. This latter situation is rare and most kimberlites show no spatial or temporal relationship to rift valleys.

5.3. TECTONIC CONTROLS ON THE DISTRIBUTION OF KIMBERLITES

5.3.1. Introduction

The factors which control the location of kimberlite provinces in cratonized regions have not yet been determined. Several contradictory hypotheses have been presented and are summarized below. Typically each hypothesis has been developed to explain the distribution of kimberlites within a given province and is not necessarily applicable to other provinces. A feature common to the hypotheses is that kimberlites are believed to define linear or arcuate trends related to the presence of major fracture zones. The proposals differ with respect to the mechanisms suggested for the activation of partial melting in the mantle and ascent of the magma along these fracture zones.

5.3.2. Epeirogenic Faulting

The essence of this hypothesis is the belief that the lithosphere is traversed by a limited number of deep fault zones that extend into the upper mantle. The

configuration of this crustal architecture may be revealed in deeply eroded terrains by the occurrence of significant linear features (lineaments) defined by major fault, shear, fracture, or disjunctive zones. Groups of igneous rocks distributed in linear belts may also record the trace of such faults. The locations of the zones are believed to be established during the growth and consolidation of the cratons (Bardet 1964, Kirillov 1961). Faulting associated with epeirogenic uplift is focused at zones of weakness within the generally rigid craton. Once established, such regions become perennial zones of faulting and provide persistent channelways that control the access of mantle-derived magmas into the crust. The existence of these fault zones may explain the occurrence of repeated cycles of magmatic activity within restricted regions of the craton.

Bardet (1956, 1964, 1965) Arsenyev (1962), and Kirillov (1961) were the principal initial advocates of the hypothesis that the location of kimberlite fields within the craton is controlled by such deep-seated fractures. The idea has been reiterated in various forms in many subsequent publications, for example, Dawson (1970), Nixon (1973b), Mitchell (1976), Zartmann (1977), and Haggerty (1982).

Figure 5.10 illustrates the distribution of kimberlite fields within the Yakutian province according to the Bardet (1965), Arsenyev (1962) model. In this example the locations of kimberlites are used to determine the trends of the deep faults beneath the platform sedimentary cover. Bardet (1956, 1964) has provided similar interpretations of African kimberlite provinces. Caution must be em-

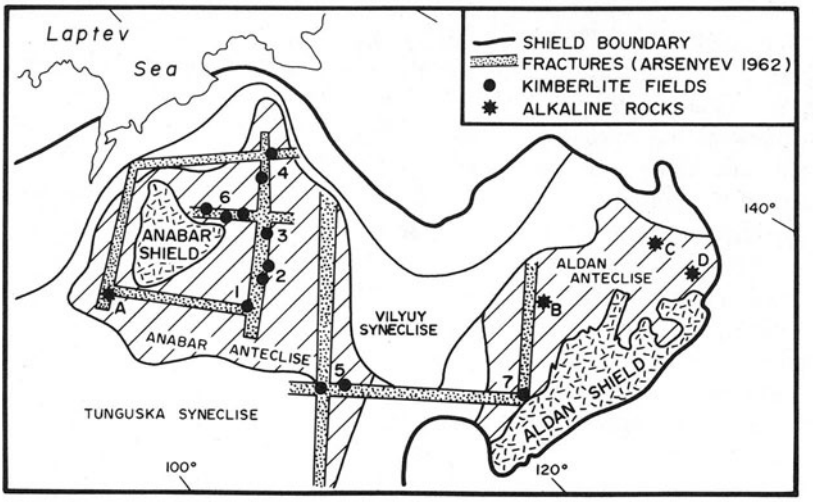

Figure 5.10. Relationship of Yakutian kimberlite fields and alkaline complexes to deep-seated fractures as proposed by Arsenyev (1962) and Bardet (1965). Kimberlites: 1, Daldyn-Alakit; 2, Muna; 3, Middle Olenek; 4, Lower Olenek, 5, Malo-Butuobinsk; 6, Luchakan (Upper Anabar); 7, Aldan. Alkaline complexes; A, Maimecha-Kotui, B, Tobukski; C, Ingili; D, Arbarastakh.

ployed in the interpretation of such diagrams as the disposition of kimberlite intrusions may not reflect the underlying structural controls of emplacement in some regions. It can be expected that the locations of deep fault zones might be best determined in provinces which have been eroded to root zone–feeder-dike levels and/or are emplaced in Precambrian basement terrains.

As many kimberlites do appear to be related to linear features (Bardet 1964, Dawson 1970), it follows that if deep fractures can be identified then they can be used to predict the locations of undiscovered kimberlites. This particular form of linearomancy has been employed by Haggerty (1982) in an analysis of the regional crustal structure of the Liberian kimberlite province. Lineaments identified from satellite-based imagery of the region were found to coincide with trends defined by known kimberlites. The lineaments are therefore considered as possible sites for further discoveries of kimberlite.

Lineament analysis is less useful in regions where the cratons are covered by platform sedimentary and volcanic rocks. Fracture analysis may lead to the prediction of the high-level structural controls of kimberlite emplacement but not the deeper fundamental structures responsible for the location of the field. Chains of intrusions may delineate the traces of the major fracture zones but indirect geological and/or geophysical methods of locating these faults may have to be employed.

Kimberlite fields in the Yakutian province are considered to be located at or close by flexure points in the structure of the sedimentary cover of the platform. The flexures separate large positive epeirogenic uplifts (anteclises) from large, negative downwarps (syneclises). The flexure point is believed to mark the location of deep faults in the basement. During epeirogenic movements the platform rocks are uplifted or downwarped about this hinge point (Bardet 1964, 1973). Kimberlites are injected into the platform rocks at this flexure point. There is some disagreement as to whether kimberlites are preferentially associated with the syneclisal or anteclisal side of the flexure. Bardet (1964, 1965), Arsenyev (1962) and Malkov (1976) favour intrusion at the margins of the syneclises followed by epeirogenic uplift. Milashev (1974) believes that positive (uplift) structures control the emplacement at all times and therefore favors association with anteclises. Regardless of which interpretation is correct it is considered that the Yakutian kimberlite fields are not found at the centers of the anteclises or syneclises, although kimberlites in the latter situation may be hidden by younger deposits.

Bardet (1964, 1974) has applied these concepts to the distribution of African kimberlites and suggested that kimberlite fields occur at the margins of large basins; thus the southern African, Kundelungu, Bakwanga, and Lucapa fields are inferred to lie in concentric arcs at the margin of the Okavango-Kalahari basin. The western African province is similarly located with respect to the Taoudeni basin. Major fault zones are predicted to exist at the margins of these basins.

Bardet's proposals do not agree with modern interpretations of the crustal structure of southern Africa (Pretorius 1973), the emplacement of kimberlites during times of uplift in a tensional stress regime (Dawson 1970), the occurrence of kimberlite at the basin center, or the long history of kimberlite emplacement in this region. These observations demonstrate that it is inappropriate to apply hypotheses developed for any given province to another region.

Despite the problems associated with locating kimberlite fields in cratons covered with platform rocks, it is apparent that many kimberlite fields can be considered to be related to large-scale linear features. Epeirogenic fault control provides an explanation for this distribution. Why some faults have apparently more kimberlites associated with them than others is not explained.

The deep fracture zones provide channels for the ascent of mantle-derived magmas. The tectonic events which trigger partial melting can be described as passive or active (Sengor and Burke 1978). Passive mechanisms attribute faulting and rifting to tensional failure as a consequence of plate motions. Active mechanisms consider that failure is due to the impingement of a mantle plume on the base of the continental lithosphere. There is no agreement regarding which process has occurred in any given region. Staritski (1963) considers that magmatism in the East Siberian Platform is not related to tectonism in the surrounding mobile belts, i.e., failure is not due to passive effects. Turcotte (1983) believes that the crustal swells and rifts of eastern Africa are due to active rifting. In contrast Bailey (1983) believes that the same features are due to passive plate motion mechanisms causing metasomatism and magmatism which result in uplift (see Section 9.7.2).

5.3.3. Transform Fault Extensions

This hypothesis proposes that kimberlites and alkaline rocks located at continental margins define distinct linear features that can be correlated with the landward extension of oceanic transform faults. It is believed that the locations of transform faults are controlled by the presence of pre-existing continental fractures (Wilson 1965, Sykes 1978). During the opening of the oceans these planes of weakness are continually reactivated and it is this passive mechanism which is responsible for the initiation of magmatism along the continental fault zone. The hypothesis was developed by Marsh (1973) to explain the distribution of alkaline rocks and kimberlites in Angola and Namibia, and has subsequently been extended to kimberlite fields in western Africa (Williams and Williams 1977, Haggerty 1982), eastern North America (Parrish and Lavin 1982, Taylor 1984), and southern Australia (Stracke *et al.* 1979). Proponents of the hypothesis are concerned mainly with the tectonic events that trigger magmatism and not with the origins of the pre-existing continental fractures. These latter zones of weakness appear to correspond to Bardet–Arsenyev epeirogenic fault zones.

5.3.3.1. Angola–Namibia

Kimberlites in Angola (Figure 5.9) and Namibia (Figure 5.7) are situated at the northeastern extremity of southwest–northeast trending linear zones of alkaline rocks. Many of the intrusions have been emplaced at the intersection of these zones with a set of northwest–southeast striking fractures (Marsh 1973, Reis 1971).

In Angola, alkaline rocks and kimberlites define a belt 55–85 km in width that stretches over 800 km from the coast to the Lunda region (Figure 5.9). The kimberlites of the Mbuji-Mayi field (Zaire) lie directly on the extension of this line. This major, approx. 1600-km lineament has the same orientation as other major fractures in the African continent (Furon 1963) and appears to represent a fundamental and persistent line of weakness. The Lunda region has been termed the Lucapa graben (Reis 1971). It is not clear whether this region is a true rift zone or simply a series of sub-parallel normal faults, although the latter seems the more likely. Kimberlite magmatism in this area is contiguous with carbonatite and alkaline magmatism to the southwest. The Nova Lisboa region appears to be a transitional area where carbonatites and kimberlites occur together (Reis 1971, 1972). Unfortunately, information regarding the petrography of the latter kimberlites is not available and it cannot be determined whether the rocks referred to are indeed *bona fide* kimberlites.

In Namibia, linear features defined by alkaline rocks and kimberlites differ from the Angolan lineament in that the linear zone of intrusions is in general less well-defined, and appears to terminate at the contact of the accreted belt with the older craton. Age determinations have demonstrated that olivine melilitites, nephelinites and phonolites occurring at the oceanic extremities of these zones are younger than the kimberlites (Figure 5.7).

The Angolan–Namibian lineaments and their South American counterparts can be correlated with the transform faults formed during the opening of the South Atlantic (Marsh 1973, A. H. G. Mitchell and Garson 1981). Importantly, the alkaline magmatism was not associated with the initial stages of ocean rifting and continental breakup. This rules out the proposal by Neill (1973) that seeks to link the intrusions with the failed arms of triple junctions. Only at a relatively advanced stage of ocean basin development does it appear that motions in the transform fault zone have reactivated Precambrian fractures.

5.3.3.2. West Africa

The kimberlites occurring at the southern margin of the West African craton provide an interesting example of how different tectonic interpretations of the same province can be devised. Bardet (1956, 1964) considered that the kimberlites and an earlier swarm of basaltic dikes were arranged along a system of northwest–southeast trending faults at the southern margin of the Taoudeni syneclise (Figure 5.11A). In contrast Williams and Williams (1977) drew attention

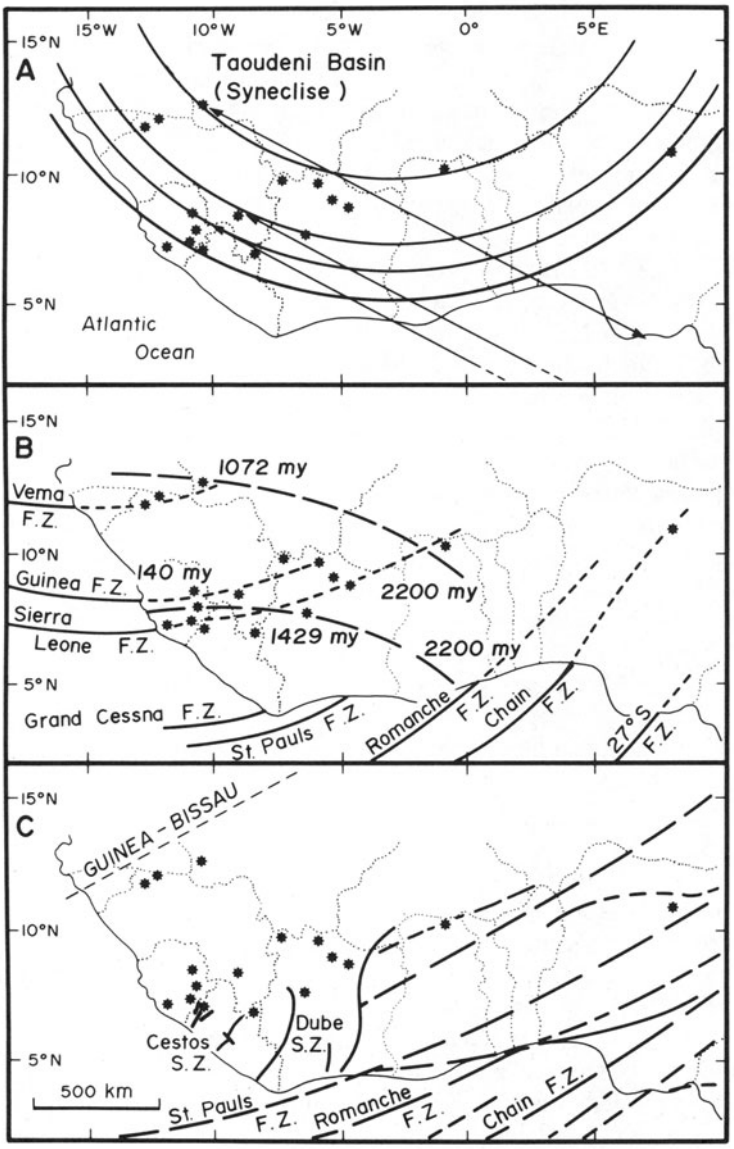

Figure 5.11. Relationship of West African kimberlites to tectonic features as proposed by A., Bardet (1956, 1964), B., Williams and Williams (1977) and Hastings and Sharp (1979), C., Haggerty (1982).

to the coincidence of oceanic transform fault zones and their continental extensions as defined by the same kimberlites (Figure 5.11B). Hastings and Sharp (1979) rejected both these hypotheses and suggested that kimberlites lie on two arcuate trends and decrease in age from east to west (Figure 5.11B). This hypothesis (which relates kimberlites to a mantle plume) has received little support as it is not based upon any reliable age determinations and includes alluvial diamond deposits in the arcuate trends.

The most recent interpretation by Haggerty (1982) relates kimberlite emplacement to "post-plate motion crustal flexuring" that has reactivated Precambrian basement sutures. Haggerty's (1982) hypothesis is based upon lineament analysis of the West Liberian kimberlite field. Here the kimberlites occur in linear zones that are parallel to prominent megashear directions in the basement gneisses (Figure 5.11C). The kimberlites are believed to be emplaced in faults formed by brittle fracture when the shear zone was reactivated. The shear zones are considered to be a part of the Pelusium megashear zone. Haggerty (1982) notes that only a few of the kimberlite dike orientations can be correlated with transform fault extensions, but does not explain how these faults are related to the megashear zones or how plate motion reactivates these old zones of weakness. The hypothesis does not explain adequately the different controls on kimberlite emplacement in the adjacent eastern Sierra Leone field in which dikes are oriented east–west, in contrast to the north to northeast trends in Liberia. Further studies are required if the controls on emplacement are to be determined unambiguously. Unfortunately, this task is hampered by the very poor exposure.

The West African province is similar to the Angolan–Namibian fields in that kimberlites are emplaced subsequent to the opening of the ocean. The province differs in that linear zones of contrasting types of alkaline magmatism are not present.

5.3.3.3. Eastern North America

The emplacement of kimberlites in eastern North America is believed to be related to stresses generated during the opening of the Atlantic, although they show no direct relationship to the continental extension of transform faults in the North Atlantic. Meyer (1976), Zartman (1977), Parrish and Levin (1982), and Taylor (1984) provide summaries of the distribution of alkaline rocks and kimberlites in the region. Two distinct zones of alkaline rock can be recognized. One defines the 38th parallel lineament (Zartman 1977) and consists of alnöites, mica peridotites (*sensu lato*), and lamproites but not kimberlites. This lineament can be considered to be a Bardet–Arsenyev type of epeirogenic fault zone. The second zone consists of kimberlites and alkaline rocks that extend from eastern Kentucky to the Ithaca–Syracuse region of New York (Figure 5.12). The lineament defined by these intrusions is parallel to the Appalachian fold belt and the

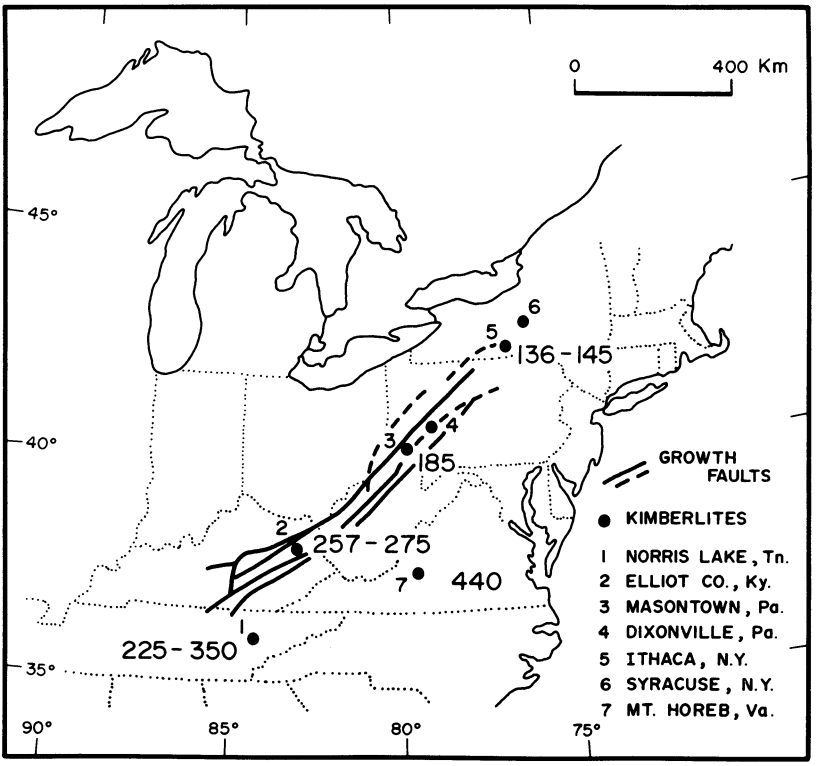

Figure 5.12. Distribution of kimberlites in eastern North American after Parrish and Lavin (1982) and Taylor (1984). Radiometric ages (mostly K–Ar) given in millions of years.

axis of Triassic basins. The kimberlites decrease in age from Carboniferous–Permian in the southwest to Late Jurassic–Cretaceous in the northeast (Taylor 1984).

Parrish and Levin (1982), Dennison (1983), Foland and Faul (1977), McHone (1981), Basu and Rubury (1980), and Taylor (1984) all have suggested that the kimberlite magmatism was a consequence of development or reactivation of fractures by plate motions. The decrease in age from southwest to northeast, being correlated with the opening of the Atlantic in this direction. Parrish and Levin (1982) claim that kimberlites are emplaced where fractures in the platform sediments formed in response to the Appalachian orogeny are cross-cut by basement fractures. The latter correspond to fractures which appear to be the continental extensions of transform faults in other areas. Taylor (1984) believes that the faults which lie parallel to the Appalachian fold belt are rift faults formed in response to plate rebound.

5.3.3.4. Comments

The major drawback to the transform fault extension hypothesis is that it is not applicable to most kimberlite fields and is clearly inappropriate for those situated far from continental margins. The idea seems most appropriate for the Angolan–Namibian fields, but is far less convincing when extended to the West African and eastern North American fields, where no direct connection between transform fault extensions and kimberlite locations is evident. Wilson's (1965) original concept of tranform fault extension did not allow for any motion in the continental fracture zone once ocean basin development has commenced. Reactivation of faults to initiate continental magmatism (Marsh 1973, Sykes 1978) implies fault motion. The proposed extensions of transform faults do not record any strike-slip movements. If motion has occurred it must have been vertical and not continuous as only at relatively advanced stages of ocean basin development does it appear that pre-existing fractures are reactivated. Proponents of the hypothesis provide no satisfactory explanation as to why magmatism is not continuous, why it occurs only subsequent to oceanic rifting and why it has a different character along different lineaments.

As carbonatite, melilitite, and kimberlite magmatism is not contemporaneous in Angola and Namibia, it seems highly probable that their apparent relationships are merely geographic and not genetic. The restriction of kimberlites to the continental extremity of the lineaments and their presence in regions where no transform fault extension can be envisaged, indicates that plate motion may not be responsible for initiating magmatism. It is not unrealistic to expect that the same zone of weakness may be activated simultaneously or sequentially by unrelated passive or active mechanisms. Magmas generated in response to either process will utilize the same ascent channel. It may not be possible to determine which process produces a particular magma type and emplacement may be correlated with the incorrect tectonic event. Further possibilities are that there is no motion on the transform fault or that if movement does occur it does not initiate magmatism. It is suggested here that transform fault formation and kimberlite emplacement are unrelated and merely reflect different processes operating at the same pre-existing zone of weakness.

5.3.4. Hot Spot Magmatism

Hot spots or mantle plumes are believed to be caused by convective upwelling of material from the deeper parts of the mantle. Partial melting may occur as pressure is reduced on the rising material and results in volcanism. Continental lithosphere above a hot spot may be thinned, uplifted, and ultimately rifted (Bott 1982, Morgan 1972). The concept arose from Wilson's (1963) suggestion that linear chains of oceanic islands were tracks reflecting the movement of oceanic lithosphere over a stationary hot spot in the mantle. The hypothesis

proved useful in describing oceanic intra-plate volcanism. Subsequent zealous promotion of the idea, primarily by geophysicists, has resulted in a veritable rash of hot spots, as attempts were made to explain all continental intra-plate volcanism by the same process (Thiessen *et al.* 1979, Morgan 1983).

Crough *et al.* (1980) and Crough (1981) applied the hypothesis to kimberlite distribution and showed, on the basis of reconstructions of plate motion, that many post-Jurassic kimberlites formed within five degrees of a mantle hot spot. The kimberlites in North America, South America, and Africa were thus believed to be related to the Great Meteor, Trindade, and Tristan hot spots, respectively.

In a modification of the hot spot hypothesis, England and Houseman (1984) have suggested, on the basis of a convection model of the upper mantle, that kimberlites result from the incidence of thermal plumes on the base of a slowly moving lithospheric plate. This conclusion is in direct contrast to Hargraves and Onstott's (1980) suggestion, based on paleomagnetic data, that kimberlite emplacement coincides with rapid plate motion.

Objections to the hot spot hypothesis can be raised specifically in relationship to kimberlites and more generally with regard to the whole spectrum of continental alkaline intra-plate magmatism. With reference to kimberlites the model does not explain the following.

1. The distribution of kimberlites which cannot be related to hot spot tracks. Crough *et al.* (1980) conveniently excluded from consideration in their study, kimberlites in eastern Kentucky, Pennsylvania, and Tennessee. These lie between supposed hot spot tracks. Although most kimberlite fields can be related to linear features, these are not hot spot paths. To account for such kimberlites a separate hot spot must be proposed for each line of intrusions. This approach taken to the extreme, as in application to all of the African fields, leads to a tangled web of tracks, that may conflict with proposed plate motions. This type of analysis is ultimately as unrewarding as the construction of Ptolemaic epicycles.

2. The hypothesis cannot explain satisfactorily the repeated occurrence of kimberlite intrusion over a long period in a relatively restricted area. In the case of the southern African province, it strains credibility that several different kimberlite-producing hot spots should pass under the same region over the last 1200 Ma and with the result that kimberlites are emplaced only in that region.

3. In the southern African and Yakutian provinces, kimberlites have been emplaced at the same time over a wide region and not sequentially along linear trends.

4. Proponents of the hypothesis provide no explanation of why every hot spot does not generate kimberlite. There is no attempt to place kimberlites in an overall framework of alkaline magmatism.

With respect to alkaline magmatism in general, the hot spot hypothesis has been challenged principally by Bailey (1974, 1977, 1983) and Turcotte and Oxburgh (1978). Bailey considers that the concept cannot account for repeated cycles of alkaline magmatism in particular regions of the crust and therefore

believes that the sources of the magmas are within the lithosphere plate. The implication of this hypothesis is that mantle plumes do not exist. Turcotte and Oxburgh (1978) have noted that magmatism in western North America and Africa shows no consistent relationship to plate motion and that many volcanic rocks do not lie in supposed hot spot tracks. Turcotte and Oxburgh (1978) have also challenged the now conventional viewpoint that chains of oceanic volcanic islands define hot spot paths. They note that the same distribution of volcanoes can be produced by propagating tensional fractures. Further, it may be incorrect to draw analogies between oceanic plumes generating large quantities of magma and supposed continental plumes producing small quantities of alkaline rocks.

5.3.5. Subduction-Related Magmatism

Sharp (1974) proposed that kimberlites are produced by the partial melting of subducted oceanic crust at depths as great as 700 km. It was suggested that this process should result in the formation of belts of kimberlite parallel to fold mountains, with diamond-bearing types occurring at the greatest distances inland from the plate margins. Sharp (1974) cited the distribution of kimberlites in the southern African and eastern North American provinces in relationship to the Cape Fold Belt and the Appalachians, respectively, as evidence in favor of his concept.

The hypothesis has been strongly criticized by Newton and Gurney (1975) on a variety of tectonic and petrological grounds. Foremost among their criticisms are that Sharp (1974) has failed to consider all of the known southern African kimberlites in his model and has incorrectly interpreted the Cape Fold Belt as a subduction-related feature. Newton and Gurney (1975) consider that there is no parallelism between kimberlite locations, which are apparently random (Dawson 1980) and the strike of the Cape Fold Belt. Sharp (1974) proposes that the subducted oceanic crust initially undergoes partial melting to form andesites, leaving an eclogitic or peridotitic residue. The latter is presumed to melt further at greater depths and form kimberlites. Newton and Gurney (1975) have argued that such a depleted source is geochemically inappropriate for deriving the high contents of incompatible elements that occur in kimberlites.

Helmstaedt and Schulze (1979) and Helmstaedt *et al.* (1979) believe that eclogites occurring in the Colorado Plateau minettes and the Zagadochnaya (Yakutia) kimberlite are remnants of subducted oceanic crust. On this evidence Helmstaedt and Schulze (1979) and Helmstaedt and Gurney (1984) have suggested that shallow subduction zones existed under the southwest United States and sourthern Africa, respectively. Helmstaedt and Gurney (1984) thus propose that all of the kimberlites in Africa occur in a broad (3000-km) belt parallel to the reconstructed Gondwanide fold belt. Dehydration and decarbonation reactions of subducted oceanic crust are believed to cause metasomatism and partial melting

(Wyllie 19880) in the overlying upper mantle. The subduction zone is believed to be shallow (150–300-km depth) and essentially horizontal under much of southern and western Africa.

The hypothesis has many tectonic, petrologic, and geochronologic deficiencies. The major drawback is that there is no evidence for any shallow subduction zone under the African cratons. In particular it seems highly improbable that horizontal subduction of a slab of oceanic crust from the Southern Cape to Northern Tanzania could occur. The hypothesis fails to explain the distribution of barren and diamondiferous kimberlites and their relationship to other forms of alkaline magmatism. No explanation is presented as to why kimberlites are not found above active zones of shallow subduction in South America.

In summary, hypotheses which attempt to link kimberlites to subduction are interesting and provocative but are untenable being largely speculative and unsupported by petrological, tectonic, and geochemical evidence.

5.3.6. Concentric and Radial Anteclises and Syneclises (CRAS Model)

Pretorius (1973) has presented a model of the southern African craton which resembles models of the Siberian craton in that a central hub of shield rocks is surrounded by a concentric succession of anteclises and syneclises. Basing his model upon the regional gravity field, Pretorius (1973) considers that the southern African craton has an elliptical shape (3000 × 2000 km) and is centered upon the Rhodesian shield. A Precambrian basement is believed to exist over the whole craton, the limits of which are not seen in southwest or southeast Africa. The fundamental structural framework of the craton consists of first-order anteclises and syneclises surrounding the Rhodesian shield. In order, from the shield toward the craton margins, there are: the Zimliss syneclise, the Bookub anteclise, the Duske syneclise, and the Swisa anteclise. Within these structures are second-order concentric and radial upwarps and downwarps and third-order anticlines and synclines. Older basement, lower grades of metamorphism, and a more negative gravity field characterize the anteclises, while the syneclises show enhanced regional metamorphism, younger basement terraines, and a more positive gravity field. Cratons as defined by Clifford (1966) are located over anteclises, mobile or accreted belts, over syneclises. Pretorius (1973) considers that the craton has existed since the early Proterozoic and that the mobile belts and shields together constitute this craton.

Pretorius (1973) has shown that the CRAS model can be used to predict the distribution of gold and coal deposits. It might be expected that the model could also have significance with regard to the distribution of kimberlites. In particular the domes formed at the intersection of radial and concentric upwarps might be favorable sites for kimberlite emplacement.

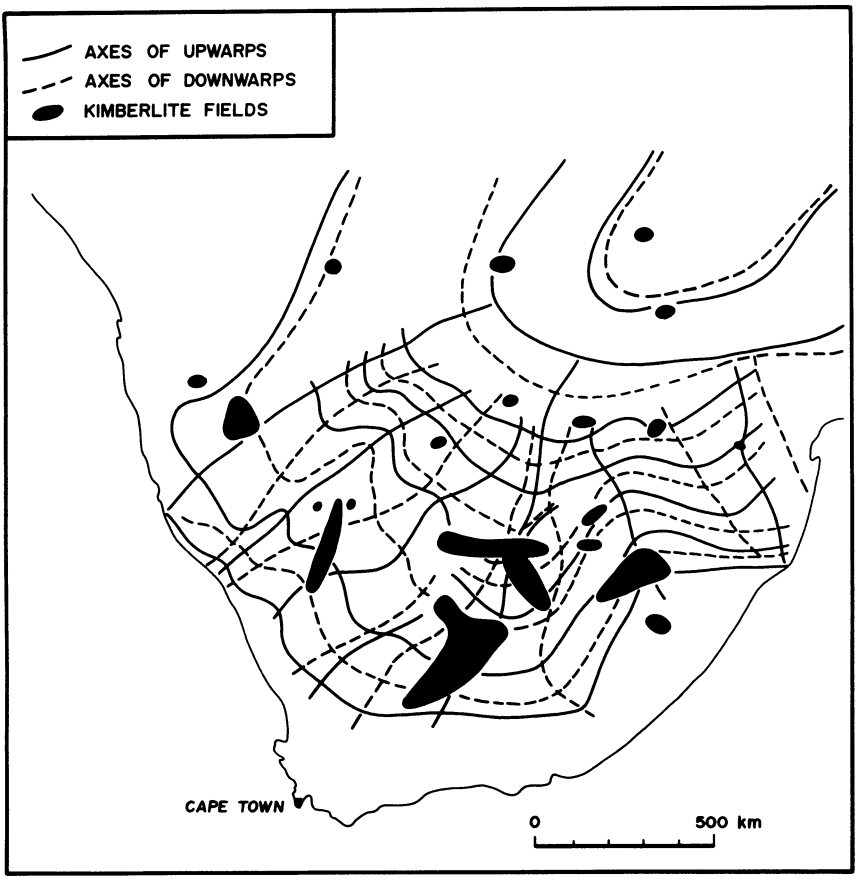

Figure 5.13. Relationship of kimberlite field to the CRAS model of the structure of southern Africa (Pretorius 1973).

Figure 5.13 shows the distribution of kimberlite fields with respect to the CRAS model. No simple relationships are evident, kimberlites being found on the shield and within three of the first-order tectonic domains. Many, but not all, diamond-bearing kimberlites are found within the Bookub anteclise. Barren kimberlites lie primarily within the Duske syneclise. There are no clear relationships of the fields to the intersection of radial and concentric upwarps. Some fields, e.g., N. Lesotho and Swartruggens, do appear to coincide with such "domes" but others, e.g., Kimberley, show no such relationship. Radial structures in southwestern Africa are parallel to the lineaments believed to mark the continental extensions of transform faults and may mark the sites of fundamental fracture zones. The drawback of the CRAS model as currently presented is that modifications resulting from faulting are not portrayed. Subsequent studies should

include the distribution of fractures and kimberlites relative to the interference patterns formed by intersection of the upwarps and downwarps. Pretorius' (1973) model would make no distinction between craton and off-craton kimberlites.

5.4. CONCLUSIONS

Kimberlites occur in clusters, fields, and provinces. Particular regions of the lithosphere appear to have acted as focii for repeated cycles of kimberlitic magmatism. The structural controls on the high level emplacement of kimberlites are different from those which control ascent of the magma from the upper mantle. The former reflect the local and regional fracture pattern, the latter reflect deep-seated controls which have not been identified unambiguously. The reactivation of major zones of weakness in the lithosphere appears to play a role in the emplacement of kimberlite; thus intrusions commonly are associated with major lineaments and fault zones. The initiation of magmatism may be associated with the rise of sub-lithospheric mantle plumes or with intra-lithospheric metasomatic processes, but no simple relationships to tectonic events occurring at plate margins are evident; thus kimberlite magmatism is not associated with transform fault extensions, subduction zones, or hot spots. Kimberlites are not found in or close to major continental rift valleys.

Without the hard little bits of marble which are called "facts" or "data" one cannot compose a mosiac; what matters, however, are not so much the individual bits, but the successive patterns into which you arrange them, then break them up and rearrange them.
Arthur Koestler

6

MINERALOGY OF KIMBERLITES

6.1. INTRODUCTION

The mineralogy of kimberlites is a result of crystallization of the parent magma over pressure and temperature conditions ranging from those of the upper mantle to those of the upper crust, and is complicated by the presence of the enigmatic megacryst suite and numerous mantle-derived xenocrysts. The approach adopted in this work is to describe the minerals approximately in their paragenetic sequence of formation as determined by petrographic studies (Chapter 3). In some cases, e.g., mica, olivine, and garnet, it is impossible to draw a firm distinction between a megacrystal or phenocrystal status; consequently it has been found convenient to describe megacrysts and phases of undoubted primary origin together. This approach facilitates comparisons and avoids repetition. Minerals of minor importance or of uncertain paragenesis are described in the latter sections of the chapter.

Diamond is *not* described in this chapter as recent investigations have concluded that it is a *xenocryst* (Meyer 1985, Richardson *et al.* 1984, Robinson 1978). Information regarding the mineralogy and chemistry of diamond can be found in the reviews by Meyer (1985), Dawson (1980), Orlov (1977), and Robinson (1978). Diamond is of importance in that its presence serves to place constraints upon conditions prevailing in the source region of kimberlite. The relationships between diamond and kimberlite are discussed in Section 9.13.

6.2. GARNET

Garnet is one of the characteristic minor minerals in kimberlite. Within any given kimberlite the amounts, sizes, and colors of the garnets vary widely. Many

sources apparently contribute to the overall assemblage of garnets and much effort has been expended in an attempt to assign the garnets to particular xenocrystal or phenocrystal sources.

The recognition of distinctively colored lilac or purple-red pyropes forms the basis of many exploration programs for kimberlite as these Cr-rich garnets unambiguously indicate the presence of upper mantle-derived material. Garnets are particularly suitable as a kimberlite tracer mineral because of their resistance to weathering and the ease with which they can be concentrated from rock, colluvium, or alluvium by heavy liquid or hydraulic separation techniques.

Sampling of garnets can be undertaken either by obtaining a heavy mineral concentrate from the crushed kimberlite or by selecting garnet megacrysts (>1 cm) by hand picking from colluvium or mine concentrates. The former method can be applied to all kimberlites and provides a random sample of the garnet population in a kimberlite. The latter technique is restricted in general to weathered or exploited kimberlites and is biased toward garnets of a particular composition.

6.2.1. Size and Color

Garnets range in size from small (0.1–1 mm) irregularly shaped fragments to isolated rounded crystals 1 mm to 15 cm in diameter. Many of the smaller garnets exhibit conchoidal fracture surfaces and are clearly derived by the fragmentation of larger crystals, whereas many of the larger megacrysts are commonly rounded, "grapefruit-like" bodies, or are disk shaped. Polycrystalline aggregates and euhedral crystals are notably absent. Lasko (1975) has shown by X-ray studies that even the largest megacrysts are single crystals. Commonly the garnets are surrounded by a corona of fine grained secondary minerals termed kelyphite (see Section 6.2.6).

Garnet colors may be lilac, red-purple, red-brown, orange, pink, yellow, or green. In many kimberlites there exists a correlation between size and color of the garnets. Red-purple garnets commonly fall below the 1-cm-diameter range, while the red-brown garnets typically comprise the megacryst population (Dawson and Stevens, 1975).

Many studies (e.g., Dawson and Stevens 1975, Yevdokimov and Bagdasarov 1982) have documented the influence of composition upon garnet color. Commonly red-purple garnets are Cr-pyropes, red-brown garnets are Ti–low Cr-pyropes, orange garnets are pyrope-almandines, and green garnets are knorringite-uvarovite-pyropes. These latter garnets rarely exhibit the alexandrite effect. Subjective attempts to correlate the color within composition have been made by Shee (1978) and Hearn and McGee (1982) and have demonstrated that no clear-cut divisions exist between color groups and that chemical gradations exist within and between groups.

Matsyuk *et al.* (1980a,b) have proposed that quantitative relationships exist between the color (CIE chromacity diagrams) and the composition of garnets derived from eclogites and lherzolites. They further suggest that the color of garnets is dependent upon the depth of formation of their source rocks. In a similar study Manson and Stockton (1981), however, find no correlation between the color and composition of pyrope-almandine garnets.

6.2.2. Statistical Classifications

The goal of statistical classifications of the compositions of kimberlite-derived garnets is to assign garnets to distinct paragenetic sources. The procedure enables the exploration geologist to identify upper mantle-derived pyropes. For the petrologist the object is to distinguish between xenocrystal and phenocrystal garnets.

Existing statistical classifications involve initially defining the compositional ranges of garnet from known parageneses. These data are then compared by multivariate statistical techniques, such as multiple discriminant analysis or cluster analysis (Le Maitre 1982), to establish standard groups of garnets. Garnets of unknown paragenesis can then be compared with these groups and the probability of membership of the sample in any of the defined groups assessed.

Dawson and Stevens (1975) have presented a statistical classification of garnets which has gained wide acceptance due to its ease of application and apparent ability to classify satisfactorily a wide range of mantle-derived garnets. Using the variation of the MgO, FeO, CaO, TiO_2, and Cr_2O_3 contents of 352 garnets, Dawson and Stevens (1975) formulated by cluster analysis (Wishart 1969) the 12 cluster groups given in Table 6.1 Groups 1 and 2 are mainly derived from red-brown megacrysts, groups 3, 4, 5, 6, and 8 from eclogites, and groups 7, 9, 10, and 12 from lherzolites and inclusions in diamonds. The limitations of the scheme include the small data base, the over-representation of some localities, and the incorporation of garnets of unknown paragenesis, e.g., isolated garnets in kimberlite, into paragenetically defined groups. The occurrence of garnets from different parageneses in one group is a further weakness. Thus group 1 for example contains garnets derived from megacrysts and porphyroclastic lherzolites.

Despite these problems, the application of the discriminant function and/or classification flow sheet to the classification of garnets provides a useful quantitative measure of the proportions of garnets of different origins present in a kimberlite.

Table 6.2 presents the Dawson and Stevens (1975) classification of garnets derived from four kimberlites and clearly demonstrates that individual kimberlites are characterized by different garnet assemblages; thus the Inugpasugsuk and Elwin Bay kimberlites contain megacryst (groups 1 and 2) and lherzolitic garnets

Table 6.1. Means of Distinguishing Oxides of Garnets in the Cluster Groups Recognized by Dawson and Stephens (1975)

Group name	TiO_2	Cr_2O_3	FeO	MgO	CaO
1. Titanian pyrope	0.58	1.34	9.32	20.00	4.82
2. High-titanium pyrope	1.09	0.91	9.84	20.30	4.52
3. Calcic pyrope-almandine	0.31	0.30	16.49	13.35	6.51
4. Titanian, calcic, magnesian almandine	0.90	0.08	17.88	9.87	9.41
5. Magnesian almandine	0.05	0.03	28.33	7.83	2.44
6. Pyrope-grossular almandine	0.24	0.27	10.77	10.38	14.87
7. Ferro-magnesian uvarovite-grossular	0.29	11.52	5.25	8.61	21.60
8. Ferro-magnesian grossular	0.25	0.04	6.91	4.69	24.77
9. Chrome-pyrope	0.17	3.47	8.01	20.01	5.17
10. Low-calcium chrome-pyrope	0.04	7.73	6.11	23.16	2.13
11. Uvarovite-pyrope	0.51	9.55	7.54	15.89	10.27
12. Knorringitic uvarovite-pyrope	0.18	15.94	7.47	15.40	9.51

(groups 9 and 11). The New Elands kimberlite, in contrast, apparently contains only xenocrystal garnets derived by the fragmentation of eclogite (group 3) and lherzolite (group 9), together with a high proportion of low-Ca, Cr-rich garnets (group 10) similar to the garnets found as inclusions in diamond. The Orapa suite (Shee 1978) contains a mixture of megacrysts, eclogite, and lherzolite-derived garnets but lacks group-10 garnets. Scott Smith *et al.* (1984) and Mitchell

Table 6.2. Classification of Garnets in Kimberlites from Canada and Southern Africa by the Dawson and Stevens (1975) Method

Garnet group	Inugpasugsuk[a] (201)[c] %	Elwin Bay[a] (265) %	New Elands[a] (64) %	Orapa[b] (163) %
1	12.44 (25)	13.58 (36)	—	7.36 (12)
2	0.49 (1)	32.08 (85)	—	15.34 (25)
3	—	—	29.69 (19)	15.34 (25)
4	—	—	—	0.61 (1)
5	0.49 (1)	—	—	—
6	—	—	—	3.68 (6)
7	—	—	—	—
8	—	—	—	—
9	77.6% (156)	54.34 (144)	29.69 (19)	57.67 (94)
10	—	—	40.63 (26)	—
11	8.96 (18)	—	—	—
12	—	—	—	—

[a] Data for Inugpasugsuk, Elwin Bay (Canada), and New Elands (S. Africa) from this work.
[b] Data from Orapa (Botswana) from Shee (1978).
[c] Number of samples in parentheses.

(1979b) have also shown by these methods that individual kimberlites within a kimberlite province each contain distinctively different assemblages of garnet.

Danchin and Wyatt (1979) have extended Dawson and Stevens' (1975) work by the cluster analysis (Parks 1970) of 1777 garnets. The analysis generated 52 clusters which could be considerably reduced in number by a suitable choice of similarity levels. The 52 clusters in fact can be grouped into 11 associations which are broadly similar to the Dawson and Stevens' (1975) groups. Although supported by a larger data base, Danchin and Wyatt's (1979) classification has not yet found general acceptance due to the lack of a published classification algorithm.

6.2.3. Compositional Variation

Garnets in kimberlites are members of solid solutions between pyrope ($Mg_3Al_2Si_3O_{12}$), almandine ($Fe_3Al_2Si_3O_{12}$), grossular ($Ca_3Al_2Si_3O_{12}$), uvarovite ($Ca_3Cr_2Si_3O_{12}$), and knorringite ($Mg_3Cr_2Si_3O_{12}$). Titanium contents are typically low (O%–2%) and schlorlomitic, andraditic, and kimzeyitic garnets are typically absent. The compositional variation can be adequately represented by ternary cation plots (Mg–Fe–Cr or Mg–Ca–Cr), binary plots [TiO_2–Cr_2O_3, Mg/(Mg + Fe)–Cr_2O_3] or by representation in *n*-dimensional space by principal component analysis or factor analysis (Jago 1982, Yevdokimov and Bagdasarov 1982).

Systematic studies of the compositional variation of garnets within and between provinces, or in relation to crystal size, have not yet been undertaken. Some common trends have emerged from the studies so far undertaken but no consensus has yet been reached regarding the interpretation of these trends.

Figure 6.1 illustrates data for *megacryst* garnets from the Monastery and Lekkerfontein kimberlites (Gurney *et al.* 1979, Robey and Gurney 1979). These garnets define trends of varying Mg/(Mg + Fe) ratio at essentially constant calcium contents. Garnets richest in iron in some cases co-exist with ilmenite and are considered by Gurney *et al.* (1979) to be poorer in titanium than the ilmenite-free samples (Figure 6.2). All of the garnets are typically poor in Cr_2O_3 (O%–2.1%). This compositional trend is termed the *Cr-poor megacryst trend* and is found in most of the kimberlites so far examined. Garnets belonging to this trend are mainly titanian and high-titanium pyropes. Representative compositions are given in Table 6.3.

Figure 6.3 illustrates data for *megacryst* garnets from the Sloan-Nix and Fayette County kimberlites (Eggler *et al.* 1979, Hunter and Taylor 1984). In these occurrences two compositional trends are evident. One is a Cr-poor trend analogous to the Monastery-Lekkerfontein trend. The other is defined by garnets of variable Ca/(Ca + Mg) ratio at essentially constant iron content. The garnets are Cr_2O_3 rich (6%–13%; Eggler *et al.* 1979), increasing Ca being correlated

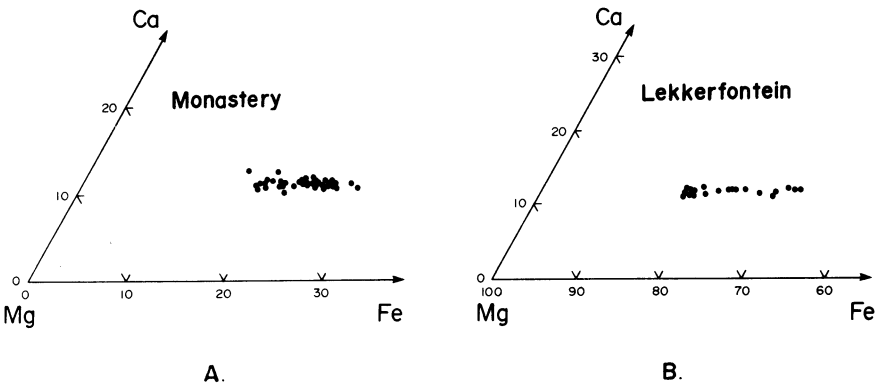

Figure 6.1. Composition of Cr-poor garnet megacrysts from the Monastery (Gurney *et al.* 1979) and Lekkerfontein (Robey and Gurney 1979) kimberlites.

with increasing Cr indicating solid solution toward uvarovite. The garnets fall into Dawson and Stephens' (1975) group 9 (chrome pyrope). The trend is termed the *Cr-rich megacryst trend*. Representative compositions are given in Table 6.3

Eggler *et al.* (1979) have noted that these Cr-rich garnets are similar in composition to garnets occurring in lherzolite xenoliths found within the same kimberlite. Figure 6.4 shows clearly the compositional overlap in terms of their TiO_2 and Cr_2O_3 contents. Despite this similarity, Eggler *et al.* (1979) and Hunter and Taylor (1984) do not consider the Cr-rich megacryst suite to be derived

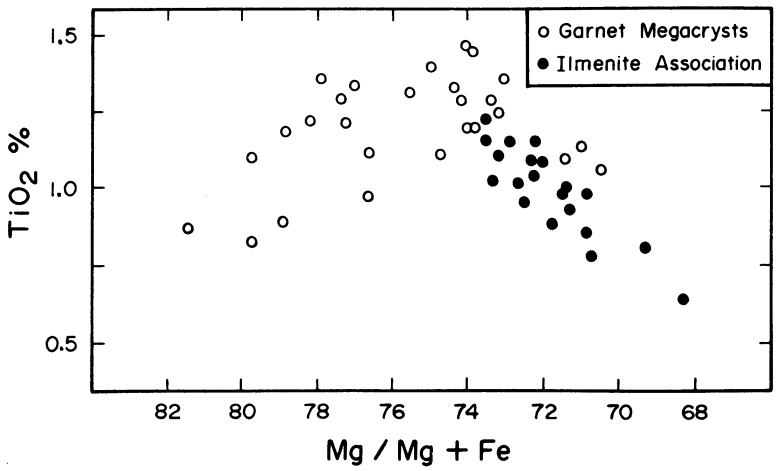

Figure 6.2. Variation of TiO_2 content with Mg/Mg + Fe ratio for Cr-poor garnet megacrysts from the Monastery Mine (Gurney *et al.* 1979). Megacrysts richest in iron coexist with ilmenite.

Table 6.3. Representative Analyses of Megacryst Garnets[a]

	Cr-rich megacrysts			Cr-poor megacrysts												
	1	2	3	4	5	6	7	8	9	10	11	12	13	14	15	16
SiO_2	40.7	39.5	41.4	42.9	41.6	41.7	41.66	41.13	41.47	41.93	42.04	42.25	41.75	41.28	41.6	41.9
TiO_2	0.70	0.74	0.68	0.56	0.98	0.63	0.88	0.64	1.00	0.16	0.92	0.77	0.32	1.04	0.55	1.25
Al_2O_3	14.9	12.6	17.5	20.3	21.2	21.9	20.66	21.99	21.81	22.00	21.84	21.16	18.77	19.39	23.2	21.2
Cr_2O_3	10.2	12.7	6.13	2.61	0.65	0.07	2.09	0.00	0.74	1.69	0.43	1.03	2.40	0.10	0.39	1.83
FeO[b]	6.7	6.7	7.85	7.5	10.6	13.0	8.11	14.19	9.75	9.26	9.24	9.04	7.23	11.83	11.8	9.42
MnO	0.39	0.38	0.43	0.28	0.33	0.44	0.31	0.32	0.31	0.51	0.24	0.26	0.28	0.45	0.28	0.27
MgO	19.0	17.6	20.2	21.3	19.8	18.2	20.02	17.22	19.56	19.79	20.51	21.10	22.55	20.03	18.3	20.1
CaO	7.6	8.9	6.64	5.2	5.0	4.4	5.06	4.34	4.98	4.42	4.37	4.28	5.55	4.79	4.62	4.58
Na_2O	0.01	0.03	—	0.03	0.06	0.06	—	—	—	—	—	—	0.13	0.09	0.15	0.09
	100.20	99.15	100.63	100.68	100.22	100.39	98.79	99.83	99.73	99.85	99.59	99.94	98.99	100.00	100.90	100.70

[a] 1, 2, Colorado-Wyoming (Eggler *et al.* 1979); 3, Fayette County (Hunter and Taylor 1984); 4–6, Colorado–Wyoming (Eggler *et al.* 1979); 7, 8, Monastery Mine (Gurney *et al.* 1979); 9, 10, Tunraq (this work); 11, 12: Thaba Putsoa (Nixon and Boyd 1973b); 13, 14, Kuonam (Yevdokimov and Bagdasarov 1982); 15, 16, Orapa (Shee 1978).

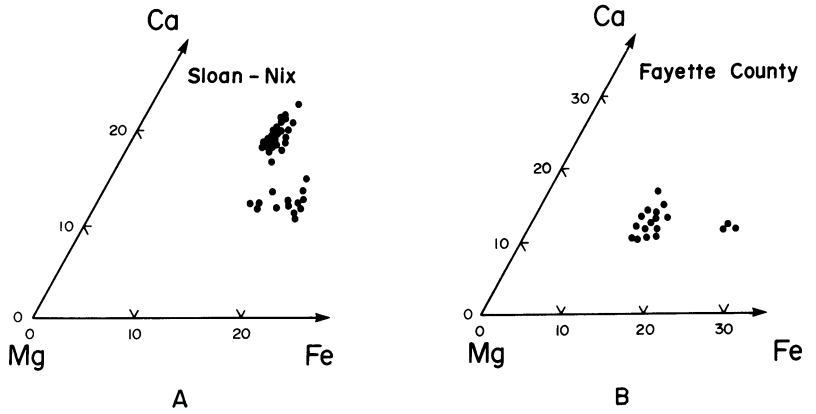

Figure 6.3. Composition of garnet megacrysts from the Sloan-Nix (Eggler *et al.* 1979) and Fayette County (Hunter and Taylor 1984) kimberlites.

from lherzolite xenoliths as the garnets in these rocks are very small (<1 cm) compared to the size (>1 cm) of the megacrysts.

Commonly it is not possible to collect a large number of garnets belonging to the megacryst suite from a particular kimberlite and consequently garnets from heavy mineral concentrates must be examined. Garnets separated from the Tunraq kimberlite (Mitchell 1979b) illustrate some of the problems in the interpretation

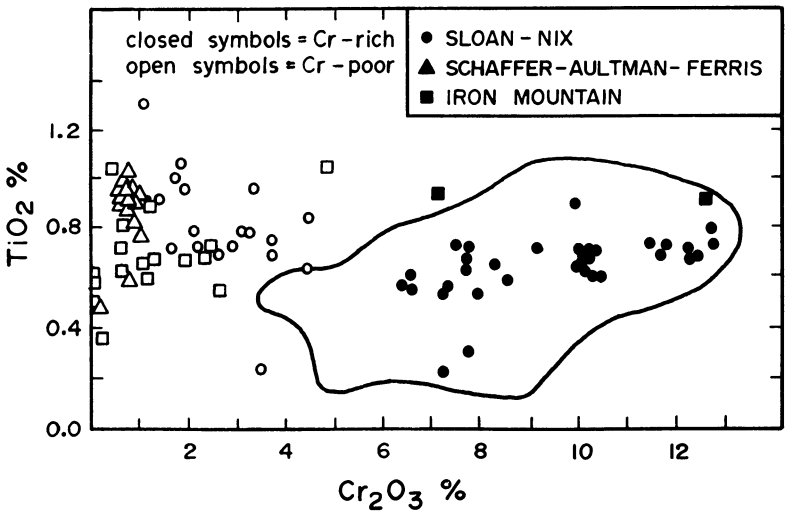

Figure 6.4. TiO_2 versus Cr_2O_3 content for Cr-rich and Cr-poor garnet megacrysts from Colorado–Wyoming kimberlites (Eggler *et al.* 1979). The solid line delineates compositions of garnets in lherzolite xenoliths from this area.

of data obtained from this type of sampling. Tunraq garnets fall into three of Dawson and Stephens' (1975) classification groups: group 1 (34%), group 2 (3%), and group 9 (63%). Groups 1 and 2 are actually best regarded as a continuum of compositions rather than as two discrete groups (Mitchell 1979b). Group 9 is bimodal and incorporates a relatively iron-rich low-Cr_2O_3 (<2.5%) group and a relatively iron-poor high-Cr_2O_3 (> 2.5%) group of variable Ca content.

Figure 6.5 shows that group-1, -2, and low-Cr group-9 garnets are very similar to Monastery and other megacryst garnets. These garnets undoubtedly belong to the Cr-poor megacryst suite. Figure 6.5 also shows that the high-Cr group-9 garnets are similar to garnets occurring in lherzolite xenoliths found within other Somerset Island kimberlites. They are also similar to the garnets of the Cr-rich megacryst trend. The garnets therefore cannot be unambiguously assigned to any one paragenetic source. Mitchell (1979b) suggests that the garnets most probably are lherzolite-derived xenocrysts. Scott Smith *et al.* (1984) have presented a similar study of the garnets in the Orroroo kimberlites, South Australia.

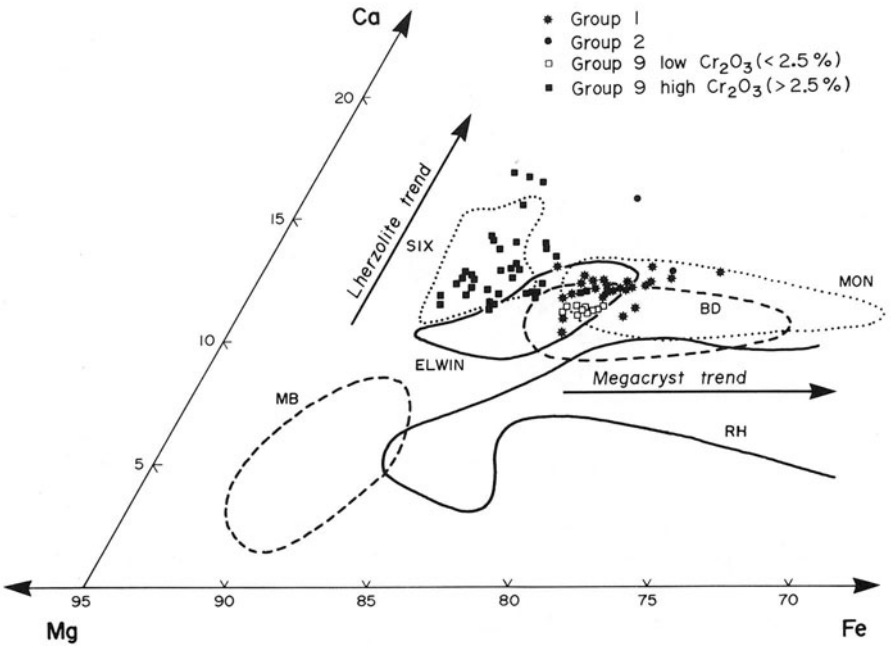

Figure 6.5. Composition of garnets in the Tunraq kimberlite and in garnet lherzolite xenoliths from Somerset Island (SIX), after Mitchell (1979b). Garnets are grouped according to the Dawson and Stevens' (1975) method. ELWIN, Elwin Bay megacrysts (Mitchell 1978a), BD, Frank Smith and Monastery megacrysts (Boyd and Dawson 1972), RH, kimberley megacrysts (Reid and Hanor 1970), MB, garnet inclusions in diamonds (Meyer and Boyd 1972). MON, Monastery megacrysts (Gurney *et al.* 1979).

The statistical classifications and compositional variations noted above demonstrate that each kimberlite contains a characteristic suite of garnets. Many of the Cr-poor garnets can be assigned to an eclogitic or lower crustal source and are therefore xenocrysts. Chrome-rich pyrope garnets belong to Dawson and Stephens' (1975) lherzolitic (group 9) or diamond-inclusion garnet (group 10) parageneses. The group-9 garnets are commonly regarded as lherzolite- or harzburgite-derived xenocrysts (Sobolev 1977, Mitchell 1979b, Boyd and Gurney 1982, Gurney 1985). However, Frantsesson (1970), Lazko (1971), Eggler *et al.* (1979), and Hunter and Taylor (1984) regard group-9 garnets of large size as megacrysts or phenocrysts. The Cr-rich sub-calcic group-10 garnets which show a positive correlation with the presence of diamond in southern African kimberlites (Gurney 1985), are considered to be xenocrysts derived from the fragmentation of garnet dunites or garnet harzburgites (Pokhilenko *et al.* 1977, 1979). Consideration of the composition of lherzolitic and harzburgitic garnets is beyond the scope of this work and the reader is referred to the detailed discussion by Sobolev (1977). Garnets belonging to the Cr-poor megacryst suite are considered to be either phenocrysts (this work) or xenocrysts (Boyd and Nixon 1975, Nixon and Boyd 1973b). The problem of their origin is discussed in Sections 6.2.4 and 9.11.

6.2.4. Cr-Poor Megacryst Suite Pyrope

The studies listed in Table 6.4 have established that the low-Cr megacryst garnets are titanium-bearing pyropes (0%–1.5% TiO_2) of variable Cr_2O_3, (0%–3%) content and Mg/(Mg + Fe) ratio (0.86–0.68). Increasing Fe contents are correlated with decreasing Cr_2O_3, and megacrysts richest in iron commonly contain inclusions of ilmenite. Representative compositions are given in Table 6.3.

The major element variations established for several representative suites of megacrysts are compared in Figure 6.6, from which it can be determined that, on a worldwide basis, the megacrysts have very similar compositions. They differ only in the range of the Mg/(Mg + Fe) ratios. Unfortunately insufficient data have been published to allow a detailed statistical comparison of their compositions. Data for Soviet occurrences are limited and systematic studies of megacryst garnets by modern analytical techniques have not been undertaken. Most data are qualitative and based upon identification of broad groups of compositions from refractive index and unit cell information. Megacryst garnets are present in most Yakutian kimberlites (Kharkiv and Abaginskaya 1975). Compositional data given by Yevdokimov and Bagdasarov (1982), Ponomarenko *et al.* (1972), and Smirnov (1959) indicate that the garnets are similar to South African and North American megacrysts.

Mitchell (1979b) has noted that, despite the overall similarity, subtle differences exist between the megacryst compositions from different kimberlites; thus garnets from the Tunraq kimberlite are slightly richer in Fe [Mg/

Table 6.4. Sources of Garnet Megacryst Data

Canada		
	Elwin Bay, Somerset Island	Mitchell (1978a)
	Tunraq, Somerset Island	Mitchell (1979b)
	Ham, Somerset Island	Jago (1982)
U.S.A.		
	Sloan-Nix, Colorado	Eggler *et al.* (1979)
	Schaffer-Aultman-Ferris, Colorado	Eggler *et al.* (1979)
	Iron Mountain, Wyoming	Eggler *et al.* (1979)
	Williams, Montana	Hearn and McGee (1982)
	Elliot Co., Kentucky	Garrison and Taylor (1980)
	Fayette Co., Pennsylvania	Hunter and Taylor (1984)
	Ithaca, New York	Kay *et al.* (1983)
	Stockdale, Kansas	Rost *et al.* (1975)
	Lake Ellen, Michigan	McGee and Hearn (1984)
Southern Africa		
	Kimberley, R.S.A.	Reid and Hanor (1970)
	Monastery, R.S.A.	Gurney *et al.* (1979)
	Lekkerfontein, R.S.A.	Robey and Gurney (1979)
	Frank Smith, R.S.A.	Boyd and Dawson (1972)
	E. Griqualand, R.S.A.	Nixon and Boyd (1979a)
	Northern Lesotho	Nixon and Boyd (1973b)
	Artur de Paiva-Camutue, Angola	Boyd and Danchin (1980)
	Orapa, Botswana	Shee (1978)
		Shee and Gurney (1979)
Others		
	Orroroo, South Australia	Scott Smith *et al.* (1984)
	Koidu, Sierra Leone	Tompkins and Haggery (1984)

(Mg + Fe) = 0.82–0.76] and poorer in TiO_2 than garnets from the Elwin Bay kimberlite [Mg/(Mg + Fe) = 0.83–0.79].

These differences can be put on a quantitative basis by procedures such as multiple discriminant analysis (Le Maitre 1982). Table 6.5 compares groups of garnets from seven Somerset Island kimberlites by means of a canonical discriminant function (Klecka 1975) established from their TiO_2, Al_2O_3, Cr_2O_3, FeO, MgO, and CaO contents. The procedure essentially assesses the amount of overlap between the groups in six-dimensional space. The probability of membership of any garnet within one of the 7 defined groups can be calculated from the discriminant function and is expressed as a "predicted group membership." Table 6.5 indicates, for example, that out of 61 garnets from the Nord kimberlite, 33 garnets (54%) can be established as being characteristic of this kimberlite. However six garnets (9.8%) and 22 garnets (36.1%) have compositions similar to garnets from the Elwin Bay and Tunraq kimberlites, respectively. This "misclassification" of Nord garnets reflects the compositional overlaps between the three groups. The group centroid calculated from the discriminant

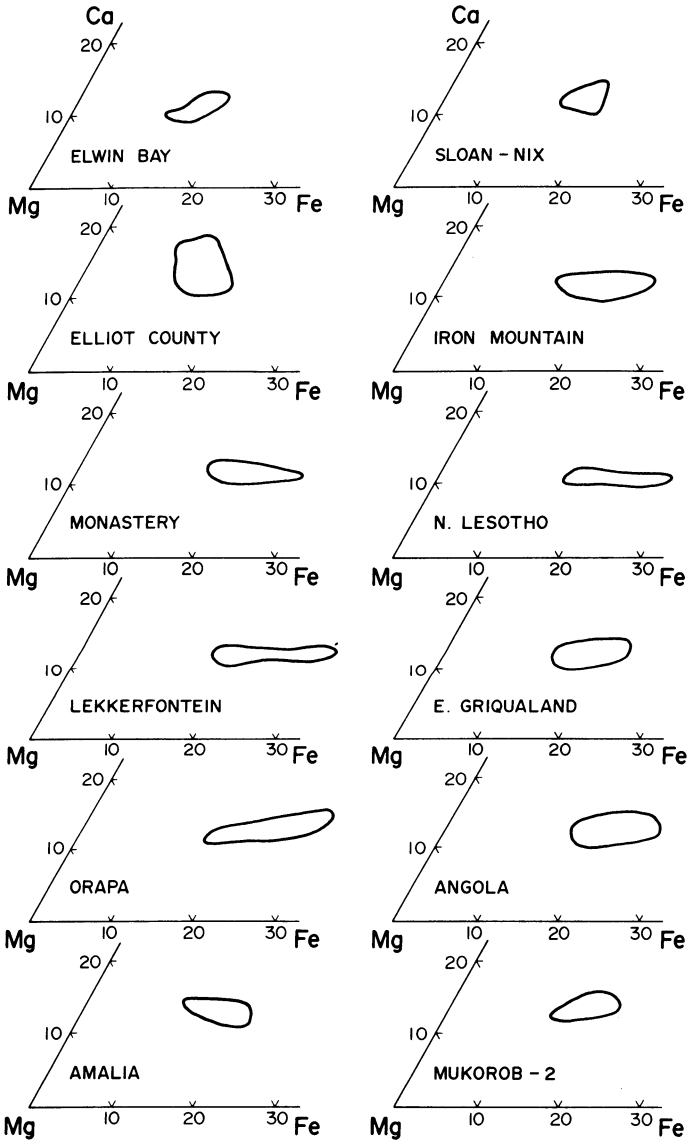

Figure 6.6. Compositional fields of Cr-poor megacryst garnets from diverse kimberlites. Data sources given in Table 6.4. (Mukorob-2 and Amalia, this work).

Table 6.5. Classification of Garnet Megacrysts from Somerset Island Kimberlites by Discriminant Function Analysis

Actual group	Predicted group membership							Group centroid
	1	2	3	4	5	6	7	
1. Nord (61)[a]	54.1%(33)	0	0	0	0	9.8%(6)	36.1%(22)	0.726
2. Inugpasugsuk (33)	42.4%(44)	0	0	0	0	15.2%(5)	42.4%(14)	0.541
3. Amayersuk (42)	64.3%(27)	0	0	0	0	9.5%(4)	26.2%(11)	0.659
4. Ham West (10)	40.0%(4)	0	0	0	0	20.2%(2)	40.0%(4)	0.404
5. Ham Dike (42)	61.9%(26)	0	0	0	0	9.5%(4)	28.6%(12)	0.746
6. Elwin Bay (121)	6.6%(8)	0	0	0	0	83.5%(101)	9.9%(12)	−1.026
7. Tunraq (76)	26.3%(20)	0	0	0	0	46.1%(35)	27.6%(21)	−0.013

[a] Number of cases given in parentheses.

scores for samples within each group is a measure of the compositional differences between the groups. In total, Table 6.5 demonstrates that megacryst garnets from the Nord, Inugpasugsuk, Amayersuk, and Ham kimberlites are compositionally similar. Garnets from the Elwin Bay and Tunraq kimberlites differ from each other and the five other groups.

A similar multiple discriminant analysis of the compositions of low-Cr pyrope megacrysts from four Namibian kimberlites is given in Table 6.6. Intra-province compositional variations are demonstrated even more clearly. Garnets from Deutsche Erde and Amalia are similar to each other but differ from garnets found at Mukorob-1 and Mukorob-2. Garnets from Deutsche Erde however have a range of composition which overlaps that of the Mukorob-2 garnets.

The intra-provincial compositional differences demonstrated above and the regular chemical variations observed within any given suite of megacrysts as described by Gurney *et al.* (1979) and Robey and Gurney (1979) are unlikely to be observed if the garnets are merely xenocrysts.

Pyrope megacrysts, similar in composition to the low-Cr kimberlite megacrysts, occur in diatremes and vents formed by alnöitic, basanitic, nephelinitic,

Table 6.6. Classification of Garnet Megacrysts from Namibian Kimberlites by Discriminant Function Analysis

Actual group	Predicted group membership				Group centroid
	1	2	3	4	
1. Deutsche Erde (20)[a]	40.0%(8)	30.0%(6)	0	30.6%(6)	1.277
2. Amalia (15)	80.0%(12)	13.3%(2)	0	6.7%(1)	1.722
3. Mukorob-1 (10)	0	0	90.0%(9)	10.0%(1)	−3.075
4. Mukorob-2 (28)	3.6%(1)	0	7.1%(2)	89.3 (5)	−0.736

[a]Number of cases given in parentheses.

Table 6.7. Representative Compositions of Garnets from Undersaturated Basic Rocks[a]

	1	2	3	4	5	6	7	8	9	10	11	12
SiO_2	41.79	41.64	41.45	42.82	42.47	41.6	39.80–40.80	42.47	42.28	42.32	41.3	40.9
TiO_2	0.36	0.42	0.51	0.54	0.59	0.49	0.01– 0.58	0.50	0.69	0.74	0.9	1.1
Al_2O_3	23.44	23.41	23.50	23.13	23.14	23.3	20.77–23.09	22.99	21.90	22.39	21.7	22.4
Cr_2O_3	0.08	0.06	—	0.10	0.08	0.06	0.00– 0.42	0.63	1.03	0.95	1.7	—
FeO[b]	9.96	10.66	10.76	10.67	10.73	11.2	15.34–20.14	10.33	9.38	9.03	10.2	8.5
MnO	0.35	0.38	0.28	0.33	0.33	0.39	0.13– 0.86	0.21	0.29	0.29	0.3	0.2
MgO	18.64	18.30	18.51	19.43	19.09	17.4	11.90–15.09	19.93	20.28	20.38	19.0	18.7
CaO	5.33	5.53	5.09	4.64	4.60	5.30	5.32– 6.72	4.86	4.91	5.11	5.2	5.8
Na_2O	—	—	—	0.04	0.05	—	0.01– 0.05	0.05	0.06	0.06	0.2	0.1
	99.99	100.20	100.25	101.70	101.08	99.7	— —	101.97	100.82	101.27	100.5	97.7

[a] 1, 2, Elie Ness (Chapman 1976); 3, Kakanui (Mason and Allen 1973); 4, 5, Malaita (Nixon and Boyd 1979b); 6, Nigerian basalt (Frisch and Wright 1971); 7, range of composition Azov region (Gonshakova *et al.* 1975); 8–10, Colorado Plateau (Ehrenberg 1982); 11, garnet formed at 40 kbar, 1100°C, 0.3% H_2O from pyrolite less 40% olivine (Green and Sobolev 1975); 12, garnet formed at 30 kbar, 1280°C, 4.5% H_2O from olivine basanite (Green and Sobolov 1975).

[b] Total Fe calculated as FeO.

and minette volcanism. Pyropes (Table 6.7) from the Elie Ness Vent (Colville 1968, Chapman 1976), the Kakanui melanephelinite breccia (Mason and Allen 1973), Nigerian alkali basalts (Frisch and Wright 1971), and the Malaita alnöite (Nixon and Boyd 1979b) are typically poorer in Cr_2O_3 (<0.5%) and TiO_2 (<0.5%) than kimberlite megacrysts, but are similar in their Mg/(Mg + Fe) ratios (0.80–0.76). Garnets from the basaltic diatremes of the Azov region (Gonschakova *et al.* 1975) and the Onega Penninsula (Kaminskii 1977) are mainly pyrope-almandines, richer in Fe than the kimberlite pyropes. In these diatremes, garnets derived from eclogitic and granulitic sources are also common; chrome-pyropes occur rarely.

The minettes of the Colorado Plateau contain a heterogeneous assemblage of garnets derived from lherzolites, eclogites, and lower crustal sources, together with a suite of low-Ti, low-Cr pyropes (Table 6.7; Ehrenberg 1978, 1982, Aoki 1981, Hunter 1979, Switzer 1977). Ultramafic breccias in the region referred to previously as kimberlites (Aoki 1981, Switzer 1977) are now considered to be manifestations of diatreme-like activity associated with minette magmatism (Jones and Smith 1983, Ehrenberg 1982).

The above observations are important in that they demonstrate the occurrence of garnet megacrysts in a wide spectrum of magma types. Petrologists studying these garnets, with the exception of Nixon and Boyd (1979b), have concluded that low-Cr pyropes and other megacrysts represent high pressure phenocrysts formed at depths below 60 km. Strong support for this conclusion is provided by Green and Sobolev's (1975) experimental studies which have shown that garnets of identical composition (Table 6.7) are primary liquidus phases in undersaturated magmas at 21–40 kbar pressures and 900–1100°C. Although no kimberlitic compositions were studied it appears reasonable to suggest that the kimberlite pyropes are also high pressure phenocrysts. The Ti and Cr enrichment relative to other garnet megacrysts is undoubtedly a bulk compositional effect. The problem of the origins of megacrysts is discussed further in Section 9.11.

6.2.5. Trace Elements (Megacrysts)

Few data are available. Nixon *et al.* (1963), Gurney *et al.* (1973), and Mitchell and Keays (1981) have demonstrated the following ranges in trace element content (ppm): Co, 50–75; Sc, 40–100; V, 35–400; Ni, 70–190; Ga, 2–8; Pb, 2–6; Cu, 0.6–0.9. Gurney *et al.* (1973) have noted an inverse relationship between Sc and Cr contents. Pd, Ir, and Au contents are all less than 0.1 ppb (Mitchell and Keays, 1981). Eggler *et al.* (1979) have shown that rare earth element (REE) distribution patterns (two samples only) of Colorado garnets are relatively flat (5–10 times chondrites) with Cr-rich garnets being depleted in heavy REE relative to Cr-poor garnet. Taylor *et al.* (1983) state that eastern North American megacrysts are depleted in light REE (2 times chrondrites) and

enriched in heavy REE (10–20 times chrondrites) with no significant differences between Cr-rich and Cr-poor suites. Gurney *et al.* (1973) showed that REE abundances are very low (<10 ppm total) and that red (Cr-rich) garnets are depleted in Yb relative to orange (Cr-poor) garnets.

6.2.6. Kelyphite

Kelyphite is the name given to the complex intergrowth of fine grained minerals occurring as coronas upon garnets. It forms as a consequence of the breakdown and reaction of garnet during transport from regions in which it is a stable phase. Kelyphite is most commonly developed upon lherzolite-derived garnets and is rarely found on megacrysts. Removal of the kelyphite during transport in the kimberlite reveals a characteristically etched (Dawson 1980) or sculpted (Frantsesson, 1970) surface, formed by the growth of acicular orthopyroxenes. Kelyphite typically consists of ortho- and clinopyroxenes, spinel, phlogopite, and serpentine and forms at 900–1300°C at 10–20 kbar (Garvie and Robinson, 1982).

6.3. MAGNESIAN ILMENITE

Magnesian ilmenite is one of the most characteristic minerals of kimberlite. It plays a key role in kimberlite exploration programs because of its ease of concentration combined with its resistance to physical and chemical weathering. Its characteristic bright metallic luster aids in its easy recognition.

The amount of ilmenite present in kimberlites varies widely from trace quantities up to about 10 wt. % (Frantsesson 1970). Some kimberlites, e.g., Peuyuk, Finsch, and Koffiefontein appear to be devoid of ilmenite. Within a given kimberlite province some intrusions may be relatively rich in ilmenite while others contain only trace amounts, e.g., the Tunraq and Elwin Bay kimberlites of the Somerset Island kimberlite province (Mitchell 1979b). Different kimberlites within a single diatreme also vary in their ilmenite content; e.g., the K7, K6, K2, and K5 kimberlites of the Letseng-La-Terae main pipe contain 1680, 690, 100, and 8 ppm ilmenite, respectively (Bloomer and Nixon 1973). Kimberlites which are considered to be relatively rich in ilmenite include Monastery, 0.9%–5.0 wt. %; Morkoka, 3.9 wt. %; and Mir, 0.6–1.2 wt. % (Frick 1973, Bobrievich *et al.* 1964).

The following paragenetic types of ilmenite have been recognized:

1. Large rounded single crystals or polycrystalline megacrysts and macrocrysts (Boyd and Nixon's 1975 discrete nodule suite).
2. Lamellar intergrowths with clinopyroxene and less commonly orthopyroxene.

3. Euhedral to anhedral primary groundmass or matrix ilmenite.
4. Rounded-to-subhedral inclusions in olivine and/or phlogopite macrocrysts.
5. Intergrowths with groundmass spinel and perovskite.
6. Intergrowths with spinel (sub-solidus reduction).
7. Intergrowths with ilmenite (exsolution).
8. Intergrowths with rutile (armalcolite breakdown products).
9. Concentric multiple overgrowths upon rounded macrocryst olivine (only developed at Mukorob, Namibia).

In the kimberlitic environment ilmenite is also found as anhedral inclusions in megacryst garnet, clinopyroxene, orthopyroxene, phlogopite, and zircon. Magnesian ilmenites occur also in metasomatized lherzolites and eclogites and in MARID-suite xenoliths.

6.3.1. Megacryst/Macrocryst Ilmenite (Paragenesis 1)

Megacryst/macrocryst ilmenites typically occur as rounded-to-ellipsoidal nodules up to 10 cm in diameter. Their surfaces are commonly coated with alteration products such as leucoxene or perovskite or by thin skins of very fine grained kimberlite. Many are fractured, the exposed internal surfaces being alteration-free. Fractures are commonly filled with carbonates. Internal structures consist of tubules that contain in some instances sulfides or their alteration products (Dawson 1980, Haggerty *et al.* 1979).

It should be stressed that a distinction between megacryst/macrocryst ilmenite and groundmass ilmenite in some instances cannot be unambiguously made. Groundmass ilmenites are commonly considered to be any ilmenites that are smaller than 0.5–5 mm (Apter *et al.* 1984, Shee 1984); however, fragmentation of macrocrysts (0.5–5 mm) and megacrysts (>5 mm) can produce similar size or smaller particles which are indistinguishable from anhedral groundmass ilmenites. Mantling of such fragments by spinel and perovskite reaction rims further blurs the distinction between the two paragenetic types.

The megacrysts display a wide range of textures which have been described in detail by Frick (1973), Mitchell (1973b), Pasteris *et al.* (1979), and Pasteris (1980a). These form a continuum ranging from single crystals exhibiting weak undulose extinction and minor kink banding, through porphyroclastic textures to equilibrium granoblastic polygonal textures. In the porphyroclastic ilmenites, zones of weakly anisotropic, coarse grained (1–10 mm) crystals are separated by sub-parallel bands of fine grained (0.1–0.5 mm) strongly anisotropic material. Grain boundaries in the latter are strongly curved non-equilibrium boundaries. Decoration of subgrain boundaries of crystals within these zones by spinels is common. The textures have been interpreted as representing the effects of high-temperature deformation, recrystallization, and annealing of large single crystals

of ilmenite or cumulate-like bodies of ilmenite at upper mantle temperatures and pressures (Mitchell 1973b).

The majority of the ilmenite megacrysts are monomineralic; however, many crystals are characterized at their margins by the presence of rod-like or lamellar spinels oriented parallel to ilmenite {0001} planes. Less common are exsolution lamellae of secondary ilmenite. The nature and origin of the intergrowths is discussed in Sections 6.3.5–6.3.7.

Megacryst ilmenites are essentially members of solid solutions between ilmenite ($FeTiO_3$), geikielite ($MgTiO_3$), and hematite (Fe_2O_3). Significant amounts of Cr_2O_3 (0.1%–11.0%) are commonly present. Typically they contain minor amounts of Al_2O_3 (<1%), SiO_2 (<0.5%), and MnO (<1%), although enrichments of up to 21% MnO have been noted in some rare occurrences. The major compositional variation is within the ilmenite–geikielite series at relatively constant, low (<25 mol %) hematite contents. Ilmenite can, however, contain up to 45 mol % hematite, and such ilmenites are typically poor in MgO. Representative compositions covering the range in MgO content are given in Table 6.8.

Studies of megacryst ilmenite compositions from many kimberlites allow the following generalizations to be drawn:

1. Ilmenites from kimberlite provinces located in South Africa (Mitchell 1973b, 1977, Frick 1973, Pasteris 1980, Gurney *et al.*1973, 1979), Siberia (Garanin *et al.* 1979, 1983, Frantsesson 1970), Angola (Boyd and Danchin 1974), Liberia and Sierra Leone (Haggerty 1982, Tomp-

Table 6.8. Representative Compositions of Ilmenite Megacrysts[a]

	1	2	3	4	5	6	7	8	9
TiO_2	35.96	38.43	47.70	48.80	51.12	51.92	53.27	56.37	47.73
Al_2O_3	0.80	0.72	0.00	0.05	0.66	0.00	0.77	0.04	0.00
Cr_2O_3	0.60	0.14	1.80	2.54	0.33	0.30	0.12	0.95	0.66
Fe_2O_3	32.12	29.59	13.80	11.61	10.06	10.28	7.88	3.21	23.55
FeO	25.29	26.44	29.63	27.81	27.85	25.04	23.01	21.33	10.94
MnO	0.11	0.15	0.50	0.39	0.21	0.35	0.00	0.24	0.21
MgO	3.89	4.47	7.16	8.80	10.05	11.95	13.97	16.34	17.83
	98.77	99.94	100.59	100.00	100.28	99.54	99.02	98.48	100.92
mol %									
$FeTiO_3$	54.1	55.2	60.8	56.6	55.1	48.8	44.7	40.9	20.4
$MgTiO_3$	14.8	16.6	25.8	31.9	35.5	41.5	48.4	55.7	59.4
$MnTiO_3$	0.2	0.3	1.0	0.8	0.4	0.7	0.0	0.5	0.4
Fe_2O_3	30.9	27.9	12.4	10.6	9.0	9.0	6.9	2.9	19.8

[a] 1, 2 Mir, (Garanin *et al.* 1983); 3, Kamfersdam (Parfenoff 1982); 4, Wesselton (Shee 1984); 5, Orroroo (Scott Smith *et al.* 1984); 6, Festival'naya (Frantsesson 1970); 7, Ison Creek (Mitchell 1973b); 8, Zimnyaya (Rozova *et al.* 1979); 9, Frank Smith (Mitchell 1977).

kins and Haggerty 1984), Colorado-Wyoming (Eggler *et al.* 1979), Brazil (Parfenoff 1982, Svisero *et al.* 1984), S.E. and N.W. Australia (Scott Smith *et al.* 1984, Atkinson *et al.* 1982, 1984), and China (Zhou *et al.* 1982) are all of broadly similar composition. No inter- or intra-provincial differences have been established and any given province can contain high and low MgO ilmenites. Figure 6.7 illustrates the compositional variation of ilmenites in the ternary system ilmenite–geikielite–hematite for a representative selection of kimberlites.

2. Within a given province each kimberlite contains a characteristic suite of ilmenite as defined by its major element compositional range and mean. Thus Mitchell (1977) has shown that ilmenites from Frank Smith (MgO = 8.5%–17.8%) and Premier (MgO = 4.0%–23.1%) are distinctly more magnesian than ilmenites from Sekameng (MgO = 4.6%–8.6%) or Kao (MgO = 7.7%–12.5%). In the Yakutian kimberlites, ilmenites from Mir (MgO = 3.3%–9.2%, Garanin *et al.* 1983) are poorer in magnesium and richer in hematite (4.5–21.0 mol %) than those from Udachnaya (MgO = 8.2%–9.3%, Garanin *et al.* 1979), and Zarnitsa (MgO = 5.6%–9.9%, Frantsesson 1970). It should be noted that ilmenite compositional variation is more obvious than that of garnet megacrysts and multivariate statistical methods are generally not required to demonstrate the presence of distinctive populations. Mitchell (1977), however, using factor analysis has shown that inter-intrusion compositional variations are statistically significant.
3. Compositional variations within a single kimberlite can be as great as found for all occurrences within a province. Thus kimberlites from Wesselton contain macrocrystal ilmenites ranging from 6%–16% MgO (Mitchell 1973b, Shee 1984). Similar large ranges can even be found within a single, hand specimen of kimberlite. This latter phenomenon has been attributed to the random mixing during transport of crystals derived from fragmented compositionally zoned ilmenite cumulates (Mitchell 1973b).
4. Kimberlites that are geographically close exhibit gross differences in the composition of their ilmenite assemblages. Data shown in Figure 6.8 for ilmenites from the Orroroo kimberlites (Scott Smith *et al.* 1984) clearly exemplify this observation.

Megacryst ilmenites exhibit a wide range in their Cr_2O_3 content and Haggerty (1975) on the basis of data from Lesotho and West Africa proposed that Cr_2O_3 and MgO contents were related by a parabolic function (Figure 6.9). This hypothesis was supported by data for Colorado–Wyoming ilmenites (Eggler *et al.* 1979). For these occurrences each limb of the parabola is defined by ilmenites from a particular kimberlite group of kimberlites but the overall parabolic relationship cannot be defined by ilmenites from a single intrusion. Other studies

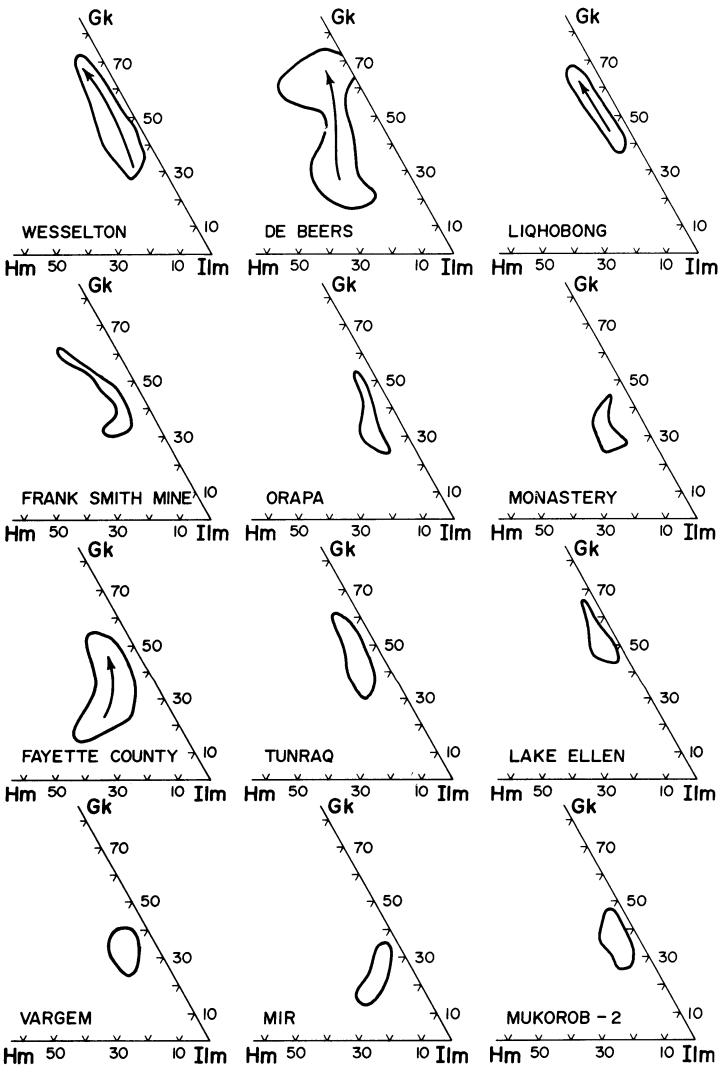

Figure 6.7. Compositional fields of ilmenite megacrysts from diverse kimberlites. Data sources: Wesselton (Shee 1984), De Beers (Pasteris 1980a), Liqhobong (Boctor and Boyd 1980), Frank Smith (Mitchell 1977), Orapa (Tollo 1982), Monastery (Mitchell 1977), Fayette County (Hunter and Taylor 1984), Tunraq (Mitchell 1979b), Lake Ellen (McGee and Hearn 1984), Vargem (Svisero *et al.* 1979), Mir (Garanin *et al.* 1979), Mukorob-2 (Mitchell, unpublished data). Arrows indicate zoning trends. Gk = geikielite, Ilm = ilmenite, Hm = hematite.

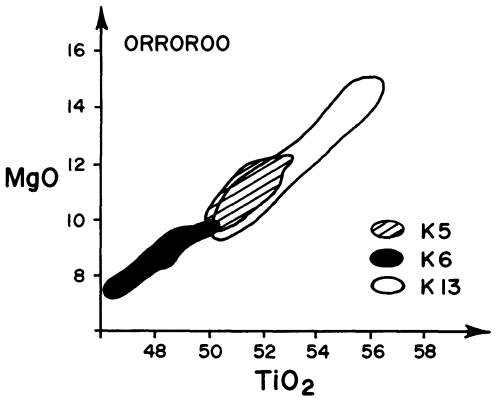

Figure 6.8. MgO versus TiO_2 (wt %) for ilmenite megacrysts from different dikes in the Orroroo kimberlite field (Scott Smith *et al.* 1984).

have not supported Haggerty's (1975) hypothesis, either Cr_2O_3 contents are independent of MgO (Mitchell 1979a) or only a weak positive correlation is present (Boctor and Boyd 1980a). Data for Orapa (Tollo 1982) and Wesselton ilmenites (Shee 1984) plot within the parabola (Figure 6.9) and appear to invalidate the basic concept.

Schulze (1984) has shown that on a Cr_2O_3-MgO plot, megacryst ilmenites from the Hamilton Branch kimberlite form an array reminiscent of Haggerty's (1975) parabola. The pattern differs in that the MgO-rich (14%–15%) limb is

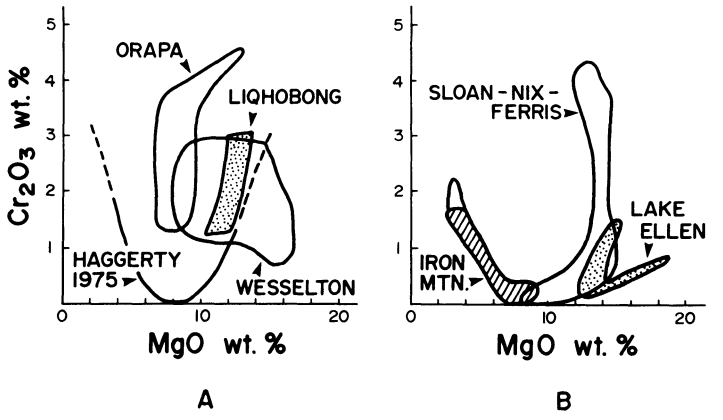

Figure 6.9. Cr_2O_3 versus MgO contents of megacrystal ilmenites from A. the Orapa (Tollo 1982), Liqhobong (Boctor and Boyd 1980), Wesselton (Shee 1984), Iron Mountain (Eggler *et al.* 1979), B. Sloan-Nix-Ferris (Eggler *et al.* 1979) and Lake Ellen kimberlites (McGee and Hearn 1984); together with Haggerty's (1975) "Cr_2O_3–MgO parabola."

vertical, the trough is horizontal (9%–14% MgO, <0.5% Cr_2O_3) and the MgO-poor limb is poorly defined, being represented by only three widely scattered data points. The curve segments can be related to textural groups. Monomineralic ilmenites define the whole array but are predominant in the Cr-poor trough. Tiny inclusions of ilmenite in silicate megacrysts, and ilmenites from graphic intergrowths with diopside, define the upper (0.5%–4.0% Cr_2O_3) and lower (0.5%–2.0% Cr_2O_3) portions of the MgO-rich limb, respectively. Ilmenite megacrysts with small silicate inclusions are confined to the MgO-rich (12%–15%) segment of the array trough.

6.3.1.1. Trace Elements (Megacrysts)

Megacryst ilmenites in addition to being Cr-rich are characterized by a distinctive enrichment in Ni, Nb, Ta, Zr, Hf, and V relative to Mg- and Cr-poor ilmenites found in basic igneous rocks. Representative ranges in the trace element content of megacrysts are given in Table 6.9.

Ni contents (2000–2320 ppm) (Nixon and Kresten 1973b, Ilupin and Nagaeva 1971, Parfenoff 1982) are well in excess of the levels found in ilmenites from basalts (40–130 ppm) (Parfenoff 1982). Ni contents correlate positively with MgO and negatively with Nb and Zr (Mitchell 1977, Parfenoff 1982).

Nb (477–2608 ppm) (Mitchell 1977) and Ta (65-440 ppm) (Mitchell *et al.* 1973a, Fesq *et al.* 1975, Ilupin 1983) contents are similar to levels found in ilmenites from syenites and granites (Nb = 200–4300 ppm, Ta = 130–640 ppm) (Mitchell 1977). The negligible Cr and Ni contents of the latter ilmenites, however, serve to distinguish them from kimberlitic megacryst ilmenites. Cr-poor, Nb-rich (1.1%–2.8%Nb_2O_5) groundmass ilmenites from the Premier carbonate kimberlite dikes are the only ilmenites from kimberlites yet found which are geochemically similar to ilmenites from carbonatites, which typically contain more than 1.0% Nb_2O_5 (Gaspar and Wyllie 1984, Garanin *et al.* 1983). Nb/Ta ratios range from 8.2–9.4 (Mitchell *et al.* 1973a).

Zr contents are the highest known for terrestrial ilmenites (mean 330 ppm) (Arhenius *et al.* 1971), similar levels only being found in ilmenites from lunar basalts. Hf shows a similar enrichment. Zr/Hf ratios range from 29 to 40 (Mitchell *et al.* 1973a).

The small amounts of rare earth elements, Pb, and anomalously high Cu contents reported from some ilmenites by Fesq *et al.* (1975), Fieremans (1966), and Dawson (1980) are probably due to the presence of small inclusions of perovskite, carbonate, or sulfides.

Inter-kimberlite trace element variations are poorly known. Mitchell (1977) showed that Frank Smith ilmenites are poorer in Zr and Nb and richer in Cu than Sekameng or Kao ilmenites, although Zr/Nb ratios are similar and not characteristic of individual occurrences.

Nixon and Kresten (1973b) proposed that individual kimberlites could be

Table 6.9. Trace Element Content (ppm) of Magnesian Ilmenite Megacrysts[a]

	Ni	Co	V	Cu	Al	Ga	Zn	Sc	Nb	Ta	Zr	Hf
Kamfersdam (1)	580–1300	185–210	1300–2000	17–30	720–1400	0–12	220–400	35–60	—	—	—	—
Kimberley (1)	440–890	160–200	1000–2000	18–22	1000–1400	10–12	180–230	40–55	—	—	—	—
Kao (2,3)	325–1069	150–287	1300–1600	15–45	1800–4200	15–20	150–300	23–50	971–1917	165–174	754–1269	24–32
Sekameng (2)	182–1359	236–366	—	16–173	—	—	133–163	—	477–1521	—	385–1005	—
Monastery (3,4)	—	139–194	—	—	—	—	—	19–22	659–1223	47–142	546–896	15–28
Japecanga (1)	1000–1250	180–190	1000–2000	22–30	1700–2000	10–12	230–240	70–80	—	—	—	—

[a] (1) Parfenoff (1982); (2) Mitchell (1977); (3) Mitchell *et al.* (1973a); (4) Gurney *et al.* (1973). Ni, Cu, V, Al, Ga, Zn determined by atomic absorption and/or emission spectrography, Co and Sc emission spectrography and/or neutron activation, Nb and Zr by XRF analysis, Ta and Hf by neutron activation.

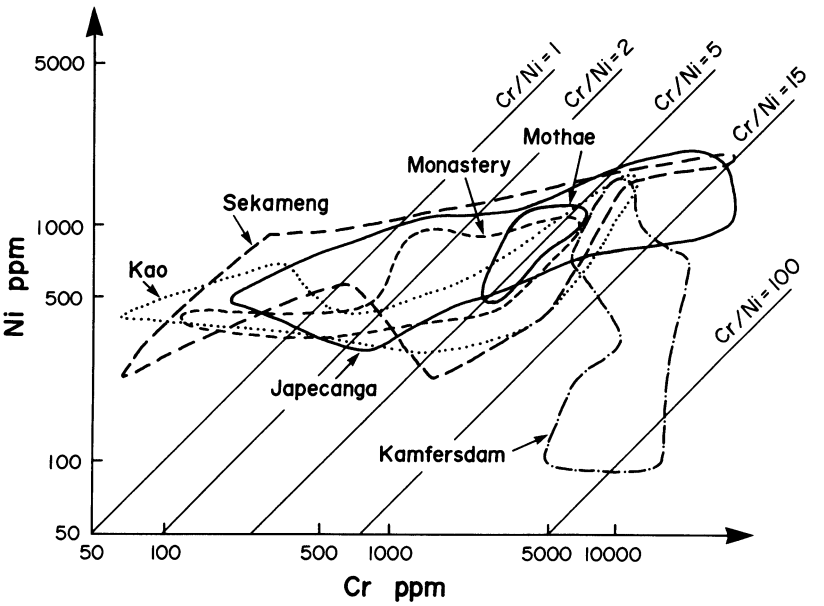

Figure 6.10. Ni versus Cr compositional fields for ilmenite megacrysts from Kao, Sekameng, Monastery, Mothae (Nixon and Kresten 1973b), Japecanga and Kamfersdam (Parfenoff 1982).

characterized by ilmenite Cr/Ni ratios. Recent data (Figure 6.10) however indicate that this hypothesis is not correct and that Cr/Ni ratios show a wide range within and between kimberlites. Most of this variation is a consequence of the wide range in Cr content at relatively constant Ni content.

Mitchell (1977) and Parfenoff (1982) have noted that Nb, Zr, and Ni correlate with Fe, Mg, and Ti variations, but that Co, Sc, Cu, and Zn abundances are independent of major element variations.

6.3.2. Zoning and Reaction Trends

Most ilmenites (single crystals or polycrystalline aggregates) are homogeneous; however, several studies have demonstrated the existence of two distinctive zoning trends.

One is a trend of increasing MgO and Cr_2O_3 coupled with decreasing or constant Fe_2O_3 and termed the *magmatic trend* by Haggerty *et al.* (1979).

The other is a trend of increasing FeO and MnO, and decreasing MgO and Cr_2O_3 leading toward ilmenite-pyrophanite ($MnTiO_3$) solid solutions, and termed the *kimberlite reaction trend* by Haggerty *et al.* (1979).

The former trend is more common than the latter, and may be characteristic in that it is only since the development of the electron microprobe that it has been possible to examine such zonations in any detail.

6.3.2.1. Magnesium-Enrichment Trend

Ilmenites zoned according to the Mg-enrichment magmatic trend have been described from Monastery (Haggerty *et al.* 1979), De Beers (Pasteris 1980), Wesselton (Elthon and Ridley 1979, Shee 1984), Liqhobong (Boctor and Boyd 1980a), Elliot County (Agee *et al.* 1982), Green Mountain (Boctor and Meyer 1979), and Fayette County (Hunter *et al.* 1984).

Typically the magnesium enrichment is confined to a narrow mantle (100–500 μm) upon a relatively uniform core (Figure 6.11A). Commonly the mantle is not symmetrical and crystals are fractured across the zonation (Tollo 1982). Clearly in some cases the development of the Mg-rich rims occurred prior to incorporation in their current host.

The pattern of magnesium enrichment shown in Figure 6.11A is better described as an overgrowth rather than as an example of continuous zoning formed by fractional crystallization. Boctor and Boyd (1980a) and Agee *et al.* (1982) consider that the overgrowths are formed by reaction of ilmenite megacrysts with a magma that is in equilibrium with, or is precipitating ilmenite that is more magnesian, than their cores. Data presented by Agee *et al.* (1982) and Shee (1984) in fact clearly demonstrate that the trend of Mg enrichment is toward the composition of the groundmass ilmenites (Figures 6.11B, 6.14) and undoubtedly represent an attempt by the megacrysts to come to equilibrium with their host magma. Continuous zonation is apparently found in ilmenites from Monastery (Haggerty *et al.* 1979), although the zoning could merely represent a greater degree of megacryst–magma interaction than experienced by the mantled megacrysts.

Haggerty *et al.* (1979) attribute the magmatic magnesium enrichment trend to reaction with a liquid caused by a decrease in total pressure. The consequent decrease in oxygen fugacity (fo_2), is manifested by the decrease in Fe_2O_3 toward

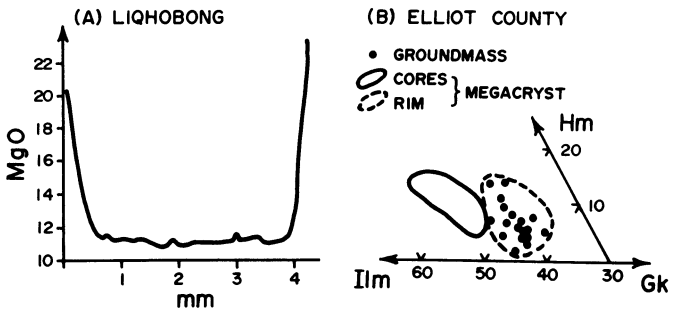

Figure 6.11. (A) Magnesium enrichment occurring at the margins of an otherwise compositionally uniform ilmenite megacryst from the Liqhobong kimberlite, after Boctor and Boyd (1980); (B) Compositional relationships between the cores and rims of megacryst ilmenite and groundmass ilmenites in the Elliot County kimberlite, after Agee *et al.* (1982).

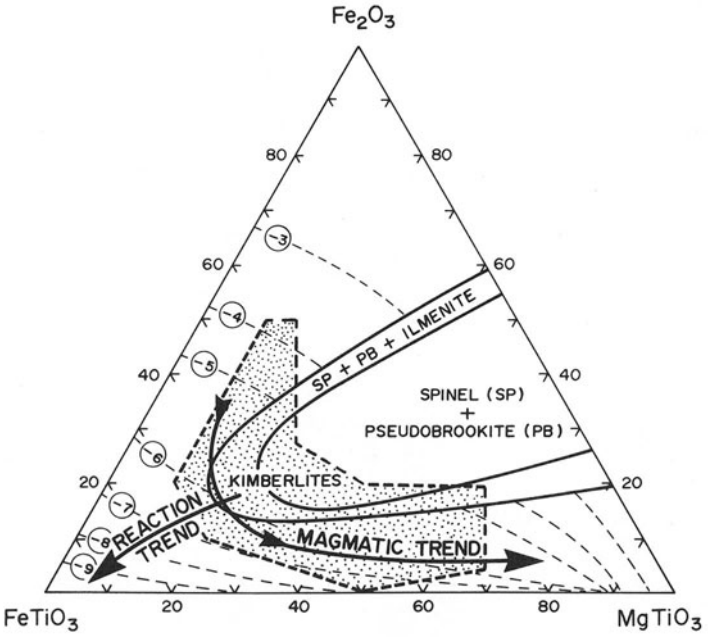

Figure 6.12. Phase relationships in the system $MgTiO_3$–$FeTiO_3$–Fe_2O_3 at 1300°C after Woermann *et al.* (1970). Stippled field indicates the compositions of megacrystal ilmenites. The arrowed heavy lines indicate Haggerty *et al.*'s (1979) reaction and magmatic trends corresponding to the magnesium and manganese-enrichment trends respectively. Dashed lines are contours of oxygen fugacity.

the magacryst rims. Figure 6.12 shows the relationship between the magnesium enrichment trend and fo_2 isobars in the system ilmenite–geikielite–hematite at 1300°C, and demonstrates that Mg enrichment is initially correlated with decreasing fo_2 and that subsequently fo_2 may rise slightly.

6.3.2.2. Manganese-Enrichment Trend

Haggerty *et al.* (1979), Mitchell *et al.* (1973b), and Agee *et al.* (1982) have noted that the margins of some megacryst and lamellar intergrowth ilmenites from Monastery are enriched in MnO (1%–5%) and FeO, and depleted in Fe_2O_3 and MgO relative to their cores (Table 6.10). This compositional trend, as shown in Figure 6.12, is opposite to the magnesium enrichment trend and is associated with greater reductions in fo_2 than the latter. Haggerty *et al.* (1979) attribute the formation of the Mn-rich rims to the onset of carbonate immiscibility during the later stages of crystallization of the kimberlite magma. This association is supported by the occurrence of Mn-rich ilmenites in the calcite-rich Green Mountain

Table 6.10. Representative Compositions of Manganese-Bearing Ilmenites[a]

	1	2	3	4	5	6	7	8	9	10
TiO_2	54.19	53.32	52.33	48.30	49.91	54.12	53.49	50.04	51.5	50.1
Al_2O_3	0.60	0.77	0.01	0.41	0.13	0.49	0.48	0.51	0.00	0.00
Cr_2O_3	0.06	0.07	0.04	0.96	0.30	1.27	1.23	1.19	0.00	0.00
Fe_2O_3	5.85	0.73	1.58	11.67	2.38	4.46	4.03	3.12	4.48	2.67
FeO	31.25	39.95	40.86	26.67	21.51	25.88	29.12	35.29	25.79	24.64
MnO	0.44	5.35	4.96	8.69	20.96	0.26	1.36	9.28	12.2	17.5
MgO	9.02	0.81	0.66	4.47	1.20	12.64	9.88	0.18	4.58	1.51
Nb_2O_5	n.d.[b]	n.d.	n.d.	n.d.	n.d.	n.d.	n.d.	n.d.	1.15	2.83
	101.41	101.00	100.44	101.17	96.39	99.12	99.59	99.60	99.70	99.3
mol %										
$FeTiO_3$	62.0	84.4	85.5	54.9	46.8	51.1	58.3	76.0	53.4	53.3
$MgTiO_3$	31.9	3.1	2.5	16.4	4.7	44.4	35.3	0.7	16.9	5.8
$MnTiO_3$	0.9	11.6	10.5	18.1	46.2	0.5	2.8	20.3	25.6	38.3
Fe_2O_3	5.2	0.8	1.5	10.6	2.3	4.0	3.6	3.0	4.2	2.6

[a] 1, 2 Core and rim Monastery (Mitchell *et al.* 1973); 3, Green Mountain (Boctor and Meyer 1979); 4, Elliot Co. (Agee *et al.* 1982); 5, De Beers (Pasteris 1980a); 6–8, core, intermediate region, and rim, Premier grey kimberlite (Wyatt 1979a); 9, 10, Premier carbonate dike (Gaspar and Wyllie 1984).
[b] n.d. = not determined.

kimberlite (Boctor and Meyer 1979). The relationship is however not supported by studies of ilmenites from the extremely carbonate-rich highly evolved kimberlites from the Benfontein sill (Boctor and Boyd 1981, Gaspar and Wyllie 1984, McMahon *et al.* 1979), the De Beers dike (Donaldson and Reid 1982), and Skinner's sill, Wesselton (Mitchell 1984a). In contrast Pasteris (1980) has reported a manganoan ilmenite containing 21% MnO and other Mn-bearing ilmenites (2.5%–5.4% MnO) forming complex intergrowths with magnesian ilmenite, spinel, and perovskite not in association with carbonate in the De Beers kimberlite (Table 6.10). Manganese enrichments of up to approx. 4.0% MnO have been found in ilmenites from Yakutian kimberlites (Garanin *et al.* 1983) and the Skerring kimberlite of the North Kimberley field, Western Australia (Atkinson *et al.* 1984).

Extreme MnO enrichment in kimberlitic megacryst ilmenites has only been consistently reported from the Premier kimberlite (Wyatt 1979a, Scott and Skinner 1979, Gaspar and Wyllie 1984). These ilmenites are strongly continuously zoned toward Mn-rich (up to 9% Mn) margins (Table 6.10) from normal Mg-rich cores. Mn-rich ilmenites are most common at the margins of the pipe. Ilmenites in the associated carbonate-rich dikes were found to be Mn-rich (12%–17% MnO) by Gaspar and Wyllie (1984), but not by Wyatt (1979a). Agreement has not been reached as to the origin of these Mn-rich ilmenites. Wyatt (1979a) believes that the enrichment was a non-magmatic phenomenon related to cir-.

culating ground waters. Gaspar and Wyllie (1984) in contrast believe that the ilmenites in the carbonate dikes are primary liquidus phases and represent the culmination of the reaction trend.

6.3.3. Lamellar Intergrowth Ilmenite (Paragenesis 2)

Coarse grained ilmenite-clinopyroxene lamellar intergrowths are found in most kimberlite provinces. Intergrowths with orthopyroxene are less common (Frick 1973) and comprise only about 5% of the lamellar intergrowth population at Monastery (Haggerty *et al.* 1979). The intergrowths range in size from a few millimeters up to 20 cm in diameter (Dawson and Reid 1970). The proportions of the constituent phases vary widely from 10%–90% ilmenite, although ilmenite:clinopyroxene ratios of 20–40:80–60 are most common. Individual nodules usually have a uniform orientation of the ilmenite lamellae within clinopyroxene with intersections at 60° and 120°. X-ray studies (Wyatt *et al.* 1975, McCallister *et al.* 1975) have shown the ilmenites to be single crystals with the planar lamellae sets oriented parallel to ilmenite {0001} and pyroxene {100} planes. The texture of the intergrowth is best described as a graphic intergrowth which is in appearance and crystallography identical to graphic quartz-feldspar intergrowths (Mitchell 1977). Single crystals in the Frank Smith intergrowths (Pasteris *et al.* 1979) have been subjected to deformation and the ilmenites exhibit the spectrum of recrystallization and annealing textures observed in monomineralic megacryst ilmenites. Haggerty *et al.* (1979) have reported tubular cavities containing pyrrhotite and pentlandite which pierce ilmenite and pyroxene crystals, and attributed their presence to the existence of a separate sulfide liquid at the time of formation of the intergrowth. Pasteris *et al.* (1979), Haggerty *et al.* (1979) and Mitchell *et al.* (1973b) have noted the common occurrence of fine grained sub-solidus reduction "exsolution" spinels (see below).

Few studies have been undertaken attempting to establish the intra- and inter-kimberlite compositional variation and to provide comparisons with respect to the compositions of associated megacrysts. Lamellar ilmenites from Frank Smith (MgO = 10.2%–12.9%, Nixon and Boyd 1973a, Pasteris *et al.* 1979) and Mukorob-2 (MgO = 10.7%–13.4%, this work) are distinctly more magnesian than lamellar ilmenites from Monastery (MgO = 8.5%–10.1%, Gurney *et al.*1973, Mitchell 1977). Data for other localities are limited to one or two analyses per occurence. Most ilmenites contain between 8% and 11% MgO, although Gurney *et al.* have found 15.3% MgO in a Riley County ilmenite. Representative compositions are given in Table 6.11.

Figure 6.13 shows that lamellar ilmenites from Mukorob-2, Frank Smith, and Monastery all exhibit a small but distinct range in composition and overlap the compositional field of associated megacryst ilmenite. Although the lamellar ilmenites do not terminate the megacryst compositional trend, it is clear that the majority of their compositions are similar only to the more Mg-rich megacrysts.

Table 6.11. Representative Compositions of Lamellar Ilmenites[a]

	1	2	3	4	5	6	7	8
TiO_2	50.11	48.77	47.05	50.05	53.09	52.84	53.79	50.92
Al_2O_3	0.53	0.50	0.75	0.81	0.63	0.87	0.98	1.08
Cr_2O_3	0.13	0.08	0.05	0.22	0.08	0.32	0.47	1.24
Fe_2O_3	9.95	16.40	15.42	10.19	6.22	9.43	6.74	12.73
FeO	29.67	22.56	26.40	27.15	28.52	24.86	24.06	18.36
MnO	0.24	0.23	0.23	0.20	0.20	0.20	0.20	0.20
MgO	8.50	11.82	8.80	9.91	10.67	12.60	13.53	15.30
	99.13	100.36	98.70	98.53	99.41	101.12	99.77	99.79
mol %								
$FeTiO_3$	59.8	44.0	53.6	54.7	56.4	48.0	46.7	35.5
$MgTiO_3$	30.6	41.1	31.8	35.6	37.6	43.3	46.9	52.9
$MnTiO_3$	0.5	0.5	0.5	0.4	0.4	0.4	0.4	0.4
Fe_2O_3	9.0	14.4	14.1	9.2	5.6	8.3	5.9	11.2

[a] 1, Monastery (Gurney *et al.* 1973); 2, Monastery (Ringwood and Lovering, 1970); 3, Pipe 200 (Kresten and Dempster 1973); 4, Mothae (Nixon 1973a); 5, Mukorob-2 (this work); 6, Mayeng (Apter *et al.* 1984); 7, Deutsche Erde-1 (this work); 8, Riley Co., Kansas (Gurney *et al.* 1973).

This observation is supported by limited data for Elliot County intergrowths and megacrysts (Agee *et al.* 1982). Figure 6.13 also indicates that the overall composition of the lamellar ilmenites is correlated with that of the megacrysts, implying a genetic relationship for both to the kimberlite in which they occur. Mitchell (1977) and Gurney *et al.* (1973) indicate that there are no substantial

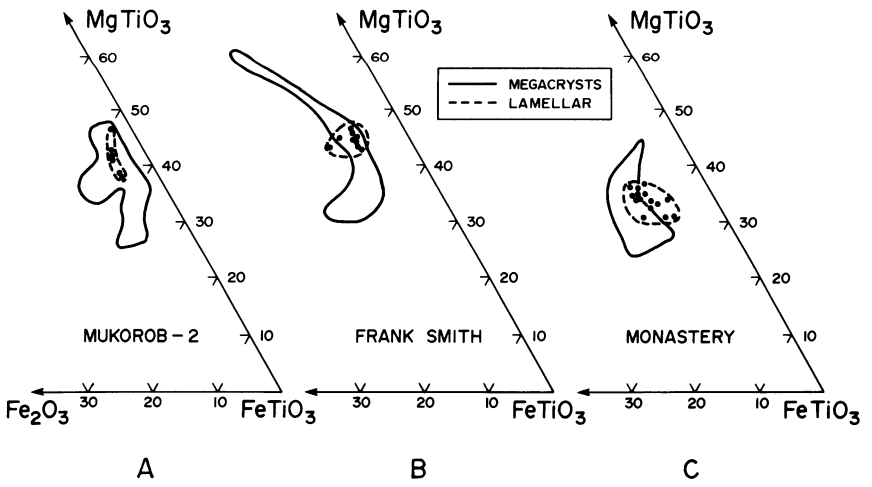

Figure 6.13. Relative compositions of ilmenite megacrysts and ilmenite–clinopyroxene lamellar intergrowths from A. the Mukorob-2, B. Frank Smith and C. Monastery kimberlites (Mitchell 1977 and unpublished data).

differences in the trace element contents of lamellar and megacryst ilmenites, although very few data are available for comparison.

6.3.4. Groundmass Ilmenite (Parageneses 3, 4, and 5)

Groundmass ilmenites are difficult to identify conclusively except in the rare instances where euhedral prisms are found, as at Liqhobong (Boctor and Boyd, 1980a) and Lepelaneng (Haggerty 1975). Typically, groundmass ilmenites are anhedral, zonation free, not polycrystalline, and show uniform extinction. Commonly, they are mantled by, or included within, perovskite and/or spinel. Complex intergrowths between ilmenite and spinel (see below) may in some instances also represent groundmass ilmenites (Pasteris 1980a, Haggerty 1973, 1975, Shee 1984, Agee *et al.* 1982). Anhedral-to-bleb-like inclusions in macrocrystal olivines, and less commonly in phlogopite, are also members of the groundmass suite (Dawson and Hawthorne 1973, Shee 1984, Apter *et al.* 1984).

Few detailed studies of their composition (Table 6.12) have been undertaken but data obtained for groundmass ilmenites from Liqhobong (Boctor and Boyd 1980) De Beers (Pasteris 1980), Elliot County (Agee *et al.* 1982), Mayeng (Apter *et al.* 1984), and Wesselton (Shee 1984) all show a constant trend of Mg enrichment relative to associated megacrysts/macrocrysts. Figures 6.11B and 6.14 show that the Mg enrichments at the rims of megacrysts converge upon the groundmass ilmenite compositions, indicating that the megacrysts either were attempting to equilibrate with the matrix liquids, or they provided nucleation sites for the crystallization of some of the primary groundmass ilmenites. Figure

Table 6.12. Representative Compositions of Groundmass Ilmenites[a]

	1	2	3	4	5	6	7	8
TiO_2	56.24	57.40	57.40	57.50	54.30	52.12	53.3	55.8
Al_2O_3	0.30	0.24	0.16	0.07	0.16	0.34	0.66	0.29
Cr_2O_3	1.13	1.16	3.94	3.37	1.99	2.55	0.13	1.69
Fe_2O_3	5.83	5.63	6.15	2.13	7.38	11.22	9.00	5.84
FeO	18.33	13.38	7.78	17.52	19.55	15.92	23.35	19.69
MnO	0.52	0.65	0.60	0.64	0.58	0.66	0.34	0.54
MgO	17.52	12.09	24.26	18.82	16.10	16.99	13.6	16.8
	99.87	99.55	100.29	100.05	100.06	99.80	100.38	100.65
mol %								
$FeTiO_3$	35.4	24.7	14.3	33.3	37.5	30.7	44.9	37.3
$MgTiO_3$	58.7	69.4	79.5	63.7	55.0	58.3	46.6	56.7
$MnTiO_3$	1.0	1.2	1.1	1.2	1.1	1.3	0.7	1.0
Fe_2O_3	4.9	4.7	5.1	1.8	6.4	9.7	7.8	5.0

[a] 1, 2, Groundmass ilmenite core and rim, Wesselton; 3, Wesselton; 4, inclusion in olivine phenocryst, Wesselton (Shee 1984); 5, Mayeng (Apter *et al.* 1984); 6, Liqhobong (Boctor and Boyd (1980a); 7, 8, Elliot Co. (Agee *et al.* 1982).

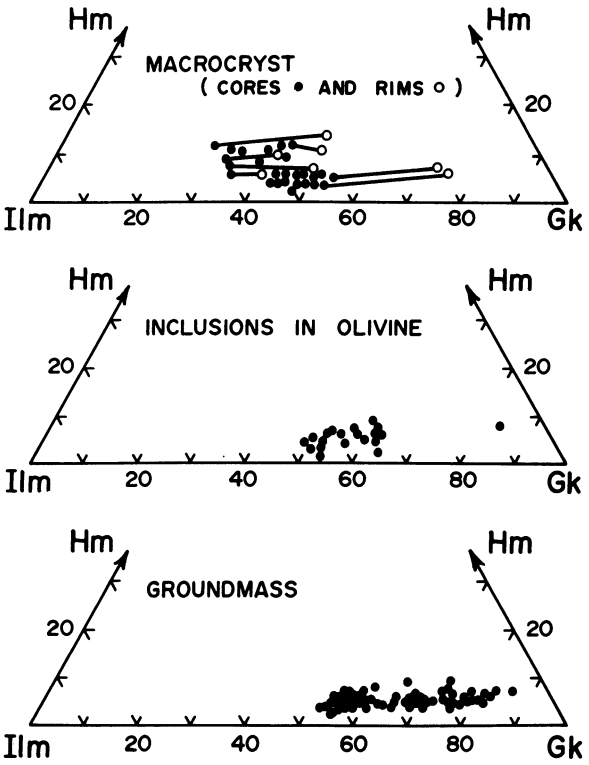

Figure 6.14. Composition of ilmenites from different parageneses in the Wesselton kimberlite, after Shee (1984).

6.14 shows that ilmenite inclusions in olivine are similar in composition to the Fe-rich members of the groundmass suite. These ilmenites probably crystallized contemporaneously with the earliest members of that suite, with enrichment of the later members in MgO being the result of the cessation of olivine crystallization (Pasteris 1980, Shee 1984).

Apter *et al.* (1984) have shown zoning in the Mayeng groundmass ilmenites to be a trend of sharply decreasing Cr_2O_3 at essentially constant or slightly increasing MgO contents (Figure 6.15). Zoning trends in groundmass and macrocrystal ilmenites converge upon the composition of ilmenites included in olivine and phlogopite.

Danchin *et al.* (1975) have demonstrated that ilmenites in fine grained globular segregations are more magnesian (MgO = 10.6%) than the macrocrysts (MgO = 5%–7%) around which they have nucleated.

The above studies indicate conclusively that ilmenite is a primary liquidus phase during the early stages of crystallization of the groundmass, and that the trend of differentiation is toward magnesium enrichment. Groundmass ilmenites

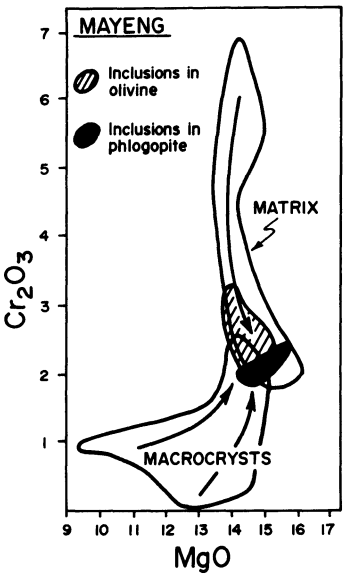

Figure 6.15. Cr_2O_3 versus MgO (wt %) contents of ilmenites from different parageneses in the Mayeng kimberlites, after Apter *et al.* (1984). Arrows indicate core-to-rim compositional variation.

have, according to Figures 6.12 and 6.14, crystallized along a trend of increasing fo_2 relative to megacryst ilmenites (Shee 1984).

6.3.5. Ilmenite–Spinel Intergrowths (Parageneses 5 and 6)

Oriented inclusions of spinel are common in many megacryst/macrocryst ilmenites (paragenesis 6), Mitchell (1973b), Pasteris *et al.* (1979), Haggerty (1975), and Garanin *et al.* (1983) have described examples from southern African and Soviet kimberlites and noted that the spinels occur as rod-like or lamellar inclusions oriented parallel to ilmenite {0001} planes. Commonly, the spinels are confined to the margins of the megacrysts. Pasteris *et al.* (1979) have noted that subgrain boundaries of deformed ilmenites are decorated by spinels. It is generally agreed that these spinels have been formed by the sub-solidus reduction of an originally homogeneous ilmenite as a consequence of decreases in temperature and/or oxygen fugacity. Pasteris *et al.* (1979) however, regard pleonaste inclusions in the Frank Smith ilmenites to be a product of exsolution *sensu stricto*.

Because of the very small size (5 mm in general) of the inclusions, few compositional data exist. Haggerty and Tompkins (1984), Garanin *et al.* (1979), Pasteris *et al.* (1979), and Danchin and d'Orey (1972) have demonstrated that the spinels are predominantly titanian chromites and aluminous magnesian ulvöspinel-magnetites. The most comprehensive account of their chemistry and origin is given by Haggerty and Tompkins (1984) for ilmenite-spinel pairs from Koidu (Sierra Leone), Antoschka (Guinea), and a Liberian kimberlite. Haggerty

and Tompkins note the composition of the host ilmenites vary widely with respect to MgO content, but the Fe_2O_3 contents are generally low (2–14 mol % Hm). Figure 6.16 shows that each locality has a specific spinel composition with very little overlap. A weak positive correlation exists between the hematite content of the ilmenite and the $[Fe^{3+}/(Fe^{3+} + 2Ti)]$ ratio of the "exsolved" spinel, with the more highly oxidized ilmenites hosting the more magnetite-rich spinels. No simple or systematic relationships between Cr_2O_3 and MgO contents of the ilmenite–spinel pairs is evident. Haggerty and Tompkins (1984) regard the trend shown in Figure 6.16 to be one of progressively stronger reducing conditions and that the redox potential under which the Koidu pairs were formed was higher than that at Antoschka. Using experimental data for the systems FeO–MgO–TiO_2 and FeO–Cr_2O_3–TiO_2 (Knecht *et al.* 1979), Haggerty and Tompkins (1984) propose that sub-solidus reduction took place at 1050–1200°C. This conclusion is supported by Haggerty *et al.*'s (1979) synthesis of ilmenite–spinel pairs similar to those occurring at Monastery at 1100°C ($fo_2 = 10^{-8}$ atm). Decomposition of ilmenite to two phase assemblages required only a slight ($10^{0.5}$ atm) reduction in oxygen fugacity. Haggerty and Tompkins (1984) have calculated the temperatures and oxygen fugacities of equilibration of the pairs, using Lindsley and Spencer's (1982) method, to be: Koidu, 650–1250°C at 10^{-17}–10^{-7} atm; Liberia, 850–1200°C at 10^{-12}–10^{-9} atm.; Antoschka, 800–1150°C at 10^{-16}–10^{-10} atm. It

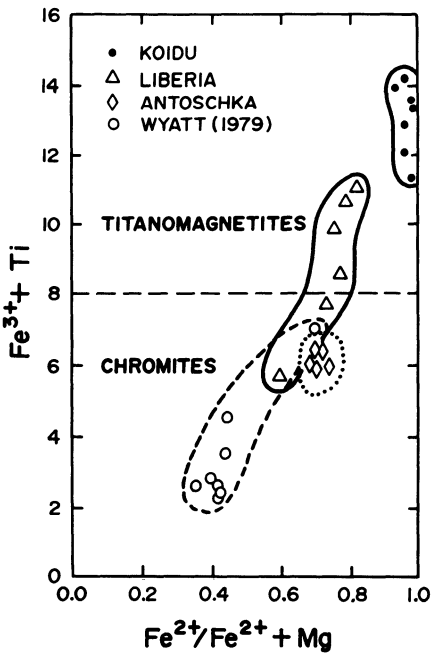

Figure 6.16. $(Fe^{3+} + Ti)$ versus $(Fe^{2+}/Fe^{2+} + Mg)$ for spinels co-existing with ilmenite, after Haggerty and Tompkins (1984).

is inferred that initial sub-solidus reduction occurred in the mantle and that re-equilibration occurred during subsequent transport.

Wyatt (1979b) has described unusually Cr-rich (up to 13% Cr_2O_3) ilmenites containing segregations and lamellae of Cr-spinel and Cr-rutile. These intergrowths are not strictly analogous to those described above because of the presence of rutile, and Haggerty and Tompkins (1984) have proposed that they are the breakdown products of a chromian titanate belonging to a crichtonite group precursor. Figure 6.16 indicates that they formed at higher temperatures and lower oxygen fugacities than the ilmenite–spinel pairs discussed above.

Ilmenite–spinel intergrowths, not related to subsolidus reduction, have been described from kimberlite groundmass assemblages (paragenesis 5) by Pasteris (1980a,b), Haggerty (1973, 1975), Elthon and Ridley (1979), and Boctor and Meyer (1979). Typically these consist of oscillatory zoned ilmenite–spinel–ilmenite–spinel/perovskite reaction mantles. For example, Pasteris (1980) described from the De Beers kimberlite, chromites mantled by ilmenite with both phases enclosed by later titanomagnetite. The ilmenites sandwiched between these contrasting spinels are typically MgO-rich groundmass types. Haggerty and Tompkins (1984) ascribe these intergrowths to the effects of fluctuating oxygen fugacities causing the precipitation of either ilmenite or spinel, as the bulk composition of the magma falls alternately within or outside of the ilmenite decomposition loop shown in Figure 6.12. This decomposition loop probably also limits the extent to which groundmass ilmenites in general can become enriched in Fe_2O_3 before they decompose or are replaced by spinel as the stable liquidus phase.

6.3.6. Ilmenite–Ilmenite Intergrowths: Exsolution Pairs (Paragenesis 7)

True exsolution of ilmenite from an originally homogeneous hypersolvus ilmenite is apparently rare. Exsolution intergrowths of contrasting types have been described by Tompkins and Haggerty (1984) and Haggerty and Tompkins (1984). Ilmenites from Koidu are hematite-rich and have exsolved hematite-poor geikielitic ilmenites, whereas hematite-poor ilmenites from Monastery have exsolved hematite-rich lamellae (Table 6.13). The differences are a consequence of the parent bulk composition with respect to the position of the solvus. The initially exsolved ilmenites are also subjected to subsolidus reduction resulting in spinel formation. The process commonly has occurred where ilmenites and co-existing sulfides are in contact. Haggerty and Tompkins (1984) have concluded that the exsolved ilmenite pairs are consistent with decomposition at 1300°C at 1 atm.

A rare type of exsolution is one in which the host ilmenite breaks down into two ilmenites, one of which is Mg rich and the other Mn rich, together with spinel formation. At Koidu, Tompkins and Haggerty (1984) have considered such exsolution to be associated with the formation of a carbonate rich fluid.

Table 6.13. Representative Compositions of Ilmenite-Ilmenite Intergrowths[a]

	1	2	3	4	5	6	7
TiO_2	49.05	44.01	36.68	50.39	8.61	54.13	47.74
Al_2O_3	0.48	1.02	0.44	0.01	3.64	0.02	0.58
Cr_2O_3	0.26	0.44	0.84	0.16	8.60	0.53	1.47
Fe_2O_3	12.61	21.09	32.39	7.80	73.62+	35.89+	40.52+
FeO	28.03	25.76	25.44	35.11	—	—	—
MnO	0.20	0.30	0.16	0.19	0.19	0.19	0.19
MgO	8.92	7.60	4.10	5.55	5.06	11.73	10.38
	99.55	100.22	100.05	99.21	99.72	102.42	100.83
$FeTiO_3$	56.5	52.8	53.7	72.4	0.0	55.7	52.9
$MgTiO_3$	32.0	27.8	15.5	20.3	33.3	42.1	40.4
Fe_2O_3	11.5	19.4	30.8	7.3	66.7	2.2	6.7

[a] 1, 2, Host and exsolved ilmenite, Monastery (Haggerty and Tompkins 1984); 3, 4, Host and exsolved ilmenite Koidu, (Haggerty and Tompkins 1984); 5, co-existing ilmenite and 6, 7, hosts, Udachnaya (Garanin *et al.* 1983). +, total iron expressed as Fe_2O_3

Garanin *et al.* (1983) have described from the Udachnaya pipe an unusual Cr-rich geikielitic-hematite associated with a hematite-poor geikielitic-ilmenite.

6.3.7. Ilmenite–Rutile Intergrowths (Paragenesis 8)

Lamellar intergrowths with rutile described by Haggerty (1975) and Tollo (1982) are considered to be derived by the breakdown of Ti^{3+}-bearing chromian armalcolite ($FeMgTi_2O_5$) and thus are not strictly comparable to the megacryst or groundmass ilmenites. They are however, clearly kimberlitic in character containing 10.5%–17.4% MgO and 2.7%–7.3% Cr_2O_3 with approximately 5 mol % hematite. Lamellar ilmenites from Orapa are more magnesian and poorer in Fe_2O_3 than Orapa megacrysts. Those from Jagersfontein are poorer in Fe_2O_3 than associated megacrysts (Tollo 1982). The origins of these intergrowths are discussed further in Sections 6.17.5 and 6.18.1.

6.3.8. Compositionally Related Ilmenites

6.3.8.1. Basic Volcanic Rocks

Megacrystal magnesian ilmenites of similar composition (3%–7% MgO, 5–25 mol % Hm) to kimberlitic ilmenites are common in alkali basalts and basanites (Binns 1969, Wass 1979, Reay and Wood 1974, Parfenoff 1982, Leblanc *et al.* 1982). Commonly, the ilmenites are apparently phenocrysts and

exhibit a euhedral to subhedral habit and lack perovskite reaction mantles (Parfenoff 1981). Rounded deformed polycrystalline nodules occur in the Tahalra basanites (Leblanc *et al.* 1982) and are considered to be mantle cumulates that have been subjected to shearing, recrystallization annealing, and sub-solidus reduction in a manner analogous to that proposed for polycrystalline kimberlitic ilmenites. Megacryst and lamellar ilmenite–clinopyroxene intergrowths are found in the Malaita alnöite (Nixon and Boyd 1979b).

Table 6.14 and Figure 6.17 show that these ilmenites overlap the Mg-poor portion of the kimberlitic ilmenite field. However, they differ markedly from the latter in being poor in Cr (<500 ppm), Ni (<100 ppm), and Nb (<100 ppm).

A cumulate or phenocrystal origin has in general been favored as appropriate for these ilmenites. Nixon and Boyd (1979b) are the exception in believing that the Malaita ilmenites are simple mantle xenocrysts. A cognate relationship is, however, strongly supported by Green and Sobolev's (1975) demonstration that magnesian ilmenites (Table 6.14) form over a wide range of high pressures and temperatures as primary liquidus phases in melts derived from pyrolite-related or basanitic compositions.

It is therefore unreasonable to expect that magmas derived from increasing depths, e.g., the sequence basalt–basanite–alnöite–kimberlite, each pass during their eruption through a zone in the mantle where ilmenite xenoliths only of the appropriate MgO and Fe_2O_3 content can be picked up. It is suggested here that

Table 6.14. Representative Compositions of Ilmenites from Basic Volcanic Rocks[a]

	1	2	3	4	5	6	7	8	9
TiO_2	41.6	53.6	53.63	52.20	49.49	52.51	46.09	53.7	57.1
Al_2O_3	1.0	0.1	0.13	0.30	0.41	0.65	0.96	0.7	0.6
Cr_2O_3	0.0	0.1	0.00	0.00	0.00	0.00	0.01	0.0	1.6
Fe_2O_3	24.4	3.4	3.92	8.89	10.38	9.26	13.88	2.1	0.0
FeO	30.6	35.0	35.6	27.94	36.58	29.40	35.68	37.3	27.4
MnO	0.04	0.07	—	—	0.31	0.35	0.26	0.3	0.2
MgO	3.6	7.0	7.05	10.56	4.27	9.80	3.09	6.0	12.9
	101.6	99.9	100.39	99.69	100.44	101.97	99.97	100.2	99.8
mol %									
$FeTiO_3$	63.2	70.4	71.3	55.0	74.4	57.2	74.8	75.7	54.2
$MgTiO_3$	13.3	25.1	13.0	37.1	15.5	34.0	11.5	21.9	45.3
$MnTiO_3$	0.8	1.4	0.3	0.0	0.6	0.7	0.6	0.6	0.5
Fe_2O_3	22.7	3.1	3.5	7.9	9.5	8.1	13.1	1.9	0.0

[a] 1, 2, Alkali basalt, Mts. Bamenda-Bambouto, Cameroon (Parfenoff 1982); 3, 4, basanite Tahalra, southern Algeria (Leblanc *et al.* 1982); 5, 6, alnöite, Malaita (Nixon and Boyd 1979b); 7, melanephelinite, Kakanui (Reay and Wood 1974); 8, ilmenite crystallized at 27 kbar, 1050°C, 4.5% H_2O from a basanite melt; 9, ilmenite crystallized at 40 kbar, 1100°C, 0.3% H_2O from pyrolite less 40% olivine melt (Green and Sobolev 1975).

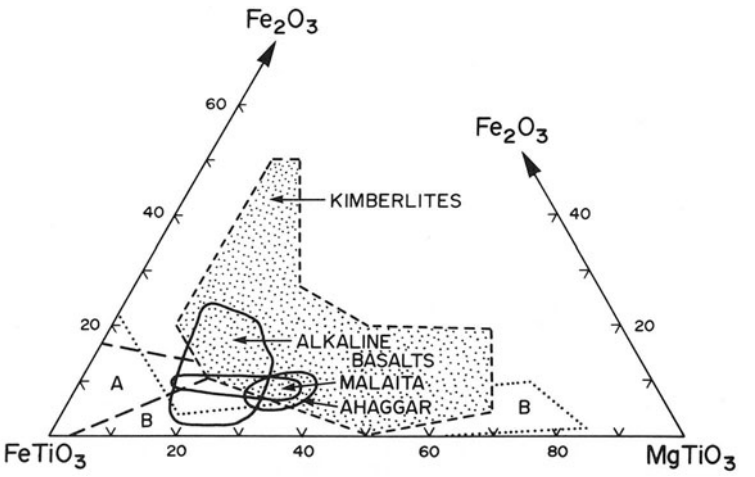

Figure 6.17. Compositional field of kimberlite ilmenites in the system $MgTiO_3$–$FeTiO_3$–Fe_2O_3 compared with those of alkaline basalts (Parfenoff 1982), Malaita alnöites (Nixon and Boyd 1979b) and Ahaggar basanites (Le Blanc *et al.* 1982). Fields A and B delineate the compositions of ilmenites from granites and basalts, and carbonatites, respectively (Gaspar and Wyllie 1983, Mitchell 1978c).

the MgO content of ilmenite in such magmas may be a function of the degree of undersaturation and/or depth of formation of the parent magma and ranging from Mg-poor ilmenites in tholeiites to Mg-rich varieties in kimberlites.

6.3.8.2. Carbonatites

Ilmenites in carbonatites are typically poor in MgO (<5%) and Cr_2O_3 (<0.1%). rich in Nb (<0.5%) and of variable MnO (0.5%–20.0%) content relative to kimberlitic ilmenites. Ilmenites from the Jacupiranga carbonatite are unusual in exhibiting a very wide range in MgO (0%–25%) content. (McMahon and Haggerty 1979, Mitchell 1978c, 1979a, Garanin *et al.* 1979, Gaspar and Wyllie 1983, 1984). Ilmenites from carbonatites and kimberlites can thus be easily distinguished on the basis of their Cr, Nb, and Mn contents.

With respect to the major elements, Figure 6.17 illustrates the compositional range of ilmenites from kimberlites and carbonatites and demonstrates, although some overlap is present, that the compositions are distinctly different. Most kimberlitic ilmenite is relatively rich in hematite and the bulk of the carbonatite data actually clusters near the ilmenite apex (Mitchell 1979a, Gaspar and Wyllie 1983, 1984). Figure 6.18 shows that the compositional overlaps seen in Figure 6.17 are resolved when MnO contents are taken into consideration. Thus Mg-rich, MnO-rich Jacupiranga ilmenites are clearly separated from kimberlite ilmenites of similar MgO content.

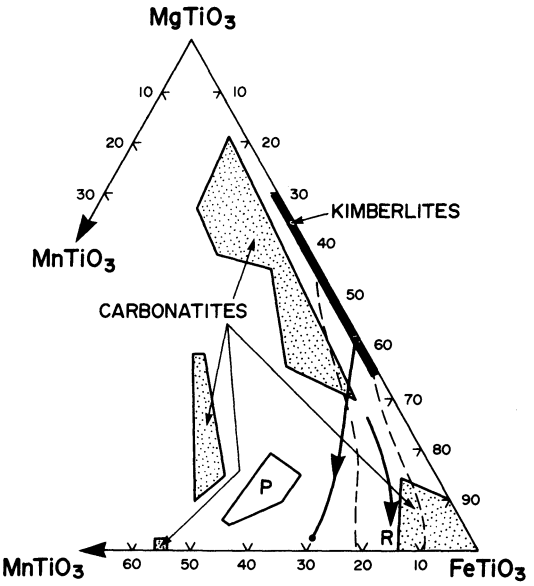

Figure 6.18. Compositional fields of kimberlite ilmenites in the system $MgTiO_3$–$FeTiO_3$–$MnTiO_3$. Stippled fields for carbonatite ilmenites from Gaspar and Wyllie (1983) and Mitchell (1978c). Field P, ilmenites from Premier calcite kimberlite dikes (Gaspar and Wyllie 1984). Field R outlined by dashed lines from Wyatt (1979a) for Premier kimberlites. Points joined by arrow are core (Mg rich) and margin (Mn rich) of an ilmenite from the Premier calcite kimberlite dike (Wyatt 1979a).

As noted above Mn-rich ilmenites do occur in kimberlites. They are, however, rare and most examples are of indeterminate origins or are produced by reaction with late-stage fluids and thus may not be primary liquidus phases. Megacryst, macrocryst, and primary groundmass ilmenites are not Mn-rich. The manganoan ilmenites from Premier (Figure 6.18) are anomalous, of uncertain origin (Wyatt 1979a, Gaspar and Wyllie 1984), and not characteristic of carbonate-rich kimberlites or kimberlites in general.

On the basis of the available data it is unwise to postulate genetic links between kimberlites and carbonatites using ilmenite compositions (Gaspar and Wyllie 1984) and in attempting to compare ilmenites the paragenesis must be taken into account. Many of the Mn-rich ilmenites from carbonatites occur as sub-solidus oxidation "exsolution" lamellae in spinels. The Mn enrichment is a result of the preferential partitioning of Mn into the rhombohedral phase and is not therefore a magmatic feature. Ilmenites originating by this process should not be directly compared with kimberlite ilmenites. One example only of oxidation "exsolution" ilmenites has been reported from a kimberlite. This ilmenite from the Wesselton pre-pipe dike (Gaspar and Wyllie 1984) is enriched in MnO (2%–9%) due to a subsolidus partitioning of Mn into the "exsolved" phase.

6.4. PYROXENE

Clinopyroxenes are common as megacryst and groundmass phases. Orthopyroxenes are relatively much rarer and occur only as megacrysts or exsolution intergrowths with clinopyroxene. The amounts, sizes, and proportions of pyroxenes vary widely between intrusions.

Stephens and Dawson (1977) have attempted statistically to classify pyroxenes found in the kimberlitic environment, in a manner analogous to their scheme for garnets (Dawson and Stephens 1975). The classification has not been extensively utilized, perhaps because of the relative paucity of pyroxene in many kimberlites, its rapid decomposition in the weathering environment, and the ease with which many pyroxenes can be characterized by color alone.

6.4.1. Clinopyroxene

Clinopyroxene occurs primarily in the following parageneses: (1) monomineralic megacrysts, (2) lamellar intergrowths with ilmenite, (3) granular intergrowths with and inclusions in ilmenite and garnet, (4) macro- and micro-exsolution intergrowths with orthopyroxene, (5) as a microphenocrystal or groundmass phase in hypabyssal kimberlites, (6) as cryptocrystalline primary or deuteric groundmass aggregates as microlites in diatreme facies kimberlite.

Parageneses 1–3 may all be considered as part of, or related to, the megacryst suite, and for convenience are discussed together. Megacryst pyroxenes have been divided into a Cr-poor and a Cr-rich suite by Eggler *et al.* (1979). The Cr-poor suite is, however, the characteristic pyroxene megacryst suite of most kimberlites.

6.4.2. Megacrysts and Clinopyroxene–Ilmenite Intergrowths (Parageneses 1 and 2)

Low-Cr megacrysts are typically smoothly rounded nodules up to 15 cm in diameter. They are commonly covered by a creamy-white alteration coat consisting of a very fine grained mixture of serpentine, calcite, and chlorite. Similar alteration occurs adjacent to fractures within the crystal. The pyroxenes range in color from grey-green (subcalcic diopsides) to dark, bottle green (low Cr-diopsides). Fragmented megacrysts are thus easily distinguished from bright, emerald green Cr-rich diopsides of lherzolitic parentage but not from jadeitic pyroxenes derived from eclogites. Megacrysts occur as single crystals; deformed and recrystallized aggregates appear to be absent. Small rounded-to-anhedral inclusions of ilmenite or garnet occur rarely. Bimineralic nodules, consisting of low Cr-garnet and low Cr-megacryst pyroxene, are termed griquaite by Nixon and Boyd (1973b) to distinguish them from modally similar, but mineralogically

different eclogites. Some pyroxenes contain exsolved orthopyroxenes and garnet (see Section 6.4.3). Lamellar intergrowths with ilmenite have been described above (Section 6.3.3); pyroxenes in these intergrowths are single crystals.

Megacrystal pyroxenes are known from all kimberlite provinces; however, few detailed studies of their compositional variation have been undertaken. The principal investigations to date are the following: various Lesotho occurrences (Boyd and Nixon 1973), Monastery (Gurney *et al.* 1979), Colorado–Wyoming (Eggler *et al.* 1979), Orapa (Shee and Gurney 1979, Tollo 1982), East Griqualand (Nixon and Boyd 1979a), Lekkerfontein (Robey and Gurney 1979), Koidu (Haggerty and Tompkins 1984), Hamilton Branch (Schulze 1984). Other studies which include megacryst pyroxene data are for kimberlites from Kao (MacGregor 1979), various Kimberley area pipes (Boyd and Nixon 1978), Camutue (Boyd and Danchin 1980), Fayette County (Hunter and Taylor 1984), Lake Ellen (McGee and Hearn 1984), Mzongwana (Boyd *et al.* 1984b), Bellsbank, Frank Smith, and Koffiefontein (Meyer and McCallister 1984).

Representative megacryst compositions are given in Table 6.15. From the above-cited works the following generalizations can be advanced:

(1) Megacrysts are more Fe-rich than comparable pyroxenes in lherzolites found in the same intrusion (Figure 6.21).

(2) They are characterized by low Cr_2O_3 (<1%), TiO_2 (<1%), Al_2O_3 (<3%), and Na_2O (<2%) contents (Table 6.15). The low Al_2O_3 and Na_2O serve to distinguish them from eclogitic pyroxenes and the low Cr_2O_3 from lherzolite Cr-diopsides.

(3) Megacrysts show a substantial range in their Ca/(Ca+Mg) ratios, corresponding to compositions ranging from subcalcic diopside to diopside. Each megacryst suite appears to be characterized by a slightly different range in Ca/(Ca + Mg), although the overall compositional trends are similar, e.g., Monastery (0.31–0.43), Colorado–Wyoming (0.36–0.47), Letseng-la-Terae (0.31–0.36), and Camutue (0.35–0.43). Representative compositional trends are illustrated in Figure 6.19.

(4) Pyroxenes occurring as lamellar intergrowths with ilmenite have consistently higher Ca/(Ca + Mg) ratios than ilmenite-free megacrysts from the same intrusion (Figure 6.19). The most calcic pyroxenes are found as small inclusions in ilmenite megacrysts (paragenesis 3). The most magnesian ilmenite megacrysts within any one kimberlite are associated with the pyroxenes having the highest Ca/(Ca + Mg) ratios.

(5) Changes in the Ca/(Ca + Mg) ratio are not accompanied by correspondingly significant changes in Mg/(Mg + Fe) ratios. At Monastery and Sloan-Nix the Mg/(Mg + Fe) decreases slightly until the pyroxenes become associated with ilmenite, after which Mg/(Mg + Fe) remains constant (Figure 6.19). Other suites however show no inflec-

Table 6.15. Representative Compositions of Clinopyroxenes[a]

	1	2	3	4	5	6	7	8	9	10	11	12	13	14	15	16	17	18
SiO_2	55.27	55.20	54.79	54.12	54.55	55.31	54.02	55.0	55.4	55.4	53.60	54.08	53.7	54.3	53.94	54.73	54.8	54.1
TiO_2	0.33	0.33	0.29	0.42	0.46	0.39	0.52	0.32	0.19	0.13	0.50	0.50	0.60	0.57	0.48	0.54	0.01	0.07
Al_2O_3	2.55	2.54	2.56	2.67	2.76	2.53	2.30	1.93	1.43	1.20	2.56	2.85	3.04	2.32	2.25	2.36	4.29	0.86
Cr_2O_3	0.33	0.30	0.27	0.44	0.20	0.02	0.01	0.83	2.43	1.50	0.08	0.06	0.18	0.38	0.08	0.04	1.17	0.52
FeO[b]	5.76	5.34	5.79	4.96	5.76	6.36	5.52	3.7	2.9	2.6	6.25	6.48	5.60	4.54	4.46	5.47	1.34	3.78
MnO	0.15	0.14	0.15	0.16	0.16	0.13	0.11	0.09	0.12	0.11	0.16	0.15	0.15	0.15	0.16	0.13	0.06	0.12
MgO	21.26	20.78	19.89	19.48	18.90	16.91	17.40	17.6	18.4	18.8	17.95	17.99	17.8	18.3	18.06	17.28	15.8	17.1
CaO	13.11	13.62	14.20	14.99	15.52	17.29	18.75	19.3	17.8	19.8	16.13	15.44	16.4	16.8	18.30	19.11	19.1	22.4
Na_2O	1.49	1.52	1.63	1.96	1.92	1.84	1.51	1.44	1.55	0.99	1.79	2.07	2.00	1.55	1.38	1.32	2.80	0.66
	100.25	99.77	99.57	99.20	100.23	100.78	100.15	100.17	100.20	99.5	99.02	99.62	99.5	98.91	99.13	101.03	99.3	99.6
Structural formula based on 6 oxygens																		
Si	1.973	1.979	1.977	1.963	1.965	1.991	1.963	1.978	1.987	1.971	1.964	1.967	1.956	1.977	1.968	1.968	1.972	1.978
Al	0.107	0.107	0.109	0.114	0.117	0.011	0.098	0.081	0.061	0.051	0.111	0.122	0.130	0.099	0.096	0.099	0.182	0.037
Ti	0.009	0.009	0.008	0.011	0.012	0.107	0.013	0.009	0.005	0.004	0.014	0.014	0.016	0.015	0.013	0.014	0.000	0.002
Cr	0.009	0.009	0.008	0.013	0.006	0.001	0.000	0.024	0.069	0.043	0.002	0.002	0.005	0.010	0.002	0.001	0.030	0.015
Fe	0.172	0.160	0.175	0.150	0.174	0.191	0.167	0.111	0.087	0.079	0.192	0.197	0.171	0.138	0.136	0.164	0.040	0.116
Mn	0.005	0.004	0.005	0.005	0.005	0.004	0.003	0.003	0.004	0.003	0.005	0.005	0.005	0.004	0.004	0.003	0.002	0.004
Mg	1.132	1.111	1.070	1.054	1.015	0.907	0.942	0.944	0.985	1.016	0.981	0.976	0.968	0.993	0.982	0.925	0.848	0.933
Ca	0.501	0.523	0.059	0.583	0.599	0.667	0.729	0.756	0.685	0.770	0.633	0.602	0.638	0.653	0.715	0.736	0.738	0.879
Na	0.103	0.106	0.114	0.138	0.134	0.128	0.105	0.101	0.108	0.070	0.127	0.142	0.141	0.109	0.097	0.092	0.196	0.047
Ca/(Ca + Mg)	0.307	0.320	0.339	0.356	0.371	0.424	0.436	0.445	0.410	0.431	0.392	0.381	0.397	0.397	0.429	0.443	0.465	0.485
Mg/(Mg + Fe)	0.868	0.874	0.860	0.875	0.854	0.826	0.849	0.895	0.919	0.927	0.837	0.832	0.850	0.878	0.878	0.849	0.955	0.889

[a] 1, Solane (Nixon and Boyd 1973b); 2, 3, Thaba Putsoa (Nixon and Boyd 1973b); 4, 5, Letseng-1a-terae (Bloomer and Nixon 1973); 6, Monastery (Gurney *et al.* 1973); 7, Mukorob-2 (this work); 8, Cr-poor, Colorado–Wyoming (Eggler *et al.* 1979); 9, 10, Cr-rich, Colorado–Wyoming (Eggler *et al.* 1979); 11–16, clinopyroxenes in lamellar intergrowths with ilmenite from Mothae (Nixon 1973a), Kao (Rolfe 1973), Artur de Paiva (Boyd and Danchin 1980), Hamilton Branch (Garrison and Taylor 1980), Deutsche Erde-1 (this work), respectively; 17, 18, clinopyroxenes from intergrowths with orthopyroxenes (Table 6.17, analyses 15, 16), Koffiefontein (Meyer and McCallister 1984).

[b] Total Fe calculated as FeO.

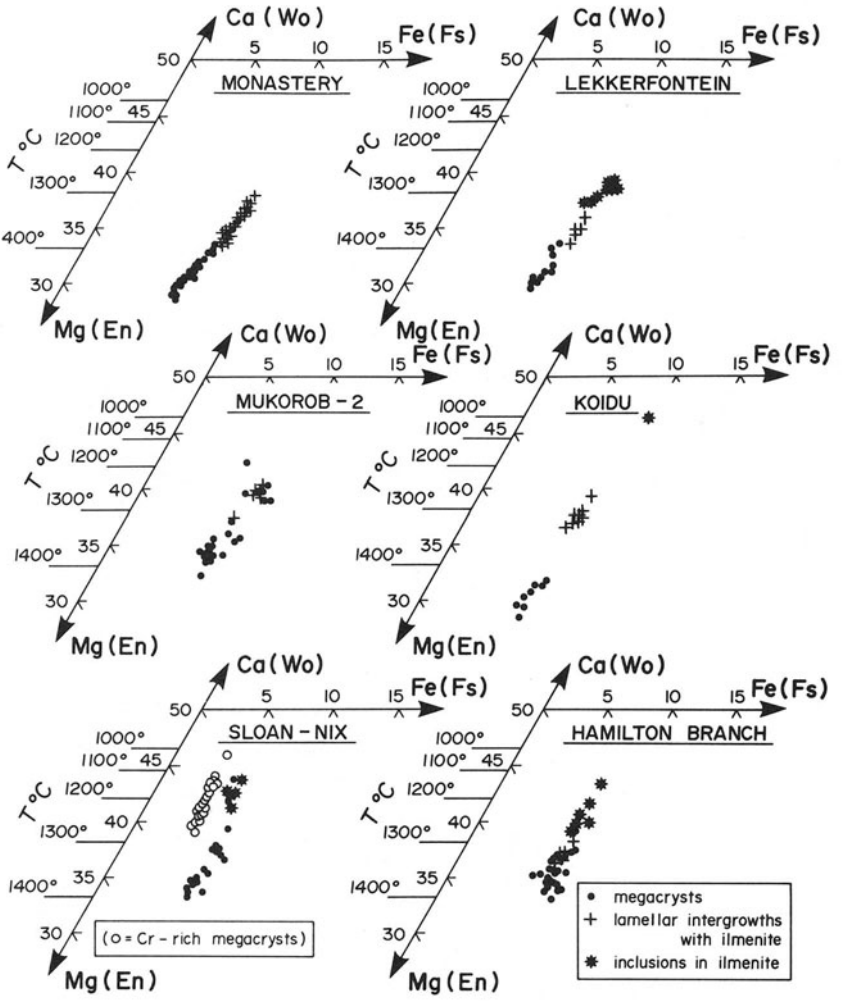

Figure 6.19. Representative compositional trends of megacryst clinopyroxenes from the Monastery (Gurney *et al.* 1979), Lekkerfontein (Robey and Gurney 1979), Mukorob-2 (this work), Koidu (Tompkins and Haggerty 1984), Sloan-Nix (Eggler *et al.* 1979), and Hamilton Branch (Schulze 1984) kimberlites.

tion in the Ca/(Ca + Mg) trend which can be correlated with the crystallization of ilmenite, and the Mg/(Mg + Fe) ratio remains constant, e.g., Lekkerfontein, Hamilton Branch (Figure 6.19) or increases slightly, e.g., Iron Mountain, with respect to increasing Ca/(Ca + Mg) ratios.

(6) Compositional trends for minor elements are not systematic. At Monastery Cr_2O_3 decreases with increasing Ca/(Ca + Mg); however, no

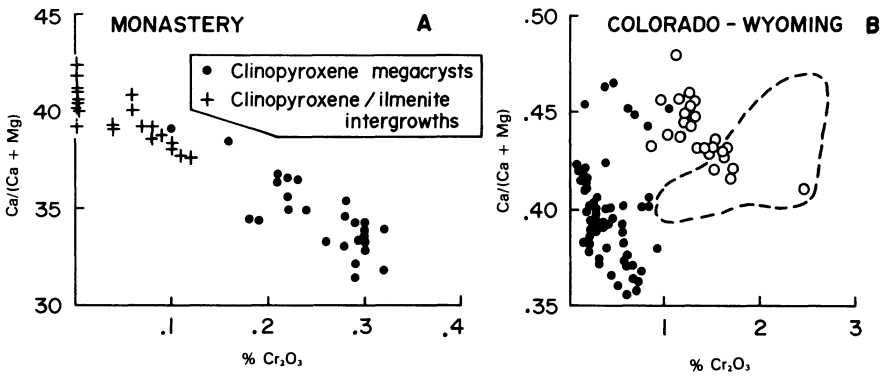

Figure 6.20. Variations of Ca/(Ca + Mg) versus Cr_2O_3 content for megacryst clinopyroxenes from (A) Monastery (Gurney *et al.* 1979) and (B) Colorado–Wyoming (Eggler *et al.* 1979) kimberlites. Solid points are Cr-poor pyroxenes, open circles are Cr-rich pyroxenes. Field defined by the dashed line is for Cr-diopsides in Colorado–Wyoming lherzolites.

correlation is found for Colorado–Wyoming megacrysts (Figure 6.20). Also, at Monastery TiO_2 increases as Ca/(Ca + Mg) increases until ilmenite becomes associated with the pyroxene, after which TiO_2 decreases. In contrast, Hamilton Branch megacrysts show no TiO_2–Ca/(Ca + Mg) correlation. Where Mg/(Mg + Fe) is found to vary, decreases in this ratio are accompanied by a decrease in Cr_2O_3 content (Figure 6.21). The Al_2O_3, Cr_2O_3, and Na_2O contents are apparently independent of each other.

(7) Assuming that the megacrysts crystallized together with orthopyroxene and garnet (Boyd and Nixon 1973) it is possible to estimate their temperatures of formation. Regardless of the geothermometer chosen, the range of Ca/(Ca + Mg) indicates crystallization over a wide range of temperatures, and that the ilmenite–pyroxene intergrowths have consistently formed at lower temperatures than the ilmenite-free pyroxenes. Figure 6.19 illustrates pyroxene compositional trends with respect to the Lindsley and Dixon (1976) pyroxene solvus at 20 kbar and shows that for this geothermometer, Koidu pyroxenes for example crystallized from 1450°C to 1000°C.

(8) If the range in Ca/(Ca + Mg) actually reflects the temperatures of formation of the pyroxenes, then the trends seen in Figures 6.19, 6.20, and 6.21 are consistent with the initial crystallization of pyroxene megacrysts followed by the pyroxene–ilmenite intergrowths as the parent magma differentiates. The constant or slightly increasing Mg/(Mg + Fe) ratios are compatible with this model only if the magma is buffered with respect to Fe and Mg. Schulze (1984) has shown that the crystallization of silicate alone will lead to a decrease in their Mg/(Mg + Fe) ratios, but once ilmenite begins to crystallize this ratio

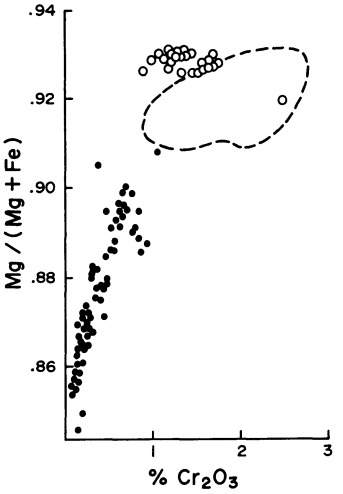

Figure 6.21. Variation of Mg/(Mg + Fe) with Cr_2O_3 content for megacryst clinopyroxenes from Colorado–Wyoming kimberlites (Eggler *et al.* 1979). Symbols and dashed line as in Figure 6.20.

will be held constant or will decrease depending upon the amount of ilmenite formed. For trends of approximately constant Mg/(Mg + Fe) the amount of ilmenite fractionation cannot exceed 15 wt % using reasonable values for Fe and Mg distribution coefficients. Hence the subtle differences in the pyroxene compositional trends shown in Figure 6.19 may be attributed to differences in the amounts of ilmenite crystallization.

(9) Temperature–compositional relations between megacrystal pyroxenes and intergrowth pyroxenes are compatible with a crystallization origin for the lamellar intergrowths, and that sub-solidus breakdown of TiO_2-rich garnets and pyroxenes (Ringwood and Lovering 1970, Dawson and Reid 1970) can be discounted. Williams (1932), Gurney *et al.* (1973) and Wyatt (1975) have proposed that the intergrowths are a product of eutectic crystallization. Such an explanation is not tenable in that ilmenites and pyroxenes both show a range of compositions and that this range is but a part of a broader compositional trend (Figure 6.19). Such relationships are not possible unless the eutectic composition and temperature were changing with respect to pressure and vapour composition. It is unlikely that random changes in such parameters would produce the similar trends seen in Figure 6.19.

Wyatt's (1977) study of the crystallization of an ilmenite–clinopyroxene mixture does not actually demonstrate a eutectic. The bulk composition chosen for study is considered to be eutectic by inference, yet this composition does not crystallize eutectically, although the crystallization sequence observed results in an apparent binary eutectic after crystallization of clinopyroxene alone. The

join ilmenite–clinopyroxene is thus a pseudobinary system and the intergrowth may be the result of cotectic crystallization of skeletal ilmenite surrounded by faster growing pyroxene plates (Frick 1973). Importantly, Wyatt's (1977) study mirrors the crystallization sequence of pyroxenes deduced from pyroxene geothermometry.

Williams (1932) and Mitchell (1977) noted that pyroxene–ilmenite lamellar intergrowths are crystallographically analogous to quartz–feldspar graphic intergrowths, i.e., a trigonal mineral enclosed in a monoclinic single-crystal host. Smith (1974), reviewing the evidence for the origin of graphic granite, concluded that lamellar or graphic intergrowths are not the result of either eutectic or cotectic crystallization, but are the product of simultaneous crystallization of quartz and feldspar under vapor-rich conditions, their formation depending upon epitaxial kinetic factors. A similar origin must be considered for the ilmenite–pyroxene intergrowths.

6.4.2.1. Cr-Rich Megacryst Suite

High Cr_2O_3 megacryst pyroxenes (Table 6.15) were initially recognized by Eggler and McCallum (1976) from the Colorado–Wyoming kimberlites. These differ from their low-Cr counterparts (Cr_2O_3 = 0.08%–1.0%; Mg/(Mg + Fe) = 0.83–0.91) in being richer in Cr_2O_3(0.8%–2.4%) and magnesium (Mg/(Mg + Fe) = 0.92–0.93). Their Ca/(Ca + Mg) ratios (0.41–0.48) are similar to those of the low-Cr suite. The compositional distinction between the two groups is shown in Figures 6.19, 6.20, and 6.21. These Cr-rich pyroxenes are very similar to pyroxenes in lherzolite xenoliths (Figures 6.20 and 6.21) and they are considered to be a part of the megacryst suite primarily on the basis of their size.

Subsequently, Shee and Gurney (1979) reported the presence of Cr-rich and Cr-poor pyroxenes at Orapa, although, unlike the Colorado–Wyoming occurrences these high Cr-pyroxenes are not accompanied by other Cr-rich megacrysts. Orapa Cr-rich pyroxenes have similar Cr_2O_3 contents (0.7%–2.9%) and Ca/(Ca + Mg) ratios (0.44–0.49) and a wider range in Mg/(Mg + Fe) ratios (0.86–0.92) as compared with Colorado–Wyoming pyroxenes.

Hunter and Taylor (1984) consider that Cr-rich (1.86%–2.3% Cr_2O_3) pyroxene inclusions in Cr-rich olivines from the Fayette County dike are also a part of the Cr-rich megacryst suite.

Boyd *et al.* (1984a) consider that the only *bona fide* occurrence of the Cr-rich megacryst suite is in the Colorado–Wyoming kimberlites. The high-Cr_2O_3 pyroxenes from Orapa are similar, e.g., Na < Al + Cr, to Cr-rich pyroxenes found in sheared ilmenite and phlogopite-bearing "Granny Smith diopsides" megacrysts (Boyd *et al.* 1984a) and MARID-suite xenoliths. These latter nodules are considered not to be cognate with kimberlite.

6.4.3. Pyroxene–Garnet Intergrowths (Paragenesis 3)

As noted in Chapter 2, polymineralic intergrowths of megacryst phases are rare and low-Cr-pyroxene–low-Cr-garnet intergrowths are absent in most kimberlites. Two examples have been reported from Monastery (Gurney *et al.* 1979). The intergrowths seem to be relatively abundant at Thaba Putsoa, where they occur as griquaite nodules (Boyd and Nixon 1973). Figure 6.22 illustrates the compositions of co-existing garnets and pyroxenes from these two localities and demonstrates clearly that these phases are compositionally identical to single crystal megacrysts of pyroxene or garnet. Equilibration temperatures calculated from either the pyroxene solvus or garnet–pyroxene Fe–Mg equilibria, are in agreement that increasing Ca/(Ca + Mg) and decreasing Mg/(Mg + Fe) occurs in response to fractional crystallization of the parent magma with decreasing temperature.

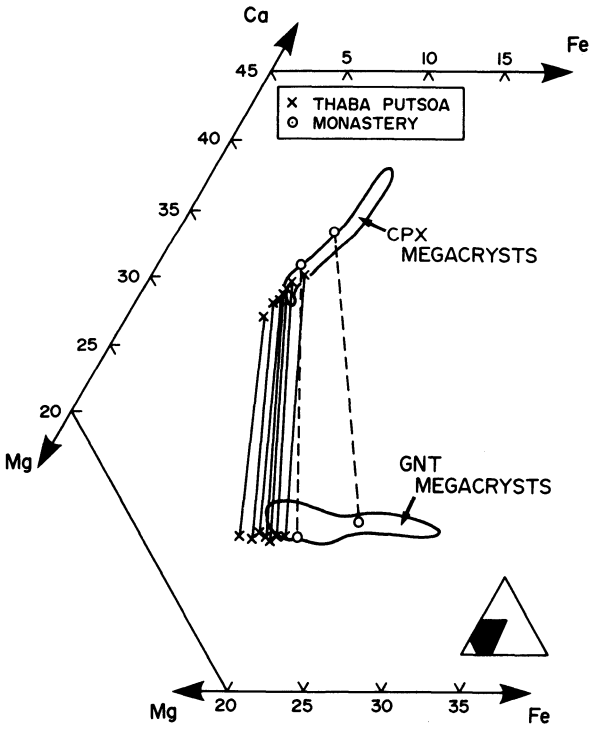

Figure 6.22. Co-existing garnet and clinopyroxene in griquaites (Nixon 1973c) from Thaba Putsoa (Nixon and Boyd 1973b) and megacrysts from Monastery (Gurney *et al.* 1979). Fields of clinopyroxene (CPX) and garnet (GNT) megacrysts for Monastery after Gurney *et al.* (1979).

6.4.4. Pyroxene–Exsolution Intergrowths (Paragenesis 4)

Macroscopic intergrowths of pyroxene formed by exsolution have been described by Aoki *et al.* (1980), Clarke and Pe-Piper (1983), and Meyer and McCallister (1984) from the Koffiefontein, Bellsbank, and Frank Smith kimberlites. The intergrowths consist of clinopyroxene hosts with exsolved orthopyroxenes or *vice versa*. The former are better developed than the latter due to the assymetry of the two pyroxene solvus, the steep Mg-rich limb precluding a large amount of exsolution of clinopyroxene from orthopyroxene hosts. Many examples also contain discontinuous lamellae of garnet, and Clarke and Pe-Piper (1983) have reported exsolution of ilmenite, chromite, and rutile in an intergrowth from Frank Smith. The pyroxenes have exsolved as lamellae parallel to their host's {100} planes, followed by garnet, in cases in which the pyroxenes are sufficiently aluminous, along pyroxene {110} and {010} planes. Some of the lamellar intergrowths are partially recrystallized to granular intergrowths.

Figure 6.23 shows compositional relationships between the exsolved phases

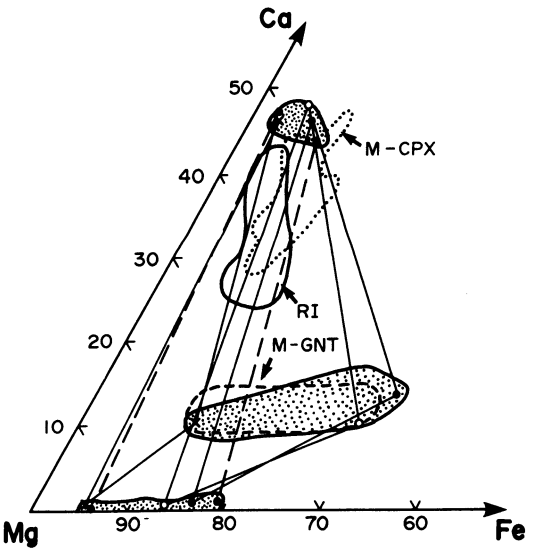

Figure 6.23. Compositions of co-existing clinopyroxene, orthopyroxene, and garnet (stippled fields) from two pyroxene exsolution intergrowths. Three phase triangles illustrate the compositions of representative co-existing phases from Bellsbank and Monastery (Meyer and McCallister 1984). Compositional fields of megacryst clinopyroxenes (M-CPX) and garnets (M-GNT) are from Figures 6.19 and 6.6, respectively. RI is the compositional field of reconstituted intergrowths from Aoki *et al.* (1980) and Meyer and McCallister (1984).

and the homogeneous megacrysts. The clinopyroxenes have high Ca/(Ca + Mg) ratios (0.45–0.49) and are Fe-poor relative to the megacrysts. The orthopyroxenes are similar to megacrystal orthopyroxenes (Section 6.4.8) in their Mg/(Mg + Fe) ratios (0.80–0.95) and are characterized by very low CaO contents (0.05%). Pigeonites are notably absent. Garnets are low-Cr–low-Ti varieties, very similar in composition to megacryst garnets.

Estimation of the original bulk compositions prior to exsolution (Figure 6.23) indicates that the precursor phases were subcalcic diopsides, which Meyer and McCallister (1984) consider to have formed at temperatures from 1500–1300°C. Calculated sub-solidus equilibration parameters demonstrate that exsolution occurred over a wide range of pressures and temperatures and was not isobaric, e.g., Bellsbank 960–740°C from 52–33 kbar, Koffiefontein 930–820°C from 43–34 kbar. Sub-solidus exsolution of pyroxene is analogous to sub-solidus reduction "exsolution" found in ilmenites. No correlation between the occurrence of two pyroxene intergrowths and ilmenite–spinel intergrowths is evident. Although both types are common at Frank Smith, two pyroxene intergrowths are apparently absent at Monastery. In this context however Meyer and McCallister (1984) have noted that kimberlites containing two pyroxene macroscopic intergrowths are apparently poor or lacking in homogeneous subcalcic diopsides and *vice versa*. Clearly, some subcalcic pyroxenes have been held at sub-solvus temperatures sufficiently long enough for exsolution to occur while others have been rapidly quenched. Meyer and McCallister (1984), on the basis of experimentally determined diffusion coefficients for pigeonite–diopside intergrowths (Brady and McCallister 1983), believe it would take at least 60 Ma. for these intergrowths to form. This observation, together with the apparent geotherm defined by the intergrowth equilibration parameters, is taken as evidence that the intergrowths are not cognate with their host kimberlite; however, Meyer and McCallister (1984) have neglected to consider the effects of megacryst–kimberlite interaction during transport and the validity of the application of volatile-free solid state diffusion data to exsolution in crystals in a volatile-rich kimberlite magma.

McCallister and Nord (1981) have demonstrated that many, apparently homogeneous, subcalcic diopsides exhibit exsolution microstructures which can be recognized only by transmission electron microscopy. Significant exsolution of pigeonite as coherent (001) lamellae occurs only in subcalcic pyroxenes with Ca/(Ca + Mg) $\leq$ 0.32. McCallister and Nord (1981) attribute the exsolution to spinoidal decomposition and the megacrysts have been quenched at various stages of completion of the decomposition process. The presence of a minor jadeite component in the pyroxenes results in the inhibition of exsolution at pressures greater than those equivalent to a depth of 15 km. Thus spinoidal decomposition is considered to have occurred at shallow levels (less than 15 km) and at temperatures initially in excess of 1000°C.

6.4.5. Microphenocrystal/Groundmass Pyroxenes in Hypabyssal Kimberlite (Paragenesis 5)

In hypabyssal facies of micaceous kimberlite, diopside is a characteristic microphenocrystal and/or groundmass phase, and can comprise 10%–40% of such kimberlites (Skinner and Clement 1979, Scott 1981). It occurs rarely and only as a late crystallizing groundmass phase in other varieties such as serpentine–calcite kimberlites, but it is important to realize that most hypabyssal kimberlites, including apparently *all* monticellite-bearing types, lack diopside entirely.

Microphenocrystal diopsides are prismatic euhedral to subhedral crystals up to 1.5 mm in length but typically less than 0.5 mm. Commonly they are flow aligned and contain tiny inclusions of phlogopite, spinels, and fluids. Usually they are corroded and apparently not in equilibrium with their current hosts. The pyroxenes are rarely twinned and very weakly zoned from colorless cores to very pale yellow-green margins.

Groundmass diopsides are acicular-to-prismatic (0.1–0.5 mm) euhedral crystals randomly incorporated in phlogopite plates or forming the borders of calcite–serpentine segregations. Euhedral crystals project from the diopside-phlogopite-rich groundmass into such segregations indicating that crystallization of diopside occurred contemporaneously with and after phlogopite formation. In some kimberlites there occur radial aggregates of acicular crystals in ocelli-like structures which have either a sharp or gradational margin towards their host groundmass. Some of these structures may represent replaced micro-xenoliths (Clement 1982), as similar diopsides can be found partially replacing crustal micro-xenoliths, earlier diopsides or other minerals. Very fine grained (<0.1 mm) brownish cryptocrystalline aggregates, similar to those found in diatreme-facies kimberlites, occur in some hypabyssal kimberlites.

Table 6.16 and Figure 6.24 demonstrate that the phenocrystal and groundmass pyroxenes are essentially pure diopsides with very little solid solution toward other end-member pyroxenes, although some examples from Premier and Schuller are sufficiently iron-rich to be considered salites. The pyroxenes typically contain less than 1 wt % TiO_2, Al_2O_3, or Na_2O and are notably Cr_2O_3 poor (<0.5%). In many examples, Na > Al + Cr, implying the presence of some Fe^{3+} (Table 6.16). Generally insufficient Si or Al^{IV} is present to occupy fully all of the tetrahedral sites, and Al^{IV} is thus typically absent.

Characteristic compositional trends have not yet been identified. Available data (Figure 6.24) indicate that, unlike pyroxenes in many alkaline rocks, primary late-stage kimberlite pyroxenes have a very restricted compositional range. Individual pipes appear to be characterized by pyroxenes of a particular composition but it should be emphasized that most of the fields shown on Figure 6.24 are defined by few (<10 in most cases) analyses, and that studies of pyroxene

Table 6.16. Representative Compositions of Groundmass Clinopyroxene[a]

	1	2	3	4	5	6	7	8	9	10
SiO_2	54.39	53.78	54.79	54.27	53.80	53.75	54.19	52.47	53.94	54.63
TiO_2	0.22	0.57	0.14	0.26	0.62	0.79	0.57	0.20	1.08	0.25
Al_2O_3	0.01	0.01	0.00	0.02	0.25	0.43	0.29	1.61	0.39	1.22
Cr_2O_3	0.00	0.00	0.12	0.12	0.15	0.15	0.25	0.13	0.12	0.13
Fe_2O_3[b]	0.36	0.70	1.26	2.52	0.77	0.93	0.88	1.93	3.17	4.20
FeO	1.32	2.43	1.55	2.53	2.10	2.68	2.03	8.98	3.96	0.76
MnO	0.13	0.21	0.09	0.16	0.09	0.11	0.06	0.44	0.17	0.18
MgO	17.78	16.70	16.75	15.64	16.92	17.21	17.36	11.71	14.12	15.46
CaO	25.58	25.11	24.68	23.93	24.52	24.56	24.50	22.21	22.90	21.88
Na_2O	0.14	0.27	0.49	0.98	0.30	0.36	0.34	0.75	1.23	1.63
	99.90	99.78	98.88	100.43	99.53	100.96	100.47	100.43	101.08	100.34
Structural formula based on 6 oxygens										
Si	1.998	1.971	1.994	1.981	1.970	1.948	1.965	1.961	1.969	1.997
Al^{IV}	0.000	0.000	0.000	0.001	0.011	0.018	0.012	0.039	0.017	0.023
Al^{VI}	0.000	0.000	0.000	0.000	0.000	0.000	0.000	0.032	0.000	0.029
Ti	0.006	0.016	0.004	0.007	0.017	0.022	0.016	0.006	0.030	0.007
Cr	0.000	0.000	0.004	0.004	0.004	0.004	0.007	0.004	0.004	0.004
Fe^{3+}	0.010	0.019	0.035	0.069	0.021	0.025	0.024	0.054	0.087	0.114
Fe^{2+}	0.040	0.075	0.047	0.077	0.065	0.081	0.062	0.281	0.121	0.023
Mn	0.004	0.007	0.003	0.005	0.003	0.003	0.002	0.013	0.005	0.006
Mg	0.964	0.913	0.909	0.852	0.924	0.930	0.939	0.653	0.769	0.835
Ca	0.998	0.987	0.964	0.937	0.963	0.955	0.953	0.891	0.897	0.850
Na	0.010	0.019	0.035	0.070	0.021	0.025	0.024	0.054	0.087	0.115
$Mg/Mg+Fe^{2+}$	0.960	0.924	0.951	0.917	0.934	0.920	0.938	0.699	0.898	0.974
Ca/Ca+Mg	0.509	0.519	0.515	0.523	0.512	0.507	0.504	0.577	0.582	0.504

[a] 1, 2, Orroroo (Scott Smith *et al.* 1984); 3, 4, Premier Type 3 (Scott and Skinner 1979); 5, 6 New Elands (this work); 7, 8, Swartruggens (Skinner and Scott 1979); 9, 10, Schuller (Scott and Skinner 1979).

[b] Fe_2O_3 calculated from Na content as acmite.

compositions to date have been of an exploratory rather than a systematic nature. Robey (1981) considers that the Silvery Home pyroxenes show a calcium enrichment trend with slightly decreasing or virtually constant Mg/(Mg + Fe) ratio. Scott Smith *et al.* (1984) have noted that pyroxenes occurring in reaction coronas around micro-xenoliths are richer in Al_2O_3 than isolated groundmass pyroxenes.

6.4.6. Pyroxenes in Diatreme Facies Kimberlite (Paragenesis 6)

As noted in Chapter 3, diatreme facies kimberlites commonly contain pelletal lapilli and xenoliths which have been replaced by crypto-crystalline aggregates of diopside and phlogopite and that similar pyroxenes occur as irregular segregations. Analyses of this very fine grained material are not available. Diop-

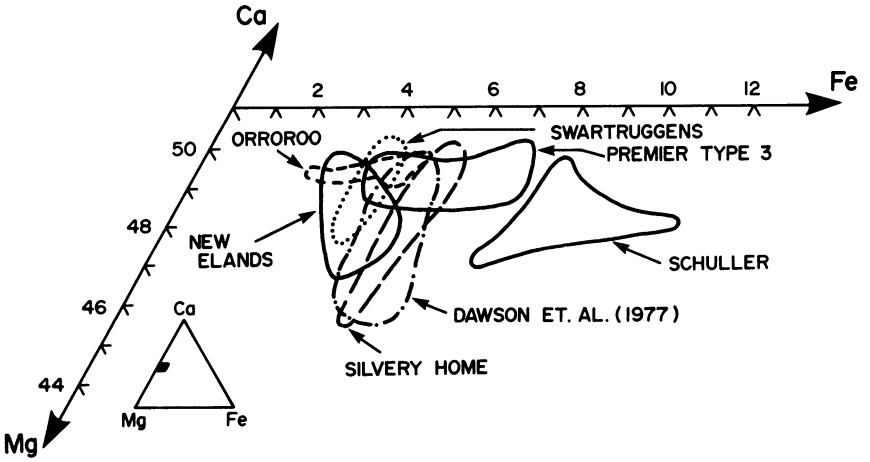

Figure 6.24. Compositional fields of groundmass clinopyroxenes from the Orroroo (Scott Smith *et al.* 1983), Swartruggens (Skinner and Scott 1979), Premier (Scott and Skinner 1979), Schuller (Scott and Skinner 1979), New Elands (this work), Silvery Home (Robey 1981), and diverse South African (Dawson *et al.* 1977) kimberlites.

sides in the Premier type-3 kimberlite (Scott and Skinner 1979), which is the closest in character to diatreme facies kimberlite, are not significantly different in composition from the other pyroxenes.

Regarding parageneses 5 and 6, it is clear that diopside can occur as a primary liquidus phase or be formed as a result of reactions between xenoliths and the host magma. The formation of diopside and its antipathetic relationship to monticellite are discussed in Section 9.9.

6.4.7. Clinopyroxenes of Similar Compositions in Alkaline Rocks

Megacrystal pyroxenes are found in many alkaline magmas, e.g., minettes (Ehrenberg 1982), the alnöitic diatremes at Malaita, Fen, and Ile Bizard (Nixon and Boyd 1979b, Mitchell 1979a, 1983), nephelinites, basanites, and alkali basalts (Binns 1969, Wilkinson 1975, Chapman 1976, Berger and Vannier 1984). They are similar in occurrence to megacrysts found in kimberlite in that they form as large rounded glassy single crystals or lamellar intergrowths with garnet and are commonly associated with a variety of mantle-derived ultramafic nodules. The megacrysts differ in being aluminous (>4%Al_2O_3) and richer in FeO than kimberlite megacrysts, and thus are predominantly aluminous subcalcic diopside, aluminous augites, and salites. Ehrenberg (1982) considered that the Al_2O_3 content of megacrystal pyroxenes increases in the order kimberlite–minette–alnöite–basanite–alkali basalt, reflecting the different pressures of formation of these magmas, with the calcium tschermak's component prefer-

entially partitioning into co-existing garnet with increasing pressure. Experimental studies by Thompson (1974) do not support this conclusion as the Al_2O_3 content of liquidus pyroxene crystallized from a variety of magmas, was found to increase with pressure regardless of the presence or absence of garnet. Thompson (1974) concludes that it is not possible to deduce the relative P–T conditions of pyroxenes from these diverse magmas.

Petrologists studying megacrysts from alkaline magmas are, however, unanimous, with the exception of Nixon and Boyd (1979b), in thinking that the pyroxenes are high-pressure liquidus phases, a conclusion supported by several experimental studies (Chapman 1976, Thompson 1974), and there seems to be no *a priori* reason why their conclusions should not be extended to include kimberlitic megacrysts.

Al-poor diopsides, with a Si and Al tetrahedral site deficiency, identical in composition to kimberlite microphenocrysts and groundmass pyroxenes, are found in lamproites as phenocrysts. Pyroxenes in lamproites crystallize early and do not form late-stage microcrystalline aggregates analagous to those of the kimberlite groundmass, as K-Ti-richterite replaces diopside as a liquidus phase during the later stages of crystallization (Mitchell 1985, Scott Smith and Skinner 1984a).

Pyroxenes in potassic rocks and lamprophyres are easily distinguished from all kimberlite pyroxenes in that they are enriched in TiO_2 (1%–6%) and Al_2O_3 (1%–13%), form euhedral strongly zoned crystals and evolve from Ti–Al salites and augites to acmitic varieties (Mitchell 1979a, Rock 1977, 1984).

6.4.8. Orthopyroxene

Orthopyroxene occurs primarily as megacrysts up to 17 cm in diameter, and is generally less abundant than other megacrysts and subordinate to clinopyroxene. Some kimberlites, e.g., Frank Smith and Letseng-la-terae, are however particularly rich in orthopyroxene and in such kimberlites it is more abundant than clinopyroxenes. In other kimberlites orthopyroxenes are known only as inclusions in garnets and ilmenites, e.g., Lekkerfontein and Koidu. Megacryst orthopyroxenes are not as well-rounded as other megacrysts, and orthopyroxene is commonly found as prismatic fragments exhibiting "cockscomb" ridges and terminations (Bloomer and Nixon, 1973, Nixon and Boyd 1973a), probably as a consequence of the exceptionally well-developed cleavage. The orthopyroxene megacrysts are brownish in color and easily distinguished from pale green lherzolitic orthopyroxene. Exsolution intergrowths with clinopyroxene and orthopyroxene–ilmenite lamellar intergrowths are described above (Sections 6.4.2 and 6.4.4).

Representative compositions are given in Table 6.17, which shows the orthopyroxenes to be essentially Ti-bronzites (Stephens and Dawson 1977) characterized by low CaO (<1.5%), Al_2O_3 (<1.5%), and Cr_2O_3 (<1.5%). Relatively

Table 6.17. Representative Compositions of Orthopyroxenes[a]

	1	2	3	4	5	6	7	8	9	10	11	12	13	14	15	16
SiO_2	56.45	55.47	57.31	55.49	58.85	57.05	56.4	55.25	57.0	58.4	57.2	57.1	56.7	56.7	58.2	55.6
TiO_2	0.20	0.16	0.20	0.16	0.00	0.08	0.25	0.04	0.34	0.04	0.13	0.18	0.29	0.23	0.01	0.05
Al_2O_3	1.12	0.80	1.30	0.75	0.92	0.78	0.81	3.07	1.16	0.68	0.71	1.12	1.00	0.82	0.91	0.43
Cr_2O_3	0.14	0.02	0.12	0.02	0.28	0.17	0.31	0.98	0.17	0.34	0.61	0.41	0.16	0.02	0.09	0.15
FeO[b]	6.96	9.93	7.30	10.94	3.63	8.28	6.3	6.41	6.91	5.04	4.9	5.98	7.23	8.09	4.03	11.6
MnO	0.16	0.19	0.10	0.13	0.09	0.13	0.15	0.16	0.09	0.09	0.14	0.16	0.18	0.16	0.06	0.20
MgO	32.26	31.41	32.12	30.89	35.63	33.44	34.2	33.79	33.3	35.6	35.3	34.0	33.8	33.2	36.6	31.7
CaO	1.43	0.76	1.53	0.80	0.29	0.24	0.70	0.31	1.09	0.43	0.95	1.20	1.17	0.93	0.25	0.32
Na_2O	0.32	0.19	0.27	0.26	0.07	0.00	0.12	0.04	0.22	0.09	0.20	0.24	0.20	0.16	0.04	0.01
	99.04	98.93	100.25	99.51	99.77	100.17	99.24	100.04	100.28	100.71	100.19	100.39	100.73	100.27	100.19	100.06
Si	1.978	1.970	1.984	1.970	2.003	1.979	1.962	1.911	1.970	1.985	1.962	1.968	1.957	1.969	1.979	1.964
Al	0.046	0.033	0.053	0.031	0.037	0.032	0.033	0.125	0.046	0.027	0.029	0.044	0.041	0.034	0.000	0.002
Ti	0.005	0.004	0.005	0.004	0.000	0.002	0.007	0.001	0.008	0.001	0.003	0.004	0.008	0.006	0.023	0.011
Cr	0.004	0.001	0.003	0.001	0.007	0.005	0.009	0.026	0.004	0.009	0.017	0.010	0.004	0.000	0.002	0.004
Fe	0.204	0.295	0.211	0.325	0.103	0.240	0.183	0.185	0.200	0.143	0.141	0.172	0.209	0.235	0.114	0.343
Mn	0.005	0.006	0.003	0.004	0.003	0.004	0.004	0.004	0.002	0.002	0.004	0.004	0.005	0.005	0.002	0.006
Mg	1.685	1.663	1.657	1.634	1.808	1.729	1.775	1.741	1.713	1.803	1.806	1.745	1.740	1.718	1.857	1.670
Ca	0.054	0.029	0.057	0.030	0.011	0.009	0.026	0.011	0.040	0.015	0.035	0.043	0.043	0.035	0.009	0.012
Na	0.022	0.013	0.018	0.018	0.005	0.000	0.008	0.002	0.014	0.006	0.013	0.016	0.013	0.010	0.003	0.001
Mg/(Mg + Fe)	0.892	0.849	0.887	0.834	0.946	0.878	0.907	0.904	0.895	0.927	0.928	0.910	0.893	0.880	0.942	0.830

[a] 1, 2, Letseng-la-terae (Bloomer and Nixon 1973); 3, 4 and 5, 6, groups I and II, respectively, Monastery (Gurney *et al.* 1979); 7, Cr-poor Colrado–Wyoming (Eggler *et al.* 1979); 8, Mukorob-1 (this work); 9, 10, groups I and II, respectively, Hamilton Branch (Garrison and Taylor 1980); 11, Cr-rich Colorado–Wyoming (Eggler *et al.* 1979); 12, Cr-rich Fayette County (Hunter and Taylor, 1984); 13, lamellar intergrowth with ilmenite, Frank Smith (Pasteris *et al.* 1979); 14, intergrowth with lamellar and granular ilmenite, Weltevreden (Meyer *et al.* 1979); 15, 16 macroscopic intergrowths with clinopyroxenes (Table 6.15, analyses 17, 18), Koffiefontein (Meyer and McCallister 1984).

[b] Total Fe expressed as FeO.

Al_2O_3-rich (2.2%–4.7%) orthopyroxenes are, however, found at Mukorob-1 (Table 6.17).

Cr-rich [Mg/(Mg + Fe) = 0.93–0.92, Cr_2O_3 = 0.69%–0.39%] and Cr-poor [Mg/(Mg + Fe) = 0.92–0.89, Cr_2O_3 = 0.31%–0.06%] groups have been recognized from Colorado–Wyoming kimberlites by Eggler *et al.* (1979). The Cr-rich orthopyroxenes outnumber the Cr-poor types by a factor of 4 in the Sloan-2 kimberlite. Like other members of the Cr-rich megacryst suite, they are distinguished from lherzolitic pyroxenes solely on the basis of their larger size (3 cm). Inclusions of Cr-rich orthopyroxene [Mg/(Mg + Fe) = 0.93–0.91, Cr_2O_3 = 0.60%–0.20%] occurring in a Cr-rich olivine from the Fayette County dike, (Hunter and Taylor 1984) may also be a part of the Cr-rich suite.

From the few studies of orthopyroxene compositional variations that have been undertaken the following generalizations can be drawn:

1. Mg/(Mg + Fe) ratios range from 0.92–0.83 (Figure 6.25). Most of the orthopyroxenes are thus bronzites and are richer in iron than the enstatites of lherzolites (Nixon and Boyd 1973a,b).
2. The most Fe-rich orthopyroxenes are associated with ilmenite, e.g., Lekkerfontein (Robey and Gurney 1979), Hamilton Branch (Schulze 1984).
3. Where discrete ilmenites and lamellar intergrowths with orthopyroxene occur together, e.g. Frank Smith, the most magnesian ilmenites are found in the intergrowths (Pasteris *et al.* 1979).
4. For the Cr-poor suite the Cr_2O_3 content decreases as Mg/(Mg + Fe) decreases, e.g., Colorado–Wyoming (Eggler *et al.* 1979), Letseng-la-terae (Bloomer and Nixon 1973). Cr_2O_3 shows no correlation with CaO and Al_2O_3 in the Colorado–Wyoming megacrysts. For the Cr-rich suite,

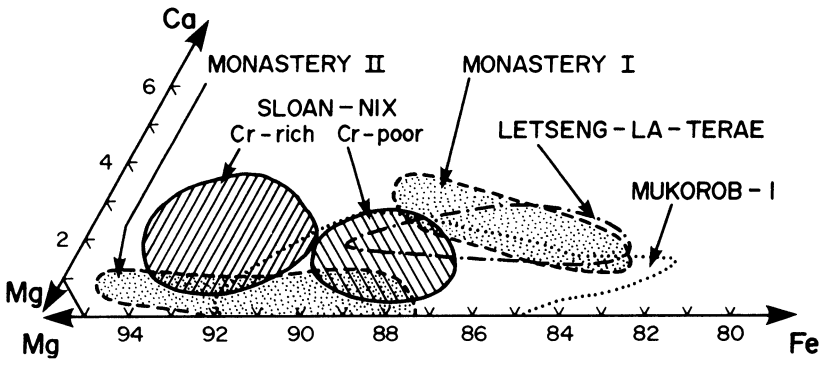

Figure 6.25. Compositional fields of orthopyroxenes from the Monastery (Gurney *et al.* 1979), Sloan-Nix (Eggler *et al.* 1979), Letseng-la-terae (Bloomer and Nixon 1973) and Mukorob-1 (this work) kimberlites.

Cr_2O_3 and Mg/(Mg + Fe) or CaO show no correlation. In contrast, Cr_2O_3 decreases with CaO decrease in the Fayette County Cr-rich inclusions.

5. Minor element variation trends are not consistent, TiO_2 and Al_2O_3 contents fall with decreasing Mg/(Mg + Fe) at Letseng-la-terae (Bloomer and Nixon 1973) and Monastery (Gurney *et al.* 1979), but remain constant at Hamilton Branch (Schulze 1984).
6. Cr-poor orthopyroxenes can be subdivided on the basis of their CaO contents. At Monastery (Figure 6.25), Gurney *et al.* (1979) recognize as group I, homogeneous bronzites with or without ilmenite, defining a trend of decreasing CaO (1.43–0.85) with decreasing MgO [Mg/(Mg + Fe) = 0.88–0.83]. Group-II orthopyroxenes are characterized by Cr-diopside and garnet exsolution and exhibit a wide range in Mg/(Mg + Fe) (0.95–0.88) at approximately constant CaO contents (0.29–0.24). Garrison and Taylor (1980) have distinguished three groups of orthopyroxene in the Hamilton Branch kimberlite. Groups Ia and Ib are relatively high in CaO (1.16%–0.86%), Al_2O_3 (1.01%–0.95%) and iron [Mg/(Mg + Fe) = 0.90–0.88]. Group-Ib pyroxenes are marginally more Fe-rich, but Al_2O_3- and CaO-poor compared to group-Ia pyroxenes, the subgrouping being made upon the differing Cr_2O_3 contents (Ia = 0.18%–0.21%; Ib = 0.03%). Group-II megacrysts are poor in CaO (0.46%–0.35%), Al_2O_3 (0.74%–0.64%) and rich in magnesium [Mg/(Mg + Fe) = 0.93–0.92] relative to group-I megacrysts. Cr_2O_3 contents (0.34%–0.18%) overlap those of group Ia. The groups appear to be equivalent to groups I and II established by Gurney *et al.* (1979) for Monastery orthopyroxenes. Schulze (1984) does not confirm Garrison and Taylor's (1980) findings and considers that many of the pyroxenes discussed by Garrison and Taylor (1980) are xenocrysts. Schulze (1984) notes that bronzites associated with ilmenite are less calcic [Ca/(Ca + Mg + Fe) = 0.19–0.16] and less aluminous (Al_2O_3 = 0.98%–0.96%) than ilmenite-free pyroxenes [Ca/(Ca + Mg + Fe) = 0.25–0.22; Al_2O_3 = 1.3%–1.2%].
7. Ranges in Ca/(Ca + Mg) imply formation or equilibration over a range of temperatures. Estimates using the empirical geothermometer of Boyd and Nixon (1973) for the steep Mg-rich limb of the pyroxene solvus, indicate temperature ranges similar to those determined for megacryst diopsides; e.g., at Monastery; group-I bronzites and diopsides range from 1410–1190°C and 1385–1220°C respectively (Gurney *et al.* 1979). Group-I and -II orthopyroxenes from both Monastery and Hamilton Branch have differing equilibration parameters. Group-II pyroxenes have undergone relatively low-temperature equilibration together with exsolution at 900–1000°C, implying a different origin or thermal history to the associated group-I pyroxenes.

The systematic compositional variations and range in formation temperatures parallel those determined for clinopyroxenes, and support the hypothesis that clino- and orthopyroxenes crystallized contemporaneously from a differentiating parent magma. Evidence in support of the existence of such a parent liquid has been provided by Rawlinson and Dawson's (1979) study of a quench textured pyroxene-ilmenite megacryst from the Weltevreden kimberlite. This large (14-cm) megacryst consists mainly of acicular Ti-bronzite and Mg-ilmenite and exhibits comb-layering and spherulitic textures. The textures were reproduced experimentally by rapidly quenching melts of the megacryst from supraliquidus temperatures (>1450°C) to solidus temperatures (≈ 1200°C) at 20 kbar pressure by Rawlinson and Dawson (1979). The megacryst also contains rare Ti-pyropes similar to megacryst garnets, together with ilmenite–clinopyroxene intergrowths that are interpreted, on the basis of the high Ca/(Ca + Mg) ratios of the pyroxene to be formed from residual fluids after the quench ilmenite–bronzite intergrowths.

Acicular and fasciculate textures in garnet pyroxenites from the Mzongwana kimberlite are interpreted by Boyd *et al.* (1984b) to be rapidly crystallized liquids.

6.4.9. Orthopyroxene–Garnet Intergrowths

Intergrowths with garnet are not common. Boyd (1974b) has described garnet and Cr-diopside which have apparently exsolved from orthopyroxenes in the Frank Smith kimberlite. Dawson (1980), however, is of the opinion that the intergrowths are derived from a lherzolite paragenesis and are not a part of the megacrystal suite.

Meyer *et al.* (1979) have described a unique, large (17-cm), single-crystal, bronzite megacryst from Weltevreden which contains lamellae and granular intergrowths of magnesian ilmenite (12% MgO), and inclusions of polyphase garnets. The most abundant of these are similar in composition to megacryst garnet, are rounded or irregular in habit, and contain spherical inclusions of a pink Cr-rich pyrope. The interface between the garnets contains rounded crystals of ilmenite, olivine, and Cr-diopside. The origins of the textures and the intergrowths remain enigmatic but appear to have formed at high pressures (60 kbar) and temperatures (1200°C).

6.5. OLIVINE

Olivine, the commonest and most characteristic mineral of kimberlite, has three main modes of occurrence: (1) large (>1.0-cm) rounded megacrysts and related porphyroclastic dunites, (2) euhedral-to-subhedral microphenocrysts (<0.5 mm) or groundmass olivines, (3) rounded macrocrysts (0.5–1.0 cm) of indeterminate origins.

The combination of olivines belonging to parageneses 2 and 3 gives rise to the characteristic inequigranular texture of kimberlite (see Chapter 2). Despite the ubiquity of olivine in kimberlite, there have been few detailed studies of its (unfortunately limited) composition variation.

6.5.1. Megacrysts (Paragenesis 1)

Megacrysts which appear to be a part of the discrete nodule suite have been recognized from only a few localities. They form rounded-to-pale yellow or pale brown single crystals from 2–5 cm in diameter and rarely, up to 15 cm. Polycrystalline dunites exhibiting a mosaic porphyroclastic texture are, on the basis of their similar composition and included phases, considered to be deformed and recrystallized megacrysts. The textures are analogous to those developed in megacrystal ilmenites. The inclusions consist of low-Ti and low-Cr megacryst garnets and magnesian ilmenite. Representative compositions are given in Table 6.18.

Initial studies by Nixon and Boyd (1973b) established that megacrystal olivines are typically richer in iron (Fo_{87}) than olivines from porphyroclastic (Fo_{90}) and coarse granular (Fo_{93}) lherzolites from the same localities (Thaba Putsoa and Solane) and thus must have a different origin. The Monastery kimberlite contains megacrysts which fall into two groups, one ranging from Fo_{88-84} with relatively high NiO (>0.2%) contents and another ranging from Fo_{81-78} with low NiO (<0.12%) contents (Gurney *et al.* 1979, Boyd 1974a). Megacryst-type garnets occur as inclusions in the former and magnesian ilmenite in the latter. Insufficient data are available to distinguish whether or not the groups are part of a continuum.

Rare megacryst olivines belonging to Cr-rich (>0.05% Cr_2O_3, Fo_{92-91}) and Cr-poor (<0.05% Cr_2O_3, Fo_{89-88}) groups are known from the Sloan-2 kimberlite (Eggler *et al.* 1979). Hunter and Taylor (1984) and Garrison and Taylor (1980) consider that similar groups are present in the Fayette and Elliot County kimberlites, respectively. However, many of these olivines, in terms of their size, are best described as macrocrysts rather than megacrysts and Schulze (1984) considers that the Cr-rich suite are xenocrysts derived from lherzolites. Cr-poor, Fe-rich (Fo_{85-81}) olivines are, however, present in the Fayette County dike and are undoubtedly a part of the megacryst suite. Porphyroclastic dunites (Fo_{89-88}, NiO = 0.18%–0.32%) containing inclusions of megacrystal garnet and pyroxenes, occur in the Hamilton Branch kimberlite.

Megacrysts from Letseng-la-terae (Dawson *et al.* 1981, Boyd and Nixon 1975) range from Fo_{83}–Fo_{87}, have low NiO (<0.1%) contents, and contain sulfide segregations (pentlandite, godlevskite, heazlewoodite, chalcopyrite) derived from a Ni-rich iron monosulfide precursor fluid that was trapped in the megacrysts during their growth.

Dawson *et al.* (1980) have described porphyroclastic dunites containing

Table 6.18. Representative Compositions of Megacryst Olivines[a]

	1	2	3	4	5	6	7	8
SiO_2	40.30	38.16	40.1	41.2	40.0	40.8	39.3	40.2
TiO_2	0.03	0.02	0.04	0.00	0.04	0.00	0.00	0.03
Al_2O_3	0.08	0.04	0.00	0.04	0.02	0.00	0.00	0.03
Cr_2O_3	0.03	0.00	0.00	0.11	0.01	0.07	0.00	0.01
FeO[b]	11.70	20.40	13.2	8.1	12.0	8.05	15.2	13.65
MnO	0.13	0.20	0.14	0.10	0.16	0.06	0.18	0.12
MgO	48.80	41.30	47.6	50.8	48.2	51.2	45.8	46.2
CaO	0.09	0.03	0.06	0.06	0.04	0.04	0.04	0.08
NiO	0.37	0.06	0.25	0.30	0.20	0.37	0.20	0.27
	101.53	100.21	101.39	100.67	100.51	100.59	100.72	100.59
Si	0.984	0.983	0.986	0.996	0.985	0.988	0.981	0.997
Ti	0.001	0.000	0.001	0.000	0.000	0.000	0.000	0.001
Al	0.002	0.001	0.000	0.001	0.001	0.000	0.000	0.001
Cr	0.001	0.000	0.000	0.002	0.000	0.001	0.000	0.000
Fe	0.239	0.439	0.272	0.164	0.247	0.162	0.317	0.283
Mn	0.003	0.004	0.003	0.002	0.003	0.001	0.003	0.003
Mg	1.776	1.586	1.744	1.832	1.771	1.849	1.708	1.710
Ca	0.002	0.001	0.002	0.002	0.001	0.001	0.000	0.002
Ni	0.007	0.001	0.005	0.005	0.003	0.007	0.003	0.005
Mg/Mg + Fe	0.881	0.783	0.865	0.918	0.878	0.919	0.843	0.858

[a] 1, 2, High- and low-Ni olivine, Monastery (Gurney *et al.* 1979); 3, Frank Smith (Boyd 1974); 4, 5, Cr-rich and Cr-poor olivine, Sloan-2 (Eggler *et al.* 1979); 6, 7, Cr-rich and Cr-poor olivine Fayette County (Hunter and Taylor 1984); 8, mean of 4 megacrysts, Letseng-la-terae, Satellite pipe (Dawson *et al.* 1981).
[b] Total Fe expressed as FeO.

minor magnesian ilmenite, bronzite, and phlogopite from Bultfontein. The olivines (Fo_{94-84}) are similar in their chemistry and size (up to 6.5 cm), to megacryst olivines. Dawson *et al.* (1980) consider that the rocks are cumulates but discount kimberlite as the parent magma and favor a basaltic (Karoo) non-cognate source, despite the similarity of the nodules to the megacryst suite. Similar conclusions are advanced by Carswell *et al.* (1984) for megacrysts (Fo_{84}) from Ngopetsoeu.

Large (10–14-cm) megacrysts described from the Udachnaya pipe have no counterparts in other kimberlites. The olivines are highly magnesian (Fo_{95-93}), poor in Cr_2O_3 (0.03%–0.05%), and CaO (<0.09), and are a part of a diamond-bearing garnetiferous dunite xenolithic paragenesis unrelated to the Fe-rich kimberlite megacrysts (Pokhilenko *et al.* 1977, 1979; Kostrovitskiy and Fiveyskaya 1983).

6.5.2. Groundmass or Microphenocrystal Olivines (Paragenesis 2)

Groundmass olivines occur as small (<0.5 mm) euhedral-to-subhedral single crystals. Clement (1982) estimates that 95% of such olivines in the Kimberley

pipes are smaller than 0.2 mm. Multiple growth aggregates, acicular, skeletal, or hopper crystals are absent. The morphology of the crystals can be modified by alteration and/or minor magmatic corrosion, but there is no evidence that the crystals were grossly out of equilibrium with their host magma. Colors range from very pale green to pale yellowish-brown with increasing Fe content.

The crystals are commonly altered at their margins and along fractures, to several varieties of serpentine with or without magnetite. The serpentinization procedes in several discrete stages, each being recognizable by the formation of an optically distinct serpentine. The alteration is a deuteric phenomenon. Complete pseudomorphing by serpentine is typical of many of the smaller crystals. Serpentine pseudomorphs may be themselves replaced by late-stage calcite, phlogopite, or magnetite. Clement (1982) and Verhoogen (1938) have reported that olivine may be replaced by diopside or monticellite.

Williams (1932), Dawson (1980), and Clement (1982) have listed a wide variety of less common alteration and replacement minerals including brucite, bowlingite, iddingsite, chlorite, clay minerals, talc, quartz, barite, and pyrite. Most of these phases are only developed locally and in general are the result of secondary processes involving groundwater or alteration of deuteric precursors in the weathering environment (Fairbairn and Robertson 1966, Ruotsala 1975).

Magnesian ilmenite, chrome spinel (Dawson 1980, Apter *et al.* 1984), and needle-like rutile (Pasteris 1980a) are present as inclusions in some olivines.

Representative analyses are given in Table 6.19 and the compositional variation summarized in Table 6.21. The principal compositional characteristics of groundmass olivines are:

1. Cores of euhedral olivines in individual kimberlites show a wide range in composition. Boyd and Clement (1977) have shown that these are relatively homogeneous or exhibit weak normal zoning.
2. The margins of the crystals commonly have narrow rims (<200 μm) of olivine which is Fe-rich or Fe-poor relative to the cores. Regardless of whether the "zoning" is normal or reversed, mantle compositions are found to converge upon Fo_{90-87}. These thin mantles are not always observable because of their common replacement during marginal serpentinization. Strong continuous zoning appears to be absent in these olivines.
3. CaO (<0.4%), MnO (<0.5%), Cr_2O_3 (<0.05), Al_2O_3 (<0.05%), and TiO_2 (<0.05%) are all extremely low. Increases in Fe are correlated with increases in CaO (Mitchell 1979a, Jago and Mitchell 1985, Kostrovitskiy and Fiveyskaya 1983).
4. NiO contents range from 0.1% to 0.5% and do not necessarily correlate with Fe or Mg contents, although a general trend of decreasing NiO with increasing FeO is observed (Mitchell 1973a, Apter *et al.* 1984, Tompkins and Haggerty 1984).

Table 6.19. Representative Compositions of Euhedral Groundmass Olivines[a]

	1	2	3	4	5	6	7	8	9	10	11	12
SiO_2	41.30	40.72	40.34	40.39	40.40	40.23	40.5	38.3	40.18	42.34	40.61	40.70
TiO_2	0.00	0.02	0.00	0.00	0.01	0.04	0.00	0.04	0.03	0.00	0.02	0.04
Al_2O_3	0.00	0.05	0.00	0.00	0.02	0.02	0.00	0.05	0.04	0.02	0.06	0.40
Cr_2O_3	0.02	0.00	0.00	0.00	0.00	0.00	0.03	0.03	0.03	0.00	0.03	0.01
FeO[b]	7.29	10.08	12.62	10.71	7.71	8.83	6.77	12.5	14.07	4.70	11.42	10.30
MnO	0.09	0.17	0.14	0.16	0.09	0.14	0.09	0.14	0.14	0.06	0.15	0.07
MgO	50.35	49.40	47.45	48.88	51.38	50.69	50.9	47.6	46.26	54.28	48.18	47.48
CaO	0.04	0.05	0.08	0.18	0.03	0.13	0.03	0.08	0.06	0.00	0.09	0.35
NiO	0.34	0.32	0.18	0.11	0.34	0.25	0.38	0.32	0.25	0.34	0.38	0.28
	99.43	100.41	100.81	100.43	99.98	100.33	98.70	99.06	101.06	101.74	100.94	99.23
Si	1.005	0.992	0.993	0.989	0.984	0.981	0.994	0.967	0.994	0.997	0.995	1.005
Ti	0.000	0.000	0.000	0.000	0.000	0.000	0.000	0.000	0.001	0.000	0.000	0.001
Al	0.000	0.000	0.000	0.000	0.001	0.001	0.000	0.001	0.001	0.001	0.002	0.012
Cr	0.000	0.000	0.000	0.000	0.000	0.000	0.000	0.000	0.001	0.000	0.001	0.000
Fe	0.147	0.205	0.259	0.219	0.157	0.180	0.137	0.263	0.291	0.093	0.234	0.213
Mn	0.001	0.002	0.002	0.002	0.002	0.003	0.001	0.003	0.003	0.001	0.003	0.002
Mg	1.828	1.794	1.841	1.786	1.867	1.844	1.862	1.789	1.706	1.906	1.760	1.749
Ca	0.001	0.001	0.001	0.004	0.001	0.003	0.000	0.001	0.002	0.002	0.004	0.002
Ni	0.006	0.005	0.002	0.001	0.006	0.005	0.007	0.006	0.005	0.006	0.006	0.005
Mg/Mg + Fe	0.929	0.895	0.877	0.891	0.922	0.911	0.931	0.872	0.851	0.953	0.883	0.891

[a] 1, 2, Core and rim, Elwin Bay (Mitchell 1978a); 3, 4, Core and rim, Tunraq (Mitchell 1979b); 5, 6, Core and rim,Orroroo (Scott Smith *et al.* 1984); 7, 8, De Beers Peripheral kimberlite (Clement personal communication); 9, Holsteinsborg (Scott 1981); 10, 11, Liqhobong (Nixon and Boyd 1973c); 12, Udachnaya (Kostrovitsky and Fiveyskaya 1983).

[b] Total Fe expressed as FeO.

It is apparent that groundmass primary liquidus olivines, richer in Fe than Fo_{85}, are not characteristic of kimberlites. The olivines show only a limited range of compositions, implying buffering at constant Mg/Fe ratios or crystallization over a very small temperature interval. The latter is the more likely in view of the paucity of inclusions of contemporaneous phases and the extreme rarity of perovskite and titaniferous spinel inclusions. Crystallization of groundmass olivine apparently ceases prior to the development of the bulk of the groundmass assemblage.

The range in the core compositions observed in any kimberlite, and the uniform composition of their mantles, implies that the groundmass olivine population is the result of mixing of batches of magma containing phenocrysts of slightly different compositions. The normal and reverse zoned mantles reflect attempts by the crystals to equilibrate with the final hybrid magma, precipitating olivines in the compositional range Fo_{90-87}.

6.5.3. Macrocrystal Olivines (Paragenesis 3)

Macrocrysts (0.5–1.0 cm) occur as round-to-elliptical single crystals. Many are embayed and otherwise corroded and it is evident that their shape has been developed by resorption of a precursor crystal of unknown habit. In any given kimberlite the proportions of macrocrysts to groundmass olivines vary widely, even on a centimeter scale, and concentration of macrocrysts by flow differentiation is common. Many of the crystals are strained and exhibit undulose extinction, and in some examples contain marginal or internal zones of mosaic-textured recrystallized olivines. Macrocrysts contain inclusions of, or are intergrown with, enstatite, Cr-pyrope, Ti-pyrope, diopside, ilmenite, chromite, phlogopite, rutile, and Cu–Ni sulfides, and many are characterized by curved planes of secondary, CO_2 fluid inclusions. The greater diversity of inclusions and the presence of deformation features indicate the mixed provenance of macrocrystal olivines.

Alteration and replacement by deuteric and secondary minerals are as described for the groundmass olivines. Commonly relict cores of macrocryst olivines are preserved, while groundmass olivines are entirely pseudomorphed (Mitchell 1973b, Boyd and Clement 1977, Dawson 1980). Graphite has been reported as a replacement mineral by Pasteris (1981) and Scott Smith *et al.* (1984).

Table 6.20 gives representative compositions and Table 6.21 demonstrates that the macrocrysts range in composition from Fo_{76}–Fo_{94}. Boyd and Clement (1977) have shown that the crystals are homogeneous and that zoning is present only as narrow rims (<200 μm) at the crystal margins. These mantles (Table 6.20) are identical to those found upon groundmass olivine and converge upon similar compositions. Due to the wider compositional range of the macrocrysts, reverse zoning is more common.

Table 6.20. Representative Compositions of Macrocrystal Olivines

	1	2	3	4	5	6	7	8	9	10	11	12
SiO_2	41.05	40.63	40.25	40.71	39.3	40.1	37.8	41.36	39.50	41.35	40.75	41.72
TiO_2	0.00	0.00	0.02	0.02	0.00	0.00	0.04	0.00	0.04	0.01	0.05	0.00
Al_2O_3	0.02	0.00	0.02	0.02	0.00	0.00	0.05	0.00	0.03	0.15	0.26	0.17
Cr_2O_3	0.00	0.00	0.00	0.00	0.00	0.00	0.00	0.00	0.00	0.02	0.01	0.10
FeO[b]	7.27	10.78	7.65	9.00	15.2	11.2	15.4	5.87	13.28	5.92	12.75	7.52
MnO	0.10	0.14	0.09	0.11	0.18	0.16	0.17	0.01	0.14	0.12	0.10	0.05
MgO	51.32	48.41	51.06	49.85	45.8	48.5	45.2	51.81	46.24	51.77	46.04	50.05
CaO	0.02	0.07	0.03	0.07	0.04	0.11	0.08	0.00	0.05	0.11	0.12	0.30
NiO	0.25	0.08	0.33	0.32	0.20	0.23	0.32	0.22	0.26	0.50	0.33	0.39
	100.03	100.11	100.05	100.10	100.72	100.30	99.06	99.27	99.54	99.95	100.41	100.29
Si	0.994	0.999	0.985	0.995	0.981	0.989	0.996	1.002	0.990	0.999	1.007	1.009
Ti	0.000	0.000	0.001	0.001	0.000	0.000	0.000	0.000	0.001	0.000	0.000	0.000
Al	0.000	0.000	0.001	0.001	0.000	0.000	0.001	0.000	0.001	0.004	0.008	0.005
Cr	0.000	0.000	0.000	0.000	0.000	0.000	0.000	0.000	0.000	0.000	0.000	0.002
Fe	0.147	0.221	0.157	0.184	0.317	0.229	0.329	0.119	0.278	0.120	0.264	0.152
Mn	0.001	0.002	0.002	0.002	0.003	0.002	0.003	0.000	0.003	0.003	0.002	0.001
Mg	1.855	1.774	1.864	1.817	1.708	1.781	1.721	1.872	1.729	1.865	1.698	1.806
Ca	0.000	0.001	0.001	0.002	0.000	0.002	0.001	0.000	0.001	0.003	0.003	0.008
Ni	0.004	0.001	0.006	0.006	0.003	0.004	0.006	0.003	0.004	0.009	0.006	0.005
Mg/Mg + Fe	0.927	0.889	0.922	0.908	0.843	0.886	0.840	0.940	0.861	0.939	0.865	0.922

[a] 1, 2, Core and rim, Tunraq (Mitchell 1978); 3, 4, Core and rim, Orroroo (Scott Smith *et al.* 1984); 5, 6, Core and rim, Fayette County (Hunter *et al.* 1974); 7, De Beers Peripheral kimberlite (Clement, personal communication); 8, 9, Liqhobong (Nixon and Boyd 1973c); 10, 11, Udachnaya (Kostrovitsky and Fiveyskaya 1983); 12, Eastern Qi-Lu, North China (Zhang and Liu 1983).

[b] Total Fe expressed as FeO.

Table 6.21. Representative Ranges in Composition (mol % forsterite) of Some Phenocrystal and Macrocrystal Olivines

	Phenocrysts		Macrocrysts		
Kimberlite	Core	Rim	Core	Rim	Reference
Peuyuk	91–88	88	93–90		Mitchell and Fritz 1973
Elwin Bay	93.5–88		93.5–88		Mitchell 1978a
Tunraq	92–90	87	92.5–90	90–88	Mitchell 1979b
Jos	93–86		93–86		Mitchell and Meyer 1980
Ham	93–90		93.5–90		Jago and Mitchell 1985
Wesselton	91–88.5	89	94–85.5	90	Mitchell 1973b
Wesselton	89–88		94–91	89	Elthon and Ridley 1979
De Beers	93–87	89	93–84	90	Boyd and Clement 1977
Benfontein	93–88	90–88	91–88	90–85	Dawson and Hawthorne 1973
Mayeng	90–88	88	93–87	88	Apter *et al.* 1984
Orroroo	92–89	90.5	92–91	90.5	Scott Smith *et al.* 1984
W. Greenland			92–76	91–87	Emeleus and Andrews 1975
W. Greenland	85		92.5–78		Scott 1981
Udachnaya	90.5–86.5		93.5–97.5		Kostrovitsky and Fiveyskaya 1983
Udachnaya		90.5	90.5		Ukhanov *et al.* 1982

The range in composition of the macrocrysts includes compositions equivalent to those of the Fe-rich megacrysts and olivines in lherzolite xenoliths and completely overlaps that of the groundmass olivine. Figure 6.26 shows that olivine compositions from the Peuyuk kimberlite (Mitchell and Fritz 1973) have a bimodal distribution with very little overlap between macrocryst and groundmass olivines, and that the macrocrysts have compositions identical to those of lherzolitic olivines. In contrast, in the Elwin Bay kimberlite (Mitchell 1978a) groundmass and megacryst olivines have identical ranges of composition which overlap those of lherzolite olivines. Similar relationships can be observed at other localities, e.g., Jos (Mitchell and Meyer 1980) Tunraq (Mitchell 1979b, De Beers, Boyd and Clement 1977), Wesselton (Mitchell 1973a), Liqhobong (Nixon and Boyd 1973c).

Figure 6.27A shows that the liebenbergite, Ni_2SiO_4 (Ni-olivine), content of the macrocryst olivines from Peuyuk is practically unchanged over a wide range of Fo content, and that the groundmass olivines exhibit a considerable spread in Ni-olivine content at essentially constant Fo content. Overlap of the trends occur at Fo_{91-90}, and Ni_2SiO_4 = 0.3%–0.4%. Similar trends have been determined for olivines from the Tunraq (Mitchell 1979b), Elwin Bay (Mitchell 1978a), and Ham kimberlites (Jago and Mitchell 1985).

Figure 6.27B shows that both Mg-rich and Fe-rich megacrystal and macrocrystal olivines from Fayette County (Hunter and Taylor 1984) are mantled by overgrowths of identical Fo content. The mantles of both types are rich in CaO (>0.1%) relative to their cores (CaO < 0.1%). Mantles of the Mg-rich,

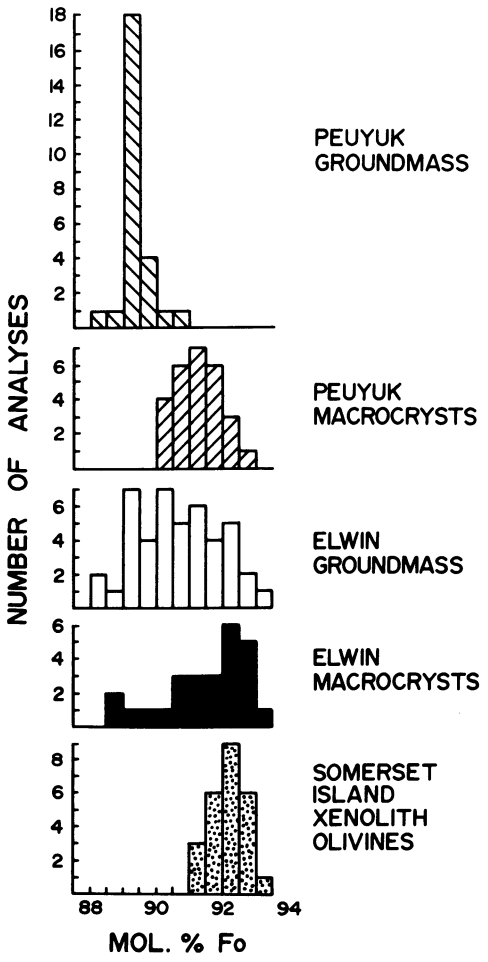

Figure 6.26. Compositions (mol % forsterite) of macrocryst and groundmass olivines from the Peuyuk (Mitchell and Fritz 1973), and Elwin Bay (Mitchell 1978a) kimberlites.

Cr-rich types are depleted in NiO (<0.3%) relative to their cores (NiO > 0.3%). Hunter and Taylor (1984) unfortunately do not present compositional data for groundmass olivines, but it is evident that the megacryst rims are identical to the common groundmass olivine convergence composition of Fo_{90-87}. Similar CaO enrichments and NiO depletions between macrocryst cores and groundmass olivines have been noted by Mitchell (1973a, 1979b) and Kostrovitskiy and Fiveyskaya (1983).

Figure 6.27C shows that Wesselton olivines are very similar to Fayette County olivines and that macrocrystal olivines range from relatively Fe-rich to

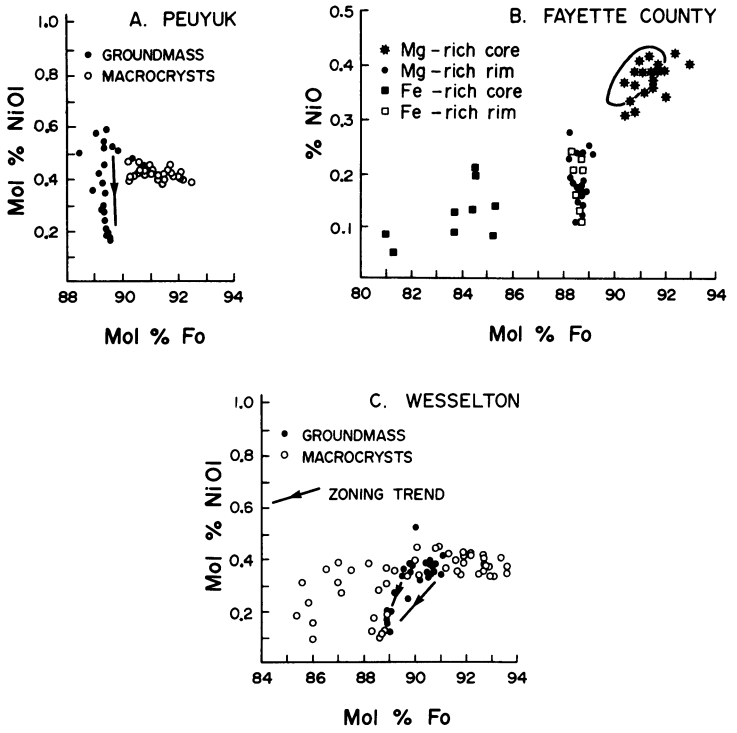

Figure 6.27. Variation of forsterite (Fo) content with nickel content (mol %) Ni_2SiO_4 = Niol or % NiO) for macrocryst and groundmass olivines from (A) Peuyuk (Mitchell and Fritz 1973), (B) Fayette County (Hunter and Taylor 1984), (C) Wesselton (Mitchell 1973).

relatively Mg-rich compositions and have rim compositions that converge upon groundmass olivine compositions.

Conclusions which can be drawn from Figures 6.26 and 6.27 and Table 6.21 are (1) that the macrocryst population may be composed of olivines derived from at least three sources, fragmented megacrysts and porphyroclastic dunites, olivines derived from dis-aggregated lherzolite xenoliths, and true phenocrysts; (2) the macrocrysts and groundmass microphenocrysts have all been randomly mixed and transported in a hybrid magma; (3) all of these olivines have been mantled by olivines crystallizing in equilibrium with this final liquid.

The iron-rich macrocrysts are probably derived from a megacryst source and/or possibly from Fe-rich porphyroclastic lherzolites. However, it is impossible to determine the source of the more magnesian macrocrysts, as phenocrystal and xenocrystal olivines cannot be characterized by any chemical criteria. Even textural criteria, e.g., strain, are unreliable in view of the relative ease with which olivines can be deformed and recrystallized. It is unreasonable to suggest

that all of the Fo-rich macrocrysts are xenocrysts, as the studies of the groundmass olivines have shown that kimberlite magmas can crystallize microphenocrysts of identical composition. There is no *a priori* reason why larger crystals should not form under suitable conditions. These may then form cumulate bodies or phenocrysts which could be collected, resorbed and rounded during extraction of individual batches of magma. Unfortunately it is as yet impossible to estimate the proportions of xenocrystal to phenocrystal olivine in the macrocryst population.

6.6. PHLOGOPITE

Kimberlite phlogopites are divisible into two broad groups: megacrystal and macrocrystal micas, and microphenocrystal and groundmass micas. Minor parageneses are as rims upon olivines or garnets (Hunter *et al.* 1984), as metasomatic replacements of xenoliths and as rare phlogopite-ilmenite nodules (Apter *et al.* 1984).

6.6.1. Megacryst/Macrocryst Phlogopite (Paragenesis 1)

The phlogopites occur as silvery bronze, single crystals ranging from 5 mm up to 10 cm in length. Commonly they are rounded, broken, distorted, or kink banded and show undulose extinction. Replacement by calcite, chlorite, and serpentine, especially along cleavage planes, is common. The margins of most crystals are corroded and embayed and decorated with many small crystals of spinel that are formed during the resorption process. Inclusions are typically absent. In most kimberlites, smaller (<5-mm) micas of identical characteristics can be found. Such micas are considered to be a part of this paragenesis.

The abundance of megacrystal/macrocrystal micas varies widely from rare scattered crystals (<1%) to abundant oriented plates giving the rock a pronounced foliation. In many serpentine–calcite kimberlites they form the bulk of the mica population and groundmass micas may be absent or present only as a minor late stage phase. In some cases there appears to be a definite hiatus in the crystallization sequence of phlogopite, e.g., Elwin Bay and Wesselton. Other kimberlites, e.g., Ngopoetsoeu, appear to have crystallized a continuum of micas ranging from macrocrysts through to tiny groundmass plates and laths. Many macrocrysts are mantled by micas optically and compositionally identical to groundmass micas. The cores may exhibit normal or reversed pleochroism (see Section 6.6.3.9), while mantles commonly show normal pleochroism. The cores may be irregular or rounded with euhedral overgrowths or may be identical in habit to the overgrowth, with the contact between the two phases being sharply defined. Micas of diverse habit and mantling occur in juxtaposition in most kimberlites.

6.6.2. Groundmass/Microphenocryst Phlogopite (Paragenesis 2)

Micas in micaceous kimberlites, e.g., New Elands and Swartruggens, form closely packed mosaics of tabular-to-square cross section microphenocrysts (0.05–1 mm). Many of the crystals are rounded, corroded, and distorted. Some examples are flow-aligned, but the commonly randomly orientated crystals typically grade into reticulate intergrowths of very small plates and euhedral prisms. Extremely fine grained intimate intergrowths with cryptocrystalline diopside occur in many diatreme facies kimberlites.

Groundmass micas typically contain inclusions of spinel and perovskite which can be sufficiently abundant to produce sieve-textured plates and laths. Micas occur within calcite–serpentine segregations (Section 3.7.2), having nucleated at the margins of bounded segregations. They project into less well-defined segregations from the adjacent groundmass. Many groundmass micas are unevenly zoned, apparently as a result of reactions with deuteric fluids. Others are complexly mantled by distinct overgrowths of eastonitic phlogopites and/or tetraferriphlogopites. Cores and mantles can exhibit either normal or reversed pleochroism.

6.6.3. Composition

Representative compositions given in Tables 6.22, 6.23, and 6.24 demonstrate that kimberlitic micas are essentially phlogopites and tetraferriphlogopites that in some cases may contain significant amounts of TiO_2 and Cr_2O_3.

Unfortunately, few systematic studies of mica compositional variation have been undertaken and it is as yet difficult to formulate any but the broadest generalizations regarding crystallization trends. Consequently, individual investigations are described below in order to illustrate the varied character of the mica populations of kimberlites.

6.6.3.1. Diverse South African Kimberlites (Dawson and Smith 1975, Smith et al. 1978)

Dawson and Smith (1975) proposed that megacrystal micas could be characterized on the basis of their Cr_2O_3 (<1.1%) and TiO_2 (<2.0%) contents, and that two groups of megacrysts could be recognized. One group is relatively rich in Cr_2O_3 (>0.5%) and poor in TiO_2 (<0.6%) and FeO (<3.7%), the other being poorer in Cr_2O_3 (<0.5%) and having greater FeO (>3.75) and TiO_2 (0.60%–2.0%) contents (Figure 6.29). The former group is considered to have compositions equivalent to those of primary phlogopites in lherzolites (Carswell 1975, Delaney *et al.* 1980) and therefore possibly to be xenocrysts derived from such a source. The latter group is considered to be made up of phenocrysts. Dawson and Smith (1975, 1977) also note that megacrysts, in terms of their Cr_2O_3–TiO_2 contents,

Table 6.22. Representative Compositions of Megacryst and Macrocryst Phlogopites[a]

	1	2	3	4	5	6	7	8	9	10
SiO_2	39.9	41.45	41.0	41.9	41.5	41.94	38.6	38.10	41.6	42.4
TiO_2	5.4	1.29	1.4	3.0	1.01	1.57	4.52	4.72	1.96	0.6
Al_2O_3	13.8	12.38	11.7	12.3	12.6	12.58	14.4	14.33	12.8	10.1
Cr_2O_3	0.4	0.93	0.1	0.1	0.17	0.18	1.52	1.03	0.24	0.2
FeO[b]	4.8	3.05	5.0	4.4	3.84	4.72	4.89	6.09	4.86	6.5
MnO	0.0	0.06	0.0	0.0	0.03	0.00	0.08	0.06	0.0	0.0
MgO	21.6	26.55	25.3	23.3	25.1	24.47	20.7	20.52	24.6	25.1
CaO	0.0	0.02	0.1	0.0	0.01	0.06	0.0	0.03	0.0	0.1
Na_2O	0.3	0.09	0.3	0.2	0.18	0.02	0.33	0.37	0.15	0.2
K_2O	10.1	9.21	9.6	10.2	10.4	9.85	9.85	9.67	10.4	10.6
NiO	0.1	0.14	0.0	0.0	0.0	0.00	0.00	0.05	0.0	0.0
	96.1	95.17	94.5	95.4	94.54	95.37	94.89	94.97	96.61	95.8
Structural formulas based on 22 oxygens										
Si	5.606	5.836	5.873	5.926	5.901	5.924	5.546	5.499	5.835	6.059
Al	2.304	2.055	1.976	2.051	2.113	2.096	2.440	2.439	2.117	1.702
Ti	0.575	0.137	0.151	0.319	0.108	0.167	0.488	0.513	0.207	0.065
Cr	0.045	0.104	0.011	0.011	0.019	0.020	0.173	0.118	0.027	0.023
Fe	0.569	0.359	0.559	0.521	0.457	0.558	0.588	0.736	0.571	0.777
Mn	0.000	0.007	0.000	0.000	0.004	0.000	0.009	0.007	0.000	0.000
Mg	4.562	5.577	5.406	4.916	5.324	5.156	4.436	4.419	5.148	5.350
Ca	0.000	0.003	0.015	0.000	0.002	0.009	0.000	0.005	0.000	0.015
Na	0.082	0.025	0.083	0.055	0.050	0.055	0.092	0.104	0.041	0.056
K	1.826	1.656	1.756	1.842	1.888	1.776	1.807	1.782	1.863	1.934
Ni	0.010	0.016	0.000	0.000	0.000	0.000	0.000	0.008	0.000	0.000

[a] 1, Tunraq (Mitchell 1979b); 2, Elwin Bay (Mitchell 1978a); 3, 4, Type-A and -B micas, respectively Jos (Mitchell and Meyer 1980); 5, Dutoitspan (Jones and Smith 1984); 6, Swartruggens (Skinner and Scott 1979a); 7, Fayette County (Hunter *et al.* 1984); 8, Holsteinsborg (Scott 1981); 9, Elliot County (Garrison and Taylor 1980; 10, average of eight reversed pleochroic megacrysts, De Beers (Farmer and Boettcher 1981).

[b] Total Fe calculated as FeO.

are similar to those of micas in MARID-suite xenoliths, but that they could be distinguished from the latter on the basis of their higher Mg/(Mg + Fe) contents (Figures 6.30, 6.32).

Smith *et al.* (1978) presented data showing that two types of microphenocrystal and groundmass micas were present in a suite of micaceous kimberlites. Rare, relatively iron-rich types [(Mg/(Mg + Fe) = 0.45–0.65, TiO_2 = 3%–6%, Al_2O_3 = 14%–16%)] with no tetrahedral site deficiency with respect to Si and Al, are designated type-I micas. The ubiquitous groundmass micas, designated type II, are more magnesian [Mg/(Mg + Fe) = 0.82–0.93] and poorer in TiO_2 (0.7%–4.0%) and Al_2O_3 (6.8%–14.2%), resulting in a substantial tetrahedral site deficiency and probably entry of Fe^{3+} into those sites. Type-II micas form mantles upon type-I micas. Smith *et al.* (1978) found no systematic correlations between tetrahedral site deficiency, FeO, TiO_2, Cr_2O_3, and NiO contents or sizes

Table 6.23. Representative Compositions of Groundmass Phlogopite[a]

	1	2	3	4	5	6	7	8	9	10
SiO_2	35.7	40.8	35.9	35.6	40.12	38.95	38.35	37.18	37.78	37.5
TiO_2	3.2	1.4	3.09	1.1	1.40	5.21	2.69	2.07	1.36	3.51
Al_2O_3	15.5	12.3	17.8	18.0	12.54	13.94	13.75	15.40	15.18	14.2
Cr_2O_3	0.0	0.71	0.17	0.0	1.25	0.63	0.04	0.03	0.04	0.17
FeO[b]	21.7	3.7	8.26	3.4	5.08	5.11	5.93	4.42	6.33	5.77
MnO	0.0	0.0	0.13	0.1	0.06	0.03	0.08	0.05	0.09	0.02
MgO	9.9	25.7	19.1	22.4	24.60	21.42	22.95	23.44	22.75	21.6
CaO	0.0	0.0	0.0	0.2	0.09	0.02	0.09	0.01	0.16	0.16
Na_2O	0.1	0.21	0.0	0.1	0.19	0.19	0.13	0.11	0.25	0.39
K_2O	9.5	10.7	10.3	9.2	9.80	10.13	10.08	9.27	8.35	9.48
BaO	n.d.[c]	n.d.	n.d.	n.d.	n.d.	n.d.	n.d.	3.01	2.86	n.d.
NiO	0.0	0.24	0.05	0.1	0.0	0.11	0.03	0.02	0.00	0.0
	95.6	95.76	94.8	90.2	95.13	95.74	94.12	95.01	95.15	92.8
Structural formulas based on 22 oxygens										
Si	5.495	5.792	5.250	5.313	5.739	5.554	5.578	5.422	5.509	5.519
Al	2.813	2.059	3.069	3.168	2.116	2.344	2.359	2.648	2.610	2.465
Ti	0.371	0.149	0.339	0.124	0.151	0.559	0.294	0.227	0.149	0.389
Cr	0.000	0.080	0.020	0.000	0.142	0.071	0.005	0.004	0.005	0.020
Fe	2.795	0.439	1.011	0.425	0.608	0.610	0.722	0.539	0.772	0.711
Mn	0.000	0.000	0.016	0.013	0.007	0.004	0.010	0.006	0.011	0.003
Mg	2.273	5.442	4.167	4.987	5.252	4.556	4.980	5.099	4.949	4.743
Ca	0.000	0.000	0.000	0.032	0.014	0.003	0.014	0.002	0.025	0.025
Ka	0.030	0.058	0.000	0.029	0.053	0.053	0.037	0.031	0.071	0.111
K	1.867	1.939	1.923	1.753	1.791	1.844	1.872	1.726	1.554	1.781
Ba	—	—	—	—	—	—	—	0.172	0.164	—
Ni	0.000	0.026	0.008	0.010	0.000	0.012	0.004	0.003	0.000	0.000

[a] 1, 2, Type-I and -II micas from Montelo and Roberts Victor, respectively (Smith *et al.* 1978); 3, Pyramidefjeld (Emeleus and Andrews 1975); 4, Chloritized Jos type C (Mitchell and Meyer 1980); 5, Swartruggens (Skinner and Scott 1979); 6, 7, Mayeng dark and pale, respectively, (Apter *et al.* 1984); 8, Orroroo (Scott Smith *et al.* 1984); 9, Skinner's sill, Wesselton (Mitchell 1984a); 10, Fayette Co. (Hunter *et al.* 1984).

[b] Total Fe calculated as FeO.

[c] n.d., not determined.

of crystals in type-II micas. Although most crystals were shown to be relatively uniform, considerable inter-grain compositional variation (similar to that found in groundmass olivine cores) was evident. Smith *et al.* (1978) attribute these inter-grain variations to changes in the bulk composition of the parent magma on a millimeter scale, rather than any batch mixing process. Some type-II micas have foxy-red reversed pleochroic margins of tetraferriphlogopite. Both type-I and -II micas are also strongly serpentized at their margins as a result of deuteric alteration. The provenance of the type-I micas is unknown; type-II micas however form as a groundmass liquidus phase. Individual micaceous kimberlites appear to be characterized by subtly different populations of type II micas (Figure 6.28).

Table 6.24. Representative Compositions of Tetraferriphlogopite[a]

	1	2	3	4	5	6	7
SiO_2	39.7	42.6	40.10	42.12	42.51	40.96	41.09
TiO_2	1.7	0.07	0.02	0.32	0.33	4.68	5.40
Al_2O_3	7.6	1.09	0.38	2.23	0.57	1.88	1.05
Cr_2O_3	0.3	0.0	0.0	0.01	0.01	0.0	0.09
FeO[b]	9.7	14.8	15.07	13.82	11.99	28.94	13.46
MnO	0.0	0.27	0.43	0.14	0.14	0.25	0.14
MgO	24.9	25.0	26.29	25.16	27.39	9.91	22.19
CaO	0.0	0.16	0.09	0.34	0.12	0.20	0.0
Na_2O	0.3	0.0	0.06	0.20	0.26	0.24	0.0
K_2O	9.4	8.83	9.80	10.14	10.18	9.25	9.62
BaO	n.d.	n.d.	0.09	0.0	n.d.	0.09	0.52
NiO	0.0	0.0	0.01	0.05	0.01	0.11	0.0
	93.6	92.8	92.44	94.43	93.52	96.25	93.59
Structural formulas based on 22 oxygens							
Si	5.921	6.547	6.313	6.392	6.466	6.516	6.319
Al	1.337	0.198	0.071	0.399	0.102	0.354	0.189
Ti	0.191	0.008	0.002	0.025	0.038	0.563	0.623
Cr	0.035	0.000	0.000	0.001	0.001	0.000	0.009
Fe	1.211	1.903	1.985	1.755	1.526	3.875	1.729
Mn	0.000	0.035	0.057	0.018	0.018	0.034	0.018
Mg	5.540	5.731	6.175	5.696	6.215	2.365	5.087
Ca	0.000	0.026	0.015	0.055	0.020	0.034	0.000
Na	0.087	0.000	0.018	0.059	0.077	0.075	0.000
K	1.789	1.733	1.969	1.964	1.977	1.889	1.887
Ba	—	—	0.006	0.000	—	0.005	0.027
Ni	0.000	0.000	0.002	0.008	0.002	0.015	0.000

[a] 1, Star (Smith *et al.* 1978); 2, Pyramidefjeld (Emeleus and Andrews 1975); 3, Orroroo (Scott Smith *et al.* 1984); 4, Skinner's Sill, Wesselton (Mitchell 1984); 5, Mayeng (Apter *et al.* 1984); 6, Rice Hill lamproite (Mitchell 1981); 7, Hills Pond lamproite (Mitchell 1985).
[b] Total Fe calculated as FeO.

6.6.3.2. Somerset Island Kimberlites (Mitchell 1978a, 1979b, Clarke and Mitchell 1975, Mitchell and Meyer 1980, Jago and Mitchell 1985)

Micas in Somerset Island kimberlites are predominantly macrocrystal in character and, except for the Jos dike micas, are not typically mantled and zoned. Figure 6.29 shows that the macrocrysts exhibit a wide range in their TiO_2 and Cr_2O_3 contents, e.g., Elwin Bay (TiO_2 = 0.6%–3.2%, Cr_2O_3 = 0.0%–1.3%), Tunraq (TiO_2 = 1.5%–5.5%, Cr_2O_3 = 0.0%–1.3%), Peuyuk (TiO_2 = 2.0%–3.5%, Cr_2O_3 = 0.1%–1.0%), Ham (TiO_2 = 0.3%–4.5%, Cr_2O_3 = 0.0%–2.1%), Jos B micas (TiO_2 = 2.5%–5.6%, Cr_2O_3 = 0.0%–0.5%). Although considerable overlap occurs, there is a general trend of increasing TiO_2 from Elwin Bay to Ham/Jos to Tunraq, indicating that individual kimberlites

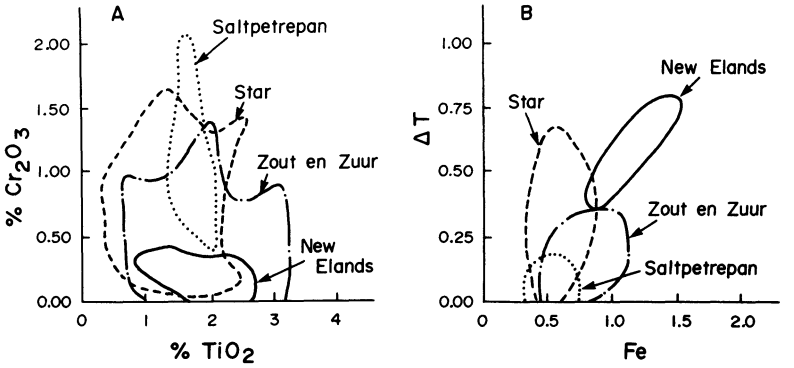

Figure 6.28. A. Cr_2O_3 versus TiO_2 B. Tetrahedral site deficiency (ΔT) versus Fe content for micas from South African kimberlites, after Smith *et al.* (1978).

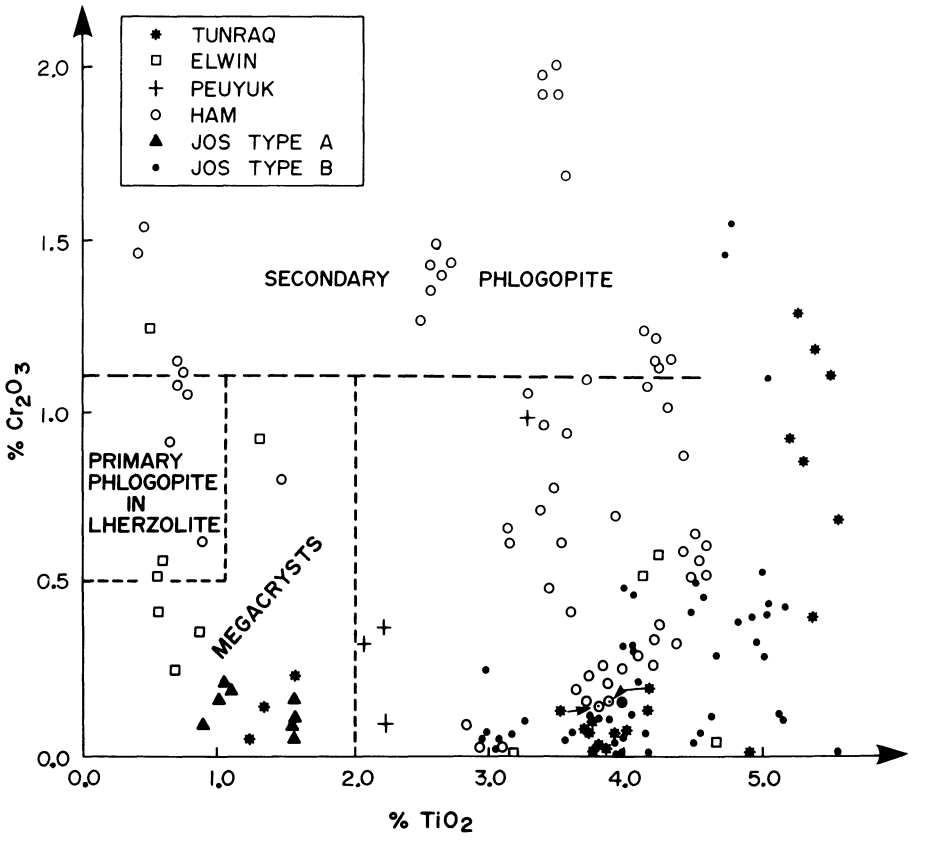

Figure 6.29. Cr_2O_3 versus TiO_2 for macrocrystal micas from Somerset Island kimberlites. See Section 6.6.3.2 for data sources. Fields for megacrystal phlogopite, and primary and secondary phlogopite in lherzolite, from Carswell (1975), and Dawson and Smith (1975).

may be characterized by distinctive macrocryst suites. Few of the macrocrysts have compositions similar to those of primary phlogopite in lherzolites, although some, e.g., Ham, are similar to secondary micas in lherzolites. The major element variation is relatively small and Mg/(Mg + Fe) ratios are similar (0.93–0.87) in all intrusions. Figure 6.29 also indicates that Dawson and Smith's (1975) field of megacryst/macrocryst compositions is too restricted and should be extended up to 6% TiO_2. Figure 6.30 illustrates the oxide range in NiO content of the macrocrysts at essentially constant Mg/(Mg + Fe) ratios and that the Tunraq and Ham micas are richer in NiO than Jos micas. The macrocrysts are similar, in terms of their NiO-Mg/(Mg + Fe) parameters, to South African megacrysts and differ from those of MARID-suite xenoliths.

Three varieties of mica are present in the Jos calcite kimberlite dike. Type-A micas are yellow-brown phlogopites [Mg/(Mg + Fe) = 0.93–0.87] with low Cr_2O_3 (<0.25%) and low TiO_2 (<2.0%) forming anhedral crystals zoned to relatively Fe-rich margins. Type-B phlogopites are darker in color and richer in TiO_2 [2.5%–5.6%, Mg/(Mg + Fe) = 0.93–0.84, Cr_2O_3 = 0.0%–0.6%] and exhibit complex Ti–Cr zonations (Figure 6.31). Considerable intergrain com-

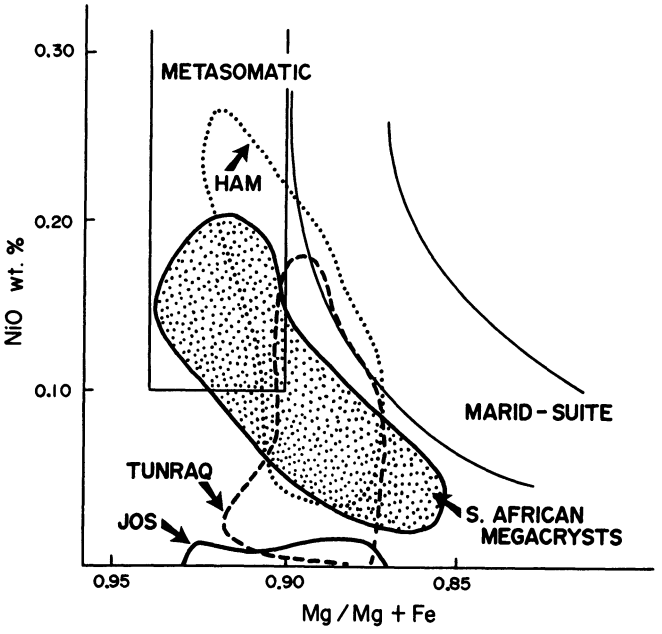

Figure 6.30. NiO versus Mg/Mg + Fe for macrocrystal micas from the Jos (Mitchell and Meyer 1980), Tunraq (Mitchell 1979b), and Ham (Jago and Mitchell 1985) kimberlites. Fields for South African megacrysts, metasomatic and MARID-suite phlogopites, from Dawson and Smith (1975, 1977).

positional variation, analogous to that found by Smith *et al.* (1978) for groundmass mica, is evident. Figure 6.31 shows that a compositional gap in terms of the TiO_2 content exists between type-A and -B micas. Type-B micas show no correlation between size, habit, composition, or degree of distortion. Type-C micas are relatively poor in SiO_2, TiO_2, FeO, and Cr_2O_3 and rich in Al_2O_3 relative to types A and B. Many have been partly replaced by chlorite and/or serpentine but the high Al_2O_3 contents indicate that they originally were eastonitic phlogopites.

Type-A micas are mantled by type B and/or type C, and type B by type-C micas. Type A and B are macrocrysts and have not crystallized *in situ* as have the type-C groundmass micas. Similar Al-rich late-stage micas occur as sieve-textured laths and groundmass plates adjacent to calcite–serpentine segregations

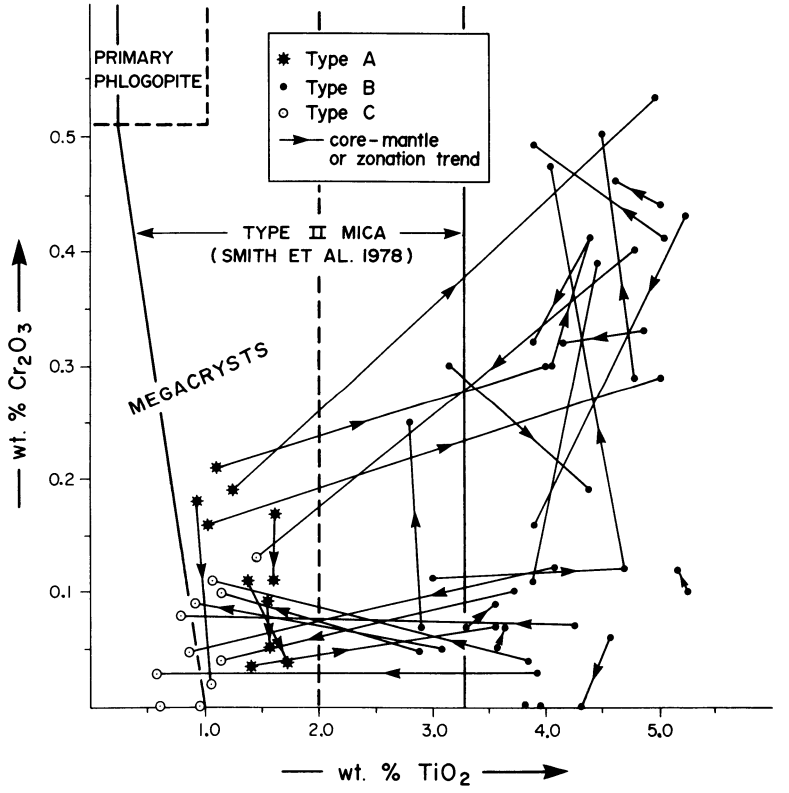

Figure 6.31. Mantling and zonation trends in macrocrystal (type A and B) and groundmass (type C) phlogopites in the Jos (Mitchell and Meyer 1980) kimberlite. Primary phlogopite and megacryst phlogopite fields from Carswell (1975) and Dawson and Smith (1975), respectively.

in the Elwin Bay kimberlite. Red tetraferriphlogopites are not present in the Somerset Island kimberlites.

Figure 6.29 shows that many of the Somerset Island mica macrocrysts have compositions similar to Smith *et al.*'s (1978) type-II micas; however, it is important to note that the latter are groundmass micas, and the two groups may not be directly comparable.

6.6.3.3. Mayeng (Apter et al. 1984)

The Mayeng Sills contain three distinct types of micas (Figure 6.32). Rare macrocrysts are pale-colored, strained phlogopites [Mg/(Mg + Fe) = 0.91–0.89, TiO_2 = 1.2%–1.4%, Cr_2O_3 = 0.02%] identical in their composition to micas in ilmenite-phlogopite nodules (see below). Groundmass micas are either dark-colored titaniferous (TiO_2 = 4%–6%) varieties of variable Cr_2O_3 (0%–1.0%), and relatively constant FeO (4.5%–5.4%) content, or pale, relatively TiO_2-poor, (2.5%–2.9%) low-Cr_2O_3 (<0.2%) types which exhibit a wider range in FeO (5%–8%) content. The dark micas contain inclusions of ilmenite, and in different sills are rimmed either by the pale micas or by tetraferriphlogopite. These latter phases appear to be mutually exclusive and reflect vastly different redox conditions during the final stages of groundmass formation. The pale micas are similar to Smith *et al.*'s (1978) type-II micas and the dark micas are akin to Mitchell and Meyer's (1980) type-B macrocrysts. All of the Mayeng sills contain the dark groundmass micas which probably crystallized over a wide interval, overlapping matrix ilmenite, and followed by later TiO_2-poor phlogopites containing groundmass spinel inclusions. The rare macrocrysts are probably derived from dis-aggregated phlogopite-ilmenite nodules and correspond in composition to some megacrysts from South African kimberlites or to micas in MARID-suite xenoliths (Figure 6.32). Compositions of co-existing ilmenites are similar to macrocryst ilmenites (MgO = 11%–16%, Cr_2O_3 = 1.1%–1.5%). Similar ilmenites occurring as inclusions in olivine indicate that there was an overlap in the crystallization times of olivine, Cr-poor ilmenite and Ti-rich phlogopite.

6.6.3.4. Fayette County (Hunter et al. 1984)

Macrocrysts (0.5–1.0 cm) are rimmed by stronger pleochroic micas similar in optical properties and composition to groundmass laths (100 × 10 μm). The macrocryst cores are richer in Cr_2O_3 (1.3%–1.8%) and TiO_2 (4.5%–5.0%) and slightly poorer in FeO (4.6%–5.5%) than the rims (Cr_2O_3 = 0.1%–1.0%, TiO_2 = 3.6%–4.5%, Fe 0.49%–6.0%). Groundmass micas are Cr_2O_3-poor (<0.2%) and have a wider range in TiO_2 (1.7%–4.5%) and FeO (5.4%–8.3%) content. Figure 6.33 shows clearly that the evolutionary trend of the Fayette County micas was toward decreasing Cr_2O_3 at relatively constant TiO_2 and FeO,

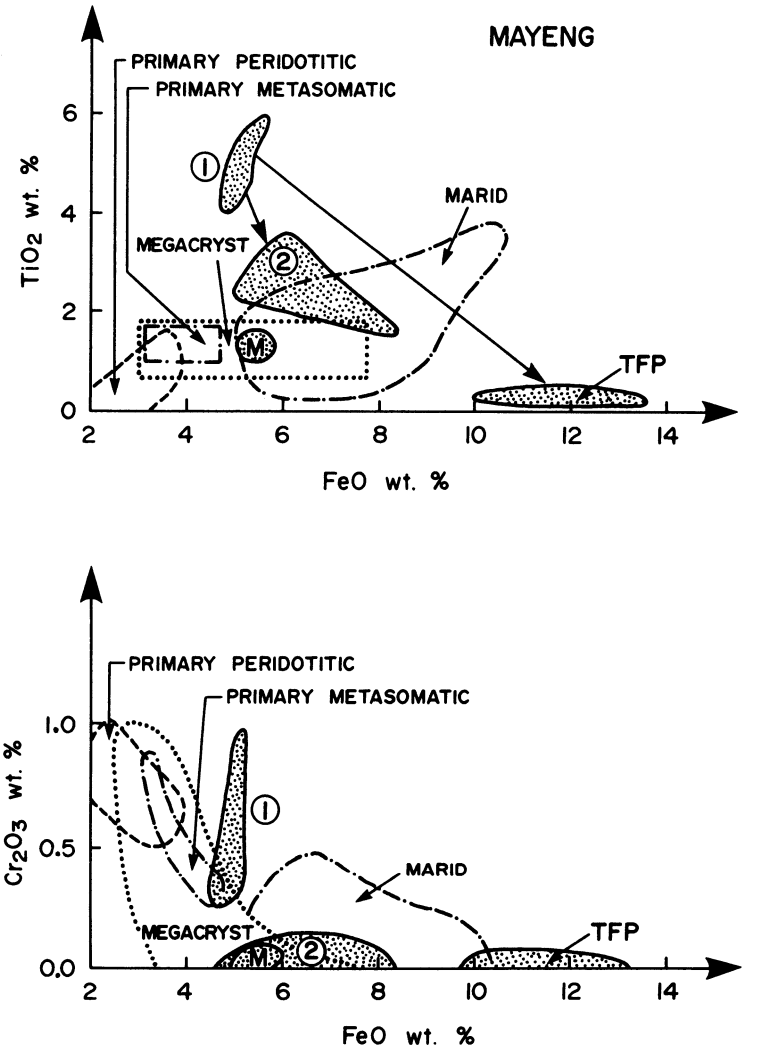

Figure 6.32. Compositional fields of mica from the Mayeng kimberlite. Stippled fields: 1, dark colored phlogopite; 2, pale-colored phlogopite; M, megacryst phlogopite from ilmenite-phlogopite intergrowths; TFP-tetraferriphlogopite. Data sources for other fields as in Figures 6.30 and 6.31.

followed by decreasing TiO_2 and increasing FeO. The trend is similar to that found by Apter *et al.* (1984) for the Mayeng micas, with the exception that tetraferriphlogopites are not found in the Fayette County dike. Macrocrysts are similar to Somerset Island macrocrysts and groundmass micas are similar to Smith *et al.*'s (1978) type-II micas. Eastonitic phlogopites are absent.

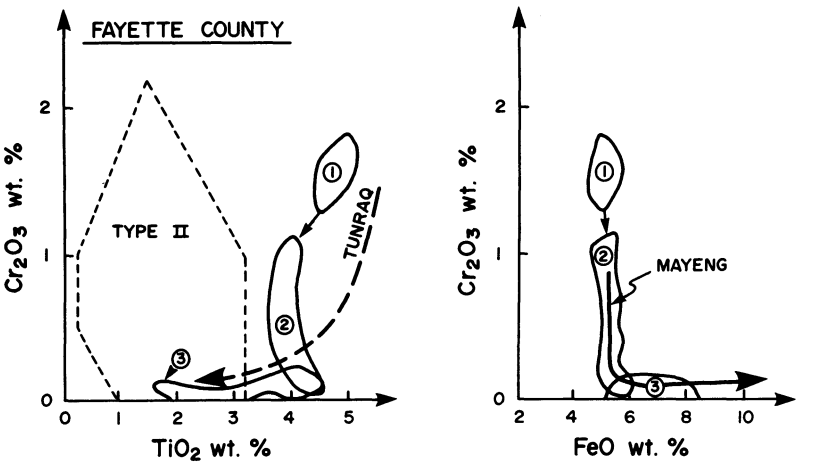

Figure 6.33. Compositional fields of mica from the Fayette County kimberlite, after Hunter *et al.* (1984). Field: 1, phenocryst cores; 2, phenocryst rims; 3, groundmass. Compositional trends for micas in the Tunraq (Mitchell 1979b) and Mayeng (Apter *et al.* 1984) kimberlites indicated by arrows. Field of type-II groundmass mica from Smith *et al.* (1978).

6.6.3.5. Orroroo (Scott Smith et al. 1984)

Dikes in the Orroroo region contain two-phase euhedral groundmass micas crowded with inclusions of spinels and perovskites. Lath-like crystals up to 1 mm in length with a normal colorless-to-pale-brown pleochroism are mantled by reversely pleochroic orange-brown micas. The sharp contact with the euhedral core suggests that the mantles are overgrowths rather than reaction rims. The pale cores [Mg/(Mg + Fe) = 0.90–0.94] are weakly zoned toward decreasing Al_2O_3, TiO_2, and BaO contents. They are rather richer in Al_2O_3 (15%–13%), BaO (1.0%–3.9%), and F (0.9%–2.2%) than other kimberlitic groundmass micas. Their TiO_2 (0.9%–2.2%) and Cr_2O_3 (0.0%–0.1%) contents are similar however to Smith *et al.*'s (1978) low Cr_2O_3 type-II micas. The tetraferriphlogopite mantles are extremely poor in Al_2O_3 (<1.0%) and consequently these micas contain substantial tetrahedrally coordinated Fe^{3+}. (Table 6.24, analysis 5). Crystallization of tetraferriphlogopite overgrowths upon aluminous phlogopite precursors indicates that gross changes in the chemistry and redox conditions of fluids occurred during the hiatus in the crystallization sequence of these phlogopites. Macrocrysts are absent.

6.6.3.6. Swartruggens (Skinner and Scott 1979)

Phlogopite occurs as anhedral macrocrysts (up to approx. 10 mm), euhedral-to-subhedral crystals of various sizes and as euhedral microlites. The majority

of the smaller crystals have dark reversed pleochroic rims. The micas have a relatively uniform composition regardless of their habit, with most containing 1.5% TiO_2 and having Mg/(Mg + Fe) ratios of 0.91. Some Fe-rich varieties [Mg/(Mg + Fe) = 0.82] are considered to be altered. The dark rims are Al_2O_3-deficient tetraferriphlogopites.

6.6.3.7. *West Greenland (Emeleus and Andrews 1975, Scott 1981, Scott Smith et al. 1983)*

Dikes in the Nigerdlikasik and Pyramidefjeld regions contain rare corroded, sieve-textured, low-TiO_2 (0.3%) macrocrysts and euhedral pale-brown to greenish-brown groundmass laths of eastonitic phlogopite. The latter are zoned from TiO_2-rich (3.0%) cores to paler TiO_2-poor (0.6%) margins. Narrow incomplete rims of red-brown tetraferriphlogopite are common (Table 6.24, analysis 2).

Scott (1981) has described a similar mica paragenesis in dikes from the Holsteinsborg area and noted that the phlogopite compositions show no correlation with crystal size. TiO_2 contents (2%–7%) are higher than found in many kimberlite phlogopites and Mg/(Mg + Fe) ratios (0.85–0.78) are unusually low (Scott Smith *et al.* 1983a).

6.6.3.8. *Bellsbank (Boctor and Boyd 1982)*

In these micaceous kimberlite dikes, phlogopite occurs primarily as macrocrysts and groundmass laths. The macrocrysts are deformed, low-TiO_2 (0.5%–0.7%) varieties [Mg/(Mg + Fe) = 0.93]. Groundmass phlogopites are richer in TiO_2 (1.5%) and FeO [Mg/(Mg + Fe) = 0.88]. Rarely, macrocrysts show reversed pleochroic cores and have TiO_2 enriched mantles identical to the groundmass phlogopites. Eastonitic phlogopites and tetraferriphlogopite are absent.

6.6.3.9. *Phlogopite Macrocrysts with Reversed Pleochroism*

Macrocrysts exhibiting reversed pleochroism (α = light to medium red-brown, $\gamma = \beta$ = light pink, light green, or light brown) mantled by micas with normal pleochroism (α = colorless, $\gamma = \beta$ = pale yellow, pale brown, light green) are particularly abundant in the De Beers kimberlite (Farmer and Boettcher 1981, Pasteris 1983) and are also found in the Elliot County (Garrison and Taylor 1980), Bellsbank (Boctor and Boyd 1982), and Koidu (Tompkins and Haggerty 1984) kimberlites. The phlogopites are very different in composition (Table 6.22, analysis 10) to the Fe^{3+}-rich, Al_2O_3-deficient groundmass tetraferriphlogopites which also exhibit reversed pleochroism (Table 6.24). Typically the macrocryst cores are euhedral and have sharp contacts with the overgrowths. The latter originally were similar in habit to the cores but commonly have been modified

by extensive corrosion. Farmer and Boettcher (1981) showed that the macrocrysts are identical in composition to euhedral primary phlogopites in lherzolite xenoliths, also characterized by reversed pleochroism, and suggesting therefore that these macrocrysts are probably xenocrysts. Mantles upon the macrocrysts are in some examples (Bellsbank, Elliot County) identical to groundmass micas, in others (De Beers) they are similar to Mitchell and Meyer's (1980) type-B-macrocrysts or Smith *et al.*'s (1978) type-II micas.

At Koidu there exists also a separate generation of groundmass micas and an apparent continuum from the outer margins of the macrocrystal mantles (4%–2% TiO_2) to groundmass laths (<2% TiO_2) to tetraferriphlogopite overgrowths (Tompkins and Haggerty 1984).

6.6.4. Trace Elements

The trace element content of kimberlite micas is inadequately known. Smith *et al.* (1979) have shown that type-1 groundmass micas contain 240–630 ppm Rb_2O and 1030–4300 ppm BaO, respectively (av. K/Rb = 209, av. K/Ba = 42). Type-II micas contain 90–820 ppm Rb_2O and 470–5800 ppm BaO, respectively (av. K/Rb = 330, av. K/Ba = 74). Allsopp and Barrett (1975) report wide ranges in the Rb (202–952 ppm) and Sr (55–281 ppm) content of groundmass micas in the Roberts Victor, Swartruggens and Wesselton kimberlites. K/Rb ratios range from 100–160 (Barrett 1975), in contradiction to Smith *et al.*'s (1979) values for similar groundmass micas. Megacrystal micas from Monastery contain 624–880 ppm Rb and 36–402 ppm Sr (Allsopp and Barrett 1975).

Rimsaite (1971) determined that groundmass phlogopites from the Upper Canada Mine contained 0.01% Li_2O, 0.05% ZnO, 0.3% BaO, 0.09% Rb_2O, 0.04% SrO, 0.3% F, and 0.08% Cl. Jones and Smith (1984) found 0.09%–0.11% Rb_2O, 0.48%–0.83% F, 0.02%–0.64% Cl, 1.4–16.2 ppm Li, and 1.9–2.9 ppm B in megacrysts from several South African kimberlites.

6.6.5. General Characteristics of Kimberlite Phlogopites

The above studies have demonstrated that although no single characteristic compositional trend is evident, some generalizations can be made concerning the nature of kimberlite micas:

1. Subtle differences exist between the compositions of populations of macrocrysts(megacrysts) and/or groundmass micas from different kimberlites.
2. Within any given kimberlite there exist significant inter-grain compositional variations between macrocrysts (megacrysts) and/or groundmass micas. These differences can be attributed to batch-mixing pro-

cesses or to heterogeneities in the magma composition during the later stages of crystallization.

3. Phlogopite precipitation is not continuous in all kimberlites during the whole period of crystallization of the groundmass.
4. Most megacrysts and macrocrysts, especially TiO_2-rich varieties, are probably phenocrysts. Only the macrocrysts exhibiting reversed pleochroism or having compositions similar to primary micas in lherzolites might be xenocrysts.
5. In some kimberlites (Fayette County, Mayeng) there is evidence for an evolutionary trend of decreasing TiO_2 and Cr_2O_3 and increasing FeO as macrocryst mica is followed by groundmass mica crystallization. In others (Swartruggens) no such trend is evident.
6. Primary groundmass micas can occur as titanian phlogopites, eastonitic phlogopites, or TiO_2-poor tetraferriphlogopites. The latter micas can also form as a reaction product between earlier aluminous phlogopites and late-stage fractions of the magma.

Comparisons between micas from kimberlites and other alkaline rocks have been made by Bachinski and Simpson (1984), Scott Smith and Skinner (1984a), and Mitchell (1985). These studies have demonstrated that the least evolved (i.e., highest Mg[Mg + Fe] ratio) phlogopites from minettes, lamproites, and kimberlites have similar and broadly overlapping compositions with respect to their Mg/(Mg + Fe) ratios, Al_2O_3, TiO_2, and Cr_2O_3 contents, but that their subsequent evolutionary compositional trends are very different (Figure 6.34).

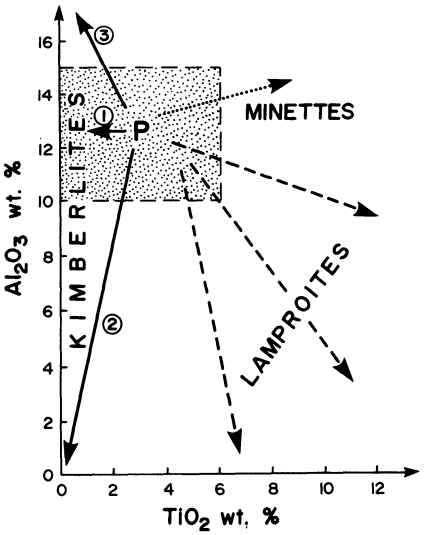

Figure 6.34. Compositional trends of micas in kimberlites (this work), minettes (Bachinsky and Simpson 1984) and lamproites (Mitchell 1985) with respect to Al_2O_3 and TiO_2 contents. All trends originate from a field (P) of phlogopites of similar composition, but subsequently evolve to either increasing or decreasing TiO_2 contents. The three trends exhibited by kimberlite phlogopite depend upon whether Al_2O_3 is constant (1), decreasing (2), or increasing (3).

Micas in lamproites are typically richer in TiO_2 and poorer in Al_2O_3 than kimberlitic micas and evolve toward Fe-rich titanian tetraferriphlogopites (Table 6.24) unlike those found in the kimberlite groundmass, and never toward eastonitic phlogopites. Micas in minettes are in general much richer in TiO_2 and FeO than kimberlite micas and evolve towards increasing TiO_2 and FeO at constant or increasing Al_2O_3 contents (Ehrenberg 1978, Jones and Smith 1983, Bachinski and Simpson 1984). The Ba-Ti-rich micas commonly found in alkaline volcanic rocks (Mansker *et al.* 1979, Wendlandt 1977) are not found in kimberlites although some enrichment in Ba can occur in the later stages of crystallization (Table 6.23, analyses 8 and 9.) Sodium and calcium bearing micas and biotite are absent. Biotites described from the Moses Rock dike and Cane Valley diatremes (McGetchin *et al.* 1973) occur in minettes, not kimberlites.

6.7. SPINEL

Spinels are ubiquitous and occur as (1) macrocrysts and fragmented macrocrysts, (2) primary groundmass minerals, (3) reaction or replacement products formed during the serpentinization of olivine, (4) subsolidus reduction intergrowths with ilmenite, (5) part of ilmenite decomposition and reaction assemblages.

Parageneses 4 and 5, because of their relationship to ilmenite, are discussed under ilmenite parageneses 5 and 6.

6.7.1. Macrocrystal Spinel (Paragenesis 1)

Macrocrystal spinels are typically large (0.1–0.5 mm), rounded, and transparent crystals. Their color varies from bright reddish-brown through orange to deep red and they ultimately become opaque as their Cr_2O_3 and Al_2O_3 contents increase and decrease, respectively. Identical euhedral spinels can very rarely be found as inclusions in olivine. Macrocrystal spinels were not in equilibrium with the magma that formed their host groundmass and they are typically mantled by irregular opaque rims of groundmass spinel or have acted as nucleation points for the growth of euhedral crystals of such spinels. Macrocrystal spinels can be found in all varieties of kimberlites and are even present in highly evolved, flow-differentiated, calcite-rich kimberlites. Macrocrystal spinels have previously been termed pre-fluidization phenocrysts (Mitchell and Clarke 1976). The term macrocryst is preferable in that these spinels are present in hypabyssal kimberlites and the rounding is probably due to resorption rather than abrasion. Although smaller than the associated olivine and phlogopite macrocryst population, it is useful to refer to these spinels by this non-genetic descriptive term because of their diverse origins (see Section 6.7.10), and distinctive size and chemistry with respect to other generations of spinel.

6.7.2. Primary Groundmass Spinels (Paragenesis 2)

Small (0.001–0.1-mm) euhedral to subhedral spinels comprise a significant proportion of the groundmass mineral assemblage. Their abundance typically ranges from 1–30 vol % (Skinner and Clement 1979) but may vary widely on a centimeter scale, owing to their concentration by flow differentiation, preferential nucleation about pre-existing crystals (especially olivine) or the presence of oxide-free carbonate–serpentine segregations. Spinels can occur as discrete, homogeneous, or continuously zoned crystals, or as relatively large crystals containing euhedral inclusions of earlier generations of spinels. Complexly zoned and epitaxially mantled crystals are common. Most spinels crystallized with a euhedral hexahedral (chromites) or octahedral habit (Ti-rich spinels) but have subsequently been subjected to widely varying degrees of resorption. The instability of the earliest groundmass minerals, with respect to the later stages of groundmass formation, is one of the hallmarks of the kimberlite groundmass spinel assemblage. Resorption can be limited to minor corrosion and modification of the crystal margins or to almost complete dissolution leaving tiny (<0.005-mm) irregular relicts scattered throughout the groundmass. Resorption of complex epitaxially mantled spinels gives rise to atoll-textured spinels (see Section 6.7.3). Many kimberlites contain large corroded anhedra of spinel, similar in composition to much smaller groundmass spinels, that have apparently been formed elsewhere and transported in their current hosts. Oxidation along margins or fractures in primary spinels, leads in some cases to the formation of titanomaghemite. Spinels of cruciform or skeletal habit, characteristic of rapidly cooled magmas, are typically absent. Spinels commonly occur as inclusions in perovskite.

6.7.3. Atoll Spinels

The term *atoll spinel* was applied by Mitchell and Clarke (1976) to resorbed complexly mantled spinels which resemble an island surrounded by a barrier reef. Typically a euhedral-to-subhedral core of chromite or titanomagnetite is separated by a distinct gap (1–10μm) from a fretted, spongy, narrow (<5 μm) rim of Ti-free magnetite (Figure 6.35). In some examples the relatively thick outer rim encloses several very thin (<1 μm) discontinuous parallel rims. The space between the core and the rim is occupied by a fine grained serpentine–calcite intergrowth. This material is identical to the groundmass mesostatis in which the early crystallizing spinels are set. Small anhedral crystals of rutile and/or perovskite can occur in the fretted rims. Increasing degrees of resorption result in disruption of the atoll rims and the scattering of tiny irregular fragments of magnetite throughout the groundmass. Importantly the habit of the magnetite rim exactly parallels that of the core, implying that the "lagoon" was originally occupied by a spinel that grew in crystallographic continuity with the core spinel.

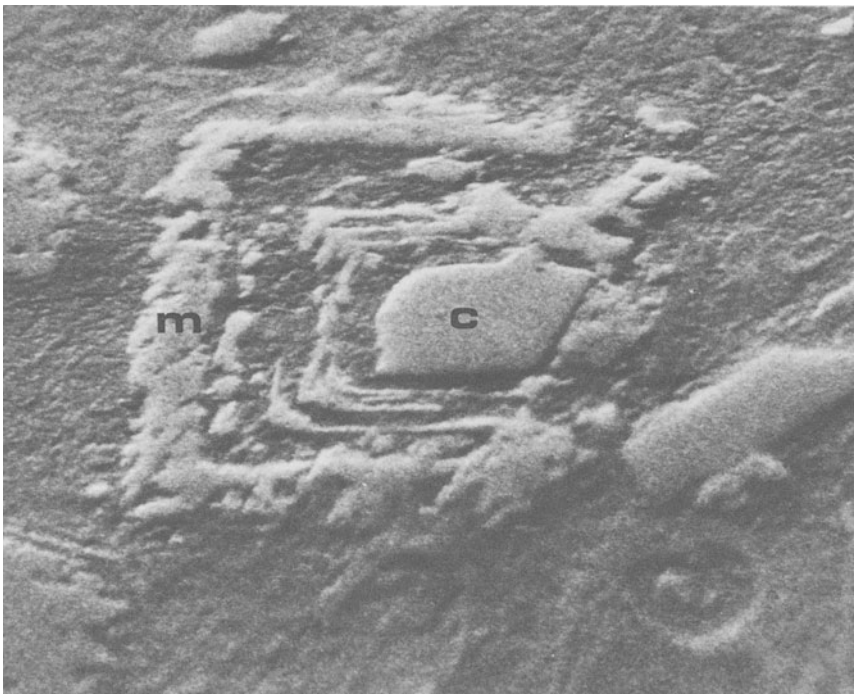

Figure 6.35. Atoll spinel, Peuyuk kimberlite. Scanning electron micrograph. A uniform core of chromite (c), 10 μm (diagonal), is surrounded by multiple atolls of resorbed spinel. Outer rim is magnetite (m).

Whether the outer rim developed prior to, or contemporaneously with, resorption of this intermediate spinel is uncertain. In the latter case the intermediate spinel must have been preserved for a sufficient time for it to act as a substrate for the growth of the outer epitaxial mantle. While there is general agreement that the atoll texture is produced by the resorption of this intermediate phase by dissolution in the fluids which formed the serpentine–calcite groundmass, there is no consensus as to the nature of this phase.

Mitchell and Clarke (1976) believe that atolls in the Peuyuk B kimberlite were formed by resorption of magnesian ulvöspinel-ulvöspinel-magnetite (MUM spinels), that originally formed mantles upon less titanian Cr-rich spinels, and which may themselves have been mantled in turn by Ti-free magnetite. Resorption is considered to be due to the instability of MUM spinels, but not Ti-free magnetite, in the late stage, carbonate-rich fluids which formed the groundmass, replaced olivines with a mixture of calcite and magnetite and formed late veins of the same mineralogy. Evidence in favor of this hypothesis is the presence of partially resorbed MUM spinels in the Peuyuk C kimberlite. In this facies the

titanian spinels were preserved by the separation of the late-stage carbonate-rich fluid into discrete segregations which did not subsequently pervade throughout the silicate-oxide groundmass.

In contrast, Pasteris (1980b, 1983) has presented evidence that in the De Beers kimberlite the intermediate phase was pleonaste. Kimberlites adjacent to the intrusion margins contain well-preserved epitaxial mantles of pleonaste upon chromite or titanomagnetite cores, and Pasteris describes a continuum from these crystals to atoll-textured spinels entirely lacking in pleonaste. Resorption of pleonaste by the late-stage groundmass fluids is considered to be accompanied by the deposition of Ti-free magnetite as the atoll rims.

Atoll spinels are common in many kimberlites and in view of Mitchell and Clarke's (1976) and Pasteris' (1980b, 1983) contrasting hypotheses, may have a multiplicity of origins. Each case must be considered on its own merits.

6.7.4. Reaction Product Spinels (Paragenesis 3)

During the retrograde serpentinization of olivine under relatively oxidizing conditions iron is released as tiny (< 1 μm) euhedral magnetite crystals scattered throughout an iron-poor serpentine matrix. As a consequence of prograde replacement of serpentinized olivines by deuteric fluids, pseudomorphs of calcite and magnetite can be produced. The magnetite in both cases is very pure Ti-free magnetite.

Marginal serpentinization of olivines also induces the crystallization of primary groundmass spinels. These occur as "necklaces" around groundmass olivines which have acted as nucleation centers.

6.7.5. Macrocrysts and Groundmass Spinel Compositions

The compositions of most kimberlite spinels fall within the eight-component system $MgCr_2O_4$(magnesiochromite)–$FeCr_2O_4$ (chromite)–$MgAl_2O_4$ (spinel)–$FeAl_2O_4$(hercynite)–Mg_2TiO_4(magnesian ulvöspinel)–Fe_2TiO_4 (ulvöspinel)–$MgFe_2O_4$(magnesioferrite)–Fe_3O_4(magnetite). Manganese contents are typically low and the Mn_2TiO_4 (maganoan ulvöspinel) or $MnFe_2O_4$ (jacobsite) end members are usually unimportant.

The compositional variation of Ti-free spinels can be illustrated by conventional bivariate plots of Cr/(Cr + Al) versus Fe/(Fe + Mg) ratios. Ti- and Fe^{3+}-bearing spinels present problems in the graphical representation of their chemistry, owing to the extensive solid solution between the eight common end-member spinel molecules. Conventionally, such spinels are represented by projections into six-component modified Johnson spinel prisms (Irvine 1965, Haggerty 1976). In the "reduced" spinel prism (Figure 6.36A) total iron is calculated as FeO. This type of projection is useful for many kimberlite spinels which are known to have formed under relatively reducing conditions (Mitchell 1973a).

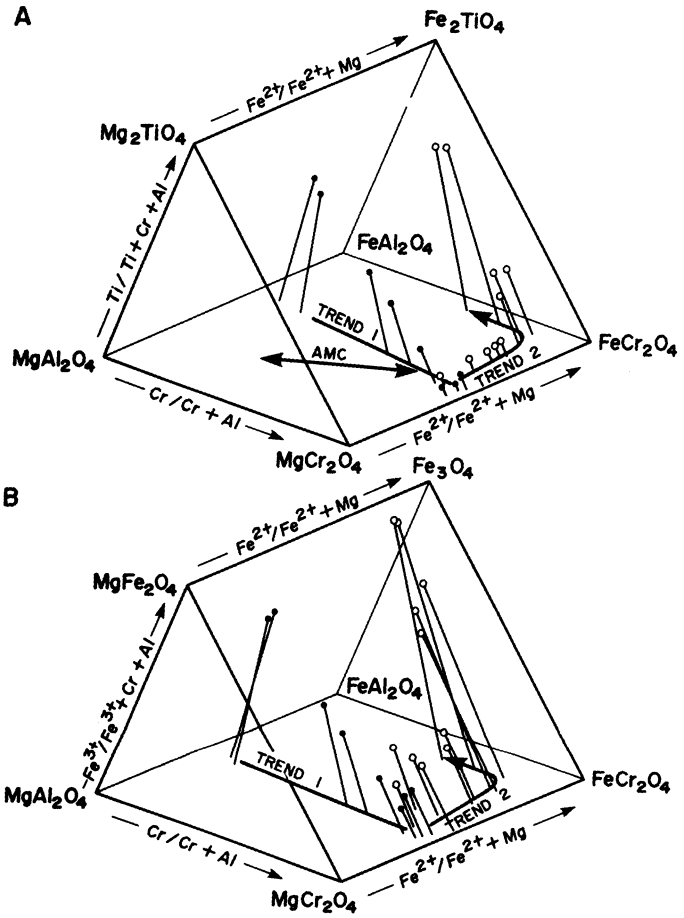

Figure 6.36. Representation of Trend-1 and -2 spinels in the "reduced" (A) and "oxidized" (B) spinel prisms (Haggerty 1976). Closed circles, Trend 1, data from the Tunraq kimberlite (Mitchell 1979b). Open circles, Trend 2, data from Zagodochnaya (Rozova *et al.* 1982) and Bellsbank (Boctor and Boyd 1982). NB. For an accurate representation of molecular proportions of spinel end-member molecules the Ti/(Ti + Cr + Al) axis should be given as 2Ti/(2Ti + Cr + Al). Haggerty's (1976) representation is retained here for consistency with the existing literature.

The projection, however, fails to illustrate variations in Fe_3O_4 or $MgFe_2O_4$ content, but has the merit that all of the major elements present are included in the prism. For projections in the "oxidized" prism (Figure 6.36B) spinel analyses are recalculated on a stoichiometric basis or by Carmichael's (1967) method to assess their Fe^{2+} and Fe^{3+} contents. "Oxidized" prisms fail to illustrate the significant Mg_2TiO_4 and Fe_2TiO_4 contents of kimberlite spinels.

Haggerty and Tompkins (1984) have attempted to improve graphical representation by plotting spinels in sections of an eight-component trapezoid. This cumbersome procedure, however, requires three sections, with the repetition of data points connected by tie-lines (Figure 6.37), and the procedure has not yet been generally accepted.

Multivariate methods such as principal component analysis (Le Maitre 1982) have proved satisfactory in separating different evolutionary trends of spinels

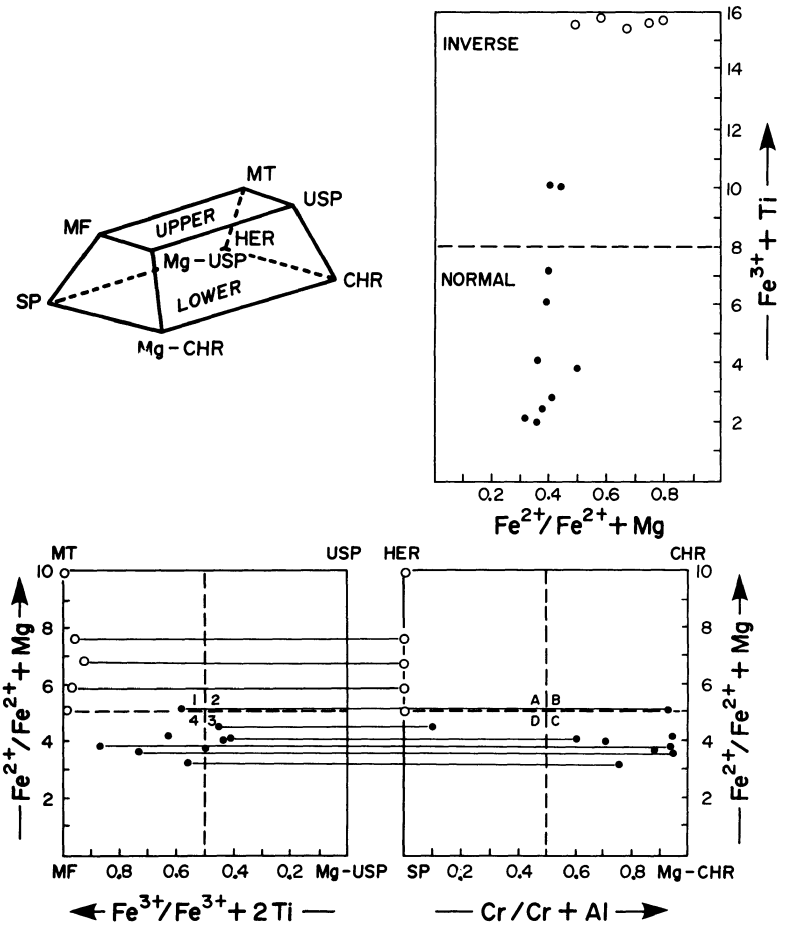

Figure 6.37. Representation of the compositions of spinels from the Tunraq kimberlite (Mitchell 1979b, closed circles) and the Premier carbonate dikes (Gaspar and Wyllie 1984, open circles) in Haggerty and Tompkins' (1984) spinel trapezoid. Projections of the upper and lower faces together with tie lines are shown in the lower two diagrams. The Fe^{2+}/Fe^{2+} + Mg versus Fe^{3+} + Ti diagram provides a measure of the octahedral site occupancy and approximates to a vertical section through the trapezoid.

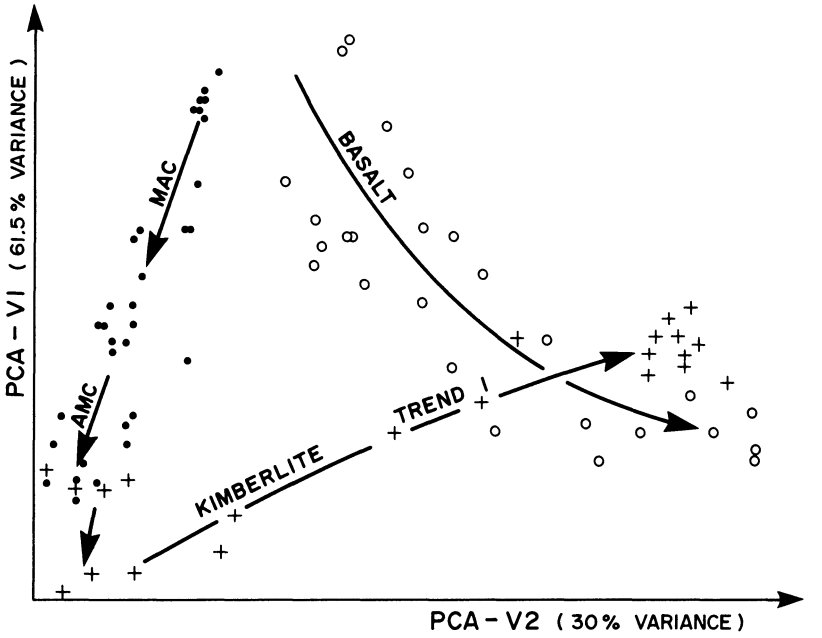

Figure 6.38. Principal components analysis of spinels from the Tunraq and Jos kimberlites (Mitchell 1979b, Mitchell and Meyer 1980), Ti-poor chromites (AMC-MAC) from kimberlites Mitchell and Clarke 1976, Mitchell 1978a) and spinels from mid-Atlantic ridge (Sigurdsson and Schilling 1976) and Scottish Tertiary (Ridley 1977) basalts. Two vectors (PCA-VI, PCA-V2) account for 91.5% of the variance in seven-dimensional space and can be used to delineate compositional trends.

from diverse environments in seven-dimensional space (Figure 6.38). The method has the disadvantages of requiring the whole data base to be subjected to the analysis each time new data are added to the data base, and computing facilities capable of handling large matrices in the calculations of eigenvectors.

Further discussion of plotting procedures and of less commonly used methods can be found in Irvine (1965), Haggerty (1976), Pasteris (1982), and Boctor and Boyd (1982).

Figures 6.36A and 6.36B illustrate representative spinel compositions plotted in "reduced" and "oxidized" spinel prisms to illustrate the differences between the projections. For most purposes the reduced prism is superior to the oxidized prism and is employed in most of the following discussions. It should, however, be borne in mind that significant amounts of Fe^{3+} are present in all of the more evolved Ti-bearing spinels.

Four general spinel compositional trends so far have been observed in kimberlites: (1) the macrocrystal or aluminous magnesian chromite (AMC) trend, (2) magmatic trend 1 or the magnesian ulvöspinel trend, (3) magmatic trend 2 or the Ti-magnetite trend, (4) the pleonaste reaction trend.

6.7.6. Macrocrystal (AMC) Trend

Macrocrystal spinels belong essentially to the quaternary system $MgAl_2O_4$–$MgCr_2O_4$–$FeCr_2O_4$–$FeAl_2O_4$ (Table 6.25) and plot on or near the basal plane of the spinel prism (Figure 6.36A). They typically contain less than 1% TiO_2 and exhibit a wide range in their Cr/(Cr + Al) [0.3–0.95] and Fe/(Fe + Mg) [0.3–0.6] ratios. The spinels are best described as magnesian aluminous chromites (MAC) or aluminous magnesian chromites (AMC). Individual crystals are typically homogeneous and it is therefore not possible to determine evolutionary trends. Ti-bearing magnesian chromites similar to the more Cr-rich AMC macrocrysts mantle these latter spinels and occur as a primary groundmass phase, indicating that if these macrocrysts are phenocrysts (Mitchell and Clark 1976, Section 6.7.10) then their compositional evolution is towards Cr and Fe enrichment at the expense of Al and Mg. The compositional trend of the MAC–AMC macrocrysts overlaps the compositions of the least evolved, ie., Ti-poor, Cr-rich primary groundmass spinels, and possibly there may be a continuum between the two groups (see Figures 6.36, 6.39A, and 6.41D).

Table 6.25. Representative Compositions of Macrocrystal (AMC) Spinels[a]

	1	2	3	4	5
TiO_2	0.10	0.63	0.10	0.5	0.45
Al_2O_3	36.82	17.31	13.94	10.5	3.51
Cr_2O_3	26.88	46.44	52.29	55.5	62.37
FeO[b]	14.84	21.82	18.79	20.5	20.47
MnO	9.15	0.34	0.41	0.3	0.49
MgO	17.46	12.80	13.93	13.0	11.76
	98.03	99.34	99.46	100.3	99.05
Recalculated analyses					
Fe_2O_3	4.76	7.18	6.89	7.00	6.79
FeO	10.55	15.36	12.58	14.1	14.36
	98.51	100.36	100.14	100.9	99.73
Mol % end member spinel molecules					
$MgAl_2O_4$	60.6	30.6	24.9	19.0	6.7
Mg_2TiO_4	0.3	2.1	0.3	1.6	1.6
$MnCr_2O_4$	0.4	0.9	1.1	0.8	1.3
$MgCr_2O_4$	11.6	23.8	37.7	38.4	47.6
$FeCr_2O_4$	19.6	30.4	24.1	28.0	30.5
Fe_3O_4	7.5	12.2	11.8	12.2	12.3

[a] 1,2, Peuyuk (Mitchell and Clarke 1976); 3, Elwin Bay (Mitchell 1978a); 4, Jos (Mitchell and Meyer 1980); 5, Chang Ma Chuan (Dong and Zhou 1980).

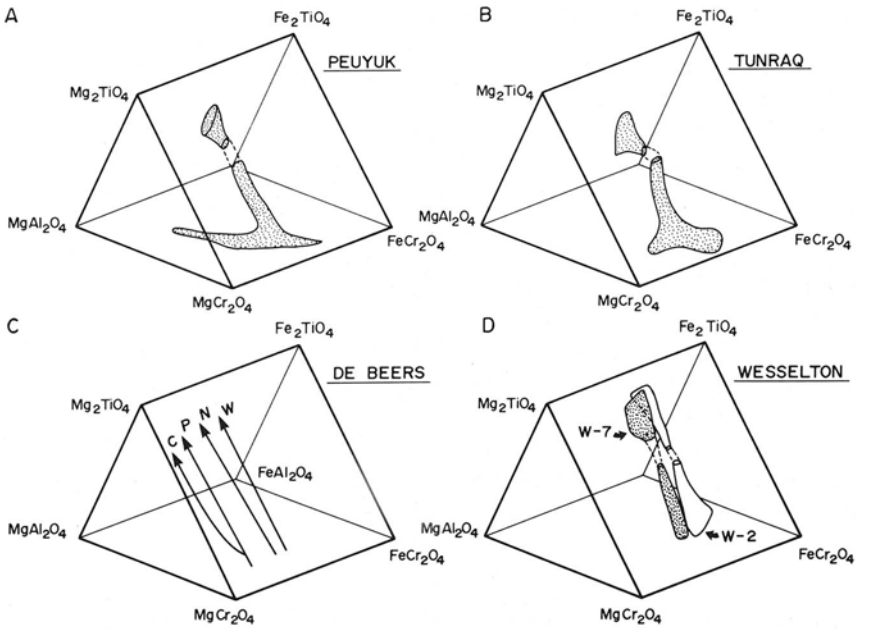

Figure 6.39. Compositions of spinels in the (A) Peuyuk (Mitchell and Clarke 1976), (B) Tunraq (Mitchell 1979b), (C) De Beers (Pasteris 1980), and (D) Wesselton (Shee 1979) kimberlites.

6.7.7. Magmatic Trend 1—The Magnesian Ulvöspinel Trend

The magnesian ulvöspinel trend (Figure 6.36) appears to be confined to serpentine, calcite, monticellite, and diopside kimberlites. Micas, when present are macrocrystal phlogopites or groundmass eastonitic phlogopites. The trend has not yet been described from isotopic group-II (Smith 1983) micaceous kimberlites.

The trend was initally established for spinels from the Peuyuk kimberlite by Mitchell and Clarke (1976) and substantiated by the detailed studies of spinels from the Tunraq (Mitchell 1979b), De Beers (Pasteris 1980b, 1983), and Wesselton (Shee 1979, 1984) kimberlites. For all of these occurrences the trend was defined on the basis of core–mantle relationships, the presence of extensive compositional zoning, and/or inter-grain compositional variation. Petrographically distinct intrusions within any one kimberlite occurrence provide near-complete coverage of the whole trend, e.g., Peuyuk C (Mitchell and Clarke 1976), the De Beers Intrusion Breccia (Pasteris 1983), or the Wesselton W2 kimberlite (Shee 1979).

The compositional trend is across the spinel prism from the base near the $MgCr_2O_4$–$FeCr_2O_4$ join [commonly Cr/(Cr + Al) = 0.80–0.95, Fe/

(Fe + Mg) = 0.4–0.6] toward the rear rectangular face and upward toward the Mg_2TiO_4–Fe_2TiO_4 (or $MgFe_2O_4$–Fe_3O_4) apex (Figure 6.36A and 6.36B). Spinel evolution is from titanian magnesian aluminous chromites (TIMAC) or titanian magnesian chromites (TMC) containing 1%–12%TiO_2 toward members of the magnesian ulvöspinel-ulvöspinel-magnetite (>15% TiO_2) series (MUM spinels), and is a trend of increasing Ti, Fe^{3+}/Fe^{2+}, and total Fe and decreasing Cr at approximately constant $Fe^{2+}/(Fe^{2+}$ + Mg) ratios. Aluminum may decrease, increase, or remain constant over this trend. MnO contents are typically low (<1%) but may increase slightly in the more evolved spinels. The Fe-enrichment trend culminates with the development of Ti- and Mg-free magnetite. The presence of Ti-rich spinels containing substantial proportions of the magnesian ulvöspinel molecule, is the hallmark of spinels belonging to Trend 1 (Table 6.26).

Important aspects of, and variations within, Trend 1 are as follows:

1. The trend traverses the prism at similar Fe/(Fe + Mg) ratios in petrographically distinct kimberlites within a given intrusion, e.g., the Peuyuk A and B kimberlites (Mitchell and Clarke 1976), the De Beers West and Intrusion Breccia kimberlites (Pasteris 1983), and the Wesselton W2 and W3 kimberlites (Shee 1984).
2. Similar Fe/(Fe + Mg) ratios for the trend are found in kimberlites from different kimberlite provinces, e.g., Peuyuk, Wesselton, Hatzium (Figures 6.39A, 6.39D, and 6.41C).
3. Different facies of kimberlite within the same intrusion contain spinels which exhibit the same overall compositional trend, but the positions of these trends are displaced along the axis of the spinel prism. Thus for kimberlites from the root zone of the De Beers pipe, Pasteris (1980b, 1983) finds that the cross-prism trends for the Peripheral, Core, Neck, and West Kimberlites occur at increasing Fe/(Fe + Mg) ratios (Figure 6.39C). Similar, though not as pronounced, relationships have been noted (Shee 1979) for spinels from the Weselton kimberlites (Figure 6.39D).

Pasteris (1980b, 1983) believes that the increasing Fe/(Fe + Mg) ratios reflect increasing degrees of differentiation of a single batch of parent magma from which the various De Beers kimberlites are sequentially derived. It is important to realize that despite the different degrees of Fe enrichment, Cr-rich as well as Fe-Ti-rich spinels are present in all facies. A single differentiating magma would not produce such an assemblage and later members of the sequence would be expected to contain only Cr-free highly evolved MUM spinels, such as are found in evolved kimberlites from Jos or Benfontein (see below). The common, but parallel, trends may thus reflect parallel evolutionary trends of spinel compositions from *unevolved* parents of slightly different bulk composition, perhaps formed by mixing of batches of similar magmas at different stages of differentiation in the source regions at depth.

Table 6.26. Representative Compositions of Spinels from Magmatic Trend 1[a]

	1	2	3	4	5	6	7	8	9	10	11	12	13	14	15	16	17	18
Ti_2O_3	1.20	3.81	5.24	9.17	12.90	16.48	19.82	21.51	22.59	0.9	1.5	3.0	4.8	7.6	11.5	14.7	16.7	18.2
Al_2O_3	15.34	7.67	8.90	10.69	9.24	10.69	7.26	5.99	7.80	2.7	2.3	1.8	2.3	3.9	7.5	8.0	8.7	8.4
Cr_2O_3	47.77	47.27	40.57	25.03	10.84	1.25	4.59	3.97	0.86	58.7	61.0	55.4	47.8	43.9	27.1	19.3	2.4	1.5
FeO[b]	21.19	25.13	30.04	38.82	48.67	53.63	48.17	45.55	50.26	25.1	21.9	26.6	33.2	28.3	36.9	41.2	52.2	52.4
MnO	0.33	0.44	0.49	0.47	0.50	0.47	0.99	1.21	0.45	0.5	0.4	0.4	0.5	0.5	0.5	0.5	0.5	0.5
MgO	12.71	13.40	12.62	13.33	13.24	13.57	16.42	18.06	16.80	11.4	12.1	11.1	9.6	13.8	14.5	15.3	15.7	15.0
	98.54	97.72	97.86	97.01	95.30	96.09	97.25	96.26	98.76	99.2	99.3	98.3	98.1	97.8	98.8	96.1	97.2	97.3
Recalculated analyses																		
Fe_2O_3	6.39	11.01	13.45	19.78	28.10	30.61	26.19	24.56	25.60	11.0	8.0	10.4	13.2	12.1	18.1	20.6	32.2	30.5
FeO	15.44	15.23	17.94	20.52	23.28	26.61	24.60	23.45	27.22	15.2	14.7	17.2	21.3	17.4	20.6	22.6	23.2	25.9
	99.18	98.82	99.21	98.99	98.21	99.10	99.84	98.72	101.32	100.3	100.0	99.3	99.5	99.1	99.7	100.8	99.3	99.9
Mol % end member spinel molecules																		
$MgAl_2O_4$	27.5	13.4	15.1	16.7	13.6	14.9	9.9	8.1	10.3	4.5	4.3	3.2	4.1	6.6	11.5	11.6	12.0	11.5
Mg_2TiO_4	4.1	12.8	17.0	27.0	26.7	24.7	35.0	40.2	34.3	3.0	5.3	10.4	16.4	24.3	33.7	33.5	31.9	30.0
Mn_2TiO_4	—	—	—	0.5	0.8	0.7	1.5	1.8	0.6	—	—	—	—	—	0.2	0.8	0.7	0.7
Fe_2TiO_4	—	—	—	—	8.8	18.6	15.2	13.7	22.1	—	—	—	—	—	—	6.6	11.7	16.6
$MnCr_2O_4$	0.9	1.1	1.2	0.5	—	—	—	—	—	1.4	1.2	1.0	1.2	1.1	0.7	—	—	—
$MgCr_2O_4$	24.6	28.8	16.3	—	—	—	—	—	—	44.2	45.6	34.4	17.0	19.9	—	—	—	—
$FeCr_2O_4$	32.0	25.5	28.6	25.8	10.7	1.2	4.2	3.6	0.8	27.0	29.4	32.6	38.8	28.5	27.2	18.8	2.2	1.4
Fe_3O_4	11.0	18.4	21.8	29.6	39.5	40.0	34.3	32.7	31.9	19.4	14.2	18.2	22.4	19.6	26.7	28.7	42.2	39.8

[a] 1, 5, Titanian magnesian aluminous chromites (TIMAC), Peuyuk B (Mitchell and Clarke 1976); 6–9, magnesian ulvöspinel-ulvöspinel magnetites (MUM); 6, Peuyuk C (Mitchell and Clarke 1976); 7, 8, Wesselton (Shee 1979); 9, Benfontein, (Boctor and Boyd 1971); 10–16, titanian magnesian chromite (TMC); 14–18, magnesian ulvöspinel-ulvöspinel-magnetites (MUM), Tunraq (Mitchell 1979b).

[b] Total Fe calculated as FeO.

In many kimberlites the complete trend of compositional variation is not present and the spinel assemblage consists of early crystallizing TIMAC or TMC, mantled by discrete rims of MUM whose composition is identical to that of euhedral or resorbed groundmass spinels. Zonation trends, when present, are identical to the more extensive compositional variations found in the spinels from kimberlites used to define Trend 1. Representative examples from the Upper Canada Mine, Pipe 200, Nqechane, and Elliot County kimberlites are illustrated in Figure 6.40. Similar spinel assemblages are also known from the Kao (Haggerty 1975), Peuyuk C (Mitchell and Clark 1976), Wesselton (Elthon and Ridley 1979), Holsteinsborg (Scott 1981), and Fayette County (Hunter *et al.* 1984) kimberlites.

These studies demonstrate that there is a distinct hiatus in the crystallization sequence of spinel in many kimberlites and that there is not typically a continuous series of solid solutions between TIMAC/TMC and MUM compositions. This hiatus may reflect the presence of a solvus in this spinel system, as demonstrated experimentally by Muan *et al.* (1972), who showed that solvii exist in the ternary systems Fe_2TiO_4–$FeAl_2O_4$–$FeCr_2O_4$ and Mg_2TiO_4–$MgAl_2O_4$–$MgCr_2O_4$ (Figure 6.40A). Spinel solid solutions lying within these solvii will breakdown into

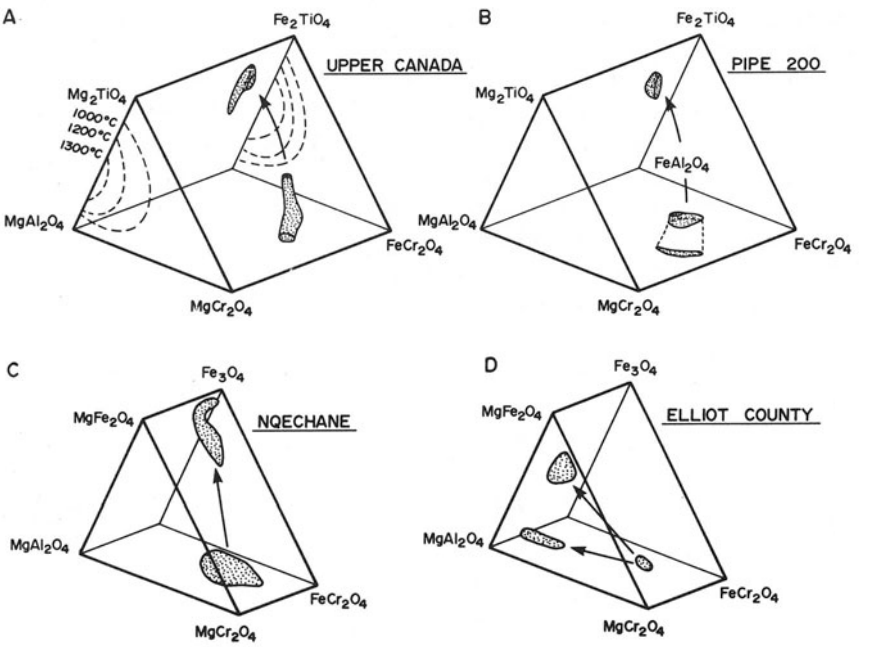

Figure 6.40. Compositions of spinels in the (A) Upper Canada (Mitchell 1978b), (B) Pipe 200 (this work), (C) Nqechane (Haggerty 1975), and (D) Elliot County (Agee *et al.* 1982) kimberlites. Solvus data in (A) are from Muan *et al.* (1972).

normal (Cr-rich) and inverse (Ti-rich) spinels with falling temperature. Although Muan *et al.*'s (1972) sub-solidus data are not directly applicable to spinels crystallizing from complex kimberlite melts, they are instructive in indicating that a solvus may intersect the solidus of such melts. The observed phase relationships are commensurate with the initial crystallization of high-temperature Cr-spinel followed by resorption of this spinel at a reaction point. Subsequently, after a period of no spinel crystallization, a Ti-Fe^{3+}-rich spinel is formed as a stable phase. The extensive solid solutions shown by some spinels which cut across possible miscibility gaps, in the Peuyuk, Tunraq, and Wesselton kimberlites, may be due to metastable preservation of these spinels by rapid quenching (Mitchell and Clarke 1976).

Similar compositional gaps between normal and inverse spinels are known in ultrabasic and basic rocks (Haggerty 1976) and have been interpreted as being due to a peritectic relationship between spinel and pyroxene and/or variations in oxygen fugacity. Hill and Roedder (1974), for example, have found that at relatively high fo_2 spinel precipitation from basaltic compositions is continuous, but that a "spinel-absent and pyroxene-present" field is encountered with falling temperature and fo_2. Peritectics related to pyroxene formation are not appropriate for pyroxene-free kimberlites, but such studies serve to emphasize that spinel precipitation is controlled by many variables. Until experimental studies of synthetic analogs of kimberlite magma are undertaken the origin of the bimodel spinel assemblage will remain uncertain; however, the existing data favor the existence of a miscibility gap in the spinel compositional trend.

Some kimberlites contain spinels belonging primarily to the initial or final portions of Trend 1; thus in the Elwin Bay, Peuyuk A, Chang Ma Chuan, and Hatzium kimberlites (Figure 6.41) only TIMAC or TMC spinels are found and the MUM series never appears to have crystallized. Similar spinels occur in the Orroroo kimberlites (Scott Smith *et al.* 1984b).

Three modes of origin are possible for these assemblages: bulk compositions of the magmas involved may have been such that the field of MUM spinels was not encountered during crystallization; crystallization was rapid and completed before MUM spinels could nucleate; MUM spinels originally formed but have since been resorbed. This latter possibility must be suspected wherever TIMAC/TMC form the cores of atoll structures, e.g., Peuyuk B, Hatzium. Careful consideration of the associated phases should enable a distinction to be made between the first and second options. Thus Peuyuk A appears to have been rapidly quenched, while Elwin Bay, a highly evolved segregation-textured monticellite-calcite serpentine kimberlite appears to have an inappropriate bulk composition.

At the other extreme are kimberlites which are characterized predominantly by MUM spinels and magnetite; e.g., Green Mountain (Boctor and Meyer 1979), Jos (Mitchell and Meyer 1980), the Tunraq fissile macrocrystal phlogopite kimberlite (Mitchell 1979b), the Benfontein sill (Boctor and Boyd 1982), the Wes-

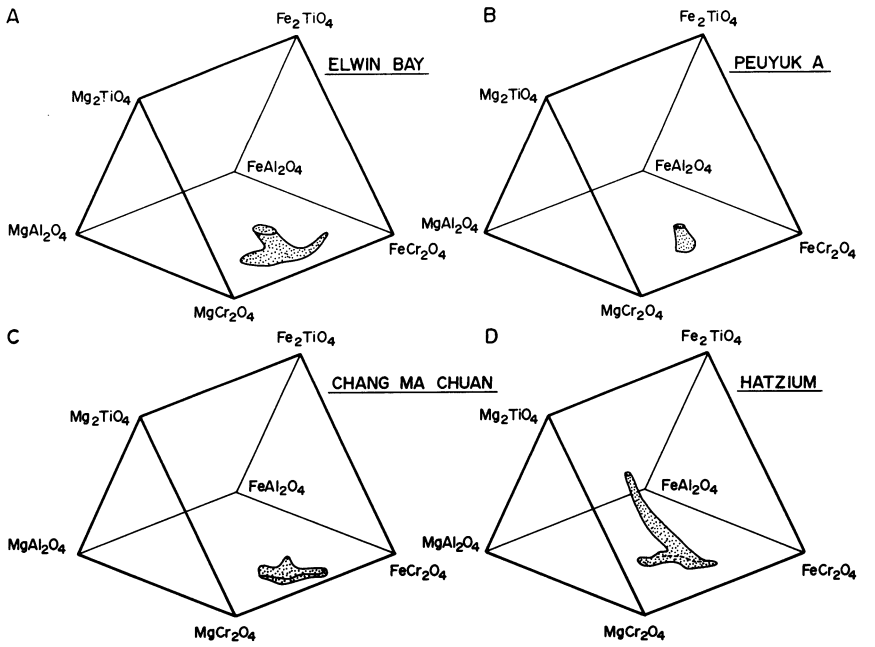

Figure 6.41. Compositions of spinels in the (A) Elwin Bay (Mitchell 1978b), (B) Peuyuk A (Mitchell and Clarke 1976), (C) Chang Ma Chuan (Dong and Zhou 1980), and (D) Hatzium (this work) kimberlites.

selton Water Tunnel sills (Mitchell 1985, Shee 1984), and late-stage carbonate-rich dikes in the Premier (Gaspar and Wyllie 1984) kimberlite (Figure 6.42). In these kimberlites TIMAC/TMC are present as rare, highly corroded inclusions in discrete crystals of MUM spinels. These, and rare AMC, are relicts of an earlier generation of spinels which have been preferentially, physically separated out of the magma, or extensively resorbed. Spinels in the carbonate-rich segregations of the Benfontein sill are aluminous MUM, or rarely, magnesioferrite and/or magnetite (Gaspar and Wyllie 1984, Boctor and Boyd 1982, McMahon *et al.* 1979). Inclusions of TIMAC in olivines from the Benfontein sill demonstrate that these kimberlites initially crystallized contemporaneously olivine and Cr spinel. Spinels from the carbonate-rich dikes of the Premier kimberlite are low TiO_2 (0.6%–2.7%) and low MgO (4%–9%) magnetites with a significant magnesioferrite component or pure Ti-Mg-free magnetites (Gaspar and Wyllie 1984, Mitchell 1979a). Such spinels appear to represent the extreme development of Trend 1 and occur only in highly evolved calcite kimberlites.

Mitchell and Meyer (1980) have noted that spinels with similar Fe/(Fe + Mg) ratios may have different Al_2O_3 contents (Table 6.26); thus the Jos and Tunraq Ti-rich spinels are poor in the $MgAl_2O_4$ component (<30% ml%) compared to

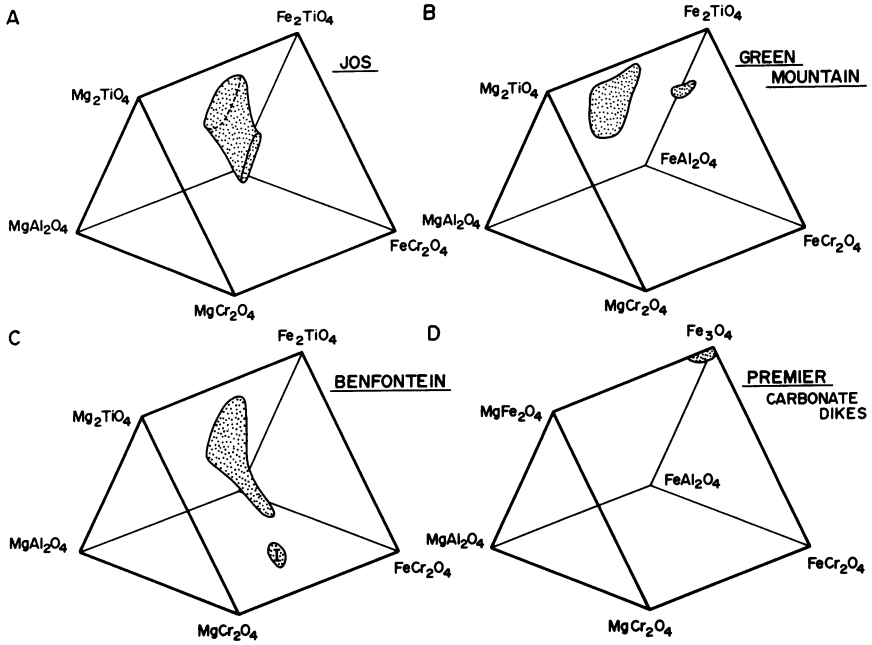

Figure 6.42. Compositions of spinels in the (A) Jos (Mitchell and Meyer 1980), (B) Green Mountain (Boctor and Meyer 1979), (C) Benfontein (Boctor and Boyd 1981), I = inclusions in olivine, and (D) Premier (Gaspar and Wyllie 1984, Mitchell 1979a) kimberlites.

the Peuyuk spinels (<30 mol%). In these examples the crystallization of abundant macrocrystal phenocrystal phlogopite has probably depleted the magma in Al_2O_3 prior to the onset of spinel formation. Increases in the Al_2O_3 content of the latest MUM to form are, however, noted in the Jos (Mitchell and Meyer 1980) and Elwin Bay (Mitchell 1978a) kimberlites. These increases are a reflection of the progressive increase of Al_2O_3 in the magma, which culminates in the formation of groundmass eastonitic phlogopite.

6.7.8. Magmatic Trend 2—The Titanomagnetite Trend

This less common spinel compositional trend was first recognized in the Tunraq kimberlite (Mitchell 1979b) but is best developed in spinels from Bellsbank (Boctor and Boyd 1982), Zagadochnaya (Rozova *et al.* 1982) and Koidu (Tompkins and Haggerty 1985). Rare spinels apparently belonging to this trend have also been noted in the Elwin Bay (1978a), De Beers Peripheral (Pasteris 1980b), and Marushkaya (Rozova *et al.* 1982) kimberlites.

Trend-2 spinels range in composition (Table 6.27) from aluminous magnesian chromites (AMC) to titanian magnesian chromites (TMC) to titanian chrom-

Table 6.27. Representative Analyses of Spinels from Magmatic Trend 2[a]

	1	2	3	4	5	6	7	8	9	10	11	12	13	14	15	16	17
Ti_2O_3	1.91	3.55	4.44	9.30	1.32	2.88	5.55	7.45	6.2	7.0	1.93	2.98	5.78	7.18	13.04	16.7	21.51
Al_2O_3	1.33	1.11	0.66	0.14	8.28	3.97	1.84	2.03	0.3	0.2	7.95	5.61	4.23	3.73	4.68	3.91	0.68
Cr_2O_3	58.50	54.79	50.74	1.16	48.54	46.75	15.36	18.15	26.5	11.0	53.58	53.83	47.7	42.62	23.98	10.44	4.18
FeO[b]	25.49	28.13	30.61	76.57	30.64	37.78	70.94	66.25	58.1	70.4	23.19	25.26	29.74	32.82	43.29	61.08	68.71
MnO	1.11	0.94	0.97	1.45	0.58	0.58	0.71	0.61	0.3	0.3	0.53	0.53	0.47	0.50	0.57	3.4	2.98
MgO	10.61	10.46	10.63	5.46	9.05	6.07	3.11	4.53	5.2	5.2	12.37	11.30	11.38	10.66	12.78	0.72	0.00
	98.95	98.98	98.05	94.08	98.41	98.04	97.51	99.02	94.1	96.1	99.55	99.51	99.30	97.51	98.34	96.25	98.06
Recalculated analyses																	
Fe_2O_3	10.00	10.86	13.41	52.16	12.00	14.16	43.46	38.18	32.5	46.0	8.43	8.28	10.80	12.33	21.16	21.9	23.02
FeO	16.49	18.36	18.54	29.64	19.84	25.04	31.83	31.89	28.9	29.0	14.61	17.81	20.02	21.73	24.25	41.38	48.00
	99.95	100.1	99.39	99.3	99.61	99.46	101.90	102.8	99.8	98.7	100.40	100.30	100.40	98.74	100.50	98.44	100.40
Mol % end member spinel molecules																	
$MgAl_2O_4$	2.5	2.0	1.2	0.2	15.1	7.3	2.9	3.1	0.4	0.3	14.3	10.1	7.3	6.5	7.1	2.9	—
Mg_2TiO_4	6.8	12.3	15.2	14.9	4.6	10.1	7.0	10.9	15.8	15.0	6.6	10.3	19.2	23.8	31.4	—	—
Mn_2TiO_4	—	—	—	2.3	—	—	1.2	1.0	0.6	0.5	—	—	—	—	0.9	5.9	4.9
Fe_2TiO_4	—	—	—	8.7	—	—	8.3	10.1	3.0	5.1	—	—	—	—	5.4	45.8	57.5
$MnCr_2O_4$	3.0	2.5	2.5	—	1.5	1.5	—	—	—	—	1.4	1.4	1.2	1.2	—	—	—
$MgCr_2O_4$	38.3	29.6	26.6	—	20.5	7.4	—	—	—	—	33.1	27.8	17.0	8.5	—	—	—
$FeCr_2O_4$	31.6	34.7	31.7	1.1	37.3	48.7	16.0	18.7	29.1	11.3	30.1	36.1	37.4	39.7	24.4	11.3	4.2
Fe_3O_4	17.8	18.9	22.9	72.7	20.9	24.9	64.6	56.2	51.1	67.7	14.5	14.3	17.9	20.4	30.7	34.0	33.4

[a] 1–4, Bellsbank (Boctor and Boyd 1982); 5–8 Zagadochnaya (Rozova *et al.* 1982); 9, 10 Tunraq; 11–17, Koidu (Tompkins and Haggerty 1985).
[b] Total Fe calculated as FeO.

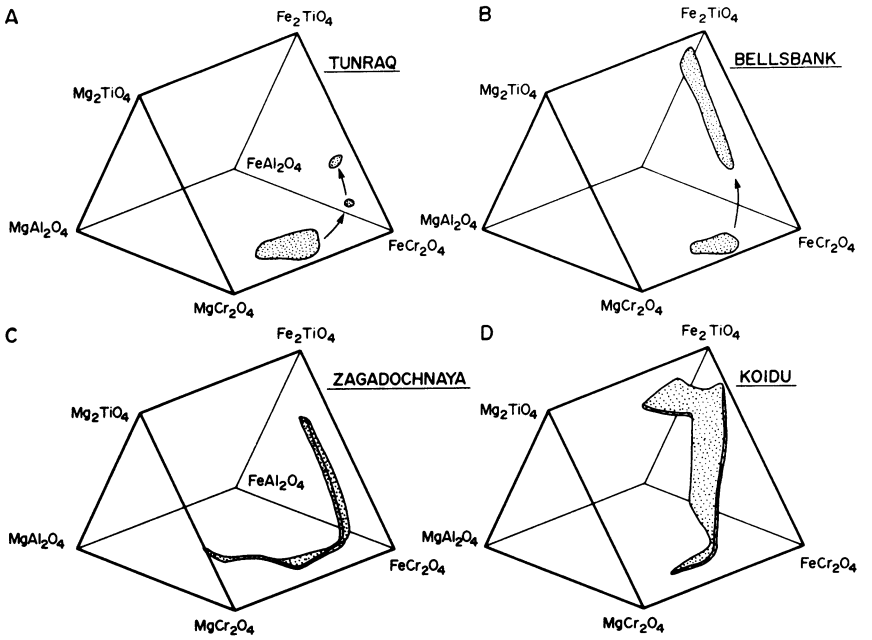

Figure 6.43. Compositions of spinels in the (A) Tunraq (Mitchell 1979b), (B) Bellsbank (Boctor and Boyd 1982), (C) Zagodochnaya (Rozova *et al.* 1982), and Koidu (Tompkins and Haggerty 1985) kimberlites.

ites (TC) to members of the ulvöspinel-magnetite (Usp-Mt) series. As shown in Figure 6.43, Trend 2 is initially along the axis of the spinel prism toward increasing Fe/(Fe + Mg) ratios at relatively constant but low Ti contents and high Cr/(Cr + Al) ratios (>0.7), followed by a rapid increase in Ti at high Fe/(Fe + Mg) ratios (>0.8) toward the Fe_2TiO_4 (or Fe_3O_4) apex. Manganese enrichment (>1.0% MnO) also occurs in the most evolved spinels. The trend is characterized by rapid Mg depletion and spinels rich in the Mg_2TiO_4 component are not formed. All the spinels in Trend 2 are poor in Al relative to Trend 1 spinels.

Petrographically, the spinel assemblage is similar to Trend 1 in that early cores of AMC are mantled in succession by TMC and Usp-Mt with the latter spinels also being present as abundant discrete corroded groundmass spinels. Atoll textures are common. The hiatus in the crystallization sequence of Trend 2 spinels, as described for Trend 1, is probably related to a miscibility gap.

The common feature of kimberlites characterized by Trend-2 spinels is that they appear to have crystallized abundant phlogopite prior to the formation of the bulk of the groundmass spinels. Boctor and Boyd (1982) have noted that phlogopites are included in Usp-Mt spinels at Bellsbank. Trend 2 is therefore

apparently initiated as a consequence of the depletion of the magma in Mg and Al by extensive phlogopite crystallization.

Spinel crystallization trends in the Tunraq kimberlite are important in that they demonstrate that the kimberlite magma may develop Trend-1 or -2 spinels depending upon the amount of phlogopite crystallization; thus Trend-2 spinels are only developed in the high micaceous (macrocrystal phlogopite) facies of the Tunraq kimberlites (Mitchell 1979b).

6.7.9. Pleonaste Reaction Trend

Al-rich groundmass spinels (Table 6.28, analyses 5–8) that do not belong to magmatic Trends 1 or 2 or the macrocrystal AMC trend, occur as epitaxial mantles upon Trend-1 spinels in some kimberlites.

Pasteris (1980b, 1983) has described from the De Beers kimberlites, chromites (TIMAC), and MUM spinels epitaxially mantled successively by pleonaste ($MgAl_2O_4$) and magnetite (Figure 6.44). The mantled spinels are best developed in kimberlites adjacent to the intrusion margins. In other facies, extensive resorption of the pleonaste has occurred and only remnants of former continuous mantles remain. Atoll spinels lacking pleonaste are considered to be the result of complete resorption. Pasteris (1980b, 1983) suggests that the Al content of the magma was initially controlled by the crystallization of phenocrystal phlogopite and Al-poor spinel, and that during the ascent of the kimberlite, phlogopite ceased to form. The available Al_2O_3 was therefore partioned into pleonaste. Subsequent increases in fo_2 in the later stages of crystallization caused breakdown of the pleonaste and deposition of magnetite as atoll rims. Pleonaste mantles are best preserved in the wall rock regions where it is believed that rapid cooling

Table 6.28. Representative Compositions of Magnesioferrites, Magnetites, and Pleonastes[a]

	1	2	3	4	5	6	7	8
TiO_2	0.64	1.51	0.81	0.0	2.36	2.05	20.61	19.47
Al_2O_3	2.24	1.05	0.10	0.79	49.32	50.5	10.99	12.53
Cr_2O_3	0.00	0.00	0.05	0.0	2.56	5.78	1.88	0.97
Fe_2O_3	70.3	66.9	66.28	68.9	14.38	9.78	24.23	26.96
FeO	18.7	26.4	29.82	28.2	9.74	11.00	18.02	14.48
MnO	0.0	0.14	0.27	0.48	0.29	0.21	0.72	1.04
MgO	8.81	3.96	1.89	1.64	20.32	19.8	22.80	23.20
	100.69	99.95	99.42	100.01	98.97	99.12	99.25	98.65

[a] 1, 2, magnesioferrite-magnetite, Premier (Gaspar and Wyllie 1984); 3, magnetite, Premier (Mitchell 1979a); 4, magnetite, Benfontein (Gaspar and Wyllie 1984); 5, 6, pleonaste reaction mantles De Beers (Pasteris 1983) and Elliot Co. (Agee *et al.* 1982), respectively; 7, 8, titanian ferrian pleonaste, Liqhobong (Haggerty 1973, Boctor and Boyd 1980, respectively).

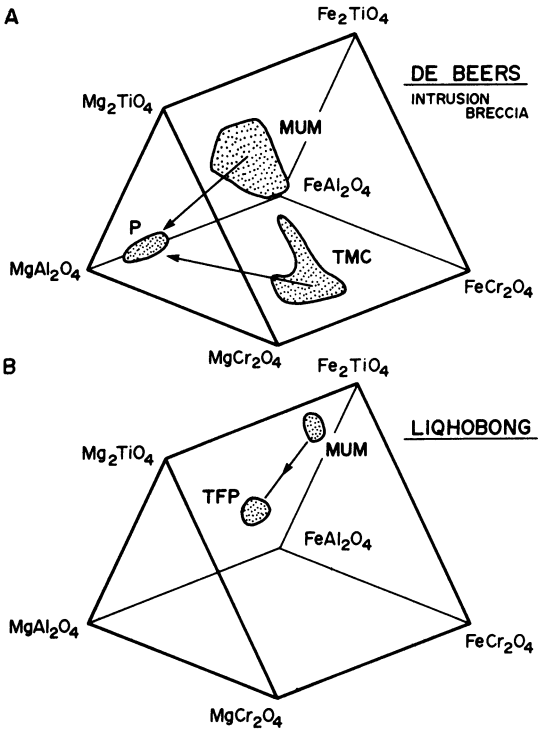

Figure 6.44. Reaction trend spinels in the De Beers (Pasteris 1983) and Liqhobong (Haggerty 1973) kimberlites.

prevented the resorption process from being completed. Pasteris (1980b, 1983) discounts wall rock reaction as a means of enhancing the Al content of the melt, as pleonaste is found in several facies of the intrusion and because of the lack of significant bulk compositional differences between facies.

Similar pleonaste mantles about titanomagnetites occur in the Igwisi Hills extrusives. In this example phenocrystal phlogopite is, however, absent (Reid *et al.* 1975, Pasteris 1983).

Mantles of pleonaste on cores of TIMAC have been described from the Elliot County kimberlite (Figure 6.40D); however, Agee *et al.* (1982) do not advance any hypotheses as to their origin.

Al-rich spinels are known from the Liqhobong kimberlite (Haggerty 1973, Boctor and Boyd 1980) where they occur exclusively in association with reaction mantles on megacrystal ilmenites. Haggerty (1973) described a reaction sequence of primary ilmenite–MUM–secondary Mg–ilmenite–titanian ferripleonaste (TFP)–perovskite. Discrete crystals of TFP detached from and crystallizing in the immediate vicinity of the reacting ilmenite also occur. The TFP are similar to Trend-1 MUM spinels but are distinctly more aluminous (Table 6.28, Figure

6.44). Ti-bearing chromites occurring in the groundmass are not mantled by Al-rich spinels (Boctor and Boyd 1980).

Spinels in the Lipelaneng kimberlite consist of hercynitic-pleonastes and aluminous magnesian chromites mantled by aluminous MUM spinels (Haggerty 1975). Pleonaste mantles are absent. The Lipelaneng kimberlite is unusually rich in spinel lherzolite and spinel wehrlite xenoliths (Carswell *et al.* 1984) and a xenocrystal origin for the Al-rich spinels seems highly probable.

Al-rich spinels clearly have a multiplicity of origins and a hypothesis advanced to account for one occurrence is not necessarily applicable to others.

6.7.10. Kimberlite Spinel Compositional Trends Compared to Those of Other Basic and Alkaline Rocks

Spinels overlapping the compositional range of MAC–AMC macrocrysts, are found in a wide variety of basic and ultrabasic rocks and as inclusions in diamonds (Figure 6.45). The overall similarity, and identical compositional trends, to those of spinels in lherzolite xenoliths in kimberlite, and to spinels in alpine peridotites indicates that some of the macrocrysts could be xenocrysts derived from such sources. On the other hand, the common occurence of AMC-type spinels as primary liquidus phases in such diverse magmas as those forming midoceanic ridge basalts, meimechites, komatiites and layered basic intrusions

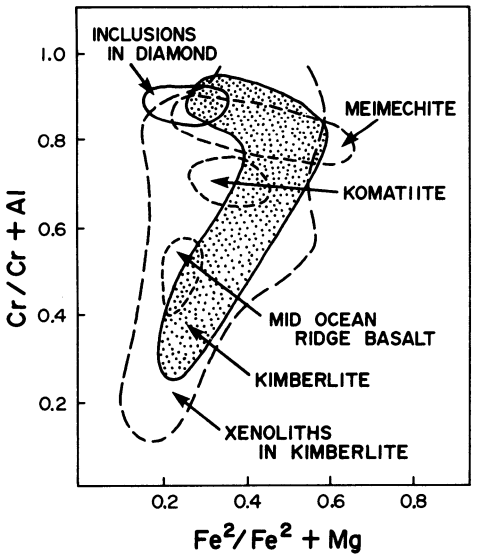

Figure 6.45. Compositions of Ti-poor spinels from kimberlites (stippled field), inclusions in diamonds (Meyer and Boyd 1972), meimechite, komatiite (Bagdasarov *et al.* 1981), mid-ocean ridge basalts (Sigurdsson and Schilling 1976) and xenoliths in kimberlite (Haggerty 1976).

(Figure 6.45), clearly supports a case for other macrocrysts being true phenocrysts. Textural and chemical criteria for distinguishing between these diverse origins are lacking and the problem of identifying provenance is identical to that posed by the olivine macrocrysts. The macrocrystal spinels are best regarded as being composed of a mixed population of xenocrysts and phenocrysts of indeterminate proportions. It is possible that most of the high-Cr spinels are phenocrysts and that most the Al-rich spinels are xenocrysts. Shee (1984), regards all macrocrystal spinels as being xenocrysts. Mitchell and Clarke (1976) in contrast propose that the macrocrysts are phenocrysts formed when garnet ceases to be a liquidus phase in the rising kimberlite magma in response to falling pressure.

Magmatic Trend 1 appears to be unique to kimberlites. The determination of spinel compositional trends thus allows a distinction to be drawn between

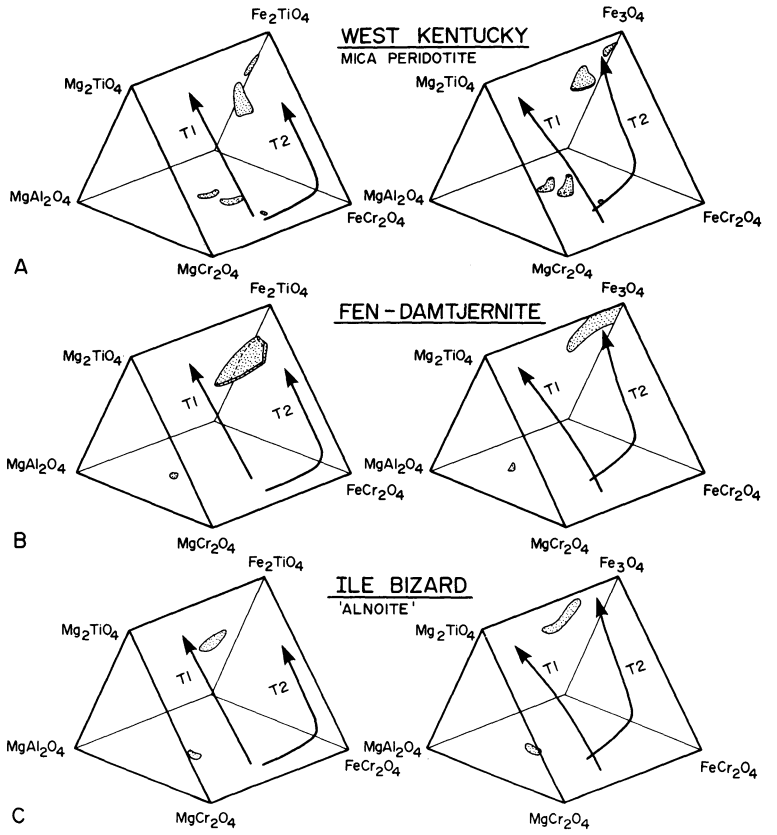

Figure 6.46. Composition of spinels in alnöitic rocks (Mitchell 1979a, this work) compared with kimberlite spinel compositional trends (T1, T2).

petrographically similar rocks, such as mica peridotites, alnöites, and lamprophyres (*sensu lato*), and kimberlites, using weathered, deuterically altered, or fresh material. Mitchell (1979a), Nixon *et al.* (1981), Platt and Mitchell (1982), and Mitchell (1983) have discussed the characteristics of spinels in the former rocks and noted the following:

1. For a given Ti content, they are poorer in Mg, reflecting a lack of solid solution toward Mg_2TiO_4. Titanium is accommodated as ulvöspinel-magnetite solid solutions.
2. They are richer in total Fe and have greater Fe^{3+}/Fe^{2+} ratios, reflecting their higher Fe_3O_4 contents.
3. They are typically lacking in spinels with $Cr/(Cr + Al) > 0.8$ (Figures 6.46, 6.47). Chromites are thus more aluminous, in keeping with the common anchibasaltic parentage of the magmas and co-existence with groundmass and/or megacrystal aluminous pyroxenes.
4. They have a different evolutionary trend (Figure 6.46, 6.47). Lamprophyric spinels trend from low-to-high Ti with increasing $Fe^{2+}/(Fe^{2+} + Mg)$ and $Fe^{3+}/(Fe^{3+} + Cr + Al)$ ratios, that is, diagonally upward from the

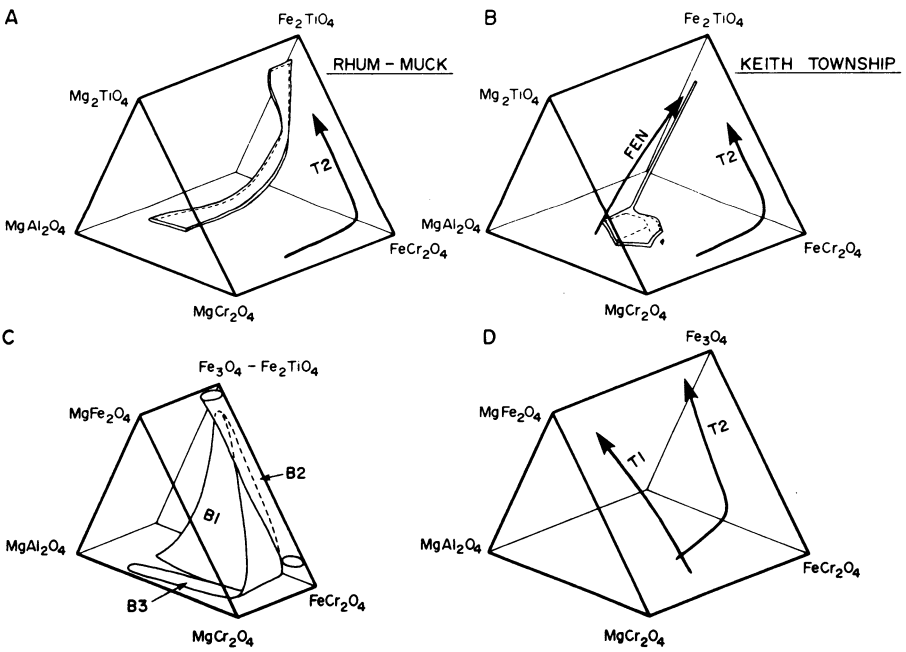

Figure 6.47. Composition of spinels in (A) basalts (Ridley 1977), (B) the Keith Township lamprophyre (Watson *et al.* 1978). (C) and (D) compare basalt (Haggerty 1976) and kimberlite spinel compositional trends in the oxidized spinel prism, respectively.

base of the spinel prism toward the Fe_2TiO_4 (or Fe_3O_4) apex. Commonly, cores of chromite are mantled by ulvöspinel-magnetite.

5. They are typically richer in MnO (1.0%–2.5%) than Trend 1 kimberlite spinels which usually contain less than 1% MnO.

In contrast, magmatic Trend 2 is not unique to kimberlites. Trend 2 and the lamprophyric trends described above appear to be variants of a common trend in spinels from a wide variety of "basaltic" rocks (Figure 6.47). The trends are similar in that their initial evolution is along the prism axis [increasing $Fe^{2+}/(Fe^{2+}Mg)$] followed by the rapid Ti and Fe^{3+} increase toward the Fe_2TiO_4 (or Fe_3O_4) apex. The trends differ in their Cr/(Cr + Al) ratios, with the kimberlite trend being a Cr-rich variant(Figure 6.47).

Spinels of high Cr/(Cr + Al) ratio, very similar to Trend-2 spinels, are found in lamproites. In these rocks, evolved Mg-poor titaniferous magnetites (Usp-Mt) occur as discrete crystals and as mantles upon titanian magnesian chromites (Mitchell 1985). Figure 6.48 shows that the kimberlite and lamproite trends originate from Ti-poor spinels of similar composition and that Trend-2 and the lamproite trend diverge sharply from Trend 1 in the early stages of the compositional evolution.

Magmatic Trend 2 is in itself not diagnostic of a kimberlitic paragenesis. The Cr-rich members of the trend, by virtue of their high Cr/(Cr + Al) ratios, are indicative of kimberlite or lamproite, but the final identification must be made on the basis of the occurrence of groundmass titanian potassian richterite in lamproite. The Ti-rich evolved spinels are not characteristic of a particular paragenesis and are known from a wide variety of basic alkaline rocks (Haggerty 1976, Nixon *et al.* 1980, Platt and Mitchell 1979, 1982).

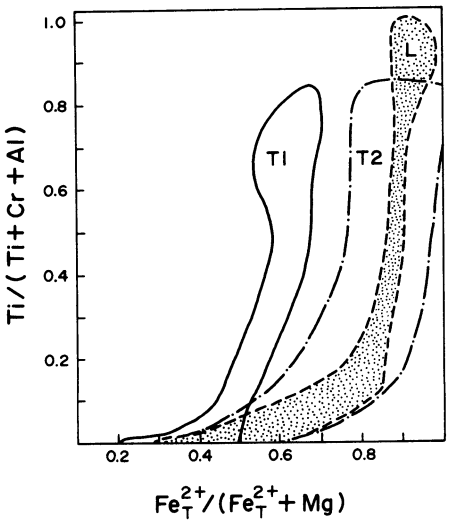

Figure 6.48. Compositional trends of kimberlite (T1, T2) and lamproite (L) spinels.

The principal characteristics of carbonatite spinels are lack of Cr_2O_3, low TiO_2, and low MgO relative to kimberlite spinels. The spinels are essentially members of the magnesioferrite-ulvöspinel-magnetite series. MgO contents (0–10%, Haggerty 1976, Gaspar and Wyllie 1983, Mitchell 1979a) are variable, but those containing appreciable MgO are easily distinguished from kimberlite spinels as the Mg content reflects solid solution toward magnesioferrite rather than magnesian ulvöspinel. Such spinels, therefore, lack appreciable TiO_2 and may contain significant MnO. High levels of MnO (2%–12%) occur but should not be regarded as being characteristic, as relatively pure magnetite is also very common (Haggerty 1976, Prins 1972, Mitchell 1979a). Oxidation-exsolution lamellae of ilmenite (commonly Mn rich) are characteristic features of many carbonatitic titaniferous magnetites (Mitchell 1978c).

Cr spinels such as TIMAC, TMC, and TC and Mg-Ti-rich spinels (MUM) are not found in carbonatites. Conversely, jacobsite-magnesioferrite-magnetites are not characteristic of kimberlites.

It should be noted that spinel compositions in kimberlites, carbonatites, and lamprophyres all converge upon Fe_3O_4; thus the calcite-rich segregations and veins in the Benfontein and Peuyuk kimberlites (Gaspar and Wyllie 1984, Mitchell and Clarke 1976) have crystallized Ti-Mg-poor magnetites identical in composition to many carbonatite magnetites. The carbonate dikes cutting the Premier kimberlite likewise contain magnesioferrite (Mn poor) and pure magnetite (Gaspar and Wyllie 1984, Mitchell 1979a). This mineralogical convergence can be expected as minerals of similar composition will form wherever the correct physicochemical conditions for stability are met in magmas of diverse origins, and the simple presence of magnetite should not be used as an argument in favor of a genetic relationship of kimberlite with carbonatites (see Section 9.12).

6.8. PEROVSKITE

Perovskite is a ubiquitous accessory phase. Modal abundances typically range from trace amounts up to 10% (Skinner and Clement 1979), but can rise rarely to major levels(>25%) in occurrences where perovskite and spinel have been locally concentrated by magmatic processes, e.g., the Benfontein Sill (Dawson and Hawthorne 1973). Perovskite is usually less abundant than the earlier-formed spinel assemblage, although this relationship may be reversed in examples in which extensive spinel resorption has occurred.

The bulk of the perovskite occurs as discrete euhedral-to-subhedral or rounded crystals ranging in size from 0.05 to 0.2 mm in their largest dimension. The crystals can be scattered randomly throughout the groundmass or be concentrated together with spinels as "necklaces" around earlier-formed pseudomorphed olivines. The habit is commonly characterized by re-entrant angles indicative of the presence of complex interpenetrant twins (Blagulkina and Tarnovskaya 1975).

Colors range from yellow-brown through brown to reddish-brown.

Perovskite also occurs as simple mantles upon earlier-formed ilmenite, rutile, magnesian chromite, and magnesian ulvöspinel-ulvöspinel-magnetite (MUM) or as part of a more complex epitaxial mantling sequence, e.g., ilmenite-Cr-spinel-perovskite or ilmenite-MUM-perovskite-rutile. Decomposition of megacrystal ilmenites leads to the development of complex reaction mantles of intimately intergrown anhedral crystals of MUM, perovskite, serpentine, sulfides and rutile (Mitchell 1972, Haggerty 1973, Elthon and Ridley 1979, Boctor and Meyer 1979, Pasteris 1980b, Hunter *et al.* 1984). The occurrences of complex intergrowths and aggregates with MUM spinels indicate some contemporaneous crystallization, although the bulk of the perovskite post-dates spinel formation.

The perovskite mantling relationships reflect the instability of earlier-formed phases in liquids saturated with perovskite. Their decomposition releases Ti which combines with the Ca present to precipitate a reaction mantle which is chemically identical to contemporaneous liquidus perovskite (Mitchell 1972).

Perovskite crystallizes after olivines and spinels and prior to monticellite, eastonitic phlogopite, serpentine, and calcite. It is also rarely found as inclusions in microphenocrystal phlogopite.

The mineral is not stable in the residual fluids and perovskites are commonly resorbed and/or mantled by thin rims of rutile (Mitchell and Clarke 1976, Boctor and Meyer 1979).

6.8.1. Composition

Kimberlitic perovskites are relatively pure $CaTiO_3$ with very little solid solution toward other perovskite-structured compounds (Table 6.29). The principal substitutions for Ca and Ti are by the rare earth elements (REE) and Nb. Perovskite is the major carrier of these elements in kimberlites.

Grantham and Allan (1960) initially reported the presence of substantial amounts of REE and recent studies have demonstrated that perovskite may contain from 2–16 wt% total REE oxides (Table 6.29). Although all studies are in agreement that perovskites are enriched in the light REE (La-Gd), there is no agreement concerning the abundance of the individual REE.

Jones and Wyllie (1984) have argued that the electron microprobe data of Boctor and Boyd (1979, 1980a, 1981, 1982) and Boctor and Meyer (1979) contain serious analytical errors arising from a combination of a poor choice of analytical lines and backgrounds, inadequate assessment of interferences and less than optimum sensitivity for the REE with the beam current and accelerating voltages employed. The basis for Jones and Wyllie's (1984) assertions lies in their demonstration that Exley and Smith's (1982) analytical scheme produces data that give smooth curves on chondrite normalized REE distribution plots that are similar to the REE distribution patterns obtained by neutron activation

on whole rock kimberlites. Jones and Wyllie (1984) thus believe that the analytical errors inherent in the Boctor–Boyd method leads to over-estimation of the heavy REE, under-estimation of Sm, and highly irregular REE distribution patterns. Table 6.29 and Figure 6.49 illustrate clearly the differences in the REE abundances and distribution patterns for Benfontein perovskites obtained by the Boctor–Boyd and the Jones–Wyllie methods.

Figure 6.49 also indicates that analytical errors, especially with respect to Pr and Dy abundances, are present in the REE obtained by Blagulkina and Tarnovskaya (1975) and Ilupin *et al.* (1971) by X-ray spectrometric methods.

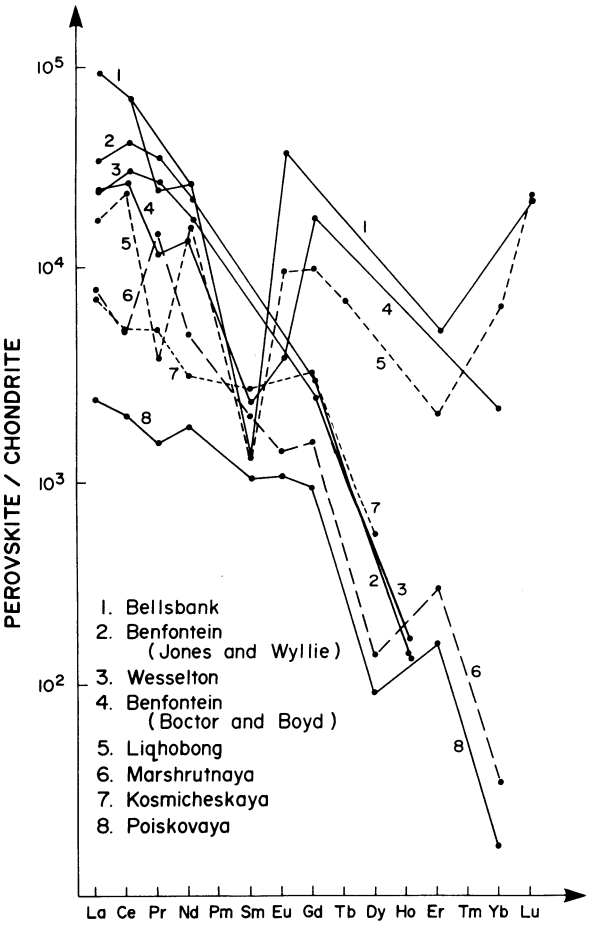

Figure 6.49. Rare earth element distribution patterns for kimberlite perovskite: 1, Boctor and Boyd (1982); 2, 3, Jones and Wyllie (1984); 4, Boctor and Boyd (1981); 5, Boctor and Boyd (1980a); 6–8, Blagulkina and Tarnovskaya (1975).

Table 6.29. Representative Compositions of Perovskites from Kimberlites, Alkaline Rocks, and Carbonatites[a]

	1	2	3	4	5	6	7	8	9	10	11	12	13	14	15
TiO_3	52.43	52.1	53.9	55.8	54.28	50.04	43.00	55.20	53.6	52.3	55.25	36.20	10.05	41.43	39.65
SiO_2	—	0.04	0.04	0.05	0.04	0.22	0.03	1.00	0.15	0.03	—	0.09	0.45	—	0.38
ZrO_2	—	0.36	0.67	—	—	—	0.01	0.05	0.2	0.2	0.03	—	—	0.14	—
Nb_2O_5	0.55	1.33	0.80	0.90	—	2.18	11.50	0.24	0.8	1.5	0.08	16.79	43.90	2.67	9.74
Al_2O_3	—	0.51	0.28	0.17	—	—	—	1.12	0.9	0.4	—	—	—	—	0.20
Y_2O_3	—	0.032	0.044	0.018	—	—	0.08	0.03	0.1	0.1	—	—	—	—	—
FeO^b_T	1.54	1.75	1.06	0.94	1.24	1.62	2.58	1.64	1.9	2.7	0.97	4.88	7.86	1.00	0.36
MnO	—	0.04	0.06	0.02	—	—	—	0.02	0.03	0.06	—	—	0.77	—	—
MgO	0.83	0.11	0.11	0.11	0.34	0.37	0.34	0.37	—	—	0.06	0.46	2.20	—	—
CaO	37.60	35.7	35.5	39.5	36.54	27.44	30.00	38.41	38.2	32.3	37.56	35.43	25.95	2.64	5.00
SrO	—	0.23	0.19	0.08	—	—	—	0.26	0.5	1.2	0.48	—	—	23.85	3.42
BaO	—	0.14	0.19	0.16	—	—	—	—	—	—	0.17	—	—	0.39	—
Na_2O	0.53	0.33	0.67	0.36	0.79	1.54	1.88	0.32	0.3	0.8	0.33	0.98	4.03	3.47	8.32
K_2O	—	0.02	0.02	0.02	—	—	—	0.11	0.08	0.05	0.12	—	0.03	0.28	0.13
La_2O_3	0.93	1.037	0.877	0.320	0.67	3.70	1.98	0.12	0.5	1.4	—	1.13	—	8.02	—
Ce_2O_3	2.70	3.053	2.830	0.797	2.41	7.90	5.88	0.26	1.0	2.8	—	2.19	—	10.85	—

Pr_2O_3	0.16	0.341	0.335	0.062	0.05	0.99	0.81	0.05	0.2	0.6	—	0.10	—	—	—
Nd_2O_3	0.98	1.261	1.292	0.302	1.14	1.75	1.64	0.13	0.7	1.9	—	0.11	—	—	—
Sm_2O_3	0.05	0.140	0.147	0.040	0.03	0.07	—	0.03	0.1	0.2	—	—	—	—	—
Eu_2O_3	0.03	—	—	—	0.08	0.23	—	0.01	0.1	0.1	—	0.09	—	—	—
Gd_2O_3	0.54	0.075	0.084	0.019	0.29	0.54	—	0.03	0.2	0.4	—	—	—	—	—
Tb_2O_3	—	—	—	—	0.04	0.15	—	0.01	—	—	—	—	—	—	—
Dy_2O_3	—	—	—	—	—	—	—	—	—	—	—	—	—	—	—
Ho_2O_3	—	—	—	—	—	—	—	—	—	—	—	0.41	—	—	—
Er_2O_3	—	—	—	—	0.05	0.20	—	—	—	—	—	0.06	—	—	—
Tm_2O_3	—	—	—	—	—	—	—	—	—	—	—	—	—	—	—
Yb_2O_3	0.05	0.005	—	—	0.16	—	—	—	—	—	—	—	—	—	—
Lu_2O_3	—	—	—	—	0.09	—	—	—	—	—	—	—	—	—	—
TR_2O_3[b]	—	—	—	—	—	—	—	—	—	—	—	—	2.03	5.87	30.80
	98.92	98.604	99.099	99.668	98.24	98.94	99.73	99.41	99.56	99.04	95.05	99.09	97.27	100.61	98.00

[a] 1, Benfontein sill (Boctor and Boyd 1981); 2–4, Benfontein sill, Wesselton and Premier, respectively (Jones and Wyllie 1984); 5, Liqhobong (Boctor and Boyd 1980); 6, Bellsbank (Boctor and Boyd 1982); 7, Green Mountain (Boctor and Meyer 1979); 8, Turmannosti (Blagulkina and Tarnovskaya (1975); 9, melilitite, Dwinberg Czechoslovakia (Smith 1970); 10, nephelinite, Etinde, Cameroon (Smith 1970); 11, lamproite Prairie Creek, Arkansas (Scott Smith and Skinner 1984); 12, carbonatite, Oka (Boctor and Yoder 1980); 13, Nb-perovskite, carbonatite, Oka (Nickel and McAdam 1963); 14, Sr-loparite, Sarambi-fenite (Haggerty and Mariano 1983); 15, loparite, Kola (Vlasov 1966).

[b] FeO_T = total iron expressed as FeO; Tr_2O_3 = total rare earth element oxides.

Although Ilupin (1977) believes that the Blagulkina and Tarnovskaya (1975) data are in error, these latter data are more in keeping with Jones and Wyllie's (1984) data than Boctor and Boyd's analyses and are in reasonable agreement with whole rock REE distribution patterns.

Although Table 6.29 lists the abundances of individual REE in perovskite, it should be borne in mind that these data, especially for the heavy REE, may be substantially in error. All of the studies however demonstrate that La, Ce, Pr, Nd, Sm (and Y) are the most significant of the REE present. Sufficient and/or accurate data are not as yet available to establish the nature of the solid solutions present. These may be toward loparite (Na, Ce, Ca)(Nb, Ti, Fe)O_3, or $CaCeO_3$ if Ce^{4+} is present, although the substitutions of REE^{3+} for Ca^{2+} and Ti^{4+} are complicated by the occurrence of site vacancies and distortion of the ideal perovskite structure.

Niobium contents ranging from 0.5% to 2.0% Nb_2O_5, coupled with the presence of significant amounts (0.3%–0.88%) of Na_2O (Mitchell 1972, Boctor and Boyd 1979, 1980a, 1981, 1982, Jones and Wyllie 1984), are indicative of minor solid solution toward $NaNbO_3$ (leushite), and that perovskite is a major host for Na_2O in kimberlites. Boctor and Meyer (1979) have reported the presence of perovskites that are unusually rich in Nb_2O_5 (6.8%–11.5%) in the Green Mountain kimberlite. The elevated Nb_2O_5 contents are, however, not accompanied by concomittant Na_2O enrichment.

Other elements present in minor quantities (Table 6.29) include FeO_T (1%–2%), ZrO_2 (0.3%–1.5%), and Al_2O_3 (0.2%–1.1%). Significant levels of SrO (0.08%–0.25%) and BaO (0.14%–0.19%) are reported by Jones and Wyllie (1984). Uranium is concentrated in perovskite (Figure 7.11) and the mineral has been found suitable for U–Pb geochronology (Kramers and Smith 1983).

Most perovskites appear to be homogeneous, although minor core-to-rim zonation has been reported for Fe (increasing), Nb (decreasing), and Al (increasing) by Shee (1984), Boctor and Meyer (1979) and Elthon and Ridley (1979), respectively.

Mitchell (1972) and Hunter *et al.* (1984) have shown that there are no significant compositional differences between discrete and reaction-rim perovskites. Mitchell (1972) found no inter- or intra-kimberlite compositional variations. Boctor and Boyd (1981) showed that the REE contents of perovskite from both the carbonate-oxide layers and the silicate-rich layers of the Benfontein sill are similar.

The low Fe content of kimberlite perovskite, even in reaction rim perovskite where the activity of iron must be high, is important. Kimura and Muan (1971a) studied the system CaO–iron oxide–TiO_2 in air and found that perovskite can contain up to 83% Fe substituting for Ti; however in the same system under a strongly reducing environment there is no appreciable solid solution (Kimura and Muan 1971b). Mitchell (1972) interpreted the paucity of Fe in kimberlitic perovskite to be indicative of formation under low oxygen fugacities.

Perovskite of similar composition (Table 6.29) to kimberlite perovskites is found in alkaline pyroxenites (Frank-Kamentskii and Veselskii 1961), melilitites, ugandites, mafurites, and nephelinites (Smith 1970) and madupitic lamproites (Scott Smith and Skinner 1984b).

Carbonatites, in contrast, contain perovskites that are enriched in Fe, Na, Nb, Ta, Sr, Ba, and REE (Table 6.29) relative to kimberlite perovskite and thus show extensive solid solution toward leushite and loparite end members (Nickel and McAdam 1963, Boctor and Yoder 1980, Haggerty and Mariano 1983). Eby (1975) has also noted that carbonatitic perovskite from Oka exhibits significant negative Eu anomalies.

6.9. MONTICELLITE

Until recently monticellite was considered to be a relatively rare and minor mineral, its presence being only tentatively identified on the basis of optical criteria in kimberlites from Zaire (the calcic olivine of Verhoogen 1938), South Africa and Lesotho (Wagner 1929, Dawson 1962), and Siberia (Nikishov and Nikishova 1966, Frantsesson 1970).

Clement *et al.* (1975), Mitchell (1978a) and Skinner and Clement (1979), however, provided positive identification using electron microprobe analysis and demonstrated that in some kimberlites, monticellite is a major groundmass phase.

Monticellite occurs principally as discrete euhedral-to-subhedral small (0.005–0.08 mm) crystals (Figure 3.19) in amounts ranging from trace quantities to 60%–80% of the groundmass (Skinner and Clement 1979, Nikishov and Nikishova 1966). Although the crystals are typically colorless and zonation free, Mitchell (1978a) has noted zonation from pale-yellow cores to colorless margins in monticellites from the Elwin Bay kimberlite. Many crystals exhibit patchy extinction and relief due to incipient alteration (Snowden 1981, Clement 1982). Monticellites, typically, are free of inclusions of silicate and oxide phases, although Nikishov and Nikishova (1966) have reported (unconfirmed) the presence of periclase inclusions. Small fluid inclusions are, however, common.

Monticellite has also been found replacing serpentinized olivines (Kornilova *et al.* 1983, Clement 1982) and as apparent reaction coronas about olivine (Verhoogen 1938, Nikishov and Nikishova 1966). Limestone and/or dolomite xenoliths commonly exhibit reaction rims of monticellite precipitated during the attempted assimilation of the xenolith by the kimberlite magma.

Monticellite crystallizes after spinel and perovskite and prior to late-stage primary groundmass serpentine and calcite. The apparent rarity of monticellite, especially in calcite-rich kimberlites (Kornilova *et al.* 1983), may be due to the ease with which it is replaced by calcite. Groundmass plates of eastonitic phlogopite commonly poikilitically enclose euhedral monticellite crystals. Diopside

and monticellite do not cyrstallize contemporaneously; the appearance of either phase being controlled by the local silica activity (see Section 9.9).

6.9.1. Composition

Although few compositional data exist, Table 6.30 and Figure 6.50 demonstrate that kimberlitic monticellites are relatively pure $CaMgSiO_4$, exhibiting in some cases significant solid solution toward kirschsteinite (5–20 mol% $CaFeSiO_4$) and forsterite (3–12 mol% Mg_2SiO_4). The solid solution towards Mg_2SiO_4 is more extensive than that predicted at low temperatures (900°C, 2 kbar) by Warner and Luth's (1973) study of the iron-free Mg_2SiO_4–$CaMgSiO_4$ solvus.

Clement *et al.* (1975) noted that minor increases in the Fe content of De Beers monticellite were correlated with decreasing crystal size. In contrast Mitchell (1978a) found that Elwin Bay monticellites were zoned from Fe-rich cores to Fe-poor margins. The majority of crystals are, however, zonation free. Figure 6.50 shows that Elwin Bay monticellites have a wider compositional range than monticellites from other kimberlites. Significant intergrain compositional variations (Table 6.30) appear to be common. Figure 6.50 also suggests that individual kimberlites are characterized by monticellites of a particular composition; however, too few data are available to establish this observation firmly.

Few comparative data are available for monticellites from alkaline ultrabasic rocks, although the presence of this mineral has been reported from several occurrences considered to have "kimberlitic" or alnöitic affinities, e.g., the Williams diatremes (Hearn 1968), the Blue Hills monticellite peridotite (Janse 1971), Isle Cadieux (Bowen 1922), and the Kuonamka-Luchakan River alnöitic intrusions (Nikishov *et al.* 1979).

Table 6.30 and Figure 6.50 show that monticellites in the Blue Hills per-

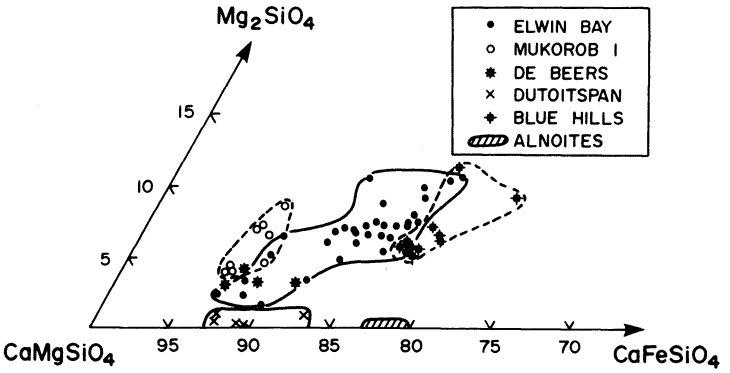

Figure 6.50. Composition of monticellite from the Elwin Bay (Mitchell 1978a), Mukorob 1 (this work), De Beers (Clement *et al.* 1975) and Dutoitspan (Snowden 1981) kimberlites. Data for Blue Hills peridotite and Yakutian alnöites from this work and Nikishov *et al.* (1979).

Table 6.30. Representative Compositions of Monticellites from Kimberlites, Alnöites[a]

Wt. %	1	2	3	4	5	6	7	8	9	10	11	12	13	14	15
SiO_2	37.26	37.66	37.31	37.41	37.52	36.95	37.45	36.91	36.84	36.95	37.25	37.87	37.39	36.68	37.61
Al_2O_3	0.04	0.04	0.00	0.00	0.00	0.00	0.09	0.10	0.00	0.00	0.06	0.11	0.48	0.07	0.07
FeO[b]	3.16	5.38	3.36	5.88	3.02	3.97	7.87	5.45	7.38	3.73	8.05	7.41	9.59	8.07	8.01
MnO	0.00	0.00	0.28	0.27	0.37	0.43	0.40	0.27	0.47	0.19	0.29	0.35	0.48	0.44	0.34
MgO	24.33	23.02	23.73	22.16	24.57	24.09	23.41	24.13	23.04	23.64	21.63	22.27	20.71	20.37	19.51
CaO	34.27	33.90	34.93	34.92	33.83	33.51	31.48	33.05	31.63	34.19	32.46	32.82	30.36	34.21	33.16
	99.06	100.01	99.61	100.64	99.36	98.99	100.76	100.00	99.36	98.70	99.74	100.83	99.01	99.84	98.70
Mol % end member molecules															
Ks	7.0	12.0	7.4	13.1	6.7	8.8	17.5	12.0	16.6	8.3	18.3	16.6	22.5	18.3	18.8
Mo	90.1	84.7	91.6	86.2	89.5	86.8	72.2	81.3	74.5	89.4	76.1	77.7	68.6	81.1	80.9
Fo	2.9	3.3	1.0	0.7	3.8	4.4	10.3	6.7	8.9	2.3	5.7	5.7	8.9	0.6	0.3

[a] 1, 2, De Beers (Clement *et al.* 1975); 3, 4, Dutoitspan (Snowden 1981); 5, 6, Mukorob 1 (this work); 7, 8, 9, 10, cores and rims, respectively, Elwin Bay (this work); 11, Lattavaram 1 (Akella *et al.* 1979); 12, 13, Blue Hills peridotite, Gros Brukkaros (this work); 14, 15, Tamakh and Victoriya alnöites (Nikishov *et al.* 1979).

[b] Total iron expressed as FeO; Ks = $CaFeSiO_4$, Mo = $CaMgSiO_4$, Fo = Mg_2SiO_4.

idotites are very similar to Fe-rich monticellites from kimberlites. In contrast monticellites from the Tamakh and Viktoriya alnöites (Nikishov *et al.* 1979) do not exhibit solid solution toward Mg_2SiO_4 and are essentially monticellite-kirschsteinite solid solutions. Kornilova *et al.* (1983) consider that monticellites from kimberlites and alnöites do not differ in their compositions. An important difference, however, is that in the alnöitic paragenesis the monticellite is always accompanied by melilite or its decomposition products.

6.10. APATITE

Apatite is a late-crystallizing groundmass phase occurring in quantities ranging from less than 1% (vol) to as much as 10% (vol) in some apatite phlogopite kimberlites or calcite-rich segregations (Skinner and Clement 1979, Apter *et al.* 1984). The crystals are typically euhedral to subhedral hexagonal prisms rarely exceeding 0.2 mm in length, and in most kimberlites are smaller than 0.01 mm (Clement 1982). Apatites are particularly abundant in carbonate-rich portions of the groundmass and in calcite-rich segregations (Figure 3.20). In calcite-rich kimberlites, apatites tend to be larger (0.2–0.8 mm) than those in calcite-poor kimberlites, and to enclose poikilitically earlier-formed monticellite, perovskite, and spinel. Apatites in segregations, in some cases appear to have nucleated at the margins of the segregations, while in others appear to have formed prior to the development of the segregation as they traverse the margins of the segregation. Dawson and Hawthorne (1973) and Clement (1975) have described from the Benfontein and Andreisfontein kimberlites respectively, acicular radial aggregates of apatites. These are similar to quench apatites produced experimentally by Wyllie *et al.* (1962). Skeletal crystals indicative of rapid growth are also illustrated by Wagner (1914).

Apatite is commonly replaced by later-forming calcite resulting in the formation of "ghosted" and resorbed irregular crystals. Textural evidence indicates that most apatite forms prior to calcite and late-stage primary serpentine.

6.10.1 Composition

Little is known of the compositional variation of kimberlite apatite. Representative compositions given in Table 6.31 demonstrate that they are very pure fluor-hydroxy apatites, although significant quantities of silicon may replace phosphorous. The only other elements present in appreciable amounts include the rare earth elements (REE) and strontium. The high Na_2O content reported by Zhang and Liou (1983) appears anomalous.

Ilupin *et al.* (1971) have shown by X-ray spectrometric methods that apatites from Siberian kimberlites contain 0.38%–1.23% total $(REE)_2O_3$. Chondrite normalized distribution patterns (Figure 6.51) are irregular, and experimental error,

Table 6.31. Representative Compositions of Apatite[a]

	1	2	3	4	5	6	7
SiO_2	0.69	—	2.23	2.16	1.59	0.04	—
Al_2O_3	—	—	0.36	0.02	—	—	—
FeO	0.18	0.11	0.23	0.11	—	0.08	0.13
MnO	—	—	—	0.07	0.02	—	—
MgO	0.09	0.72	0.13	0.13	0.82	0.23	0.23
CaO	56.41	55.23	55.93	54.26	54.78	54.59	52.68
Na_2O	0.05	0	2.28	0.07	—	—	—
K_2O	0.05	0	0	0	0	0.05	0.06
BaO	0.02	0	0	0		0.20	0.19
SrO	0.68	—	—	—	0.58	2.51	—
P_2O_5	38.97	36.88	37.16	36.83	37.04	38.58	36.65
F	3.62	—	2.24	—	2.37	5.91	—
	100.76	92.94	100.56	93.65	97.20	102.19	89.94

[a] 1, Orroroo (Scott Smith *et al.* 1984); 2, Wesselton (Mitchell 1984); 3, China, location unknown (Zhang and Liu 1983); 4, Holsteinsborg (Scott 1981); 5, Benfontein, includes Cl = 0.08%, Y_2O_3 = 0.024%, La_2O_3 = 0.224%, Ce_2O_3 = 0.372%, Nd_2O_3 = 0.139%, (Exley and Smith 1982); 6, lamproite, Prairie Creek (Scott Smith and Skinner 1984); 7, lamproite Leucite Hills (Keuhner *et al.* 1981).

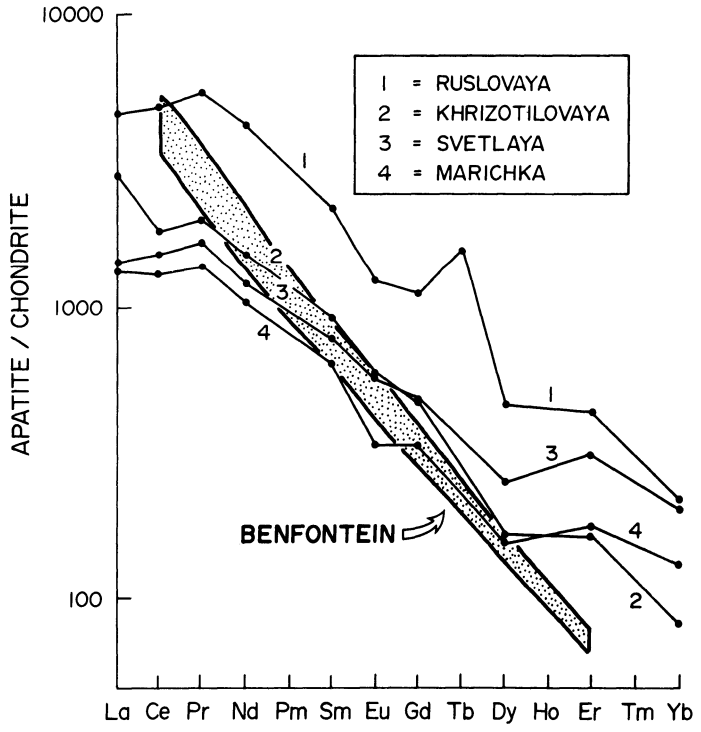

Figure 6.51. Rare earth distribution patterns for kimberlite apatite. Data for Yakutian (1–4) kimberlites and the Benfontein sills from Ilupin *et al.* (1971) and Jones and Wyllie (1984), respectively.

particularly in the determination of Pr, Dy, and Tb, must be suspected. The slopes of the distribution patterns are however similar to those of the better quality data presented by Jones and Wyllie (1984). Figures 6.49 and 6.51 show that the chondrite normalized abundances of the light REE in apatite are a factor of 10 less than those of perovskite, and that the enrichment of the light REE is not quite as extreme. Carbonate-rich highly evolved kimberlitic sills contain apatites that are poor in REE (Jones and Wyllie 1984, Mitchell 1984a). REE abundances in apatites are consistent with crystallization of apatite from a liquid that has been depleted in REE by the prior crystallization of perovskite.

Kimberlitic apatites appear to be similar in their composition to apatites from a wide variety of rocks including lamproites (Table 6.31); however, insufficient data are available for meaningful comparisons to be made.

6.11. SERPENTINE

Serpentine is one of the dominant groundmass minerals of many kimberlites (20%–50%, Skinner and Clement 1979). Despite the ubiquity of serpentine, few studies have been made of its compositional variation or of the polymorphs and polytypes present. The paucity of information is a consequence of the extremely small size of the serpentine crystals and their common intergrowth with other phases, rendering them intractable to routine X-ray or chemical investigations.

Serpentine-group minerals occur in three parageneses:

1. As pseudomorphic replacements of earlier minerals, including macrocrystal and microphenocrystal olivines and such groundmass phases as phlogopite, monticellite, calcite, and pre-existing serpentines.
2. As a primary groundmass mineral, forming veins and segregations (Clement 1975, Emeleus and Andrews 1975, Clarke and Mitchell 1975, Mitchell 1978a).
3. As non-pseudomorphic prograde replacements (terminology of Wicks and Plant 1979) of pre-existing pseudomorphic serpentines (Jago 1982, Jago and Mitchell 1985).

No two kimberlites exhibit exactly the same pattern of olivine replacement or have identical groundmass textures; even individual kimberlites vary widely on a centimeter scale.

6.11.1. Pseudomorphic Replacements

Petrographic studies have demonstrated that the serpentinization of olivine is a complex process. Commonly, the small euhedral-to-subhedral groundmass olivines are completely pseudomorphed while the larger macrocrystal olivines

are only partially replaced. In some kimberlites extensive serpentinization of olivines occurs only in zones surrounding xenoliths.

In most examples several stages of serpentinization are evident. The earliest stage, observed predominantly in macrocrysts, is a network of anastomozing yellow-brown to pale yellow veins. The veins may be composite and sometimes contain minute magnetite crystals. This serpentinization event occurred prior to the incorporation of the crystals in their current host, as the veins are terminated by marginal serpentines of a different character. These latter serpentines envelop the olivines and were developed *in situ*. The vein-type serpentines are identical to serpentines found in olivines in ultramafic xenoliths and may represent a pre-kimberlite serpentinization event (Helmstaedt 1982), if the macrocrysts are derived from such a source. Large euhedral-to-subhedral macrocrysts, possibly of phenocrystal origin, are typically not serpentinized to the same degree and commonly only along well-defined cleavages or partings. (The nature of the serpentinization may in fact provide a means of distinguishing between phenocrystal and xenocrystal populations of olivine.)

Marginal pseudomorphic serpentines form complex mantles about remnant macrocrystal and microphenocrystal olivines or completely pseudomorph the latter. Two (or more) optically distinct (color, texture, inclusions) zones of widely variable width are commonly present. These zones may represent growth mantling, reflecting changing serpentine compositions in response to changing conditions in the fluid phase from which it forms. Alternatively the zones may represent partial replacements of pre-existing serpentines by later groundmass and segregation serpentines. Both cases may be present in some examples.

Serpentinization is accompanied by the formation of nickel sulfide as acicular crystals in the Lattavaram kimberlite (Akella *et al.* 1979) and as globules in the De Beers (Pasteris 1980b) and Sydney-on-Vaal kimberlites (this work). Release of Fe from the olivine as magnetite is not typical of marginal pseudomorphic serpentinization.

6.11.2. Segregation and Groundmass Serpentine

Serpentines, in this paragenesis, are extremely fine grained homogeneous pale-green-to-brown amorphous-appearing masses. Typically, they are isotropic or very weakly birefringent. Such serpentines have been termed "serpophite" (Lodochinkov 1933). This name is useful as a descriptive term but has no strict mineralogical meaning, as Wicks and Zussmann (1975) have shown that serpophites are not amorphous but are extremely fine grained aggregates of identifiable minerals. As noted in Section 3.7.2, serpophite segregations and the silicate-oxide groundmass serpentine are related, both being apparently the last primary phases to form. Some serpophites replace pre-existing pseudomorphic serpentines and calcite. Serpophites may be the result of the crystallization of

gel-like matter deposited from low-temperature $MgO–SiO_2–H_2O$-rich residua. Textures indicative of colloidal parentage are, however, lacking.

6.11.3. Prograde Serpentine

Non-pseudomorphic prograde serpentine results in the total replacement and recrystallization of pseudomorphic and serpophitic serpentines. In the Ham kimberlite, it occurs as a uniform very fine-grained pale yellow mosaic-type multilayer lizardite replacing earlier single-layer fibrous lizardites (Jago and Mitchell 1985). In the Ham example the development is due to the alteration of an earlier facies of the intrusion by residual fluids emanating from a later intrusion. The formation of antigorite and magnetite together with the introduction of calcite is a feature of the alteration process, and results in complete replacement of the original textures. Prograde serpentinization may be more common than currently realized due to the insufficient attention which has been given to highly "altered" serpentine-calcite kimberlites.

Serpentine, in all of the above parageneses, is usually considered to be of deuteric origin. This assumption is not necessarily correct, especially in the cases of serpentines formed in diatreme facies rocks or in association with "de-watered" xenoliths. Sheppard and Dawson (1975) and Ukhanov and De Virts (1983) have demonstrated that a significant fraction of the water in serpentines is of meteoric origin. Incorporation of this water into the magma prior to crystallization, however, results in late-stage serpentinization which in a petrographic sense is deuteric.

6.11.4. Structural Types

Few studies have attempted to identify the serpentine species. Brookins and McDermott (1970) reported abundant lizardite and antigorite, but rare chrysotile in Kansas kimberlite. Kresten (1973b) detected chrysotile and lizardite in Lesotho kimberlite by X-ray diffraction (XRD) and differential thermal analysis (DTA). McCallum and Eggler (1971) showed by XRD that the commonest groundmass serpentine in the Sloan diatreme is a mixture of single- and double-layer lizardite and chrysotile and that pseudomorphic serpentines are mixtures of antigorite and lizardite. Peyve *et al.* (1977) reported that groundmass serpentines in Yakutian kimberlites are flaky and lamellar antigorites and less commonly fibrous chrysotile. Podvysotskiy *et al.* (1981) note that, owing to the very poor crystallinity of kimberlite serpentine, it is not possible to identify unequivocably lizardite, chrysotile, or any of their polytypes by conventional XRD techniques. Jago and Mitchell (1985), using X-ray micro-diffraction techniques (Wicks and Zussmann 1975), have shown that pseudomorphic, primary groundmass serpentines and serpophite are all aggregations of 1T lizardite and that non-pseudomorphic prograde serpentine is 6H lizardite.

6.11.5. Composition

Detailed studies have not yet been undertaken and the limited data available (Emeleus and Andrews 1975, Mitchell 1978a, Smith *et al.* 1978, Scott 1981, Pasteris 1982, Donaldson and Reid 1982, Scott Smith *et al.* 1984, Jago and Mitchell 1985) have been obtained as an adjunct to other studies. The principal compositional variation is, with respect to FeO_T and Al_2O_3 content, with pseudomorphic and serpophitic serpentine containing from 2%–14% FeO_T and up to 7.5% Al_2O_3. Compositions are widely variable even within a single intrusion (Table 6.32). The nature of the solid solutions has not been established, as the above analyses are not accompanied by XRD and DTA data. Compositional variation may be toward greenalite or septechlorite (Mitchell 1978a) or talc and minnesotaite (Smith *et al.* 1978).

Pasteris (1980b) considers that serpentine color in the De Beers kimberlite is not related to FeO_T content. Blue serpentines from Elwin Bay however contain more FeO (4.0%–4.5%) and NiO (0.4%) than colorless serpentines (FeO = 3.0%, NiO = 0.1%). Serpophitic segregations are uniform with and between segregations and commonly are richer in Al_2O_3 and FeO than pseudomorphic serpentines, e.g., Orroroo, Lake Ellen, Peuyuk (Table 6.32). At Elwin Bay both varieties have similar compositions but groundmass serpentines are Al rich. This enrichment is variable (0–5%) and relates to whether or not the serpentine is primary or has replaced eastonitic phlogopite. Similar high-Al serpentines have been noted by Smith *et al.* (1978) in micaceous kimberlites. Pasteris (1980b) considers that high levels of Al are related to the breakdown of phlogopite. High Fe contents may be related to the breakdown of Fe-rich spinels.

Non-pseudomorphic prograde 6H lizardite in the Ham kimberlite is relatively uniform in composition and richer in SiO_2 than the 1T lizardites that it replaces (Jago and Mitchell 1985).

6.12. CARBONATES

The dominant carbonate present in kimberlites, as established by XRD and alizarin staining methods (Clement 1982, Kobelski *et al.* 1979), is calcite. The amounts present can range from trace quantities to over 50% (vol) in calcite kimberlites and the carbonate-rich portions of some dikes and sills (Skinner and Clement 1979). Calcite is least abundant in diatreme facies rocks (Clement 1973, 1982) and most abundant in segregation-textured hypabyssal kimberlites. The mineral exhibits a wide range of habits including anhedral grains in the silicate-oxide groundmass; anhedral, euhedral, or acicular crystals in carbonate-rich segregations; euhedral tabular microphenocrysts that are commonly flow-aligned and dendritic; and acicular crystals that have apparently grown during the rapid quenching of carbonate-rich liquids. Textural varieties of calcite kimberlites and

Table 6.32. Representative Compositions of Serpentine[a]

	1 Ps	2 Ps	3 S	4 S	5 Ps	6 Ps	7 S	8 S	9 Ps	10 S	11 Ps	12 S	13 Ps	14 Ps	15 Ps	16 Ps	17 Ps	18 V	19 S	20 —
SiO_2	39.99	42.01	42.66	39.12	39.15	39.27	38.61	35.33	41.70	41.50	40.55	39.52	41.64	41.84	42.79	41.88	40.33	39.63	41.03	41.79
Al_2O_3	0.95	0.47	0.29	0.63	0.01	0.31	3.39	8.37	0.82	2.09	0.36	0.82	0.13	0.08	0.07	0.11	1.05	0.53	0.64	0.19
FeO[b]	5.33	14.36	3.82	9.78	6.16	9.19	7.89	9.64	4.80	7.47	4.62	5.58	5.94	3.98	4.07	7.45	4.41	4.46	4.88	5.07
MnO	0.11	0.24	0.09	0.13	0.03	0.22	0.23	0.27	0.00	0.06	0.00	0.00	0.04	0.11	0.07	0.07	0.14	0.07	0.11	0.07
NiO	0.44	0.52	0.01	0.46	0.33	0.50	0.03	0.01	0.00	0.00	0.15	0.23	0.01	0.00	0.00	0.06	0.34	0.11	0.05	0.09
MgO	38.11	27.66	37.11	33.82	37.46	34.18	33.86	31.01	37.16	33.25	38.23	37.88	37.39	37.65	38.11	36.03	37.76	38.16	38.59	37.67
CaO	0.63	0.34	0.31	0.67	0.04	0.11	0.18	0.26	0.25	0.41	0.15	0.12	0.04	0.04	0.07	0.10	0.19	0.24	0.05	0.06
	85.56	85.60	84.29	84.74	83.18	83.78	84.19	84.89	84.73	84.78	84.06	84.12	85.19	83.70	85.18	85.70	84.22	83.20	85.35	84.94

[a] 1–4, De Beers (Pasteris 1980); 5–8, Orroroo (Scott Smith *et al.* 1983, 1984); 9, 10, Lake Ellen (this work); 11, 12, Peuyuk A (this work); 13–16, successive optically and texturally distinct zones of pseudomorphic serpentine, Syndey-on-Vaal (this work); 17–19, Elwin Bay (this work); 20, prograde non-pseudomorphic 6H-lizardite, Ham (this work).

[b] Total Fe expressed as FeO; Ps, pseudomorphic serpentine; S, serpophite; V, vein serpentine.

segregations are described in Section 3.7.2. In addition, calcite occurs as pseudomorphs after earlier phases, especially olivine, monticellite, apatite and phlogopite; and as late cross-cutting thin veins. Most of the carbonate is of undoubted primary origin (see Chapter 8), although the upper levels of some diatremes can be expected to have undergone secondary carbonatization related to groundwater circulation.

The few compositional data available indicate that the calcites, in all habits, are very pure, with low MgO (0–1.0%) and FeO (<0.5%) contents (Mitchell 1984a, Donaldson and Reid 1982, Smith *et al.* 1978). Donaldson and Reid (1982) have noted that microphenocrystal laths contain less MgO (0.16%) and FeO (0.05%) than calcites in segregations (MgO = 0.75%, FeO = 0.24%). The principal minor element present is Sr, and Scott Smith *et al.* (1984) and Smirnov (1959) report 0.44% and 0.55% SrO in calcites from the Orroroo and Mir kimberlites, respectively. Rare earth element (REE) contents are below the limits of microprobe detection (Mitchell 1984a). Frey *et al.* (1977) found approximately 100 ppm total REE in Benfontein calcite. The chondrite normalized distribution pattern is enriched in the light REE and similar to whole rock kimberlite and perovskite REE distribution patterns. Carbon and oxygen isotopic studies of calcite are discussed in Section 7.6.

Dolomite is present as an accessory phase in many kimberlites, e.g., Sloan (McCallum and Eggler 1971), Midtaernes and Nigerdlikasik (Emeleus and Andrews 1975), Excelsior (Smith *et al.* 1978), and more rarely occurs in major quantities as at Norris Lake (Meyer 1975) and Peuyuk C (Clarke and Mitchell 1975). The dolomite forms anhedral and euhedral crystals and appears to be primary. In contrast to carbonatites, dolomite is never found in kimberlites as calcite-dolomite intergrowths of exsolution origin. Dolomite can form as a secondary phase (Smirnov 1959). Scott Smith *et al.* 1984 have shown that weathering of the dolomite-free primary kimberlites from Orroroo results in the replacement of coarse grained magmatic calcite by fine grained sugary dolomite.

The few compositional data available (Donaldson and Reid 1982, Smith *et al.* 1978, Clarke and Mitchell 1975, Mitchell and Fritz 1973) demonstrate that the dolomites are ferroan (CaO = 26%–32.5%, MgO = 16.4%–21%, FeO = 1.92%–5.2%, MnO = 0.2%–0.6%). Strontian dolomite has been reported from the Excelsior kimberlite (Smith *et al.* 1978). Donaldson and Reid (1982) have noted that the margins of segregations in the De Beers dike are dolomite (CaO = 31.95%, MgO = 18.82%, FeO = 1.92%), while the cores are calcite (MgO = 0.75%, FeO = 0.24%).

Dawson (1980) has shown that the root zone of Benfontein sill contains magnesian calcite ($Ca_{99}Mg_1$) and that detached diapirs are zoned with an outer rim of dolomite ($Ca_{55}Mg_{44}Fe_1$) and an inner core of ankeritic siderite ($Ca_{13}Mg_{11}Fe_{76}$).

Other carbonates reported from kimberlites include aragonite, strontianite, calciostrontianite, shortite, and (?)benstonite.

Aragonite occurs as fibrous and radial aggregates in the Malyutka, Marshrutnaya, Udachnaya, and Yakutskaya kimberlites (Bobrievich *et al.* 1959a,b, 1964), and Dawson (1980) reports stellate aragonite needles in vesicles in the Igwisi extrusive. Strontianite and calciostrontianite are found in the upper levels of the Udachnaya and Zarnitsa kimberlites (Bobrievich *et al.* 1959a,b, Smirnov 1959) as radiating aggregates of needles and as reniform masses intergrown with iron hydroxides. The formation of aragonite and strontianite is undoubtedly secondary and related to circulating groundwater.

Shortite, $Na_2Ca_2(CO_3)_3$, occurs in the groundmass of micaceous kimberlite dikes of the Upper Canada Mine kimberlite (Watkinson and Chao 1973), in association with primary serpentine and calcite. Watkinson and Chao (1973) consider that the shortite was precipitated as a primary phase together with calcite and serpentine even though experimental studies have shown that shortite is unstable in the presence of water at temperatures above 304–428°C at 2 kbar pressure. Cooper and Gittins (1974), however, believe that the presence of shortite is due to the subsolidus breakdown of nyerereite, $Na_2Ca(CO_3)_2$. Neither of the above studies have addressed the problem of the formation of this sodic mineral in a sodium-poor environment. The apparent primary nature of the shortite may be analogous to the occurrence of pectolite (Section 6.19) in some kimberlites and related to assimilation of Na-bearing materials or metasomatic introduction of Na-bearing fluids.

Scatena-Wachel and Jones (1984) have reported the occurrence of a primary groundmass Ba-Ca-carbonate, related to benstonite, $Ba_6Ca_7(CO_3)_{13}$, in the lower Benfontein sill.

6.13. CHLORITE AND CLAY MINERALS

Although chlorite is commonly mentioned in petrographic descriptions of kimberlites, there have been few X-ray studies or investigations of its compositional variation. Chlorites have been found to occur in four parageneses: (1) replacing serpentinized olivine, (2) as discrete nodules, (3) replacing macrocrystal and groundmass phlogopites, (4) as a primary groundmass phase.

6.13.1. Replacements Of Serpentine

Olivines are initially pseudomorphed by serpentines with the latter in turn being altered to chlorite, and ultimately to vermiculite (Kresten 1973b). Little is known of the structure or composition of such chlorites. Fieremans and Ottenburgs (1979b) identified, by X-ray diffraction, kammererite-kotschubeite chlorites replacing serpentinized-phlogopitized olivine phenocrysts at Mbuji-Mayi. Blue and colorless septechlorites (Table 6.33) formed after Fe-rich lizardite in the

Table 6.33. Representative Compositions of Chlorites[a]

	1	2	3	4	5	6	7	8	9
SiO_2	31.96	41.65	37.73	29.64	27.60	30.48	32.67	36.32	33.52
TiO_2	0.00	0.22	0.19	0.14	—	0.32	0.16	0.36	0.23
Al_2O_3	0.05	11.84	10.91	8.12	15.62	8.42	10.20	3.72	9.35
Cr_2O_3	0.00	0.16	0.13	0.08	—	0.26	0.07	0.22	0.40
FeO[b]	7.09	6.66	13.06	22.31	13.72	13.38	18.50	11.20	17.27
NiO	0.33	—	—	—	—	0.13	—	0.05	—
MnO	0.12	0.01	0.01	0.06	—	0.06	0.09	0.07	0.07
MgO	45.17	26.21	27.95	23.79	29.78	25.18	26.38	30.87	26.33
CaO	0.20	0.00	0.09	0.14	—	3.70	0.43	0.38	0.12
Na_2O	0.03	0.00	0.00	0.02	—	0.00	0.14	0.13	0.00
K_2O	0.00	0.15	0.02	0.01	—	0.30	0.13	0.70	0.01
	84.97	86.95	84.31	84.31	86.72	82.23	88.77	84.18	87.30

[a] 1, Septechlorite after olivine, Elwin Bay (Mitchell 1978a); 2, 3, and 4, low, intermediate, and high Fe clinochlores from chlorite nodules, Koidu (Tompkins *et al.* 1984); 5, calculated composition of chlorite in nodule, Mbuji-Mayi (Fieremans and Ottenburgs, 1979b); 6–8 chlorites replacing phlogopite from Mir (Frantsesson 1970), Koidu (Tompkins and Haggerty 1983), and New Elands (this work); 9, primary groundmass chlorite (Tompkins *et al.* 1984).

[b] Total Fe expressed as FeO.

Elwin Bay kimberlite (Mitchell 1978a) are themselves Fe-rich (7%–10% FeO_T) and Al_2O_3 poor (<0.2%).

6.13.2. Chlorite Nodules

Discrete chlorite nodules (1–4 cm) from Koidu (Tompkins *et al.* 1984) occur with fibrous, platy, tectonized, or multiply cleaved textural habits. Some nodules contain networks of cross-cutting fibers of chlorites of distinctly different optical properties and composition. The chlorites are essentially trioctahedral Mg-Fe clinochlores (Table 6.33) containing 8%–12% Al_2O_3, 29%–41% SiO_2, and 19%–28% MgO. The chlorites are classified into high-Fe (17%–29% FeO), intermediate-Fe (12%–14% FeO), and low-Fe (7%–10% FeO) varieties. X-ray studies show that the bulk of the chlorites have layer–interlayer structures of the Ia type of Bailey and Brown (1962), a variety ubiquitous in vermiculites, but very rarely found in other chlorites. Type-Ia chlorites require a 1M phlogopite precursor for their formation, and Tompkins *et al.* (1984) propose that the chlorite nodules were formed by the chloritization of phlogopite megacrysts under CO_2-poor conditions. Some of the platy nodules contain a mixture of Ia and IIb structural types. Tompkins *et al.* (1984) suggest that at least some of the chlorites (i.e., IIb) are not pseudomorphs, as experimental studies of IIb clinochlores show that such chlorites can be stable at low temperatures (<900°C).

Similar chlorite nodules have been reported from the Mbuji-Mayi kimber-

lites (Fieremans and Ottenburgs 1979b). The nodules have been replaced by quartz along chlorite cleavage planes. The chlorites identified by X-ray diffraction as clinochlore have similar calculated compositions to Tompkins *et al.*'s (1984) low Fe chlorites (Table 6.33). Fieremans and Ottenburgs (1979b) regard the chlorites as a primary phase. Pre-existing enstatite, olivine, and spinel are considered to react with melt to form chlorite and phlogopite.

6.13.3. Pseudomorphs after Phlogopite

Macrocrystal, microphenocrystal, and groundmass phlogopites are commonly replaced by chlorite (Tompkins *et al.* 1984, Mitchell and Meyer 1980, Skinner and Scott 1979, Frantsesson 1970, Mitchell 1970). The replacement initially occurs along cleavages and at grain margins. The chloritization is commonly accompanied by the introduction of quartz and calcite resulting in expansion of the mica along cleavage planes (Fieremans and Ottenburgs 1979). The chlorites vary in their color from colorless to pale green to bright emerald green. The strongly colored varieties are commonest in kimberlites which have been altered by groundwater, and are particularly characteristic of the weathered portions of micaceous kimberlites found at Bellsbank (Bosch 1971) Swartruggens (Skinner and Scott 1979), Roberts Victor, and New Elands (this work). Many micas which are apparently fresh optically, are, upon analysis, found to be partially altered to chlorite, i.e., hydromica. Fieremans and Ottenburgs (1979b) determined by XRD that chlorites in the Mbuji-Mayi kimberlites were possibly kammererite-kotschubeites, although Cr contents were not determined. Few compositional data exist for chlorites from this paragenesis. Chlorites from Mir, Koidu, and New Elands (Table 6.33) are all Fe-rich clinochlores, and are Al-rich relative to chlorites replacing serpentines.

Chloritization of phlogopite is considered to be either a primary and/or deuteric phenomenon (Tompkins *et al.* 1984, Mitchell and Meyer 1980), or secondary and associated with weathering (Bosch 1971). Zinchuk and Kharkiv (1978) have shown that complete pseudomorphing of phlogopite macrocrysts in the Mir Pipe is confined to the upper 35–40 m. From 40 to 335 m, phlogopites are partially chloritized, and below 335 m are unaltered.

6.13.4. Primary Chlorite

Primary groundmass chlorite has only been conclusively identified in kimberlites from Koidu (Tompkins *et al.* 1984). Here it forms euhedral blue-green platelets (0.05 mm) disseminated throughout the calcite-silicate groundmass or aggregates of crystals in carbonate segregations. Primary chlorites are abundant only in samples rich in calcite, and are rare in kimberlites rich in phlogopite and serpentine. Tompkins *et al.* (1984) have shown these chlorites to be Fe-rich

clinochlores similar in their composition to the high Fe chlorites occurring in chlorite nodules, and as pseudomorphs after phlogopite.

6.13.5. Clay Minerals

A wide variety of clay minerals and related phyllosilicates have been reported from kimberlites. These include montmorillonite, nontronite, halloysite, kaolinite, sepiolite, stevensonite, vermiculite, and saponite. Hydromicas, interstratifications of vermiculite and other phyllosilicates, are common (Ruotsala 1975, Kresten 1973b, Fairbairn and Robertson 1966, Smirnov 1959).

Talc has been identified by optical and X-ray methods in the Sloan diatreme (McCallum and Eggler 1971), Yakutian kimberlites (Milashev *et al.* 1963), and the Premier kimberlite (Scott Smith and Skinner 1979). Kresten (1973b) has proposed that the deuteric alteration of kimberlites proceeds via three stages: a talc-serpentine stage, a chlorite-vermiculite stage, and a saponite stage. However most of the kimberlites studied by Kresten (1973b) appear also to have been subjected to weathering (Clement 1982) and it is considered unlikely that saponite and vermiculite formation is related to deuteric alteration. Kresten's (1973b) scheme, together with the ultimate stage of laterite formation (Fairbairn and Robertson 1966), provides a satisfactory guide to the late-stage deuteric alteration and weathering of kimberlite. Detailed discussion of secondary alteration is beyond the scope of this work.

6.14. BRUCITE AND RELATED MINERALS

Few investigations have reported the presence of brucite, $Mg(OH)_2$, despite the H_2O- and MgO-rich nature of kimberlite. Malkov (1974) identified brucite in the East Udachnaya and Novinka kimberlites by X-ray and DTA methods. It was shown that brucite occurred only in rocks which had undergone complete serpentinization of the olivines, and that partially serpentinized or phlogopite-bearing rocks lack brucite. The deuteric alteration of olivine to serpentine-brucite mixtures is apparently an isochemical process accompanied by volume increase and density decrease. Zinchuk *et al.* (1983) noted that kimberlitic brucite is a very pure magnesian variety showing very little solid solution with other cations. Brucites were also shown to contain chlorine either replacing hydroxyl groups (iowaite) or occurring as sub-microscopic impurities. Malkov (1974) considers that the presence of brucite should be suspected in any kimberlites that contain an excess of MgO over SiO_2 in terms of serpentine stoichiometry.

Zinchuk *et al.* (1984) have discussed the genesis of pyroaurite, rhombohedral $Mg_6Fe_2(CO)_3(OH)_{16}.4H_2O$, in Yakutian kimberlites where it occurs in thin veins together with halite and calcite, and in segregations composed of calcite

and serpentine. The pyroaurite seems, for the most part, to be a secondary mineral formed and deposited in consolidated kimberlite whose serpentine comes into contact with Na, and $(CO_3)^{2-}$-bearing ground water. Pyroaurite is an unstable mineral and decomposes to $Fe(OH)_3$, $MgSO_4$ and $Mg(HCO_3)_2$ in groundwaters. The presence of amakinite, $Fe(OH)_2$, a brucite-like mineral (Kozlov and Levshev 1962) and epsomite $MgSO_4.7H_2O$, in the Yakutian kimberlites (Bobrievich *et al.* 1964) may be a result of pyroaurite decomposition.

The prograde alteration of kimberlite by residual H_2O-and CO_2-rich fluids provides a suitable environment for the formation of pyroaurite and other minerals related to brucite. Detailed study of serpentinized kimberlites may reveal the presence of primary deuteric pyroaurite, sjögrenite, iowaite, brugnatellite and coalingite.

6.15. SULFIDES

Sulfides are a common but volumetrically insignificant phase in most kimberlites. Although detailed studies of their occurrence and composition have not yet been undertaken it is possible to recognize five distinct sulfide parageneses: (1) sulfurization assemblages associated with serpentinization, (2) polysulfide globules, (3) primary immiscible sulfide, (4) primary low-temperature pyrite, (5) epitaxial overgrowths on perovskites and spinel.

6.15.1. Sulfurization Assemblages

The serpentinized margins and fractures of olivines commonly contain needlelike (2–10 μm) triangular prisms of nickel sulfides. These have been optically identified as millerite (NiS) or heazlewoodite (Ni_3S_2) in the Swartruggens, Premier and De Beers kimberlites (Skinner and Scott 1979, Scott and Skinner 1979, Pasteris 1980b). Analysis has confirmed the presence of heazlewoodite in the Lattavaram (Akella *et al.* 1979) and Green Mountain (Boctor and Meyer 1979) kimberlites. In this latter occurrence the heazlewoodite occurs as veinlets and irregular masses in serpentine and rarely as oriented plates. Bornite forms thin discontinuous rims upon the heazlewoodite. Globules of nickel sulfide (unidentified) occur in serpentinized olivines from the Sydney-on-Vaal dike (this work).

Sulfides in this paragenesis form during the sulfurization of olivine that accompanies serpentinization, with the Ni being derived from the original olivine. The sulfur may be derived by the breakdown of primary immiscible sulfides in the associated magma. If sulfur fugacities are not sufficient to stabilize sulfides then Ni–Fe or metallic Fe may form in their place (Haggerty 1975).

6.15.2. Polysulfide Globules

Polysulfide globules have been found in megacrystal and macrocrystal olivines (Hunter and Taylor 1984, Botkunov *et al.* 1980, Haggerty 1975), zircons (Botkunov *et al.* 1980), and megacrystal ilmenite or ilmenite–clinopyroxene intergrowths from Monastery (Haggerty *et al.* 1979), Frank Smith (Clarke 1979) and an unidentified Yakutian kimberlite (Boctor and Boyd 1980b). The globules (0.05–2-mm diameter) are composed primarily of pyrrhotite or nickeliferous pyrrhotite that contains flame-like exsolution lamellae of pentlandite or cobaltian pentlandite. Chalcopyrite is a minor phase forming a thin discontinuous mantle at the periphery of the globules and rarely occurring as exsolution lamellae in pyrrhotite. Boctor and Boyd (1980b) have determined that the bulk compositions of the globules (e.g., Cu = 1.57%, Ni = 9.75%, Co = 0.39%, Fe = 51.53%, S = 37.47%), lie within the boundaries of monosulfide solid solution compositions in the system Cu–Fe–Ni–S. Formation of the globules is ascribed to inclusion of immiscible sulfide liquid droplets at high temperature (1100°C). The liquids ultimately crystallized to homogeneous Fe–Ni monosulfide, which, upon cooling to below 610°C, decomposed into pyrrhotite, pentlandite, and chalcopyrite. Subsequent to the initial exsolution, chalcopyrite migrated to the globule margins (Boctor and Boyd, 1980b, Haggerty *et al.* 1979). In some examples the primary exsolved sulfide assemblage has been subjected to alteration involving oxidation of the pyrrhotite to magnetite and marcasite, together with replacement of chalcopyrite by bornite. Exsolution and alteration took place after emplacement of the kimberlite.

These polysulfide globules are identical to those occurring in lherzolite and eclogite xenoliths (Keays *et al.* 1981, Tsai *et al.* 1979, Bishop *et al.* 1975) and for which a similar origin has been proposed.

Clarke (1979) has described metasomatic, low-temperature replacement of the primary exsolved sulfide assemblage by djerfisherite ($K_6Fe_{26-x}S_{26}Cl$) and a Cl-free K–Fe–Cu sulfide, intermediate between djerfisherite and Fe–Ni monosulfide. Formation of these rare sulfides was due to interaction between the preexisting sulfides and a fluid rich in K, Cl, and Cu that was derived from a postmagmatic gaseous phase associated with the kimberlite. Dobrovolskaya *et al.* (1978) have noted that Ni-bearing mackinawite forms in association with djerfisherite during such metasomatic alteration.

6.15.3. Primary Immiscible Sulfides

Pentlandite, cobaltian pentlandite, millerite, heazlewoodite, chalcopyrite, and pyrite occur as ragged, irregular, single crystals and rarely as distinct globules disseminated throughout the silicate-oxide groundmass (Smith *et al.* 1978, Mitchell and Clarke 1976, Clarke and Mitchell 1975).

All of the crystals have undergone extensive resorption in the fluids which formed the groundmass. The sulfides, with the exception of pyrite, may be relicts of an original high-temperature immiscible sulfide assemblage which has undergone dissolution in the late-state low-temperature sulfur-undersaturated magma (Mitchell and Clarke 1976).

The origins of the pyrite are enigmatic; in some examples it may be a primary low temperature phase (see Section 6.15.4) or it may have formed as a result of contamination of the magma by pyritiferous shale (Dawson 1980) or evaporites (Ilupin 1962). The latter processes are highly probable in diatreme facies kimberlites. Preliminary sulfur isotopic studies are inconclusive, a wide range of $\delta^{34}S$ values (1.2‰–16.1‰) being found (Dawson 1980, Tsai *et al.* 1979). Low $\delta^{34}S$ values are consistent with a primary igneous origin; however, the higher $\delta^{34}S$ values could result from hydrothermal processes and are in themselves not indicative of an evaporitic source. Negative $\delta^{34}S$ values, perhaps indicative of sedimentary (biogenic) pyrite, were not found by Dawson (1980).

Sphalerite, wurtzite, galena, cinnabar, marcasite, and molybdenite reported from Yakutian kimberlites (Bobrievich *et al.* 1959(b), 1964, Milashev *et al.* 1963) may result from hydrothermal or secondary alteration processes.

6.15.4. Primary Low-Temperature Pyrite

Euhedral crystals (laths and cubes) associated with carbonate-rich segregations have been described from the Peuyuk C (Mitchell and Clarke 1976) and Skinner's Sill kimberlite (Mitchell 1984a). Pyrite from the Peuyuk kimberlite contains 0.7% Ni. Similar Ni-poor pyrite mantles irregular heazlewoodite or forms discrete grains in the associated silicate-oxide groundmass (Clarke and Mitchell 1975).

These pyrites show no sign of resorption and were evidently formed in equilibrium with the carbonate-rich residual fluid. They appear to have crystallized directly from this fluid and not from a separate immiscible sulfide liquid.

6.15.5. Epitaxial Sulfides

Mitchell and Clarke (1976) have described epitaxial mantles upon resorbed perovskites in the Peuyuk B kimberlite. In this paragenesis the pyrite is sandwiched between a perovskite core and a rutile rim. Nickel contents range from 0 to 11% Ni, individual mantles being homogeneous with respect to their Ni content. The pyrite mantle is irregular and commonly discontinuous. Perovskites with sulfide mantles do not differ in composition from perovskites which lack them.

In the Peuyuk C kimberlite, mantles of heazlewoodite occur upon groundmass spinels (Clarke and Mitchell 1975). Pasteris (1980b) has noted spinel mantled by Ni-poor pyrite and (?)violarite (Ni_2FeS_4) in the De Beers kimberlites.

From Koidu, Tompkins and Haggerty (1984) have described a spinel mantle on magnesian ilmenite that is in turn mantled by pyrrhotite, pentlandite, and chalcopyrite.

The genesis of these epitaxial sulfides remains unclear. Mitchell and Clarke (1976) have proposed that steep diffusional gradients in the vicinity of dissolving crystals may lead to local zones of sulfur saturation, but offer no explanation of the processes involved.

6.16. ZIRCONIUM MINERALS

6.16.1. Zircon

Although zircon ($ZrSiO_4$) is a rare accessory phase in most kimberlites, occurring in amounts ranging from 10–50 ppm, it is commonly found in heavy mineral concentrates together with diamond. Zircons are useful for U/Pb and fission track age determinations (Davis 1977, Haggerty *et al.* 1983a).

Kimberlitic zircons form rounded-to-subrounded grains, euhedral crystals being very rare. Their surfaces typically have a frosted and pitted appearance due to the development of a variety of crystallographically controlled etch pits and dissolution features (Krasnobayev 1980). Bartoshinski *et al.* (1982) believe that this microrelief was developed in two stages, with an initial period of slow etching in a melt being followed by rapid dissolution in a gas-rich environment.

Zircon colors range from colorless to grey, yellow, honey-colored, pink and reddish-brown. Strongly colored zircons are usually xenocrystal (Xu, 1982, Krasnobayev 1980). Individual kimberlites or groups of closely related kimberlites are characterized by zircons of a distinctive coloration (Kresten *et al.* 1975). Krasnobayev *et al.* (1981) and Krasnobayev (1980) have noted that the distinctive X-ray and UV fluorescence of kimberlitic zircon is probably related to the low number of paramagnetic centers in these zircons as compared to zircons from other parageneses.

Kimberlitic zircons are deformed and exhibit a strong parting not related to their tetragonal symmetry (Krasnobayev 1980, Kresten *et al.* 1975). This parting and distortion of the zircon lattice, noted by Kresten *et al.* (1975), may be due to formation, followed by shearing, in a high-pressure environment.

Minerals found as inclusions in zircon are diamond, magnesian ilmenite, phlogopite, chrome-spinel (46%–57% Cr_2O_3), chrome diopside [Ca/(Ca + Mg) = 0.492–0.498], (?)zirconia (ZrO_2), and pyrrhotite mantled by chalcopyrite (Botkunov *et al.* 1980, Kresten *et al.* 1975). Intergrowths with pyroxene (Williams 1932) and magnesian ilmenite (Whitelock 1973) are known from the Bultfontein and Monastery kimberlites, respectively. Kresten *et al.* (1975) have shown that some zircons contain abundant secondary tubular and spherical fluid inclusions that delineate healed fractures. The common large size (up to 1 cm),

and association with diamond and magnesian ilmenite, have led Kresten *et al.* (1975) to propose that zircons are a part of the megacryst suite.

Kimberlitic zircons show limited solid solution with $HfSiO_4$ and may contain up to 3% HfO_2. Zr/Hf ratios vary widely, e.g., Lesotho, 16.4–79.3; South Africa, 28.8–49.5; Tanzania, 43.7–52.5; Yakutia, 39–59; Zaire, 30.2–46.6 (Fieremans and Ottenburgs 1979, Kresten *et al.* 1975, Nekrasova and Rozhdestvenskaya 1970). The Zr/Hr ratios of zircons from some kimberlite diatremes vary within narrow limits; e.g., Mothae, 34–40; Wesselton, 44–49; Pipe 200, 30–36; however, other diatremes (e.g., Kao, 17–35) and dikes, e.g., Dike 170; Butha Butte, 24–79, exhibit wider variations that may be related to crustal contamination (Kresten *et al.* 1975). Zr/Hf ratios are similar to those of zircons from granitic rocks (Nekrasova and Rozhdestvenskaya 1970) and to those of whole rock kimberlites (Kable *et al.* 1975).

Few data are available for trace elements. The U contents (ppm) are typically low, e.g., Lesotho, 7.3–23.7; South Africa, 6.0–66; Tanzania, 6.3–22.4; Yakutia, 14–35; Zaire, 12–45, with most zircons containing less than 25 ppm U (Haggerty *et al.* 1983a, Krasnobayev 1980, Fieremans and Ottenburgs 1979a, Davis 1977, Kresten *et al.* 1975, Ahrens *et al.* 1967). Thorium contents ranging from 4 to 23 and 1.8 to 7.2 ppm are found in Yakutian and South African zircons, respectively (Krasnobayev 1980, Ahrens *et al.* 1967). The Th/U ratios (0.2–0.7) are low and similar to those found in zircons from granitic rocks. The very low Th and U content of kimberlitic zircons, however, serves to differentiate them from zircons in granites which typically contain greater than 100 ppm Th and U (Krasnobayev 1980).

Rare earth contents in general appear to be very low (Ilupin *et al.* 1971). Nekrasova and Gamyanina (1968) reported only 2–60 ppm total REE, and Krasnobayev (1980), although finding some higher contents, recorded only 15–23 ppm total REE in colorless zircons. The zircons are preferentially enriched in the heavy REE. Zircon from kimberlite has REE contents lower by factors of 100 or more than those for zircon from other rocks (Nekrasova and Gamyanina 1968).

Yttrium contents are similarly low (14–270 ppm) relative to amounts found in other zircons (Krasnobayev 1980).

6.16.2. Baddeleyite and Tetragonal ZrO_2

Baddeleyite (monoclinic ZrO_2) has been found as coatings upon zircon crystals, as discrete grains in heavy mineral concentrates, as primary groundmass crystals, and in complex subsolidus reaction assemblages with rutile, ilmenite, and zircon.

Kimberlitic zircons are typically covered by a white to yellowish, thin (0.04–0.45 mm) alteration or reaction coat having a vitrous, crystalline, or chalky

appearance. First described as baddeleyite by Nixon *et al.* (1963), this coat was subsequently shown by Kresten (1973a) and Kresten *et al.* (1975) to be a mixture of baddeleyite and tetragonal ZrO_2. The proportions of the phases vary widely with some examples containing up to 70% of the tetragonal polymorph. The coatings appear to have formed by reaction or desilicification of the substrate, perhaps during transport in the kimberlite. It has not been established whether the baddeleyite was formed by the inversion of the tetragonal ZrO_2 or vice versa. The former would seem the more probable in view of the metastable nature of tetragonal ZrO_2 below 1150°C (1 atm).

The U content (60–190 ppm) of the coatings is much greater than that of the associated zircon.

Fieremans and Ottenburgs (1979a) and Fieremans (1966) have described large (0.5–1-cm) rounded-to-subrounded brown-black baddeleyite crystals in heavy mineral concentrates from Mbuji-Mayi. Commonly these crystals are coated by zircon. The baddeleyites contain significant amounts of U, Hf, and Nb with average contents of 1200, 9200, and 120 ppm, respectively. Fieremans (1966) reports 9.78% TiO_2 in one crystal but believes that this may reflect contamination or the presence of rutile inclusions. However, this TiO_2 content may be real in view of Raber and Haggerty's (1979) recognition of titanian baddeleyite.

Single crystals (0.5 mm) of baddeleyite have also been found in concentrates from the Aykhal kimberlite (Marshintsev 1970). The crystals were derived from a diatreme facies sample containing 40%–60% calcite, apatite, and barite. Marshintsev (1970) regards the baddeleyite as a secondary mineral and not as a primary magmatic phase.

Primary baddeleyite has been recognized as a late-stage groundmass phase in the lowermost Benfontein sill, by Scatena-Wachel and Jones (1984). The baddeleyite apparently crystallized contemporaneously with Al-Ti-magnetite and perovskite and was concentrated in oxide-rich layers by cumulus processes. The baddelyite is very pure, averaging 96.4 + 1.3% ZrO_2 and 1.72 ± 0.08% HfO_2 and containing only 0.32–0.80 TiO_2.

Raber and Haggerty (1979) have described baddeleyite formed by reaction at interfaces between rutile and zircon or ilmenite and zircon. In the former case associated minerals are zirconolite and diopside, in the latter, sphene and baddeleyite co-exist. The common factor in the reaction assemblages is the presence of calcite, and Raber and Haggerty (1979) attribute baddeleyite formation to introduction of a carbonate-rich fluid along grain boundaries inducing an intercrystalline reaction between zircon and ilmenite or rutile. This reaction product baddeleyite is notably enriched in TiO_2 (3.7%–6.1%).

Although baddeleyite is an apparently rare phase, the presence of primary baddeleyite places constraints upon the silica activities of kimberlite magmas (see Section 9.9).

6.16.3. Other Zirconium-Bearing Minerals

Raber and Haggerty (1979) have found zirconolite ($CaZrTi_2O_7$) accompanied by baddeleyite in reaction assemblages between ilmenite and zircon. The ZrO_2 contents vary from 41.9% to 71.3% and are higher than those found in zirconolites from alkaline or lunar rocks. Formation of zirconolite is attributed to the presence of an intergranular carbonate- and Ca-rich fluid which induced reaction between ilmenite and zircon.

Micaceous kimberlites from New Elands contain abundant brown euhedral groundmass crystals of kimzeyitic garnets (SiO_2 = 23.4%, TiO_2 = 13.53%, FeO = 14.14%, MgO = 2.4%, CaO = 30.08, Na_2O = 1.06%, ZrO_2 = 14.40%; Mitchell, unpublished data).

Haggerty (1983) reports an unidentified Zr-silicate in lindsleyite and mathiasite-bearing xenocrysts (ZrO_2 = 38.9%, SiO_2 = 53.6%, Na_2O = 2.33%, CaO = 2.71%).

6.17. RUTILE

Rutile is found in five parageneses as (1) a primary groundmass phase, (2) reaction mantles upon perovskite, (3) discrete crystals (megacrysts?), (4) rutile–silicate intergrowths, (5) rutile–ilmenite intergrowths.

Rutiles belonging to parageneses 1–3 may represent primary phases. The origins of rutiles from parageneses 4–5 are enigmatic, they may be a part of the megacryst suite or be derived from metasomatized mantle xenoliths.

6.17.1. Groundmass Rutile

Primary groundmass late-stage needles and tabular crystals of rutile have been described from the Fayette County and Benfontein kimberlites (Hunter *et al.* 1984, Boctor and Boyd 1981). In the latter occurrence, Boctor and Boyd (1981) have shown the rutile to be Nb-bearing (0.9%–1.22% Nb_2O_5) and low in Cr_2O_3 (0–0.04%).

Thin needles (0.10–0.02 mm) of rutile, commonly aligned parallel to the margins of euhedral-to-subhedral olivines, have been noted in the De Beers, Kimberley, Dutoitspan, and Tunraq kimberlites (Pasteris 1980b). Their abundance differs in each facies of the De Beers kimberlite. The rutiles are high-Cr_2O_3, low-Fe_2O_3, low-Nb_2O_5 varieties. Pasteris (1980b) discounts an exsolution origin and believes that rutiles nucleated epitaxially at the margins of the olivines and were subsequently encapsulated by further olivine growth. Precipitation of olivine is considered to be related to the cessation of crystallization or instability of ilmenite and/or perovskite. Rutiles not preserved in olivines, or less commonly

in phlogopite (Elthon and Ridley 1979), may have been subsequently resorbed into the melt.

6.17.2. Mantles on Perovskite

Thin (1–10 μm), complete to discontinuous epitaxial mantles of rutile are found upon rounded perovskites in Somerset Island and the Green Mountain kimberlites (Mitchell and Clarke 1976, Mitchell 1978a, Boctor and Meyer 1979). Such rutiles appear to have been directly precipitated in the immediate environment of perovskites that were undergoing resorption. The mantles are commonest in facies that have been replaced by fluids depositing calcite, serpentine, and magnetite. Total resorption of perovskite leads to the development of discontinuous doughnut-like rings of rutile which are ultimately disaggregated and strewn throughout the groundmass. Resorption of these fragments (<1 μm) indicates rutile is unstable in the evolving fluids. In the Peuyuk B kimberlite (Mitchell and Clarke 1976), epitaxial mantles of nickeliferous pyrite are sandwiched between the perovskite and the rutile outer mantle.

Pasteris (1980b) considers that perovskites are replaced by anatase in the De Beers kimberlites.

6.17.3. Discrete Crystals

Large (0.04–02-mm), homogeneous, rounded-to-anhedral single crystals of rutile, commonly mantled by magnesian ilmenite, are found in heavy mineral concentrates from the Tunraq kimberlite (Mitchell 1979b). Similar rutiles have been noted from Wesselton (Mitchell 1973b). Elthon and Ridley (1979) also describe from Wesselton discrete small crystals of rutile disseminated throughout the groundmass and mantled by perovskite and/or groundmass spinels. Some grains protected from reaction by phlogopite megacrysts have reacted with the latter to produce an unidentified potassian titanate. Rutiles from Tunraq are low-Cr_2O_3 (0.4%), low-Nb_2O_5 (0.3%–1.8%) varieties. A single megacrystal rutile from Orapa (Tollo 1982) is, in contrast, Nb_2O_5 (6.5%) and Cr_2O_3-rich (5.2%) and similar to the niobian rutiles from coarse rutile-ilmenite intergrowths (Section 6.17.5).

Mitchell (1979b) believes that rutile is a high-pressure phenocryst, although a xenocrystal origin cannot be ruled out as rutiles of similar composition are common in eclogites.

6.17.4. Rutile–Silicate Intergrowths

Rutiles and silicates, intergrown in graphic or symplectic textures analogous to those of pyroxene–ilmenite intergrowths, are common in the Jagersfontein kimberlite (Haggerty 1983) and are known also from the Kampfersdam (Schulze

1983) and Mbuji-Mayi kimberlites (Ottenburgs and Fieremans 1979). The primary silicates have, in most examples, been replaced by serpentine, sepiolite, and palygorskite-attapulgite, although Haggerty (1983) and Schulze (1983) report the occurrence of fresh olivine ($Fo_{91.5}$), pyroxene, and amphibole. Fine lamellae of ilmenite are present in the rutiles, which contain 2%–6% Cr_2O_3, 0.3%–3.0% Nb_2O_5, and less than 1% Fe_2O_3. The Nb_2O_5 contents are less than those of metasomatic rutiles (7%–13% Nb_2O_5) (Haggerty 1983), and similar to those of rutiles from paragenesis 3 or MARID-suite rutiles (2%–5% Nb_2O_5) (Dawson and Smith 1977). Ottenburgs and Fieremans (1979) and Schulze (1983) believe that these intergrowths crystallized directly from a kimberlite melt, although Haggerty (1983) considers that they are a part of the megacryst suite and therefore of indeterminate origin. A xenocrystal relationship with MARID-suite xenoliths cannot be ruled out.

6.17.5. Rutile–Ilmenite Intergrowths

Large (0.5–3.0-cm) rutile–ilmenite megacrysts occur at Jagersfontein (Haggerty 1983) and Orapa (Tollo 1982). Fragments of similar material, presumably derived from megacrysts, are also known from Wesselton (Shee 1979, Elthon and Ridley 1979), Green Mountain (Boctor and Meyer 1979), De Beers (Pasteris 1980b), Letseng-la-terae (Gurvich *et al.* 1982), and Elliot County (Agee *et al.* 1982). The intergrowths are commonly mantled by magnesian ilmenite and/or Cr-spinel and rarely by manganoan ilmenite. Haggerty (1983) has distinguished two groups of rutile in the intergrowths on the basis of their texture and Nb and Cr contents.

One group contains fine sigmoidal-oriented lenses of ilmenite, is intergrown with silicates (Section 6.17.4), and has low Nb_2O_5 (<6%) and variable Cr_2O_3 (1%–9%). This rutile is associated with decomposition assemblages (ilmenite–sphene–spinel) after LIMA-type phases (Section 6.18.2).

The second group contains orientated lamellae of ilmenite, is Nb_2O_5 rich (4%–13%), and of restricted Cr_2O_3 content (4%–8%). Rutiles in this group commonly enclose LIMA (Section 6.18.2). Many of the intergrowths exhibit textures analogous to those found in megacrystal ilmenites (6.3.1) indicating deformation and long-term annealing. Thus deformation twins and polygonal granoblastic textures with equal angle triple points are common.

Ilmenites in this paragenesis are of distinctly different composition to megacrystal ilmenites from the same intrusion (see Section 6.3.10).

Rutile-ilmenite intergrowths have been interpreted by Haggerty (1975), Elthon and Ridely (1979), Boctor and Meyer (1979), and Pasteris (1980b) to be the decomposition products of precursor armalcolite (Section 6.18.1). Although Haggerty (1983) has shown that the bulk composition of some of the Jagersfontein-Orapa intergrowths is broadly similar to Jagersfontein Cr–Ca (ZrNb)

armalcolites, he believes that a different precursor must be sought. This conclusion is based upon the failure to homogenize intergrowths experimentally, the low Ca content of the intergrowths, the occurrence of armalcolite as mantles upon the intergrowths, and the fact that armalcolite breakdown is a prograde reaction. Possible precursors suggested by Haggerty (1983) include compounds with PbO_2-type crystallographic shear structures or LIMA (Section 6.18.2).

It is not clear whether these intergrowths are a part of the megacryst suite or are xenocrysts derived from metasomatized mantle. In the latter case, however, the metasomatizing fluids may be derived from kimberlitic magmas (Jones *et al.* 1982).

6.18. TITANATES

Armalcolite and several rare titanates have been recovered from heavy mineral concentrates, or recognized as groundmass minerals. Similar titanates have also been recognized in metasomatized lherzolite xenoliths, where their origin has been ascribed to metasomatic activity either pre-dating kimberlite formation (Erlank *et al.* 1982) or associated with ascending kimberlite magmas (Jones *et al.* 1982).

6.18.1. Armalcolite

Armalcolite, (Fe,Mg) Ti_2O_5, first described from lunar rocks, is the intermediate member of the solid solution series between $FeTi_2O_5$ (ferropseudobrookite) and $MgTi_2O_5$ (karooite-magnesio-ferropseudobrookite). Terrestrial armalcolites which contain Fe^{3+} can be considered to have compositions within the ternary system Fe_2TiO_5(pseudobrookite)–$FeTi_2O_5$–$MgTi_2O_5$. Armalcolites exhibit a wide compositional range with respect to their Ca, Cr, Nb, and Zr contents (Table 6.34).

Armalcolites from Dutoitspan (Haggerty 1975) are Cr-, Zr-, Ca-poor and intergrown with ilmenite and rutile. Those from Mothae (Raber and Haggerty 1979) are Zr rich and formed only at an interface between zircon and rutile. Jagersfontein armalcolites fall into two compositional groups, Cr-armalcolite (Type 1), and Ca-Cr (NbZr) armalcolite (Type 2). Type-1 armalcolites are euhedral crystals, enclosing rutile and ilmenite, which are poor in Cr_2O_3 (2%), Nb_2O_5 (1%), and ZrO_2 (0.5%), relative to Type-2 armalcolites (Cr_2O_3 = 5%–12%, Nb_2O_5 = (1%–3%), ZrO_2 = (1%–3%), CaO = 3.5%) which mantle or vein rutile–ilmenite intergrowths (Haggerty 1983). The compositional groups are similar to groups established for lunar armalcolites (Haggerty 1983). Only the Dutoitspan example is similar to the only other primary terrestrial armalcolite occurring in the Smoky Butte lamproite (Table 6.34) (Mitchell 1985, Velde 1975).

Table 6.34. Representative Compositions of Armalcolite and Other Titanates[a]

	1	2	3	4	5	6	7	8	9	10
TiO_2	76.92	66.08	70.12	70.11	68.70	54.28	61.55	53.16	75.73	72.56
ZrO_2	—	6.71	0.44	1.14	—	4.02	4.48	—	—	—
Al_2O_3	0.02	0.19	0.02	0.41	0.12	0.09	0.55	0.27	—	—
Cr_2O_3	—	0.13	2.65	7.91	0.89	16.22	16.32	17.98	—	—
V_2O_3	—	—	—	—	0.44	—	—	8.46	4.51	—
Fe_2O_3	—	—	6.17	—	6.51	—	—	—	—	—
FeO	13.47	15.23	5.91	6.47	11.67	11.20	6.68	11.28	3.17	11.07
MgO	7.08	4.16	13.43	5.87	9.67	3.54	4.22	3.66	0.94	1.30
MnO	0.54	0.20	0.08	0.14	0.19	0.19	0.19	0.14	0.17	—
CaO	0.06	1.61	0.02	4.38	—	0.42	0.80	0.39	—	—
SrO	—	1.63	—	—	—	1.69	0.78	—	—	—
BaO	—	2.37	0.51	0.63	—	4.60	1.00	4.07	3.92	7.37
Na_2O	—	—	0.01	0.26	—	0.01	0.09	—	—	—
K_2O	—	0.52	—	0.30	—	0.21	0.97	—	8.69	7.37
Nb_2O_5	—	—	0.85	2.13	—	0.02	—	—	—	—
Ta_2O_5	—	—	0.05	0.27	—	0.03	—	—	—	—
La_2O_3	—	—	0.05	0.05	—	0.05	0.33	—	—	—
Ce_2O_3	—	—	0.05	0.09	—	1.36	0.61	—	1.52	—
$(REE)_2O_3$	—	—	0.03	—	—	0.80	0.59	—	—	—
	98.09	98.83	100.39	100.16	98.18	98.73	99.16	99.41	98.15	99.67

[a] 1–5, Armalcolites; 1, Dutoitspan (Haggerty 1975); 2, Mothae (Raber and Haggerty 1979); 3, type-1 Jagersfontein (Haggerty 1983); 4, type-2 Jagersfontein (Haggerty 1983); 5, Smoky Butte (Mitchell 1985); 6, Lindsleyite, De Beers (Haggerty *et al.* 1983); 7, Mathiasite, Jagersfontein (Haggerty *et al.* 1983); 8, unnamed titanate, De Beers (Haggerty 1975); 9, unnamed titanate, New Elands (Mitchell and Haggerty, unpublished data); 10, priderite, W. Kimberley lamproite (Mitchell 1985).

Armalcolite decomposes to rutile plus ilmenite with increasing pressure or decreasing temperature (Lindsley *et al.* 1974, Friel *et al.* 1977), and its presence implies formation at low pressures and high temperatures, e.g., less than 10 kbar, at 1200°C. The formation of armalcolite mantles upon rutile–ilmenite intergrowths may be a primary growth feature, consequent upon decreasing pressure, during their transport in kimberlite.

Tatarintsev *et al.* (1983) have reported the presence of co-existing skeletal crystals of manganoan (MnO = 3.7%) armalcolite, and manganoan (MnO = 19.9%, MgO = 1.0%) ilmenite within spherical glassy particles, resembling Pele's Tears, from the West Udachnaya kimberlite. The glass is extremely heterogeneous and rich in MnO (11%–17%) and K_2O (8%–14%). Co-existing minerals include native iron, wüstite, ulvöspinel, rutile, magnetite, and hematite. The assemblage is clearly not in equilibrium and may represent oxidation of an original reduced assemblage or vice versa as postulated by Tatarintsev *et al.* (1983). The glass is unlikely to represent quenched kimberlite magma and its origin remains enigmatic.

6.18.2. Crichtonite Series

Crichtonites have the general formula $AM_{21}O_{38}$, where A is a large radius cation (Sr, Pb, La, Ca, Na, Ba, K) and M is a smaller cation (Fe^{2+} Mg, Al, Cr, Zr, Ti). In the kimberlitic environment, Haggerty *et al.* (1983) and Haggerty (1983) have recognized the Ba and K end member crichtonites, lindsleyite and mathiasite (Table 6.34). Solid solutions between these end members and other crichtonites are designated by the acronym LIMA (Haggerty 1983). LIMA is the dominant opaque phase in heavy mineral concentrate from the Kolonkwanen kimberlite (Haggerty *et al.* 1983). Other occurrences are found in concentrates from Jagersfontein (Haggerty 1983) and De Beers (Haggerty 1975) and in metasomatized xenoliths from Bultfontein (Erlank and Rickard 1977, Jones *et al.* 1982). LIMA is associated with Nb-Cr-rutile, magnesian ilmenite, and spinel at Jagersfontein (Haggerty 1983). No data are available regarding the stability of LIMA, but its presence as a stable phase in the source regions of kimberlite is unquestionable, and has important ramifications with regard to the sequestration of incompatible elements in the mantle. LIMA, as currently found, appears to be a xenocrystal phase; however, Jones *et al.* (1982) argue that it was deposited in mantle rocks by fluids derived from kimberlites.

6.18.3. Unnamed Titanates

Haggerty (1975) has described, from the De Beers kimberlite, a Ba–Cr–V titanate (Table 6.34) enclosed in phlogopite and mantled by ilmenite and perovskite.

The New Elands kimberlite contains a K–Ba–V titanate (Table 6.34) which occurs as clusters of radiating prisms and which is apparently a primary groundmass mineral (Mitchell and Haggerty, unpublished data). This mineral is similar in composition to priderite, (K, Ba)$(Ti,Fe)_8O_{16}$ (Norrish 1951) but is different in its habit and optical properties, i.e., light reddish-brown, monoclinic prisms, no etched basal cleavage.

A Ba-rich titanate (TiO_2 = 51%–54%, BaO = 16.1%–16.7%, Fe_2O_3 = 15.6%–16.1%) has been reported from the groundmass of the Benfontein sill (Scatena-Wachel and Jones 1984).

Zr-rich titanates (ZrO_2 = 0–7%, TiO_2 = 14%–50%, FeO = 23%–48%, CaO = 0.24%, MgO = 5%–17%) occur as complexly zoned mantles upon LIMA "xenocrysts" at Jagersfontein (Haggerty 1983).

Dawson (1980) has described the occurrence of subhedral crystals of a hydrated manganese-rich titanosilicate (SiO_2 = 16.4%, TiO_2 = 29.8%, FeO = 15.6%, MnO = 12.0%, MgO = 17.4%) apparently of primary origin in serpophitic segregations in a late dike at Dutoitspan.

A titanate with the general formula $K(Cr, Ti, Fe, Mg)_{10}O_{17}$ has been reported from a Shandong region kimberlite (Zhou 1980).

6.19. PECTOLITE

Pectolite, $Ca_2NaHSi_3O_9$, has been identified in the De Beers, Dutoitspan, Letseng-la-terae (Scott Smith *et al.* 1983), Elliot County (Agee *et al.* 1982) and Lattavaram (Akella *et al.* 1979) kimberlites. The pectolite occurs in the groundmass as radiating aggregates of colorless acicular or fibrous crystals set in a base of serpentine. It is also found in altered xenoliths. The occurrence of a Na-bearing mineral (7.2%–9.3% Na_2O) in this environment is unusual (see shortite, 6.12). On textural evidence it appears to be a primary groundmass phase. In some kimberlites, however, pectolite is developed only adjacent to altered xenoliths. Scott Smith *et al.* (1983b) propose two origins. It may occur as an apparently primary phase where the composition of the kimberlite has been modified by the partial digestion of, and reaction with Na-bearing xenoliths, or it may occur as a secondary mineral, in veins, as at Wesselton, formed by the metasomatic introduction of Na-bearing fluids. Scott Smith *et al.* (1983b) consider that the mineral identified as cebollite by Kruger (1980, 1982) is in fact pectolite.

6.20. MISCELLANEOUS MINOR MINERALS

Apart from diamond there have been numerous reports of the occurrence of native elements in kimberlites. Flecks of native Cu (5–10 μm) of unknown origin, are common in the De Beers, Letseng-La-Terae (Pasteris 1980b), and other Lesothan (Haggerty 1975) kimberlites.

Wagner (1914) and Pasteris (1980b) mention the occurrence of unidentified platinum group element minerals in association with ilmenite and spinels in the Kimberley group kimberlites.

Metallic iron and iron–nickel alloys occur in serpentinized olivines in the Koidu, De Beers, and Ramatseliso kimberlites (Tompkins and Haggerty 1985, Pasteris 1980b, Haggerty 1975). These have been produced when serpentinization of olivine occurs under unusually low oxygen and sulfur fugacities (see 6.15.1).

Graphite occurs as small flakes disseminated throughout the groundmass of the De Beers and Premier kimberlites (Pasteris 1980b, Wagner 1914), as an intergrowth with pyrrhotite (Haggerty 1975), and as pseudomorphs after olivine (Scott Smith *et al.* 1984, Pasteris 1981). The graphite may be a primary phase derived from methane or a xenocryst derived from graphitized diamond, dis-

aggregated graphite-bearing eclogites and lherzolites (Dawson 1980) or metamorphosed Carboniferous tree fragments (Williams 1932).

A postulated occurrence of native silver (reviewed by Dawson 1980) has been discredited (Clark and Mitchell 1975).

Quartz, of primary origin, is found together with magnetite and ankeritic siderite in carbonate-rich segregations in the Benfontein Sill (Dawson and Hawthorne 1973).

Primary barite ($BaSO_4$) occurs in serpophite segregations together with an unidentified manganese titanosilicate in the Dutoitspan kimberlite (Dawson 1980).

Periclase (MgO) has been postulated to occur as inclusions in monticellite and olivine and in the groundmass of several Yakutian kimberlites (Nikishov and Nikishova 1966). Positive X-ray identification has not been made.

Titan-olivine reported from the Ruslovaya kimberlite (Voskrensenskaya *et al.* 1965) has been shown to be titanian clinohumite (Shchalelkova and Brovkin 1969). This is apparently the only occurrence of humite group minerals in kimberlite. Titanoclinohumites described by McGetchin *et al.* (1970) and Aoki *et al.* (1976) from Moses Rock and Buell Park are considered now to be derived from minette diatremes.

Tompkins and Haggerty (1985) have described the occurrence of a Mg-Al-Ti-Cr wüstite (FeO = 63%–67%, MgO = 9%–11%, TiO_2 = 14%–18%, Cr_2O_3 = 1%–13%, $Al_2O_3 \approx 2.0\%$) type mineral (M_6O_7) mantling spinels in Koidu dike kimberlite. The presence of this mineral implies unusually low oxygen fugacities during the initial stages of crystallization of this dike.

6.21. SECONDARY AND XENOCRYSTAL MINERALS

Many zeolitic, halide and sulfate minerals are found only in the upper levels of kimberlite diatremes and especially adjacent to xenoliths of basalt and shale. The commonest of these secondary minerals are halite (Pavlov and Ilupin 1973, Zinchuk *et al.* 1984), barite, gypsum, anhydrite, epsomite (Bobrievitch *et al.* 1964), afwillite (Parry and Wright 1925), bultfonteinite (Parry *et al.* 1932), phrenite, chabazite, and natrolite (Williams 1932). In addition many kimberlites have been subjected to secondary silicification leading to the deposition of quartz and chalcedony. Dolomite, calcite, aragonite and iron oxides and hydroxide are also common secondary phases.

The presence of these secondary minerals is clearly related to deposition from circulating groundwaters that have interacted with the consolidated kimberlite and xenoliths. The minerals provide no information regarding the petrogenesis and evolution of kimberlite magmas, and discussion of the reactions leading to their formation is beyond the scope of this work.

A wide variety of xenocrystal minerals, e.g., anthophyllite, moissanite

coesite, epidote, corundum, have been described from kimberlites or heavy mineral concentrates (Dawson 1980, Williams 1932). These xenocrysts are derived from xenoliths of crustal and mantle rocks which have been fragmented during transportation in the kimberlite magma. The most important of the xenocrysts are diamonds and the constituents of eclogites and lherzolites, as these phases serve to place limits upon the depths and temperatures of formation of kimberlite magmas (see Chapter 9).

However much you knock at nature's door,
she will never answer you in comprehensible
words.

Ivan Turgenev

7

GEOCHEMISTRY OF KIMBERLITES

7.1. INTRODUCTION

Investigation of the geochemistry of kimberlite is hampered by problems inherent in the intrusive styles characteristic of this volatile-rich magma; by the hybrid nature of the rocks formed from magmas which carry a high proportion of crystalline phases at their time of emplacement; and by the high probability of contamination of some facies by crustal materials and/or groundwater.

A severe impediment to studies of geochemistry of kimberlites is the absence of aphyric or glassy extrusive rocks which could serve as a reference point for understanding either the relationships of the primitive liquids to their mantle sources or of the differentiation processes which may have acted upon the liquids.

Whole-rock major and trace element analyses have been undertaken upon three types of material: diatreme facies rocks, hypabyssal dikes and sills, and autoliths (globular segregations). Each of these materials has its particular sampling problems which impart a bias to the compositions determined on whole rock samples.

The severest problems are associated with diatreme facies rocks: these rocks may contain significant amounts of crustal xenoliths, and have undergone weathering and/or alteration associated with groundwater circulation even at considerable depths. In addition the magmas were devolatilized during their emplacement.

Many of the earlier studies of kimberlite geochemistry paid little heed to the above problems and there exist in the literature analyses of highly contaminated diatreme facies rocks. Dawson (1980) has noted that attempts to extract visible xenoliths from kimberlites prior to analysis (Ilupin and Lutts 1971) are simplistic, as the presence of finely comminuted sub-microscopic particles of

crustal xenoliths can produce unacceptable levels of contamination. Scott Smith *et al.* (1983) have also demonstrated that complete assimilation of xenoliths can lead to the formation of contaminated Na-rich kimberlites which crystallize Na-bearing minerals, e.g., pectolite, of apparently primary aspect.

Hypabyssal kimberlites, in general, contain very few crustal xenoliths, and contamination from this source may be of minor importance. However, compositions are biased because of the increased importance of mantle-derived components, e.g., megacrysts and high-pressure phenocrysts, which can be concentrated by differentiation processes. Although volatiles are retained, their concentration leads to the formation of inhomogeneous segregation-textured kimberlites, highly evolved calcite-enriched residua, or to oxide-rich cumulates whose compositions are vastly different from those of their parent magmas.

Danchin *et al.* (1975) consider autoliths (globular segregations) to be equivalent to the chilled margins of dikes or lavas. However, these bodies appear to form only in diatreme facies kimberlites; thus they are subject to the contamination problems associated with this environment. Their compositions, in addition, are biased because they have been depleted in volatiles.

7.2. MAJOR ELEMENT GEOCHEMISTRY

7.2.1. Contamination and Alteration

Recognition of the above problems has led to attempts at estimating the degree of contamination or alteration of analyzed kimberlites. Ilupin and Lutts (1971) proposed that Si/Mg and Mg/(Mg + Fe) atomic ratios provide a good estimate of crustal contamination as, in general, crustal rocks have higher Si and lower Mg contents than ultramafic rocks, such as kimberlite. Contaminated rocks are considered to have Si/Mg > 0.88 and Mg/(Mg + Fe) < 0.85. Fesq *et al.* (1975), in a modification of Ilupin and Lutts' (1971) proposal, suggested on the basis that olivine (Fo_{87-93}, Si / Mg$\sim$0.60) and phlogopite (Si / Mg$\sim$1.21) may comprise the bulk of kimberlite, that Si/Mg ratios in excess of 1.2 indicate contamination.

Clement (1982) introduced the concept of a contamination index (C.I.) to evaluate the effects of crustal contamination and/or weathering:

$$\text{C.I.} = (SiO_2 + Al_2O_3 + Na_2O)/(MgO + 2K_2O)$$

This index is in effect a measure of the proportions of clay minerals and tectosilicates relative to olivine and phlogopite. Contamination indices close to unity are considered to indicate uncontaminated or fresh kimberlites, although Clement (1982) notes that some apparently contamination-free fresh phlogopite and/or diopside-rich kimberlites may have C.I.'s of 1 to 1.5

Table 7.1. Representative Compositions of Contaminated and Altered Kimberlites[a]

	1	2	3	4	5	6
SiO_2	45.55	34.92	38.10	38.67	30.4	33.78
TiO_2	1.66	0.78	2.11	1.06	0.90	1.40
Al_2O_3	4.78	6.61	6.95	7.19	1.90	2.27
Cr_2O_3	—	—	0.13	0.11	0.14	0.28
Fe_2O_3	8.78	5.11	9.60	6.41	4.0	7.81
FeO	—	—	1.51	2.94	2.0	1.62
MnO	0.14	0.08	0.19	0.14	0.13	0.18
MgO	22.70	10.87	16.92	23.38	25.9	32.13
CaO	6.42	15.85	6.45	5.91	14.8	5.41
Na_2O	0.78	0.41	0.11	0.13	0.04	0.11
K_2O	1.32	2.09	0.29	0.25	0.29	0.33
P_2O_5	0.28	0.30	0.54	0.32	0.35	0.69
H_2O+	4.43	5.30	8.51	9.30	10.2	10.94
H_2O-	2.78	5.34	6.56	3.35		—
CO_2	0.16	11.79	1.68	0.11	8.9	3.15
	99.78	99.56	99.65	99.27	99.95	100.10
C.I.[b]	2.02	2.79	2.58	1.93	1.22	1.10
Si/Mg	1.56	2.49	1.75	1.28	0.91	0.81

[a] 1, Brown kimberlite contaminated with shale and quartzite, Premier Mine (Fresq *et al.* 1975); 2, shale contaminated kimberlite, Ebenhaezer West (Fesq *et al.* 1975); 3, weathered kimberlite, Lemphane (Gurney and Ebrahim 1973); 4, contaminated diatreme facies from Liqhobong, described as fresh by Gurney and Ebrahim (1973); 5, 6, contamination-free diatreme facies kimberlites from Sloan, U.S.A. (Smith *et al.* 1979) and Qi Lu-Shangdong region, China (Zhang and Liu 1983), respectively.

[b] C.I. = $(SiO_2 + Al_2O_3 + Na_2O)/(MgO + 2K_2O)$.

The above indices of contamination are useful, as demonstrated in Table 7.1, which presents comparative data for weathered and contaminated diatreme facies kimberlites and apparently contamination-free fresh diatreme rocks.

Contamination by crustal rocks usually results in the addition of SiO_2, Al_2O_3 and Na_2O to kimberlites. Weathering to mixtures of chlorite, montmorillonite, and serpentine, and in extreme cases to lateritic assemblages will lead to increased SiO_2 and Al_2O_3, as Mg^{2+} and other soluble cations are removed. Either process will result in increased SiO_2 and Al_2O_3 contents relative to those of the pristine kimberlite. Figure 7.1 illustrates these effects in terms of a simple mixing model between uncontaminated fresh kimberlite and some possible crustal contaminants and secondary alteration products. The composition of Malibamatso dike 202 (Gurney and Ebrahim 1973) is used as the kimberlite end member in deriving the mixing lines shown on Figure 7.1. This kimberlite is representative of the more SiO_2-rich varieties of apparently uncontaminated hypabyssal kimberlites and therefore least modified by the differentiation process which can affect kimberlite magmas (see below).

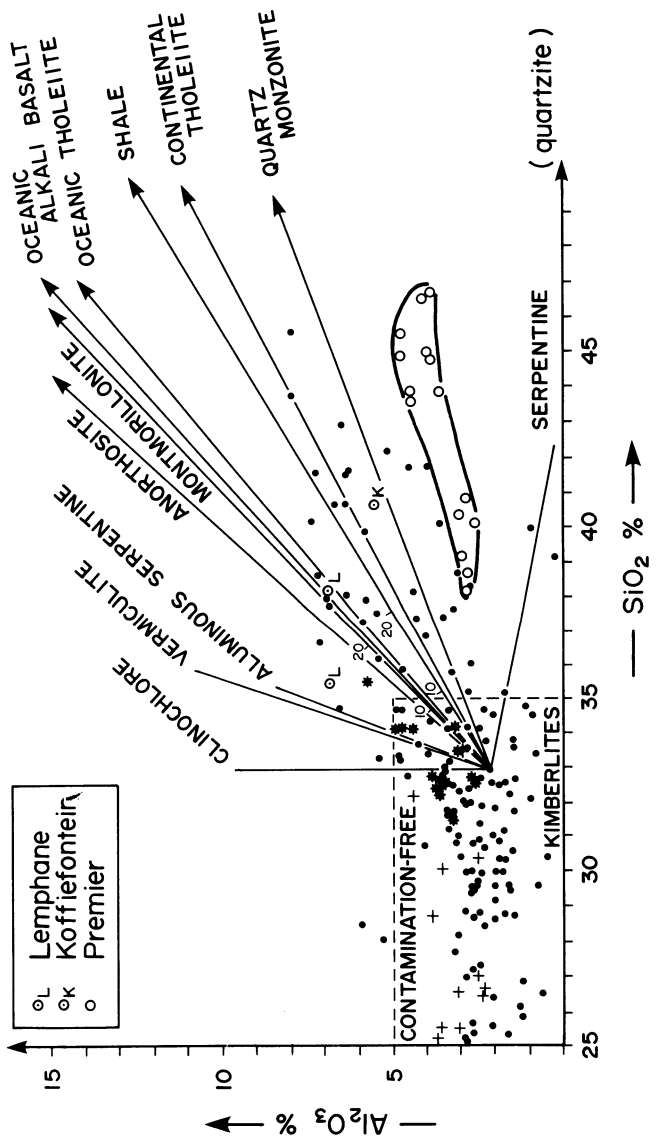

Figure 7.1. Relationship between Al_2O_3 and SiO_2 in contaminated and contamination-free(?) kimberlites. Solid lines are simple mixing lines between Malibamatso dike 202 (Gurney and Ebrahim 1973) and various contaminants and weathering products (Brownlow 1979). Kimberlite data from; Gurney and Ebrahim (1973), Fesq *et al.* (1975), Scott (1979), Nixon *et al.* (1981), Muramatsu (1983), Smith *et al.* (1979), Zhang and Liu (1983), He (1984), Apter *et al.* (1984). Also plotted are data for autoliths(*) (*sensu* Danchin *et al.* 1975) and the average compositions (+) of Soviet kimberlites (Ilupin *et al.* 1974).

Kimberlite whole-rock compositions plotted on Figure 7.1 fall into two groups: a relatively tight band of data points of low Al_2O_3 (0–5%) and widely varying SiO_2 (25%–35%) contents, and a group with widely varying and relatively higher SiO_2 and Al_2O_3 contents, that plot within the envelope defined by the array of mixing lines. The former group is composed of hypabyssal, and diatreme facies rocks and autholiths (*sensu* Danchin *et al.* 1975) which on the basis of their C.I. and Si/Mg ratios are considered to be fresh and contamination free. The latter group contains kimberlites which are known to be weathered (Lemphane) or contaminated (Premier, Koffiefontein). The effects of contamination are particularly well illustrated by the Premier kimberlite which contains microxenoliths of shale and quartzite (Fesq *et al.* 1975). Compositions define an array, reflecting variable degrees of contamination, that plots between the mixing lines for shale and quartzite contaminants. Kimberlites falling within this array are thus considered to be altered or contaminated. Overlap between the groups occurs at low levels (< 10 wt %) of contamination, and for such materials the Si/Mg ratios and C.I. appear not to reflect the effect of contamination.

Application of the above criteria to some of the kimberlite compositions presented by Gurney and Ebrahim (1973) or Muramatsu (1983) indicates that many of their apparently fresh kimberlites are in fact altered or contaminated, e.g., Liqhobong (Table 7.1). The average kimberlite compositions defined by Gurney and Ebrahim (1973) and Muramatsu (1983) are thus not based entirely on fresh samples and are biased toward high Al_2O_3 and SiO_2 contents.

7.2.2. Compositional Variation of Contamination-Free Kimberlites

Figure 7.1 indicates the compositional field, in terms of SiO_2 (<35%) and Al_2O_3(0–5%), of kimberlites which, on the basis of their contamination indices and Si/Mg ratios, are considered to be contamination-free. Representative compositions are given in Table 7.2.

The most significant feature of these data is the extreme variation shown by SiO_2, CaO, MgO, CO_2, and H_2O. The Al_2O_3 and Na_2O contents are extremely low relative to those of other basic and alkaline ultrabasic rocks and are a hallmark of kimberlite magmatism.

The extensive compositional variation is a consequence of the hybrid nature of kimberlites and the differentiation processes that act upon these magmas. The hybrid nature arises from the occurrence of a suite of macrocrystal phases (olivine, phlogopite) which were present in the magma prior to emplacement together with similar phases that were formed *in situ*. The relative proportions of the two components are impossible to estimate, and their presence precludes an estimate of the composition of primitive kimberlite liquids.

Differentiation processes can lead to the concentration of macrocrystal and groundmass microphenocrystal olivines and to increased MgO and SiO_2 contents (Table 7.2, analyses 1 and 4) or to the formation of carbonate-rich residua

Table 7.2. Representative Compositions of Kimberlites[a]

	1	2	3	4	5	6	7	8	9	10	11	12	13	14
SiO_2	32.07	32.53	30.42	29.2	28.63	25.19	16.9	3.41	38.90	36.12	31.00	32.43	26.53	16.40
TiO_2	0.83	1.38	2.95	4.70	1.07	1.89	0.93	12.23	1.67	1.45	1.33	3.88	1.84	1.94
Al_2O_3	0.94	2.12	3.09	2.03	2.01	2.87	0.79	7.81	3.97	4.38	3.05	3.77	0.61	1.28
Cr_2O_3	0.22	0.23	0.15	—	—	—	—	0.10	0.31	—	—	—	—	—
Fe_2O_3	5.45	5.10	5.08	11.85[b]	4.02	3.72	7.04	19.66	8.57[b]	6.80	8.90[b]	4.18	6.68	3.49
FeO	3.22	3.78	6.28	—	5.38	6.72	3.47	12.12	—	2.68	—	9.49	6.50	5.45
MnO	0.16	0.15	0.18	0.85	0.14	0.22	0.24	0.43	0.15	0.22	0.15	0.19	0.22	0.19
MgO	38.45	31.35	25.14	31.11	34.02	29.69	16.6	11.93	19.92	22.82	23.99	26.63	32.78	17.24
CaO	5.67	7.59	9.72	7.47	11.92	13.59	26.4	17.15	7.06	8.33	11.43	8.04	9.58	24.81
Na_2O	0.05	0.05	0.08	0.13	0.20	0.01	—	0.26	0.28	0.29	0.05	0.26	0.06	0.99
K_2O	0.22	1.63	2.15	0.88	0.05	0.15	0.02	0.09	4.68	5.04	1.55	2.10	0.09	0.14
P_2O_5	0.37	0.54	1.17	0.69	0.27	2.20	1.36	2.42	1.34	1.46	0.63	0.25	0.66	1.80
CO_2	—	4.46	5.30	—	8.99	12.83	19.23	9.45	—	3.80	—	5.88	10.58	23.39
H_2O+	8.70	7.56	6.25	—	2.75	1.15	5.13	2.34	—	4.89	—	3.16	5.64	3.16
H_2O-	0.69	0.44	0.64	—	0.23	—	0.28	0.30	—	1.28	—	—	—	—
L.O.I.	3.09	—	—	9.94	—	—	—	—	11.39	—	16.33	—	—	—
	100.33	98.91	98.60	98.18	99.69	99.62	98.39	99.80	98.24	99.56	98.41	100.25	101.77	100.78

[a] 1, Shandong, China (Zhang and Liu 1983); 2, Dike 202, Malibamatso River, Lesotho (Gurney and Ebrahim 1973); 3, Pipe 200, Lesotho (Gurney and Ebrahim 1973); 4, base of macrocrystal-rich sill, Mayeng (Apter *et al.* 1984); 5, olivine-magnetite-perovskite cumulate, Benfontein (Dawson and Hawthorne 1973); 6, composite sample of Benfontein sill (Dawson and Hawthorne 1973); 7, magnetite-calcite-serpentine dike, Premier (Robinson 1975); 8, magnetite perovskite cumulate, Benfontein (Dawson and Hawthorne 1973); 9, Swartruggens Main dike (Skinner and Scott 1979); 10, New Elands dike (Dawson 1972); 11, Orroroo dike (Scott Smith *et al.* 1984); 12–14, Holsteinsborg dikes, Greenland (Scott 1979).

[b] Total Fe calculated as Fe_2O_3; L.O.I. = loss on ignition.

depleted in MgO and SiO_2 and enriched in CaO, CO_2, and H_2O (Table 7.2, analyses 7 and 14). In some cases crystal sorting processes lead to the formation of oxide-rich cumulates of extreme composition (Table 7.2, analysis 8). The variation in K_2O contents reflects the petrographic division into micaceous K_2O-rich (Table 7.2, analyses 9–14) and mica-poor, K_2O-poor kimberlites (Table 7.2, analyses 1–8).

The most important conclusion which can be drawn from the above observations is that kimberlite whole-rock compositions do not represent the compositions of the magmas from which they formed.

The use of standard variation diagrams to represent the compositional variations found in kimberlites is, in many cases, inappropriate as the data cannot define liquid lines of descent. Much of the compositional variation shown in the ternary diagrams employed, for example by Dawson (1967b), Meyer (1976), and He (1984), simply reflects differing proportions of olivine to calcite in the samples.

Scott (1979) discussed the problems of representation of kimberlite analyses in several types of variation diagrams (Harker, molar ratio, FMA, CMAS) and concluded that the data must be considered on a volatile-free basis. The rationale for this conclusion is that an attempt must be made to account for the random loss or relative movement of either volatiles or an immiscible volatile-rich fluid during emplacement. Such a proposal however introduces an element of unreality into the problem by ignoring the major modal amounts of calcite that have formed *in situ* in many kimberlites. The artifice may generate smooth curves on variation diagrams but their significance is debatable in that similar "corrections" to the data are not made for the random amounts of macrocrystal and phenocrystal olivine that are present. It is, therefore, not surprising that the variation diagrams presented by Scott (1979) or Danchin *et al.* (1975) can be interpreted in terms of olivine control lines. Clearly variation diagrams are of use in depicting the compositional variation of kimberlite; however, any conclusions reached by the use of such diagrams must be regarded critically with respect to the hybrid nature of kimberlites.

7.2.2.1. Intra-kimberlite Compositional Variation

Systematic studies of the compositional variation within a single intrusion, or between individual members of a composite intrusion, have not been undertaken. Compositional data for most kimberlites are limited to a few samples generally taken at random, or to material considered to be representative of the whole intrusion. The approach is clearly inappropriate for complex diatremes and root zones, but may be adequate for relatively homogeneous dikes. General geochemical principles and the data of Table 7.2 indicate that differentiation will lead to the depletion of MgO and SiO_2 and the enrichment of CaO, TiO_2, and H_2O in the derivative liquids, with concomitant formation of Mg-rich "cu-

mulate" fractions. The few data available indicate that very wide ranges in composition occur within the Dutoitspan (Clement 1982) and Mir (Frantsesson 1970) kimberlites. Analyses of the Benfontein sill (Dawson and Hawthorne 1973) confirms the expected trend of CaO enrichment (Table 7.2). Unfortunately the limited data do not allow any significant conclusions to be drawn.

7.2.2.2. *Inter-kimberlite Compositional Variation*

Relationships between randomly selected samples of kimberlites are difficult to assess as there are no common reference points with regard to their relative phenocryst/macrocryst content, or extent of differentiation, that will allow comparison of their composition at the same stage of evolution, or of their primitive compositions. Kimberlites within a given field may be consanguineous, but this may not hold with respect to more distantly related occurrences.

Scott's (1979, 1981) studies of the Holsteinsborg micaceous kimberlites are the only significant studies of the compositional variation within a closely related group of kimberlites. Scott (1979) demonstrated that with decreasing MgO there is a poorly defined increase in K_2O, Al_2O_3, and CaO (Figure 7.2). Bulk compositions, when recalculated on a volatile-free basis, define linear arrays on variation diagrams (Figures 7.3 and 7.4) that are interpreted to be a consequence of olivine and spinel fractionation, but which do not allow identification of the

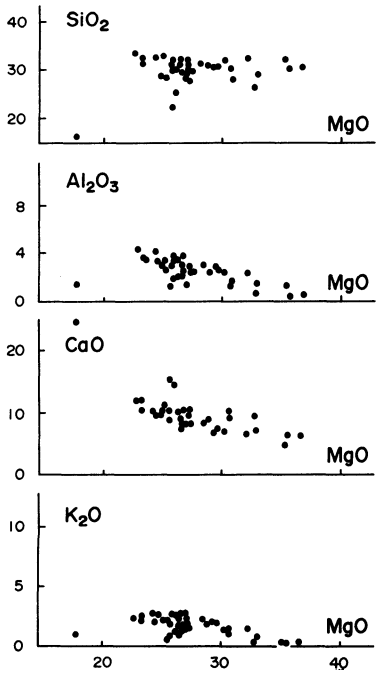

Figure 7.2. Representative major oxide (wt %) variation diagrams for the Holsteinsborg kimberlites, after Scott (1979).

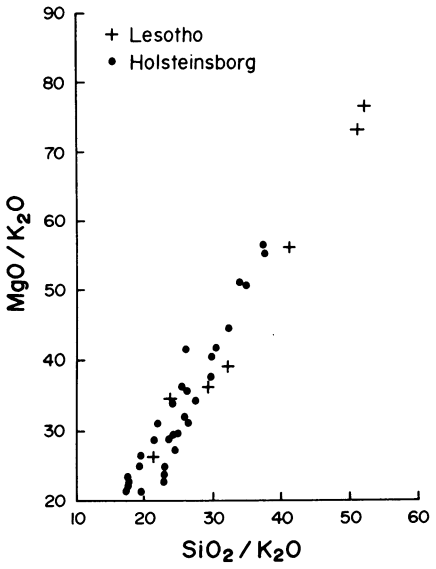

Figure 7.3. MgO/K_2O versus SiO_2/K_2O molar ratio variation diagram for Holsteinsborg (Scott 1979) and Lesotho (Gurney and Ebrahim 1973) kimberlites.

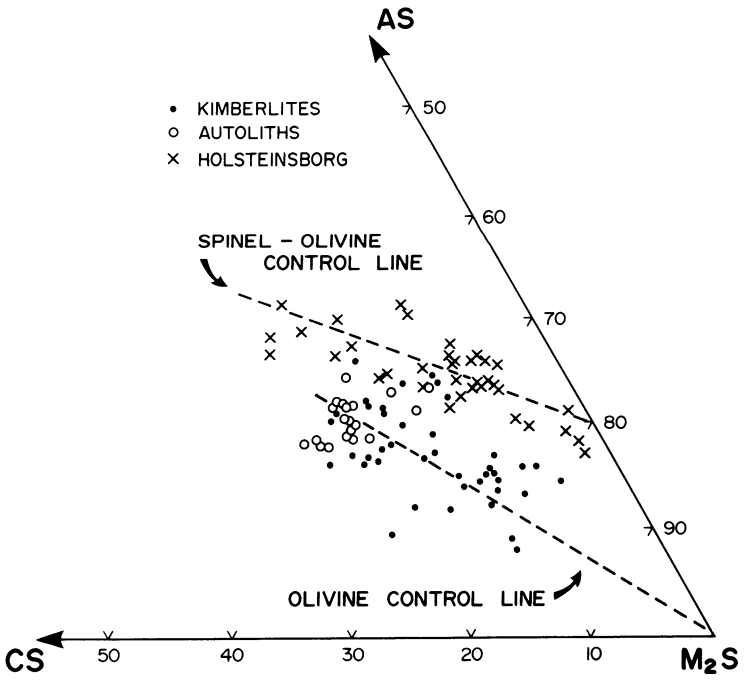

Figure 7.4. Projection from or toward silica onto the plane M_2S–CS–AS in the CaO–MgO–Al_2O_3–SiO_2 (CMAS) system (O'Hara 1968) of kimberlite and autolith (*sensu* Danchin *et al.* 1975) compositions from Holsteinsborg (Scott 1979) and southern Africa (Danchin *et al.* 1975).

parental liquids. As noted above those compositional "control lines" may be artifacts of the data presentation method and reflect modal variations in olivine content. Figure 7.3 also shows that data for fresh Lesotho kimberlites define a linear trend on a molar ratio variation diagram, similar to that of the Holsteinsborg dikes.

Scott's (1979) study is important in that it demonstrates that some closely related groups of kimberlites exhibit well-defined geochemical trends which may be interpreted as being indicative of consanguineity. Such trends are however more difficult to discern when more distantly related kimberlites are compared. Figure 7.4 thus shows that southern African kimberlites in general form a diffuse array as compared with the Holsteinsborg linear array in the CMAS system. Kimberlites from the Shandong region illustrate well the problems of comparing data on a regional basis in Figure 7.5 in which no simple compositional relationships are evident.

It has long been recognized that two compositionally and mineralogically distinct groups of kimberlites are present in South Africa. The older micaceous group, not surpisingly, contains more K_2O and Al_2O_3 than the younger mica-poor group (Table 7.3). Isotopic and age relationships (Smith 1983) clearly indicate that the magmas are not consanguineous and demonstrate the existence of contrasting types of kimberlite magmatism within this region. It is not known whether similar bimodal magmatism exists in other kimberlite provinces. Micaceous kimberlites, such as Tunraq in the Somerset Island province (Mitchell 1979), or Zagodochnaya in the Daldyn-Alakit field (Lebedev 1964), may or may not be simple modally enriched variants of a single magma type.

Ilupin *et al.* (1974) have proposed that major differences exist between the composition of kimberlites from the individual provinces of Yakutia and suggest that the southern groups of Paleozoic diamond-bearing kimberlites are relatively poorer in K, Ti, Fe, and Al than the northern groups of Mesozoic barren (un-

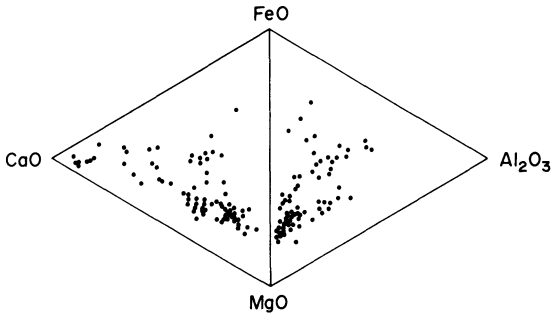

Figure 7.5. Compositions of kimberlites from China (He 1984) plotted in the ternary variation diagrams CaO–FeO–MgO and FeO–MgO–Al_2O_3.

Table 7.3. Representative Average Compositions of Kimberlites[a]

	1	2	3	4	5	6	7	8	9	10	11	12
SiO_2	35.2	31.1	33.21	36.36	34.03	30.18	30.00	27.64	27.03	25.51	26.58	32.15
TiO_2	2.32	2.03	1.97	0.98	1.52	3.39	1.52	1.65	1.47	1.17	1.89	2.82
Al_2O_3	4.4	4.9	4.45	5.13	3.37	2.48	2.45	3.17	2.46	3.00	3.06	4.37
Cr_2O_3	—	—	0.17	0.22	0.20	0.22	0.25	0.14	0.15	0.11	0.11	0.15
Fe_2O_3	—	—	6.78	—	4.58	3.92	5.98	5.40	5.53	3.90	5.61	5.99
FeO	9.8[b]	10.5[b]	3.43	7.71[b]	3.78	8.68	2.99	2.75	1.71	2.39	3.00	3.98
MnO	0.11	0.10	0.17	0.16	0.16	0.19	0.16	0.13	0.10	0.12	0.12	0.16
MgO	27.9	23.9	22.78	17.43	25.39	27.53	28.57	24.31	25.53	17.00	25.45	22.54
CaO	7.6	10.6	9.36	11.16	9.45	9.65	10.12	14.13	13.56	21.37	13.45	10.87
Na_2O	0.32	0.31	0.19	0.42	0.48	0.25	0.18	0.23	0.12	0.19	0.14	0.28
K_2O	0.98	2.1	0.79	1.52	1.60	1.82	0.46	0.79	0.34	0.47	0.78	1.73
P_2O_5	0.7	0.7	0.65	0.55	1.12	0.51	0.65	0.55	0.46	0.56	0.77	0.67
CO_2	3.3	7.1	4.58	n.d.	5.08	7.39	n.d.	10.84	11.12	16.21	10.91	6.38
H_2O+	7.4	5.9	8.04	n.d.	7.26	3.70	n.d.	7.89	10.15	7.59	7.86	7.76
H_2O	—	—	2.66	n.d.	0.99	—	n.d.	0.24				
	100.30	99.24	99.23	81.64	99.01	99.91	83.33	99.86	99.73	100.15	99.73	99.85
No.	—	—	(25)	(80)	(11)	(41)	(14)	(63)	(229)	(61)	(42)	(29)

[a] 1, kimberlite (Dawson 1967); 2, micaceous kimberlite (Dawson 1967); 3, Lesotho (Gurney and Ebrahim 1973); 4, South Africa (Gurney and Ebrahim 1973); 5, South Africa (Muramatsu 1983); 6, Holsteinsborg, Greenland (Scott 1979); 7, Shandong and Liaoning, China (Zhang and Liu 1983); 8, Siberian kimberlites (Ilupin and Lutts 1971); 9–12 Alakit, Malaya Botuoba, Chomurdakh and Luchankan fields, Siberia (Ilupin *et al.* 1974).
[b] Total Fe calculated as FeO. No. = number of samples.

economic) kimberlites (Table 7.3). Perchuk and Vaganov (1980) also propose that, while the Paleozoic kimberlites have relatively constant SiO_2 contents, their H_2O and CO_2 contents are inversely correlated. Mesozoic kimberlites, in contrast, show very wide variations in their SiO_2 content and no correlations between the volatiles. Illupin *et al.* (1974) and Perchuk and Vaganov (1980) consider that these differences are due to formation of the magmas under different PT conditions and that the Mesozoic kimberlites underwent a greater degree of differentiation than the Paleozoic ones. Care must be taken in accepting the above generalizations in view of their being based upon average compositions of kimberlites within a given field.

7.2.2.3. Average Compositions

In view of the wide ranges in composition that exist within and between kimberlites it is unlikely that average compositions have any real geochemical significance. Averages are useful in that they illustrate the overall compositional characteristics of the clan and allow broad comparisons to be made with the

compositions of other rock types. Representative average compositions are given in Table 7.3. These data should not be used to draw conclusions regarding intraprovincial compositional differences, as some of the averages are probably based upon samples that were weathered or contaminated. A further drawback is that no assessment of the variance of the data is available.

Table 7.3 indicates that kimberlites may be considered to be undersaturated ultrabasic rocks (SiO_2 = 25%–35%) of unusually low Al_2O_3 content (generally less than 5%). Their Na_2O/K_2O ratios are very low (<0.5), illustrating their potassic nature. Molar $(Na_2O + K_2O)/Al_2O_3$ ratios of less than unity demonstrate their miascitic affinities.

The only rocks which have petrographic and chemical affinities with kimberlites are a diverse group of ultrabasic alkaline rocks of lamprophyric aspect, e.g., alnöites and mica periodotites. Table 7.4 presents representative compositions of such rocks and shows that they are typically richer in Al, Ti, and Fe than kimberlites and that they can even be sodic in character. Some of the Al-poor alnöitic rocks are however similar in composition to kimberlite. Such rocks are mineralogically very different in that they contain andraditic garnets, Na–Al bearing pyroxenes (see Section 2.5) and a distinctive suite of spinels (see Section 6.9.10).

Table 7.4. Representative Compositions of Alnöites and Micaceous Ultrabasic Rocks[a]

	1	2	3	4	5	6	7	8	9	10
SiO_2	30.90	33.26	39.19	38.00	25.79	27.30	26.20	29.80	33.84	30.00
TiO_2	4.28	2.15	0.40	1.90	3.32	3.68	3.60	2.24	3.78	4.50
Al_2O_3	3.66	5.90	8.41	10.69	7.35	8.95	11.34	7.90	5.88	9.32
Cr_2O_3	—	0.05	—	—	—	0.07	—	—	0.18	—
Fe_2O_3	10.29	5.30	3.47	7.34	1.63	8.87	3.97	6.90	7.04	4.11
FeO	5.80	6.54	5.51	4.52	10.72	7.01	13.89	4.13	5.16	7.49
MnO	0.27	0.05	—	0.21	0.40	0.27	0.22	—	0.16	—
MgO	19.25	26.41	22.78	10.12	13.78	12.34	9.33	17.90	22.96	9.20
CaO	14.37	14.47	8.90	14.76	18.90	17.18	12.36	15.90	9.46	12.31
Na_2O	0.31	1.23	3.23	5.83	0.52	0.38	0.67	0.20	0.33	0.92
K_2O	0.95	0.82	2.14	2.60	2.83	2.99	1.46	1.72	2.04	4.03
P_2O_5	0.78	0.76	0.53	0.70	3.20	2.90	1.40	0.93	0.89	3.31
CO_2	4.62	1.10	0.00	1.50	7.93	2.17	6.42	7.04	0.43	
H_2O+	5.04	1.91	3.66	0.42	3.44	3.95	7.19	4.05	7.05	14.83
H_2O		0.09	0.56	1.41	2.30	1.32	2.22	0.94		
	100.52	100.04	98.78	100.00	102.11	99.38	100.27	99.65	99.65	100.02

[a] 1, Ultrabasic lamprophyre, McKellar Harbour, Ontario (Platt and Mitchell 1982); 2, alnöite, Isle Cadieux, Quebec (Bowen 1922); 3, alnöite, Winnett, Montana (Ross 1926); 4, alnöite, Maimecha-Kotui, Siberia (Egorov 1970); 5–7, alnöite, Alnö, Sweden (Von Eckermann 1948); 8–9, ultrabasic lamprophyres Claylick Creek and Flanery, respectively (Koenig 1956); 10, mica peridotite, Bokaro Coalfield, Bihar (Mukherjee 1961).

7.3. TRACE ELEMENT GEOCHEMISTRY

7.3.1. Introduction

Studies of kimberlite trace element geochemistry are subject to many of the sampling and contamination problems discussed above with respect to the major elements. The bulk of the data have been obtained on randomly selected samples and upon material which may have been contaminated to varying degrees. Aspects of this latter problem have been discussed by Fesq *et al.* (1975) and Kable *et al.* (1975), who have concluded that the elements Ti, Nb, Ta, Zr, Hf, P, and the rare earths are insignificantly affected by crustal contamination.

In addition the trace element geochemistry is poorly characterized due to problems associated with the analytical techniques utilized. Many of the analyses (especially in the 1960s) were made by emission spectrographic methods which although adequate for trace elements present in relatively high concentrations, (for example, Co, Ni, Cr), are subject to matrix interference effects of unknown magnitude or to erratic behavior in the arc, e.g., Cs (Gurney *et al.* 1966). Much emission spectrographic data is, at best, semiquantitative, e.g., all of Litinskii's (1961) data. Many of the elements determined occur at concentration levels close to the sensitivity limits of the technique employed and the data should be regarded as providing only an indication of the true concentration, e.g., Re by compleximetric titration (Ilupin *et al.* 1975), Se by fluorimetry (Sobolev *et al.* 1975), and the heavy rare earths by X-ray fluorescence spectrometry (Burkov and Podporina 1966). Significant interferences may also be inherent in all these methods.

Further, discrepancies exist between individual groups of determinations using the same technique, such as Ni determinations by Litinskii (1961) and Dawson (1962), and between determinations of the same element by different methods, such as the rare earth data of Burkov and Podporina (1966) and Mitchell and Brunfelt (1975).

The overall characteristics of the trace element geochemistry of kimberlite, initially recognized by Dawson (1962, 1967b) and subsequently reiterated by Dawson (1980), Wedepohl and Muramatsu (1979), and Muramatsu (1983), are that two major groups of trace elements are present in significant amounts: (a) elements with abundances similar to those found in ultramafic rocks, e.g., Cr, Ni, Co; and (b) elements with abundances similar to those found in alkaline rocks such as melilitites, carbonatites, and potassic lavas, e.g., Nb, Zr, Sr, and the rare earths.

In this work these groups are referred to as the *compatible* and *incompatible* element groups, respectively. The latter group is divided into three subgroups: (1) alkaline earths, Nb, Zr, Ta, Hf, U, Th; (2) rare earth elements; (3) alkali and volatile elements.

7.3.2. Compatible Elements

Compatible elements are those which are preferentially incorporated into the phases crystallizing from the magma and are therefore rapidly depleted during fractional crystallization. Such elements have solid/liquid distribution coefficients greater than unity, and for kimberlites are taken to include the first series of transition elements and the siderophile/chalcophile platinum-group elements.

The mean abundances and ranges, respectively, of Sc (14, 6–38 ppm), V (100, 21–760 ppm), Cr (893, 430–2554 ppm), Co (65, 9–125 ppm), Ni (965, 471–1800 ppm), Cu (93, 6–1320 ppm), and Zn (69, 10–287 ppm) are fairly well established, and data obtained by a variety of analytical techniques are in good agreement.

General geochemical principles, supported by the meager data of Marshintsev and Sukneva (1970) and Muramatsu (1983), indicate that incompatible elements are hosted essentially by spinels and olivines, and to a lesser degree by perovskite (Sc), sulfides (Cu, Ni), and diopside (Cr, V, Ni).

The abundances of compatible elements are directly related to the modal proportions of olivine and spinel and are inversely proportional to the amount of crustal xenoliths (Fesq *et al.* 1975); however, some groups of kimberlites, e.g., the Lesotho dikes (Kresten 1973a, Dempster and Tucker 1973), appear to be poor in Cr and Ni relative to other kimberlites. The Holsteinborg dikes (Scott 1979) and the Lesotho dikes (Dempster and Tucker 1973) are enriched in V and Zn, respectively. Kable *et al.* (1975) have shown that micaceous kimberlites are richer in Sc (mean 19.4 ppm) than mica-poor varieties (mean 9.6 ppm). Highly evolved carbonate-rich kimberlites are relatively poor in incompatible elements (Scott 1979, Dawson and Hawthorne 1973).

Few systematic studies of interelement relationships have been undertaken. Scott (1979) showed that the Cr and Ni content decrease as MgO decreases in the Holsteinsborg dikes is related to spinel and olivine fractionation. Other elements Zn, Cu, and V, however, do not correlate with MgO variations. Figure 7.6 shows that the Holsteinsborg dikes exhibit a strong positive correlation between their Cr and Ni contents. This relationship is, however, poorly defined for the apparently consanguineous Lesotho dikes and not surprisingly is absent from the random samples from the Yakutian kimberlites (Tomanovskaya 1974) and the Kimberley area (Muramatsu 1983).

Marshintsev and Lapin (1976) have noted that Ni, Co, and Cr contents, and Ni/Co, Ni/V, and Cr/V ratios, apparently decrease with depth in the West Udachnaya kimberlite. These authors also propose that there exists a regional decrease in the Sc, V, Cr, Ni, and Co contents of kimberlites from the diamond-bearing older varieties of the center of the Siberian platform to the barren younger types at the margins. This assertion would, however, seem improbable given the difficulty of establishing the transitional element content of undifferentiated

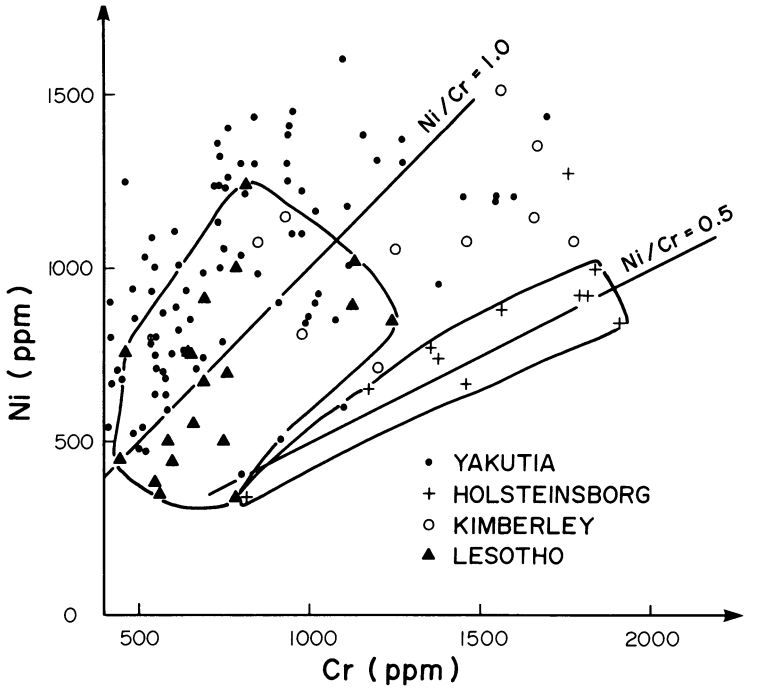

Figure 7.6. Ni versus Cr content of kimberlites from Yakutia (Tomanovskaya 1964), Holsteinsborg (Scott 1979), South Africa (Muramatsu 1983), and Lesotho (Dempster and Tucker 1973).

kimberlite. Average abundances, as employed by Marshintsev and Lapin (1976), are clearly inadequate.

Figure 7.7 demonstrates that Cr and Ni show no correlation with La or Th in closely related groups of kimberlites. This lack of coherent relationships indicates that the enhancement of incompatible element abundances is unlikely to be the result of fractional crystallization of a kimberlite magma initially poor in these elements. The data clearly show that fractional crystallization has probably not played a significant role in the evolution of kimberlite magmas prior to their emplacement. This conclusion is supported by the fact that groundmass olivines and spinels which have crystallized *in situ* are rich in Ni and Cr, respectively.

Compatible element abundances are clearly not representative of the liquids from which the kimberlites form, and their variability is due to the widely varying macrocryst/phenocryst-matrix ratios. Estimates of their "primitive" concentrations in undifferentiated kimberlites are difficult to obtain and these elements cannot be used in geochemical models of evolution beyond the broad generalizations noticed above.

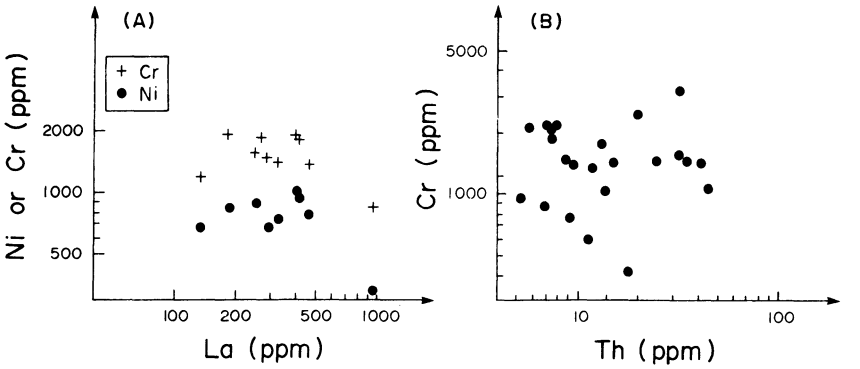

Figure 7.7. (A). Ni or Cr versus La content of Holsteinsborg kimberlites (Scott 1979). (B) Cr versus Th content of some Kimberley area kimberlites (Mitchell and Clement, unpublished data).

Platinum-group element (PGE) abundances are very poorly characterized. Few data are available and those obtained by chemical techniques are at variance with those obtained by neutron activation analysis (Table 7.5). Averages quoted by Muramatsu (1983) and Wedepohl and Muramatsu (1979) are too high, as Kaminskii *et al.*'s (1974), and Ilupin *et al.*'s (1975) chemical methods clearly over-estimate PGE relative to data obtained by neutron activation (Morgan and Lovering 1967, Paul *et al.* 1979). The PGE can be expected to be hosted mainly by spinels and sulfides (Mitchell and Keays 1981). The current data base should not be used to infer anything about the evolution of kimberlite magmas or their relationship to the upper mantle.

7.3.3. Incompatible Trace Elements: I. Ba–Sr, Zr–Hf, Nb–Ta, U–Th

Incompatible trace elements have solid/liquid distribution coefficients in common rock-forming silicates of approximately zero. Their abundances may be reduced by the presence of olivine macrocrysts and/or crustal contamination, but their inter-element relationships remain unaffected and may be used to obtain information regarding the source regions of the magmas. In kimberlites these elements may not be removed from the liquid until the later stages of the crystallization of the groundmass; therefore whole-rock analyses may provide reasonable estimates of their abundances and ratios.

7.3.3.1. Barium and Strontium

Ba (mean 1100, range 128–5690 ppm) is hosted primarily by phlogopite; consequently, micaceous kimberlites, e.g., New Elands (4841 ppm), the Main Bobbejaan dikes, Bellsbank (3714 ppm), and Holsteinsborg (1013 ppm), are

Table 7.5. Abundances of Some Trace Elements in Kimberlites for (A) Platinum Group and Related Elements (ppb) and (B) Other Elements (ppm)[a]

(A)	Range	Mean	No.	Method	Source
Ru	2–18	6.5	17	CHEM	1
Rh	0.2–23	7.1	17	CHEM	1
Re	34–221	37.1	9	CHEM	2
		0.069	1	NAA	3
Os	2–12	5.0	17	CHEM	1
	26–65	45.5	2	CHEM	2
		1.34	1	NAA	3
Ag	5–250	134	19	CHEM	4
Pd	4–170	53	17	CHEM	1
	1.3– 19	8.1	11	NAA	5
Ir	2.0– 11.0	7.6	17	CHEM	1
	0.49– 5.9	3.0	11	NAA	5
Pt	30–430	187	17	CHEM	1
		250(a)	26	?	6
		87(b)	11	?	6
Au	0.5– 8.4	2.94	46	NAA	4
	0.11– 43.0	12	11	NAA	5
		95(a)	26	?	6
		80(b)	11	?	6
	1.2– 18	3.9	14	NAA	7

(B)	Range	Mean	No.	Method	Source
Be		1.6(a)	53	?	6
		2.2(b)	37	?	6
	1–3	—	3	ES	8
		1	38	ES	9
Ga		6(a)	31	?	6
		9(b)	5	?	6
	1–5	2.6(a)	7	?	10
	<1–8	5.5(b)	7	?	10
		9	14	ES	11
		1	10	ES	12
		30	3	ES	8
Ge		0.5	48	CHEM	9
Mo	3–12	—	14	ES	11
		2(a)	25	?	6
		2.7(b)	5	?	6
	0.3–0.9	0.5	7	?	10
	<0.1–1.7	0.9	7	?	10
Sn		6.4(a)	25	?	6
		12(b)	5	?	6
	0.4–2	1(a)	7	?	10
	<1–2	1.6(b)	7	?	10
		30	3	ES	8

[a] No., numbers of samples; CHEM, chemical methods of analysis; NAA, neutron activation; ES, emission spectrography. (a), diamond-rich (b), diamond-poor kimberlite. Data sources: 1, Kaminskii *et al.* 1974; 2, Ilupin *et al.* 1975; 3, Morgan and Lovering 1967. 4, Ivanov *et al.* 1977; 5, Paul *et al.* 1979; 6, Marshintsev and Lapin 1976; 7, Rozkhov *et al.* 1973; 8, Nixon and Kresten 1973a; 9, Burkov and Podporina 1965; 10, Ilupin *et al.* 1974; 11, Dawson 1962; 12, Borisenok 1959.

enriched in Ba relative to mica-poor types. High Ba content may also result from the presence of K–Ba titanates (New Elands) or barium carbonates (Benfontein). In mica-poor kimberlites, Ba is concentrated in residual fluids until it is incorporated into groundmass micas or carbonates. K/Ba ratios range from 1 to 45 (Fesq *et al.* 1975, Scott 1979, Muramatso 1983) with the lowest ratios being found for micaceous kimberlites.

Sr (mean 851, range 120–2727 ppm) is hosted by apatite, perovskite, groundmass diopside, and carbonates. Calcite-rich residua are enriched in Sr (Dawson and Hawthorne 1973, Scott 1979).

No systematic studies of Ba–Sr variations have been undertaken. Scott (1979) showed no correlation between Ba and Sr abundances and the MgO content of Holsteinborg dikes. Figure 7.8 demonstrates that no significant correlation exists between Ba and Sr in kimberlites as a group and is no doubt a reflection of widely variable mica/carbonate ratios. Ba/Sr ratios can be greater or less than unity. The Ba and Sr contents of kimberlites are less than those of lamproites (Scott Smith and Skinner 1984) and carbonatites (Gold 1966) but similar to those of alkali basalts and melilitites.

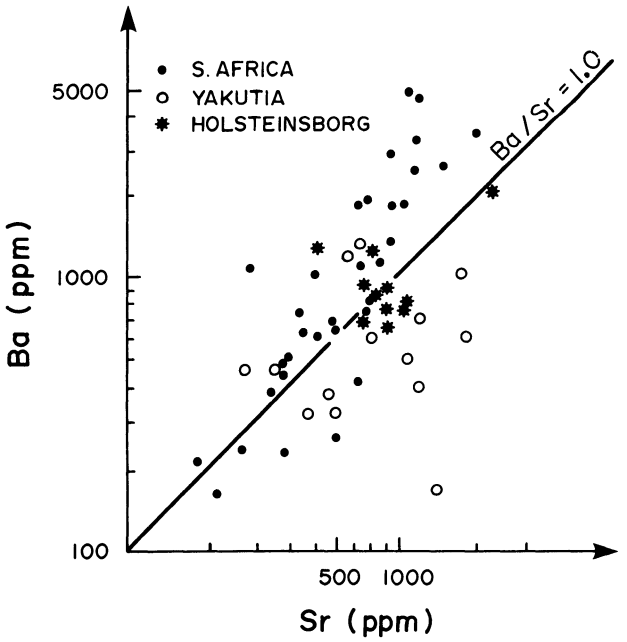

Figure 7.8. Ba versus Sr content of kimberlites from Yakutia (Ilupin *et al.* 1974), Holsteinsborg (Scott 1979), and southern Africa (Fesq *et al.* 1975, Nixon *et al.* 1981, Muramatsu 1983).

7.3.3.2. Zirconium and Hafnium

Zirconium (mean 184, range 47–1300 ppm) and hafnium (mean 5.6, range 1.0–29.7 ppm) are hosted primarily by perovskite (Kaminskii *et al.* 1977). Zircons, although rich in Hf and Zr, are unlikely to control the whole rock abundances of these elements because of their extreme rarity. High contents of macrocrystal ilmenite can result in increased Zr and Hf abundances. The elevated contents of Zr (≈2300 ppm) in the oxide cumulates of the Benfontein sills (Dawson and Hawthorne 1973) can be correlated with the presence of baddeleyite (Scantena-Wachel and Jones 1984).

Zr and Hf abundances show a high degree of correlation (Figure 7.9), with the highest amounts being found in the micaceous kimberlites. The slope of the plot of the logarithmic abundances is close to unity indicating that these elements are highly incompatible, with bulk distribution coefficients close to zero. The Zr/Hf ratios may, therefore, reflect those of the sources of the magmas. The scatter in Figure 7.9 is due principally to errors associated with Hf determination which result in high Zr/Hf ratios (32–102) for some of the Yakutian kimberlites. The majority of the samples analyzed by Kamenskii *et al.* (1977), however, have Zr/Hf ratios between 30 and 60, in agreement with Fesq *et al.*'s (1975) data for South African kimberlites (Zr/Hf = 35–50). Importantly the Zr–Hf coherence is observed on a worldwide basis and is independent of the age of magmatism, implying that the sources of all kimberlites so far examined have similar Zr/Hf ratios (29–40; Mitchell *et al.* 1973a). The differences in the Zr and Hf abundances of rocks of similar Zr/Hf ratio may reflect derivation of the magmas either from sources of differing Zr and Hf contents, or by different degrees of partial melting of a single source, or the effects of fractional crystallization of phases other than ilmenite.

Kimberlites are poor in Zr relative to lamproites, which typically contain more than 1000 ppm Zr (Scott Smith and Skinner 1984). The Zr/Hf ratios are similar to those of a wide variety of mantle-derived basic rocks.

7.3.3.3. Niobium and Tantalum

Whole rock abundances of Nb (mean 141, range 29–400) and Ta (mean 11, range 1.2–42.5 ppm) are controlled principally by the presence of perovskite as other phases, with the exception of ilmenite, contain relatively insignificant quantities of Nb and Ta (Mitchell 1977, 1972; Kaminskii *et al.* 1977). Enrichment in these elements can be caused by the presence of significant quantitites of macrocrystal ilmenite (Kable *et al.* 1975). Micaceous kimberlites do not appear, in general, to be enriched in Ta (and hence Nb) relative to other varieties of kimberlite (Mitchell and Brunfelt 1975, Paul *et al.* 1977).

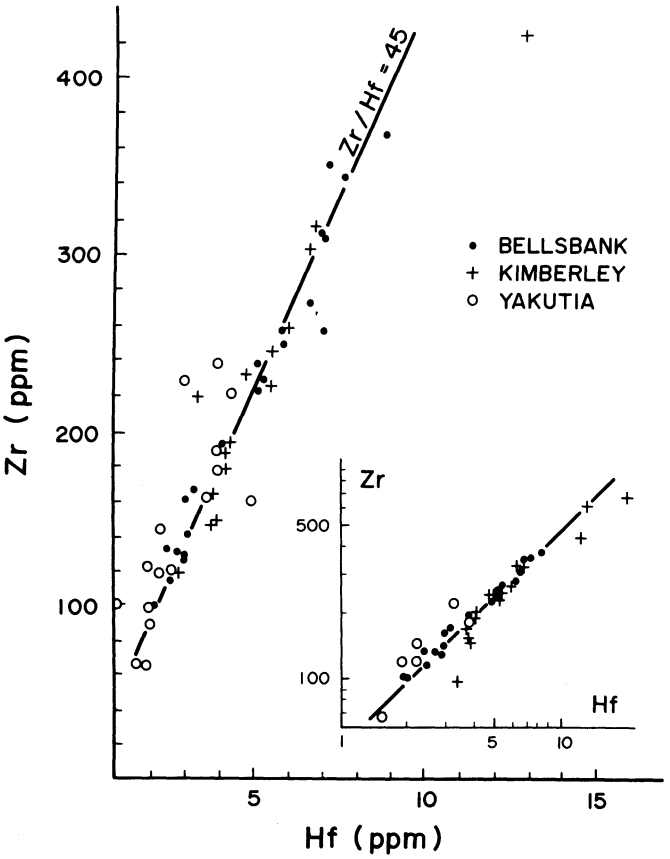

Figure 7.9. Zr versus Hf content of kimberlites from Bellsbank, South Africa (Kable *et al.* 1975), the Kimberley area (Mitchell and Clement, unpublished data) and Yakutia (Kaminskii *et al.* 1977). Insert—logarithmic plot of the same data.

In contrast to the close Zr–Hf coherency, Nb and Ta in kimberlites as a whole are not highly correlated. Individual groups of closely related kimberlites however define parallel arrays on logarithmic plots (Figure 7.10.) demonstrating that within each group Nb and Ta behave as incompatible elements. The differing Nb/Ta ratios of the Kimberley group (11.4–15.7), Bellsbank (14.2–28.0), and the Premier (samples not enriched in Ta) (8.3–11.0) kimberlites may reflect differing sources or the effects of ilmenite fractionation. This latter process can lead to increased Nb/Ta ratios, as Ta is preferentially incorporated into ilmenite relative to Nb (Mitchell *et al.* 1973).

The mean Nb/Ta ratio (20.4) of Yakutian kimberlites (Kamenskii *et al.* 1977) is similar to that of the Bellsbank kimberlites (av. Nb/Ta = 20.5) although the greater range of Nb/Ta ratios (12.8–50.4) can be attributed to errors associated

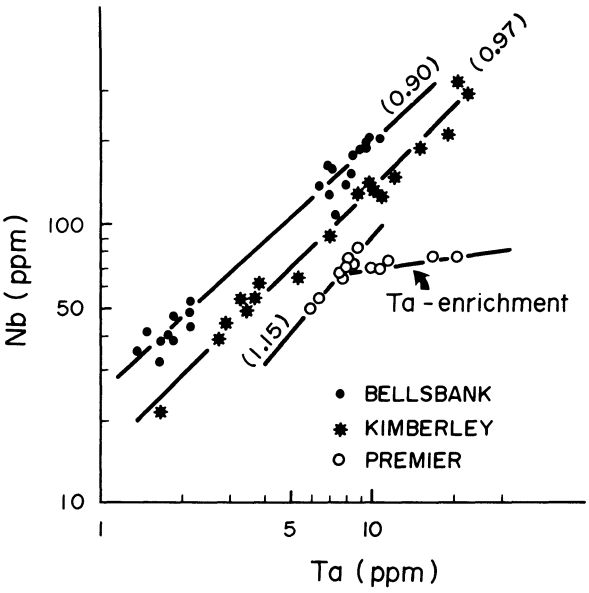

Figure 7.10. Zr versus Hf content of kimberlites from South Africa (Kable *et al.* 1975).

with the determination of Ta by spectrometric methods. Kamenskii *et al.* (1977) consider that Nb/Ta and Zr/Hf ratios of kimberlites decrease from the center to the margins of the Siberian platform. Insufficient data for individual groups of kimberlites are presented to substantiate this claim.

7.3.3.4. Uranium and Thorium

Uranium (mean 3.1, range 0.5–22.9 ppm) and thorium (mean 17, range 2.8–920 ppm) are hosted primarily by perovskite (Figure 7.11) and apatite. Perovskites may contain up to 150 ppm U (Kresten 1974). Apatites are estimated by Kresten (1974) to contain at least 300 ppm U. No data for Th are available, but Fesq *et al.* (1975) report very high Th contents (630–920 ppm) in apatite-rich dikes from Bellsbank. Significant amounts of U (8–40 ppm) occur in zircon and baddeleyite (Davis 1977, Davis *et al.* 1980, Kresten 1974), but these minerals are insufficiently abundant to control whole-rock abundances. Kresten (1974) determined that late-stage apatite is the major host for U in Lesothan micaceous kimberlites and that in other types perovskite is the principal host. Bookins *et al.* (1979) proposed that Kresten's (1974) suggestion, regarding the positive correlation between perovskite content and U abundance, was valid only for kimberlites containing little or no calcite. This assertion was not supported by analyses of kimberlitic carbonates or by discussion of the role of apatite. Com-

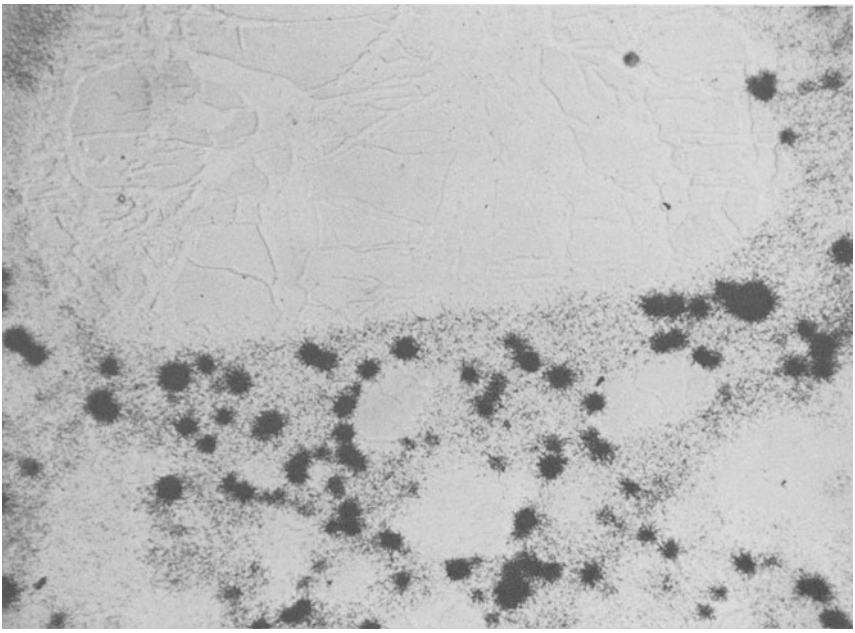

Figure 7.11. Distribution of uranium in the Jos kimberlite as revealed by induced fission tracks. The track density, recorded here in an etched Lexan external track detector, is proportional to the uranium content of the phases present. Dense stellate clusters of tracks correspond to U-rich perovskite, and track-free areas to macrocrystal and groundmass olivines. Note that U is distributed uniformly within the serpentine-calcite groundmass. (Field of view 10 mm.)

parisons with carbonatites in which U may occur in rare earth carbonates is unwarranted.

Individual kimberlites, for the most part, exhibit a wide range in their U and Th contents, e.g., De Beers (Th = 8–22 ppm, U = 1.8–5.0 ppm; Gurney and Hobbs 1973), Bellsbank group (Th = 13.9–920 ppm, U = 5–22.9 ppm; Fesq *et al.* 1975). Kimberlites from India (Gangadharam and Aswathanarayana 1969, Paul *et al.* 1977), and Lesotho (Kresten 1974) have low and restricted ranges in their U content (0.6–3.8 ppm), coupled, in the case of the Indian examples, with a wide range in Th content (17–60 ppm). Generally micaceous kimberlites have higher U (2.5–23 ppm) and Th (14–60 ppm) contents than other varieties (U = 0.7–5.0 ppm, Th = 7–24 ppm).

Akimov and Semenov (1970), Lutts and Mineyeva (1973) and Marshintsev and Lapin (1976) consider that the diamondiferous kimberlites from the center of the Siberian platform have lower U (1.2 ppm) and Th (6.7 ppm) contents than barren marginal kimberlites (U = 2.5 ppm, Th = 17.5 ppm). The conclusion is not supported by data for South African kimberlites.

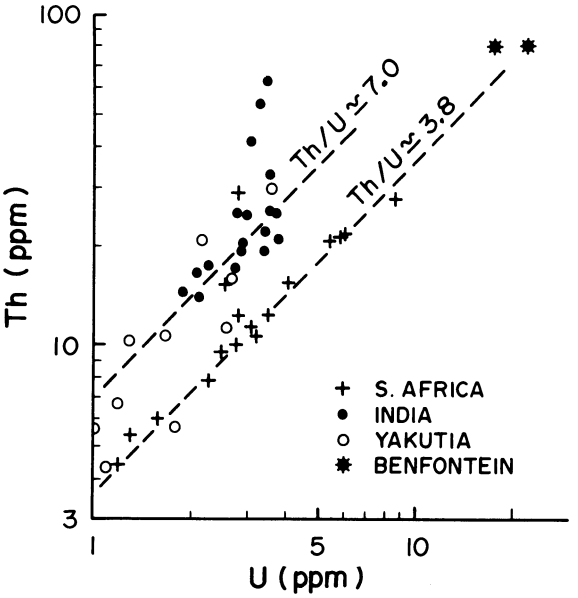

Figure 7.12. Th versus U content of kimberlites from India (Paul *et al.* 1977), Yakutia (Akimov and Seminov 1970), South Africa (Fesq *et al.* 1975) and the Benfontein sill, South Africa (Dawson and Hawthorne 1973).

Figure 7.12 demonstrates that Th and U are highly incompatible elements. Kimberlites from southern Africa may thus be derived from sources with relatively low Th/U ratios (≈3.8). Indian and Siberian kimberlites have widely variable Th/U ratios but define a trend with a Th/U ratio of about 7. The high Th/U ratios (>8) found in Indian kimberlites may be due to the removal of U as the highly soluble uranyl (U^{6+}) ion during weathering (Fesq *et al.* 1975). In this case the low U contents represent a base level of insoluble U. Paul *et al.* (1977), however, believe that the concentration level of U, but not Th, in the magma has been buffered at 2–3 ppm U by the fractionation of apatite. Gurney and Hobbs (1973) have concluded that the Th/U ratios of micaceous kimberlites (5.7–11) are greater than those of other types (Th/U = 3.5–6.6). Samples which may have been subjected to weathering do not appear to have lost U and thus have Th/U ratios similar to those of fresh samples. Lutts and Mineyeva (1973), using a very limited data base, consider that the Th/U ratio of barren kimberlite (7.0) is greater than that of diamondiferous kimberlite (Th/U = 5.6).

Gurney and Hobbs (1973), Komarov and Ilupin (1975), and Ilupin and Komarov (1979) have noted a general, but poorly correlated, increase in K/U ratios with K and Ca content, and no correlation with MgO content. Akimov and Semenov (1970) have proposed that the K/U ratio of diamondiferous kimberlite (0.08×10^4) is less than that of barren kimberlite (0.26×10^4).

7.3.3.5. Other Inter-element Relationships

Figure 7.13 demonstrates that Sm and Th behave as a pair of incompatible elements. In the Kimberley group samples both elements appear to be incompatible with bulk distribution coefficients of zero. In the Bellsbank group the slope of the data array indicates that Sm is not completely incompatible and has a bulk distribution coefficient of about 0.3. Th however appears to be highly incompatible. The differences between the behavior of Sm in the two groups may be due to the presence of abundant apatite in the Bellsbank suite.

Kable *et al.* (1975) and Kaminskii *et al.* (1977) have noted the high degree of coherence between Zr and Nb and that Zr/Nb ratios are typically less than 3, and thus much less than those of most basaltic rocks.

Fesq *et al.* (1975) and Kable *et al.* (1975) have found strong positive correlations between the light REE, Sr, Th, U, and P in some South African kimberlites (Figure 7.14). A weak positive correlation betwen U and P was noted by Ilupin and Komarov (1979) in Yakutian kimberlites. In addition, Kable *et al.* (1975) have shown that individual kimberlites appear to have distinct Nb/P ratios. The data plot as parallel linear arrays on logarithmic plots (Figure 7.14) implying possible derivation from sources of different Nb/P ratios. These correlations imply that two distinct hosts for the incompatible elements must exist

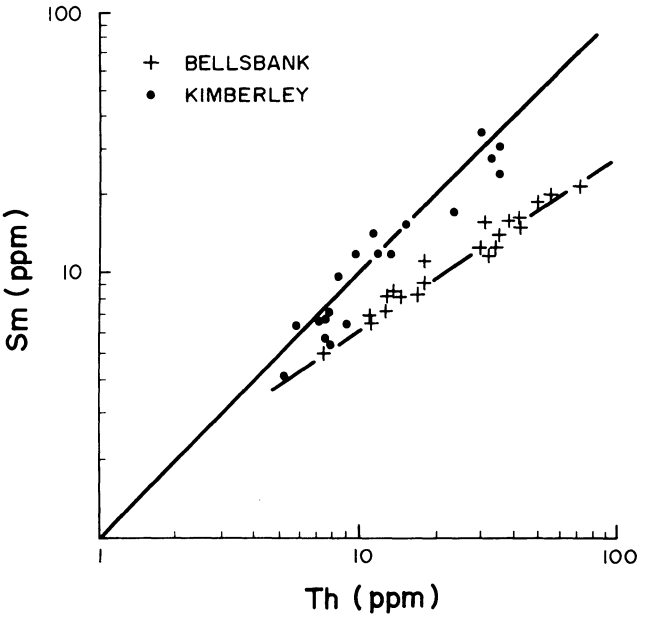

Figure 7.13. Sm versus Th content of kimberlites from Bellsbank (Fesq *et al.* 1975), and the Kimberley area (Mitchell and Clement, unpublished data.)

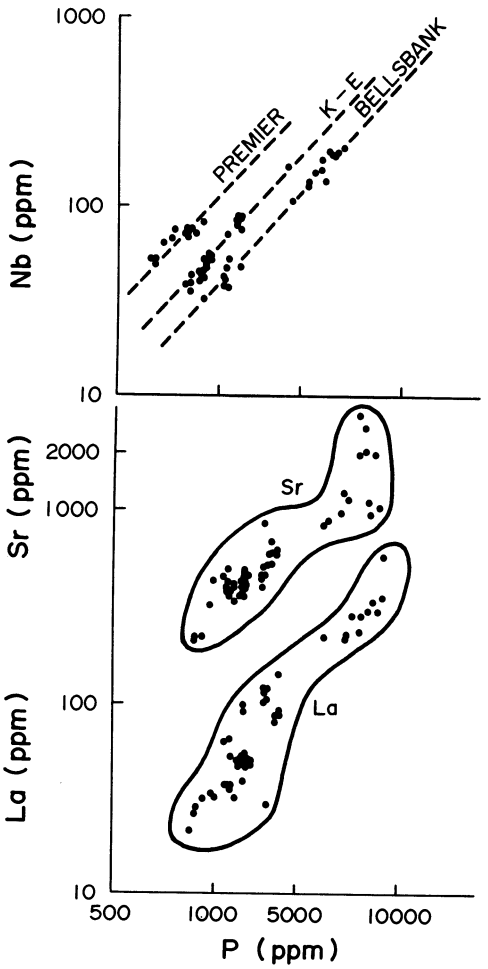

Figure 7.14. La, Sr, or Nb versus P content of kimberlites from South Africa (Fesq *et al.* 1975, Kable *et al.* 1975). K-E, Koffiefontein-Ebenhaezer.

in the upper mantle. One must be a phosphate, e.g., apatite, capable of hosting REE, Sr, Th, U, and the other must be a titanate which incorporates Nb, Ta, Zr, and Hf. Possible candidates for the latter are ilmenite (Kable *et al.* 1975) or LIMA-type phases (Haggerty 1983).

7.3.4. Incompatible Trace Elements: II. Rare Earth Elements

Rare earth element (REE) abundances have been determined in kimberlites from Africa (Haskin *et al.* 1966, Frey *et al.* 1971, 1977, Philpotts *et al.* 1972,

Table 7.6. Representative Rare Earth Element Contents of Kimberlites

	La	Ce	Nd	Sm	Eu	Gd	Tb	Yb	Lu	La/Yb	Ref.[a]
Kimberlites											
Mir	21.5	43.4	10.7	2.2	0.4	2.6	—	0.1	0.03	215	1
Wesselton	106	239	—	13.7	3.28	—	1.21	1.09	0.13	97	2
Ison Creek	114	226	—	10.3	2.69	—	0.66	0.68	0.08	168	2
Wajrakarur	117	249	95	16.6	4.4	7.8	1.79	1.38	0.15	85	3
Kundulungu	133	241	79	9.1	2.33	—	0.61	0.49	—		4
Tayezhnaya	182	356	161	28.5	11.2	28.6	2.6	0.9	0.26	202	1
Bala	301	529	—	18.5	5.2	—	1.19	1.38	0.30		5
Micaceous kimberlites											
Pyramidefjeld	63	149	72	14.4	3.0	5.7	0.8	0.68	—	188	6
Majhgawan	156	372	159	22.5	5.0	8.0	1.32	0.98	0.11	159	3
Swartruggens	238	378	—	22.9	4.10	—	1.8	1.24	0.17	192	2
Bellsbank	1120	2080	780	185	6.44	—	18.8	4.4	0.52		7

[a] References: 1, Kaminskii *et al.* 1978; 2, Mitchell and Brunfelt 1975; 3, Paul *et al.* 1975; 4, Fieremans *et al.* 1984; 5, Cullers *et al.* 1982; 6, Paul and Potts 1976; 7, Fesq *et al.* 1975.

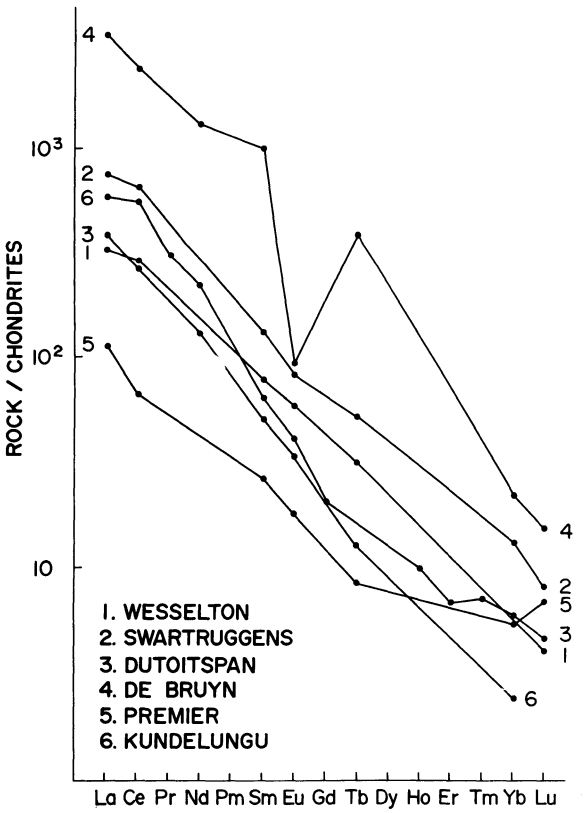

Figure 7.15. Rare earth element distribution patterns for kimberlites from South Africa and Zaire. Data sources: 1,2, Mitchell and Brunfelt (1975), 3, Haskin *et al.* (1966); 4,5 Fesq *et al.* (1975); 6, Fieremans *et al.* (1984).

Mitchell and Brunfelt 1975, Fesq *et al.* 1975, Nixon *et al.* 1981, Fieremans *et al.* 1984), Siberia (Burkov and Podporina 1966, Kaminskii *et al.* 1978), North America (Michell and Brunfelt 1975, Cullers *et al.* 1982) Greenland (Paul and Potts 1976), and India (Paul *et al.* 1975).

Although these data serve to illustrate the basic features of the REE geochemistry it should again be emphasized that systematic studies of REE abundances within a given intrusion, or between kimberlites within a province, have not yet been undertaken.

Representative REE contents and chondrite normalized distribution patterns are given in Table 7.6 and Figures 7.15–7.17, respectively.

Individual kimberlites exhibit wide variations in their total REE contents ranging from approx. 100 (Mir) to approx. 4000 (De Bruyn) ppm (Table 7.6). In general, micaceous kimberlites, and the hypabyssal facies of other varieties, contain significantly greater REE abundances than diatreme facies kimberlites. Nixon *et al.* (1981) consider that the enrichment of REE in the dikes is due to closed-system crystallization preventing loss of REE along with volatiles. However, the lower abundances in the diatremes may be a simple dilution effect caused by the presence of large volumes of REE-poor materials. Nixon *et al.*

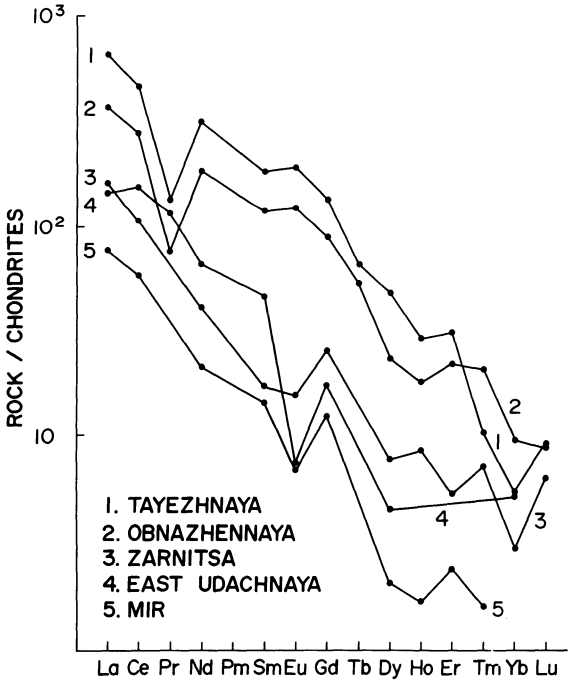

Figure 7.16. Rare earth element distribution patterns for kimberlites from Yakutia. Data sources: 1–3, Kaminski *et al.* (1978); 4,5, Burkov and Podporina (1966).

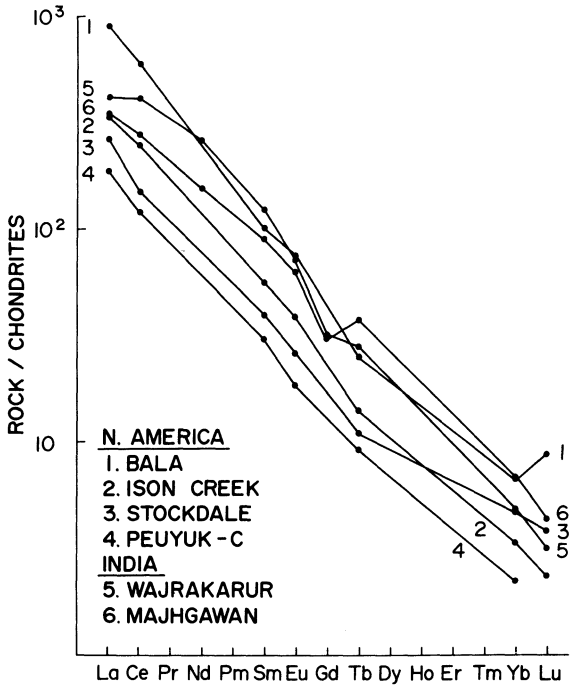

Figure 7.17. Rare earth element distribution patterns for kimberlites from North America and India. Data sources: 1,3, Cullers *et al.* (1982); 2,4, Mitchell and Brunfelt (1975), 5,6 Paul *et al.* (1975).

(1981) also claim that on-craton kimberlites contain more REE, Rb, Ba, and Sr than marginal kimberlites. Insufficient data are presented to substantiate this hypothesis which is contradicted by their own data for a Mothae dike.

Although the absolute REE abundances are variable, Figures 7.15–7.17 indicate that most kimberlites are characterized by simple linear REE distribution patterns showing extreme light REE enrichment. La and Yb are enriched 100–1000 and 2–10 times chondritic abundances, respectively. La/Yb ratios range from 50 to 500, with the majority ranging from 80 to 200; thus being significantly higher than the La/Yb ratios (<60) of most other mantle-derived mafic magmas. The average La/Yb ratios of micaceous kimberlites (e.g., Swartruggens = 139, Bellsbank = 172) are in general higher than those of other varieties (e.g., Wesselton = 103, Koffiefontein = 54) Kaminskii *et al.* (1978) consider that the average La/Yb ratios of Siberian and American kimberlites (164–198) are greater than those of African and Indian kimberlites (95–102) and that two groups of kimberlites, the Gondwana and Laurasia groups, can be distinguished on the basis of their total REE content and light REE enrichment. These conclusions are based upon average La/Yb ratios and are doubtful in view of the limited data

base; bias, in the case of the Siberian kimberlites, toward diatreme facies rocks; and by the fact that kimberlites with extremely high and low La/Yb ratios occur in each province.

Figures 7.15 and 7.16 demonstrate some problems in the interpretation of kimberlite REE distribution patterns. Data presented in Figure 7.15 obtained by neutron activation analysis produce smooth REE distribution patterns which are modified, in the case of the Swartruggens and Bellsbank kimberlites, by the presence of slight-to-significant negative Eu anomalies. These anomalies appear to be real and not an artifact of the analytical method as they are not found in all samples analyzed by this method.

In contrast, the distribution patterns depicted in Figure 7.16, obtained by X-ray spectrometric techniques, are not smooth curves. The data for the heavy REE show considerable scatter, and significant negative Eu and Pr anomalies are evident in the bulk of the data given by Burkov and Podporina (1966) and Kaminskii *et al.* (1978), respectively. Neumann *et al.* (1966) and Mitchell and Bell (1976) have discussed the accuracy of Soviet X-ray spectrometric data and concluded that the method is particularly insensitive for Eu and is very poor for all the heavy REE and that significant errors may also be introduced during the hydroxide-oxalate precipitation pre-concentration step in the procedure. Consequently the large scatter in heavy REE distributions and the Pr and Eu anomalies can be considered as being mainly due to analytical error. Further it is impossible to determine whether or not real Eu anomalies occur in Siberian kimberlites. In conclusion, it would appear that some kimberlites do exhibit negative Eu anomalies. These anomalies should not, however, be considered characteristic of kimberlites as proposed by Loubet *et al.* (1972).

Modification of the linear REE distribution patterns is also seen in kimberlites that have been contaminated by crustal xenoliths, e.g., the tuffisitic kimberlite breccias at Premier (Figure 7.15) and Bala (Figure 7.17). Contamination results in a significant increase in the abundance of the heavy REE, resulting in a decrease in the slope of the distribution pattern from Tb to Lu. La/Yb ratios in such rocks are less than those of the original uncontaminated magmas.

Boctor and Boyd (1982), Jones and Wyllie (1984), and Ilupin *et al.* (1971) have shown that the principal carrier of REE in kimberlites is perovskite and that apatite, while containing significant amounts of REE, is of subordinate importance. Other phases (e.g., olivine, spinel, serpentine) do not have significant REE contents and most whole-rock abundances and distribution patterns must be controlled primarily by perovskite, which is usually more abundant than apatite. Systematic studies of REE contents with respect to the perovskite/apatite ratio have not yet been undertaken. REE abundances should be directly proportional to the REE content and modal amount of perovskite. The extremely high REE abundances found in the Bellsbank kimberlites (Fesq *et al.* 1975) may be correlated with the presence of apatites or perovskites that are unusually rich

in REE (Boctor and Boyd 1982). Jones and Wyllie (1984) have shown that the distribution pattern of perovskite from the Wesselton kimberlite is similar to that of the whole-rock, although a significant positive Ce anomaly occurs in the former. The similarity of the REE distribution patterns for diverse kimberlites shown in Figures 7.15–7.17 is evidence in favor of control of the whole-rock pattern by this one phase. Kaminskii *et al.* (1978), however, believe that perovskite is not the only major carrier of REE and that the balance is due to the presence of a REE-rich phlogopite. Such a conclusion is however untenable on crystallochemical grounds and the well-known low REE contents of mica (Haskin *et al.* 1966).

The Eu anomaly observed in some kimberlites has not yet been satisfactorily explained. Mitchell and Brunfelt (1975) proposed that the anomaly was due to the presence of a Eu-deficient perovskite, a conclusion based upon the recognition of such perovskites in the Oka carbonatite (Eby 1975). Such anomalies have not been detected by reliable analytical methods in kimberlite perovskites (Jones and Wyllie 1984) and the hypothesis must be regarded as unsubstantiated. Fesq *et al.* (1975) showed that Bultfontein phlogopite exhibited a negative Eu anomaly and proposed that the presence of similar phlogopite explains the Eu anomalies seen in some micaceous kimberlites. The hypothesis was not verified by analysis of mica from such rocks. Fesq *et al.* (1975) and Reitan (1974) proposed that low oxygen fugacities may result in the formation of Eu^{2+} and subsequent preferential exclusion of this ion from lattice sites relative to $(REE)^{3+}$. Following Reitan's (1974) arguments it is possible that the crystallization of large amounts of megacryst pyroxene under reducing conditions could lead to Eu-depleted residual magmas.

Frey *et al.* (1977) and Mitchell (1984a) have noted that late-stage carbonate-rich residua are relatively poor in REE. This is a consequence of depletion of the magma in REE by the earlier crystallization of perovskite. In this context it is important to realize that REE appear to be removed from the magma only during the later stages of the crystallization of the groundmass by perovskite and apatite formation. These minerals are, in most cases, retained *in situ* until final consolidation. Whole-rock distribution patterns and La/Yb ratios of such samples will therefore reflect those of the parent magma.

Highly fractionated light REE-enriched distribution patterns are not unique to kimberlites. Figure 7.18 shows that similar distribution patterns occur in lamproites and highly undersaturated potassic lavas. The similarity of the REE distributions may imply that the REE, if representative of the initial magmas, are derived from similar sources in the upper mantle. The clearly differing mineralogy and evolution of these diverse magma types, however, require that the major element composition of the source rocks be very different. Addition of a common "metasomatic" component to a variety of mantle source rocks may be the origin of the similar incompatible element content.

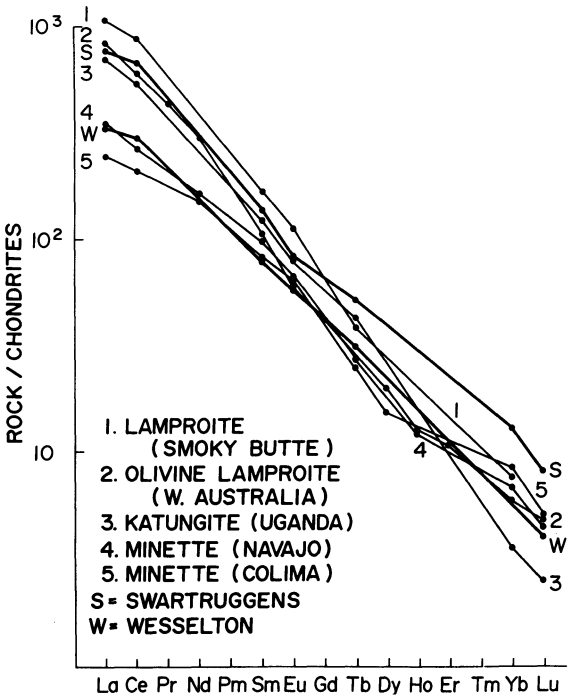

Figure 7.18. Rare earth element distribution patterns for kimberlites compared with those of other alkaline rocks that are enriched in light REE. Data sources: 1, Mitchell (unpublished data); 2, Nixon *et al.* 1984); 3, Mitchell and Bell (1976); 4, Roden (1981); 5, Luhr and and Carmichael (1981). Average kimberlites from Swartruggens (s) and Wesselton (w) from Mitchell and Brunfelt (1975).

Melilitites, alnöites and minettes are in general not as enriched in light REE as kimberlites (Figure 7.18), implying derivation from different sources, if their REE distribution patterns have not been modified by other processes.

7.3.4.1. Rare Earth Elements and Partial Melting Models

Models of partial melting of the type described by Shaw (1970) are useful in placing constraints upon the nature of the source regions of kimberlites, *assuming* that the REE distribution patterns have not been substantially modified by fractional crystallization. Mitchell and Brunfelt (1975), Paul *et al.* (1977) and Cullers *et al.* (1982) have shown that melts with high La/Yb ratios (100–200) can be produced by small (0.1%–0.9%) amounts of partial melting of a phlogopite-garnet lherzolite source. Such melts are however insufficiently enriched in REE to account for the observed REE contents of kimberlites, if the source is considered to have either chondritic REE abundances (Figure 7.19) or to be

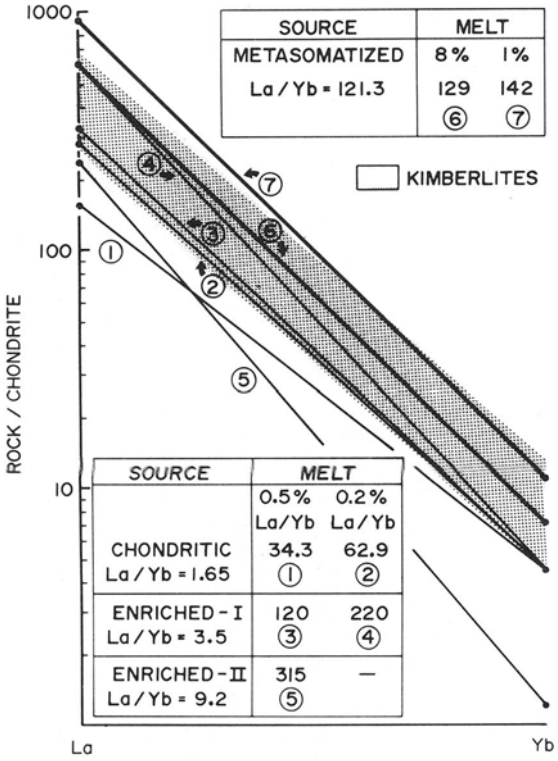

Figure 7.19. Rare earth element distribution patterns for melts derived from diverse lherzolitic sources (see text). Cryptically enriched (Dawson 1984) sources from Mitchell and Carswell (1976). Patently enriched (Dawson 1984) or metasomatized source (this work). Distribution coefficients from Frey *et al.* (1978) and Kyle (1981) were used in Shaw's (1970) partial melting model.

slightly enriched in light REE. The latter source corresponds to Dawson's (1984) cryptically metasomatized mantle, and Figure 7.19 shows that 0.5% melting of such a source (La/Yb = 3.5, Mitchell and Carswell 1976) will only produce melts with REE abundances (La = 107.8, Yb = 0.898, La/Yb = 120) at the lower limit of the spectrum of kimberlite REE abundances. The even smaller degrees (0.2%) of partial melting (Figure 7.19) that are required to explain the REE contents of highly enriched kimberlites such as Bellsbank or Swartruggens are also inappropriate in that it is unlikely that such small volumes of melt would ever escape from their source regions.

Accumulated mineralogical (Dawson 1984) and geochemical evidence (Menzies and Wass 1983, Vollmer and Norry 1983) indicates that the source regions of most alkaline rocks may be some variety of metasomatized mantle. The application of partial melting models to such sources is rendered difficult

by the wide variations that are possible in the modal mineralogy of the metasomatites and by inadequate knowledge of the solid/liquid distribution coefficients of the phases involved in the melting. Nevertheless, some discussion of partial melting of metasomatized mantle is instructive in that Figure 7.19 shows that 1%–8% partial melting of a source containing apatite (2.5%), potassian titanian richterite (2.5%), clinopyroxene (5.0%), garnet (10%), orthopyroxene (20%), and olivine (60%) can account for the observed REE contents and La/Yb ratios of many kimberlites. The mantle mineralogy chosen is reasonable in view of the common occurrence of metasomatically introduced titanates and potassic richterites in garnet lherzolite xenoliths, and by the requirement that kimberlites contain apatite and titanates in their sources (Section 6.3.3.5). A barren garnet harzburgite residua could be produced by 10% melting of this source.

For metasomatized sources the La and Yb enrichments of the melts are relatively insensitive to the degree of partial melting and their La/Yb ratios essentially reflect those of the source. Thus, high La/Yb ratios in this model are not the result of element fractionation during partial melting, but are controlled by the presence of apatites of high La/Yb ratio.

Production of kimberlites from a metasomatized mantle has the further advantage that the relatively large volumes of melt can segregate from the source and escape from the mantle.

The hypothesis is unfortunately unsatisfactory, in that the metasomatized mantle mineralogy can be preset to produce any desired REE distribution pattern.

7.3.5. Incompatible Trace Elements: III. Alkali and Volatile Elements

7.3.5.1. Lithium

Lithium abundances (mean 29 ppm, range 2–207 ppm) are inadequately known and apparently vary widely between individual kimberlites (Muramatsu 1983, Ilupin *et al.* 1974, Borodin 1976). The major host for Li is phlogopite (see Section 6.6.4.), although positive correlations between Li, Ca, and P indicate that apatite may contain some Li (Lebedev-Zinovyev and Ilupin 1976). Systematic studies of Li distribution within and between kimberlites have not been undertaken apart from the work of Lebedev-Zinovyev and Ilupin (1976). They have noted that kimberlites from the center of the Daldyn field contain higher Li (20–80 ppm) than those of the margins (10–40 ppm). This zonation is considered to be a result of late stage autometasomatism. Two groups of kimberlites are present in the Alakit field with a northern group having lower Li contents (12 ppm) than others in the field (42 ppm). In the Lena region an eastern group of kimberlites contains less than 27 ppm Li, while a western group contains 34–93 ppm Li. Discrete sources of kimberlite magmatism are postulated to account for these groups within each field rather than differentiation of a single magma.

7.3.5.2. Rubidium

Rubidium abundances (mean 73 ppm, range 4–267 ppm) are in general correlated with the abundance of phlogopite which acts as the host for Rb (see Section 6.6.4.). The lowest Rb contents are thus found in calcite-rich residua such as the Benfontein sills (<10 ppm, Dawson and Hawthorne 1973) and the highest in micaceous kimberlites such as Swartruggens (63–265 ppm, Mitchell and Crocket 1971a). Weathering of kimberlites results in loss of Rb (Mitchell and Crocket 1971a, Barrett and Berg 1975).

Studies of several South African kimberlites by Gurney and Berg (1969) have demonstrated wide variations in the Rb contents of individual kimberlites, e.g., Bultfontein (77–111 ppm), Wesselton (88–107 ppm) De Beers (26–91 ppm), Roberts Victor (73–136 ppm), Jagersfontein (51–107 ppm). Ilupin *et al.* (1974) have suggested that the Rb content of diamondiferous kimberlites (mean 23 ppm) from Yakutia is less than that of barren kimberlites (mean 64 ppm). Such a generalization is clearly not applicable to the southern African kimberlites studied by Gurney and Berg (1969) Mitchell and Crocket (1971a), and Nixon *et al.* (1981).

The K/Rb ratios of most kimberlites (Figure 7.20) range from 93–271 (Gurney and Berg 1969, Fesq *et al.* 1975, Scott 1979, Nixon *et al.* 1981, Kramers, 1977) with no significant differences being observed within and between kimberlites. Micaceous kimberlites do not possess different K/Rb ratios from mica-poor varieties (Gurney and Berg, 1969). The K/Rb ratios are similar

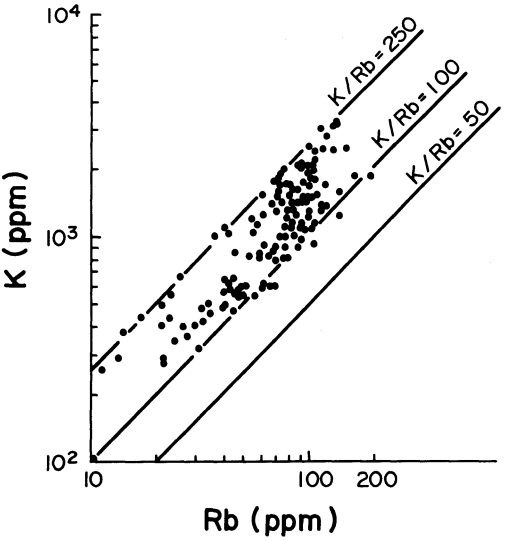

Figure 7.20. K versus Rb content of kimberlites. See text for data sources.

to those of many mantle-derived basic undersaturated magmas and are in general less than the crustal average of 250. Figure 7.20 demonstrates the high degree of correlation between K and Rb abundances and that they act as incompatible elements. The K/Rb ratios of unaltered kimberlites may thus reflect those of their source regions.

In contrast to the above observations Lebedev-Zinovyev and Ilupin (1976) have noted that kimberlites from the center of the Daldyn field have higher K/Rb ratios (170–530) than those of the margins (55–200). Kimberlites in the Alakit field fall into two groups within a northern group, having lower K/Rb ratios (60–100) than the other intrusions (K/Rb = 90–230). In the Lena field, eastern and western kimberlites have K/Rb ratios of 280–580 and 80–180, respectively. The zoning of the Daldyn field is believed to be due to magmatic differentiation of a single parent magma, the central kimberlites with the highest K/Rb ratios being less evolved and emplaced earlier than the peripheral kimberlites. Distinct magmatic sources are postulated to account for the groupings within the Alakit and Lena fields. The possibility that the high K/Rb ratios of some of the Yakutian kimberlites could be a consequence of weathering is not discussed by Lebedev-Zinovyev and Ilupin (1976).

7.3.5.3. Cesium

Cesium abundances are inadequately known as there are serious discrepancies between the data obtained by emission spectrography, flame photometry, or neutron activation analysis. The analytical problems noted by Gurney and Berg (1969) have undoubtedly resulted in the over-estimation of Cs abundances in the Bultfontein (7–76 ppm), Wesselton (17–46 ppm), and De Beers kimberlites (10–76 ppm), consequently the data for Roberts Victor (5–8 ppm), Jagersfontein (5–21 ppm), and Dutoitspan (2–6 ppm) must also be considered suspect. Neutron activation (Fesq *et al.* 1975) and flame photometric (Burkov and Podporina 1965) data indicate much lower Cs contents (mean 2.2, range 0.4–4.5 ppm). K/Cs ratios are apparently low (1000–5800). Interpretation of the Cs data is rendered difficult by the extreme mobility of the element. Cs may be lost during emplacement or by leaching during weathering or alteration (Fesq *et al.* 1975). Gurney and Berg (1969) have postulated that Cs contents may be enhanced in zeolite-rich kimberlites by late hydrothermal activity or groundwater leaching.

7.3.5.4. Volatile Elements

Insufficient data are available for volatile elements to allow the formation of any but the broadest generalizations regarding their abundance and distribution.

Boron abundances are inadequately known. Markedly different ranges in B content, 300–3000 ppm and 5–52 ppm, have been reported by Malinko *et al.*

(1982) and Higgins (1984). Burkov and Podporina (1965) and Cherepanov (1967) quote average abundances of 149 and 190 ppm, respectively. Ilupin *et al.* (1974) consider that the average B contents of diamondiferous (58 ppm) and barren kimberlites (46 ppm) differ. Cherepanov (1967) has stated that micaceous kimberlites are poorer in B than mica-poor types and that hypabyssal kimberlites are richer in B than diatreme facies rocks. Malinko *et al.* (1982) have shown that the bulk of the B is associated with serpentines replacing olivines. High levels of B in Yakutian kimberlites in some cases can be correlated with the presence of datolite and danburite of undoubtedly secondary origin. Assimilation of evaporitic horizons during emplacement (Bobrievich *et al.* 1964) may be the origin of such high B contents. Cherepanov (1967) and Higgins (1984) consider that B is enriched in kimberlites relative to other igneous rocks. Cherepanov (1967) believes that the B is juvenile, while Higgins (1984) suggests that it is recycled subducted material.

Wide variations in the F (mean 2774, range 210–7490 ppm) and Cl (mean 202, range 9–740 ppm) contents exist within and between kimberlites (Muramatsu 1983, Paul *et al.* 1976). The latter authors reported a significant correlation between P_2O_5 and F content and suggested that apatite and mica were the hosts for F and Cl, respectively. This conclusion was not supported by Muramatsu (1983), who found no correlation between P_2O_5 and F. The correlation may have no significance in that P_2O_5-rich kimberlites are commonly rich in phlogopite, which Paul *et al.* (1976) have determined to be rich in F (0.44%–1.24%). Regional and local differences in the F and Cl contents of kimberlites are considered by Paul *et al.* (1976) to reflect magmatic differentiation and/or mantle heterogeneity.

Sulfur and selenium abundances are inadequately known and both elements exhibit wide inter-kimberlite variations. Principal hosts for S and Se are undoubtedly sulfides and the high S contents of some kimberlites may be attributed to assimilation of pyrite-rich shales (Dawson 1980). Sulfur abundances (mean 1687, range 280–1959 ppm) have been determined by Muramatsu (1983) and Ilupin *et al.* (1974). Sobolev *et al.* (1975) have reported Se abundances (mean 0.15, range 0.04–0.60 ppm) for Yakutian kimberlites and suggested that diamondiferous (0.13 ppm) and barren (0.24 ppm) kimberlites differ in their Se content.

Lead abundances (mean 15.3, range 2–41 ppm) vary widely within and between kimberlites (Smith 1983, Kramers 1977, Marshintsev and Lapin 1976, Ilupin *et al.* 1974). Data presented by Smith (1983) demonstrate that micaceous kimberlites (mean 29 ppm) contain more lead than mica-poor types (mean 8.3 ppm). Lead may be hosted by sulfides or mica.

Muramatsu (1983) has presented data for Cd (mean 0.073, range 0.040–0.115 ppm), Hg (mean 0.008, range 0.0060–0.012 ppm), Tl (mean 0.219, range 0.087–0.650 ppm), and Bi (mean 0.024, range 0.010–0.038 ppm). The data for Bi are in reasonable agreement with those of Dunin-Barkovskaya and Ukhanov

(1974), who report 0.011–0.083 ppm Bi in Yakutian kimberlites. The latter authors consider that Bi is enriched by volatile transfer in diatreme facies kimberlites relative to hypabyssal types. Muramatsu's (1983) data for Hg is in agreement with that (0.007–0.025 ppm) of Ozerova *et al.* (1976) but not that (0.2 ppm) of Ehmann and Lovering (1967).

7.3.6. Other Elements

The abundance and distribution of Be, Ga, Ge, Sn, Mo (Table 7.5) is inadequately known. Gallium abundances are not sufficiently well established to assert that Ga/Al ratios are typical of late differentiates. Data are not available for In, W, As, Sb, Te, Br, and I.

7.4. AVERAGE ABUNDANCES OF TRACE ELEMENTS

The average trace element contents of kimberlites have been summarized by Wedepohl and Muramatsu (1979) and Muramatsu (1983). The averages presented in Table 7.7 are based upon Muramatsu's (1983) compilation together with new weighted mean averages for the compatible and incompatible elements discussed above. The data must be regarded with caution, bearing in mind the difficulty of obtaining geochemically significant averages for such heterogeneous rocks. Further, the averages for some elements (e.g., B, Ru, Rh, Ag, Pt, Ga) are based upon data obtained by unreliable analytical techniques. Despite these

Table 7.7. Average Trace Element Abundances in Kimberlites (ppm)[a]

Li	29	Ge	0.5*	Sb	—	Yb	(1.2)
Be	1.6*	As	—	Te	—	Lu	(0.16)
B	(36)*	Se	0.15*	I	—	Hf	5.6
F	2774	Br	—	Cs	2.2*	Ta	11
P	(3880)	Rb	73	Ba	1100	W	—
S	1687	Sr	851	La	(150)	Re	0.069*
Cl	202	Y	(22)	Ce	(200)	Os	1.34*
Sc	14	Zr	184	Pr	(22)	Ir	0.003*
Ti	(11800)	Nb	141	Nd	(85)	Pt	(0.19)*
V	100	Mo	1.7*	Sm	(13)	Au	0.012*
Cr	893	Ru	0.065*	Eu	(3.0)	Hg	(0.008)*
Mn	(1160)	Rh	0.0071	Gd	(8.0)	Tl	(0.219)*
Co	65	Pd	0.0081*	Tb	(1.0)	Pb	15.3
Ni	965	Ag	0.134*	Dy	—	Bi	(0.024)*
Cu	93	Cd	(0.073)	Ho	(0.55)	Th	17
Zn	69	In	—	Er	(1.45)	U	3.1
Ga	5.7*	Sn	5.4*	Tm	(0.23)		

[a] Values in parentheses from Muramatsu (1983). * = unreliable data or inadequate data base.

drawbacks, the averages are useful in demonstrating gross depletions or enrichments of trace elements with respect to other magma types or to the parental upper mantle.

Figure 7.21 shows that kimberlites are enriched in Sc, V, Cu, and Zn, and depleted in Cr, Co, and Ni with respect to a pyrolite mantle (Jagoutz *et al.* 1979). This compatible trace element distribution pattern is similar to that of other mantle-derived magmas with the exception that kimberlites are markedly depleted in V. The low Cr, Co, and Ni abundances in all magmas imply derivation of the magmas from a source that retains these elements during partial melting e.g., garnet lherzolite or harzburgite. The high Cr, Co, and Ni contents of kimberlites with respect to other magmas is due to the high content of macrocrystal olivine coupled with their relatively unevolved nature.

Figure 7.22 demonstrates that kimberlites are strikingly enriched in Cs, Rb, Ba, Th, U, Ta, Nb, La, Sr, and P relative to primitive upper mantle and to other mantle-derived magmas. Muramatsu (1983) has noted that incompatible element abundances increase in the sequence tholeiitic basalts, alkaline olivine basalts, nephelinites, and kimberlites. The incompatible element enrichment of kimberlites relative to other magma types could be the result of either smaller degrees of partial melting of similar source rocks or derivation from a different incompatible element-rich source. The latter possibility would seem the more likely in view of the constraints imposed upon the nature of the source by the REE geochemistry (see Section 7.3.4.1).

7.5. RADIOGENIC ISOTOPES

7.5.1. Strontium

Reconnaissance studies by Powell (1966), Bardet and Vachette (1966), Mitchell and Crocket (1971a), Bolivar and Brookins (1977), and Brookins *et al.* (1979), indicated that the initial $^{87}Sr/^{86}Sr$ ratios of kimberlites range from 0.706 to 0.716. Powell (1966) suggested that the high ratios might be due to the presence of micro-xenoliths of crustal materials. Brookins (1967) analyzed carbonates extracted from Kansas kimberlites and concluded that their high $^{87}Sr/^{86}Sr$ (0.705–0.707) ratios were due to contamination of "carbonatitic Sr" with Sr derived from the country-rock limestones and shales.

Mitchell and Crocket (1971a) and Barrett and Berg (1975) presented calculations which show that the bulk assimilation of typical basement or crustal materials is unlikely to account for the high $^{87}Sr/^{86}Sr$ ratios. Extremely large amounts of such low-Sr materials are required to change the isotopic composition of Sr-rich kimberlites. Barrett and Berg (1975) also demonstrated that the country rocks adjacent to the De Beers diatreme were not thermally affected by the

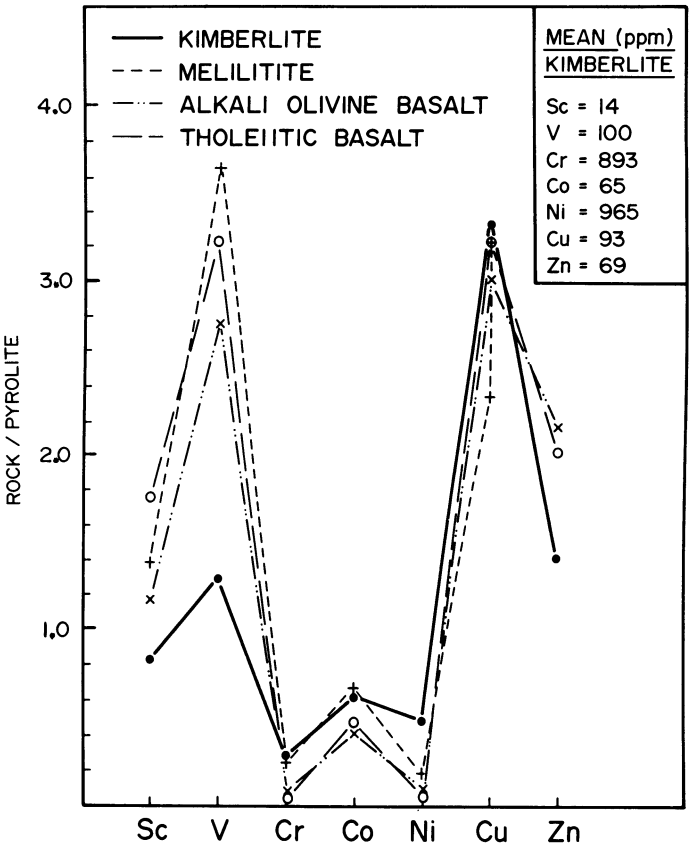

Figure 7.21. Mean contents of some compatible elements in kimberlites compared with those of melilitite and basalts. Kimberlite means are based upon the following: Burkov and Podporina (1965), Cullers *et al.* (1982), Dawson (1962), Dempster and Tucker (1973), Fieremans *et al.* (1984), Gangadharam and Aswatharanarayana (1969), Gurney and Ahrens (1973), Ivanov *et al.* (1977), Kable *et al.* (1975), Kresten (1973a), Lee and Lawrence (1968), Marshintsev and Lapin (1976), Marshintsev and Sukneva (1970), Mitchell and Brunfelt (1975), Muramatsu (1983), Nixon *et al.* (1981), Scott (1979), Steuber and Goles (1967), Tomanovskaya (1974), Young *et al.* (1954), Zhang and Liu (1983). Alkaline olivine basalt and tholeiitic basalt data are from Wedepohl and Muramatsu (1979). Melilitite data is for olivine melilitite from the Balcones province, Texas (Mitchell, unpublished data). Pyrolite abundances are from Jagoutz *et al.* (1979).

intrusion, and concluded that thermally induced migration of radiogenic ^{87}Sr was unlikely to have increased the $^{87}Sr/^{86}Sr$ ratios.

Berg and Allsopp (1972) and Barrett and Berg (1975), on the basis of the analysis of some exceptionally "fresh" hypabyssal kimberlites, concluded that all high initial ratios are due to alteration of the kimberlite subsequent to intrusion.

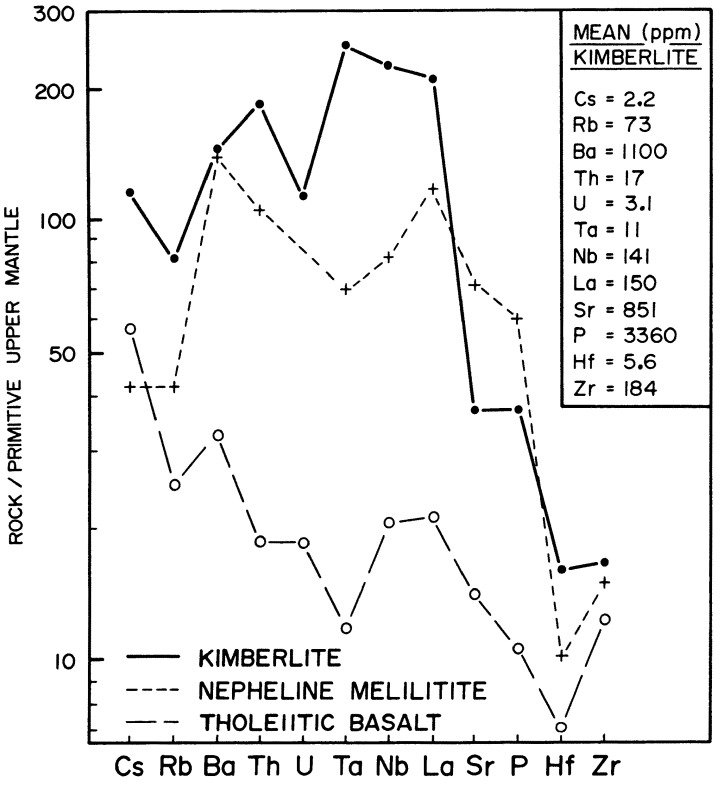

Figure 7.22. Mean contents of some incompatible elements in kimberlites compared with those of nepheline melilitite and tholeiitic basalts (Wedepohl and Muramatsu 1983). Data sources for kimberlites are given in the text. Primitive mantle composition from Wood (1979).

The initial ratios of fresh kimberlites were postulated to be ≈0.7040. The hypothesis was predicated upon the assumption that sources of high $^{87}Sr^{86}Sr$ do not exist in the mantle. Later studies have demonstrated that this assumption is incorrect (Smith 1983).

Criteria presented for judging the "freshness" of kimberlite included relative hardness, degree and appearance of serpentinization, apparent permeability and porosity, coloration, and general geology. Barrett and Berg (1975) outlined three specific petrographic criteria: (1) olivine morphology and alteration, (2) nature of the groundmass serpentinization, (3) uniformity of the groundmass texure.

These criteria are clearly subjective, although the presence of unserpentinized macrocrystal and groundmass olivines, especially of euhedral habit, is undoubtedly a useful guide to "freshness." Barrett and Berg (1975) regard the common pseudomorphing of groundmass olivines as a deuteric phenomenon. Uniform groundmass serpentinization and calcite/opaque oxide ratios are not

suitable criteria in view of the common occurrence of irregular serpentine and/or calcite segregations and/or pervasive prograde serpentinization.

Using Barrett and Berg's (1975) criteria, Paul (1979) found that Indian kimberlites classified as "fresh" had higher initial $^{87}Sr/^{86}Sr$ (0.7102–0.7142) ratios than those considered to be altered (0.7036–0.7073). Demaiffe and Fieremans (1981) also noted that highly "altered" kimberlites from Zaire had low $^{87}Sr/^{86}Sr$ (0.7040–0.7045) ratios.

Despite such contradictions, Barrett and Berg (1975), supported by Kramers *et al.* (1981) and Smith (1983), consider that all $^{87}Sr/^{86}Sr$ ratios falling between 0.705 and 0.707 are due to the introduction of crustally derived ^{87}Sr by percolating groundwater. Barrett and Berg (1975) did not discuss the possibility of ^{87}Sr introduction by groundwater in phreatomagmatic systems as discussed by Lorenz (1975) and supported by the O and H isotopic studies of Sheppard and Dawson (1975).

Recent studies of fresh kimberlites by Kramers (1977), Kramers *et al.* (1981), and especially Smith (1983) have demonstrated the existence of two isotopically distinct groups (see Section 7.5.2). Serpentine-calcite kimberlites (group I) and micaceous kimberlites (group II) have $^{87}Sr/^{86}Sr$ initial ratios of 0.7033–0.7049 and 0.7064–0.7109, respectively, indicating that the sources of group-II kimberlites are enriched in Rb relative to those of group I; Sr isotopic compositions are inversely correlated with Nd and Pb isotopic compositions (Smith 1983).

7.5.2. Neodymium

Because of the different analytical techniques utilized in different laboratories (O'Nions *et al.* 1979), initial Nd-isotopic ratios are commonly expressed as the deviation from the bulk-earth chondritic value of $^{143}Nd/^{144}Nd$ at the time of formation (T) of the sample by the relation

$$\varepsilon = \left[\frac{(^{143}Nd/^{144}) \text{ initial sample}}{(^{143}Nd/^{144}Nd)_{\text{CHUR}} \text{ at T}} - 1 \right] \times 10^4$$

where CHUR is the isotopic composition of a chondritic uniform reservoir that is used to represent the Sm/Nd ratio and isotopic composition of the bulk earth (DePaolo and Wasserburg 1976, O'Nions *et al.* 1979). Values of ε_{Nd} of zero or near zero in mantle-derived rocks indicate undifferentiated primitive mantle sources in terms of their Sm/Nd ratios. Positive or negative values require that at least one episode of fractionation has increased or decreased the source Sm/Nd ratio, relative to the chondritic ratio.

Basu and Tatsumoto (1980), Kramers *et al.* (1981), and Smith (1983) have determined that kimberlites fall into two distinctive groups with respect to their initial $^{143}Nd/^{144}Nd$ ratios or ε_{Nd} values (Figure 7.23).

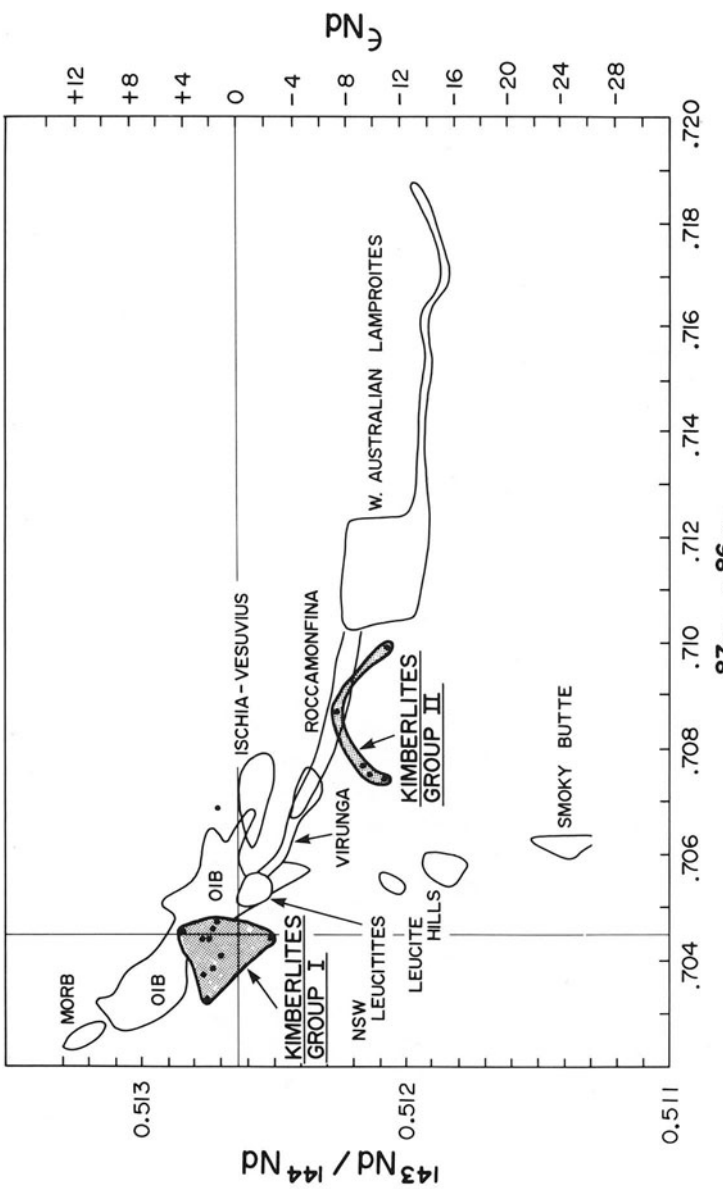

Figure 7.23. Nd versus Sr isotopic composition of kimberlites and other mantle-derived volcanic rocks. Kimberlite data is from Basu and Tatsumoto (1980), Kramers *et al.* (1981) and Smith (1983). All other data is from compilations given by Vollmer and Norry (1983), Hawkesworth and Vollmer (1979), Mitchell and Hawkesworth (1984), McCulloch *et al.* (1983).

One group, termed group I (Smith 1983), has ε_{Nd} values ranging from -0.5 to $+6.0$ and low $^{87}Sr/^{86}Sr$ (0.703–0.705) ratios. This group includes serpentine, monticellite and calcite kimberlites ranging in age from 80 to 114 Ma Kimberlites from Southern Africa, India, Siberia, and the U.S.A., fall within this group.

Group-II (Smith (1983) kimberlites have negative ε_{Nd} (-7 to -12) values and high $^{87}Sr/^{86}Sr$ (0.707–0.711) ratios. This group comprises an older (114–150 Ma) series of predominantly micaceous kimberlites and has so far only been recognized in southern African kimberlites.

Kimberlites belonging to isotopic group I can be considered to be derived from mantle sources which were undifferentiated or slightly depleted (i.e., relatively higher Sm/Nd ratios) with respect to the bulk-earth composition. The Rb/Sr ratios of these sources were also lower than the chondritic value (Basu and Tatsumoto 1980). The Sm–Nd data indicate that the enrichment of the source regions in REE, required to explain the geochemistry of kimberlite, could not have existed for a long time period prior to the generation of the magma, and that this source must have had a chondritic REE distribution pattern (Basu and Tatsumoto 1980).

Kimberlites belonging to group II are derived from an enriched (i.e., relatively low Sm/Nd ratio) source with respect to the bulk-earth Sm/Nd ratio. Smith (1983) considers that the enrichment must have occurred at least 1.0 Ga ago and was not caused by the younger events (<300 Ma) recorded by some mantle-derived xenoliths from this region. The high $^{87}Sr/^{86}Sr$ ratios also require that the source be enriched in Rb. The isotopic characteristics of group-II kimberlites are in accord with derivation from a source that was enriched in Rb and Nd and possessed a non-chondritic REE distribution pattern for a significant time period prior to the generation of the kimberlites.

Figure 7.23 illustrates the isotopic characteristics of kimberlites relative to those of other mantle-derived igneous rocks. Isotopic group-I kimberlites have Nd and Sr isotopic ratios similar to some alkali basalts from oceanic islands. Isotopic group II are similar to potassic volcanic rocks of the Roman region and to the least ^{87}Sr-enriched Western Australian lamproites.

Not all geochemists agree with the Basu and Tatsumoto (1980) and Smith (1983) interpretation of the Nd–Sr data. McCulloch *et al.* (1983) have interpreted the approximately inverse correlation between Nd and Sr isotopic compositions from mid-oceanic ridge basalt (MORB) to the Australian lamproites to be the result of mixing of a highly enriched mantle with a depleted MORB-type mantle. According to this interpretation, the apparently primitive character of group-I kimberlites is the fortuitous coincidence of the hybrid composition with that of the bulk earth. McCulloch *et al.* (1983) estimate that about 2% of an enriched component (high Nd, and Rb) added to a depleted MORB mantle will generate hybrids with an ε_{Nd} of zero. A mixture of about 5% of the enriched component is required to produce the group-II ε_{Nd} values. An important feature of this and other mixing models (Anderson 1982) is that

rocks with positive ε_{Nd} values can have light REE enrichments and Nd/Sm ratios greater than those of chondrites.

Four pyroxene megacrysts analyzed by Kramers *et al.* (1981) have positive ε_{Nd} values (3–6) and low $^{87}Sr/^{86}Sr$ (0.70280–0.70360) ratios. Kramers *et al.* (1981) consider that the data are compatible with the crystallization of the megacrysts from kimberlite magmas. One pyroxene megacryst ($\varepsilon_{Nd} = +9.2$) is considered by Basu and Tasumoto (1981) to be unrelated to kimberlites.

7.5.3. Lead

The very few Pb isotopic data available (Kramers 1977, Smith 1983) are summarized in Figure 7.24 which demonstrates the existence of two groups of kimberlites corresponding to the groups derived from the Sr–Nd isotopic data. Group-I kimberlites contain Pb which is more radiogenic than Pb in group II. All group-I Pb's are anomalous in that they have negative (future) ages relative to their known age of intrusion and to the Stacey and Kramers (1975) two-stage growth curve for terrestrial U–Th–Pb systems. Group-II Pb's are anomalously old (i.e., radiogenic Pb-poor) relative to their known age. Kramers (1977) considered that his data defined an anomalous Pb line and the existence of a long-lived high $^{238}U/^{204}Pb$ source for kimberlite Pb's. Smith (1983) however showed that Kramers' (1977) approach was invalid as the two groups of kimberlites

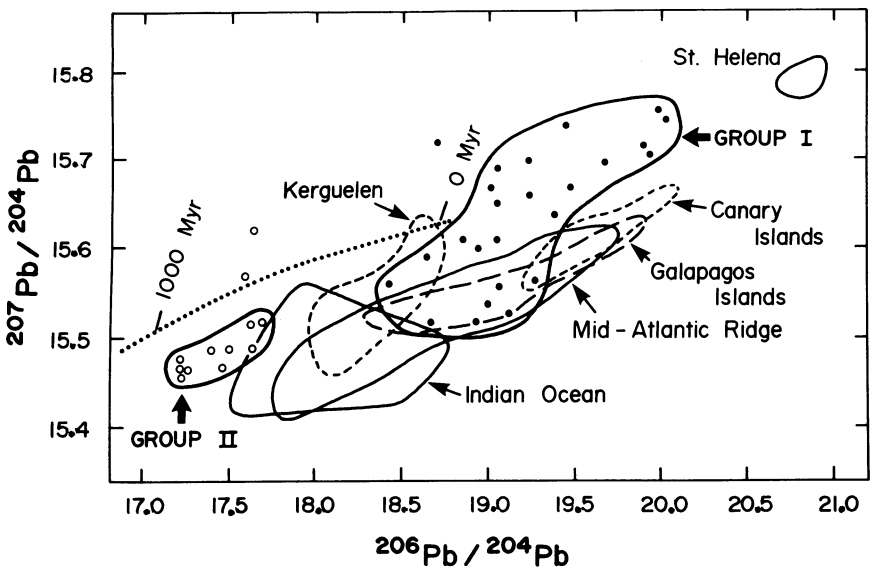

Figure 7.24. Isotopic composition of Pb in kimberlites and oceanic volcanic rocks. Kimberlite data from Kramers (1977) and Smith (1983), oceanic island data from Staudigel *et al.* (1984). The dotted curve is the Stacey and Kramers (1975) two-stage growth curve.

clearly had different Sr and Nd sources and moreover were of different age. The scatter in the data is too great to allow definition of an anomalous Pb line for either group. Group-I Pb's however were generated in a region of higher U/Pb ratio than those of group II.

Figure 7.24 also shows that group-I kimberlites are similar in their Pb isotopic composition to oceanic island basalts. The Pb in these occurrences has been interpreted in terms of a multi-stage history of continually increasing U/Pb ratios in the sources (Oversby and Gast 1970) or in terms of a mixing model involving depleted and enriched mantle reservoirs (Anderson 1982).

In summary, the radiogenic isotopic data for Sr, Nd, and Pb demonstrate either that kimberlites are derived from different sources in a heterogeneous mantle or by the mixing of two or three components of vastly differing isotopic characteristics. The choice of either model is at present purely subjective.

7.5.4. Uranium

Zverev *et al.* (1976, 1979) have determined $^{234}U/^{238}U$ ratios in Yakutian kimberlites and noted that most are depleted in ^{234}U ($^{234}U/^{238}U$ = 0.56–1.06), and that there is an inverse correlation between $^{234}U/^{238}U$ and Th/U ratios. The departure from secular equilibrium and the high Th/U ratios are attributed to uranium loss. This loss has occurred over a time commensurate with the half-life of ^{234}U (24000 yr) and could be due to either U transport by groundwater or to post-magmatic alteration.

7.6. STABLE ISOTOPES

7.6.1. Hydrogen

Sheppard and Epstein (1970) and Sheppard and Dawson (1975) determined that phlogopite megacrysts have a limited range in δD (-40 to $-80‰$) and that mixtures of groundmass micas and serpentines (Figure 7.25) are relatively depleted in D ($\delta D = -85$ to $-105‰$). Even greater D depletions ($\delta D = -137$ to $-147‰$) have been noted for serpentines by Ukhanov and Devirts (1983).

7.6.2. Carbon

Kimberlites contain several carbon-bearing phases, e.g., calcite, dolomite, graphite, diamond, moissanite, and bituminous matter. Of these only calcite can be considered to be predominantly of primary origin. Studies by Baertschi (1957), Vinogradov *et al.* (1965), Vinogradov and Kropotov (1967), Deines and Gold (1973), Sheppard and Dawson (1975), Suwa *et al.* (1975), and Mamchur *et al.* (1980) have established that kimberlitic calcites exhibit a wide range in $\delta^{13}C$

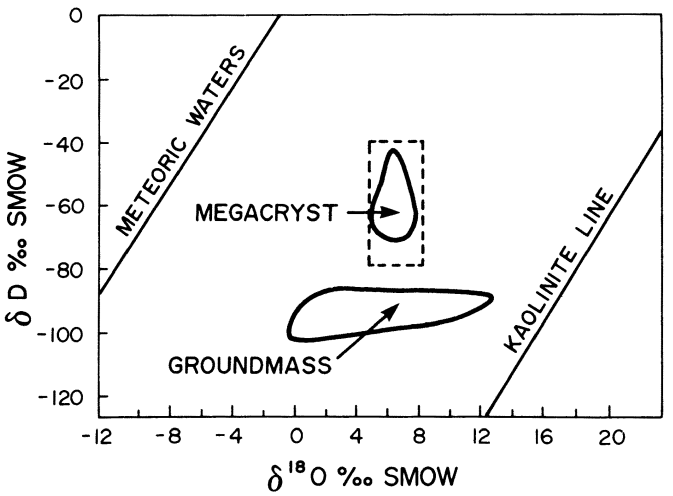

Figure 7.25. D versus ^{18}O isotopic composition of mica megacrysts and groundmass mica and serpentine. Dashed box indicates the composition of magmatic water. Adapted from Sheppard and Dawson (1975).

(−1.6 to −10‰) and that they are isotopically similar to carbonatite calcite ($\delta^{13}C$ = 2 to −8‰, Deines and Gold 1973) and diamond. Although the isotopic composition of diamond is widely variable ($\delta^{13}C$ = 0 to −30‰) most have $\delta^{13}C$ between −2 and −10‰ (Vinogradov *et al.* 1965, Deines 1980, Deines *et al.* 1984). Carbon in all of these parageneses is considered to be mantle-derived (Deines and Gold 1973).

Detailed studies by Kobelski *et al.* (1979) of southern African kimberlites also delineated a wide range in $\delta^{13}C$ carbonate (mean −5.85‰ range to +0.2 to −11.8‰). No significant differences were noted between the $\delta^{13}C$ of hypabyssal (−5.41‰) and diatreme (−5.67‰) facies carbonates, although late stage carbonate-rich dikes are enriched in ^{12}C ($\delta^{13}C$ = −7.24‰). Dolomites are enriched in ^{13}C($\delta^{13}C$ = +0.65‰) relative to coexisting calcite. Individual kimberlites exhibit a wide range in $\delta^{13}C$ values (Figure 7.26), e.g. De Beers (−1 to −12‰), Premier (−4 to −17‰), and Roberts Victor (−6 to −12‰). Although overlap in the $\delta^{13}C$ values of carbonates from individual intrusions occurs, it appears that each intrusion is characterized by a distinct mean $\delta^{13}C$ value, e.g., National (−4.41 + 1.17‰), De Beers (−5.99 + 2.29‰). Acicular calcites in the Benfontein sill are 1‰ lighter than the carbonates occurring in the ocelli and matrix, which are of similar isotopic composition.

Angular carbonate inclusions in most of the kimberlites studied by Kobelski *et al.* (1979) have similar isotopic compositions to the matrix calcite. These inclusions may be cognate inclusions or completely re-equilibrated limestone

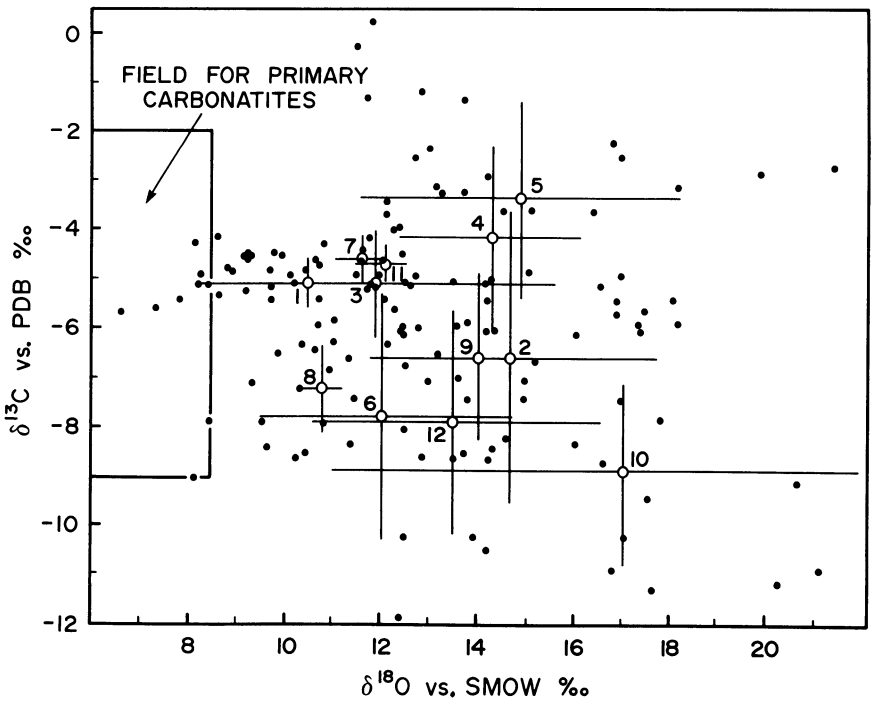

Figure 7.26. Isotopic composition of carbonates from kimberlites. (o) Means and deviations of individual kimberlite intrusions (+), after Kobelski *et al.* (1979). Field of primary carbonatite isotopic compositions from Deines and Gold (1973). 1, Benfontein; 2, De Beers; 3, Wesselton; 4, Monastery; 5, National; 6, Premier; 7, Ngopetsoeu; 8, Star; 9, Pipe 200; 10, Kao; 11, Marakabei; 12, Roberts Victor.

xenoliths. Mamchur *et al.* (1980) and Deines (1968) have found, in some kimberlites, partially re-equilibrated xenoliths which are isotopically zoned toward the composition of primary groundmass calcite from relatively ^{13}C-rich compositions ($\delta^{13}C = +12‰$ to $+34‰$).

Brown secondary calcites (Mamchur *et al.* 1980), commonly associated with bituminous matter, have distinctly different isotopic compositions from primary carbonates being enriched in ^{12}C ($\delta^{13}C = -10$ to $-32‰$).

Bitumens in Yakutian kimberlites range in $\delta^{13}C$ from -13 to $-48‰$ (Mamchur *et al.* 1980, Vyshemirskii *et al.* 1971, Vinogradov *et al.* 1965). The isotopic composition of some of these bitumens ($\delta^{13}C = -25$ to $-48‰$) is similar to that of liquid hydrocarbons in the country rocks and Vinogradov *et al.* (1965) propose that they are derived from such a source. Relatively heavier ($\delta^{13}C = -13$ to $-20‰$) bitumens are considered by Mamchur *et al.* (1980) to be of abiogenic origin and to have formed from the volatiles associated with the kimberlite magma.

7.6.3. Oxygen

Sheppard and Epstein (1970) and Sheppard and Dawson (1975) determined that phlogopite megacrysts have similar, but relatively restricted, $\delta^{18}O$ (4 to 8‰) values as compared to mixtures of groundmass micas and serpentines ($\delta^{18}O$ = 0 to 12‰).

Even wider ranges in $\delta^{18}O$ have been noted for calcites ($\delta^{18}O$ = 7 to 27‰) by Baertchi (1957), Deines and Gold (1973), Sheppard and Dawson (1975), Suwa *et al.* (1975) and Kobelski *et al.* (1979). Carbonates have a much greater variation in their $\delta^{18}O$ values than their $\delta^{13}C$ values and although the mean $\delta^{18}O$ of each kimberlite appears to be distinct, e.g., Wesselton (10.62‰), Pipe 200 (14.71‰), Kao (17.10‰), there exist broad compositional overlaps (Figure 7.26). Kobelski *et al.* (1979) have shown that diatreme facies kimberlites appear to be enriched in ^{18}O($\delta^{18}O$ = 13.9‰) relative to hypabyssal ($\delta^{18}O$ = 11.35‰) and calcite-rich ($\delta^{18}O$ = 12.6‰) varieties. No significant differences were found between the $\delta^{18}O$ values of co-existing calcite and dolomite or inclusions and matrix carbonates.

The wide range in $\delta^{18}O$ of kimberlite calcite is similar to that observed in volcanic and subvolcanic carbonatite carbonates ($\delta^{18}O$ = 7 to 26‰, Deines and Gold 1973) and the mean isotopic composition ($\delta^{18}O$ = 13.9‰, Kobelskii *et al.* 1979) is enriched in ^{18}O as compared with oxygen in primary intrusive carbonatite calcite ($\delta^{18}O$ = 6–7‰, Deines and Gold 1973).

7.6.4. Origins of the Hydrogen, Oxygen, and Carbon Isotopic Variations

Figure 7.25 shows the isotopic composition of the two groups of micas and serpentines established by Sheppard and Dawson (1975), with respect to the composition of meteoritic and magmatic waters. None of the samples has undergone H and O isotopic exchange in a low-temperature weathering environment as they do not plot on the kaolinite reference line. This line represents the composition of clay minerals found at the earth's surface in equilibrium with the local meteoritic water. (One highly weathered sample of yellow ground, analyzed by Sheppard and Dawson [1975], does in fact plot on this line). The δD and $\delta^{18}O$ values of the megacryst micas fall within the range of isotopic composition of primary magmatic water and are considered to be representative of the initial H and O isotopic composition of the kimberlite magma. Sheppard and Dawson (1975) and Ukhanov and Devirts (1983) interpret the wide range in ^{18}O and depletion in D of the groundmass mica–serpentine mixture to be a consequence of mixing of the magma with hot meteoritic waters depleted in D and enriched in ^{16}O with respect to magmatic water. The mixing process cannot be analyzed in detail because of the paucity of data, lack of knowledge of the temperature and composition of the meteoric water, the meteoric to magmatic

water ratio, and the CO_2/H_2O ratio of the associated volatile phase. Further, the isotopic composition of the hybrid magma may be subsequently modified by CO_2 and H_2O loss during degassing after emplacement. This process can result in significant changes in the isotopic composition of the late-stage serpentine-forming fluids.

Figure 7.26 demonstrates the lack of correlation between $\delta^{18}O$ and $\delta^{13}C$ of kimberlitic calcites. Very few of the samples, e.g., the Benfontein sills and hypabyssal Wesselton and Premier kimberlites, have isotopic compositions falling within the field of primary mantle C and O as established by Deines and Gold (1973) for plutonic carbonatite complexes. Most kimberlites have C isotopic compositions close to that of mantle C but are significantly enriched in ^{18}O, implying that isotopic fractionation, occuring during and after intrusion, has modified the oxygen isotopic compositions to a much greater extent than those of carbon.

The ^{13}C variation is difficult to explain and could be the result of any of the following processes acting alone or in concert:

1. Contamination of the kimberlite by relatively heavy crustal limestones (mean $\delta^{13}C = +0.56 \pm 1.55‰$; Keith and Weber 1964).
2. Isotopic fractionation during crystallization. Kobelskii *et al.* (1979) have proposed that the enrichment in ^{12}C in late-stage calcite-rich kimberlites is a consequence of C isotopic fractionation between an initial silicate-CO_2 phase and a later fluid capable of precipitating carbonates. Deposition of ^{13}C-rich carbonates from the CO_2-rich phase results in enrichment of ^{12}C in the later phase.
3. Degassing of isotopically heavy CO_2 subsequent to emplacement.

In addition, some of the ^{13}C variation may be inherited from the upper mantle sources of the magma. That such heterogeneities exist is demonstrated by the variations in the $\delta^{13}C$ of diamond (Deines 1984, Deines *et al.* 1984).

The enrichment in ^{18}O over the mantle $\delta^{18}O$ values may be due to: loss of isotopically light water during emplacement, equilibration of some of the carbonates with magmatic waters to low temperatures, or an influx of meteoric water at relatively low (<250°C) temperatures.

The latter process is in accord with the conclusions reached from the hydrogen isotopic data, and with the estimated temperatures of serpentinization (150–75°C) proposed by Sheppard and Dawson (1975) on the basis of oxygen isotopic fractionation between co-existing calcite and serpentine–mica mixtures.

7.6.5. Boron

Cherepanov (1967) considers that kimberlites are enriched in ^{11}B ($\delta^{11}B = +28.7‰$) relative to basalts ($\delta^{11}B = -7.0\%$ to $+15.0‰$) and that this enrichment is due to mantle degassing. The process is assumed to generate

a $\delta^{11}B$ gradient in the mantle, with the lighter ^{10}B being concentrated in the crust. The different $\delta^{11}B$ values of mantle-derived rocks are thus considered to reflect their derivation from different depths. Agyei (1968), however, finds no significant variations in the isotopic composition of terrestrial B, and similar $\delta^{11}B$ values for Swartruggens kimberlite (+10.3‰) and Hawaiian basalt (+7.8‰). The contradictions between the two data sets may be a consequence of the different methods used to extract B from the samples, although both authors claim that isotopic fractionation does not occur during extraction.

7.6.6. Sulfur

Systematic studies of sulfur isotopic compositional variation have not been undertaken despite the ubiquity of sulfides in kimberlites. Vinogradov and Ilupin (1972) have reported a very wide range in $\delta^{34}S$ (−14‰–+52‰) for sulfides and sulfates in Yakutian kimberlites and ascribed the high $\delta^{34}S$ values to contamination of the kimberlite by crustal materials. Tsai *et al.* (1979) found massive pyrite in the Premier kimberlite to have a $\delta^{34}S$ of +1.3‰. Dawson (1980) reported pyrites in the Saltpetrepan and Bellsbank dikes to be enriched in ^{34}S ($\delta^{34}S$ = 1.9 and 2.5‰, and 1.2, 7.2, and 16.1‰, respectively). Muramatsu (1983) found kimberlites in the Kimberley area to range from −3.0 to +9.6‰ $\delta^{34}S$. Clearly the $\delta^{34}S$ values of kimberlites are wide ranging but because of the inadequacies of the data base they should not be used to infer the source(s) of the sulfur.

"Take away the recipient,
and rectify your menstrue, from the phlegma,
Then pour it, o' the Sol, in the curcubite,
And let 'em macerate, together."
Ben Jonson, *The Alchemist (1610)*

8

EXPERIMENTAL STUDIES RELEVANT TO THE FORMATION AND CRYSTALLIZATION OF KIMBERLITE MAGMA

8.1. EXPERIMENTAL STUDIES AT HIGH PRESSURES

8.1.1. Introduction

The mineralogy of the upper mantle is in part dependent upon the abundance and proportions of H_2O and CO_2 present. They may be fixed in hydrous and carbonate minerals and/or exist as a separate vapor phase. These volatiles also profoundly influence the composition of the magmas formed by partial melting of upper mantle peridotite.

Initial experimental studies of the melting of peridotite in the presence of *excess* volatiles demonstrated that near-solidus liquids become increasingly undersaturated with increasing CO_2/H_2O ratios (Kushiro 1972, Eggler 1974, Boettcher *et al.* 1975, Mysen and Boettcher 1975). Accordingly it was suspected that a wide spectrum of magmas could be derived by merely varying the CO_2/H_2O ratio of the source. Other studies, summarized by Green (1971) and Frey *et al.* (1978), indicated that a series of magmas ranging from tholeiitic to melilititic might be produced by varying the degrees of partial melting at any given pressure, or by similar amounts of melting with increasing depth. Kimberlites were believed to be extreme variants of these trends; that is, magmas produced by small degrees of partial melting at great depth under CO_2-rich conditions.

The experimental studies suggested that a specific set of conditions of formation could not be assigned to any one particular magma type. This unsatisfactory situation was in part resolved by the realization of the following:

1. Large quantities of volatiles are unlikely to be present in the mantle and hence experiments with excess volatiles may be unrealistic.
2. The demonstration that synthetic peridotites melt in the presence of small amounts of volatiles in a eutectic-like manner (Eggler 1977, Wyllie 1977).
3. That liquids of a constant composition are produced regardless of the CO_2/H_2O ratio of the rock–fluid system under mantle-like conditions (Eggler 1977).
4. The recognition of the existence of a series of carbonation reactions which fix CO_2 as dolomite or magnesite in the upper mantle (Wyllie and Huang 1975a,b, 1976).

From these observations new models of the melting behavior of the upper mantle were constructed. The basic features of these models are outlined below in order that some understanding may be gained of the nature of the melting processes that occur at vapor-buffered solidii. These processes control the compositions of the magmas formed at the solidii of carbonated lherzolites. An understanding of these melting relationships is essential if the merits and detractions of some recent hypotheses of kimberlite petrogenesis (Wyllie, 1980, Bailey 1980, 1984) are to be appreciated.

8.1.2. Peridotite–H_2O

Normal mantle can store only small amounts of water, and only about 0.06% H_2O or 0.4% H_2O are required to make the maximum possible amounts of phlogopite or amphibole, respectively (Wendlandt and Eggler 1980b, Wyllie 1977). Metasomatic introduction of phlogopite and/or amphibole will result in increased but unpredictable buffering capacity (Wendlandt and Eggler 1980b).

Representative experimentally based solidii of amphibole peridotite are illustrated in Figure 8.1, together with the peridotite solidus with excess water. Amphibole is stable at the solidus where its stability field overlaps the peridotite solidus at H_2O contents of less than 0.4%. For example, a separate vapor phase does not exist between A and B (Figure 8.1) on the Millhollen *et al.* (1974) solidus. With excess water the peridotite solidus extends continuously between A and B.

Figure 8.1 demonstrates that amphiboles are limited to shallow depths in the mantle whereas phlogopite is stable at higher pressures and can be expected to be the primary water-bearing phase at depths of 100–180 km.

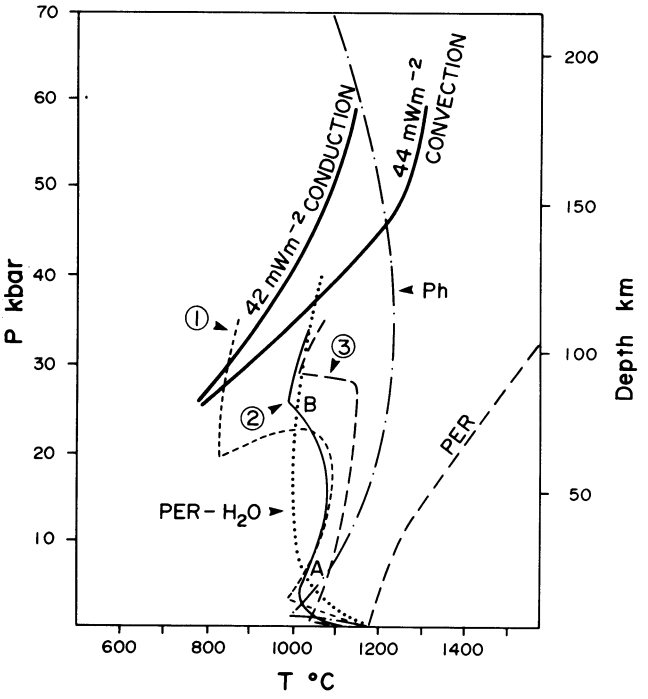

Figure 8.1. Experimentally based and deduced curves for the solidus of amphibole peridotite with less than 0.4% H_2O. Curves 1, 2, and 3 are from Boettcher (in Wyllie 1977), Millhollen *et al.* (1974), and Green (1973), respectively. Representative shield geotherms are from Gurney and Harte (1980). Curve Ph is the solidus for vapor-absent phlogopite peridotite (Wyllie 1977). PER–H_2O and PER are solidii for water-saturated and anhydrous peridotite, respectively (Wyllie 1977).

8.1.3. Peridotite–CO_2

Studies of the system CaO–MgO–SiO_2–CO_2 (synthetic peridotite) have demonstrated that dolomite and magnesite can be stable in the mantle at solidus temperatures (Eggler 1975, 1978, Wyllie and Huang 1975a,b).

Reaction of CO_2 with mantle minerals results in the formation of a carbonate mineral by a *carbonation* reaction. The three most important carbonation reactions in order of increasing pressure of reaction defined by Wyllie and Huang (1976) are as follows:

$$\text{olivine} + \text{clinopyroxene} + CO_2 \rightleftharpoons \text{orthopyroxene} + \text{dolomite}_{ss} \quad (6)$$

$$\text{olivine} + \text{dolomite} + CO_2 \rightleftharpoons \text{orthopyroxene} + \text{magnesite}_{ss} \quad (4)$$

$$\text{orthopyroxene} + \text{dolomite}_{ss} + CO_2 \rightleftharpoons \text{quartz/coesite} + \text{magnesite}_{ss} \quad (2)$$

A further sub-solidus exchange reaction determining the stability relationships between dolomite and magnesite lherzolite is:

$$\text{enstatite} + \text{dolomite} \rightleftharpoons \text{diopside} + \text{magnesite} \qquad (0)$$

It requires about 5% CO_2 to complete reaction (6) for a lherzolite containing 10%–15% clinopyroxene. Because of the much greater buffering capacity of olivine, about 23% CO_2 is required to convert lherzolite into coesite marble by reactions (4) and (2). Such high concentrations of CO_2 are unlikely to be encountered in the mantle, and carbonation reaction (6) will usually not result in complete elimination of clinopyroxene. Schematic phase diagrams for model mantle peridotites with excess and limited amounts of CO_2 are depicted in Figures 8.2A and B, respectively. Figure 8.2B shows that carbonated garnet lherzolite will exist at all pressures and temperatures above carbonation reaction (6) and below the solidus.

An important feature of the solidii for peridotite–CO_2 is the dramatic decrease in solidus temperature where dolomite becomes a stable solidus phase. This is due to a significant increase in the solubility of CO_2 in the liquid coexisting with olivine, ortho- and clinopyroxene, and CO_2 (vapor) over a small pressure interval below the pressure and temperature at which carbonation reaction (6) intersects the solidus.

At this invariant point (I_6) six phases (opx, cpx, ol, dol, L, V) co-exist. Below I_6, because carbonate is not stable at the solidus, there is no fluid buffering. Above I_6 the fluid composition is buffered (see below), by the presence of dolomite or magnesite.

The sub-solidus exchange reaction (0) has recently (Brey *et al.* 1983, Olafsson and Eggler 1983) been found to occur at much lower pressures than previously estimated (Kushiro *et al.* 1975). The recent studies indicate that magnesite will be the stable carbonate throughout much of the upper mantle in the regions where kimberlites might be generated (Figures 8.10 and 8.11).

8.1.4. Peridotite–CO_2–H_2O

Wyllie (1977, 1978, 1979a,b, 1980) has discussed in detail the topology of the system peridotite–CO_2–H_2O. Wyllie's analysis is based upon the melting behavior of natural and synthetic peridotites together with extrapolation of the data to higher pressures and temperatures. Wyllie (1979a) cautions that although the topology of the system may be correct, the assignment of pressure and temperatures to the phase relationships gives the phase diagrams a "semblance of accuracy" (Wyllie 1979a, p. 472) which does not actually exist. In fact serious conflict exists between Wyllie's analysis of this system and the recent experimental studies by Brey *et al.* (1983) and Olafsson and Eggler (1983). The

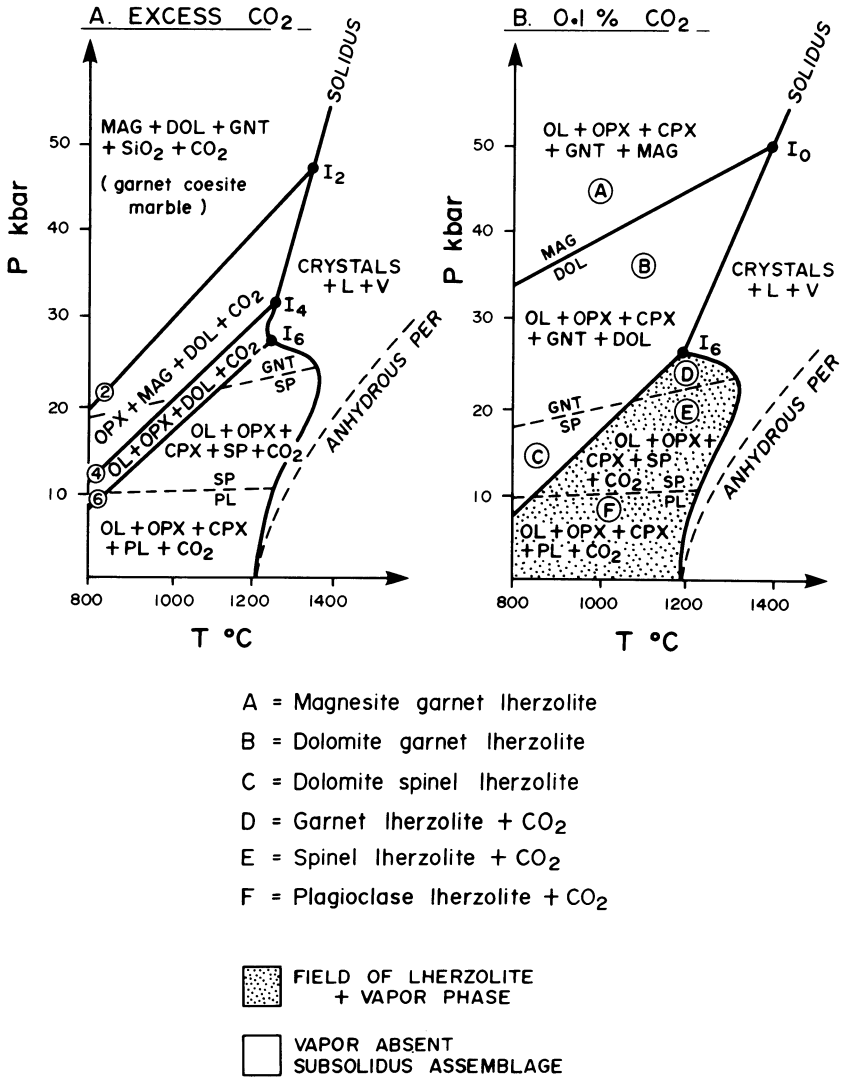

Figure 8.2. Phase relationships in the system peridotite–CO_2 based on experimental data and deductions from CaO–MgO–SiO_2–CO_2 (Wyllie and Huang 1976, Wyllie 1977, 1978) (A) with excess CO_2 the peridotite mineral facies are traversed by three carbonation reactions (6), (4), and (2) (see text); (B) with 0.1% CO_2 all CO_2 is absorbed in reaction (6) leaving a vapor-absent dolomite peridotite which experiences a sub-solidus exchange reaction (○) among carbonates and pyroxenes, along the curve (MAG–DOL) extending to point I_0. MAG, magnesite; DOL, dolomite; GNT, garnet; OPX, orthopyroxene; OL, olivine; CPX, clinopyroxene; SP, spinel; PL, plagioclase.

differences are not trivial and have important consequences with respect to Wyllie's (1980) models of kimberlite magmatism.

Detailed discussion of the phase relationships of peridotite–CO_2–H_2O is beyond the scope of this work and the reader is referred to Wyllie (1978, 1979a,b) for further details. Two aspects of the system are of particular importance with respect to kimberlite petrology, namely, (1) the shape of the solidus and which phases are stable at the solidus, and (2) the nature of melting at the fluid buffered carbonated peridotite solidus.

An analysis of the system according to Wyllie (1978, 1979a) is presented initially as a guide to understanding these topics.

8.1.4.1. Solidus Phase Relationships

Adding H_2O to the system CaO–MgO–SiO_2–CO_2 changes each univariant curve to a divariant surface which can be represented in P–T space by contours of constant vapor composition. Figure 8.3A shows the position of the divariant carbonation surface for reaction (6) with respect to the peridotite solidus surface as a function of X_{CO_2} [molar $CO_2/(CO_2 + H_2O)$]. The invariant point I_6 of the quaternary system is now a univariant line located at the intersection of three divariant surfaces; the carbonation surface of reaction (6); the solidus surface for carbonated peridotite; and the solidus surface for peridotite–vapor with no carbonate (Figure 8.4A). The locations of the latter two surfaces with respect to changing volatile composition are illustrated in Figures 8.3B and 8.3C, respectively.

Figures 8.3A–C are combined in Figure 8.4A to illustrate the shape of the peridotite–CO_2–H_2O solidus in P–T–X space and to show that its location is dependent upon the composition of the volatile phase, but lies between the limits established for peridotite–H_2O (Figure 8.1) and peridotite–CO_2 (Figure 8.2).

The thermal ridge on the solidus surface (Figure 8.4A), which appears as a maximum in an isocompositional section (Figure 8.4B), is the most important feature of Wyllie's model of this system. This maximum plays an important role in Wyllie's (1980) model of diapiric ascent of magmas as it acts as a thermal barrier at which crystallization and vapor liberation occur. A melt ascending along the line A–B in Figure 8.4B will encounter the maximum at B and crystallize. The liberated vapor will, according to Wyllie (1980), initiate crack propagation through the overlying lithosphere followed by explosive eruption of the magma from depths of about 90 km. The hypothesis is discussed in Section 9.7.1.

The stability fields of amphibole and dolomite are especially important with respect to the presence or absence of a thermal maximum on the peridotite–vapor solidus. Figure 8.5 shows that increasing proportions of H_2O (decreasing X_{CO_2}) lead to the appearance of amphibole at the solidus. Wyllie (1980) indicates that at all X_{CO_2} compositions, regardless of which estimate of amphibole stability is

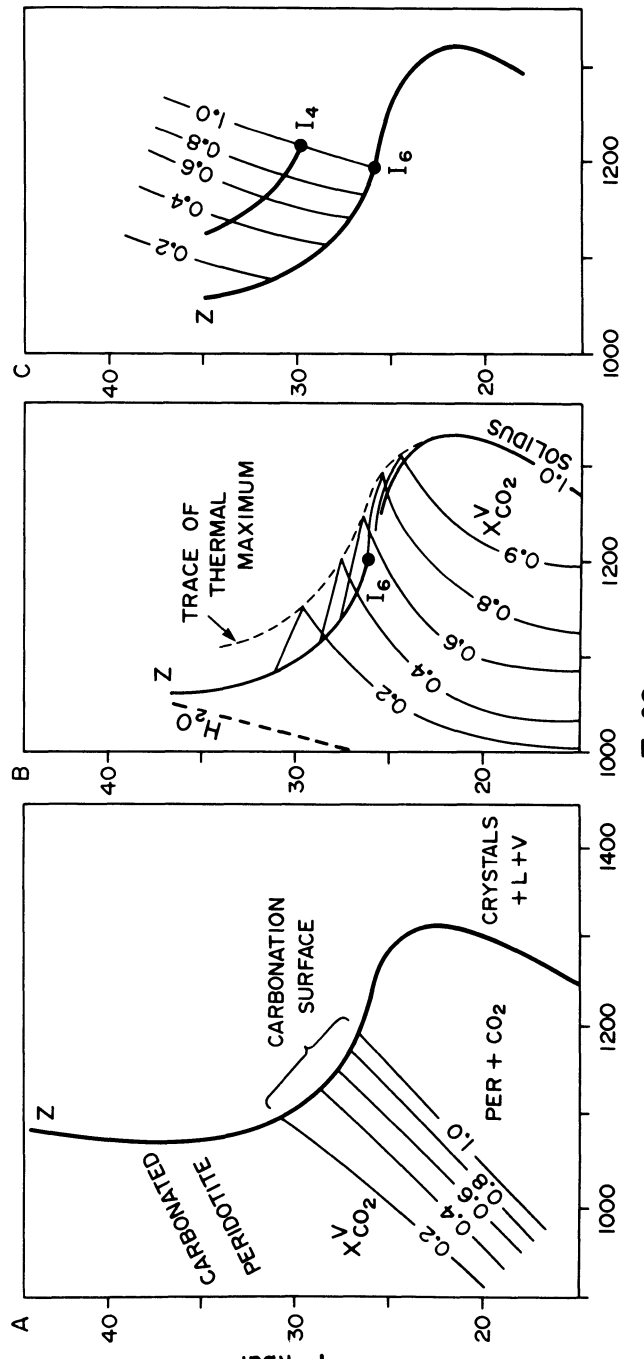

Figure 8.3. Vapor phase contours (mole fraction) of three divariant surfaces for peridotite–CO_2–H_2O adapted from Wyllie (1977, 1978): (A) The carbonation surface for reaction (6), (B) the solidus surface for peridotite–vapor. This surface passes over a temperature maximum and then down to the buffer line extending from I_6; (C) The solidus surface for carbonated peridotite with vapor. Invariant points I_6 and I_4 correspond to similar points on Figure 8.2.

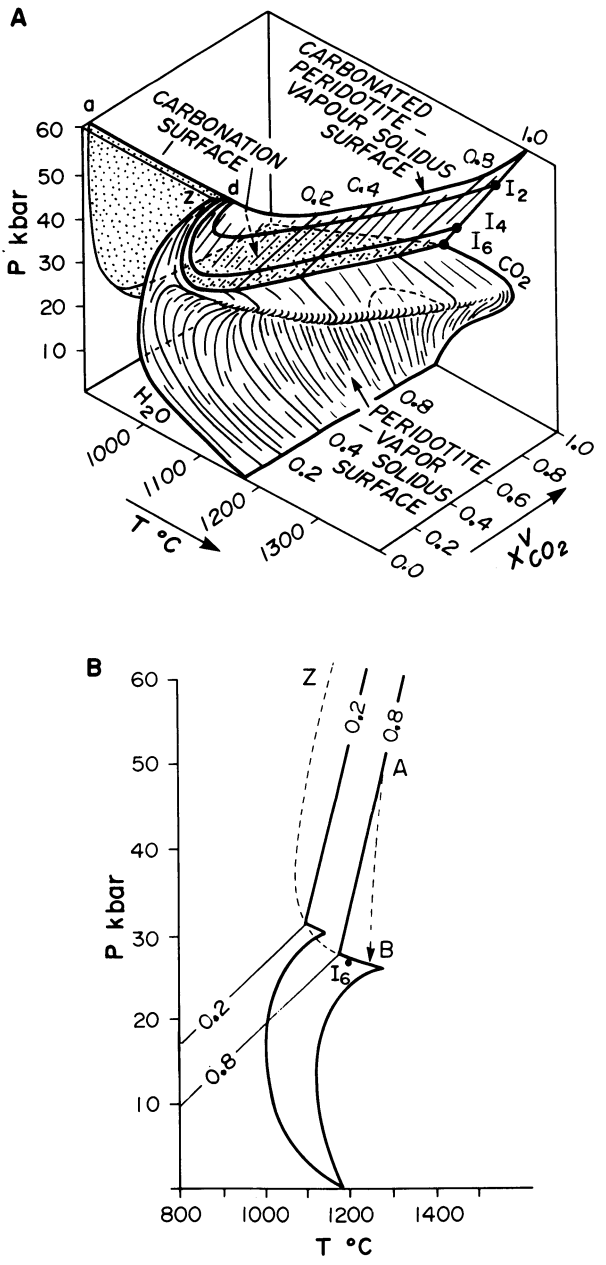

Figure 8.4. (A) The solidus surfaces for peridotite–CO_2–H_2O and the carbonation surface for reaction (6) represented schematically in P–T–X space. (B) Isocompositional sections showing the shape of the solidus surface at two fixed vapor phase compositions. Note the decreasing size of the thermal maximum on the peridotite–vapor solidus with increasing H_2O content. Dashed line Z–I_6 represents the trace of the invariant points each pertaining to a specific vapor phase composition which correspond to I_6 in the pure CO_2 system. A–B represents the ascent path of partially melted adiabatic diapirs (see Section 9.7.1).

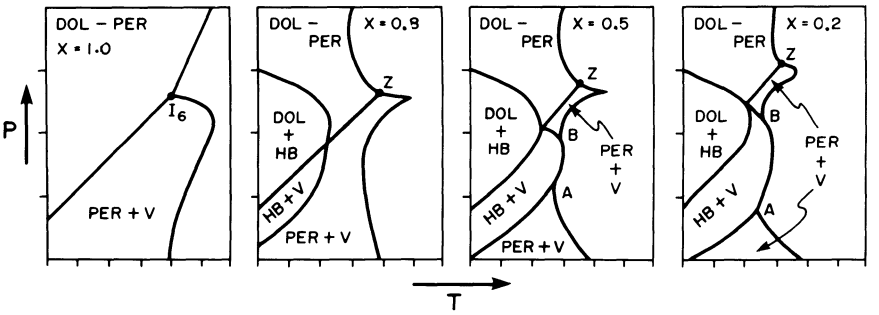

Figure 8.5. Phase fields intersected by peridotite–CO_2–H_2O as a function of changing vapor phase composition (x = mole fraction CO_2), after Wyllie (1979a). Points Z and I_6 correspond to similar points in Figure 8.4. PER, peridotite; DOL, dolomite; HB, hornblende; V, vapor.

used, there is no overlap with the thermal maximum on the solidus. Figure 8.5 also shows that amphibole and dolomite co-exist only as a sub-solidus assemblage.

Wyllie's schematic phase diagram for peridotite with small amounts of H_2O and CO_2 is compared in Figure 8.6 with recent experimental determinations of the solidus by Olafsson and Eggler (1983) and Green (in Brey *et al.* 1983). These data are clearly at variance with Wyllie's model in that:

1. Amphibole and dolomite coexist at the solidus in both of the experimental studies.

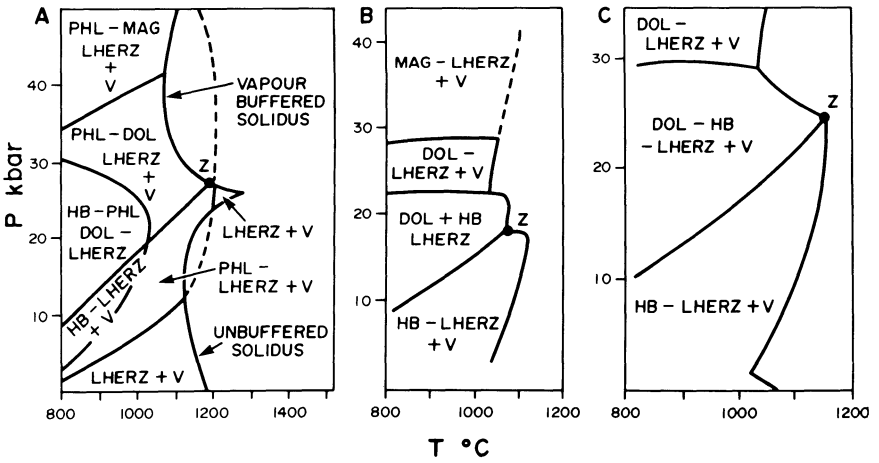

Figure 8.6. Phase relationships at the solidus for lherzolite (LHERZ)–CO_2–H_2O as proposed by (A) Wyllie (1979a,b),(B) Olafsson and Eggler (1983), and (C) Brey *et al.* (1983) and Wyllie (personal communication, 1985). Note the position of point Z in each representation. Abbreviations as in Figures 8.1 and 8.5.

2. A thermal maximum on an unbuffered peridotite–vapor solidus is not present.
3. Amphibole is present as a vapor buffer on the solidus at all pressures below those of the carbonation surface.
4. Vapor is absent at the Olafsson and Eggler (1983) amphibole–dolomite–peridotite solidus, but possibly present (Wyllie, personal communication) at the Brey *et al.* (1983) solidus.
5. There is no agreement between the positions of the experimentally determined solidii or between these and Wyllie's (1979a) schematic solidus. Especially important is the appearance of dolomite at pressures as low as 18 kbar on the Olafsson and Eggler (1983) solidus.

These data clearly demonstrate that phase relationships in the system peridotite–H_2O–CO_2 are poorly understood. This must be borne in mind when considering Wyllie's (1980) model of kimberlite magmatism, as the absence of a thermal maximum on the peridotite–vapor solidus will invalidate the hypothesis. All of the data are however in agreement that the mantle from which kimberlite magmas are derived could be a carbonated peridotite. The melting behavior of such a mantle as discussed in the next section is commensurate with the undersaturated Mg–CO_2–rich nature of kimberlites.

8.1.4.2. Melting at Fluid-Buffered Solidii (ZIVC Solidii)

When magnesite, dolomite, or amphibole exist at the solidus of closed peridotite systems containing small quantities of CO_2 or H_2O it has been found (Wyllie 1977, Eggler 1977) that the vapor phase composition is buffered by reactions involving these hydrated or carbonated phases. Vapor, and co-existing liquid compositions, are constrained by the intersection of carbonation reaction (6) with the carbonated peridotite solidus when insufficient CO_2 is present in the peridotite. Thus, for low contents of H_2O and CO_2 and for a wide range in X_{CO_2}, melting begins not on the divariant solidus surfaces shown in Figure 8.4, but at the univariant line which traverses these surfaces. If a carbonated peridotite is heated or cooled, dolomite or magnesite will dissociate or be formed in sufficient amounts to maintain a vapor whose composition is fixed with respect to X_{CO_2}, at a given pressure. The composition of the buffered vapor phase is determined by the intersection of the carbonation surface with the carbonated peridotite solidus, as shown with respect to changing pressure in Figure 8.7 and projected in P–T space in Figure 8.4B. The buffered solidus corresponds to the locus of points defined by the migration of I_6 in P–T–X space. Note that the composition of the buffered vapor phase becomes increasingly richer in H_2O as pressure increases (Figure 8.7). This type of buffered solidus has been termed a zone of invariant vapor composition or ZIVC solidus by Eggler (1977). Along this solidus a volatile-bearing mineral co-exists with a multicomponent vapor

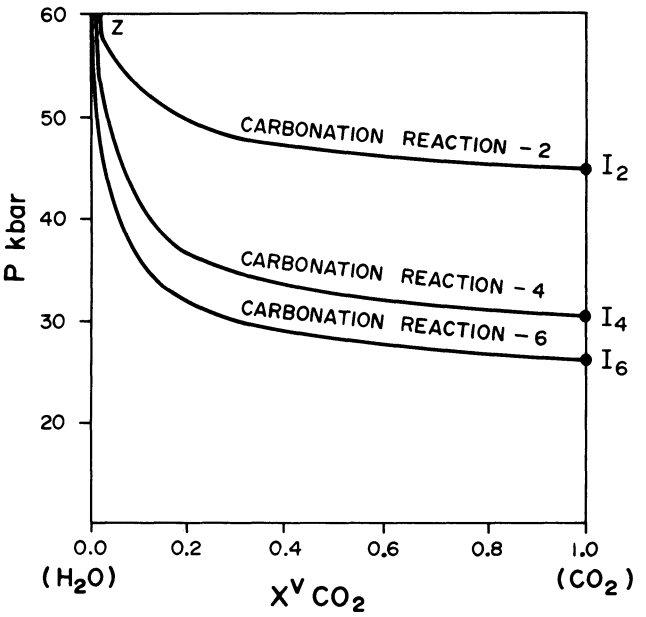

Figure 8.7. PX projection of the peridotite–CO_2–H_2O solidus surface expressed in terms of the composition of the vapor at the solidus. Adapted from Wyllie (1978).

and with its breakdown products, in a reaction relation that buffers vapor composition. Wyllie (1977, 1979b) has suggested that the term ZIVC is inappropriate and misleading in that the defined zone extends through a wide range of pressures and is therefore not invariant. Eggler's (1979) term may be applied specifically to univariant assemblages where, under *isobaric* conditions (i.e., invariant), both liquid and vapor compositions are fixed. Wyllie (1977) prefers to refer to these reactions as univariant solidus reactions with buffered vapor phases. Melting at such solidii is eutectic-like.

Figure 8.8 demonstrates the buffering effects upon the vapor composition at the solidus of an amphibole–dolomite–peridotite under closed system conditions. At low pressures where amphibole is not stable (A–B,C–D, Figure 8.8), the vapor composition equals the system vapor composition. Where amphibole is stable (B–C) at the solidus the vapor becomes enriched in CO_2. Where dolomite is stable (D–E) the vapor becomes increasingly rich in H_2O as CO_2 is withdrawn from the vapor to maintain dolomite at the solidus.

The composition of the liquids produced at vapor-buffered melting curves of carbonated peridotites have not yet been characterized in any detail, although there is general agreement that they are rich in CO_2. Eggler (1978) and Wyllie and Huang (1975a,b, 1976) postulate that liquids produced at I_6 in

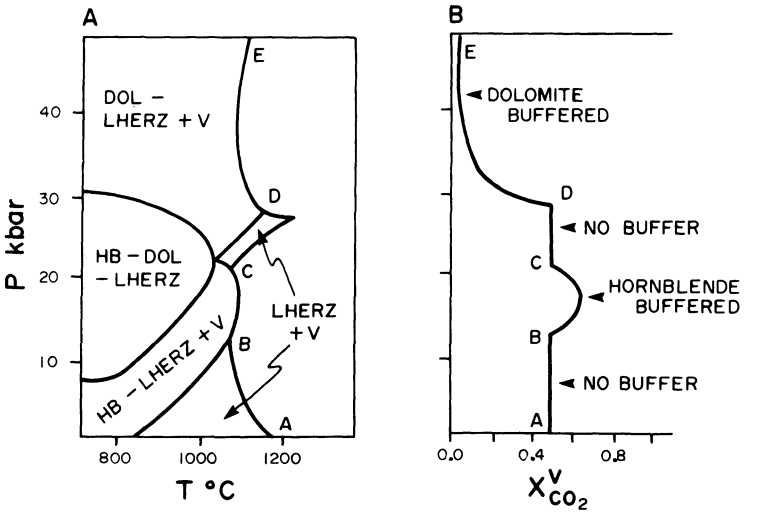

Figure 8.8. (A) Phase relationships for lherzolite–CO_2–H_2O with $CO_2/(CO_2 + H_2O) = 0.5$. (B) Composition of the vapor phase at the solidus of A. Letters correspond to similar points on each diagram. Abbreviations as in Figure 8.5. Adapted from Wyllie (1979a).

CaO–MgO–SiO_2–CO_2 contain 27% and 35%–40% CO_2, respectively. Further discussion of the nature of the melting products is presented in Section 8.1.5.

8.1.4.3. Melting Behavior of Cobaltian Kimberlite

The only studies of the melting behavior of kimberlitic compositions that include volatiles at high pressure are those of Eggler and Wendlandt (1979). In these experiments the phase relationships of anhydrous average Lesotho kimberlite were studied at 30–55 kbar with 0 to 11 wt % water contents. CoO was substituted for FeO to decrease the loss of divalent transition elements to the platinum capsules used in the experiments. This substitution results in liquidus and solidus temperatures being about 50°C higher than in analogous Fe-bearing systems. The major conclusions derived from Eggler and Wendlandt's (1979) work are as follows:

1. Below the solidus for a wide range in CO_2/H_2O ratios this bulk composition is represented by the assemblage garnet, orthopyroxene, clinopyroxene, olivine, phlogopite, dolomite (30 kbar, Figures 8,9A) or magnesite (55 kbar, Figure 8.9B) and H_2O-rich vapor.
2. The decarbonation boundary [reaction (6)] between carbonated and carbonate-free garnet lherzolite is shifted toward increasingly H_2O-rich compositions with increasing pressure due to the higher H_2O content of the buffered vapor (Figure 8.7).

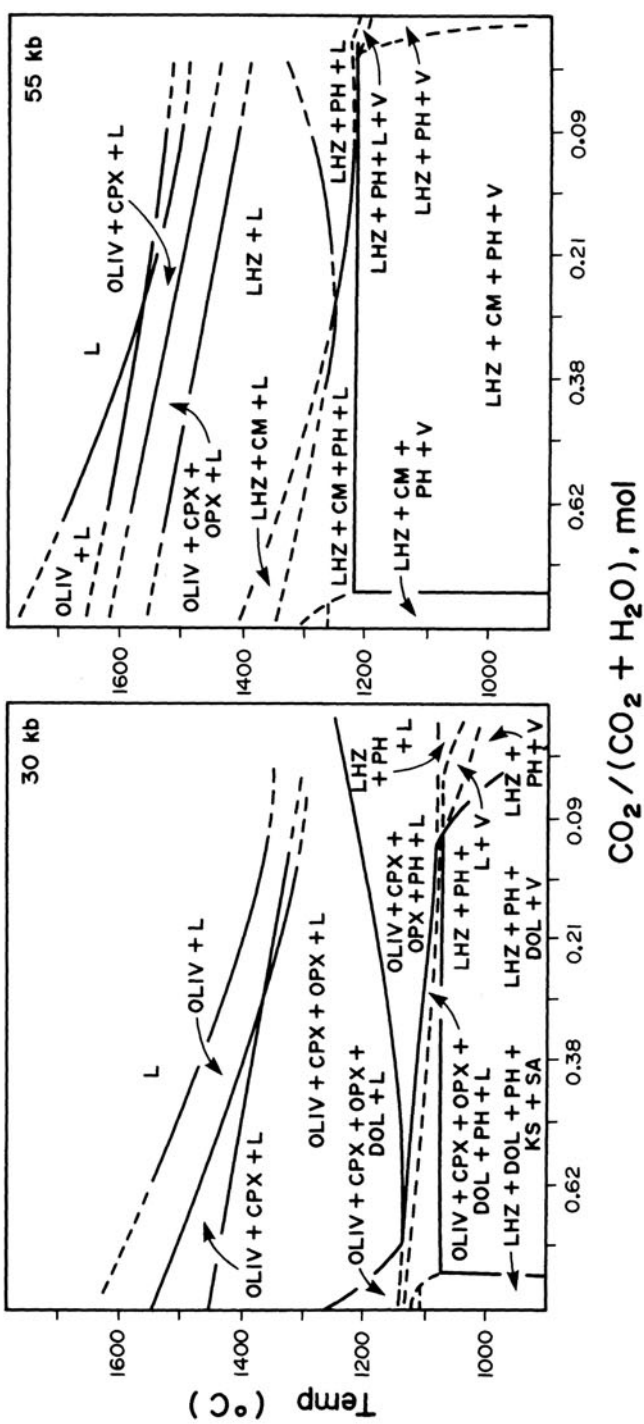

Figure 8.9. Phase relations on the join cobaltian kimberlite–5.2% CO_2–H_2O at 30 and 55 kbar pressure, with various amounts of water added, after Eggler and Wendlandt (1979). Abbreviations as in Figure 8.1. CM, magnesite; KS, kalsilite; SA, sanidine; L, liquid; LHZ, garnet + OPX + CPX + OLIV.

3. The melt is enriched in CO_2 relative to the co-existing vapor and becomes more olivine-rich with increasing pressure regardless of the H_2O/CO_2 ratio of the system. Melting is isobaric and invariant, the liquid and vapor composition being buffered by the carbonate phase. The solidus is thus a ZIVC solidus (Eggler 1977) or a buffered melting curve (Wyllie 1979).
4. An extensive supra-solidus field of garnet exists at 55 kbar pressure. Eggler and Wendlandt (1979) interpret this to indicate that garnet megacrysts are cognate with kimberlite magma.
5. The supra-solidus and sub-solidus phase assemblages indicate that kimberlite could have formed in equilibrium with a garnet lherzolite at 55 kbar but not 30 kbar pressure.
6. During melting, dolomite and phlogopite are consumed prior to other phases (Figure 8.10). Initial carbonate-rich liquids will thus become increasingly richer in SiO_2 as melting progresses.

8.1.4.4. Melting Behavior of Anhydrous Kimberlite

Ito *et al.* (1968) have determined the melting and phase relationships of an anhydrous kimberlite at pressures from 42 to 88 kbar. The sample used in the investigation was from the Dutoitspan mine and contained 11.2 wt % total volatiles before dehydration and decarbonation. This kimberlite was undoubtedly contaminated with crustal material in that it contains 6.98% Al_2O_3, 2.04% Na_2O and has a contamination index (Section 7.2.1; Clement 1982) of 1.89. The assemblage olivine–garnet–clinopyroxene plus a trace of kalsilite is stable at the solidus from 42 to 50 kbar. Above 50 kbar, only olivine, garnet, and clinopyroxene are stable. Melting of the kimberlite begins at 40 kbar at 1450°C and at 70 kbar at 1750°C. Olivine is the initial liquidus phase at all pressures below 80 kbar. At 88 kbar olivine and garnet crystallize simultaneously.

The study is not especially relevant to kimberlite crystallization at high pressures in that CO_2 and H_2O are absent and solidus temperatures are consequently very high. The phase relationships do however suggest that olivine and garnet may be high-pressure liquidus phases.

8.1.5. Partial Melting of the Upper Mantle

The experimental studies cited above are in agreement with petrological observations that CO_2 is present in the mantle and must play some role in the formation of highly undersaturated magmas (Wyllie 1977, Brey 1978, Olafsson and Eggler 1983). The restriction of the sources of hydrous and oversaturated-

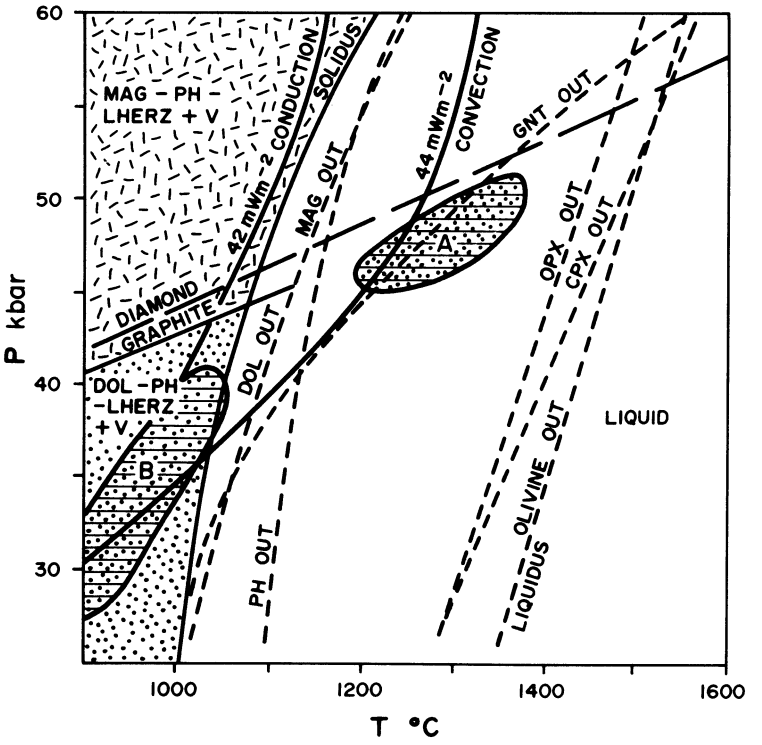

Figure 8.10. Phase relations of a kimberlite composition containing 5.0% CO_2 and 5.0% H_2O (wt.) interpolated and extrapolated from Figures 8.9A and 8.9B. Representative shield geotherms are from Gurney and Harte (1980). Field of equilibration (Wells–Wood) of porphyroclastic and mosaic-textured (A) and granular-textured (B) garnet lherzolites from Thaba Putsoa and Mothae (Boyd and Nixon 1975).

to-slightly undersaturated magmas to relatively high levels in the mantle, and the eruption of CO_2-bearing highly undersaturated magmas from much greater depths, provides strong support for the concept of carbonation of the upper mantle at pressures above approx. 25 kbar.

Olafsson and Eggler (1983) have also noted that the presence of diamond or graphite is not diagnostic of reducing conditions and the absence of carbonates. The co-existence of elemental carbon and carbonate can be predicted if oxygen fugacities are buffered by enstatite–magnesite–olivine–graphite/diamond (EMOG/EMOD) assemblages (see Section 9.10.1).

A troubling aspect of the carbonation hypothesis is that samples of carbonated mantle have not yet been found. This is surprising in view of the fact that only small amounts of CO_2 are required to form carbonate. Mantle-derived

xenoliths commonly contain phlogopite and/or potassian titanian richterite but not dolomite or magnesite. The single exception is the report by McGetchin and Besancon (1973) of two calcite inclusions and one dolomite inclusion in chromian pyrope garnets from the Cane Valley diatreme, Utah. These authors suggest that the carbonates are primary and that the pyrope is derived by the disaggregation of a carbonated garnet lherzolite.

Wyllie (1978) believes that the general absence of carbonates in mantle-derived xenoliths is due to their rapid dissociation during transport from depth and the impossibility of metastably quenching the carbonated assemblage. Alternatively, oxygen fugacities in the lower lithosphere may stabilize elemental carbon rather than carbonates (Section 9.10.1). Carbonates may not be stable in the magmas derived from carbonated mantle and small amounts of dolomite or magnesite present in xenoliths will dissociate during transport or subsequent serpentinization.

The experimental studies demonstrate that, at the depths at which kimberlites are generated (Figures 8.10 and 8.11), phlogopite and a carbonate mineral are likely to be present at the solidus. Amphibole may or may not be present (Figure 8.6). The presence of these minerals will influence the character of the magma derived by the partial melting of carbonated peridotite at the vapor-buffered solidus. Importantly, solidus temperatures and melt compositions will vary principally as a function of the pressure of magma generation and will be independant of volatile composition (Wendlandt and Eggler 1980b).

Magnesite, dolomite, amphibole, and phlogopite should melt at the solidus (Figure 8.10). If the melting process is invariant and isobaric (ZIVC-type solidus), a phase should melt completely and produce an appropriately large amount of liquid. This observation is important in that it alleviates the problems associated with the extraction of small amounts (<1%) of magma from the mantle. The formation of relatively large amounts of eutectic-like melts is, moreover, in agreement with conclusions drawn from the rare earth element geochemistry of kimberlite (Section 7.3.4.1) which indicates that the REE contents and distribution patterns *might* originate by 1%–8% partial melting of a metasomatized phlogopite-bearing source.

The melting process is not simple, the nature of the products and the residual phases being determined by the presence or absence of a vapor at the onset of melting and whether or not any of the phases melt incongruently (Wendlandt and Eggler 1980b, Olafsson and Eggler 1983). As yet the compositions of the melts produced by the melting of natural peridotite or their synthetic analogues in the presence of CO_2 and H_2O have been inadequately characterized. This is a consequence of their small volume and failure to quench unambiguously to a glass (Wendlandt and Eggler 1980b). General principles indicate that melts derived from phlogopite peridotites or carbonated peridotites will be K_2O and MgO-rich or carbonate-rich, respectively. The MgO/CaO ratio of the latter will

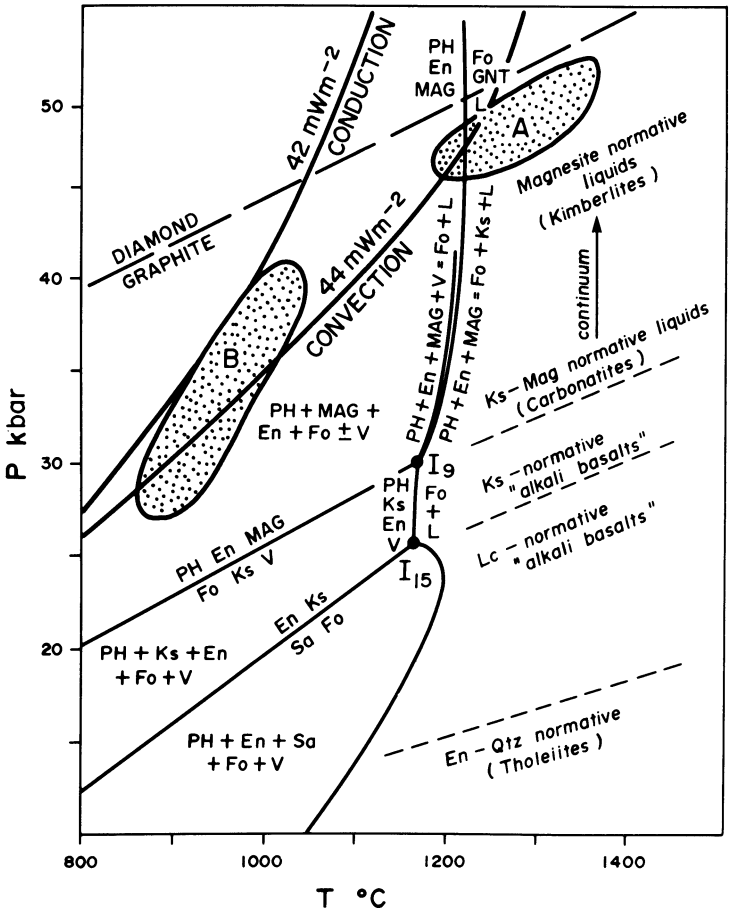

Figure 8.11. Phase relations and reactions in the system $KAlSiO_4$–MgO–SiO_2–H_2O–CO_2 after Wendlandt and Eggler (1980b). The normative composition of liquids produced by melting near the solidus is shown to the right of the solidus. Sub-solidus assemblages are stable in the presence of small amounts of volatiles. Geotherms and lherzolite equilibration fields as in Figure 8.10.

depend upon whether dolomitic or magnesitic solid solutions are stable at the solidus.

It was recognized by Wyllie and Huang (1975a,b, 1976) that initial melts in the system CaO–MgO–SiO_2–CO_2 will be carbonate rich and that increased degrees of melting will lead to increasing MgO and SiO_2 contents. These observations prompted Wyllie and Huang (1975a,b) to state that increasing degrees of partial melting of carbonated mantle at depths greater than 80 km will result in the successive formation of carbonatite, kimberlite, and basaltic magmas. The

initial carbonate-rich melts are termed haplocarbonatites by Wyllie and Huang, but no agreement has been reached upon the actual composition of these liquids (Wyllie and Huang 1975b, Eggler 1976). Carbonate-rich ultrabasic liquids with normative larnite are termed haplokimberlites by Wyllie and Huang (1975b) although the composition of these liquids has not been determined.

Holloway and Eggler (1976) showed that the liquid produced by the melting of phlogopite–dolomite–garnet lherzolite at 1125°C at 30 kbar was enriched in CO_2 and probably of melilititic composition. The initial melting was eutectic-like. At temperatures above the solidus, phlogopite or dolomite melt out over a temperature range of 100°C and produce a diversity of liquid compositions depending upon the bulk composition. Brey and Green (1977) concluded that a Tasmanian olivine melilitite could have been derived by 5% partial melting of pyrolite at 27 kbar at 1160°C with 7%–8% H_2O and 6%–7% CO_2 dissolved in the melt. Subsequently, Brey (1978) proposed that the MgO/CaO ratios of upper-mantle-derived melts depended upon the nature of the carbonate present in the source. Increasing MgO/CaO and (CaO + MgO)/SiO_2 ratios in melilititic magmas were correlated with increasing amounts of CO_2 in the source, decreasing degrees of partial melting, or increasing depth of origin. A dolomite-bearing peridotite was proposed as a source for all types of melilitite. To account for the greater MgO/CaO ratios of kimberlites, Brey (1978) inferred that they were produced at greater depths (>35 kbar) in the stability field of magnesite. Brey *et al.* (1983) believe that near solidus liquids at depths greater than 100 km are highly magnesian and enriched in incompatible elements, but are relatively poor in CaO and Al_2O_3. These liquids described as "kimberlitic" are considered to be in equilibrium with olivine, pyroxenes, garnet, phlogopite, and possibly ilmenite.

Figure 8.10 shows the position of Eggler and Wendlandt's (1979) cobaltian kimberlite solidus with respect to continental shield geotherms, and the equilibration pressures and temperatures of mantle xenoliths that have been transported in kimberlites. The figure demonstrates that partial melting of phlogopite magnesite peridotite will produce liquids rich in carbonate, K_2O, and MgO as phlogopite and magnesite melt at the solidus. Increased degrees of melting will result in the liquids becoming increasingly SiO_2 rich. The disposition of the geotherms indicates that melting could occur at pressures of 35–50 kbar at 1000–1300°C. These values are in accord with the equilibration conditions of garnet lherzolite xenoliths.

Wendlandt and Eggler (1980b) have demonstrated that in the system $KAlSiO_4$–MgO–SiO_2–H_2O–CO_2 the composition of near solidus melts is dependent upon the pressure of melting. At low pressures (<30 kbar) melts are carbonate-free and oversaturated-to-undersaturated "haplobasaltic" compositions. At higher pressures (>30 kbar) carbonate is stabilized at the solidus by a carbonation reaction which intersects the solidus at I_9 (Figure 8.11). Small degrees of partial melting at pressures just above I_9 result in carbonatitic melts.

With increasing pressure the supra-solidus stability of phlogopite decreases and the melt becomes increasingly silicic and potassic as this phase melts. Wendlandt and Eggler (1980b) therefore propose that a continuum exists between carbonatitic melts at low pressures (30 kbar) and kimberlitic melts at higher pressures (50 kbar). Figure 8.11 shows that the intersection of the 44-mW m^{-2} geotherm with the solidus, occurs at the regions in which Wendlandt and Eggler predict that kimberlite melts might be formed. Similar pressures and temperatures are defined by the equilibration conditions of the high-temperature Lesotho lherzolite xenolith suite (Figure 8.11). These conditions of formation are remarkably similar to those predicted by the melting experiments on cobaltian kimberlite, despite Wendlandt and Eggler's (1980b) system not being analogous in bulk composition to mantle lherzolite. Wendlandt and Eggler (1980b) propose that at these pressures and temperatures phlogopite is not stable and that mantle lherzolites will contain traces of an intergranular liquid rich in K_2O and H_2O. Further melting of this mantle will generate carbonate-rich potassic liquids of kimberlitic composition. The experimental study also demonstrates that olivine and pyrope could be high-pressure liquidus phases.

In summary, the high-pressure experimental data suggest that kimberlites may be produced by the eutectic-like melting of phlogopite magnesite garnet lherzolite at pressures on the order of 40–50 kbar at 1000–1300°C. The initial stages of melting of such a lherzolite might be envisaged to produce a sequence of liquids that would range from carbonate liquid to carbonate kimberlite to kimberlite as the degree of melting increases. Importantly, all of these melts will be able to reconcentrate the carbonate in their differentiates at low pressures. Melilitites appear to be formed at lower pressures (25–35 kbar) than kimberlites from a dolomitic garnet lherzolite source that does not contain phlogopite. A continuum of compositions might be expected to occur between melilitites and kimberlites, but this has not been recognized in nature. This may be due to the presence of low-temperature cusps on the solidus which confine magmas to discrete compositions at particular depths (Wendlandt 1984).

8.2. EXPERIMENTAL STUDIES AT LOW PRESSURES

A substantial proportion of the major oxide composition of kimberlite can be represented by the quinary system $CaO–MgO–SiO_2–H_2O–CO_2$ (CMSHC). Although lacking in iron and titanium, this system provides insights into the nature of, and constraints upon, the low-temperature crystallization of kimberlite. Unfortunately, liquidus phase relationships in this system are extraordinarily complex. Some appreciation of crystallization processes in CMSHC can be gained by initially considering the quaternary bounding systems $CaO–MgO–H_2O–CO_2$, $CaO–MgO–SiO_2–H_2O$, and $CaO–MgO–SiO_2–CO_2$.

8.2.1. CaO–MgO–H_2O–CO_2 (CMHC)

CMHC illustrates important aspects of crystallization in systems containing two volatile phases. Figure 8.12 depicts the four ternary bounding systems which are combined as an isobaric quaternary system in Figure 8.13 (Wyllie 1965). Within the ternary systems vapor-saturated liquidus field boundaries give the compositions of liquids in equilibrium with a crystalline phase and vapor. They represent the maximum amounts of volatiles which can be dissolved in the liquid at the given pressure. Extension of these ternary univariant field boundaries into the quaternary system produces an isobaric divariant surface termed the *vapor-saturated liquidus surface* (VSLS). This is not a normal liquidus surface, in that the liquids which lie on this surface co-exist with a crystalline phase and a vapor phase (Wyllie and Haas 1965). The composition of this vapor is given by the complementary isobaric divariant vaporous surface (VS) that extends between H_2O and CO_2. This surface lies close to the join H_2O–CO_2 because of the low solubility of CaO and MgO in H_2O or CO_2. Compositional volumes and surfaces occurring on the CaO-rich side of the VSLS give the phase relationships between

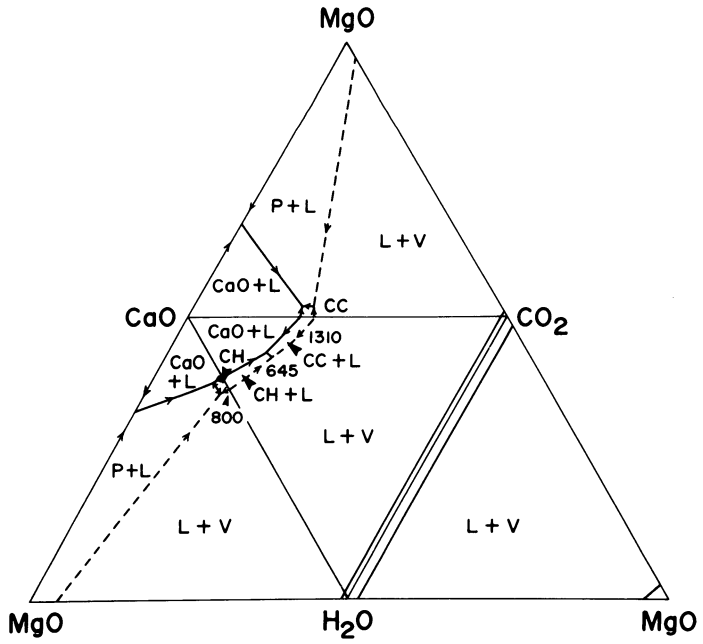

Figure 8.12. Phase relationships in the ternary bounding systems of the quaternary system CaO–MgO–H_2O–CO_2 at 0.5 kbar pressure after Wyllie (1965) and Franz (1965). P, periclase; CC, calcite; CH, portlandite; L, liquid; V, vapor. Dashed line is the vapor-saturated liquidus field boundary.

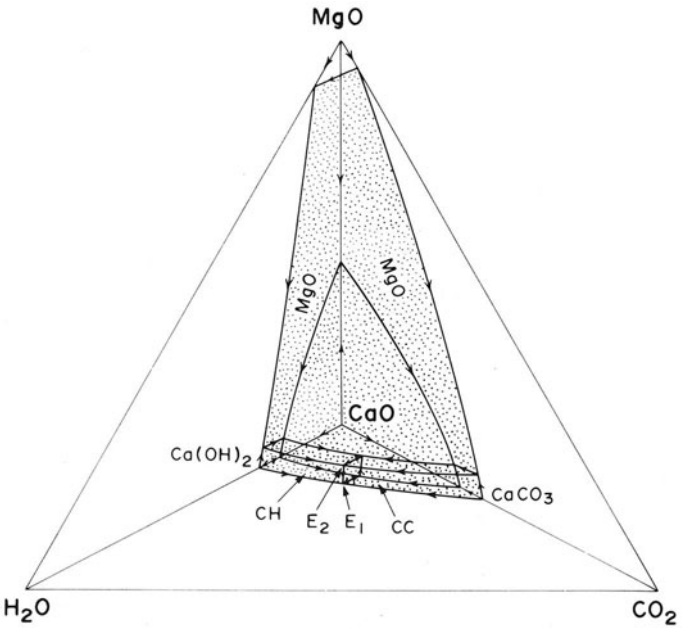

Figure 8.13. Phase relationships in the quaternary system CaO–MgO–H_2O–CO_2 at 0.5 kbar pressure after Wyllie (1965). Stippled surface is the vapor-saturated liquidus surface. E1 and E2 are quaternary eutectics. CC, calcite; CH, portlandite.

crystals and liquids lacking vapor. The VSLS includes fields for the primary crystallization of periclase, portlandite, and calcite at 0.5 kbar (Figure 8.12).

Bulk compositions lying on the H_2O–CO_2 side of the VSLS at high temperature will initially be liquid plus vapor. With falling temperature, vapor is evolved from the liquid, and the liquid moves onto the VSLS where crystallization of solid phases begins. During crystallization the liquid follows a path on the VSLS while the vapor follows a corresponding path on the vaporous surface until all the liquid is used up. At this point crystalline phases co-exist with vapor. During the crystallization process vapor is continually evolved and the composition of the vapor phase is continually changing. In CMHC, as liquids evolve from the carbonate to the hydrate side of the tetrahedron, the vapor changes from being CO_2 rich to H_2O rich. At the quaternary eutectics (E_1, E_2, Figure 8.13) the vapor is extremely rich in H_2O (<2 wt % CO_2) despite coexisting with calcite and a liquid containing abundant carbonate.

At low pressures, dolomite does not occur as a liquidus phase as the dissociation curve for dolomite does not intersect the liquidus surface. Wyllie's

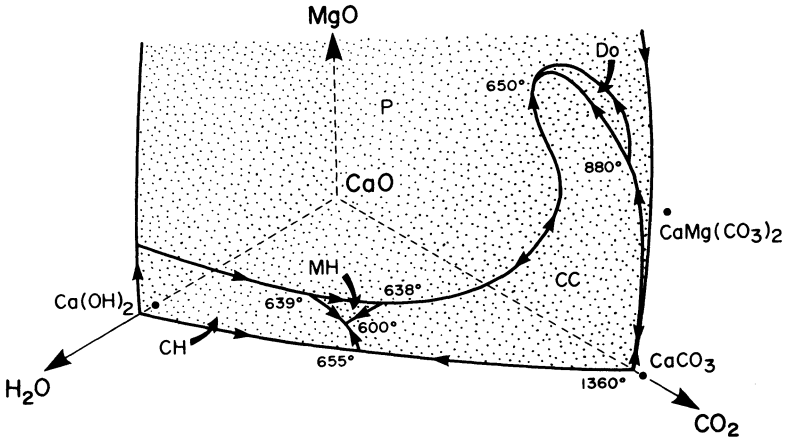

Figure 8.14. Phase relationships for the system CaO–MgO–H_2O–CO_2 at 2 kbar pressure after Fanelii *et al.* (1985). Stippled surface is the vapor-saturated liquidus surface. P, periclase; DO, dolomite; MH, brucite; CC, calcite; CH, portlandite.

(1965) analysis of the system suggested that brucite and dolomite should appear on the VSLS with calcite at high pressures. Boettcher *et al.* (1980) studied the solidus of CMHC to 40 kbar pressure but did not find dolomite co-existing with liquid. Fanelli *et al.* (1985) have shown that this is due to the presence of a previously undetected eutectic at 650°C in CMHC at higher pressures (Figure 8.14). This eutectic, involving calcite, dolomite, and periclase, is separated from the 600°C calcite, brucite, and portlandite eutectic by a thermal divide on the calcite–periclase field boundary at about 900°C (Figure 8.14). Depending upon their bulk composition, liquids will evolve toward either of these low-temperature regions. Fanelli *et al.* (1985) show that at 2 kbar pressure calcite and dolomite can crystallize together from about 880–650°C. Liquids with high Mg/Ca ratios will precipitate calcite with very low $MgCO_3$ contents.

Several features of CMHC are relevant to the crystallization of kimberlites, given the assumption that in the natural systems periclase is represented by spinels (magnesian ulvöspinel-magnetite) and brucite by serpentine. Petrographic studies have shown that the sequence spinel (magnetite), calcite, calcite plus serpentine, serpentine is observed during the final stages of groundmass crystallization. Dolomite is not found. These observations indicate that the bulk compositions of kimberlite liquids are such that they evolve toward the natural analog of the calcite–brucite–portlandite eutectic or the calcite–periclase–portlandite eutectic, thus explaining the absence of dolomite. The assemblage spinel, calcite, and serpentine does not occur together, indicating that crystallization is non-equilibrium. The synthetic system suggests that calcite can crystallize alone down to very low temperatures (<650°C) after the initial crystallization of mag-

netite and crossing of the periclase (magnetite)–calcite field boundary. Conditions suitable for the crystallization of portlandite are never apparently reached in natural systems. The newly recognized eutectic (Fanelli *et al.* 1985) is more appropriate as an end point for the evolution of carbonatite magmas than kimberlitic magmas.

Late-stage vapors in CMHC are H_2O rich. These may interact with previously formed crystals and result in the resorption of calcite in late-stage segregations or the sepentinization of olivine. After crystallization these H_2O-rich vapors will co-exist with the sub-solidus assemblage and produce post-consolidation deuteric alteration effects, e.g., further serpentinization.

Crystallization at the VSLS takes place with evolution of vapor. This may result in turbulence and boiling of the liquids and generation of conditions suitable for the formation of globular segregations.

In the experimental studies it is not possible to quench the liquids to glasses. Instead, fine grained aggregates of crystalline phases are formed. Quenched vapor deposits consist of amorphous isotropic aggregates (Boettcher *et al.* 1980). These observations may explain the absence of glassy selvedges to kimberlitic dikes, and the lack of glassy extrusives or pyroclastic shards. The quenching of a vapor phase containing dissolved Ca–Mg, etc., has direct application to the interclast matrices of diatreme facies kimberlites (see Section 3.6.2).

All of the above features of CMHC are present during the crystallization of more complex systems.

8.2.2. $CaO–MgO–SiO_2–H_2O$ (CMSH) and $CaO–MgO–SiO_2–CO_2$ (CMSC)

The system CMSH investigated by Franz (1965) and Franz and Wyllie (1966), is illustrated in Figure 8.15. The VSLS is divided into two regions by a thermal barrier on the liquidus which corresponds to the temperature maximum along the join Ca_2SiO_4–MgO in the anhydrous system. The vaporous surface occurs as a small surface close to the H_2O apex. Phase relationships above the thermal divide (XYB) are similar to those of the anhydrous system. Liquidus temperatures are slightly reduced as a result of the dissolution of a small amount (<5%) of H_2O in the liquid: no new phases are introduced. Only two compounds, dicalcium silicate (Ca_2SiO_4) and periclase (MgO), have stability fields on the VSLS which straddle the thermal divide. Phase relations below the divide (XYB) are more complex than in the anhydrous system due to an increase in size of the stability field of Ca_2SiO_4, elimination of Ca_3SiO_5 and CaO as VSLS phases, and the appearance of calciochondrodite $[Ca_5(SiO_4)_2(OH)_2]$ and portlandite $[Ca(OH)_2]$ at low temperatures. The composition of portlandite marks the maximum amount of H_2O that can be dissolved in the liquids on the VSLS in CMSH. The lowest temperatures on the VSLS occur at 725°C at a quaternary eutectic involving portlandite, calciochondrodite, periclase, vapor, and liquid.

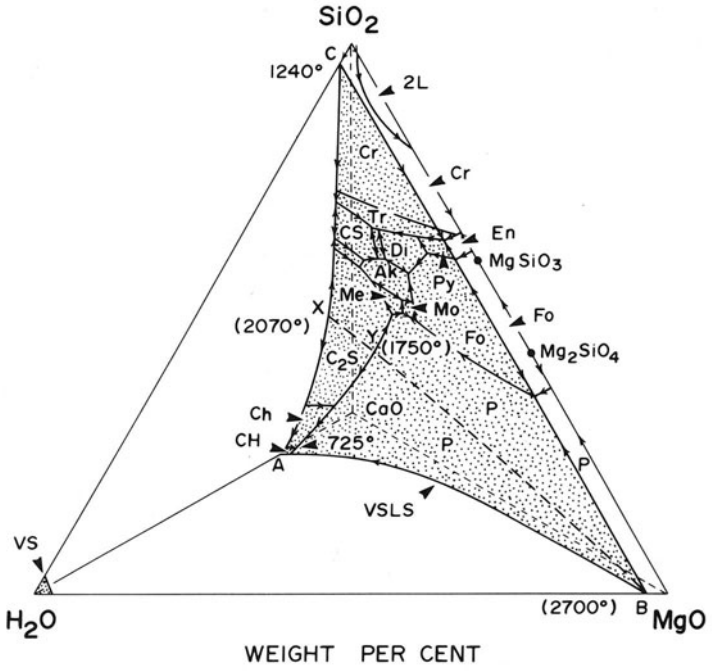

Figure 8.15. Phase relationships for the system CaO–MgO–SiO_2–H_2O at 1 kbar pressure after Franz and Wyllie (1966). VSLS, vapor-saturated liquidus surface; VS, vaporous surface. The dashed line XYB marks a thermal maximum on the VSLS. Cr, cristobalite; Tr, tridymite; Cs, wollastonite; Di, diopside; En, enstatite; Py, pyroxene; Fo, forsterite; Ak, akermanite; Mo, monticellite; Me, merwinite; C_2S, larnite; Ch, calciochondrodite; CH, portlandite; P, periclase; L, liquid.

The system CMSC has not been experimentally investigated. The phase relationships shown in Figure 8.16 are hypothetical and modeled upon CMSH and the ternary bounding systems (Franz 1965). The principal differences between CMSC and CMSH are the replacement of portlandite by calcite and calciochondrodite by spurrite [$Ca_5(SiO_4)_2.CO_2$]. Liquidus temperatures are higher than in CMSH as a result of CO_2 being less soluble in the liquids than H_2O. The lowest temperature on the VSLS is at a quaternary eutectic involving calcite, spurrite, periclase, vapor, and liquid at about 1180°C. The thermal divide (X′–X″–X, Figure 8.16) between Ca_2SiO_4-MgO is believed to persist.

CMSH and CMSC have several features in common. The most significant with respect to kimberlite is the presence of the thermal divide. Franz and Wyllie (1966) believe that this barrier persists on the VSLS over a very wide range of pressures. Liquids cannot cross this barrier by either fractional or equilibrium crystallization; thus, high-temperature silicate liquids with compositions richer

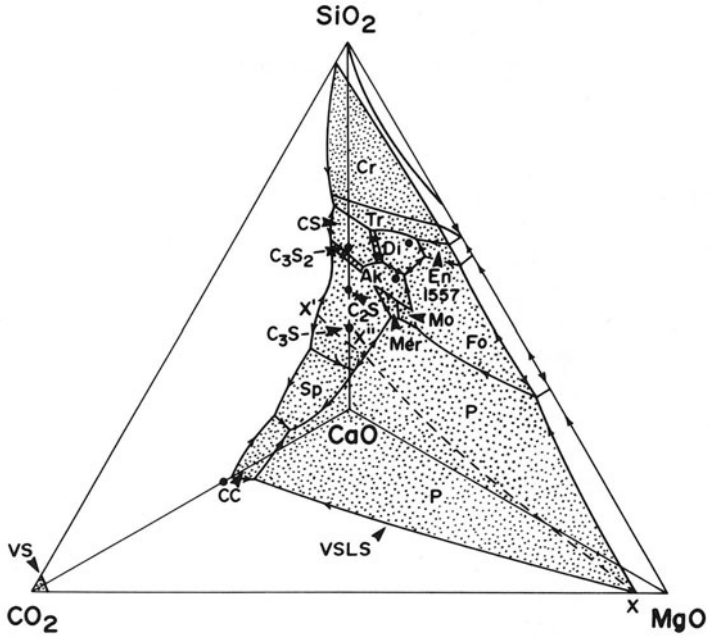

Figure 8.16. Phase relations for the system CaO–MgO–SiO_2–CO_2 at 1 kbar pressure after Franz (1965). The dashed line X′–X″–X marks a thermal divide on the VSLS. C_3S_2 = $Ca_3Si_2O_7$, C_3S = Ca_3SiO_5, Sp = spurrite. Other abbreviations as in Figure 8.15.

in SiO_2 than this barrier, are unable to evolve to liquids which are capable of crystallizing hydrated or carbonated phases. Their crystallization will produce silicates that co-exist with a vapor. Liquids with compositions poorer in SiO_2 than the barrier can, upon fractional crystallization, form residua which will crystallize hydrates and carbonates.

The thermal divide indicates that a high-temperature volatile-bearing magma which initially crystallizes olivine, pyroxenes, and monticellite is incapable of differentiating to a calcite-bearing residuum. This conclusion is at variance with the crystallization history of kimberlites. The thermal barrier must therefore be inoperative in more complex Fe–Ti-bearing systems, or the bulk composition of kimberlite liquids must lie below the SiO_2 levels of the barrier.

Most of the minerals crystallizing on the low-temperature side of the thermal divide, e.g., larnite, calciochondrodite, portlandite, and spurrite, are never found in kimberlite. As CMSH and CMSC are relatively good analogs of kimberlite compositions, the absence of these phases must indicate that the bulk composition of kimberlite liquids lies toward the MgO apex of the system.

8.2.3. $CaO–MgO–SiO_2–H_2O–CO_2$ (CMSHC)

The quinary system CMSHC is basically a combination of CMSH and CMSC. It contains a VSLS upon which a thermal divide exists. Low-temperature liquids will be able simultaneously to precipitate hydrated and carbonated phases. Crystals and liquids will co-exist with a vapor phase whose composition lies on the vaporous surface extending between CO_2 and H_2O. Residual vapors can be expected to be H_2O-rich.

Franz (1965) and Franz and Wyllie (1967) have investigated the join calcite–portlandite plus various amounts of forsterite. One such temperature-composition section is illustrated in Figure 8.17. In this "pseudobinary" projection of quinary phase relationships, the horizontal lines give the temperature of isobaric invariant six-phase assemblages. Above and below these lines are fields of isobaric univariant five-phase assemblages.

Particularly important with respect to kimberlites is the termination of a decarbonation reaction at an invariant point involving a liquid (Figure 8.18).

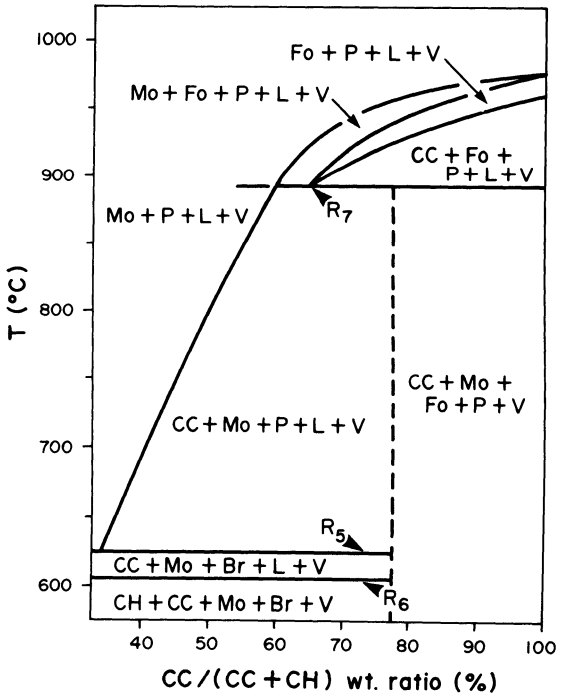

Figure 8.17. Phase elements intersected by the 30 wt % forsterite TX section on the composition triangle portlandite(CH)–calcite(CC)–forsterite(Fo) in the system $CaO–MgO–SiO_2–CO_2–H_2O$ at 1 kbar pressure after Franz (1965) and Franz and Wyllie (1967). Mo, monticellite; P, periclase; V, vapor; L, liquid. Point R_7 is an invariant point where CC, Mo, Fo, P, L, and V coexist.

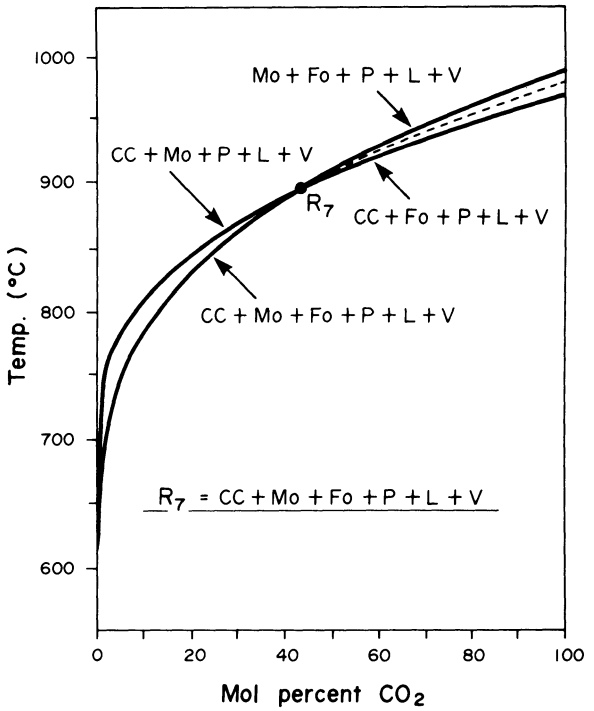

Figure 8.18. T–X section of the quinary system CaO–MgO–SiO_2–CO_2–H_2O at 1 kbar illustrating the intersection of a decarbonation reaction with the liquidus that permits calcite and forsterite to crystallize together. Univariant assemblages are located about the invariant point R_7 which corresponds to a similar point in Figure 8.17.

The intersection of this reaction with the liquidus occurs on the low-temperature side of the thermal divide and permits calcite and forsterite to crystallize together.

Phase relationships in CMSHC are best represented by a flow sheet. Figure 8.19 shows the flow sheet for a portion of the VSLS for MgO-rich liquids poorer in SiO_2 than the Ca_2SiO_4–Mg_2SiO_4 join. Isobaric univariant assemblages are represented by lines, isobaric invariant assemblages by points. Upon fractional crystallization, liquids will move toward the vapor-saturated quinary eutectic R_6, where portlandite, calcite, monticellite, periclase, and brucite co-exist with liquid, and a vapor that is extremely H_2O rich (<0.2% CO_2). The flow sheet indicates that at the invariant point, R_7, forsterite will react with the liquid, and will therefore not be present in low-temperature assemblages. Crystallization paths in this system are very complex and vary depending upon whether bulk composition or vapor composition is held constant.

With increasing pressure, Franz (1965) found that forsterite becomes stable at the solidus (2–3 kbar). This is a consequence of the field of forsterite crystallization becoming larger at the expense of that of monticellite. Franz (1965)

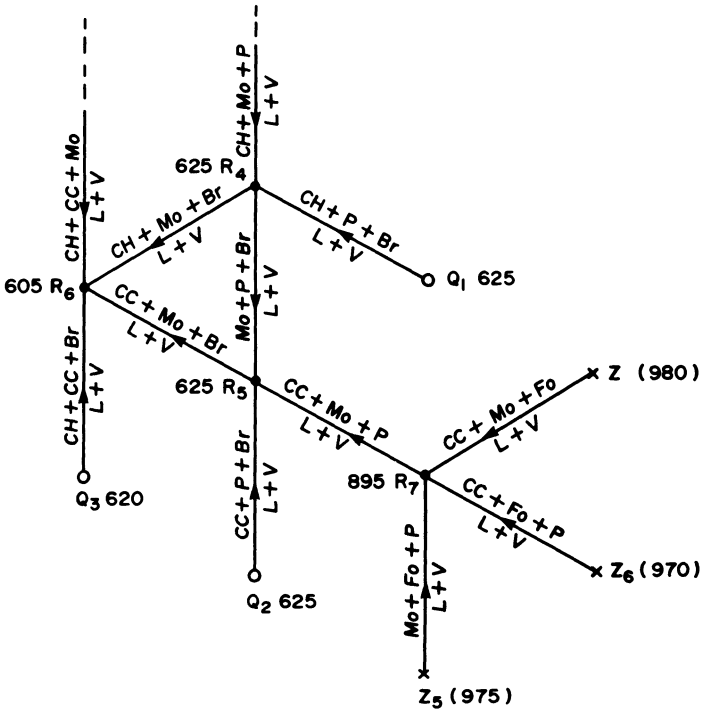

Invariant points

R_4 = CH + Mo + P + Br + L + V
R_5 = CC + Mo + P + Br + L + V
R_6 = CH + CC + Mo + Br + L + V
R_7 = CC + Mo + Fo + P + L + V

Univariant Assemblages (Invariant points in the quaternary bounding systems)

Q_1 = CH + P + Br + L + V
Q_2 = CC + P + Br + L + V
Q_3 = CH + CC + Br + L + V
Z_4 = CC + Mo + Fo + L + V
Z_5 = Mo + Fo + P + L + V
Z_6 = CC + Fo + P + L + V

Figure 8.19. Flow sheet showing univariant and invariant assemblages on the vapor-saturated liquidus surface in a part of the system CaO–MgO–SiO_2–CO_2–H_2O after Franz (1965). Abbreviations as in Figure 8.17. Br, brucite.

demonstrated that forsterite, calcite, and brucite can co-exist with vapor and liquid at temperatures as low as 605°C, down to pressures as low as 2 kbar. Below this pressure monticellite, calcite, and brucite co-exist with liquid and vapor. Polybaric crystallization of liquids containing forsterite crystals, which are precipitating portlandite, calcite, and forsterite from 4 kbar at 620°C, to 2 kbar at 605°C, results in the dissolution of forsterite and the precipitation of monticellite. If pressure is reduced slowly all of the olivine will be resorbed, and at a pressure of 1 kbar at 605°C the liquid will crystallize completely to portlandite, calcite, monticellite, and brucite. If pressure is reduced rapidly, unreacted relict olivine will remain.

Franz's work correctly predicts the observed sequence of orthosilicate formation in kimberlites, assuming polybaric polythermal crystallization. It also demonstrates that low-temperature carbonate-rich silicate liquids are capable of crystallizing olivine, and that their differentiates will precipitate calcite. Significantly, diopside and melilite are *absent* on the low-temperature VSLS. This explains their absence in the groundmass, and supports the hypothesis advanced in Section 3.6.2 that much of the diopside that occurs in kimberlites is a consequence of contamination of the magma by SiO_2-rich materials. (N.B. CMSHC is not applicable to the aluminous potassic magmas that form micaceous kimberlites and in which diopside is common.) Typically, kimberlitic liquids are not sufficiently polymerized to be able to form soro- or inosilicates despite containing dissolved CO_2. Only after the crystallization of olivine, monticellite, apatite, and oxides do the liquids become sufficiently polymerized to form phyllosilicates. Petrographic studies show that olivine, monticellite, and calcite all exhibit a reaction relationship to later liquids. Crystallization paths of kimberlitic liquids thus do not follow field boundaries and/or are non-equilibrium. Crossing of field boundaries on the VSLS by varying the bulk composition and/or vapor composition can result in the sequential non-equilibrium crystallization of olivine, monticellite, and calcite.

Obvious drawbacks in the application of CMSHC to kimberlites are the lack of Ca–Fe–Ti oxides in the synthetic system and the absence of periclase, brucite, and portlandite in kimberlites. The lack of portlandite may be due to failure to attain the extremely H_2O-rich vapor compositions in equilibrium with the final liquids required to form this phase (Wyllie and Biggar 1966). In natural systems periclase might be replaced by Fe–Ti oxides and brucite by serpentine. The general topology of the system may remain intact.

8.2.4. Other Systems

Studies of the system $CaO–P_2O_5–H_2O–CO_2$ have demonstrated that only a limited amount of $Ca_3(PO_4)_2$ is soluble in liquids near the calcite–portlandite join (Wyllie 1966, Wyllie and Biggar 1966). Magmas containing a few wt % P_2O_5 will therefore begin to precipitate apatite before calcite. The work also

shows that calcite and apatite can co-precipitate over a wide temperature range (654– approx. 1150°C). Crystallization in this system terminates at a quaternary eutectic on the VSLS at 639°C where calcite, apatite, portlandite, liquid, and H_2O-rich vapor co-exist. The experimental studies correctly predict the sequence of formation of apatite before calcite as observed in carbonate-rich kimberlites such as the Benfontein (Dawson and Hawthorne 1973) and Wesselton Sills (Mitchell 1984a). The co-existence of apatite and calcite in carbonate segregations indicates that temperatures as low as approx. 650°C are achieved during this stage of crystallization of the groundmass.

Seifert and Von Schreyer (1966) have investigated the system K_2O–MgO–SiO_2–H_2O at 1 kbar at temperatures from 500 to 900°C. Within this system, fields of silicate liquids are found to persist to temperatures (≈700°C) below the thermal divide in CMSHC. It is possible therefore that the addition of K_2O will eliminate this thermal barrier (Wyllie and Biggar 1966). The studies also demonstrate that phlogopite and olivine can crystallize together over a wide temperature range. Yoder and Kushiro (1968) have studied the system Fo–H_2O–(Lc:Ks) at 10 kbar at 1225°C and shown that forsterite and phlogopite can co-exist as liquidus phases. Studies by Luth (1967), Wendlandt and Eggler (1980a), and Arima and Edgar (1983) demonstrate that phlogopite (±olivine) can be a liquidus phase in a variety of magmas over a wide pressure (1–10 kbar) and temperature range (approx. 900–1200°C). The systems investigated are not directly applicable to kimberlites, in that aluminous phases such as sanidine and leucite are present as liquidus phases. They do suggest that phlogopite megacrysts are likely to be early liquidus phases in kimberlite magmas.

8.3. CONCERNING MELILITE

Although some older definitions of kimberlite include the presence of melilite as an essential mineral, e.g., Shand (1934), Milashev (1963), it should be realized that fresh melilite has *never* been reported from a *bona fide* kimberlite as defined by Mitchell (1979a) or Clement *et al.* (1984). Lewis (1897) was the first to suggest that kimberlites might contain melilite. Since that time melilite has achieved a status in kimberlite petrology that is out of all proportion to the evidence concerning its supposed presence. Ideas formed around the premise that melilite is of importance in kimberlite culminate in the Soviet interpretation of the groundmass as a melilitite (Section 2.6.2) and in attempts to link kimberlites and olivine melilitites as consanguineous magmas by complex petrogenetic schemes (McIver and Ferguson 1979).

The melilite hypothesis originated as a result of the observation by Wagner (1914) that lath-shaped crystals of calcite occurring in the Franspoort dike must be pseudomorphs after some pre-existing CaO-rich mineral such as melilite.

Similar pseudomorphs have been described from the Kadi, Schuller and Jagersfontein kimberlites by Williams (1932) and from Mukorob by Frankel (1956).

The pseudomorphed melilite hypothesis gained considerable support on the following grounds:

1. The prevailing dogma until 1960 was that calcite could never crystallize as a primary magmatic mineral. This viewpoint was ardently promulgated by Shand (1934), who was opposed to a magmatic origin for carbonatites.
2. There is a geographic juxtaposition of melilitite and kimberlite petrographic provinces in southern Africa. This spatial relationship is tacitly assummed to have some petrogenetic significance (Taljaard 1936, McIver and Ferguson 1979, McIver 1981). A similar disposition of magma types has also been recognized in Siberia (Lebedev 1964, Egorov 1970).
3. Von Eckermann's (1961, 1967) definition of kimberlites was so broad as to include melilite-bearing alnöites and altered alnöites which possess a superficial petrographic similarity to genuine kimberlites (see Section 2.6.3).

The demise of the pseudomorphed melilite hypothesis commenced with Wyllie and Tuttle's (1960) experimental demonstration that calcite could actually crystallize at low temperatures as a primary liquidus phase, and with the recognition of carbonatite volcanism. The experimental studies of the system CMSHC described above (Section 8.2) demonstrate that melilite is not a liquidus phase on the VSLS at low temperatures, and indicate that calcite is a primary phase. Consequently, optically homogeneous calcite laths are now interpreted to have crystallized directly from carbonate-rich kimberlite magmas, e.g., Benfontein (Dawson and Hawthorne 1973), Jos (Mitchell and Meyer 1980). Importantly, the morphology of the calcite crystals was usually the sole criterion for postulating the presence of earlier melilite. In no case were examples described which contained relict peg structures, relict cores of fresh melilite, or its alteration products such as andradite, xonotlite, and cebollite. Prismatic calcite has been described only from hypabyssal kimberlites and its occurrence in this paragenesis is undoubtedly related to rapid crystallization or quenching (Treiman and Schedl 1983). In some kimberlites, e.g., Swartruggens (Mitchell 1970), Monastery (Sampson 1953), calcite laths appear to have formed by the replacement of phlogopite.

Current opinion holds that melilite does not crystallize from CO_2-rich kimberlite magmas and the focus of attention has now shifted toward explanations of why melilite is absent from kimberlites. The melilite hypothesis, however, lingers on in petrogenetic theories which attempt to derive melilitites from kimberlites or vice versa (see Section 8.4).

Studies of the join $CaO–CaMgSi_2O_6–CO_2$ in the system CMSC by Yoder (1975) have shown that akermanite is not stable in the presence of excess H_2O or CO_2 at pressures above 10.2 kbs or 6.1 kbar, respectively. At low pressure, akermanite is stable only at high temperatures and reacts, upon cooling, with CO_2 to form diopside and calcite. In the presence of H_2O below 685°C akermanite breaks down to monticellite and wollastonite. Yoder (1975) considers that the absence of melilite in kimberlites is due to the presence of CO_2. Only loss of volatiles during transport, or crystallization at low pressures and high temperatures in the absence of excess CO_2 will yield melilite-bearing assemblages in the upper crust.

Moore (1983) suggests that the absence of melilite is due to the crystallization history of kimberlites being unusual with respect to that of melilitites. This is a consequence of the rapid expansion and cooling postulated to occur during fluidized ascent of kimberlite magma from great depths. Moore (1983) believes that kimberlite magmas will not crystallize melilite as phenocrysts at pressures above 10 kbar as Yoder (1975) has shown this to be the maximum pressure at which melilite is stable. Formation of melilite at low pressures does not occur because the pressures and temperatures attained during the fluidized ascent do not correspond to the stability field of melilite, and lie entirely within that of diopside and calcite. Moore's (1983) hypothesis is untenable in that kimberlites are unlikely to be emplaced according to his fluidized intrusion model (see Section 4.4.2). High-temperature melilite-free kimberlites which have not undergone fluidization are present in the hypabyssal zones of diatremes. Moore's (1983) recourse to unusual intrusion conditions is rendered unnecessary by the experimental studies of CMSHC which show that melilite is not a liquidus phase at low temperatures.

Recently Clement (1982) has reported the occurrence of pseudomorphs after a lath-shaped phase in pelletal lapilli from the Koffiefontein and Ebenhaezer kimberlites (Figure 3.7). These are unlike all other pseudomorphs that have been proposed to be after melilite in that they are calcite-free, and consist of a very fine grained intergrowth of serpentine, chlorite, and clay minerals. Clement (1982) believes that a median fracture (relict peg structure) is recognizable in some examples. The laths are strikingly similar in appearance to melilite laths and/or pseudomorphed melilites in pelletal lapilli in Swabian olivine melilitites. Clement (1982) believes that the pseudomorphed mineral is melilite and not phlogopite, diopside, or apatite. If these pseudomorphs are indeed after melilite their mode of formation may be broadly in accord with Yoder's (1975) CO_2-degassing hypothesis. The formation of the lapilli by fluid–coolant interactions, coupled with degassing and contamination of the magma with SiO_2 and Al_2O_3 in the diatreme environment, may have changed the bulk composition of the magma. The liquid composition may have thus been removed from the VSLS and into the melilite stability field above the thermal divide in CMSHC.

The CO_2 degassing hypothesis may not be tenable given that melilite com-

monly co-exists stably with calcite in other parageneses, e.g., melilite laths in a calcite matrix in the Laetolil tuffs (Hay 1978), turjaites (Nielsen 1980), and alnöites (Watkinson and Wyllie 1971).

Lack of melilite in kimberlites may be related to the structure of the liquid, rather than to some degassing process. The structure of liquids is determined in part by their bulk compositions and it is important to note that melilite is common in rocks formed from magmas which are more polymerized than kimberlites, as evidenced by its common association with feldspathoids.

8.4. KIMBERLITES AND MELILITITES

The supposition that kimberlites and melilitites are genetically related stems from the idea that calcite in kimberlites is secondary and pseudomorphs melilite, and from the presence in southwestern Africa of geographically overlapping kimberlite and melilitite provinces (Taljaard 1936, Shand 1947, Marsh 1973, Cornelissen and Verwoerd 1975). The melilite pseudomorph hypothesis has been demonstrated (Section 8.3) to be untenable. The geographic association is unlikely to have any petrogenetic significance given the following:

1. The ages of kimberlite and melilitite emplacement in southwestern Africa differ (Chapter 5).
2. Kimberlite fields and melilitite-bearing petrographic provinces on a worldwide basis show no association in space, time, or tectonic setting. Melilitites are commonly associated with continental margins or rifts.
3. Melilitites are typically accompanied by significant volumes of other alkaline rocks including phonolites, nephelinites, basanites and alkali basalts, e.g. the Urach, Hegau, Balcones, Freemans Cove, Tasmanian, and southwestern African provinces (Spencer 1969, Cornelisson and Verwoerd 1975, Brey 1978, Mitchell and Platt 1984).
4. Garnet lherzolite xenoliths are rare in melilitites and related rocks. When present they have equilibrated at lower pressures (17–32 kbar) and higher temperatures (1130–1350°C) than those found in kimberlites (Sutherland *et al.* 1984). Megacrysts similarly are more aluminous and magnesian-poor relative to those of kimberlites and derived from shallower depths (Ferguson and McIver 1979).
5. Kimberlites do not differentiate to melilite-bearing residua.
6. Proponents of relationships to melilitites do not discuss how small volumes of kimberlite produce, by differentiation, the more voluminous melilitites and related rocks.
7. Experimental studies demonstrate that kimberlites and melilitites are likely to be derived from different sources at different depths. Thus Brey *et al.* (1983) and Brey (1978) consider that melilitites are produced

by the partial melting of dolomite garnet lherzolite at approx. 30–35 kbar pressure. Phlogopite is probably absent from the source. Melilitites are possibly volumetrically more abundant than kimberlites because of their formation in regions where the geotherm is steeper. Larger volumes of magma provide greater opportunities for differentiation as noted by Bailey (1983).

In summary, it would appear that kimberlites and melilitites are not genetically related except in the broad sense that they are both products of partial melting of metasomatized mantle. Despite the above evidence McIver (1981) and Ferguson and McIver (1979) have proposed ingenious schemes that attempt to derive melilitites from kimberlites by fractional crystallization. Such models are apparently an attempt "to save the appearance of the phenomena" (Koestler 1977, p. 77) and attest to the long-term influence of Shand's (1934, 1947) teaching in South African petrological thought.

The fashion in which we think changes like the fashion of our clothes and it is difficult if not impossible for most people to think otherwise than in the fashion of their own period.

George Bernard Shaw

9

PETROGENESIS AND EVOLUTION OF KIMBERLITE MAGMA

9.1. INTRODUCTION

Hypotheses regarding the petrogenesis of kimberlite and its relationships with other magmas have ranged from the commonplace, e.g., fractional crystallization of incompatible element-poor magma (O'Hara and Yoder 1967), to the bizarre, e.g., Mikheyenko's (1977) proposal that kimberlites are sedimentary rocks formed in Archean river deltas which have been subsequently mobilized as sedimentary tectonic breccias. Most petrogenetic schemes bear the imprint of the philosophy prevailing at the time of their introduction. This characteristic is no less true of current ideas than those of the 1930s; thus modern hypotheses, which hinge upon the fashionable concept of a metasomatized mantle as a panacea for all petrological problems, have heralded a resurgence of "Maxwell's Demons" and the eclipse (temporarily?) of fractional crystallization models.

Despite the diversity of opinion most petrologists have placed the sources of kimberlites in the upper mantle. Garnet lherzolites are typically regarded as xenoliths or fragments of source rocks, although some Russian geologists have proposed the existence of garnet peridotite magma (Bobrievich *et al.* 1959b, Marakushev 1982). Eclogites at various times have been regarded as cognate (Williams 1932, O'Hara and Yoder 1967) or xenolithic (Harger 1905, Holmes 1936, Dawson 1980).

9.2. EARLIER HYPOTHESES

Wagner proposed that "kimberlite magma was generated by liquefication consequent upon relief of pressure of potentially fluid portions of a universal zone or couche of holocrystalline peridotite, which at some unknown depth must be assumed to underlie the platform of granite and gneissoid rocks forming the basement of South Africa" (Wagner 1914, p. 117). Pressure relief was believed to result from the uplift of the South African shield in Cretaceous times. Wagner's ideas are remarkably similar to current models of magma generation.

Williams in contrast believed that kimberlite magma was produced by the settling of peridotite, pyroxenite, and eclogite from a reservoir of basic magma situated at some unknown depth. Williams (1932, p. 236) thus states "the crystallization of these ultrabasic rocks must have continued over a very long period during which time the composition of the original magma was undergoing changes until it eventually assumed the composition of kimberlite magma." Williams believes that the ultramafic nodules were cognate cumulates and did not recognize the hybrid nature of kimberlite as a mixture of disaggregated xenoliths transported in an ultrabasic magma.

Holmes (1936) suggested that kimberlites represent a mixture of xenolithic material and an olivine melilitite enriched in H_2O, CO_2, and P_2O_5. Taljaard (1936) and Shand (1934) proposed that kimberlites were merely hydrothermally altered olivine melilitites. These ideas were subsequently incorporated by Russian petrologists into petrogenetic schemes which propose that the groundmass of kimberlite is actually a melilitite. Shand's (1934) and Holmes' (1936) hypotheses survive today in a modified form in the petrogenetic ideas advanced by Yoder (1975), McIver and Ferguson (1979), and McIver (1981), and Moore (1983) which attempt to link melilititic and kimberlitic magmatism (see Section 8.4).

The 1960s saw the introduction of two concepts that have not yet been entirely banished from the pantheon of petrogenetic thought. These are that carbonatites and kimberlites are directly genetically related and that kimberlites are a unique form of cryoclastic volcanism.

Dawson (1966, 1967b) proposed that the incorporation of "crustal granite" in water-rich ankeritic fractions of a carbonatite magma results in reactions that produce ultrabasic rocks. Disruption and rounding of these "skarns" occurs during subsequent fluidized intrusion. The hypothesis, based upon the supposed association of kimberlites and carbonatites in alkaline complexes, is similar to ideas advocated by Holmes (1950) and represents a version of the now discredited limestone assimilation hypothesis of Daly (1933) and Shand (1947). In recognition of the xenolithic nature of garnet lherzolites Dawson (1968, 1971) abandoned the hypothesis, which has many additional petrological and geochemical drawbacks. Petrogenetic schemes that consider kimberlites to be hybrids between carbonatites and garnet lherzolites (Franz 1965, Marakushev 1982) or megacrysts and silicate liquids (Boyd and Nixon 1973) remain in vogue.

Hypotheses which consider kimberlites to be cold intrusions of gases and crystals were proposed by Mikheyenko and Nenashev (1962), Davidson (1967) and Kennedy and Nordlie (1968). These have been found to be untenable in the light of recent studies (Section 4.4.6). Variants still exist in the form of Wyllie's (1980) or McGetchin's (1968) models of kimberlitic magmatism (Section 4.4.2).

Recent hypotheses fall into four categories with respect to the processes responsible for the formation of kimberlitic magmas: hybridization, zone refining, fractional crystallization, and partial melting models. Of these some variety of the latter process is currently the most popular, although it should be realized that no single process can account for all the petrological characteristics of kimberlites (see Section 9.14). All of the models advanced seek to explain the CO_2-rich ultrabasic nature of kimberlite, the dual enrichment of compatible and incompatible elements, the small volumes of magma and the supposed association with carbonatites, melilitites, or basaltic volcanism.

9.3. HYBRIDIZATION

Several hypotheses have proposed that kimberlites are hybrids formed between carbonatite magmas and pre-existing ultramafic rocks. The ideas were formulated as a means of circumventing the difficulties of deriving CO_2-rich magmas from CO_2-poor sources and of providing the high concentrations of Sr, Nb, REE, etc. found in kimberlites. The concepts are rooted in the assumption that carbonatites and kimberlites are associated in alkaline complexes (Dawson 1966, 1967b). Introduction of a carbonatite parent in many respects is unsatisfactory in that no explanations for the origins of these magmas are presented.

Franz (1965) regards all of the ultrabasic inclusions found in kimberlite to be xenoliths of mantle material randomly incorporated into an ascending carbonatite magma. Reaction of the xenoliths with this magma is believed to produce phlogopite. Franz (1965) states that micaceous kimberlites occur in dikes and "basaltic" types in pipes; thus, as the hybrid, essentially micaceous, kimberlite magma nears the surface, dissolved vapor is explosively expelled. This results in the formation of a "basaltic" kimberlite diatreme below a carbonatite tuff cone. The vapor is believed to react with phlogopite and the xenoliths to form olivine, remove H_2O and Al_2O_3, and leave behind calcite and Ca and Mg-silicates in the form of a "basaltic" kimberlite.

Franz' (1965) hypothesis is based upon studies of the system CMSHC (Section 8.2.3) and has the merit of showing that low-temperature liquids, equivalent to the kimberlite groundmass, are possible. Carbonatite is chosen as a parent magma because of the presence of a thermal divide in CMSHC which prevents CO_2-poor ultrabasic magmas from differentiating to carbonate-rich residua. Major drawbacks to the hypothesis include the paucity of H_2O in both

parental components, the lack of petrographic evidence for any of the proposed reactions and the unsubstantiated claim that micaceous kimberlites are precursors to all other types of kimberlites.

Boyd and Nixon (1973) and Nixon and Boyd (1973, p. 75) suggest that "kimberlites originate with the eruption of carbonatite deep within the lithosphere." In their view, kimberlites are hybrids formed between carbonatites and "crystal mush magmas" occurring in a presumed low-velocity zone at 150–200 km depth beneath shield areas. The model is based upon the concept that liquids in partially melted regions of the asthenosphere will migrate upward toward the low-velocity zone where they will collect at the base of the impermeable lithosphere. Crystallization results in the concentration of Fe and Ti and it is within this zone that the megacryst suite is formed. Magmas rising from depth pass through this zone and are contaminated by the addition of residual silicate liquid, megacrysts, and garnet lherzolite xenoliths. Eruption of this mixture as kimberlite then follows. The hypothesis rests in part on the interpretation of the megacryst suite as xenocrysts. The proposal is invalidated if the megacrysts are in fact phenocrysts (see Chapter 6 and Section 9.11.4). Further difficulties lie in the absence of the required low-velocity zone beneath the shields (Bott 1982) and the failure to explain the source of the carbonatite magma involved.

Marakushev (1982) believes that garnet lherzolites crystallize from ultrabasic magmas. Garnets in such rocks are interpreted to be phenocrysts. These magmas can be emplaced in the crust where they crystallize as tubular volcanic pipes or ultrabasic plutons. As a result of differing cooling rates the former retain their diamond phenocrysts while the latter resorb diamond and form barren, layered intrusions. Subsequent replacement of the garnet lherzolite pipes by carbonatites results in the formation of the hybrid kimberlite. Depending upon the degree of replacement, a continuum from garnet lherzolite to kimberlite to carbonatite can be recognized. Marakushev (1982) states that kimberlites contain no high-pressure minerals of their own; they inherit such phases during the replacement of pre-existing rocks. The hypothesis has many detractions, not the least of which is the complete lack of evidence for the existence of garnet lherzolite magma and the failure of Marakushev (1982) to consider all recent petrological and geothermobarometric studies of lherzolites. Why carbonatites should intrude and replace pre-existing garnet lherzolite pipes is not explained.

In summary, the above hypotheses suffer from serious petrological drawbacks and are untenable in the light of recent studies of kimberlites. The discovery of reactions involving CO_2 that lead to carbonation of the upper mantle renders unnecessary the introduction of carbonatite magmas of unknown origin as a source of CO_2. The occurrence of complexly mantled and zoned olivines and phlogopites in kimberlites provides evidence that less extreme forms of hybridization, or mixing of crystals and magmas of similar type, does play some role in the evolution of kimberlite (see Sections 6.5, 6.6, and 9.14).

9.4. ZONE REFINING

Harris and Middlemost (1969) propose that kimberlites are restricted to cratonic areas as a consequence of the low heat flow observed in these regions. They consider that partial melting of slightly hydrated peridotite (0.2% H_2O) is only possible where the geothermal gradient intersects the solidus of that peridotite. This depth is considered to be at about 600 km. Partial melting is thought to give rise to a water-saturated silicate liquid of unspecified composition. This liquid then rises toward the surface by a solution stoping process that is analogous to the industrial process of zone refining. By this mechanism incompatible elements are continuously enriched in the liquid while allowing the major element composition to remain unchanged. As a consequence of the low geothermal gradient the liquid rapidly enters regions of the mantle which have a local temperature that is considerably lower than the solidus of peridotite. The liquid does not crystallize in these regions by virtue of its water content, i.e., the H_2O-saturated solidus lies at a temperature below the ambient temperature. At depths on the order of 200 km the silicate magma is thought to contain about 40% H_2O and to be highly enriched in residual elements. Crystallization of portions of the magma effect further enrichment of incompatible elements until, at depths of about 150 km, the fluid pressure exceeds the local pressure and the magma escapes rapidly to the surface as a fluidized system.

Harris and Middlemost's (1969) hypothesis may be redundant if metasomatized mantle exists as a suitable site for the storage of incompatible elements. Current models of the upper mantle therefore do not envision a 400-km zone of H_2O-poor barren mantle beneath the continental lithosphere. In addition the thermal requirements for zone refining may not be realized. Harris and Middlemost (1969) note that the magma might ascend without much heat loss when the surrounding mantle is at or above the solidus temperatures; however, as partial melting is considered to occur at depths of 600 km, then it follows that most of the mantle above this partial melting zone must be at temperatures below the solidus. Thus it would seem unlikely that a relatively cool magma could rise by solution stoping into the overlying anhydrous peridotite whose solidus is several hundreds of degrees above the water saturated solidus. Even if water in the magma assists in reducing solidus temperatures it would seem unlikely that a small volume of magma, not possessing superheat or continual heat input, would ascend very far from its source without crystallizing completely. Further drawbacks to the hypothesis include the failure to account for the high CO_2 content and hybrid nature of kimberlites. Emplacement as a fluidized drive from 150-km depth is not tenable on the basis of recent studies. Dawson (1980) suggests that the products of zone refining of the mantle might be expected to be abundant, in direct contrast to the insignificant amounts of kimberlite relative to other mantle-derived magmas.

9.5. FRACTIONAL CRYSTALLIZATION

O'Hara and Yoder (1967) have suggested that partial melting (15%–30%) of a four-phase garnet lherzolite at depths of 80–100 km will produce a liquid with the composition of hypersthene normative picrite basalt. Depending upon the amount of melting, the residual solid will be either a more refractory garnet lherzolite or a harzburgite. The initial melt will not be enriched in incompatible elements and may have a low La/Yb ratio. At 30 kbar pressure olivine and orthopyroxene exhibit a reaction relationship to the liquid and are not precipitated (O'Hara 1968). Crystallization takes place instead by the separation of the minerals of bimineralic eclogite (Cr-poor grossular-rich garnet and Cr-poor omphacitic pyroxene). The type of eclogite precipitated is believed to vary in response to changing conditions of crystallization with more calcic and aluminous varieties forming at relatively low pressures and temperatures. The geochemical effect of high-pressure eclogite fractionation is to produce residual magmas enriched in compatible and incompatible elements, akin to kimberlites or K-rich undersaturated mafic lavas. Kimberlites are thus seen to consist of a mixture of xenoliths (garnet lherzolite and harzburgite residua), cognate cumulates (eclogites) and degassed residual fluid.

A variant of this hypothesis proposed by MacGregor (1970) considers that the evolution of the crust–mantle system is a two-stage process in which an initial heating up of the earth, leading to the formation of the crust 2.5–3.0 Ga ago, was followed by cooling until the present thermal regime was attained. Basic magmas formed by the partial fusion of primitive material during the heating stage are thought to have remained trapped in the upper mantle in a liquid state long after their formation. As the mantle cooled these magmas underwent differentiation and changed in composition from picritic to kimberlitic by the separation of harzburgite, garnet harzburgite, garnet lherzolite, eclogite, and kyanite eclogite. These rocks are interpreted to be a sequence of crystal assemblages separating from the differentiating magma. MacGregor (1970) further considers that kimberlites are only intruded about 0.5 Ga after the formation of the crust and that this is the minimum time required for eclogite fractionation to raise the concentration of volatiles and trace elements in the original magmas to the levels observed in kimberlites. The magma is considered to remain fluid over this period by the continuous depression of the solidus by increasing water contents.

O'Hara and Yoder's (1967) hypothesis was developed prior to the recognition of metasomatized mantle and represents an ingenious attempt at explaining how incompatible element-enriched magmas might be produced from parents poor in such elements. Recent studies have demonstrated the impracticality of the concept by showing that eclogites and garnet lherzolites are older than the kimberlite in which they are found and are hence xenoliths, and by the experimental demonstration that olivine is likely to be a liquidous phase in kimberlites

at high pressures (Ito *et al.* 1968, Eggler and Wendlandt 1979). Further problems result from the paucity of REE, K_2O, TiO_2, CO_2, P_2O_5 etc., in the starting material and it is unlikely that extensive eclogite fractionation will ever raise the concentration of these elements to the required levels. For example Mitchell and Brunfelt (1975) and Frey *et al.* (1977) have shown that although eclogite fractionation (>70%) can raise the La/Yb ratios of the residual melt to the desired levels, this is not accompanied by a corresponding increase in La and Yb contents. Cullers *et al.* (1982) further suggest that eclogite fractionation would result in depletion of Co, Sc, and Cr relative to the levels found in kimberlite. O'Hara and Yoder (1967) fail to account for the general paucity of eclogite in general and in particular relative to garnet lherzolite xenoliths in kimberlites. Eclogites should be common in all kimberlites according to their model.

MacGregor's (1970) version of the scheme attempts to circumvent the problem of the age of the xenoliths but in doing so goes against current trends in petrological thought by assuming that garnet lherzolites are cumulates. Even if this were correct it is unlikely that xenoliths could preserve their isotopic heterogeneities over 2.0 Ga if they co-existed with the melts from which they crystallized. The concept of pockets of magma trapped at depth was popular in the early part of this century but has been discounted by most petrologists on the grounds that seismological studies have failed to disclose any such bodies.

A modified version of O'Hara and Yoder's (1967) hypothesis may be applicable to kimberlites if the bimineralic rocks, termed griquaites (*sensu* Nixon 1973c) and consisting of garnets and pyroxenes belonging to the Cr-poor megacryst suite, crystallize from kimberlite magmas at high pressure. The megacryst suite is currently considered to form by the mixing of crystals derived from several batches of kimberlite magma. O'Hara's (1977) model of a continuously fractionating replenished magma chamber may be relevant to these processes.

9.6. PARTIAL MELTING

During the 1970s geochemical studies of a variety of alkaline rocks demonstrated that partial melting of a four-phase garnet lherzolite source was inadequate as a means of explaining their incompatible element contents. The recognition of richterite- and phlogopite-bearing mantle-derived xenoliths (Dawson 1980, 1984) provided petrologists with mineralogical evidence to support the geochemical claims that incompatible elements must reside in hydrous or other phases (Haggerty 1983) in the mantle. Partial melting hypotheses thus suggest that the small volumes and high incompatible element abundances of kimberlites result from limited (<10%) amounts of melting of five- or six-phase lherzolites and that fractional crystallization plays no significant role in the evolution of the magmas until they have been emplaced at high levels in the

crust. The hypotheses differ with respect to the mineralogy of the source rocks, the extent of partial melting and the origin of the incompatible element-bearing phases.

The concept was initially applied to kimberlites by Dawson (1971, 1972) as a consequence of the discovery of primary TiO_2-bearing phlogopites in garnet lherzolite xenoliths from the Lashaine ankaramitic volcano (Dawson and Powell 1969). Similar phlogopites, although not as Ti rich, are common in lherzolite xenoliths in kimberlites (Carswell 1975, Dawson 1984); such micas can clearly act as a source for K, Ti, Mg, Rb, Ba, and H_2O. Dawson (1971, 1972) suggested that the initial stages of melting of a phlogopite garnet lherzolite involve phlogopite plus a small amount of Cr-diopside. The liquid formed would be rich in K, Ti, Ca, Mg, Fe, Cr, and H_2O and capable of crystallizing olivine, chromite, perovskite, and magnesian ilmenite. This melt, modified by the crystallization of these phases together with disaggregated and/or unfused fragments of the source lherzolites, would finally consolidate as kimberlite. Using Griffin and Murthy's (1969) partial melting model, Dawson (1971) suggests that 5%–10% melting of garnet lherzolite containing 0.2%–0.5% phlogopite could produce liquids with the K and Rb contents of kimberlite. Dawson (1972) recognizes that a serious problem with his model lies in finding a source for CO_2. He suggests that carbon may be stored in the mantle as cohenite (FeC), moissanite (SiC), inclusions of CO_2 in minerals or as hydrocarbons.

Mitchell and Brunfelt (1975) in a modification of Dawson's (1972) model suggested that partial melting involves mica, chrome diopside, and garnet, as Kushiro *et al.* (1972) showed that these phases will melt together. Partial melting models of the REE geochemistry showed that although the La/Yb ratios of kimberlites (100) and micaceous kimberlites ($\approx$140) could be produced by 0.7% to 0.9% and 0.3% to 0.4% melting of phlogopite garnet lherzolite, the predicted La and Yb abundances were much lower than actually observed. This conclusion required the further concentration of the REE by volatile transfer or by crystallization of REE-deficient phases without modifications of the La/Yb ratio. Similar conclusions using revised values for distribution coefficients have been arrived at by Paul *et al.* (1977) and Cullers *et al.* (1982). The REE geochemistry illustrates the inappropriateness of considering garnet and pyroxene as the sole sources of the REE. Small volumes of melt are required to produce the light REE enrichment and it is debatable whether such liquids could ever escape from their source regions.

Fesq *et al.* (1975) and Kable *et al.* (1975) have shown on the basis of Nb–Ti, Ta–Ti, Nb–P, and Zi–P correlations (Section 7.3.3) that a phosphate and a titanate are probably sources of incompatible elements in the mantle (Section 7.3.4.1). These conclusions are supported by the discovery of crichtonites, Mg–Cr–ilmenites, Nb–Cr–rutile, and Ca–Cr (Nb, Zr) armalcolite in metasomatized lherzolite xenoliths (Haggerty 1983). Apatite has not yet been reported from this paragenesis.

Section 7.3.4.1 demonstrates that 1%–8% partial melting of an apatite–K–Ti–richterite–garnet lherzolite source with or without phlogopite can account for the observed REE geochemistry of kimberlite.

Dawson (1972) and Mitchell and Brunfelt (1975) consider that the source regions of kimberlite are primitive upper mantle material. Recent isotopic (Section 7.5) and petrological (Haggerty 1983, Bailey 1982, Dawson 1984) studies point to the metasomatic addition of incompatible elements to evolved mantle. This addition may or may not result in partial melting as Sr and Nd isotopic studies have indicated that isolated metasomatized regions of the mantle can persist for long periods before other events trigger magmatism.

The limitations of the earlier versions of the partial melting hypotheses with respect to CO_2 were eliminated with the recognition of carbonation reactions in the system peridotite–CO_2–H_2O (Section 8.1.4). Eggler and Wendlandt (1979), Wyllie (1979), Brey (1978), Brey *et al.* (1983) and Wendlandt and Eggler (1980b) thus suggest that kimberlites are formed by small degrees of partial melting of carbonated garnet lherzolite. The products and nature of this process are described in Section 8.1.5. The major drawback to these attractive hypotheses is the absence of samples of carbonated mantle.

9.7. CAUSES OF MAGMATISM

Partial melting may occur at depths where the geotherm intersects the solidus of a suitable mantle source material; thus, Figures 8.10 and 8.11 indicate that kimberlites might be derived from the partial melting of phlogopite magnesite garnet lherzolite at pressures on the order of 40–50 kbar at 1000–1300°C. Density contrasts will cause the resulting liquid to migrate upward. Melting models of this type as advocated by Dawson (1971), Mitchell and Crocket (1971), and Mitchell and Brunfelt (1975) are based upon Ringwood's (1969) model of the mantle in which a barren dunite or harzburgite overlies fertile garnet lherzolite. Ringwood (1969) envisions that the barren–fertile mantle interface migrates downward as the crust–mantle system evolves. Consequently, the sources of magmas are found at greater depths and may become increasingly alkaline.

Current petrological thought has veered away from such essentially static models of magma generation toward dynamic interpretations that seek to link tectonism and magmatism. Two models currently in vogue, diapir melting and volatile fluxing, are derived from interpretations of vastly different phenomena and are mutually incompatible.

9.7.1. Diapir Melting

This hypothesis suggests that kimberlite magmas are formed by the decompressional melting that occurs when a diapir of mantle material rises to levels

at which it experiences PT conditions above those of its solidus. The model was developed from studies of the textures and equilibration conditions of garnet lherzolite xenoliths and is basically a variant of the mantle plume or hot spot hypothesis. The diapir is assumed to rise from within or below the asthenosphere, the ascent being initiated by a thermal or density perturbation of unknown origin. The model implies that the sources of kimberlites are entirely sublithospheric. Initially proposed by Green and Gueguen (1974), the concept has been widely accepted in recent interpretations of xenolith suites (Hearn and McGee 1984, Harley and Thompson 1984, Mitchell 1984b), or kimberlite petrogenesis (Eggler and Wendlandt 1979, Wyllie 1980, Hunter and Taylor 1984).

In its commonest expression the model assumes that melting occurs within or at the top of a rising diapir. Segregation of the melt in response to density contrasts is followed by rapid ascent of the magma into the upper crust. Ascent within the lower lithosphere may be controlled by pressure-induced fracture propagation (Anderson 1979, Spera 1984). At higher levels the magma may be channeled into pre-existing fracture zones that have been reactivated by uplift. In this scenario the uplift is a consequence of the incidence of the diapir on the base of the lithosphere causing doming and ultimately rifting (Turcotte 1983). Kimberlite magmatism is considered to be focused above the rising diapir.

A significant advantage of this model is that it provides a link between the production of kimberlite magma and the processes leading to the deformation, recrystallization, and metasomatism of the associated mantle-derived xenolith suite. Residual diapiric material may be incorporated into the segregating magma as restite and/or be metasomatized by that magma (Gurney and Harte 1980, Mitchell 1984b). Deformation textures within the xenoliths can be attributed to pre-segregation flow within the diapir or to events associated with magma formation (Green and Gueguen 1974, Harte 1978). Other mantle xenoliths unrelated to the kimberlite-forming diapir may be entrained in the ascending magma (Mitchell 1984b).

A modified version of the diapir hypothesis has been presented by Wyllie (1980), who recognizes that magnesite-phlogopite peridotite is a suitable source for kimberlite magmas. Wyllie (1980), however, suggests that CO_2, H_2O and phlogopite are present as components of a trace magma within a persistent melt zone extending from 120–260-km depth. This zone of melting is a consequence of the shield geotherm over this depth range lying at pressures and temperatures above the solidus of magnesite phlogopite peridotite. Above 120 km the mantle is composed of hornblende or phlogopite dolomite peridotite plus vapor, and below 260 km of phlogopite magnesite peridotite and vapor. Eruption of kimberlite is triggered by the rise of volatiles from deep within the asthenosphere. Partial melting is induced when the vapors reach point A (Figure 8.4B) on the carbonated peridotite solidus. Melting results in a density inversion which is followed by the uprise of a partially melted diapir along the adiabatic path A–B (Figure 8.4B). Within each diapir the percentage of melting increases during

uprise. At point B (Figure 8.4B) the diapir intersects the thermal maximum on the solidus. If equilibrium is maintained the magma will evolve vapor and crystallize completely to a phlogopite dolomite peridotite plus vapor. The hot solid diapir may continue to rise and will, upon re-crossing the solidus at lower pressures, melt to a liquid that is poor in CO_2 and possibly of alkali basaltic composition (Wyllie 1978). Alternatively if the lithosphere is under tension the evolution of vapor at B (Figure 8.4B) could result in crack formation and propagation in the overlying lithosphere as suggested by Anderson (1979). Kimberlites would then erupt explosively as vesiculating partially crystallized magma from depths of about 90 km. At or near the surface the vapor phase composition will change from being CO_2 rich to H_2O rich as a consequence of cooling and crystallization. Initial batches of magma erupted from 90-km depth will not contain diamond as they have equilibrated at depths above the stability field of diamond. Wyllie (1980) believes that once a conduit has been established by the rising diapirs and magmas, further escape of volatiles will trigger diapiric ascent from successively deeper levels and ultimately from within the diamond stability field. Thus, Wyllie (1980) suggests that individual intrusions within a single kimberlite diatreme should contain xenoliths that record successively deeper paleodepths. A corollary to this conclusion is that the initial batches of kimberlite magma in a pipe or cluster should be diamond free.

A further consequence of Wyllie's (1980) model is that if diapirs do not follow an adiabatic ascent path and do not escape from the mantle they will crystallize at depth and release vapor. This vapor will react with mantle minerals and produce hornblende, dolomite, and phlogopite. From this viewpoint mantle metasomatism is a consequence of and not a precursor to kimberlite magmatism.

Wyllie's (1980) model has been widely accepted but has several serious drawbacks including the following:

1. The low-velocity zone beneath the shields is very weakly developed or absent suggesting that these regions do not contain a persistent interstitial melt (Soloman 1976, Bott 1982).
2. The model is critically dependent upon Wyllie's (1978, 1979a,b) version of the carbonated peridotite solidus (Section 8.1.4.1). These postulated phase relationships have not been verified by Olafsson and Eggler (1983) or Brey *et al.* (1983), and the existence of the thermal maximum which plays a pivotal role in Wyllie's model is doubtful.
3. The existence of a zone of persistent melt and its extent is dependent upon the shield geotherm selected. Wyllie (1980) apparently chooses Clarke and Ringwood's (1964) static conduction-related 42-mW m^{-2} shield geotherm. Choice of other solidii or geotherms may or may not result in solidus–geotherm intersections. Wyllie's (1980) static model will be inapplicable to magmatism associated with major thermal perturbations.

4. Wyllie relies upon unknown processes to release volatiles from unknown depths and derived from unknown sources. The latter are suggested to be either deeply subducted "limestones" or dense hydrous magnesian silicates.
5. Wyllie's model of kimberlite emplacement is completely at variance with recent models as outlined in Chapters 3 and 4. There is no evidence to support direct eruption from 90-km depth and certainly none to indicate that successive batches of kimberlite magma within a single pipe have all risen through a single conduit from such depths. The hypothesis totally ignores the hypabyssal infrastructure of kimberlite fields.
6. There is no evidence from the equilibration parameters of xenoliths to suggest derivation from depths as great as suggested by Wyllie, although there does exist the possibility that xenoliths continually re-equilibrate during ascent (Mitchell 1984).

In summary, the above points demonstrate that Wyllie's (1980) version of the diapir model is unacceptable as a means of explaining the genesis and emplacement of kimberlites.

Although the diapiric hypothesis has in general been widely accepted, it has some serious drawbacks. Bailey (1977, 1983, 1984) has consistently attacked the concept and cogently argued that diapirs and hot spots do not exist beneath continents and that all alkaline magmas are derived from intra-lithospheric sources (see Section 9.7.2). Bailey (1984) believes that diapirs rising from great depths fail to account for the widespread, apparently random, distribution of diatremes within some cratons; the narrow depth range of sources as indicated by the xenolith suites; the similar "paleogeotherms" derived from kimberlites of all ages and locations; the lack of associated silicate rocks, the localization of alkaline rocks in linear zones or with rifts; and the repeated intrusion of alkaline magmas at particular sites. Bailey (1984) also requires, in contrast to Wyllie (1980), pre-eruption enrichment of the sources in volatiles and incompatible elements. Other detractions of diapiric and/or plume models with respect to kimberlite distributions are noted in Section 5.3.4.

9.7.2. Volatile Fluxing

For many years Bailey (1964, 1977, 1980, 1982, 1983, 1984) has maintained that the sources of alkaline magmas lie within the lithosphere and are generated as a result of volatile fluxing or focusing. Bailey's ideas stem primarily from his studies of volcanism in eastern Africa.

Bailey's model assumes that for long periods the lithosphere acts as a lid which permits only the pervasive slow leakage of volatiles from the astheno-

sphere. Fractures, developed or reactivated by tectonic processes external to the craton, may penetrate to the base of the lithosphere and provide channels which allow easy escape of the volatiles. These channels then act as a focus for drawing heat and volatiles to one region of the lithosphere–asthenosphere interface. The process results in the build up by metasomatism of the levels of volatile-bearing phases and incompatible elements in regions adjacent to the channel. Ultimately, heating of these regions, in conjunction with the reduction of solidus temperatures as a consequence of metasomatism, culminates in melting and formation of alkaline magmas. The production of low-density hydrous minerals and/or carbonates is believed to cause long-lived uplift, which will persist until prolonged heating results in collapse as a consequence of the decomposition of the low-density metasomatic phases. At this time magmatic activity will cease as the lithospheric lid is sealed.

As applied to kimberlites, Bailey (1980, 1984) believes that the equilibration parameters determined from garnet lherzolite xenoliths represent actual mantle geothermal gradients. These geotherms are believed to define a narrow band of pressures and temperatures that is in grazing incidence with Eggler and Wendlandt's (1979) kimberlite solidus. Volatiles rising along such geotherms will cause metasomatism and ultimately incipient melting in this zone of incidence. Postulated inflection points in the geotherms (Boyd and Nixon 1973, 1975) at about 200-km depth are believed to coincide with the solidus–geotherm intersection. Figure 8.10, incorporating revised equilibration parameters for xenoliths, shows that this intersection might occur at 40 kbar pressure at 1050°C, i.e., at considerably shallower depths than envisioned by Bailey (1980, 1984).

Bailey (1984) suggests that fluids from the deep mantle may be expected to exploit any deep channelways which may be opened up by local lithospheric stresses. Initial batches of volatiles will be consumed in metasomatic reactions, producing a metasomatically veined mantle of the type proposed by Dawson (1984). Eventually saturation will permit fluid to exist in the veins, and melting will occur where these conditions impinge upon the kimberlite solidus. Importantly, the melts are produced in veins and not in the supporting garnet lherzolite mantle. This interlocking system of veins of melt remains trapped in the mantle by virtue of its small volume until major tectonic disturbances of the craton open deep lithospheric fractures. Catastrophic gas release results in the fluidized ascent of the melt together with fragments of the associated mantle. Such volatile fluxing near the kimberlite solidus accounts for the small volumes of magma, the repetitive short-lived activity and the lack of associated magmas. The conditions pre-requisite to the formation of kimberlite magmas are thus a precursor metasomatic event and a low geothermal gradient; conditions realized only in craton interiors. At craton margins higher geothermal gradients result in a greater degree of melting, segregation and differentiation of magmas, increased volatile fluxing (or gas exsolution stoping) and lead to the formation of melilititic, nephelinitic,

and carbonatitic magmas. Bailey's hypothesis has the merit of explaining the regional distribution of alkaline volcanism, the association of such volcanism with lineaments and rifts and the repetition of activity at a particular site.

Drawbacks exist with respect to the integration of the xenolith suite into the model. Recent interpretations of equilibration parameters and textures are not in accord with Bailey's static model of the mantle. Inflected or perturbed limbs of paleogeotherms in particular are considered to result from kimberlite–xenolith thermal and chemical interactions and to have no stratigraphic significance (Mitchell 1984b, Harley and Thompson 1984, Gurney and Harte 1980). Deformation textures are commonly linked to a diapiric flow that is not permissible in Bailey's model.

The differences between the models may be simply ones of perspective rather than of substance. Volcanologists and "volatile fluxers" look down into the lithosphere, while "diapiricists" work upward from the asthenosphere. Both groups make *a priori* assumptions regarding the source depths of xenoliths.

Reconciliation of the hypotheses can be effected when exact depths of kimberlite formation and the lithosphere–asthenosphere boundary are unambiguously determined. Aspects of the former problem are discussed in Section 9.8. The latter problem will only be resolved by new geophysical interpretations of continental structure. The lithosphere–asthenosphere boundary in oceanic regions, is marked by a seismic low-velocity zone and lies at about 100-km depth. A similar structure is proposed to exist under the continents with the boundary occurring at deeper levels (Bott 1982). Unfortunately there is little supporting evidence and the low-velocity zone is either poorly developed or absent (Soloman 1976). If the boundary lies as deep as 200 km, it would seem that the sources of all xenoliths could lie within the lithosphere. Jordan (1979) has proposed that continents are underlain by a root or tectosphere that is a physically distinct entity down to depths of at least 400 km. Either of the above proposals can render diapir ascent unnecessary. The mysterious source of volatiles required by most current partial melting models could ultimately lie in deeply subducted oceanic crust that underplates the lithosphere or tectosphere. Re-interpretation of the nature of the xenolith suite in a nondiapiric model is preferable to abandoning the most important aspects of Bailey's model, which are based upon observable and indisputable alkaline rock distributions.

9.8. DEPTH OF FORMATION OF KIMBERLITE

The depth at which the upper mantle may melt to form kimberlite can be estimated from constraints imposed by the presence of diamond and coesite and from the equilibration temperatures and pressures of mantle-derived xenoliths.

Coesite is found as an inclusion in diamond (Orlov 1977) and as a constituent of a grosspydite xenolith (Wohletz and Smyth 1984). Stishovite has never been

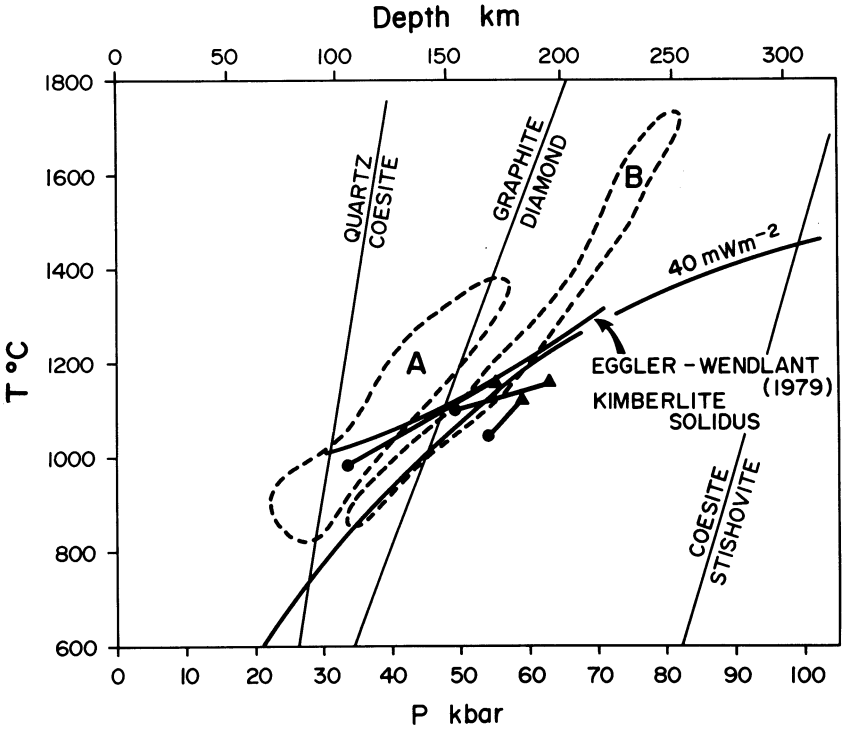

Figure 9.1. Equilibration pressures and temperatures of garnet lherzolites from Northern Lesotho kimberlites as estimated by the (A) Wells (1977)–Wood (1974) and (B) Lindsley and Dixon–MacGregor (1974) methods. Solid triangles (method B) and points (method A) connected by tie line are equilibration parameters for diamond-bearing garnet lherzolites.

reported from kimberlites; consequently the minimum depth for kimberlite generation is limited by the intersection of the stishovite–coesite inversion curve with plausible shield geotherms (Cox 1978). Figure 9.1 indicates a depth of approx. 305 km for a 40-mW m^{-2} geotherm, with the proviso that pre-existing stishovite could have inverted to coesite during slow transport (diapiric upwelling?) of material from greater depths. Coesite is of no use in establishing an upper depth limit as the quartz–coesite inversion curve (Figure 9.1) lies at lower pressures than the stability field of diamond.

The diamond–graphite inversion curve (Figure 9.1) indicates the minimum depths required for diamond stability and intersects the shield geotherm at approx. 140-km depth. All diamond-bearing rocks should have originated below this depth. Although the diamond–graphite curve is commonly used to define the stability of diamond, it should be realized that the phase diagram for the system C–O–H–N would be more realistic, as diamond stability could be assessed with reference to the diamond–CH_4 or diamond–CO univariant reactions. These re-

actions are probably more relevant to the growth and destruction of diamond in the mantle than the solid–solid phase transformation curve. Unfortunately, these phase relationships are not yet available.

The above constraints indicate that mantle-derived xenoliths and inclusions in diamonds should define equilibration pressures and temperatures between the above limits. The maximum equilibration pressures will define the minimum depths of magma generation. Garnet lherzolites are especially useful in providing estimates of equilibration parameters. The various methods of geothermobarometry that can be applied to these rocks assume that their mineral phases were in equilibrium with each other in the mantle and that the igneous activity which carried them to the surface was fast enough for equilibrium to be frozen in. Temperature estimates are based upon the pyroxene solvus, garnet–clinopyroxene, or garnet–olivine equilibria. Pressure estimates are based upon the solubility of alumina in orthopyroxene co-existing with garnet. Unfortunately there is no agreement as to which of these methods provides the most accurate *P–T* estimates or even as to the significance of the calculated *P–T* arrays for diverse suites of lherzolites. Discussion of these problems is beyond the scope of this work, but can be found in Carswell and Gibb (1980), Mitchell *et al.* (1980), Mitchell (1984b), Harley and Thompson (1984), Finnerty and Boyd (1984), and Nixon (1986).

The magnitude of the disagreement is illustrated in Figure 9.1 in which are plotted the fields of equilibration pressures and temperatures of a single suite of xenoliths from Lesotho kimberlites as calculated by the Wells (1977)–Wood (1974) and Lindsley and Dixon (1976)–MacGregor (1974) methods. As the geobarometers employed are not independent of temperature the calculated equilibration pressure is critically dependent on the geothermometer used. Consequently Wells–Wood pressures are consistently lower than Lindsley and Dixon–MacGregor pressures because the Wells (1977) formulation of the pyroxene solvus gives lower equilibration temperatures than the Lindsley and Dixon (1976) version of this solvus.

Finnerty and Boyd (1984) believe that the accuracy of any geothermobarometer can be evaluated by determining the equilibration pressures of diamond-bearing lherzolite. Figure 9.1 shows that three such lherzolites have equilibration temperatures and pressures within the diamond stability when calculated by the Lindsley and Dixon–MacGregor method, but straddle the diamond–graphite inversion curve when calculated by the Wells–Wood method. Accordingly Finnerty and Boyd (1984) consider the Lindsley and Dixon–MacGregor method to be the most accurate of all the geothermometers currently available. Caution should be exercised with regard to this conclusion, in that it is possible that xenoliths could re-equilibrate to pressures and temperatures within the graphite stability field and still contain diamond. This can arise because the equilibration of the silicates does not involve diamond which can persist metastably at low

oxygen fugacities. Mitchell *et al.* (1980) believe that the Wells–Wood method provides superior pressure and temperature estimates on the basis of comparison of calculated parameters with those of natural garnet lherzolites equilibrated at known pressures and temperatures. Bearing these problems in mind, Figure 9.1 indicates that the minimum depths of kimberlite formation are on the order of 250 km (Lindsley and Dixon–MacGregor method) or 180 km (Wells–Wood method).

Mineral inclusions in diamond belonging to the "peridotitic suite" are rarely found in combinations that permit calculations of reliable equilibration parameters. Co-existing garnet, orthopyroxene, and clinopyroxene in diamonds from the Premier and Mir kimberlites give Lindsley and Dixon–MacGregor temperatures and pressures of 1295°C at 64 kbar (≈200 km) and 1010°C at 47 kbar (≈ 150 km), respectively (Boyd and Finnerty 1980). Hervig *et al.* (1980), Finnerty and Boyd (1980), and Meyer (1985, 1986) suggest that inclusions in diamonds have equilibrated at 890–1300°C at 47–65 kbar within the diamond stability field. The wide range of equilibration conditions suggests that diamonds are xenocrysts in kimberlite and that they can form over a wide depth range in the mantle. Shee *et al.* (1982) have calculated a similar temperature range (905–1288°C) for garnet–olivine pairs in Finsch diamonds at an assumed pressure of 50 kbar using the O'Neil and Wood (1979) method. Gurney *et al.* (1984a) have indicated that inclusions in Orapa diamonds equilibrated at 1135–1212°C at 50–60 kbar pressure. Meyer (in press) notes that the average range for equilibration of ultramafic suite inclusions is approx. 50–60 kbar at 1000–1050°C. Eclogitic suite inclusions, assuming a similar pressure range, define a much wider (1100–1300°C) range of equilibration temperatures.

Eclogite xenoliths are not as useful as lherzolites in assessing the depths of kimberlite genesis as garnet–clinopyroxene equilibria are dependent upon temperature and pressure. Consequently pressure cannot be determined unambiguously and must be assessed indirectly with reference to geotherms or the diamond–graphite curve. Gurney *et al.* (1984a,b), Robinson *et al.* (1984), and Carswell *et al.* (1981) on this basis suggest that eclogites are derived from depths of 100–150 km.

The above studies demonstrate that diamond-bearing xenoliths, diamond-free lherzolites, and inclusions in diamonds all have similar maximum equilibration parameters. There is no evidence from inclusions in diamonds of derivation from deeper levels in the mantle. This observation suggests that lherzolite equilibration parameters provide a realistic estimate of the depths at which magma generation occurs e.g., 180 or 250 km depending upon the preferred geothermobarometer. The data indicate that kimberlites are derived from levels deeper in the mantle than any other magma. It is not possible to determine if kimberlite formation takes place over a range of depths above this level or is confined to a particular limited depth range by a melting cusp on the source-rock solidus.

9.9. SILICA ACTIVITY

As sphene is not found in kimberlites, and perovskite is a ubiquitous groundmass phase, one can employ a silica buffer involving these two minerals to define the maximum activity of silica in the groundmass liquid (Mitchell 1973a). Diopside is a common mineral in many kimberlites and buffers involving this mineral may be used to estimate the lower limits of silica activity. Melilite does not occur in kimberlites, thus silica activities are in general greater than those defined by the akermanite plus forsterite–diopside buffer (Mitchell 1973a). Monticellite is a common groundmass mineral and the monticellite–diopside buffer should provide a useful constraint on silica activities. Unfortunately, high-temperature thermodynamic data are not available for monticellite. The silica activity for coexisting monticellite and diopside at 25°C, however, lies between activities

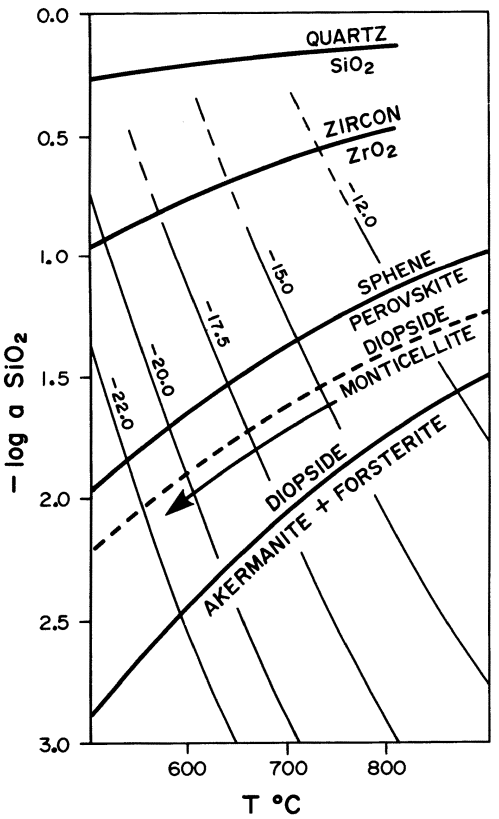

Figure 9.2. Activities of silica versus temperature at 1 kbar pressure calculated for various silica buffers relevant to the crystallization of the kimberlite groundmass. Light curves are oxygen fugacity (QFM) isobars.

defined for buffers involving perovskite and akermanite. Figure 9.2 illustrates the variation of silica activity with respect to temperature at 1 kbar pressure for various silica buffers relevant to kimberlite. The figure includes an estimate of silica activities defined by the monticellite–diopside buffer as extrapolated from the 25°C activity to higher temperatures, by assuming that the activity changes in parallel with activities defined by the sphene–perovskite buffer. The silica activities of kimberlites are considered to lie at levels between the monticellite–diopside buffer and the akermanite plus forsterite–diopside buffer. This indicates that melilitites are more undersaturated with respect to silica than kimberlites. Silica activities at the time of crystallization of the groundmass are considered to decrease from about $10^{-1.5}$ at 800°C to about $10^{-2.5}$ at 600°C. Figure 9.2 shows that the zircon–ZrO_2 buffer lies at silica activities above the sphene–perovskite buffer. This explains the absence of zircon and the presence of baddeleyite in highly differentiated kimberlites. The occurrence of quartz in the Benfontein sills (Dawson and Hawthorne 1973) and the occurrence of diopside in diatreme facies kimberlites, or in association with xenoliths in some hypabyssal kimberlites (3.6.2), may be due to local contamination by silica-rich materials which raise the silica activities above those of the silica glass–quartz or the monticellite–diopside buffers.

Silica activity decreases with increasing pressure at constant temperature for a given silica buffer. Mitchell (1973a) has shown that at high pressures the surface of activities for the olivine–enstatite buffer lies below that of the sphene–perovskite buffer. At 1200°C at 50 kbar pressure, silica activities are estimated to be on the order of $10^{-1.5}$. The zircon–ZrO_2 buffer defines similar levels of silica activity to the olivine–enstatite buffer. These relationships may explain the occurrence of orthopyroxene and zircons as megacrysts and their absence as groundmass phases, i.e., the silica activity is not sufficient to stabilize these phases except at high pressure. These conclusions must be viewed with some caution given the uncertainties involved in extrapolating low-pressure thermodynamic data to pressures of 50–60 kbar. Mitchell (1973a) has also noted that buffers involving garnet may be important at high pressures.

In summary, it should be noted that the silica activity of kimberlite is in general lower than that of most other alkaline rocks. Nepheline syenites and ijolites (nephelinites) commonly contain albite and sphene. Silica activities defined by buffers involving these minerals are higher than those discussed above.

9.10. OXYGEN FUGACITY

9.10.1. Upper Mantle and Megacrysts

Determination of the oxidation state of the upper mantle is important with respect to the growth and stability of diamond, its preservation in kimberlite,

and in assessing the nature of the fluid phase present during magma formation and crystallization at high pressures. Three methods have been used to estimate mantle redox conditions: calculation from heterogeneous phase equilibria (Eggler and Baker 1982, O'Neil *et al.* 1982); intrinsic oxygen fugacity measurements (Arculus and Delano 1981, Arculus *et al.* 1984); and Fe–Ti–oxide equilibria (Haggerty and Tompkins 1983, 1984).

Eggler and Baker (1982), O'Neil *et al.* (1982), Eggler (1983), and Ryabchikov (1983) have calculated that the oxygen fugacities (fo_2) of ilmenite megacrysts and spinel or garnet lherzolite assemblages lie between those defined by the quartz–fayalite–magnetite (QFM) and magnetite–wustite (MW) buffers (Figure 9.3). The fo_2's are compatible with the co-existence of carbonate minerals and diamond or graphite and thus lie close to fo_2's defined by the enstatite–magnetite–olivine–graphite (EMOG) or diamond (EMOD) buffers (Eggler 1983). Under these redox conditions associated fluids consist of CO_2 and H_2O mixtures.

In the intrinsic oxygen fugacity (IOF) method gas mixtures are adjusted as a function of temperature to match the redox state of the sample. Oxygen-specific Y_2O_3-stabilized ZrO_2 solid electrolyte cells are used for the fo_2 measurements (Arculus and Delano 1981). Arculus *et al.* (1984) have determined that ilmenite

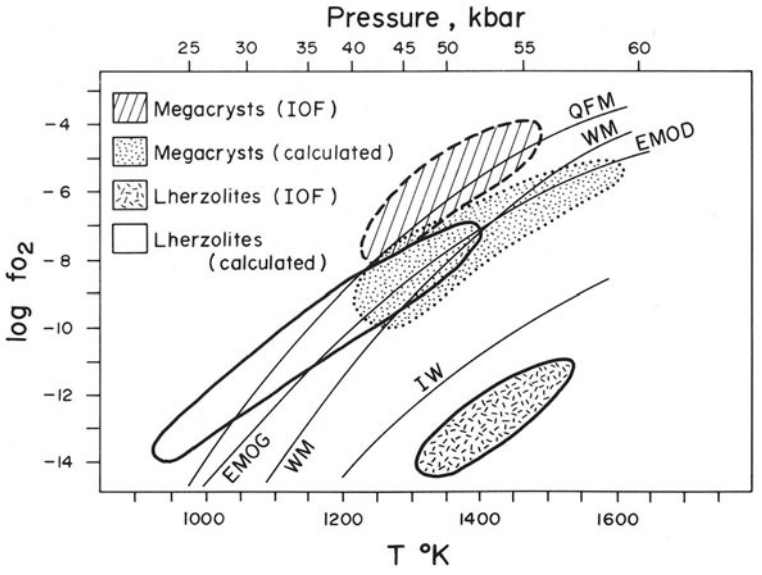

Figure 9.3. Oxygen fugacities of the upper mantle as calculated by Eggler (1983) and measured by Arculus and Delano (1981) and Arculus *et al.* (1984). IOF, intrinsic oxygen fugacity; IW, iron–wustite buffer; WM, wustite–magnetite buffer; QFM, quartz–fayalite–magnetite buffer; EMOG–EMOD, enstatite–magnesite–olivine–graphite or diamond buffers.

megacrysts and olivine pyroxenites define IOF's between QFM and nickel–nickel oxide (NNO) buffers (Figure 9.3). Exact fo_2's cannot be determined without knowledge of the temperature of formation or equilibration. At 1050°C at 1 atm IOF's range from 10^{-9} to 10^{-10} bar. At 30 kbar pressure these would increase to 10^{-7} to 10^{-8} bar.

Spinel lherzolite assemblages in contrast define lower IOF's (10^{-14} bar at 1 atm) close to the iron–wustite (IW) buffer and well below the EMOG/EMOD buffer (Figure 9.3). Under these redox conditions carbonate is not stable, diamond or graphite is stable, and fluids are mixtures of CH_4 and H_2O. The experimentally determined fo_2's are not in agreement with Eggler's (1983) calculated values. Sato (1978) and Sato and Valenza (1980) have concluded that IOF's are not representative of redox conditions in the upper mantle. The low IOF's are believed to represent auto-reduction from fo_2's near MW by the assemblage graphite–CO–CO_2 either during the experimental determination of IOF or transport of the xenoliths in the magma. Decrepitation of CO_2–CH_4-bearing fluid inclusions during heating of the samples is also believed to result in auto-reduction. These problems of the interpretation of IOF's have not yet been resolved.

Arculus *et al.* (1984), on the basis of the IOF measurements have proposed that the upper mantle is zoned with respect to its redox state and consists of a relatively reduced zone (IM–MW) of spinel lherzolite overlying a more oxidized (QFM) region which is the source of volatile rich magmas (Figure 9.4A). Reduction of portions of the upper mantle is believed to be accomplished by the diffusion of H_2 away from a rising flux of volatile-rich magma. Intrinsic fo_2's for ilmenite megacrysts are more oxidized than calculated by Eggler (1983). The

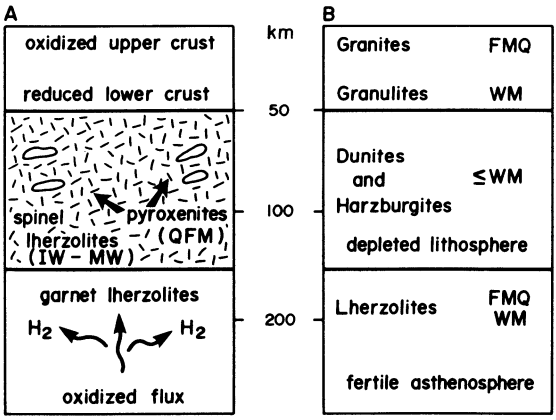

Figure 9.4. Models of upper mantle redox conditions as proposed by (A) Arculus *et al.* 1984 and (B) Haggerty and Tompkins (1983). Abbreviations for oxygen buffers as in Figure 9.3.

discrepancy may result from an inappropriate solution model employed by Eggler (1983) in his calculations or from errors inherent in the IOF measurements.

Arculus *et al.* (1984) believe that the ilmenite IOF range is well above the stability field of solid carbon and is appropriate for a dolomite or magnesite lherzolite mantle lacking diamond or graphite. Accordingly, diamonds will be unstable in kimberlites precipitating megacrystal ilmenite, and the associated fluids must consist of CO_2–H_2O mixtures. Diamond and graphite however, would be stable at the fo_2's (IW) indicated for spinel lherzolites. Unfortunately IOF data for garnet lherzolites are not available.

Haggerty and Tompkins (1983, 1984) have interpreted megacrystal ilmenite–spinel intergrowths (Section 6.3.5) to have formed by sub-solidus reduction exsolution of an originally homogeneous ilmenite. The process was initiated at high temperatures and was followed by low-temperature equilibration. Pressures at which exsolution occurred cannot be determined but Haggerty and Tompkins (1983, 1984) estimate that at 30 kbar the highest temperatures of exsolution, as determined by Fe–Ti oxide thermobarometry (Section 6.3.5), define fo_2's ranging from 10^{-5} to 10^{-9} bar. The fo_2's lie between the WM and QFM buffers and are in broad agreement with EMOG/EMOD and the IOF data. The ilmenites must have formed originally at fo_2's above these values. Haggerty and Tompkins (1984) deduced that reduction could result from a change in fo_2 of only $10^{0.5}$ bar and that this might occur simply as a consequence of pressure (5 kb) and temperature (100°C) decrease. Reduction may also be aided by the presence of the H_2 or sulfur in the associated fluid phase.

Utilizing their data together with Arculus and Delano's (1981) spinel lherzolite IOF data, Haggerty and Tompkins (1983) have constructed a model of the upper mantle that is similar to that of Arculus *et al.* (1984) and which requires a relatively reduced zone overlying a deeper more oxidized region (Figure 9.4B).

In summary, all methods of estimating the redox state of ilmenite megacrysts imply that the source regions of kimberlites are relatively oxidized and approximate to fo_2's defined by the QFM or WM buffers. These conclusions require that CO_2 and H_2O are the principal components of the fluid phase associated with kimberlites at high pressures. The redox state of the upper mantle is less well defined and it cannot yet be stated with any confidence to be either at the EMOG/EMOD, QFM or IW buffers.

9.10.2. Groundmass Crystallization

Spinel–silicate equilibria are useful in determining the redox conditions prevailing during the later stages of kimberlite evolution as the groundmass contains the assemblage olivine plus spinel. Assuming equilibrium and knowing the silica activity of the liquid which formed the groundmass, one can use the QFM buffer to calculate oxygen fugacities (Mitchell 1973a, 1975). Figure 9.2

shows the variation in fo_2 with silica activity and temperature, and demonstrates that very accurate knowledge of silica activity is not critical in estimating the fo_2 as the oxygen fugacity isobars cut the silica activity curves at a high angle. Experimental studies (Chapter 8) indicate that temperatures as low as 600°C can be expected during the final stages of groundmass formation. At these temperatures fo_2's will lie between 10^{-19} bar (sphene–perovskite buffer) and 10^{-22} bar (akermanite plus forsterite–diopside buffer). During crystallization of the groundmass at the diopside–monticellite buffer, fo_2's can be expected to decrease from about 10^{-13} bar at 800°C to 10^{-21} bar at 600°C. Figure 9.5 illustrates the trend of decreasing fo_2 to be expected in response to the changing composition of spinels at the minimum activities of silica of kimberlite magma as defined by the akermanite plus forsterite–diopside buffer (Mitchell and Clarke 1976).

Further support for the crystallization of kimberlites at the low oxygen fugacities postulated above comes from the following:

1. Ulmer *et al.'s* (1976) demonstration that the IOF of the Premier kimberlite lies on the IOF curve defined by most mantle-derived igneous rocks and which approximates to QFM.

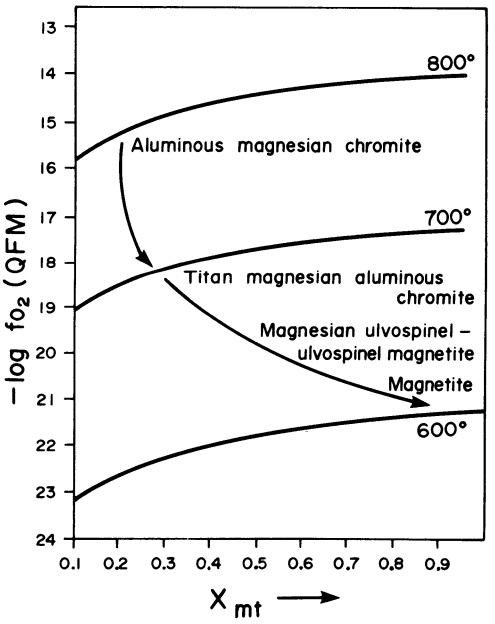

Figure 9.5. Fugacity of oxygen plotted against the mole fraction of magnetite in spinel to illustrate the possible changes (arrowed lines) in fo_2 during the formation of the groundmass spinel assemblage. Fugacities are calculated for QFM. Solid lines show fo_2 changes for this buffer under isothermal conditions.

2. The occurrence of Fe-poor perovskites which according to Kimura and Muan (1972a, b) indicate crystallization under low (IW) oxygen fugacities.
3. McMahon *et al.'s* (1979) conclusion that the composition of co-existing ilmenite and spinels in the Benfontein sills defines points in fo_2-T space that are coincident with QFM. In this occurrence strongly zoned magnesian ilmenites are mantled by strongly zoned titanomagnetites. Oxide pairs in the megacryst cores give lower equilibration temperatures (603 and 917°C) and fo_2's ($10^{-19.8}$ and $10^{-12.4}$ bar) than oxide pairs at the margins of the grains (863°C and $10^{-13.4}$ bar; 1299°C and $10^{-6.8}$ bar). The cores have apparently not equilibrated with the higher-temperature margins, and are interpreted by McMahon *et al.* (1979) to record pre-eruptive conditions. The outer mantles, in contrast, are believed to record the intrusional temperatures and fo_2's of the sill at the time of emplacement. Although giving reasonable equilibration parameters these data must be viewed with caution in that they were derived from zoned, i.e., non-equilibrium mineral assemblages.
4. Nikolskii (1983) has concluded that serpentinization of olivine can take place under reducing conditions and in the presence of graphite. Nikolskii (1983) suggests that oxygen fugacities equivalent to QFM prevail and that the fluid phase associated with serpentinization consists of H_2O, CH_4, and CO_2. The presence of metallic Fe, Fe–Ni, and Cu (Section 6.20) associated with serpentinized olivines appears to confirm these conclusions. Frost (1985) has noted that oxygen fugacities of 4 to 7 log units below the QFM buffer are possible in the development of Ni–Fe–serpentine–olivine–brucite–magnetite assemblages. The presence of carbonate requires higher fo_2 and considerable local gradients in fo_2 may exist in the carbonate and sulfide-bearing late fluids. These may have higher fo_2's than those associated with the earlier stages of serpentinization.

Whether fo_2 decreases continuously during kimberlite crystallization, or fluctuates, has not been conclusively determined. Rare samples of complex mantling between spinels and ilmenite (Section 6.3.5) have been interpreted to be a consequence of alternately decreasing and increasing fo_2's. (Haggerty 1973, Haggerty and Tompkins 1984). The occurrence of groundmass ilmenites which define a trend of increasing MgO content (Agee *et al.* 1982, Shee 1984) suggests that in some cases fo_2 increases as the magma evolves. The basis for this conclusion is that the compositional trend cuts across oxygen fugacity isobars in the system $MgTiO_3$–$FeTiO_3$–Fe_2O_3 at 1300°C (Figure 6.12; Woermann *et al.* 1970). Haggerty (1973) suggests that these variations in fo_2 are controlled by local variations in the CO/CO_2 and H_2/H_2O ratios of the late-stage melts. The introduction of groundwater may be the cause of such fluctuations.

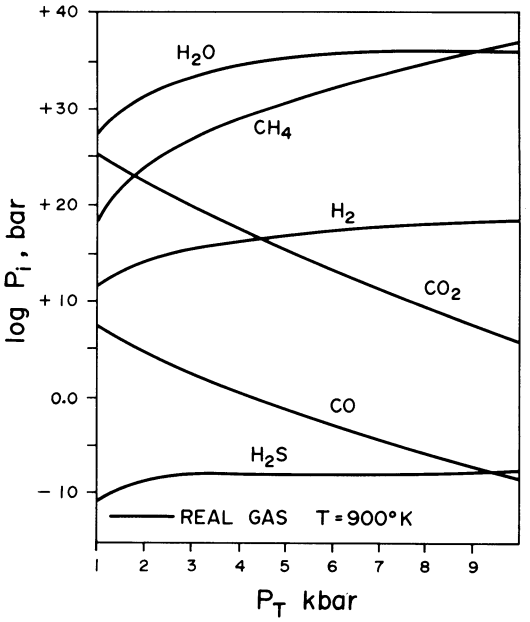

Figure 9.6. Calculated partial pressures of real gases in the system C–H–O–S in response to changing pressure at 900°K and $fs_2 = 10^{-10}$ bar.

Mitchell (1975b) has calculated gas compositions in the system C–H–O–S over a wide range of pressures and temperatures and concluded that H_2O is the dominant component of the fluid phase in equilibrium with carbon at the time of groundmass crystallization. Wide variations in the CO_2/H_2O ratio at any given fo_2 are possible in response to changes in temperature and pressure (Figure 9.6). At low pressures (<4 kbar) and temperatures (≈600°C), CH_4 and H_2O are important components of the fluid phase. Formation of these gases is also promoted by decreasing fo_2. Decreased fo_2 leads to increased partial pressures of H_2O and CO_2.

9.11. MEGACRYSTS AND THEIR RELATIONSHIP TO KIMBERLITES

The principal features of the chemistry and paragenesis of the megacryst suite have been described in Chapter 6. Any hypothesis presented to explain the genesis and relationship of the megacrysts to kimberlite must account for the following observations:

1. The wide compositional range exhibited by garnet, ilmenite, and pyroxene within any given kimberlite. Tie lines between co-existing phases suggest that the megacrysts represent a differentiated sequence (Gurney *et al.* 1979, Robey and Gurney 1979), and that the most Fe-rich garnets and lowest-temperature pyroxenes crystallized contemporaneously with ilmenite.
2. The occurrence of distinctly different inter- and intra-kimberlite megacryst assemblages. These differences can be manifested either in terms of the composition or relative abundance of the phases.
3. The existence of lamellar intergrowths of pyroxenes and ilmenites, but not garnet and ilmenite. These intergrowths may be due to the simultaneous crystallization of pyroxene and ilmenite under vapor-rich conditions and are unlikely to represent the products of eutectic or cotectic crystallization (Mitchell 1977). The compositions of lamellar ilmenites do not terminate the compositional trends defined by monomineralic ilmenites from the same intrusion. Their overall composition are characteristic for any given intrusion and similar to those of the single crystals.
4. All of the megacrysts are large single crystals that have apparently grown in a volatile-rich environment (Haggerty *et al.* 1979). It is not clear whether the megacryst suite as a whole represents disrupted pegmatites or consists of phases which grew to large size in a melt and never formed discrete solid bodies.
5. Many ilmenites show textural evidence for deformation and recrystallization at high temperatures (Mitchell 1973b, Pasteris *et al.* 1979). Such ilmenites have been interpreted to represent disaggregated cumulates. Annealed and deformation-free single crystals co-exist in the same intrusion.
6. Megacrysts appear to have formed over a wide temperature (1400–900°C) but limited depth range (50 km, Boyd and Nixon 1973, 1975). Equilibration parameters are estimated by methods devised for solid state equilibria relevant to garnet lherzolite and eclogite. It is debatable whether these thermobarometers can be extended to phases crystallizing from a liquid which is sufficiently Fe- and Ti-rich to allow ilmenite crystallization. The methods assume that all the megacrysts were originally a part of an ilmenite–clinopyroxene–orthopyroxene–garnet assemblage; however, monomineralic crystals are typical and three- and four-phase assemblages are very rare. Recent studies of the megacryst suite indicate that individual phases may crystallize in the absence of other phases.
7. The existence of Cr-rich and Cr-poor suites of megacrysts in some North American kimberlites (Eggler *et al.* 1979, Hunter and Taylor

1984) implies derivation of each suite from different sources together with subsequent mixing.

8. The general paucity of olivine relative to other megacrysts. This of course may be related to problems of recognition of megacrystal olivine; however, olivine inclusions in ilmenite or garnet are extremely rare.
9. The typical lack of correlation between the trace element assemblage and the major element variation in any given suite of megacrysts.
10. The existence of magnesium and manganese enrichment trends at the margins of zoned ilmenites. These trends indicate that the megacrysts were not in equilibrium with their transporting magmas.

It is evident from the above observations that megacrysts are products of the high-pressure fractional crystallization of magma. The crux of the megacryst problem lies in the identification of the nature of this magma. Current genetic models fall into two categories depending upon whether the megacrysts are regarded as xenocrysts or phenocrysts. Variants of the latter model depend upon whether or not the megacryst-forming magmas are believed to have crystallized isobarically.

9.11.1. Xenocrystal Models

Nixon and Boyd (1973), and Boyd and Nixon (1973, 1975) have suggested that the wide range in apparent equilibration temperatures of megacrysts is unlikely to be associated with the crystallization of a single magma or magma body of small volume. Pressure estimates are considered to indicate derivation of the megacrysts from depths ranging from 150 to 200 km. Because of the overlapping equilibration parameters with those of high-temperature Fe-rich deformed garnet lherzolites, and the geochemical similarity between the more magnesian megacrysts and minerals in such lherzolites, it is suggested that the megacrysts formed as phenocrysts in crystal mush magmas (high crystal/liquid ratios) of unspecified composition in association with the lherzolites. Megacryst and lherzolite equilibration parameters are believed to define geotherms. The more magnesian megacrysts are considered to have formed at greater depths than the Fe-rich ilmenite-bearing types. The compositional range is attributed to the fractional crystallization of small volumes of magma formed by the partial melting of the asthenosphere. Crystallization of the upward-seeping magma enriches the derivative liquids in incompatible elements, iron and titanium. The upper depth limit of the megacryst-forming magma is believed to coincide with the lithosphere–asthenosphere boundary. The crystal mush magmas occur interstitial to the deformed garnet lherzolites over a depth range of 50 km below this boundary. The presence of this liquid defines a seismic low-velocity zone extending from

150–200 km. Magmas erupting from the base of this zone will incorporate lherzolites, megacrysts, and interstitial liquids during their ascent. This conclusion requires that kimberlites are hybrid magmas formed by the mixing of liquids and crystals of diverse origins. Boyd and Nixon (1973) consider that kimberlites are formed by the incorporation of megacrysts and their associated parental silicate liquids into a carbonatite magma originating from below the low-velocity zone (see Section 9.3).

Pasteris (1980a) has modified the above hypothesis by eliminating carbonatite and suggesting that a kimberlite-bearing diapir rises through and disrupts the crystal mush magmas containing the megacrysts. Pasteris (1980a) suggests that the distinctive ilmenite megacryst suites from different intrusions do not represent chemical inhomogeneities or processes in their mantle sources, but rather partial re-equilibration of the megacrysts with the particular kimberlite that entraps them. The magnesium enrichment trends found at the margins of relatively Fe-rich ilmenites thus represent an attempt by these megacrysts to achieve equilibrium with a more magnesian magma in which a more magnesian ilmenite is a liquidus phase. Pasteris (1980a) believes that only the highly magnesian groundmass ilmenites are genetically related to kimberlite magmas and that all megacrysts are xenocrysts. Shearing and recrystallization textures recorded in many ilmenites are interpreted to have been formed by disruption of ilmenite cumulates by the rising diapir.

Neither of the above models addresses the problems posed by the Cr-rich megacryst suite and are concerned solely with the Cr-poor suite as found in South African kimberlites.

9.11.2. Phenocrystal Models—Isobaric Crystallization

Gurney *et al.* (1979), Gurney and Harte (1980), and Harte and Gurney (1981) believe that megacrysts are genetically related to kimberlites and maintain that the wide range in equilibration temperatures is inevitable for any magma body that cools *in situ* in the mantle. Concentration of volatiles as a consequence of the lack of crystallization of hydrous phases is also considered to play a role in extending the range of crystallization temperatures. Gurney *et al.* (1979) and Robey and Gurney (1979) find no evidence for differences in the pressures of equilibration of megacrysts from the Monastery and Lekkerfontein kimberlites despite wide variation in their apparent temperatures of formation. Harte and Gurney (1981) consider that the limited pressure ranges proposed by Boyd and Nixon (1973, 1975) are not real but are due to the large uncertainties associated with the methods of pressure determination. Megacrysts are thus believed to have crystallized isobarically, and their compositional range to reflect horizontal temperature gradients at essentially constant depth. Harte and Gurney (1981) propose that the parent magma originates at some depth in the mantle where temperatures are a little above those indicated by the highest temperature ($\approx$1400°C)

megacrysts. This magma moves upward into a region where the temperatures on a normal shield geotherm are the same as, or below, those of the lowest temperature (≈1000°C) megacrysts. At this level the upward flow of the magma is restricted and a magma body of limited size and vertical extent (<5 km) is formed. This magma body creates a thermal and metasomatic aureole and spreads out horizontally as a series of sheets, veins, and dikes that may range up to several tens of meters in thickness. The temperature of magma in this stockwork will decrease from the temperature of the central magma chamber down to that of the ambient geotherm at the margins. Slow cooling and differentiation will generate the megacryst suite. Harte and Gurney (1981) envisage that crystals may be forming from high temperature, undifferentiated magma in the central magma body, while crystallization is simultaneously occurring from lower-temperature differentiated magma in the apophyses. The differentiation process is believed to produce residual kimberlite liquids, which are erupted together with the megacrysts and metasomatized lherzolite xenoliths.

Schulze (1984), in applying Harte and Gurney's (1981) model to the Hamilton Branch kimberlite megacryst suite, suggests that minor crystallization only occurs in the central magma chamber while in the apophyses crystallization may be 50%–80% complete. Schulze and Hoover (1982) and Schulze (1984) have suggested that the different trends of iron-enrichment observed in different megacryst suites are related to the extent of ilmenite crystallization. In the Monastery suite, ilmenites form only at the lowest temperatures of crystallization and silicates show a trend of iron enrichment. In contrast, in the Hamilton Branch suite, ilmenites are present throughout the entire range of silicate compositions and silicates do not exhibit a trend of iron enrichment.

Harte and Gurney's (1981) model does not consider the origins of the Cr-rich suite of megacrysts. Schulze (1984) suggests that Cr-rich megacrysts in the Hamilton Branch kimberlite are xenocrysts and not phenocrysts as suggested by Garrison and Taylor (1980). A similar isobaric crystallization model was developed independently by Ehrenberg (1982) to explain the formation of megacrysts associated with a minette magma.

9.11.3. Phenocrystal Models—Polybaric Crystallization

Kimberlites in the Colorado–Wyoming province contain two compositionally distinct suites of megacrysts. One suite is Cr-poor and similar to megacrysts in South African kimberlites in exhibiting a wide range in Mg/Mg + Fe ratios and equilibration temperatures (1050–1350°C). The other suite is Cr-rich and compositionally similar to the minerals occurring in garnet lherzolite xenoliths. The megacrysts can only be distinguished from the latter on the basis of their larger size and by the lower Na, Al, and Cr contents of the clinopyroxenes relative to those lherzolites. The Cr-rich suite have constant Mg/Mg + Fe ratios. Temperatures and pressures of equilibration of orthopyroxene megacrysts from

the Cr-rich suite define an array that is interpreted as a steady-state shield geotherm. A similar geotherm is defined by the associated lherzolites. The equilibration temperatures of some of the Cr-poor orthopyroxenes fall within this array, but the temperatures of others define an extension of the array to higher temperatures (1250–1350°C), e.g., a perturbed geotherm. All megacrysts and xenoliths are believed to be derived from depths ranging from 150 to 200 km. Kimberlites and their included megacrysts and xenoliths are considered to be produced by partial melting of a rising diapir. The Cr-poor megacrysts are interpreted to crystallize from partial melts and their derivatives of undepleted peridotite in the diapir. The Cr-rich suite is considered to have crystallized from liquids derived by the melting of a mixture of undepleted peridotite and depleted lithosphere wall rocks. The latter component is required to explain the high Cr content and low equilibration temperatures of the Cr-rich suite. This model of localized melting and crystallization within a rising diapir seems adequate with respect to the Cr-poor megacrysts and can be viewed as a dynamic variant of Harte and Gurney's (1981) model. The hypothesis is far less satisfactory with regard to the Cr-rich suite. Eggler *et al.* (1979) in particular, provide no explanation how contamination and/or mixing of depleted lithosphere with melts derived from undepleted diapir peridotite occurs. Depleted Cr-rich lithosphere should presumably melt at higher temperatures in contradiction to the observed low equilibration temperatures of the Cr-rich megacrysts.

To account for the distinct assemblages of megacrysts in different kimberlites, Eggler *et al.* (1979) suggest that each cluster of pipes is fed by a distinct conduit that extends to 150–200-km depths and taps distinctly different portions of the diapir(s). These discrete main conduits only branch in their upper levels and produce pipes within a cluster. This model would seem improbable in the light of recent interpretations of diatreme infrastructure (Chapter 4).

Hunter and Taylor (1984) have attempted to explain the co-existence of Cr-rich and Cr-poor megacrysts in terms of a model that incorporates diapiric melting and magma mixing. The low-Cr megacryst suite is believed to originate when partially melting diapirs rise through the low-velocity zone with segregation of the melts in ponded magma bodies where the diapir reaches Wyllie's (1980) thermal barrier on the peridotite–CO_2–H_2O solidus (see Section 9.7.1). These melts fractionate in thermal gradients under essentially isobaric conditions according to the Harte and Gurney (1981) model. Thus, within the low-velocity zone there is believed to be a concentration of discrete magma bodies representing the various stages of high-pressure crystallization of kimberlite melts.

Once a conduit has been established and the solidus thermal barrier breached, uprise of partially melted diapirs will occur from progressively greater depths (Wyllie 1980). The absence of a barrier will prevent melt segregation and ponding. Liquids within the diapirs are therefore buffered at essentially constant Mg/Mg + Fe ratios by the low liquid/crystal ratios. Liquidus phases crystallizing from these melts will have Mg/Mg + Fe ratios typical of garnet lherzolite assem-

blages and be Cr rich. Buffering can result in major element concentrations remaining constant while minor elements can fractionate by a zone-refining type of process.

These melting diapirs rise through the low-velocity zone disrupting all of the Cr-poor megacryst-bearing crystal mushes, incorporating megacryst and host melts. The kimberlite melt that finally rises toward the surface will thus be a hybrid between a relatively Fe-rich evolved melt and relatively Mg-rich initial partial melt. The evolved Fe-rich megacrysts will back-react with the more primitive hybrid melt resulting in reverse zonation and the development of the magnesium enrichment trend rims on ilmenite megacrysts. Individual kimberlite megacryst assemblages will depend upon the degree of mixing between melts and megacrysts.

9.11.4. Conclusions

All of the above hypotheses have their merits and detractions. Although there is a concensus that megacrysts must originate by the fractional crystallization of a body of magma there is disagreement as to whether this is or is not kimberlite and as to the depths of crystallization. Acceptance or rejection of any of the hypotheses hinges upon whether the megacrysts are xenocrysts or phenocrysts. Unfortunately interpretation of their origins remains largely subjective. Given the constant association of these megacrysts of a particular composition with kimberlite there would seem to be no *a priori* reason for considering them not to be phenocrysts. There is little evidence in favor of their being xenocrysts derived by the fragmentation of some pre-existing upper mantle material formed either during the evolution of the crust–mantle system or by the high-pressure fractionation of a more common magma. Evidence in support of a phenocrystal origin is found in the following:

1. The occurrence of inclusions of calcite and phlogopite in megacrysts that are interpreted as representing trapped kimberlite liquids (Schulze 1981, Rawlinson and Dawson 1979).
2. Eggler and Wendlandt's (1979) demonstration that the megacryst assemblage could represent high-pressure liquidus phases in melts derived from carbonated lherzolites (Section 8.1.4.3).
3. Green and Sobolev's (1975) and Mysen and Boettcher's (1975) demonstration that ilmenites and garnets can be high-pressure liquidus phases in a variety of magma types.
4. The common occurrence of megacryst suites that are compositionally distinct from those of kimberlite in other magma types, e.g., minette (Ehrenberg 1979) and alnöite (Nixon and Boyd 1973). Such suites have equilibrated at lower pressures than those of kimberlite and are commonly considered to be cognate. Interpretation according to the Boyd

and Nixon (1973, 1975) model would require several zones of crystal mush magmas at different levels in the mantle.

5. It is highly probable that the injection of a body of hot magma into a cooler region would crystallize over a wide range of temperatures.

The above comments apply only to the Cr-poor megacryst suite. The Cr-rich megacrysts have been described only from the Colorado–Wyoming province (Eggler *et al.* 1979), Elliot County (Garrison and Taylor 1980), and Fayette County (Hunter and Taylor 1984) kimberlites, and are apparently absent from other occurrences. The composition of the garnets and pyroxenes corresponds closely to those of garnet lherzolites of undoubted xenolithic origin. Designation as megacrysts stems primarily from the large size of the crystals. In the Elliot and Fayette County examples, megacrysts range in size from 0.5 to 3 cm and are not significantly larger than crystals in many coarse garnet lherzolites. Extremely large (10–14 cm) crystals occur in dunite-harzburgite xenoliths found in the Udachnaya kimberlite (Pokhilenko *et al.* 1979). Such xenoliths could provide a source of Cr-rich megacrysts as found in the Colorado–Wyoming kimberlites. The typical absence of the suite is perhaps the best evidence that the Cr-rich megacrysts represent the chance incorporation of unusually large lherzolite-derived xenocrysts in kimberlite.

Despite intensive investigation the megacryst problem remains unsolved. The principal advance made in recent years is the recognition that the megacryst suite in any given kimberlite is unlikely to result from the crystallization of a single batch of magma. Mixing of megacryst-bearing magmas of similar parentage at different stages in their evolution, or disruption of pre-existing cumulates, undoubtedly plays a major role in the formation of megacryst suites. Pasteris (1980a) and Hunter and Taylor (1984) have in particular drawn attention to the importance of resorption and reaction of megacrysts with their transporting hybrid magmas.

9.12. KIMBERLITES AND CARBONATITES

The evidence for and against the kimberlite–carbonatite relationship has been discussed in detail by Mitchell (1970, 1979a, 1983), Middlemost (1974), Le Bas (1977), Dawson (1980), Gaspar and Wyllie (1983, 1984), and Jones and Wyllie (1985), and will not be reiterated here. Further comment can be found in Sections 2.6.3 and 6.9.10. Most petrologists who are familiar with the complexities of alkaline rocks now agree that there is no direct genetic connection between kimberlite and carbonatite, e.g., Dawson (1980), yet some semantic problems remain and require additional comment.

The alleged association is founded upon (1) the occurrence of kimberlites (central complex type) in alkaline rock carbonatite complexes (Dawson 1966, 1967a,b, Zhabin 1967), and (2) the occurrence of primary magmatic calcite as

a groundmass phase or as discrete segregations in kimberlites and as carbonate-rich dikes associated with kimberlites, e.g., the Premier calcite–serpentine–magnetite dikes (Robinson 1975) or the ilmenite–calcite dike at Mukorob (Frankel 1956). These carbonates are, in terms of their trace element and isotope chemistry, indistinguishable from the calcites occurring in carbonatites.

The so-called "central complex kimberlites" have been found to be alnöitic rocks unrelated to *bona fide* kimberlites on the basis of their mineralogy and petrography (Sections 2.6.3 and 6.9.10). This misleading term has been abandoned recently even by the original proponent (Dawson 1980).

Current semantic problems stem from the occurrence of calcite. It is clear that carbonate-rich rocks of magmatic derivation have been formed by the fractional crystallization of less evolved magmas. Following Heinrich (1966) on a simple petrographic basis, they may be termed carbonatites in that they are rocks dominated in their modal mineralogy by calcite. Mitchell (1979a) has argued that this approach to classification is unsatisfactory as it fails to recognize the antecedents, the comagmatic rocks and the differing mineralogy of calcite-rich rocks associated with kimberlites or with alkaline silicate rocks such as ijolites or nephelinites. Following this essentially nineteenth century approach to classification one must recognize "carbonatites" and "carbonatites" (Le Bas 1977, p. 281). To highlight these genetic differences Mitchell (1979a) has suggested that petrological science has advanced beyond this purely descriptive phase and that it is now possible to devise modern mineralogical-genetic classifications for rocks which are similar in their gross petrographic mode but different in their detailed mineralogy and are genetically unrelated. The distinction between eclogites and griquaites (Nixon 1973c) is illustrative of the benefits of this approach to terminology; thus carbonate-rich rocks resulting from the differentiation of kimberlites should be termed calcite kimberlites. Failure to emphasize the mineralogical differences between such rocks and carbonatites leads to unwarranted petrogenetic speculation. Use of the term "carbonatitic" to refer to calcite or carbonate-rich magmas in a kimberlite paragenesis, e.g., Raber and Haggerty (1979), Dawson and Hawthorne (1973), Wyllie (1979), Wyllie and Huang (1976a,b), is unwarranted unless the authors state clearly that they are using the term in a descriptive and not in a petrogenetic sense. It is recommended here that the term should not be used at all in context with kimberlite magmatism.

Mitchell (1979a,b) notes that some mineralogical convergence can be expected between calcite kimberlites and carbonatites, as minerals of similar types and composition will form wherever the correct physiochemical conditions for stability are met in magmas of diverse origins. These similarities are trivial when compared to gross mineralogical differences. The presence of Mg–Ti-poor magnetites and magnesioferrites or the development of minor Mn enrichment in ilmenites should certainly not be considered as evidence in favor of a genetic link between kimberlites and carbonatites as advocated by Gaspar and Wyllie (1984) in isolation from other mineralogical criteria.

The presence of calcite in both kimberlites and carbonatites is indicative not of a genetic relationship but of their common origin within the upper mantle. Experimental studies (Chapter 8) suggest that the sources and depths of origin of the magmas are different. The common factor is that both magmas are able to concentrate this mantle-derived carbon in their differentiates.

9.13. DIAMONDS AND KIMBERLITES

Hypotheses concerning the relationship of diamonds to kimberlite fall into the phenocrystal versus xenocrystal schools of thought. Until recently kimberlite was considered to be the only primary source of diamond. This association therefore suggested a phenocrystal relationship and accordingly Gurney *et al.* (1979a), Harte *et al.* (1980), Mitchell and Crocket (1971b), and Dawson (1971) proposed that diamonds are genetically related to the early crystallization products of kimberlite within the upper mantle. Other versions of the phenocrystal hypothesis maintain that diamonds grow in explosion chambers at high levels in crust (Leontyev and Kadenskii 1957, Trofimov 1971).

Current opinion has swung toward believing that diamonds are xenocrysts, the association of diamond with kimberlite thus being merely one of the passenger and transporting vehicle (Meyer 1985). This belief is based upon the following:

1. The discovery of diamond in lamproites (Jaques *et al.* 1984), and hence the recognition of a second primary source of diamond.
2. Richardson *et al.'s* (1984) demonstration that inclusions in diamonds from the Mesozoic Finsch and Kimberley group pipes have Rb–Sr and Sm–Nd ages of 3.2–3.3 Ga. Similarly Kramers (1979) and Welke *et al.* (1974) have indicated that diamonds are apparently much older than their host kimberlite.
3. The equilibration conditions of inclusions in diamonds suggest subsolidus growth at temperatures and pressures equivalent to those along a reasonable continental shield geotherm and within the diamond stability field. Equilibration conditions are similar to those of associated diamond-bearing garnet lherzolite and eclogite (Boyd and Finnerty 1980, Hervig *et al.* 1980, Shee *et al.* 1982, Meyer 1985, in press).
4. The absence of megacryst suite minerals as inclusions in diamonds. Their absence is inexplicable if both megacrysts and diamonds are considered to be cognate high-pressure liquidus phases.
5. The common occurrence of diamonds in eclogites which have apparently grown from a liquid that is older and unrelated to the kimberlite-forming event (Robinson 1979).
6. The resemblance in chemical composition of mineral inclusions in diamond to those of eclogite and lherzolite xenoliths, indicates a genetic relationship to these materials (Robinson 1978, Meyer 1985, in press).

Diamond is now viewed as a mineral which can occur in a variety of parageneses in the upper mantle. Several modes of origin are therefore possible. Diamond may grow as a phenocryst in melts crystallizing at high pressures, e.g., as diamondiferous eclogites (Robinson 1979, Robinson *et al.* 1984, Gurney *et al.* 1984a,b), or by solid state porphyroblastic growth in garnet lherzolites by various gas reduction/oxidation processes involving CO_4, CO_2, CO, H_2O, and NH_3 (Mitchell and Crocket 1971b, Orlov 1977, Portnov 1982, Simakov 1983). Discussion of diamond genesis is beyond the scope of this work and the reader is referred to Orlov (1977), Robinson (1978) and Meyer (1985, in press) for detailed information.

Accepting that diamonds are xenocrysts reduces the problem of their relationship to kimberlite to one of determining why some kimberlites are diamond-bearing and others are barren. Three possibilities exist:

1. All kimberlites form at the same depth; however, due to the non-uniform distribution of diamonds in the mantle, only some of these magmas will pick up diamonds as xenocrysts during their eruption. The non-random distribution of diamondiferous kimberlites indicates that although the distribution of diamonds in the mantle may not be uniform, it is not random. The association of such kimberlites with the older portions of the craton requires that the processes of diamond genesis in these areas are in some manner related to the evolution of that portion of the lithosphere; however, it is difficult to see why the formation of diamonds at great depth should be sensitive to such high-level features, unless diamond genesis occurred only during the early stages of evolution of the crust-mantle system.
2. Kimberlites form over a range of depths above and below the field of diamond stability. This interpretation would require that kimberlites in the Kimberley field formed at deeper levels in the mantle than kimberlites in the Gibeon field. Formation of kimberlites at different depths should be reflected in their mineralogy. Studies to date have not established any significant differences between the mineralogy of diamond-bearing or diamond-free kimberlites. There is no evidence in the xenolith suite to indicate derivation from a range of depths although the interpretation of the equilibration conditions of these xenoliths is subjective (see Section 9.8).
3. All kimberlites originate at the same depth and pass through regions where they can pick up diamond xenocrysts. Differences in diamond content are therefore due to processes occurring during transportation, e.g., resorption of diamond or mechanical sorting. Evidence for the action of both of these processes is found in the common occurrence of resorption features upon diamond (Robinson 1978) and in the differentiation of kimberlites to calcite-rich, megacryst-poor, and

diamond-free residua, e.g., the Benfontein sills (Dawson and Hawthorne 1973).

Detailed mineralogical studies of diamond-bearing and apparently diamond-free kimberlites are required to resolve the above problems. It is particularly important to establish whether diatreme facies kimberlites, such as occur in the Gibeon or East Griqualand fields which are not economic, were diamond-free at the time of their formation or have since resorbed their diamonds. Gurney (1985) on the basis of a positive correlation between diamond content and the presence of sub-calcic chrome pyrope (group-10 garnets of Dawson and Stevens 1975), suggests that such kimberlites have never contained diamonds. Determination of the microdiamond content (if any) may resolve such questions. Care should be exercised in applying Gurney's (1985) chrome pyrope–diamond indicator hypothesis to regions other than the Southern African province, as *both* minerals are xenocrysts.

A corollary to considering diamond to be a xenocryst is that it is not possible to derive simple algorithms relating diamond content to the bulk composition of kimberlite. Relationships such as proposed by Milashev (1965) have no universal application and are valid only for the deposits from which they were derived.

9.14. CONCLUDING REMARKS

The reader seeking a comprehensive scheme of kimberlite petrogenesis as a conclusion to this chapter is likely to be disappointed!

Construction of such a model would be satisfying emotionally but would be unsound scientifically. One must remember that long and detailed investigation of such common and abundant rocks as granite, basalt, andesite, and rhyolite has not resulted in agreement concerning their genesis; petrological studies of kimberlites and alkaline rocks in general are in their infancy as compared to studies of such rocks. It would be presumptuous to believe that a petrogenetic model, based upon our present knowledge of kimberlites, will stand the test of time.

None of the hypotheses described above can explain all of the features of the geochemistry, mineralogy, petrology, and volcanology of kimberlites; any new hypotheses must include components drawn from each model. A particular, and perhaps unique, drawback to devising a petrogenetic model, is our complete ignorance of the composition of primitive kimberlite magma. Even the apparently least differentiated hypabyssal kimberlites are the result of differentiation and hybridization of several batches of magma. In assessing the origin of partial melts in the upper mantle, too great a reliance must not be placed on the chimera of a metasomatized mantle as a source for kimberlite. Even though such a source seems reasonable in the current paradigm of petrological thought the approach

is at best proleptic. Any conclusion regarding such sources must be treated with caution as during the next decade a different nostrum may be in vogue.

Bearing these comments in mind it is suggested that the mineralogy, geochemistry and petrology of kimberlites results from a combination of the processes listed below.

1. *Metasomatism of an upper mantle source.* Incompatible trace element abundances and ratios together with radiogenic isotope studies suggest that the sources of kimberlites contain minerals that can act as sinks for REE, Sr, Nb, Ta, U, and P, etc. Experimental studies suggest that carbonates must also be a component of this source if the CO_2 content of the magma is to be explained; thus, a metasomatized magnesite garnet lherzolite containing minor amounts of phlogopite, K–Ti–richterite, a phosphate, and a titanate (ilmenite, rutile, LIMA, armalcolite, priderite) *seems* to provide a reasonable source. Partial melting may produce CO_2-bearing magnesian potassic undersaturated silicate melts with the requisite compatible and incompatible element contents. Unfortunately, this is an infinitely flexible, almost Procrustean model and the postulated source has actually not yet been shown to exist. In particular we do not know what materials were metasomatized, what the mineralogical effects of the metasomatism are, and the nature and sources of the metasomatic agents. Moreover it is unknown whether the proposed metasomatic event occurred in one or multiple stages and why random metasomatism should result in mineralogical assemblages that melt to produce similar derivative melts.

2. *Partial melting of an upper mantle source.* Kimberlites are apparently produced from melts which originate at depths of 150–200 km in the mantle (Section 9.8). The nature of the melting processes is the most poorly constrained factor in kimberlite petrogenetic models, and hence the subject of most speculation. We have no direct knowledge of the amounts, proportions, and chemistry of the phases melted. Geochemical models, based for example on REE distributions (Section 7.3.4.1) which are not constrained by major element data, must be regarded as providing only one of many partial solutions to the melting problem. The causes of melting are unknown. Current opinion holds that these could be metasomatic events in the mantle (Wyllie 1980), or the lithosphere (Bailey 1980, 1984), diapiric upwelling (Hunter and Taylor 1984) or passive tectonic disturbances (Haggerty 1982).

3. *High-pressure crystallization, magma mixing, and assimilation.* A magma once separated from its source will cool and commence crystallization. In the case of kimberlites the nature of the high-pressure liquidus phases has not yet been unequivocably determined. It is argued in Chapter 6 and in Section 9.11 that the Cr-poor megacryst suite is the normal product of crystallization of kimberlite magmas at high pressures and temperatures. The sequence of crystallization of garnet, ilmenite, pyroxenes, zircon, and possibly olivine will vary depending upon the bulk composition of the melt. Discrete crystals and pseudocotectic mineral pairs may occur. There is no requirement that all magmas, once

generated, must escape from the source regions; thus it is likely that these regions may contain the crystalline products of previous episodes of melting and the incompletely crystallized melts of contemporaneous batches of magma. It is in this environment that cumulates and pegmatites of megacryst phases will form. Incorporation of these pre-existing crystals and their associated liquids in subsequent melts combined with further differentiation is reflected in the complexities of the megacryst suite. Such high-pressure differentiation, hybridization, and assimilation of pre-existing crystals will have an effect upon the geochemistry of the melts that are subsequently erupted. To date these processes have not been evaluated.

Even if the megacryst suite is not cognate the effects of their assimilation must be determined and the nature of liquidus phases identified.

4. *Crystallization and contamination during transit from the source to the upper crust.* During ascent the magma will continue to crystallize. The nature of the liquidus phases will change in response to changing pressures and temperatures. Possible changes might involve an increase in the primary stability field of olivine and elimination of garnet as a liquidus phase as pressure decreases. This aluminous phase may be replaced by magnesian aluminous chrome spinel and/or phlogopite. These primary phases will be carried along with magma and its load of mantle-derived megacrysts or be removed by differentiation processes. Break-up, resorption, and reaction of the megacrysts will also occur during this stage of evolution. Incorporation of crystals derived by the disaggregation of lherzolite xenoliths will further modify the magma and produce the characteristic macrocrystal assemblage.

5. *Low-pressure crystallization, hybridization, and contamination.* Kimberlites are emplaced in the upper crust as a series of dikes. There is no evidence to suggest that they ascended as fluidized bodies from great depth. Diatremes are developed only above this hypabyssal infrastructure at suitable points of weakness by a series of complex brecciation, stoping, and hydrovolcanic processes. Crystallization at low pressures is dominated initially by the continued crystallization of olivine. This is soon replaced as a liquidus phase by Mg–Fe–Ti–Cr spinels, perovskite, and monticellite. These in turn are followed by a groundmass phlogopite, apatite, carbonate, and serpentine. Particularly important is the recognition of complexly mantled olivines and phlogopites, which implies that mixing of several batches of magma at slightly different stages of evolution occurs in the low-pressure environment. Mixing may occur during flow in composite dikes or within temporary magma chambers. Extensive differentiation can result in the formation of macrocryst-poor aphanitic kimberlites and carbonatite-rich residua. Crystallization of hypabyssal kimberlite is evidently a protracted process as evidenced by the common occurrence of resorption and replacement of pre-existing groundmass phases. A long crystallization interval, down to temperatures as low as 600°C, is suggested by experimental studies. In the diatreme environment opportunities for contamination are ideal. The influx of

groundwater and crustal contaminants results in an increase in the silica activity to the point where diopside becomes a stable phase in the interclast matrix.

In summary, kimberlites as we find them are the end products of a complex series of events. The problems of their origin and evolution have by no means been solved. We are still peering, as through a glass darkly, at the intangible and the inaccessible. The object of the next decade in kimberlite petrology should be to deconvolute the evidence presented to us and seek out the primitive kimberlite magma.

"Would you tell me, please, which way I ought to go from here?"

"That depends a good deal on where you want to get to" said the Cat.

"I don't much care where—" said Alice.

"Then it doesn't matter which way you go" said the Cat.

Lewis Carroll
Alice's Adventures in Wonderland

POSTSCRIPT

The Cheshire Cat's reply is, as customary, to the point. Are kimberlite studies in the next decade to meander, as they have done in the past, without a common direction; flounder in the abyss of increasing specialization with the inevitable concommitant isolationism; or progress by means of comprehensive co-operative studies of all facets of kimberlite petrology?

The basic features of the geology, mineralogy, geochemistry, and petrology of kimberlite have been established by *ad hoc* studies of random samples. Systematic studies of individual kimberlites or whole fields of kimberlites are notably lacking. There has been a fascination with trivia and exotica to the exclusion of the commonplace. The majority of investigations have been concerned with one facet of kimberlites in isolation from others. (The writer admits that he cannot plead "not guilty" in this context.) This approach leads to the accumulation of vast amounts of data which cannot be integrated into a whole, and from which conflicting conclusions are commonly drawn. The time is ripe for comprehensive and detailed studies directed toward understanding the origin and evolution of kimberlites on a broader scale.

Some specific objectives might include the following:

1. Detailed geological mineralogical–geochemical studies of individual complex kimberlites. Integration of the type of investigations undertaken by Clement (1982) and Shee (1984) would be particularly profitable. Unfortunately such studies can only be carried out on exploited kimberlites or as a result of a program of deep drilling of other bodies.
2. Comparative studies of *all* of the kimberlites within a given field. Such work would establish the nature of inter-kimberlite petrological variations and aid in the understanding of the differentiation processes occurring in kimberlite magmas. Suitable candidates for study include the State Line field (Colorado–Wyoming), the Kimberley field, the Northern Lesotho field, and the Yakutian fields, for which no comprehensive summaries are available.

3. Characterization of the isotopic group-II (Smith 1983) micaceous kimberlites as found in the Barkly West and Swartruggens fields. These rocks have affinities with both lamproites and the "classic" kimberlites belonging to isotopic group I (Smith 1983). Is it possible that they represent a third distinct class of diamond-bearing rocks?
4. Modern volcanological studies of kimberlite diatremes and epiclastic/pyroclastic kimberlites. Investigations of the Tanzanian and Kansas provinces in this context would prove valuable.
5. Further studies of the megacryst suite with a view to establishing, finally, their relationship to kimberlites. A program of age determination is required using the Sm–Nd and especially the Lu–Hf methods, the latter being particularly useful for garnet–ilmenite assemblages.
6. Experimental studies directed at reproducing the crystallization and differentiation of kimberlite magmas (assuming the primitive magma can be identified!), at high and low pressures.
7. Determination of the composition of partial melts derived from metasomatized lherzolite or magnesite garnet lherzolite.

Other studies will no doubt suggest themselves to the reader. The object of all the above studies is to delineate the evolution of kimberlite magmas from their birth in the upper mantle to their final resting place in the upper crust.

Nirvana for a kimberlite petrologist would be to witness the eruption of a kimberlite volcano. . . .

We can only hope. . . .

REFERENCES

The following non-standard abbreviations for frequently cited works are used in the interests of brevity.

SIKC 1. *Proceedings of the Second International Kimberlite Conference. Volume 1. Kimberlites, Diatremes and Diamonds: Their Geology, Petrology and Geochemistry,* F.R. Boyd Jr. and H.O.A. Meyer, eds. American Geophysical Union, Washington, D.C., 1979.

SIKC 2. *Proceedings of the Second International Kimberlite Conference. Volume 2. The Mantle Sample: Inclusions in Kimberlites and Other Volcanics,* F.R. Boyd Jr. and H.O.A. Meyer, eds. American Geophysical Union, Washington, D.C., 1979.

TIKC 1. *Proceedings of the Third International Kimberlite Conference. Volume 1. Kimberlites I: Kimberlites and Related Rocks,* J. Kornprobst, ed. Developments in Petrology 11A, Elsevier Press, New York, 1984.

TIKC 2. *Proceedings of the Third International Kimberlite Conference. Volume 2. Kimberlites II: The Mantle and Crust–Mantle Relationships,* J. Kornprobst, ed. Developments in Petrology 11B, Elsevier Press, New York, 1984.

LESOTHO KIMBERLITES. *Lesotho Kimberlites,* P.H. Nixon, ed. Lesotho National Development Corporation, Maseru, Lesotho, 1973.

Citations of Soviet literature are for the English translations except where the work is explicitly indicated as being an original citation in Russian. Such citations include an English translation of the title together with the original pagination.

Agee, J.J., Garrison, J.R., Taylor, L.A. 1982. Petrogenesis of oxide minerals in kimberlite, Elliot County, Kentucky, *Am. Mineral.* **67,** 28–42.

Agyei, E.A. 1968. Isotopic and elemental composition of boron in meteorites, tektites and terrestrial materials, Ph.D. thesis, McMaster University, Hamilton, Ontario.

Ahrens, L.H., Cherry, R.D., Erlank, A.J. 1967. Observations on the Th–U relationship in zircons from granitic rocks, *Geochim. Cosmochim. Acta* **31,** 2379–2387.

Akella, J., Rao, P.S., McCallister, R.H., Boyd, F.R., Meyer, H.O.A. 1979. Mineralogical studies of the diamondiferous kimberlite of the Wajrakharur area, Southern India, *SIKC* **1,** 172–177.

Akimov, A.P., Semenov, G.S. 1970. Radioelement contents of kimberlites from the Siberian Platform. *Dokl. Akad. Nauk SSSR* **190,** 947–950.

Allsopp, H.L., Barrett, D.R. 1975. Rb–Sr age determinations of South African kimberlite pipes, *Phys. Chem. Earth* **9,** 605–617.

Anderson, D.L. 1982. Isotopic evolution of the mantle: The role of magma mixing, *Earth Planet. Sci. Lett.*, **57,** 1–12.

Anderson, O.L. 1979. The role of fracture dynamics in kimberlite pipe formation, *SIKC* **1,** 344–353.

Andrews, J.R., Emeleus, C.H. 1975. Structural aspects of kimberlite dyke and sheet intrusion in South West Greenland, *Phys. Chem. Earth* **9,** 43–50.

Aoki, K. 1981. Chemical composition of garnets in kimberlites and their incorporated mafic xenoliths, Colorado Plateau, *Sci. Rep. Tohoku Univ. Ser III,* **15,** 121–126.

Aoki, K., Fujimaki, H., Kitamura, M., 1980. Exsolved garnet-bearing pyroxene megacrysts from some South African kimberlites, *Lithos* **13,** 269–279.

Aoki, K., Fujino, K., Akaogi, M. 1976. Titanochondrodite and titanoclinohumite derived from the upper mantle in the Buell Park kimberlite, Arizona, U.S.A., *Contrib. Mineral. Petrol.* **56,** 243–253.

Apter, D.B., Harper, F.J., Wyatt, B.A., Scott Smith, B.H. 1984. The geology of the Mayeng kimberlite sill complex, South Africa, *TIKC* **2,** 43–57.

Arculus, R.J., Dawson, J.B., Mitchell, R.H., Gust, D.A., Holmes, R.D. 1984. Oxidation states of the upper mantle recorded by megacrystal ilmenite in kimberlite and in type A and B spinel lherzolites, *Contrib. Mineral. Petrol.* **85,** 85–94.

Arculus, R.J., Delano, J.W. 1981. Intrinsic oxygen fugacity measurements: Techniques and results for spinels from upper mantle peridotite and megacryst assemblages, *Geochim. Cosmochim. Acta* **45,** 899–913.

Arima, M., Edgar, A.D. 1983. A high pressure experimental study of a magnesian-rich leucite-lamproite from the West Kimberley Area, Australia: Petrogenetic implications, *Contrib. Mineral. Petrol.* **84,** 228–234.

Arrhenius, G., Everson, J.E., Fitzgerald, R.W., Fujita, H. 1971. Zirconium fractionation in Apollo 11 and Apollo 12 rocks, *Proc. 2nd. Lunar Sci. Conf.* **2,** 169–176.

Arsenyev, A.A. 1962. The laws of the distribution of kimberlites in the Eastern part of the Siberian platform, *Dokl. Akad. Nauk SSSR* **137,** 355–357.

Artsybasheva, T.F., Blagulkina, V.A., Rovsha, V.S., Sarsadskikh, N.N. 1964. The problem of the classification of the Yakutia kimberlites based on those of the Alakit-Daldynsk diamantiferous region, *Int. Geol. Rev.* **6,** 1773–1781.

Atkinson, W.J., Hughes, F.E., Smith, C.B. 1982. A review of the kimberlitic rocks of Western Australia, *Terra Cognita* **2,** 204 (Abstract).

Atkinson, W.J., Hughes, F.E., Smith, C.B. 1984. A review of the kimberlitic rocks of Western Australia, *TIKC,* **1,** 195–224.

Bachinski, S.W., Simpson, E.L. 1984. Ti-phlogopites of the Shaw's Cove minette: A comparison with micas of other lamprophyres, potassic rocks, kimberlites and mantle xenoliths, *Am. Mineral.* **69,** 41–56.

Baertschi, P. 1957. Messung und Deutung relativer Haufigkeitsvariationen von ^{18}O und ^{13}C in Karbonatgesteinen und Mineralien, *Schweiz. Min. Pet. Mitt.* **37,** 74–152.

Bagdasarov, E.A., Landa, E.A., Markovskiy, E. 1981. Chemical composition and crystallization conditions of chrome spinels of volcanic ultramafics and other rocks of the mafic-ultramafic series, *Int. Geol. Rev.* **23,** 931–940.

Bailey, D.K. 1964. Crustal warping-possible tectonic control of alkaline magmatism, *J. Geophys. Res.* **69,** 1103–1111.

Bailey, D.K. 1974. Continental rifting and alkaline magmatism, in *The Alkaline Rocks,* H. Sorensen, ed. J. Wiley & Sons, New York, 148–159.

Bailey, D.K. 1977. Lithospheric control of continental rift magmatism, *J. Geol. Soc. London,* **133,** 103–106.

Bailey, D.K. 1980. Volatile flux, geotherms and the generation of the kimberlite-carbonatite-alkaline magma spectrum, *Mineral. Mag.* **43,** 695–699.

Bailey, D.K. 1982. Mantle metasomatism-continuing chemical change within the earth, *Nature* **296,** 525–530.

Bailey, D.K. 1983. The chemical and thermal evolution of rifts, *Tectonophys.* **94,** 585–597.

Bailey, D.K. 1984. Kimberlite: "The Mantle Sample" formed by ultrametasomatism, *TIKC* **1,** 323–333.

Bailey, S.W., Brown, B.E. 1962. Chlorite polytypism: I: Regular and semi-random one layer structures, *Am. Mineral.* **47,** 819–850.

Bardet, M.G. 1956. Note sur la relation probable entre les lignes de fractives profondes de dijonction continentale et les venues diamantiferes de l'Afrique, *Chron. Mines d'Outre Mer* **236,** 33–38.

Bardet, M.G. 1964. Controle geotectonique de la repartition des venues diamantiferes dans le monde, *Chron. Mines Rech. Miniere* 328–329, 67–89.

Bardet, M.G. 1965. Les gisements de diamant d'U.R.S.S., *Chron. Mines Rech. Minere* **65,** 1–40.

Bardet, M.G. 1973. *Geologie du Diamant,* Vol. I. Bureau de Récherches Géologiques et Minières Memoir 83, Éditions B.R.G.M., Paris, 235 pp.

Bardet, M.G. 1974. *Geologie du Diamant,* Vol. II. Bureau de Récherches Géologiques et Minières Memoir 83, Éditions B.R.G.M., Paris, 223 pp.

Bardet, M.G. 1977. *Geologie du Diamant.* Vol III. Bureau de Récherches Géologiques et Minières Memoir 83, Éditions B.R.G.M., Paris, 221 pp.

Bardet, M.G., Vachette, M. 1966. Determination of the ages of kimberlites of West Africa and an attempt at interpretation from dates the different diamondiferous advents in the world, Third Symposium Africa Geology, Commonwealth Geological Liaison Office Report GGLO(LR)88, Commonwealth Geological Liaison Office, London.

Barrett, D.R., 1975. The genesis of kimberlite and associated rocks: Strontium isotope evidence, *Phys. Chem. Earth* **9,** 637–654.

Barrett, D.R., Berg, G.W. 1975. Complementary petrographic and strontium isotope ratio studies of South African kimberlites, *Phys. Chem. Earth* **9,** 619–636.

Barrington, J., Kerr, P.F. 1961. Breccia pipe near Cameron, Arizona. *Geol. Soc. Amer. Bull.,* **72,** 1661–1674.

Bartoshinski, Z.V., Bekesha, S.N., Botkunov, A.I., Garanin, V.K., Kudryavtseva, G.P. 1982. Dissolution cones on zircon crystals from the "Mir" kimberlite pipe, *Dokl. Akad. Nauk SSSR* **267,** 1444–1448 (Russian).

Bassett, H. 1954. The Igwisi craters and lavas, *Rec. Geol. Surv. Tanganyika* **4,** 81–92.

Basu, A.R., Rubury, E. 1980. Tectonic significance of kimberlite dikes in central New York, *Geol. Soc. Am. N.E. Sect. Prog Abst.* **23.**

Basu, A.R., Tatsumoto, M. 1980. Nd-isotopes in selected mantle-derived rocks and minerals and their implications for mantle evolution, *Contrib. Mineral. Petrol.* **75,** 43–54.

Berg, G.W., Allsopp, H.L. 1972. Low $^{87}Sr/^{86}Sr$ ratios in fresh South African kimberlites, *Earth Planet. Sci. Lett.,* **16,** 27–30.

Berger, E.T., Vannier, M. 1984. Petrology of megacrysts, mafic and ultramafic xenoliths from the Pipe of Eglazines, Causses, France, *TIKC* **1,** 155–168.

Binns, R.A. 1969. High pressure megacrysts in basanitic lavas near Armidale, New South Wales, *Am. J. Sci.* **267A**, 33–49.

Bishop, F.C., Smith, J.V., Dawson, J.B. 1975. Pentlandite–magnetite intergrowth in De Beers spinel lherzolite: Review of sulphides in nodules, *Phys. Chem. Earth* **9**, 323–328.

Blagulkina, V.H., Tarnovskaya, A.N. 1975. Perovskite from Yakutian kimberlites, *Zap. Vses. Mineral. Obshch.* **104**, 703–710 (Russian).

Bloomer, A.G., Nixon, R.H. 1973. The Geology of the Letseng-la-terae kimberlite pipes, *Lesotho Kimberlites* 20–32.

Bobrievich, A.P., Bondarenko, M.N., Gnevushev, M.A., Kind, N.V., Koreshkov, B.Y., Kuryleva, N.A., Nefoca, Z.D., Popugeva, L.A., Popova, E.Z., Skuiskii, V.D., Smirnov, G.I., Yurkevtski, R.K., Fayunshteyeyuh, G.H., Shukin, V.I. 1959(a). *Diamonds of Siberia.* Gozgeolteknizdat, Moscow (Russian).

Bobrievich, A.P., Bondarenko, M.N., Gnevushev, M.A., Krasov, L.M., Smirnov, S.I., Yurkevitch, R.K. 1959(b). *The Diamond Deposits of Yakutia,* Izdatelstvo Nedra, Moscow (Russian).

Bobrievich, A.P., Ilupin, I.P., Kozlov, I.T., Lebedev, L.I., Pankratov, A.A., Smirnov, G.I., Kharkiv, A.D. 1964. *Petrography and Mineralogy of the Kimberlite Rocks of Yakutia,* Izdatelstvo Nedra, Moscow (Russian).

Boctor, N.Z., Boyd, F.R. 1979. Distribution of rare earth elements in perovskite from kimberlites, *Carnegie Inst. Washington Yearb.* **78**, 572–574.

Boctor, N.Z., Boyd, F.R. 1980(a). Oxide minerals in the Liqhobong kimberlite, Lesotho *Am. Mineral.* **65**, 631–638.

Boctor, N.Z., Boyd, F.R. 1980(b). Ilmenite nodules and associated sulphides in kimberlite from Yakutia, U.S.S.R., *Carnegie Inst. Washington Yearb.* **79**, 302–304.

Boctor, N.Z., Boyd, F.R. 1981. Oxide minerals in a layered kimberlite–carbonatite sill from Benfontein South Africa, *Contrib. Mineral. Petrol.* **76**, 253–259.

Boctor, N.Z., Boyd, F.R. 1982. Petrology of kimberlite from the DeBruyn and Martin Mine, Bellsbank, South Africa, *Am. Mineral.* **67**, 917–925.

Boctor, N.Z., Meyer, H.O.A. 1979. Oxide and sulphide minerals in kimberlite from Green Mountain, Colorado, *SIKC* **1**, 217–228.

Boctor, N.Z., Yoder, H.S. 1980. Distribution of rare earth elements in perovskite from the Oka carbonatite Quebec, *Carnegie Inst. Washington Yearb.* **79**, 304–307.

Boettcher, A.L., Mysen, B.O., Modreski, P.J. 1975. Melting in the mantle: Phase relationships in natural and synthetic peridotite–H_2O and peridotite–H_2O–CO_2 systems at high pressures, *Phys. Chem. Earth* **9**, 855–865.

Boettcher, A.L., Robertson, J.K., Wyllie, P.J. 1980. Studies in synthetic carbonatite systems: Solidus relationships for CaO–MgO–CO_2–H_2O to 40 kilobars and CaO–MgO–SiO_2–CO_2–H_2O to 10 kilobars, *J. Geophys. Res.* **85**, 6937–6943.

Bolivar, S.L., Brookins, D.G. 1977. Geophysical and Rb–Sr study of the Elliot County, Kentucky and Prairie Creek, Arkansas kimberlites, Second International Kimberlite Conference Santa Fe, New Mexico (Extended Abstracts) (unpaginated).

Bonney, T.G., 1899. The parent rock of the diamond in South Africa, *R. Soc. London Proc.* **65**, 235–236.

Borisenok, L.A. 1959. Distribution of gallium in the rocks of the Soviet Union, *Geochemistry* 52–70.

Borodin, L.S. 1976. *Petrology and Geochemistry of Ultrabasic Rocks and Kimberlites,* Izdatelstvo Nedra, Moscow (Russian).

Bosch, J.L. 1971. The petrology of some kimberlite occurrences in the Barkly West district, Cape Province, *Trans. Geol. Soc. S. Africa* **74**, 75–101.

Botkunov, A.I., Garanin, V.K., Kudryavtseva, G.P., Perminova, M.S. 1980. Mineral inclusions in olivine and zircon from the kimberlite pipe "Mir," *Dokl. Akad. Nauk SSSR* **251**, 1233–1236 (Russian).

Bott, M.H.P. 1982. *The Interior of the Earth: Its Structure, Constitution and Evolution*. Edward Arnold Ltd., London.

Bowen, N.L. 1922. Genetic features of alnöitic rocks at Isle Cadieux, Quebec, *Am. J. Sci. Ser. 5* **3,** 1–34.

Boyd, F.R. 1974a. Olivine megacrysts from the kimberlites of the Monastery and Frank Smith Mines, South Africa, *Carnegie Inst. Washington Yearb.* **73,** 282–285.

Boyd, F.R. 1974b. Ultramafic nodules from the Frank Smith kimberlite pipe, South Africa, *Carnegie Inst. Washington Yearb.* **73,** 285–293.

Boyd, F.R., Clement, C.R. 1977. Compositional zoning of olivine in kimberlites from the De Beers Mine, Kimberley, South Africa, *Carnegie Inst. Washington Yearb.* **71,** 373–378.

Boyd, F.R., Danchin, R.V. 1974. Discrete nodules from the Artur de Paiva kimberlite, Angola, *Carnegie Inst. Washington Yearb.* **73,** 278–282.

Boyd, F.R., Danchin, R.V. 1980. Lherzolites, eclogites and megacrysts from some kimberlites of Angola, *Am. J. Sci.* **280A,** 528–549.

Boyd, F.R., Dawson, J.B. 1972. Kimberlite garnets and pyroxene–ilmenite intergrowths, *Carnegie Inst. Washington Yearb.* **71,** 373–378.

Boyd, F.R., Dawson, J.B., Smith, J.V. 1984(a). Granny Smith diopside megacrysts from the kimberlites of the Kimberley area and Jagersfontein, South Africa, *Geochim. Cosmochim. Acta* **48,** 381–384.

Boyd, F.R., Finnerty, A.A. 1980. Conditions of origin of natural diamonds of peridotitic affinity, *J. Geophys. Res.* **85,** 6911–6918.

Boyd, F.R., Gurney, J.J. 1982. Low calcium garnets: Keys to craton structure and diamond crystallization, *Carnegie Inst. Washington Yearb.* **81,** 261–267.

Boyd, F.R., Nixon, P.H. 1973. Origin of the ilmenite–silicate nodules in kimberlites from Lesotho and South Africa, *Lesotho Kimberlites* 254–268.

Boyd, F.R., Nixon, P.H. 1975. Origins of the ultramafic nodules from some kimberlites of Northern Lesotho and the Monastery Mine, South Africa, *Phys. Chem. Earth* **9,** 431, 454.

Boyd, F.R., Nixon, P.H. 1978. Ultramafic nodules from the Kimberley pipe, South Africa, *Geochim. Cosmochim. Acta* **42,** 1367–1382.

Boyd, F.R., Nixon, P.H., Boctor, N.Z. 1984b. Rapidly crystallized garnet pyroxenite xenoliths possibly related to discrete nodules, *Contrib. Mineral. Petrol.* **86,** 119–130.

Brady, J.B., McCallister, R.H. 1983. Diffusion data for clinopyroxenes from homogenization and self-diffusion experiments, *Am. Mineral.* **68,** 95–105.

Brakhfogel, F.F., Kovalskii, V.V. 1979. Age of kimberlite bodies of the Siberian Platform, *Int. Geol. Rev.* **21,** 307–314.

Brey, G. 1978. Origin of olivine melilitites—chemical and experimental constraints, *J. Volcanol. Geotherm. Res.* **3,** 61–88.

Brey, G., Brice, W.R., Ellis, D.J., Green, D.H., Harris, K.L., Ryabchikov, I.D. 1983. Pyroxene–carbonate reaction in the upper mantle, *Earth Planet. Sci. Lett.*, **62,** 63–74.

Brey, G., Green, D.H. 1977. Systematic study of liquidus phase relations in olivine melilitite at high pressures and the role of CO_2 in the earth's upper mantle, *Contrib. Mineral. Petrol.* **55,** 217–230.

Brogger, W.C. 1921. Die Eruptivgesteine des Kristianagebietes IV Das Fengebiet in Telemark, Norwegen, *Skr. Norske Vidensk. Akad. i Oslo. Mat-Naturv. Kl.* (1920), No. 9.

Brookins, D.G. 1967. The strontium geochemistry of carbonates in kimberlites and limestones from Riley County, Kansas, *Earth Planet. Sci. Lett.*, **2,** 235–240.

Brookins, D.G. 1970. Kimberlite at Winkler Crater, Kansas, *Geol. Soc. Am. Bull.* **81,** 541–546.

Brookins, D.G., Dellavalle, R.S., Bolivar, S.L. 1979. Significance of uranium abundance in United States kimberlites, *SIKC* **1,** 280–288.

Brookins, D.G., McDermott, V.J. 1970. The mineralogy of the Randolph kimberlites, Riley County, Kansas, *Trans. Kansas Acad. Sci.* **73,** 31–39.

Brown, D.D., Bennett, G., George, P.T. 1967. The source of alluvial kimberlite indicator minerals in the James Bay Lowland, *Ontario Dept. Mines Misc. Paper* **7,** 33 pp.

Brownlow, A.H. 1979. *Geochemistry*. Prentice-Hall, Englewood Cliffs, New Jersey.

Brummer, J.J. 1978. Diamonds in Canada, *Can. Mining Metal. Bull.* **71,** 64–79.

Bryner, L. 1961. Breccia and pebble columns associated with epigenetic ore deposits, *Econ. Geol.* **56,** 488–508.

Burkov, V.V., Podporina, Y.K. 1965. Rare elements in kimberlite rocks, *Dokl. Akad. Nauk SSSR* **163,** 169–172.

Burkov, V.V., Podporina, Y.K. 1966. First data on rare earths in kimberlite, *Dokl. Akad. Nauk SSSR* **171,** 215–219.

Butakova, E.L., Egorov, L.S. 1962. Maimecha–Kotui complex of alkaline and ultrabasic rocks, in: *The Petrography of Eastern Siberia*. Akad. Sci. SSSR, Moscow, pp. 419–589.

Carmichael, I.S.E. 1967. The iron–titanium oxides of salic volcanic rocks and their associated ferromagesian silicates, *Contrib. Mineral. Petrol.* **14,** 36–64.

Carswell, D.A. 1975. Primary and secondary phlogopites in garnet lherzolite xenoliths, *Phys. Chem. Earth* **9,** 417–430.

Carswell, D.A., Dawson, J.B., Gibb, F.G.F. 1981. Equilibration conditions of upper mantle eclogites: Implications for kyanite-bearing and diamondiferous varieties, *Mineral. Mag.* **44,** 79–89.

Carswell, D.A., Gibb, F.G.F. 1980. Geothermometry of garnet lherzolite nodules with special reference to those from the kimberlites of Northern Lesotho, *Contrib. Mineral. Petrol.* **74,** 403–416.

Carswell, D.A., Griffin, W.L., Kresten, P. 1984. Peridotite nodules from the Ngopetsoeu and Lipelaneng kimberlites, *TIKC* **2,** 229–243.

Chapman, N.A. 1976. Inclusions and megacrysts from undersaturated tuffs and basanites, East Fife, Scotland, *J. Petrol.* **17,** 472–498.

Cherepanov, V.A. 1967. Boron in kimberlite and meimechite of Siberia, *Dokl. Akad. Nauk SSSR* **172,** 187–190.

Clark, S.P., Ringwood, A.E. 1964. Density distribution and constitution of the mantle. *Rev. Geophys.* **2,** 35–88.

Clarke, D.B. 1979. Synthesis of nickeloan djerfisherites and the origin of potassic sulphides at the Frank Smith Mine, *SIKC* **2,** 300–308.

Clarke, D.B., Mitchell, R.H. 1975. Mineralogy and petrology of the kimberlite from Somerset Island, N.W.T., Canada, *Phys. Chem. Earth* **9,** 123–136.

Clarke, D.B., Pe-Piper, G.G. 1983. Multiply exsolved clinopyroxene megacrysts from the Frank Smith Mine, Cape Province, South Africa, *Lithos* **16,** 75–84.

Clement, C.R. 1973. Kimberlites from the Kao pipe, Lesotho, *Lesotho Kimberlites* 110–121.

Clement, C.R. 1975. The emplacement of some diatreme-facies kimberlites, *Phys. Chem. Earth* **9,** 51–59.

Clement, C.R. 1979. The origin and infilling of kimberlite pipes, in Kimberlite Symposium II, Cambridge (Extended Abstracts).

Clement, C.R. 1982. A comparative geological study of some major kimberlite pipes in the Northern Cape and Orange Free State, Ph.D. thesis (2 vols.), Univ. Cape Town.

Clement, C.R., Gurney, J.J., Skinner, E.M.W. 1975. Monticellite: An abundant groundmass mineral in some kimberlites, Kimberlite Symposium I: Cambridge (Extended Abstracts), pp. 71–73.

Clement, C.R., Skinner, E.M.W. 1979. A textural genetic classification of kimberlite rocks, Kimberlite Symposium II, Cambridge (Extended Abstracts).

Clement, C.R., Skinner, E.M.W., Scott Smith, B.H. 1984. Kimberlite re-defined, *J. Geol.* **32,** 223–228.

Clifford, T.N. 1966. Tectono-metallogenic units and metallogenic provinces of Africa, *Earth Planet. Sci. Lett.* **1,** 421–434.

Cloos, H. 1941. Bau und Tatigkeit von Tuffschloten. Untersuchungen an den Schwabischen Vulkanen, *Geol. Rundsch.* **32,** 709–800.

Coe, K. 1966. Intrusive tuff of West Cork, Ireland, *Geol. Soc. London. Q. J.* **122,** 1–28.

Cohen, E. 1872. Geologische mittheilungen ueber das Workommen das Diamanten in Sued-Afrika (Letter dated September 20th. 1872), *N. Jb. Min.* **1874,** 857–861.

Colville, R.J.L. 1968. Pyrope from Elie, Fife, *Scot. J. Geol.* **4,** 283–286.

Cooper, A.F., Gittins, J. 1974. Shortite in kimberlite from the Upper Canada Gold Mine, Ontario: A discussion, *J. Geol.* **82,** 667–669.

Cornelissen, A.K., Verwoerd, W.J. 1975. The Bushmanland kimberlites and related rocks, *Phys. Chem. Earth* **9,** 71–80.

Crandall, A.R. 1885. The occurrence of trap rock in Eastern Kentucky, *Science* **6,** 222.

Crandall, A.R. 1910. Coals of the Licking Valley region and some contiguous territory including also an account of the Elliot County and its dikes, *Kentucky Geol. Surv. Bull.* **10.**

Crockett, R.N., Mason, R. 1968. Foci of mantle disturbance in Southern Africa and their economic significance, *Econ. Geol.* **63,** 532–540.

Crough, S.T. 1981. Mesozoic hot spot epeirogeny in Eastern North America, *Geology* **9,** 2–6.

Crough, S.T., Morgan, W.J., Hargraves, R.B. 1980. Kimberlites: Their relation to mantle hot spots, *Earth Planet. Sci. Lett.* **50,** 260–274.

Cullers, L.R., Mullenax, J., Dimarco, M.J., Nordeng, S. 1982. The trace element content and petrogenesis of kimberlites in Riley County, Kansas U.S.A., *Am. Mineral.* **67,** 223–233.

Daly, R.A. 1925. Carbonate dikes of the Premier diamond mine, Transvaal, *J. Geol.* **33,** 659–684.

Daly, R.A. 1933. *Igneous Rocks and the Depths of the Earth.* McGraw-Hill, New York.

Danchin, R.V., d'Orey, F. 1972. Chromian spinel exsolution in ilmenite from the Premier Mine Transvaal South Africa, *Contrib. Mineral. Petrol.* **35,** 43–49.

Danchin, R.V., Ferguson, J., McIver, J.R., Nixon, P.H. 1975. The composition of late-stage kimberlite liquids as revealed by nucleated autoliths, *Phys. Chem. Earth* **9,** 235–245.

Danchin, R.V., Wyatt, B.A. 1979. Statistical cluster analysis of garnets from kimberlites and their xenoliths, Kimberlite Symposium II, Cambridge (Extended Abstracts).

Davidson, C.F. 1964. On diamantiferous diatremes, *Econ. Geol.* **59,** 1368–1380.

Davidson, C.F. 1967. The kimberlites of the USSR, in *Ultramafic and Related Rocks,* Wyllie P.J., ed. John Wiley & Sons, New York, pp. 251–256.

Davis, G.L. 1977. The ages and uranium contents of zircons from kimberlites and associated rocks, Second International Kimberlite Conference, Santa Fe, New Mexico (Extended Abstracts).

Davis, G.L., Sobolev, N.V., Kharkiv, A.D. 1980. New data on the age of Yakutian kimberlites obtained by the uranium–lead method on zircons, *Dokl. Akad. Nauk SSSR* **254,** 53–57.

Dawson, J.B. 1960. A comparative study of the geology and petrography of the kimberlites of the Basutoland province, Ph.D. thesis, Univ. Leeds.

Dawson, J.B. 1962. Basutoland kimberlites, *Geol. Soc. Am. Bull.* **73,** 545–560.

Dawson, J.B. 1966. The kimberlite–carbonatite relationship, *Mineral. Soc. India. Internat. Mineral. Assoc. Papers 4th Gen. Mtg. 1–4.*

Dawson, J.B. 1967(a). A review of the geology of kimberlite, in *Ultramafic and Related Rocks,* P.J. Wyllie, ed. John Wiley & Sons, New York, pp. 241–251.

Dawson, J.B. 1967(b). Geochemistry and origin of kimberlite, in *Ultramafic and Related Rocks,* P.J. Wyllie, ed. John Wiley & Sons, New York, pp. 269–278.

Dawson, J.B. 1968. Recent researches on kimberlites and diamond geology, *Econ. Geol.* **63,** 504–511.

Dawson, J.B. 1970. The structural setting of African kimberlite magmatism, in *African Magmatism and Tectonics,* T.N. Clifford and I.G. Gass, eds. Oliver and Boyd, Edinburgh, pp. 321–335.

Dawson, J.B. 1971. Advances in kimberlite geology, *Earth Sci. Rev.* **7,** 187–214.

Dawson, J.B. 1972. Kimberlites and their relationship to the upper mantle, *R. Soc. London Philos. Trans. Ser. A.* **271,** 297–311.

Dawson, J.B. 1980. *Kimberlites and their Xenoliths,* Springer Verlag, New York.

Dawson, J.B. 1984. Contrasting types of upper mantle metasomatism, *TIKC* **2,** 289–294.

Dawson, J.B., Hawthorne, J.B. 1970. Intrusion features of some hypabyssal South African kimberlites, *Bull. Volcanol.* **34,** 740–757.

Dawson, J.B., Hawthorne, J.B. 1973. Magmatic sedimentation and carbonatitic differentiation in kimberlite sills at Benfontein, South Africa, *J. Geol. Soc. London* **129,** 61–85.

Dawson, J.B., Hervig, R.L., Smith, J.V. 1981. Fertile iron-rich dunite xenoliths from the Bultfontein kimberlite, South Africa, *Forts. Mineral.* **59,** 303–324.

Dawson, J.B., Powell, D.G. 1969. Mica in the upper mantle, *Beitr. Mineral. Petrogr.* **22,** 235–237.

Dawson, J.B., Powell, D.G., Reid, A.M. 1970. Ultrabasic lavas and xenoliths from the Lashaine volcano, Tanzania, *J. Petrol.* **11,** 519–548.

Dawson, J.B., Reid, A.M. 1970. A pyroxene–ilmenite intergrowth from the Monastery Mine, South Africa, *Contrib. Mineral. Petrol.* **26,** 296–301.

Dawson, J.B., Smith, J.V. 1975. Chemistry and origin of phlogopite megacrysts in kimberlite, *Nature* **253,** 336–338.

Dawson, J.B., Smith, J.V. 1977. The MARID (mica–amphibole–rutile–ilmenite–diopside) suite of xenoliths in kimberlite, *Geochim. Cosmochim. Acta* **41,** 309–323.

Dawson, J.B., Smith, J.V., Hervig, R.L. 1977. Late-stage diopside in kimberlite groundmass, *N. Jahrb. Mineral. Monats.* **1977,** 529–553.

Dawson, J.B., Stephens, W.E. 1975. Statistical analysis of garnets from kimberlites and associated xenoliths, *J. Geol.* **83,** 589–607.

Deines, P. 1968. The carbon and oxygen isotopic composition of carbonates from a mica peridotite dike, near Dixonville, Pennsylvania, *Geochim. Cosmochim. Acta* **32,** 613–625.

Deines, P. 1980. The carbon isotopic composition of diamonds: Relationship to diamond shape, color, occurrence and vapour composition, *Geochim. Cosmochim. Acta* **44,** 943–961.

Deines, P. 1984. Evidence for a systematic depletion in ^{13}C in parts of the mantle underlying Orapa, Botswana, kimberlite, Geol. Soc. America Ann. Mtg. Prog. with abstracts Reno 1984 (Abstract).

Deines, P., Gold, D.P. 1973. The isotopic composition of carbonatite and kimberlite carbonates and their bearing on the isotopic composition of deep-seated carbon, *Geochim. Cosmochim. Acta* **37,** 1709–1733.

Deines, P., Gurney, J.J., Harris, J.W. 1984. Associated chemical and carbon isotopic composition variations in diamonds from the Finsch and Premier kimberlites, South Africa, *Geochim. Cosmochim. Acta.* **45,** 325–342.

Delaney, J.S., Smith, J.V., Carswell, D.A., Dawson, J.B. 1980. Chemistry of micas from kimberlites and xenoliths. II: Primary- and secondary-textured micas from peridotite xenoliths, *Geochim. Cosmochim. Acta* **44,** 857–872.

Delaney, P.T., Pollard, D.D. 1981. Deformation of host rocks and flow of magma during growth of minette dikes and breccia-bearing intrusions near Ship Rock, New Mexico, *U.S. Geol. Surv. Prof. Paper No. 1202.*

Demaiffe, D., Fieremans, M. 1981. Strontium isotope geochemistry of the Mbuji-Mayi and Kundelungu kimberlites, Zaire, Central Africa, *Chem. Geol.* **31,** 311–323.

Dempster, A.N., Tucker, R. 1973. The geology of Sekameng (Butha-Buthe) kimberlite pipe and the associated dike swarm, *Lesotho Kimberlites* 180–189.

Dennison, J. 1983. Comment on "Tectonic model for kimberlite emplacement in the Appalachian Plateau of Pennsylvania," *Geology* **11,** 252–253.

DePaolo, D.J., Wasserburg, G.J. 1976. Nd isotopic variation and petrogenetic models, *Geophys. Res. Letts.,* **3,** 249–252.

Diller, J.S. 1885. Dikes of peridotite cutting the carboniferous rocks of Kentucky, *Science* **5,** 65.

Diller, J.S. 1886. Notes on the perodotite at Elliot County, Kentucky, *Am. J. Sci. (Ser. 3)* **2,** 121–125.

Diller, J.S. 1887. Peridotite of Elliot County, Kentucky, *U.S. Geol. Surv. Bull.* **8.**

Diller, J.S. 1892. Mica peridotite from Kentucky, *Am. J. Sci. Ser. 3,* **44,** 286–289.

Dobrovolskaya, M.G., Troneva, N.V., Ilupin, I.P., Basova, G.V. 1978. Mackinawite from Yakutian kimberlites, *Tr. Mineral. Muz. Akad. Nauk SSSR* **26,** 33–39 (Russian).

Donaldson, C.H., Reid, A.M. 1982. Multiple intrusion of a kimberlite dike, *Trans. Geol. Soc. S. Africa* **85,** 1–12.

Dong, Z., Zhou, J. 1980. The typomorphic characteristics of chromites from kimberlites in China and the significance in exploration of diamond deposits, *Acta Geologica Sinica* **54,** 284–299 (Chinese).

du Toit, A.L. 1906. Geological survey of the Eastern portion of Griqualand West, *11th Rpt. Geol. Comm. Cape Colony,* 89–176.

Dunin-Barkovskaya, E.A., Ukhavov, A.V. 1974. Bismuth in the kimberlite of Yakutia, *Geochem. Internat.* **11,** 1215–1219.

Dunn, E.J. 1873. Mode of occurrence of diamonds in South Africa, *Q. J. Geol. Soc. London* **30,** 54–59.

Eby, G.N. 1975. Abundance and distribution of the rare earth elements and ytterbium in the rocks and minerals of the Oka carbonatite complex, *Geochim. Cosmochim. Acta* **39,** 597–620.

Edwards, C.B., Howkins, J.B. 1966. Kimberlites in Tanganyika with special reference to the Mwadui occurrence, *Econ. Geol.* **61,** 537–554.

Eggler, D.H. 1974. Effect of CO_2 on the melting on peridotite, *Carnegie Inst. Washington Yearb.* **73,** 215–224.

Eggler, D.H. 1974. Peridotite–carbonate relations in the system $CaO–MgO–SiO_2–CO_2$, *Carnegie Inst. Washington Yearb.* **74,** 468–474.

Eggler, D.H. 1976. Does CO_2 cause partial melting in the low velocity layer of the mantle? *Geology* **4,** 69–72.

Eggler, D.H. 1977. The principle of the zone of invariant vapor composition: An example in the system $CaO–MgO–SiO_2–CO_2–H_2O$ and implications for the mantle solidus, *Carnegie Inst. Washington Yearb.* **76,** 428–435.

Eggler, D.H. 1978. The effect of CO_2 upon partial melting of peridotite in the system $Na_2O–CaO–Al_2O_3–MgO–SiO_2–CO_2$ to 35 kilobars, with an analysis of melting in a peridotite–$H_2O–CO_2$ system, *Am. J. Sci.* **278,** 305–343.

Eggler, D.H. 1983. Upper mantle oxidation state: Evidence from olivine–orthopyroxene–ilmenite assemblages, *Geophys. Res. Lett.* **10,** 365–368.

Eggler, D.H., Baker, D.R. 1982. Reduced volatiles in the system C–O–H: Implications to mantle melting, fluid formation and diamond genesis, in *High Pressure Research in Geophysics,* S. Akimoto and M.H. Manghnani, eds. Center for Academic Publications Japan, Tokyo, pp. 237–250.

Eggler, D.H., McCallum, M.E. 1976. A geotherm from megacrysts in the Sloan kimberlite pipes, Colorado, *Carnegie Inst. Washington Yearb.* **75,** 538–541.

Eggler, D.H., McCallum, M.E., Smith, C.B. 1979. Megacryst assemblages in kimberlite from Northern Colorado and Southern Wyoming: Petrology, geothermometry-barometry and a real distribution, *SIKC* **2,** 213–226.

Eggler, D.H., Wendlandt, R.F. 1979. Experimental studies on the relationship between kimberlite magmas and partial melting of peridotite, *SIKC* **1,** 330–338.

Egorov, L.S. 1970. Carbonatites and ultrabasic-alkaline rocks of the Maimecha-Kotui region, N. Siberia, *Lithos* **3,** 341–359.

Egorov, L.S., Goldburt, T.L., Skikhorina, K.M. 1961. Geology and petrography of the magmatic rocks of the Gulya intrusion, *Tr. Nauchno-issled. Instit. Geol. Arkt* **1961,** 3–115 (Russian).

Ehmann, D., Lovering, J.F. 1967. The abundance of mercury in meteorites and rocks by neutron activation analysis, *Geochim. Cosmochim. Acta* **31,** 357–376.

Ehrenberg, S.N. 1978. Petrology of potassic volcanic rocks and ultramafic xenoliths from the Navajo volcanic field, New Mexico and Arizona, Ph.D. thesis, University of California at Los Angeles.

Ehrenberg, S.N. 1982. Petrogenesis of garnet lherzolite and megacrystalline nodules from the Thumb Navajo Volcanic field, *J. Petrol.* **23,** 507–547.

Ellis, D.E., Wyllie, P.J. 1980. Phase relations and their petrological implication in the system $MgO–SiO_2–H_2O–CO_2$ at pressures up to 100 kilobars, *Am. Mineral.* **65,** 540–556.

Elthon, D., Ridley, W.I. 1979. The oxide and silicate mineral chemistry of a kimberlite from the Premier Mine: Implications for the evolution of kimberlitic magmas, *SIKC* **1,** 206–216.

Emeleus, C.H., Andrews, J.R. 1975. Mineralogy and petrology of kimberlite dyke and sheet intrusions and included peridotite xenoliths from South West Greenland, *Phys. Chem. Earth* **9,** 179–198.

England, P., Houseman, G. 1984. On the geodynamic setting of kimberlite genesis, *Earth Planet. Sci. Lett.* **67,** 109–122.

Erlank, A.J., Allsopp, H.L., Hawkesworth, C.J., Menzies, M.A. 1982. Chemical and isotopic characteristics of upper mantle metasomatism in peridotite nodules from the Bultfontein kimberlite, *Terra Cognita* **2,** 261–263.

Erlank, A.J., Rickard, R.S. 1977. Potassic richterite-bearing peridotites from kimberlite and the evidence they provide for upper mantle metasomatism. SIKC, Santa Fe, New Mexico (Extended Abstracts) (unpaginated).

Erlikh, E.N. 1959. The kimberlite bodies of the Ukukit group, *Tr. Nauchno-issled Instit. Geol. Arkt* **65,** 106–132 (Russian).

Exley, R.A., Smith, J.V. 1982. The role of apatite in mantle enrichment process and in the petrogenesis of some alkali basalt suites, *Geochim. Cosmochim. Acta* **46,** 1375–1384.

Fairbairn, P.E., Robertson, R.M.S. 1966. Stages in the tropical weathering of kimberlite, *Clay Minerals* **6,** 351–370.

Fanelli, M.F., Cava, N., Wyllie, P.J. 1985. Calcite and dolomite without portlandite at a new eutectic in $CaO–MgO–CO_2–H_2O$, with applications to carbonatites, *Proc. 13th. Gen. Mtg. Internat. Mineral. Assoc. 1982, Varna, Bulgaria* 313–322.

Farmer, G.L., Boettcher, A.L. 1981. Petrologic and crystal-chemical significance of some deep-seated phlogopites, *Am. Mineral.* **66,** 1154–1163.

Ferguson, J., Arculus, R.J., Joyce, J. 1979. Kimberlite and kimberlitic intrusives in southeastern Australia: a review, *Bul. Mineral Res. J. Australian Geol. Geophys.* **4,** 227–241.

Ferguson, J., Danchin, R.V., Nixon, P.H. 1973(a). Fenitisation associated with kimberlite magmas, *Lesotho Kimberlites* 207–213.

Ferguson, J., Danchin, R.V., Nixon, P.H. 1973(b). Petrochemistry of kimberlite autoliths, *Lesotho Kimberlites* 285–293.

Ferguson, J., Martin, H., Nicolaysen, L.O., Danchin, R.V. 1975. Gross Brukkaros: A kimberlite/carbonatite volcano, *Phys. Chem. Earth* **9,** 219–234.

Ferguson, J., Sheraton, J.W. 1979. Petrogenesis of kimberlitic rocks and associated xenoliths of Southeastern Australia, *SIKC.* **1,** 140–160.

Fesq, H.W., Kable, E.J.D., Gurney, J.J. 1975. Aspects of the geochemistry of kimberlites from the Premier Mine and other South African occurrences, with particular reference to the rare earth elements, *Phys. Chem. Earth* **9,** 686–707.

Fieremans, C. 1966. Contribution a l'etude petrographique de la breche kimberlitique de Bakwanga, *Mem. Inst. Geol. Univ. Louvain* **24,** 1–92.

Fieremans, M., Hertogen, J., Demaiffe, D. 1984. Petrography, geochemistry and strontium isotopic composition of the Mbuji-Mayi and Kundelungu kimberlites, *TIKC* **1,** 107–120.

Fieremans, M., Ottenburgs, R. 1979(a). The occurrence of zircon and baddeleyite crystals in the kimberlite formations at Mbuji-Mayi, Bakwanga, Zaire, *Bull. Soc. Belge Geol.* **88,** 25–31.

Fieremans, M., Ottenburgs, R. 1979(b). Kimberlite inclusions and chlorite nodules from the kimberlite breccia of Mbuji-Mayi, Eastern Kasai, Zaire, *Bull. Soc. Belge Geol.* **88,** 205–224.

Finnerty, A.A., Boyd, F.R. 1984. Evaluation of thermobarometers for garnet peridotites, *Geochim. Cosmochim. Acta* **48,** 15–27.

Fisher, R.V. 1961. Proposed classification of volcaniclastic sediments and rocks, *Geol. Soc. Am. Bull.* **72,** 1409–1414.

Fisher, R.V., Schminke, H.U. 1984. *Pyroclastic Rocks,* Springer, New York.

Foland, K.A., Faul, H. 1977. Ages of White Mountain intrusives, New Hampshire, Vermont and Maine, *U.S. Am. J. Sci.* **277,** 888–904.

Fourie, C.P. 1958. Die diamantvoorkomste in die omgewing van Swartruggens, *Transvaal. Geol. Surv. South Africa, Bull.* **26,** 16 pp.

Fozzard, P.M.H. 1956. Further notes on the volcanic rocks from Igwisi, Tanganyika, *Tangan. Geol. Surv. Rec.* **6,** 69–75.

Francis, E.H. 1960. Intrusive tuffs related to the Firth of Forth volcanoes, *Edinburgh Geol. Soc. Trans.* **18,** 32–50.

Francis, E.H. 1962. Volcanic neck emplacement and subsidence structures at Dunbar, South-east Scotland, *Trans. R. Soc. Edinburgh* **65,** 41–58.

Frank-Kamenetskii, V.A., Veselskii, I. 1961. X-ray investigation of isomorphism in perovskites, *Geochemistry* **5,** 393–403.

Frankel, J.J. 1956. An inclusion bearing olivine melilitite from Mukorob, South West Africa, *Trans. R. Soc. S. Africa,* **35,** 115–123.

Frantsesson, E.V. 1968. *The Petrology of Kimberlites,* Izdatelstvo. Nedra, Moscow (Russian).

Frantsesson, E.V. 1970. *The Petrology of Kimberlites* (translated from the Russian by D.A. Brown), Publication No. 150, Department of Geology Australian National University Canberra.

Frantsesson, E.V., Boris, E.I. 1983. Criteria for estimating the depth of erosion in kimberlite pipes, *Int. Geol. Rev.* **25,** 565–568.

Frantsesson, E.V., Prokopchuk, B.I. 1968. Kimberlites—the tectonomagmatic facies of the alkaline-ultramafic association of the platforms, in *Vulkanism and Tectogenesis,* Nauka, Moscow, pp. 159–164 (Russian).

Franz, G.W. 1965. Melting relationships in the system CaO–MgO–SiO_2–CO_2–H_2O: A study of synthetic kimberlites, Ph.D. thesis, Pennsylvania State University.

Franz, G.W., Wyllie, P.J. 1966. Melting relationships in the system CaO–MgO–SiO_2–H_2O at 1 kilobar pressure, *Geochim. Cosmochim. Acta* **30,** 9–22.

Franz, G.W., Wyllie, P.J. 1967. Experimental studies in the system CaO–MgO–SiO_2–CO_2–H_2O, in *Ultramafic and Related Rocks,* P.J. Wyllie, ed. John Wiley & Sons, New York, pp. 323–326.

Frey, F.A., Ferguson, J., Chappell, B.W. 1977. Petrogenesis of South African and Australian kimberlite suites. Second International Kimberlite Conference (Extended Abstracts) (unpaginated).

Frey, F.A., Green, D.H., Roy, S.D. 1978. Integrated models of basalt petrogenesis: A study of quartz tholeiites to olivine melilitites from South Eastern Australia utilizing geochemical and experimental petrological data, *J. Petrol.* **19,** 463–513.

Frey, F.A., Haskin, L.A., Haskin, M.A. 1971. Rare earth abundances in some ultramafic rocks, *J. Geophys. Res.* **76,** 2057–2070.

Frick, C. 1973. Kimberlitic ilmenites, *Geol. Soc. S. Africa Trans.* **76,** 85–94.

Friel, J.J., Harker, R.I., Ulmer, G.C. 1977. Armalcolite stability as a function of pressure and oxygen fugacity, *Geochim. Cosmochim. Acta* **41,** 403–410.

Frisch, T., Wright, J.B. 1971. Chemical composition of high pressure megacrysts from Nigerian Cenozoic lavas, *N. Jb. Miner. Monats.* **7,** 289–304.

Frost, B.F. 1985. On the stability of sulphides, oxides and native metals in serpentinite, *J. Petrol.* **26,** 31–63.

Furon, R. 1963. *Geology of Africa.* Hafner Pub. Co., New York.

Gangadharam, E.V., Aswathanarayana, V. 1969. Trace element content of kimberlites of South India, *Trans. Am. Geophys. Union* **50,** 341 (abstract).

Garanin, V.K., Kudryavtseva, G.B., Lapin, A.V. 1979. Typical features of ilmenite from kimberlites, alkaline-ultrabasic intrusions and carbonatites, *Int. Geol. Rev.* **21,** 1025–1050.

Garanin, V.K., Kudryavtseva, G.B., Soshkina, L.T. 1983. Genesis of ilmenites from kimberlites, *Dokl. Akad. Nauk SSSR* **272,** 102–106.

Garrison, J.R., Taylor, L.A. 1980. Megacrysts and xenoliths in kimberlite, Elliot County Kentucky: A mantle sample from beneath the Permian Appalachian Plateau, *Contrib. Mineral. Petrol.* **75,** 27–42.

Garvie, O.G., Robinson, D.N. 1982. The mineralogy, structure and mode of formation of kelyphite and associated sub-kelyphitic surfaces on pyrope from kimberlite, *Terra Cognita* **2,** 229–230.

Gaspar, J.C., Wyllie, P.J. 1983. Ilmenite (high Mg, Mn, Nb) in the carbonatites from the Jacupiranga Complex, *Am. Mineral.* **68,** 960–971.

Gaspar, J.C., Wyllie, P.J. 1984. The alleged kimberlite–carbonatite relationship: Evidence from ilmenite and spinel from Premier and Wesselton Mines and the Benfontein Sill, South Africa, *Contrib. Mineral. Petrol.* **85,** 133–140.

Geikie, A. 1902. *The Geology of Eastern Fife.* J. Hedderwick & Sons, Glasgow.

Gelperin, N.I., Einstein, V.G. 1971. The analogy between fluidized beds and liquids, in Fluidization, J.F. Davidson and D. Harrison, eds. Academic Press, London, pp. 541–568.

Gittins, J., Hewins, R.H., Laurin, A.F. 1975. Kimberlitic–carbonatitic dikes of the Saguenay River Valley, Quebec, Canada, *Phys. Chem. Earth* **9,** 137–148.

Gold, D.P. 1966. The average and typical chemical composition of carbonatites, *Min Soc. India Inter. Mineral. Assoc. Papers, 4th. Gen. Mtg. 83–91.*

Gonshakova, V.I., Zaritskiy, A.I., Kirikilitsa, I.S., Levensheyn, M.L., Strekozov, N.F., Teteryuk, P.I., Khitrov, V.G. 1975. The problem of kimberlite magmatism in the Azov region, *Int. Geol. Rev.* **17,** 175–186.

Grantham, D.R., Allen, J.B. 1960. Kimberlite in Sierre Leone, *Overseas Geol. Miner. Resour.* **8,** 5–25.

Green, D.H. 1971. Composition of basaltic magmas as indicators of conditions of origin: Application to oceanic volcanism, *R. Soc. London Philos. Trans.* **268A,** 707–725.

Green, D.H. 1973. Experimental melting studies on a model upper mantle composition at high pressure under water-saturated and water-undersaturated conditions, *Earth Planet. Sci. Lett.* **19,** 37–53.

Green, D.H., Sobolev, N.V. 1975. Co-existing garnets and ilmenites synthesized at high pressures from pyrolite and olivine basanite and their significance for kimberlitic assemblages, *Contrib. Mineral. Petrol.* **50,** 217–229.

Green, H.W., Gueguen, Y. 1974. Origin of kimberlite pipes by diapiric upwelling in the upper mantle, *Nature* **249,** 617–620.

Griffin, W.L., Murthy, V.R. 1969. Distribution of K, RB, Sr and Ba in some minerals relevant to basalt genesis, *Geochim. Cosmochim. Acta* **33,** 1389–1414.

Gurney, J.J. 1985. A correlation between garnets and diamonds in kimberlites, in *Kimberlites, Occurrence and Origin: A Basis for Conceptual Models,* J.E. Glover and P.G. Harris, eds. Geol. Dept. Univ. Western Australia Pub. **8,** 143–165.

Gurney, J.J., Ahrens, L.H. 1973. The zinc content of some ultramafic and basic rocks, *Geol. Soc. S. Africa Trans.* **76,** 301–308.

Gurney, J.J., Berg, G.W., 1969. Potassium, rubidium and cesium in South African kimberlites and their peridotite xenoliths, *Geol. Soc. S. Africa Spec. Pub.* **2,** 417–427.

Gurney, J.J., Berg, G.W., Ahrens, L.J. 1966. Observations on caesium enrichment and the potassium/rubidium/caesium relationship in eclogites from the Roberts Victor Mine, South Africa, *Nature* **210,** 1025–1027.

Gurney, J.J., Ebrahim, S. 1973. Chemical composition of Lesotho kimberlites, *Lesotho Kimberlites* 280–294.

Gurney, J.J., Fesq, H.W., Kable, E.J.D. 1973. Clinopyroxene–ilmenite intergrowths from kimberlite: A re-appraisal, *Lesotho Kimberlites* 238–253.

Gurney, J.J., Harris, J.W., Rickard, R.S. 1984(a). Silicate and oxide inclusions in diamonds from the Orapa Mine, Botswana, *TIKC* **2,** 3–9.

Gurney, J.J., Harris, J.W., Rickard, R.S. 1984(b). Minerals associated with diamonds from the Roberts Victor Mine, *TIKC* **2,** 25–32.

Gurney, J.J., Harte, B. 1980. Chemical variations in upper mantle nodules from Southern African kimberlites, *R. Soc. London Philos. Trans.* **297A,** 273–293.

Gurney, J.J., Hobbs, J.B.M. 1973. Potassium, thorium and uranium in some kimberlites from South Africa, 1st International Kimberlite Conference, Cape Town (Extended Abstracts), pp. 143–146.

Gurney, J.J., Jakob, W.R.O., Dawson, J.B. 1979. Megacrysts from the Monastery Kimberlite pipe South Africa, *SIKC* **2,** 227–243.

Gurvich, M.Y., Kozlov, A.A., Malol, Y.V., Pavlov E.G., Semenov, G.S. 1982. Decomposition structures in rutile from kimberlite pipes of Letseng-la-terae, *Geokhimiya* **1982,** 1520–1523 (Russian).

Haggerty, S.E. 1973. Spinels of unique composition associated with ilmenite reactions in the Liqhobong kimberlite pipe, Lesotho, *Lesotho Kimberlites,* 149–158.

Haggerty, S.E. 1975. The chemistry and genesis of opaque minerals in kimberlites, *Phys. Chem. Earth* **9,** 295–307.

Haggerty, S.E. 1976. Opaque mineral oxides in terrestrial igneous rocks, in *Oxide Minerals,* D. Rumble, ed. Mineral. Soc. Amer. Review in Mineralogy **3,** Hg 101–Hg 300.

Haggerty, S.E. 1982. Kimberlites in Western Liberia: An overview of the geological setting in a plate tectonic framework, *J. Geophys. Res.* **81,** 10811–10826.

Haggerty, S.E. 1983. The mineral chemistry of new titanates from the Jagersfontein kimberlite, South Africa: Implications for metasomatism in the upper mantle, *Geochim. Cosmochim. Acta* **47,** 1833–1854.

Haggerty, S.E., Hardie, R.B., McMahon, R.M. 1979. The mineral chemistry of ilmenite nodule associations from the Monastery diatreme, *SIKC* **2,** 249–256.

Haggerty, S.E., Mariano, A.N. 1983. Strontian loparite and strontio-chevkinite. Two new minerals in rheomorphic fenites from the Parana Basin carbonatites, South America, *Contrib. Mineral. Petrol.* **84,** 365–381.

Haggerty, S.E., Raber, E., Naeser, C.W. 1983a. Fission track dating of kimberlitic zircons, *Earth Planet. Sci. Lett.* **63,** 41–50.

Haggerty, S.E., Smyth, J.R., Erlank, A.J., Rickard, R.S., Danchin, R.V. 1983b. Lindsleyite (Ba) and mathiasite (K): Two new chromium titanates in the crichtonite series from the upper mantle, *Am. Mineral.* **68,** 494–505.

Haggerty, S.E., Tompkins, L.A. 1983. Redox state of Earth's upper mantle from kimberlitic ilmenites, *Nature* **303,** 295–300.

Haggerty, S.E., Tompkins, L.A. 1984. Subsolidus reaction in kimberlitic ilmenites: Exsolution, reduction and the redox state of the mantle, *TIKC* **1,** 335–357.

Harger, H.S. 1905. The diamond pipes and fissures of South Africa, *Trans. Geol. Soc. S. Afr.* **8,** 110–134.

Hargraves, R.B., Onstott, T. 1980. Paleomagnetic results from some Southern African kimberlites and their tectonic significance, *J. Geophys. Res.* **85,** 3587–3596.

Harley, S.L., Thompson, A.B. 1984. Xenolithic mineral assemblages in kimberlites, paleogeotherms and the thermal structure of the earth, *TIKC* **2,** 277–288.

Harris, P.G., Middlemost, E.A.K. 1969. The evolution of kimberlites, *Lithos* **3,** 77–88.

Harte, B. 1978. Kimberlite nodules, upper mantle petrology and geotherms, *R. Soc. London Philos. Trans.* **288A,** 487–500.

Harte, B., Gurney, J.J. 1981. The mode of formation of chromium-poor megacryst suites from kimberlites, *J. Geol.* **89,** 749–753.

Harte, B., Gurney, J.J., Harris, J.W. 1980. The formation of peridotite suite inclusions in diamonds, *Contrib. Mineral. Petrol.* **72,** 181–190.

Haskin, L.A., Frey, F.A., Schmitt, R.F., Smith, R.H. 1966. Meteoritic, solar and terrestrial rare earth distributions, *Phys. Chem. Earth* **7,** 167–321.

Hastings, D.A., Sharp, W.G. 1979. An alternative hypothesis for the origin of West African kimberlites, *Nature* **227,** 152–153.

Hawkesworth, C.J., Vollmer R. 1979. Crystal contamination versus enriched mantle: $^{143}Nd/^{144}Nd$ and $^{87}Sr/^{86}Sr$ evidence from the Italian volcanics, *Contrib. Mineral. Petrol.* **69,** 151–165.

Hawthorne, J.B. 1968. Kimberlite sills, *Geol. Soc. S. Africa Trans.* **71,** 291–311.

Hawthorne, J.B. 1975. Model of a kimberlite pipe, *Phys. Chem. Earth* **9,** 1–15.

Hawthorne, J.B., Carrington, A.J., Clement, C.R., Skinner, E.M.W. 1979. Geology of the Dokolwayo kimberlite and associated paleoalluvial diamond deposits, *SIKC* **1,** 59–70.

Hay, R.L. 1978. Melilitite-carbonatite tuffs in the Laetolil Beds of Tanzania, *Contrib. Mineral. Petrol.* **67,** 357–367.

He, G. 1984. Kimberlites in China and their major components: A discussion on the physico-chemical properties of the upper mantle, *TIKC* **1,** 181–194.

Hearn, B.C. 1968. Diatremes with kimberlitic affinities in North-central Montana, *Science* **159,** 622–625.

Hearn, B.C., McGee, E.S. 1982. Garnets in Montana diatremes: A key to prospecting for kimberlites, *U.S.G.S. Open File Report No. 82-722.*

Hearn, B.C., McGee, E.S. 1984. Garnet peridotites from Williams kimberlites, North Central Montana, U.S.A., *TIKC* **2,** 57–70.

Heinrich, E.W. 1966. *The Geology of Carbonatites.* Rand McNally Co., Chicago.

Helmstaedt, H. 1982. Possible pre-kimberlite serpentinization in ultrabasic xenoliths from Bultfontein and Jagersfontein Mines, South Africa, *Terra Cognita* **2,** 210 (Abstract).

Helmstaedt, H., Carmichael, D.M., Percival, J.A. 1979. Grospydite xenoliths from the Zagodochnaya kimberlite pipe, Yakutia-high grade metamorphic rodingites, Ann. Mtg. Geol. Soc. Amer. Absts. with programs 11,442.

Helmstaedt, H., Gurney, J.J. 1984. Kimberlites of Southern Africa—are they related to subduction processes? *TIKC* **1,** 425–434.

Helmstaedt, H., Schulze, D.J. 1979. Type A–Type C eclogitic transition in xenoliths from the Moses Rock diatreme—further evidence for the presence of metamorphosed ophiolites beneath the Colorado Plateau, *SIKC* **2,** 357–365.

Hervig, R.L., Smith, J.V., Steele, I.M., Gurney, J.J., Meyer, H.O.A., Harris, J.W. 1980. Diamonds: Minor elements in silicate inclusions: Pressure–temperature implications, *J. Geophys. Res.* **85,** 6919–6929.

Higgins, M.D. 1984. Abundance of boron in South African kimberlites, Geol. Soc. Amer. Ann. Mtg. Reno (Abstracts).

Hill, D.R.H. 1977. Field relationships and petrography of the kimberlite sills and associated dikes at the 40m level of the Wesselton Mines, Kimberley, South Africa, Unpub. B.Sc. Honours Project, Univ. of Cape Town, South Africa.

Hill, R., Roeder, P. 1974. Crystallization of spinel from basaltic liquid as a function of oxygen fugacity, *J. Geol.* **82,** 709–729.

Holloway, J.R., Eggler, D.H. 1976. Fluid absent melting of peridotite containing phlogopite and dolomite, *Carnegie Inst. Washington Yearb.* **75,** 636–640.

Holmes, A. 1936. Contributions to the petrology of kimberlite and its inclusions, *Trans. Geol. Soc. S. Afr.* **39,** 379–428.

Holmes, A. 1950. Petrogenesis of katungite and its associates, *Am. Mineral.* **35,** 772–792.

Hunt, C.B. 1938. Igneous geology and structure of the Mount Taylor volcanic field, New Mexico, *U.S. Geol. Surv. Prof. Paper No. 189-B, 51–80.*

Hunter, R.H., Taylor, L.A. 1984. Magma mixing in the low velocity zone: Kimberlitic megacrysts from Fayette County, Pennsylvania, *Am. Mineral.* **69,** 16–29.

Hunter, R.H., Kissling, R.D., Taylor, L.A. 1984. Mid to late-stage kimberlitic melt evolution phlogopites and oxides from the Fayette County kimberlite, Pennsylvania, *Am. Mineral.* **69,** 30–40.

Hunter, W.C. 1979. The Garnet Ridge and Red Mesa kimberlitic diatremes, Colorado Plateau: Geology, mineral chemistry and geothermobarometry, Ph.D., University of Texas at Austin.

Ilupin, I.P. 1962. Distribution of some hydrothermal and supergene minerals in the kimberlites of Yakutia. *Sovietskaya Geol.* **3,** 152–156 (Russian).

Ilupin, I.P. 1977. Some chemical composition characteristics of perovskite and ilmenite from Yakutian kimberlites, *Zap. Vses. Mineral Obshch.* **106,** 719–722 (Russian).

Ilupin, I.P. 1983. Tantalum in ilmenites from kimberlites and from kimberlite matrix of the Siberian Province, *Dokl. Akad. Nauk SSSR* **272,** 161–163.

Ilupin, I.P., Ivanov, V.V., Miller, A.D. 1975. Rhenium and osmium in Yakutian kimberlites, *Geochem. Int.* **12,** 209–212.

Ilupin, I.P., Khomyakov, A.P., Balashov, Y.A. 1971. Rare earths in accessory minerals of Yakutian kimberlites, *Dokl. Akad. Nauk SSSR* **201,** 272–274.

Ilupin, I.P., Komarov, A.N. 1979. New data on the geochemistry of uranium in kimberlite, *Dokl. Akad. Nauk SSSR* **249,** 168–170.

Ilupin, I.P., Lutz, B.G. 1971. The chemical composition of kimberlite and questions on the origin of kimberlite magmas, *Sovietskaya Geol.* **6,** 61–73 (Russian).

Ilupin, I.P., Nagaeva, N.P. 1971. Chromium and nickel in ilmenite from Yakutia kimberlites, in *Geol. Petrogr. Mineral. Magmat. Obrazov. Ser. Vost. Chasti Sib. Platformy,* V.V. Kovalskii, ed. Izdatelstvo Nauka, Moscow, pp. 288–300 (Russian).

Ilupin, I.P., Sobolev, S.F., Zolotarev, B.P., Lebedev-Zinovyev, A.A. 1974. Geochemical specialization of kimberlites from various parts of Yakutia, *Geochem. Int.* **11,** 357–370.

Irvine, T.N. 1965. Chromian spinel as a petrogenetic indicator. Part 1. Theory, *Can. J. Earth Sci.* **2,** 648–672.

Ito, K., Matsumoto, T., Kawai, N. 1968. Experimental study of a kimberlite at pressures between 42 and 88 kilobars, *J. Geosci. Osaka City Univ.* **11,** 1–12.

Ivanov, I.P., Ilupin, I.P., Starozhitskaya, M.I., Gross, Y.I. 1977. Distribution of Cu, Ag and Au in Yakutia plutonic xenoliths and kimberlites, *Geochem. Int.* **14,** 48–60.

Jago, B.C. 1982. Mineralogy and Petrology of the Ham Kimberlite, Somerset Island, Northwest Territories, Canada. M.Sc. Thesis, Lakehead Univ., Thunder Bay, Canada 235pp.

Jago, B.C., Mitchell, R.H. 1985. Mineralogy and petrology of the Ham kimberlite, Somerset Island, N.W.T., Canada, *Can. Mineral.* (in press).

Jagoutz, E., Palme, H., Baddenhausen, H., Blum, K., Cendales, M., Dreibus, G., Spettel, B., Lorenz, V., Wanke, H. 1979. The abundances of major, minor and trace elements in the earth's upper mantle as derived from primitive ultramafic nodules, in Proc. 10th Lunar Planet Sci. Conf., pp. 2031–2050.

Janse, A.J.A. 1964. Kimberlites and related rocks of the Nama Plateau, South West Africa, Ph.D. thesis, Univ. Leeds.

Janse, A.J.A. 1969. Gross Brukkaros, a probable carbonatite volcano in the Nama Plateau of South West Africa, *Geol. Soc. Am. Bull.* **83,** 573–586.

Janse, A.J.A. 1971. Monticellite-bearing porphyritic peridotite from Gross Brukkaros, South West Africa, *Geol. Soc. S. Africa Trans.* **74,** 45–55.

Janse, A.J.A. 1975. Kimberlite and related rocks of the Nama plateau of South West Africa, *Phys. Chem. Earth* **9,** 81–94.

Janse, A.J.A. 1985. Kimberlites—Where and when, in *Kimberlite, Occurrence and Origin: A Basis for Conceptual Models,* J.E. Glover and P.G. Harris, eds. Geol. Dept. Univ. Western Australia Pub. No. 8, 19–61.

Jaques, A.L., Gregory, C.P., Lewis, J.D., Ferguson, J. 1982. The ultrapotassic rocks of the West Kimberly region, Western Australia, and a new class of diamandiferous kimberlite, *Terra Cognita* **2,** 251–252.

Jaques, A.L., Lewis, J.D., Smith, C.B., Gregory, G.P., Ferguson, J., Chappell, B.W., McCulloch, M.T. 1984(a). The diamond-bearing ultrapotassic (lamproitic) rocks of the West Kimberley Region, Western Australia, *TIKC* **1,** 225–254.

Jaques, A.L., Webb, A.W., Fanning, C.M., Black, L.P., Pidgeon, R.T., Ferguson, J., Smith, C.B., Gregory, G.P. 1984(b). The age of the diamond-bearing pipes and associated leucite lamproites of the West Kimberley region, Western Australia, *Bur. Mineral. Res. J. Australian Geol. Geophys.* **9,** 1–7.

Jones, A.P., Smith, J.V. 1983. Petrological significance of mineral chemistry in the Agathla Peak and Thumb Minettes, Navajo volcanic field, *J. Geol.* **91,** 643–656.

Jones, A.P., Smith, J.V. 1984. Ion probe analysis of H, Li, B, F and Ba in micas, with additional data for metamorphic amphibole, scapolite and pyroxene, *N. Jahrb. Mineral. Monats.* **1984,** 228–240.

Jones, A.P., Smith, J.V., Dawson, J.B. 1982. Mantle metasomatism in 14 veined peridotites from the Bultfontein mine, South Africa, *J. Geol.* **90,** 435–453.

Jones, A.P., Wyllie, P.J. 1984. Minor elements in perovskite from kimberlites and the distribution of rare earth elements: An electron probe study, *Earth Planet. Sci. Lett.* **69,** 128–140.

Jones, A.P., Wyllie, P.J. 1985. Paragenetic trends of oxide minerals in carbonate-rich kimberlites, with new analyses from the Benfontein sill, South Africa, *J. Petrol.* **26,** 210–222.

Jordan, T.H. 1979. Mineralogies, densities and seismic velocities of garnet lherzolites and their geophysical implications, *SIKC* **2,** 1–14.

Kable, E.J.D., Fesq, H.W., Gurney, J.J. 1975. The significance of the inter-element relationships of some minor and trace elements in South African Kimberlites, *Phys. Chem. Earth* **9,** 709–734.

Kaminskii, F.V. 1972. Distribution of kimberlite (of different facies) and associated rocks on the Siberian Platform, *Dokl. Akad. Nauk SSSR* **204,** 87–90.

Kaminskii, F.V. 1977. Alkali basaltic breccias of the Onega peninsula, *Int. Geol. Rev.* **19,** 1105–1114.

Kaminskii, F.V., Frantsesson, Y.V., Khvosta, V.P. 1974. First information on platinum metals (Pt, Pd, Rh, Ir, Ru, Os) in kimberlitic rocks, *Dokl. Akad. Nauk SSSR* **219,** 190–193.

Kaminskii, F.V., Popolitov, E.I., Frantsesson, Y.V., Tsykhanskii, V.D. 1977. Zr, Hf, Nb and Ta in kimberlites, *Geochem. Int.* **14,** 193–201.

Kaminskii, F.V., Sazonova, O.F., Frantsesson, Y.V. 1978. Rare earth levels in kimberlites and ultrabasic xenoliths, *Geochem. Int.* **15,** 68–74.

Kapustin, Y.L. 1981. Damkjernites-dike equivalents of carbonatites, *Int. Geol. Rev.* **23,** 1326–1334.

Kay, S.M., Sneddon, W.T., Foster, B.P., Kay, R.W. 1983. Upper mantle and crustal fragments in the Ithaca kimberlites, *J. Geol.* **91,** 277–290.

Keays, R.R., Sewell, D.K.B., Mitchell, R.H. 1981. Platinum and palladium minerals in upper mantle-derived lherzolites, *Nature* **294,** 646–648.

Keith, M.L., Weber, J.N. 1964. Carbon and oxygen isotopic composition of selected limestones and fossils, *Geochim. Cosmochim. Acta* **28,** 1787–1816.

Kennedy, G.C., Nordlie, B.E. 1968. The genesis of diamond deposits, *Econ. Geol.* **59,** 1551–1563.

Kerr, J.W. 1980. A plate tectonic contest in arctic Canada, in *The Continental Crust and Its Mineral Deposits,* D.W. Strangway, ed. Geol. Assoc. Canad. Spec. Pap. No. 20, 457–486.

Kharkiv, A.D. 1967(a). Instances of high temperature metamorphism connected with kimberlite magmas, *Geol. Geofiz.* **1967,** 124–126 (Russian).

Kharkiv, A.D. 1967(b). Early-generated ball-shaped inclusions in kimberlite breccias, *Izv. Akad. Nauk SSSR Ser. Geol.* **1,** 87–91 (Russian).

Kharkiv, A.D., Abaginskaya, Y.A. 1975. Orange-red kimberlite garnets from Yakutia and their genetic significance, *Geol. Geofiz.* **3,** 58–66 (Russian).

Kienle, J., Kyle, P.R., Self, S., Motyka, R., Lorenz, V. 1980. Ukinrek Maars, Alaska. I: April 1977 eruption sequence, petrology and tectonic setting, *J. Volcanol. Geotherm. Res.* **7,** 11–37.

Kimura, S., Muan, A. 1971(a). Phase relation in the system CaO–iron oxide–TiO in air, *Am. Mineral.* **56,** 1332–1346.

Kimura, S., Muan, A. 1971(b). Phase relations in the system CaO–iron oxide–TiO under strongly reducing conditions, *Am. Mineral.* **56,** 1347–1358.

King, B.C. 1970. Vulcanity and rift tectonics in East Africa, in *Africa Magmatism and Tectonics,* T.N. Clifford and I.G. Gass, eds. Oliver and Boyd Ltd., Edinburgh, pp. 263–283.

Kirillov, A.S. 1961. The relation of magmatism with tectonics in the Siberian Platform, *Geol. Geofiz.* **11,** 40–46 (Russian).

Klecka, W.R. 1975. Discriminant analysis, in *Statistical Package for the Social Sciences,* 2nd. ed., N.H. Nie, C.H. Hill, J.G. Jenkins, K. Steinbrenner, D.K. Brent, eds. McGraw-Hill, New York, pp. 434–462.

Knecht, B., Woermann, E., El Goresy, A. 1979. Element distributions among spinel and ilmenite phases in the systems $FeO–Cr_2O_3–TiO_2$,$FeO–Al_2O_3–TiO_2$ and $FeO–MgO–TiO_2$, in 10th Lunar Planet. Sci. Conf. Houston, 670–672 (Abstract).

Kobelski, B.J., Gold, D.P., Deines, P. 1979. Variations in stable isotope compositions for carbon and oxygen in some South African and Lesothan Kimberlites, *SIKC* **1,** 252–271.

Kobets, N.V., Komarov, B.V. 1958. Some problems of methodology in prospecting for primary diamond deposits by aero methods, *Izv. Akad. Nauk SSSR* **1958,** 80–86.

Koenig, J.B. 1956. The petrography of certain igneous dikes of Kentucky, *Kentucky Geol. Surv. Bull.* **21,** 5–57.

Koestler, A. 1977. *The Sleepwalkers. A History of Man's Changing Vision of the Universe.* Penguin Books, New York.

Komarov, A.N., Ilupin, I.P. 1975. Potassium–uranium ratio in kimberlite, *Dokl. Akad. Nauk SSSR* **222,** 243–245.

Kornilova, V.P., Nikishov, K.N., Filippov, N.D., Makhoto, V.F. 1983. Association of monticellite and ore minerals in some kimberlite bodies of Yakutia, *Dokl. Akad. Nauk SSSR* **270,** 696–700 (Russian).

Kostrovitsky, S.I. 1976. *Physical Conditions, Hydraulics and Kinematics of Emplacement of Kimberlite Pipes.* Nauka, Novosibirsk.

Kostrovitsky, S.I., Fiveyskaya, L.V. 1983. Geochemical features of olivines from kimberlites, *Geochem. Int.* **20,** 46–57.

Kostrovitsky, S.I., Vladimirov, B.M. 1971. Energy calculations for the mechanism of formation of kimberlite pipes, *Geol. Geofiz.* **6,** 31–38 (Russian).

Kovalski, V.V. 1963. *The Kimberlitic Rocks of Yakutia,* Izdatelstvo Akad. Nauk SSSR, Moscow (Russian).

Kozlov, I.T., Levshev, P.P. 1962. Amakinite, a new mineral of the brucite-pyrochroite group, *Zap. Vses. Mineral. Obshch.* **91,** 72–77 (Russian).

Kramers, J.D. 1977. Lead and strontium isotopes in Cretaceous kimberlites and mantle-derived xenoliths from Southern Africa, *Earth Planet. Sci. Lett.* **34,** 419–431.

Kramers, J.D. 1979. Pb, U, Sr, K and Rb in inclusion-bearing diamonds and mantle-derived xenoliths from Southern Africa, *Earth Planet. Sci. Lett.* **42,** 58–70.

Kramers, J.D., Smith, C.B. 1983. A feasibility study of U–Pb and Pb–Pb dating of kimberlites using groundmass mineral fractions and whole rock samples, *Isotope Geosci.* **1,** 23–38.

Kramers, J.D., Smith, C.B., Lock, N., Harmons, R., Boyd, F.R. 1981. Can kimberlite be generated from ordinary mantle? *Nature* **291,** 53–56.

Krasnobayev, A.A. 1980. Mineralogical and geochemical features of zircons from kimberlites and problem of their origin, *Int. Geol. Rev.* **22,** 1199–1209.

Krasnobayev, A.A., Votyakov, S.L., Gramolin, A.B., Botkunov, A.I., Ilupin, I.P., Samatov, M.V. 1981. Electronic optical properties of kimberlitic zircons, *Geokhimiya* **1981,** 571–577 (Russian).

Krasnov, I.I., Lure, M.L., Masaitis, V.L. 1966. *Geology of the Siberian Platform,* Izdatelstvo Nedra, Moscow (Russian).

Kresten, P. 1973(a). The geology of Lemphane pipes and neighbouring intrusions, *Lesotho Kimberlites* 159–167.

Kresten, P. 1973(b). The coating on kimberlitic zircons: A preliminary study, *Lesotho Kimberlites* 220–223.

Kresten, P. 1973(c). Differential thermal analysis of kimberlites, *Lesotho Kimberlites* 269–279.

Kresten, P. 1974. Uranium in kimberlites and associated rocks with special reference to Lesotho occurrences, *Lithos* **7,** 171–180.

Kresten, P. 1979. The Alnö Complex: Discussion of the main features, bibliography and excursion guide, Nordic Carbonatite Symposium Alnö Sweden 1979.

Kresten, P., Dempster, A.N. 1973. The geology of Pipe 200 and the Malibamatso Dyke Swarm, *Lesotho Kimberlites* 172–179.

Kresten, P., Fels, P., Berggren, G. 1975. Kimberlitic zircons—A possible aid in prospecting for kimberlites, *Mineralium Deposita* **10,** 47–56.

Krivoshlyk, I.N. 1980. Autoliths and some corollaries of the hypothesis of their genesis from immiscible phases, *Dokl. Akad. Nauk SSSR* **252,** 81–82.

Kruger, F.J. 1980. The occurrence of cebollite in kimberlite and included zeolitized crustal xenoliths, *Mineral. Mag.* **43,** 583–586.

Kruger, F.J. 1982. The occurrence of cebollite in kimberlite and included zeolitized crustal xenoliths—A correction and discussion of the occurrence of pectolite, *Mineral. Mag.* **46,** 274–275.

Kuehner, S.M., Edgar, A.D., Arima, M. 1981. Petrogenesis of the ultrapotassic rocks from the Leucite Hills, Wyoming, *Am. Mineral* **66,** 663–677.

Kunii, D. Levenspiel, O. 1969. *Fluidization Engineering.* John Wiley & Sons, New York.

Kushiro, I. 1972. Effect of water on the composition of magmas formed at high pressures, *J. Petrol.* **13,** 311–334.

Kushiro, I., Satake, H., Akimota, S. 1975. Carbonate–silicate reactions of high pressures and possible presence of dolomite and magnesite in the upper mantle, *Earth Planet. Sci. Lett.* **28,** 116–120.

Kushiro, I., Shimizu, N., Nakumura, Y. 1972. Compositions of co-existing liquids and solid phases formed upon melting of natural garnet lherzolite and spinel lherzolite. A preliminary report, *Earth Planet. Sci. Lett.* **14,** 19–25.

Kyle, P.R. 1981. Mineralogy and geochemistry of a basanite to phonolite sequence at Hut Point Peninsula, Antarctica, based on core from Dry Valley Drilling Project drillholes 1, 2 and 3, *J. Petrol.* **22,** 451–500.

Lazko, Y.Y. 1971. Origin of garnet in the Udachnaya pipe kimberlites, *Zap. Vses. Mineral. Obsh.* **100,** 703–712 (Russian).

Lazko, Y.Y. 1975. Structural characteristics of certain minerals in kimberlites as evidence of deep-seated evolution of the ultrabasic melts, *Int. Geol. Rev.* **17,** 373–381.

Le Bas, M.J. 1977. *Carbonatite-Nephelinite Volcanism.* John Wiley and Sons, New York.

Le Maitre, R.W. 1982. *Numerical Petrology. Developments in Petrology,* Vol. 8. Elsevier, New York.

Lebedev, A.P. 1964. Kimberlites of Northeastern USSR and allied problems, *Liverpool Manchester Geol. J.* **4,** 87–104.

Lebedev-Zinovyev, A.A., Ilupin, I.P. 1976. Geochemical zoning of kimberlite fields of the Yakutian province, *Dokl. Akad. Nauk SSSR* **230,** 211–213.

Leblanc, M., Dautria, J., Girod, M. 1982. Magnesian ilmenite xenoliths in a basanite from Tahalra, Ahaggar (Southern Algeria), *Contrib. Mineral. Petrol.* **79,** 347–354.

Lee, H.A., Lawrence, D.E. 1968. A new occurrence of kimberlite in Gauthier Township, Ontario, *Geol. Surv. Canada Paper 68-22.*

Lenzen, G. 1980. South Africa and the birth of a great industry, in *Diamonds: Myth, Magic and Reality*, J. Legrand, ed. Crown Publ., New York, pp. 66–85.

Leontyev, L.N., Kadenskii, A.A. 1957. The nature of kimberlite pipes of Yakutia, *Dokl. Akad. Nauk SSSR* **115**, 368–371.

Lewis, H.C. 1887. On diamantiferous peridotite and the genesis of diamond, *Geol. Mag.* **4**, 22–24.

Lewis, H.C. 1888. The matrix of diamond, *Geol. Mag.* **5**, 129–131.

Lewis, H.C. 1897. In *Papers and Notes on the Genesis and Matrix of the Diamond*, T.G. Bonney, ed. Longmans, Green & Co., London.

Lindsley, D.H., Dixon, S.A. 1976. Diopside-enstatite equilibria at 850 degrees to 1400 degrees C, 5 to 35 Kb, *Am. J. Sci* **276**, 1285–1301.

Lindsley, D.H., Kesson, S.E., Hartzman, M.J., Cushman, M.K. 1974. The stability of armalcolite: Experimental studies in the system MgO–FeO–Ti–O, in Proc. 5th Lunar Sci. Conf., pp. 521–534.

Lindsley, D.H., Spencer, K.J. 1982. Fe-Ti oxide geothermometry: reducing analyses of coexisting Ti-magnetite (mt) and ilmenite (ilm), *EOS Trans. Amer. Geophys. Union* **63**, 471 (abstract).

Litinskii, V.A. 1961. On the content of Ni, Cr, Ti, Nb and some other elements in kimberlites and the possibility of geochemical prospecting for kimberlite bodies, *Geochemistry*, 813–821.

Lodochnikov, W.N. 1933. Serpentines and serpentinites and the petrological problems connected with them, *Prob. Sov. Geol.* **2**, 145–150 (Russian).

Lorenz, V. 1973. On the formation of maars, *Bull. Volcanol.* **37**, 183–204.

Lorenz, V. 1975. Formation of phreatomagmatic maar-diatreme volcanoes and its relevance to kimberlite diatremes, *Phys. Chem. Earth* **9**, 17–27.

Lorenz, V. 1979. Phreatomagmatic origin of the olivine melilitite diatremes in the Swabian Alb, Germany, *SIKC* **1**, 354–363.

Lorenz, V. 1984. Explosive volcanism of the West Eifel volcanic field, Germany, *TIKC* **1**, 299–307.

Loubet, M., Bernat, M., Javoy, M., Allegre, C.J. (1972). Rare earth element content of carbonatites, *Earth Planet. Sci. Lett.* **14**, 226–232.

Luhr, J.R., Carmichael, I.S.E. 1981. The Colima volcanic complex, Mexico: Part II. Late-Quaternary cinder cones, *Contrib. Mineral. Petrol.* **76**, 127–147.

Luth, W.C. 1967. Studies of the system $KAlSiO_4$–Mg_2SiO_4–SiO_2–H_2O: I: Inferred phase relations and petrologic applications, *J. Petrol.* **8**, 373–416.

Lutts, B.G., Mineyeva, I.S. 1973. Uranium and thorium in Siberian kimberlites, *Geochem. Int.*, 1278–1281.

MacGregor, I.D. 1970. A hypothesis for the origin of kimberlite, *Mineral. Soc. Am. Spec. Pap.* **3**, 51–62.

MacGregor, I.D. 1974. The system MgO–Al_2O_3–SiO_2: Solubility of Al_2O_3 in enstatite for spinel and garnet peridotite compositions, *Am. Mineral.* **59**, 110-119.

MacGregor, I.D. 1979. Mafic and ultramafic xenoliths from the Kao kimberlite pipe, *SIKC* **2**, 156–172.

Madigan, R. 1983. Diamond exploration in Australia, *Indiaqua* **35**, 27–38.

Makhlaev, L.V., Surina, N.P. 1966. Kimberlites of Maimecha-Kotui province of ultrabasic alkaline rocks, *Geol. Geofiz* **8**, 45–55 (Russian).

Malinko, S.V., Ilupin, I.P., Berman, I.B., Stolyarova, A.N. 1982. Boron in kimberlites of the Kuoika field according to local radiographic analysis data, *Dokl. Akad. Nauk SSSR* **265**, 170–172 (Russian).

Malkov, B.A. 1972. Petrological difference between kimberlite and meymechites, *Dokl. Akad. Nauk SSSR* **206**, 166–168.

Malkov, B.A. 1974. Brucite in kimberlite, *Dokl. Akad. Nauk SSSR*, **215**, 157–160.

Malkov, B.A. 1975. Carbonatite-kimberlite, a new type of diamond bearing rock, *Dokl. Akad. Nauk SSSR* **221**, 193–195.

Malkov, B.A. 1976. Tectonic patterns in the localization of kimberlite provinces, *Dokl. Akad. Nauk SSSR* **230**, 46–48.

Mamchur, G.P., Melnik, Y.M., Kharkiv, A.D., Yarynych, O.A. 1980. Origin of carbonates and bitumens in kimberlites according to carbon isotope data, *Geochem. Int.* **17,** 118–124.

Mannard, G.W. 1962. The Singida kimberlite pipes, Tanganyika, Ph.D. thesis, McGill Univ. Montreal, Quebec.

Mannard, G.W. 1968. The surface expression of kimberlite pipes, *Geol. Assoc. Canada Proc.* **19,** 15–21.

Mansker, W.L., Ewing, R.C., Keil, K. 1979. Barian–titanian biotites in nephelinites from Oahu, Hawaii, *Am. Mineral.* **64,** 156–159.

Manson, D.V., Stockton, C.M. 1981. Gem garnets in the red-to-violet color range, *Gems Gemology* **17,** 191–204.

Marakushev, A.A. 1982. The fluid regime in the formation of diamond-containing rock, *Int. Geol. Rev.* **24,** 1241–1252.

Marsh, J.S. 1973. Relationships between transform directions and alkaline igneous rock lineaments in Africa and South America, *Earth Planet. Sci. Lett.* **18,** 317–323.

Marshintsev, V.K. 1970. Discovery of baddeleyite in kimberlitic rocks of Yakutia, in *Geology Petrography and Mineralogy of Magmatic Formations of the North-Eastern Part of the Siberian Platform,* V.V. Kovalski and R.K. Yurkevich, eds. Izd. Acad. Sci. SSSR, Moscow, pp. 247–253.

Marshintsev, V.K., Lapin, A.V. 1976. Geochemical heterogeneity of kimberlite, *Dokl. Akad. Nauk SSSR* **226,** 200–203.

Marshintsev, V.K., Sukneva, L.S. 1970. Scandium in the minerals and rocks of the kimberlite bodies of Yakutia, *Geochem. Int.* **12,** 1048–1050.

Mason, B., Allen, R.O. 1973. Minor and trace elements in augite hornblende and pyrope megacrysts from Kakanui, New Zealand, *New Zealand J. Geol. Geophys.* **16,** 935–947.

Matsyuk, S.S., Platonov, A.A., Kharkiv, D. 1980(a). The typomorphic significance of color in garnets from deep-seated mineral associations, *Mineral. Zh.* **2,** 12–25 (Russian).

Matsyuk, S.S., Platonov, A.A., Kharkiv, D. 1980(b). Color as a crystallochemical indicator for garnets of deep-seated mineral associations, *Mineral. Zh.* **2,** 27–47 (Russian).

McBirney, A.R. 1959. Factors governing the emplacement of volcanic rocks, *Am. J. Sci.* **257,** 431–448.

McBirney, A.R. 1963. Breccia pipe near Cameron, Arizona: Discussion, *Geol. Soc. Am. Bull.* **74,** 227–232.

McCallister, R.H., Meyer, H.O.A., Brookins, D.G. 1975. "Pyroxene"-ilemite xenoliths from the Stockdale Pipe Kansas: Chemistry, crystallography and origin, *Phys. Chem. Earth* **9,** 287–293.

McCallister, R.H., Nord, G.L. Jr. 1981. Subcalcic diopsides from kimberlites: Chemistry, exsolution microstructures and thermal history, *Contrib. Mineral. Petrol.* **78,** 118–125.

McCallum, M.E. 1976. An emplacement model to explain contrasting mineral assemblages in adjacent kimberlite pipes, *J. Geol.* **84,** 673–684.

McCallum, M.E., Eggler, D.E. 1971. Mineralogy of the Sloan diatreme, a kimberlite diatreme in Northern Larimer County, Colorado, *Am. Mineral.* **56,** 1735–1749.

McCallum, M.E., Eggler, D.H., Burns, L.K. 1975. Kimberlite diatremes in Northern Colorado and Southern Wyoming, *Phys. Chem. Earth* **9,** 149–162.

McConnell, R.B. 1972. Geological development of the rift system of Eastern Africa, *Geol. Soc. Am. Bull.* **83,** 2549–2572.

McCulloch, M.T., Jaques, A.L., Nelson, D.R., Lewis, J.D. 1983. Nd and Sr isotopes in kimberlites and lamproites from Western Australia: An enriched mantle origin, *Nature* **302,** 400–403.

McGee, E.S., Hearn, B.C. Jr. 1984. The Lake Ellen kimberlite, Michigan, U.S.A., *TIKC* **1,** 143–154.

McGetchin, T.R. 1968. The Moses Rock Dike: Geology, petrology and mode of emplacement of kimberlite-bearing breccia dike, San Juan County, Utah, Ph.D. thesis, California Inst. Technology, Pasadena.

McGetchin, T.R., Besancon, J.R. 1973. Carbonate inclusions in mantle-derived pyrope, *Earth Planet. Sci. Lett.*, **18,** 408–410.

McGetchin, T.R., Nihan, Y.S., Chodos, A.A. 1973. Carbonatite–kimberlite relations in the Cane Valley diatreme, San Juan County, Utah, *J. Geophys. Res.* **78,** 1854–1869.

McGetchin, T.R., Silver, L.T. 1970. Compositional relations in minerals from kimberlite and related rocks in the Moses Rock dike, San Juan County, Utah, *Am. Mineral.* **55,** 1738–1771.

McGetchin, T.R., Silver, L.T., Chodos, A.A. 1970. Titanoclinohumite: A possible mineralogical site for water in the upper mantle, *J. Geophys. Res.* **75,** 225–259.

McGetchin, T.R., Ulrich, G.W. 1973. Xenoliths in maars and diatremes with inferences for the Moon, Mars and Venus, *J. Geophys. Res.* **78,** 1832–1853.

McHone, J.G. 1981. Comment on "Mesozoic hotspot epeirogeny in Eastern North America," *Geology* **9,** 341–342.

McIver, J.R. 1981. Aspects of ultrabasic and basic alkaline intrusive rocks from Bitterfontein, South Africa, *Contrib. Mineral. Petrol.* **78,** 1–11.

McIver, J.R., Ferguson, J. 1979. Kimberlitic, melilititic, trachytic and carbonatite eruptives at Saltpetre Kop, Sutherland, South Africa, *SIKC* **1,** 111–128.

McMahon, B., Haggerty, S.E. 1979. The Oka carbonatite complex: magnetite compositions and the related role of titanium in pyrochlore, *SIKC* **1,** 382–392.

McMahon, B.M., Haggerty, S.E., Bence, R.J. 1979. Oxide mineral chemistry and oxygen fugacities of the Benfontein sills, South Africa, Kimberlite Symposium II, Cambridge (Extended Abstracts).

Menzies, M.A., Wass, S.Y. 1983. CO_2- and LREE-rich mantle below Eastern Australia: A REE and isotopic study of alkaline magmas and apatite-rich mantle xenoliths from the Southern Highlands Province, Australia, *Earth Planet. Sci. Lett.* **65,** 287–302.

Meunier, S. 1982. Examen mineralogique des roches qui accompagnent le diamant dans les mines du Cap de Bonne-Esperance, *Bull. Acad. R. Sci. Lett. Beaux Arts Belge.* **3**(Ser.3), 374–404.

Meyer, H.O.A. 1975. Kimberlite from Norris Lake, Eastern Tennessee: Mineralogy and petrology, *J. Geol.* **83,** 518–526.

Meyer, H.O.A. 1976. Kimberlites of the continental United States. *J. Geol.* **84,** 377–403.

Meyer, H.O.A. 1985. Genesis of diamond: A mantle saga, *Am. Mineral.* **70,** 344–355.

Meyer, H.O.A. 1986. Inclusions in diamonds, in *Mantle Xenoliths,* P.H. Nixon, ed. John Wiley & Sons, New York, pp. 501–522.

Meyer, H.O.A., Boyd, F.R. 1972. Composition and origin of crystalline inclusions in natural diamonds, *Geochim. Cosmochim. Acta.* **36,** 1255–1273.

Meyer, H.O.A., McCallister, R.H. 1984. Two pyroxene megacrysts from South African kimberlites, *TIKC* **2,** 133–144.

Meyer, H.O.A., Tsai, H., Gurney, J.J. 1979. A unique enstatite megacryst with co-existing Cr-poor and Cr-rich garnet, Weltevreden Floors, South Africa, *SIKC* **2,** 279–291.

Meyer De Stadelhofen, C. 1963. Les breches kimberlitiques de Territoire de Bakwanga (Congo), *Archiv. Sci. Soc. Phys. d'Hist. Nat. Geneve* **16,** 87–143.

Middlemost, E.A.K. 1974. Petrogenetic model for the origin of carbonatites, *Lithos* **7,** 275–278.

Mikheyenko, V.I. 1977. Evidence for the sedimentary origin of kimberlite, *Dokl. Akad. Nauk SSSR* **237,** 198–201.

Mikheyenko, V.I., Nenashev, V.I. 1962. Absolute age of the kimberlites of Yakutia, *Int. Geol. Rev.* **4,** 914–924.

Milashev, V.A. 1963. The term "kimberlite" and the classification of kimberlitic rocks, *Geol. Geofiz.* **4,** 42–52 (Russian).

Milashev, V.A. 1965. *Petrochemistry of the Yakutian Kimberlites and Factors in their Diamond Content,* Izdatelstvo Nedra, Moscow (Russian).

Milashev, V.A. 1974. *Kimberlite Provinces,* Izdatelstvo Nedra, Moscow (Russian).

Milashev, V.A. 1983. Structure and principal stages in the formation of the Daldynsk kimberlite field, *Geol. Geofiz.* **1983,** 98–107 (Russian).

Milashev, V.A., Krutoyarski, M.A., Rabkhin, M.I., Erlich, E.N. 1963. Kimberlite rocks and picritic porphyries of the North-Eastern part of the Siberian Platform, *Tr. Nauchno Issled Inst. Geol. Arktiki* **126** (Russian).

Millhollen, G.L., Irving, A.J., Wyllie, P.J. 1974. Melting interval of peridotite with 5.7% water to 30 kilobars, *J. Geol.* **82,** 575–587.

Mitchell, A.H.G., Garson, M.S. 1981. *Mineral Deposits and Global Tectonic Settings*. Academic Press, New York.

Mitchell, R.H. 1970. Kimberlite and related rocks—A critical re-appraisal, *J. Geol.* **78,** 686–704.

Mitchell, R.H. 1972. Composition of perovskite in kimberlite, *Am. Mineral.* **57,** 1748–1753.

Mitchell, R.H. 1973(a). Composition of olivine, silica activity and oxygen fugacity in kimberlite, *Lithos* **6,** 65–81.

Mitchell, R.H. 1973(b). Magnesian ilmenite and its role in kimberlite petrogenesis, *J. Geol.* **81,** 301–311.

Mitchell, R.H. 1975(a). Geology, magnetic expression and structural control of the central Somerset Island kimberlites, *Can. J. Earth Sci.* **12,** 757–764.

Mitchell, R.H. 1975(b). Theoretical aspects of gaseous and isotopic equilibria in the system C–H–O–S with application to kimberlite, *Phys. Chem. Earth* **9,** 903–915.

Mitchell, R.H. 1976. Somerset Island kimberlites, *Geol. Surv. Canada, Paper 76-1A*, p. 501, 502.

Mitchell, R.H. 1977. Geochemistry of magnesian ilmenites from kimberlites from South Africa and Lesotho, *Lithos* **10,** 29–37.

Mitchell, R.H. 1978(a). Mineralogy of the Elwin Bay kimberlite Somerset Island, N.W.T., Canada, *Am. Mineral.* **63,** 47–57.

Mitchell, R.H. 1978(b). Composition of spinels in micaceous kimberlite from the Upper Canada Mine, Kirkland Lake, Ontario, *Can. Mineral.* **16,** 591–595.

Mitchell, R.H. 1978(c). Manganoan magnesian ilmenite and titanian clinohumite from the Jacupiranga carbonatite, Sao Paulo, Brazil, *Am. Mineral.* **63,** 544–547.

Mitchell, R.H. 1979(a). The alleged kimberlite–carbonatite relationship: Additional contrary mineralogical evidence, *Am. J. Sci.* **279,** 570–589.

Mitchell, R.H. 1979(b). Mineralogy of the Tunraq kimberlite, Somerset Island, N.W.T., Canada, *SIKC* **4,** 161–171.

Mitchell, R.H. 1981. Titaniferous phlogopites from the leucite lamproites of the West Kimberley area, Western Australia, *Contrib. Mineral. Petrol* **76,** 243–251.

Mitchell, R.H. 1983. The Ile Bizard intrusion, Montreal Quebec-kimberlite or lamprophyre?: Discussion, *Can. J. Earth Sci.* **20,** 1493–1496.

Mitchell, R.H. 1984(a). Mineralogy and origin of carbonate-rich segregations in a composite kimberlite sill, *N. Jahrb. Mineral. Abh.* **150,** 185–197.

Mitchell, R.H. 1984(b) Garnet lherzolites from the Hanaus-I and Louwrensia kimberlites of Namibia, *Contrib. Mineral. Petrol.* **86,** 178–188.

Mitchell, R.H. 1985. A review of the mineralogy of lamproites, *Geol. Soc. S. Africa Trans.* **88,** 411–437.

Mitchell, R.H., Bell, K. 1976. Rare earth element geochemistry of potassic lavas from the Birunga and Toro-Ankole Regions of Uganda, *Contrib. Mineral. Petrol.* **58,** 293–303.

Mitchell, R.H., Brunfelt, A.O. 1975. Rare earth element geochemistry of kimberlite, *Phys. Chem. Earth,* **9,** 671–686.

Mitchell, R.H., Brunfelt, A.O., Nixon, P.H. 1973(a). Trace elements in magnesian ilmenites from Lesotho kimberlites, *Lesotho Kimberlites,* 230–235.

Mitchell, R.H., Carswell, D.A. 1976. Lanthanum, samarium and ytterbium abundances in some Southern African garnet lherzolites, *Earth Planet. Sci. Lett.* **31,** 175–178.

Mitchell, R.H., Carswell, D.A., Brunfelt, A.O. 1973(b). Mineralogy and rare earth geochemistry of an ilmenite-clinopyroxene xenolith from the Monastery Mine, *Lesotho Kimberlites*, 224–229.

Mitchell, R.H., Carswell, D.A., Clarke, D.B. 1980. Geological implications and validity of calculated equilibration conditions for ultramafic xenoliths from the Pipe 200 kimberlite, Northern Lesotho, *Contrib. Mineral. Petrol.* **72,** 205–217.

Mitchell, R.H., Clarke, D.B. 1976. Oxide and sulphide mineralogy of the Peuyuk kimberlite, Somerset Island, N.W.T., Canada, *Contrib. Mineral. Petrol.* **56,** 157–172.

Mitchell, R.H., Crocket, J.H. 1971(a). The isotopic composition of strontium in some South African kimberlites, *Contrib. Mineral. Petrol.* **30,** 277–290.

Mitchell, R.H., Crocket, J.H. 1971(b).Diamond genesis—a synthesis of opposing views, *Mineral. Deposita* **6,** 392–403.

Mitchell, R.H., Fritz, P. 1973. Kimberlite from Somerset Island, District of Franklin, N.W.T., Canada, *Can. J. Earth Sci.* **10,** 384–393.

Mitchell, R.H., Hawkesworth, C.J. 1984. Geochemistry of potassic lavas from Smoky Butte, Montana, Geol. Soc. Amer. 1984 Ann. Mtg. Reno, Nevada (Abstract).

Mitchell, R.H., Keays, R.R. 1981. Abundance and distribution of gold, palladium and iridium in some spinel and garnet lherzolites: Implications for the nature and origin of precious metal-rich intergranular components in the upper mantle, *Geochim. Cosmochim. Acta* **45,** 2425–2442.

Mitchell, R.H., Lewis, R.D. 1983. Priderite-bearing xenoliths from the Prairie Creek mica peridotite, Arkansas, *Can. Mineral.* **21,** 59–64.

Mitchell, R.H., Meyer, H.O.A. 1980. Mineralogy of micaceous kimberlite from the Jos dike, Somerset Island, N.W.T., Canada, *Can. Mineral.* **18,** 241–250.

Mitchell, R.H., Platt, R.G. 1984. The Freemans Cove volcanic suite: Field relations, petrochemistry and tectonic setting of nephelinite-basanite volcanism associated with rifting in the Canadian Arctic Archipelago, *Can. J. Earth Sci.* **21,** 428–436.

Moor, C.C., Sheinmann, J. 1946. Meimechite, a new rock from the Northern border of the Siberian platform, *Dokl. Akad. Nauk SSSR* **51,** 145–148 (Russian).

Moore, A.E. 1983. A note on the occurrence of melilite in kimberlites and olivine melilitites, *Mineral. Mag.* **47,** 404–406.

Moore, J.G., Nakamura, K., Alcaraz, A. 1966. The 1965 eruption of the Taal volcano, *Science* **151,** 955–960.

Morgan, W.J. 1983. Hotspot tracks and the early rifting of the Atlantic, *Tectonophys* **94,** 123–139.

Morgan, J.W., Lovering, J.F. 1967. Rhenium and osmium abundance in some igneous and metamorphic rocks, *Earth Planet. Sci. Lett.* **3,** 219–224.

Morgan, W.J. 1972. Plate motions and deep mantle convection, in *Studies in Earth and Space Sciences (Hess Volume)*, R. Shagam, R.B. Hargraves, W.J. Morgan, F.B. Van Houten, C.A. Burk, H.D. Holland, and L.C. Holhister, eds., *Mem. Geol. Soc. Am.* **132,** 7–22.

Muan, A., Hauck, J., Lofall, T. 1972. Equilibrium studies with a bearing on lunar rocks, *Proc. 3rd Lunar Sci. Conf* **1,** 185–196.

Mukherjee, K.K. 1961. Petrology of lamprophyres of the Bokaro Coalfield, Bihar, *Mining Metall Soc. India Q. J.* **33,** 69–87.

Muller, G., Veyl, G. 1957. The birth of Nilahue, a new maar type volcano at Rininahue, Chile, 20th Internat. Geol. Cong. Mexico Sect. I, pt. 2 Cenozoic Volcanism, pp. 375–396.

Muramatsu, Y. 1983. Geochemical investigations of kimberlites from the Kimberley area, South Africa, *Geochem. J.* **17,** 71–86.

Mysen, B. O., Boettcher, A.L. 1975. Melting of a hydrous mantle: II Geochemistry of crystals and liquids formed by anatexis of mantle peridotite at high pressures and high temperatures as a function of controlled activities of water, hydrogen and carbon dioxide, *J. Petrol.* **16,** 549–593.

Neill, W.M. 1973. Possible continental rifting in Brazil and Angola related to the opening of the South Atlantic, *Nature Phys. Sci.* **245,** 104–107.

Nekrasova, R.A., Gamyanina, V.V. 1968. The composition of rare earth elements in kimberlite minerals, *Dokl. Akad. Nauk SSSR* **182,** 449–452.

Nekrasova, R.A., Rozhdestvenskaya, I.V. 1970, The ZrO_2/HfO_2 ratio in zircons from kimberlites and alluvial sediments, *Geochem. Int.* **7,** 536–542.

Neumann, H., Jensen, B. B., Brunfelt, A.O. 1966. Distribution patterns of rare earth elements in minerals, *Norsk Geol. Tidssk.* **46,** 141–179.

Newton, A.R., Gurney, J.J. 1975. Discussion of "A plate tectonic origin for diamond-bearing kimberlites," *Earth Planet. Sci. Lett.* **27,** 356–358.

Nickel, E.H., McAdam, R.C. 1963. Niobium perovskite from Oka, Quebec: A new classification for minerals of the perovskite group, *Can. Mineral.* **7,** 683–697.

Nielsen, T.F.D. 1980. The petrology of a melilitolite, melteigite, carbonatite and syenite ring dike system, in the Gardiner complex, East Greenland, *Lithos* **13,** 181–197.

Nikishov, K.N., Nikishova, V. 1966. The possibility of reaction relations between olivine and monticellite, *Geochem. Int.* **3,** 1200–1206.

Nikishov, K.N., Poberezhskiy, V.A., Makhotko, V.F. 1979. Composition of olivine and monticellite from monticellite alnöites of Siberia, *Dokl. Akad. Nauk SSSR* **224,** 116–120.

Nikitin, B.M. 1982. Deformation of country rock in the formation of kimberlite pipes, *Int. Geol. Rev.* **24,** 1057–1063.

Nikolskii, N.S. 1983. Serpentinization under reductive conditions, *Dok. Akad. Nauk SSSR* **271,** 142, 146.

Nixon, P.H. 1960. A mineralogical and geochemical study of kimberlites and the associated xenoliths, Ph.D. thesis, Univ. Leeds.

Nixon, P.H. 1973(a). The geology of Mothae, Solane, Thaba Putsoa and Blow 13, *Lesotho Kimberlites,* 39–47.

Nixon, P.H. 1973(b). Perspective, *Lesotho Kimberlites,* 300–312.

Nixon, P.H. 1973(c). Kimberlitic volcanoes in East Africa, *Overseas Geol. Mineral. Res.* **41,** 119–130.

Nixon, P.H. 1986. *Mantle xenoliths,* P.H. Nixon, ed. John Wiley & Sons, New York, in press.

Nixon, P.H., Boyd, F.R. 1973(a). Discrete nodules (megacryst) and lamellar intergrowths in the Frank Smith kimberlite pipe, in 1st Internat Kimberlite Conf. Cape Town (Extended Abstracts).

Nixon, P.H., Boyd, F.R. 1973(b). The discrete nodule association in kimberlites from Northern Lesotho, *Lesotho Kimberlites,* 67–75.

Nixon, P.H., Boyd, F.R. 1973(c). The Liqhobong intrusions and kimberlite olivine composition, *Lesotho Kimberlites,* 141–148.

Nixon, P.H., Boyd, F.R. 1979(a). The S.E. Lesotho–E. Griqualand kimberlite field and the nature of the edge cratonic lithosphere, in Kimberlite Symposium II, Cambridge (Extended Abstracts).

Nixon, P.H., Boyd, F.R. 1979(b). Garnet-bearing lherzolites and discrete nodule suites from the Malaita alnöite, Solomon Islands, S.W. Pacific, and their bearing on oceanic mantle composition and geotherm, *SIKC* **2,** 400–423.

Nixon, P.H., Kresten, P. 1973(a). Butha-Buthe dyke swarm and associated kimberlite blows, *Lesotho Kimberlites,* 197–206.

Nixon, P.H., Kresten, P. 1973(b). Chromium and nickel in kimberlitic ilmenites, *Lesotho Kimberlites,* 235–237.

Nixon, P.H., Mitchell, R.H., Rogers, N.W. 1980. Petrogenesis of alnöitic rocks from Malaita, Solomon Islands, Melanesia, *Mineral. Mag.* **43,** 587–596.

Nixon, P.H., Rogers, N.W., Gibson, I.L., Grey, A. 1981. Depleted and fertile mantle xenoliths from Southern African kimberlites, *Ann. Rev. Earth Planet. Sci.* **9,** 285–309.

Nixon, P.H., Thirwall, M.F., Buckley, F. 1982. Kimberlite, lamproite consanguinity, *Terra Cognita* **2,** 252–254.

Nixon, P.H., Thirlwall, M.F., Buckley, F., Davies, C.J. 1984. Spanish and Western Australian lamproites: Aspects of whole rock geochemistry, *TIKC* **1,** 285–296.

Nixon, P.H., Von Knorring, O., Rooke, J.M. 1963. Kimberlites and associated inclusions of Basutoland: A mineralogical and geochemical study, *Am. Mineral.* **48,** 1090–1132.

Norman, J.W., Price, N.J., Peters, E.R. 1977. Photogeological fracture trace study of controls of kimberlite intrusion in Lesotho basalts, *Trans. Instit. Mining and Metallurgy (London) Section B,* B78–B90.

Norrish, K. 1951. Priderite, a new mineral from the leucite–lamproites of the West Kimberley area, Western Australia, *Mineral. Mag.* **29,** 406–501.

Norton, D.L., Cathles, L.M. 1973. Breccia pipes-products of exsolved vapour from magmas, *Econ. Geol.* **68,** 540–546.

Novikov, L.A., Slobodskoy, R.M. 1979. Mechanism of formation of diatremes, *Int. Geol. Rev.* **21,** 1131–1139.

O'Hara, M.J. 1968. The bearing of phase equilibria studies in synthetic and natural systems on the origin and evolution of basic and ultrabasic rocks, *Earth Sci. Rev.* **4,** 69–133.

O'Hara, M.J. 1977. Geochemical evolution during fractional crystallization of a periodically refilled magma chamber, *Nature* **266,** 503–507.

O'Hara, M.J., Yoder, H.S. 1967. Formation and fractionation of basic magmas at high pressure, *Scottish J. Geol.* **3,** 67–117.

O'Neil, H. St. C., Ortez, N., Arculus, R.J., Wall, V.J., Green, D.H. 1982. Oxygen fugacities from the assemblage olivine–orthopyroxene–spinel, *Terra Cognita* **2,** 228 (Abstract).

Olafsson, M., Eggler, D.H. 1983. Phase relations of amphibole, amphibole-carbonate and phlogopite-carbonate peridotite: Petrologic constraints on the asthenosphere, *Earth Planet. Sci. Lett.* **64,** 305–315.

O'Neil, H. St. C., Wood, B.J. 1979. An experimental study of Fe–Mg partitioning between garnet and olivine and its calibration as a geothermometer, *Contrib. Mineral. Petrol.* **70,** 59–70.

O'Nions, R.K., Carter, S.R., Evensen, N.M., Hamilton, P.J.A. 1979. Geochemical and cosmochemical applications of Nd isotope analysis, *Ann. Rev. Earth Planet. Sci.* **7,** 11–38.

Orlov, Y.L. 1977. *The Mineralogy of Diamond.* John Wiley & Sons, New York.

Ottenburgs, R., Fieremans, M. 1979. Rutile–silicate intergrowths from the kimberlite formations at Mbuji-Mayi, Bakwanga, Zaire, *Bull. Soc. Belge. Geol.* **3,** 197–203.

Oversby, V.M., Gast, P.W. 1970. Lead from oceanic islands, *J. Geophys. Res.* **75,** 2097–2114.

Ozerova, N.A., Ilupin, I.P., Golovnya, S.V., Volkova, A.V. 1976. Mercury in kimberlites, *Geokhim. Rudoobrazuyushchikh Elem. Osnovn. Ultruosnovn Porod,* 166–185 (Russian).

Parfenoff, A. 1982. Une mineral traceur pour la prospection alluvionaire: L'ilmenite. Relations entre ilmenites magnesieanes, basaltes alcalins, kimberlites et diamant, *BRGM. Doc. Bur. Rech. Geol. Minieres,* No. 37.

Parks, J.M. 1970. Fortran IV program for Q-mode cluster analysis on distance function with printer dendrogram, Kansas State Geol. Surv./Univ. Kansas, Lawrence Computer Contrib. 46.

Parrish, J.B., Levin, P.M. 1982. Tectonic model for kimberlite emplacement in the Appalachian Plateau of Pennsylvania, *Geology* **10,** 344–347.

Parry, J., Williams, A.F., Wright, F.E. 1932. On bultfonteinite a new fluorine-bearing hydrous calcium silicate from South Africa., *Mineral. Mag.* **23,** 145–162.

Parry, J., Wright, F.E. 1925. Afwillite, a new hydrous calcium silicate from the Dutoitspan Mine, Kimberley, South Africa, *Mineral. Mag.* **20,** 277–286.

Pasteris, J.D. 1980(a). The significance of groundmass ilmenite and magacryst ilmenite in kimberlites, *Contrib. Mineral. Petrol.* **75,** 315–325.

Pasteris, J.D. 1980(b). Opaque oxide phases of the De Beers Pipe kimberlite (Kimberley, South Africa) and their petrologic significance, Ph.D. thesis, Yale University.

Pasteris, J.D. 1981. Occurrence of graphite in serpentinized olivine in kimberlite, *Geology* **9**, 356–359.

Pasteris, J.D. 1982. Representation of compositions in complex titanian spinels and application to the De Beers kimberlite, *Am. Mineral.* **67**, 244–250.

Pasteris, J.D. 1983. Spinel zonation in the De Beers kimberlite, South Africa: Possible role of phlogopite, *Can. Mineral.* **21**, 41–58.

Pasteris, J.D., Boyd, F.R., Nixon, P.H. 1979. The ilmenite association at the Frank Smith Mine, R.S.A., *SIKC* **2**, 257–264.

Paul, D.K. 1979. Isotopic composition of strontium in Indian kimberlites, *Geochim. Cosmochim. Acta* **43**, 389–394.

Paul, D.K., Buckley, F., Nixon, P.H. 1976. Fluorine and chlorine geochemistry of kimberlites, *Chem. Geol.* **17**, 125–135.

Paul, D.K., Crocket, J.H., Nixon, P.H. 1979. Abundance of palladium, iridium and gold in kimberlites and associated nodules, *SIKC* **1**, 272–279.

Paul, D.K., Gale, N.H., Harris, P.G. 1977. Uranium and thorium abundance in Indian kimberlites, *Geochim. Cosmochim. Acta* **41**, 335–339.

Paul, D.K., Potts, P.J. 1976. Rare earth abundances in kimberlites from Greenland and Zambia, *Chem. Geol.* **18**, 161–167.

Paul, D.K., Potts, P.J., Gibson, G.L., Harris, P.G. 1975. Rare earth abundance in Indian kimberlites, *Earth Planet. Sci. Lett.* **15**, 151–158.

Pavlov, D.I., Ilupin, I.P. 1973. Halite in Yakutian kimberlites, its relation to serpentine and the source of parent solutions. *Dokl. Akad. Nauk SSSR*, **213**, 178–180.

Perchuk, L.L., Vaganov, V.I. 1980. Petrochemical and thermodynamic evidence on the origin of kimberlites, *Contrib. Mineral. Petrol.* **72**, 219–228.

Perry, V.D. 1961. The significance of mineralized breccia pipes, *Mining Eng.* **13**, 367–376.

Peyve, A.V., Perfilyev, A.S., Savelyeva, G.N. 1977. Deep-seated inclusions, kimberlites and the problem of continental drift, *Int. Geol. Rev.* **19**, 405–415.

Philpotts, J.A., Schnetzler, C.C., Thomas, H.H. 1972. Petrogenetic implication of some new geochemical data on eclogitic and ultrabasic inclusions, *Geochim. Cosmochim. Acta* **36**, 1131–1166.

Platt, R.G., Mitchell, R.H. 1982. The Marathon dikes: Ultrabasic lamprophyres from the vicinity of McKellar Harbour, N.W. Ontario, *Am. Mineral.* **67**, 907–916.

Podvysotskiy, V.T., Vladimirov, B.M., Ivanov, S.I., Kotelnikov, V.P. 1981. Serpentinization of kimberlite, *Dokl. Akad. Nauk SSSR* **256**, 87–91.

Pokhilenko, N.P., Sobolev, N.V., Lavrentyev, Y.G. 1977. Xenoliths of diamondiferous ultramafic rocks from Yakutian kimberlites, Second International Kimberlite Conference Sante Fe (Extended Abstracts) (unpaginated).

Pokhilenko, N.P., Sobolev, N.V., Lavrentyev, Y.G. 1979. Xenoliths of peridotites from Udachnaya kimberlite pipe, Yakutia, in Kimberlite Symposium II, Cambridge (Abstract).

Ponomarenko, A.I., Ponomarenko, G.A., Kharkiv, A.D., Sobolev, N.V. 1972. New data on the mineralogy of inclusion of ilmenite-bearing ultramafic rocks from pipes, *Western Yakut ASSR. Dokl. Adak. Nauk SSSR* **207**, 156–159.

Popov, M.I., Asatkin, V.B. 1978. Nature of deformation of channels of kimberlite pipes and veins (as in a region of Siberia), *Int. Geol. Rev.* **20**, 942–946.

Portnov, A.M. 1979. Fluid diapirism as a factor in the formation of kimberlite pipes and carbonatite bodies, *Dokl. Akad. Nauk SSSR* **246**, 48–51.

Portnov, A.M. 1982. Self-oxidation of mantle fluid and the genesis of kimberlite diamonds, *Dokl. Akad. Nauk SSSR* **267**, 166–168.

Powell, J.L. 1966. Isotopic composition of strontium in carbonatites and kimberlites, in Mineral. Soc. India–Internat Mineral. Soc. Papers 4th. Gen. Mtg., pp. 58–66.

Pretorius, D.A. 1973. The crustal architecture of Southern Africa, 13th. Alex L. du Toit Memorial Lecture, *Geol. Soc. S. Africa*, **76**, 1–60 (Appendix).

Prins, P. 1972. Composition of magnetite from carbonatites, *Lithos* **5**, 227–240.

Raber, E., Haggerty, S.E. 1979. Zircon-oxide reactions in diamond-bearing kimberlites, *SIKC* **1**, 229–240.

Rabhkin, M.I., Krutoyarskii, M.A., Milashev, V.A. 1962. Classification and nomenclature of Yakutian kimberlites, *Tr. Issled Inst. Geol. Arktiti* **121**, 154–164 (Russian).

Raeside, R.P., Helmstaedt, H. 1982. The Ile Bizard intrusion, Montreal, Quebec-kimberlite or lamprophyre? *Can. J. Earth Sci.* **19**, 1996–2011.

Rawlinson, P.J., Dawson, J.B. 1979. A quench pyroxene–ilmenite xenolith from kimberlite: Implications for pyroxene–ilmenite intergrowths, *SIKC* **2**, 292–299.

Reay, A., Wood, C.P. 1974. Ilmenites from Kakanui, New Zealand, *Mineral. Mag.* **39**, 721–723.

Reid, A.M., Donaldson, C.H., Dawson, J.B., Brown, R.W., Ridley, W.I. 1975. The Igwisi Hills extrusive "kimberlite," *Phys. Chem. Earth* **9**, 199–218.

Reid, A.M., Hanor, J.S. 1970. Pyrope in kimberlites, *Am. Mineral.* **55**, 1374–1379.

Reis, B. 1971. The use of aeromagnetometry in the determination of deep-seated structures and its importance in kimberlite exploration, *Angola Serv. Geol. Minas Bol.* **23**, 11–20.

Reis, B. 1972. Preliminary note on the distribution and tectonic control of kimberlites in Angola, in Proc. 24th. Internat. Geol. Cong. Sect 4, pp. 276–281.

Reitan, P. 1974. Eu anomaly in kimberlites, *Geology* **2**, 72.

Reynolds, D.L. 1954. Fluidization as a geological process and its bearing on the problem of intrusive granites, *Am. J. Sci.*, **25**, 577–613.

Richardson, S.H., Gurney, J.J., Erlank, A.J., Harris, J.W. 1984. Origin of diamonds in old enriched mantle, *Nature* **310**, 198–202.

Ridley, W.I. 1977. Crystallization trends of spinels in Tertiary basalts from Rhum and Muck and their petrogenetic significance, *Contrib. Mineral. Petrol.* **64**, 243–255.

Rimsaite, J. 1971. Distribution of major and minor constituents between mica and host ultrabasic rocks and between zoned mica and zoned spinel, *Contrib. Mineral. Petrol.* **33**, 259–272.

Ringwood, A.E. 1969. Composition and evolution of the upper mantle, in *The Earth's Crust and Upper Mantle*, P.J. Hart, ed. *Am. Geophys. Union Monogr.* **13**, 1–17.

Ringwood, A.E., Lovering, J.F. 1970. Significance of pyroxene–ilmenite intergrowths among kimberlite xenoliths, *Earth Planet. Sci. Lett.* **7**, 371–375.

Roberts, B. 1976. *Kimberley: Turbulent City*. David Philip Publ., Cape Town.

Robey, J.V.A. 1981. Kimberlites of the Central Cape Province, R.S.A., Ph.D. thesis, Univ. of Cape Town, R.S.A.

Robey, J.V.A., Gurney, J.J. 1979. Megacrysts from the Lekkerfontein kimberlite, North central Cape. R.S.A., Kimberlite Symposium II, Cambridge (Extended Abstracts).

Robinson, D.N. 1975. Magnetite-serpentine-calcite dikes at Premier Mine and aspects of their relationship to kimberlite and to carbonatite of alkalic carbonatite complexes, *Phys. Chem. Earth* **9**, 61–70.

Robinson, D.N. 1978. The characteristics of natural diamond and their interpretation, *Minerals Sci. Eng.* **10**, 55–71.

Robinson, D.N. 1979. Diamond and graphite in eclogite xenoliths from kimberlite, *SIKC* **2**, 50–58.

Robinson, D.N., Gurney, J.J., Shee, S.R. 1984. Diamond eclogite and graphite eclogite xenoliths from Orapa, Botswana, *TIKC* **2**, 11–24.

Rock, N.M.S. 1977. The nature and origins of lamprophyres: Some definitions, distinctions and derivations, *Earth Sci. Rev.* **13**, 123–169.

Rock, N.M.S. 1984. Nature and origin of calc-alkaline lamprophyres: Minettes, vogesites, kersantites and spessartites, *R. Soc. Edinburgh Trans.* **74**, 193–227.

Roden, M.F. 1981. Origin of co-existing minette and ultramafic breccia, Navajo Volcanic Field, *Contrib. Mineral. Petrol.* **77**, 195–206.

Rolfe, D.G. 1973. The geology of the Kao kimberlite pipes, *Lesotho Kimberlites,* 101–106.

Ross, C.S. 1926. Nephelite-hauynite alnöite from Winnett, Montana, *Am. J. Sci.* **11,** 218–227.

Rozhkov, I.S., Kaminskii, F.V. Frantsesson, E.V. 1973. Gold in kimberlites and ultrabasic inclusions, *Geochem. Int.* **1973,** 1385–1389.

Rozova, Y.V., Frantsesson, E.V., Pleshakov, A.P., Botova, M.M., Filipova, L.P. 1979. Geikielitic ilmenite and titanium chromite from "Zimnyaya" kimberlite pipe, Western Yakutia, *Dokl. Akad. Nauk SSSR* **248,** 152–156.

Rozova, Y.V., Frantsesson, E.V., Pleshakov, A.P., Botova, M.M., Filipova, L.P. 1982. High-iron chrome spinels in kimberlites of Yakutia, *Int. Geol. Rev.* **24,** 1417–1425.

Ruotsala, A.P. 1975. Alteration of the Finsch kimberlite pipe South Africa, *Econ. Geol.* **70,** 587–590.

Ryabchikov, I.D. 1983. Oxidation-reduction equilibria in the upper mantle, *Dokl. Akad. Nauk SSSR* **268,** 197–199.

Sampson, D.N. 1953. The volcanic hills at Igwisi, *Rec. Geol. Surv. Tanganyika* **3,** 48–53.

Sarsadskikh, N.N. 1970. Heterogeneity of the upper mantle, *Dokl. Akad. Nauk SSSR* **193,** 1392–1395.

Sato, M. 1978. Oxygen fugacity of basaltic magmas and the role of gas-forming elements, *Geophys. Res. Lett.* **5,** 447–449.

Sato, M., Valenza, M. 1980. Oxygen fugacities of the layered series of the Skaerguard intrusion, East Greenland, *Am. J. Sci.* **280**A, 134–158.

Scatena-Wachel, D.E., Jones, A.P. 1984. Primary baddeleyite (ZrO_2) in kimberlite from Benfontein, South Africa, *Mineral. Mag.* **48,** 257–261.

Schmitt, H.H., Swann, G.A., Smith, D. 1974. The Buell Park kimberlite pipe, North Eastern Arizona, in *Geology of Northern Arizona,* T.N.V. Karlstrom, G.A. Swann, R.L. Eastwood, eds. Geol. Soc. Amer. Meeting, Flagstaff Arizona, pp. 672–698.

Schulze, D.J. 1981. Mantle-derived calcite and phlogopite in discrete nodules from a Kentucky kimberlite: Evidence for primary kimberlitic liquids, EOS, *Trans. Am. Geophys. Union* **63,** 414 (Abstract).

Schulze, D.J. 1983. Graphic rutile–olivine intergrowths from South African kimberlite, *Carnegie Inst. Washington Yearb.* **82,** 343–349.

Schulze, D.J. 1984. Cr-poor megacrysts from the Hamilton Branch kimberlite, Elliot County, Kentucky, *TIKC* **2,** 97–108.

Schulze, D.J., Hoover, J.D. 1982. Origin of compositional trends in megacrysts from kimberlites by fractional crystallization, EOS, *Trans. Am. Geophys. Union* **63,** 464.

Scott, B.H. 1979. Petrogenesis of kimberlites and associated potassic lamprophyres from Central West Greenland, *SIKC* **1,** 190–205.

Scott, B.H. 1981. Kimberlite and lamproite dykes from Holsteinsborg, West Greenland, *Medd. Gronland Geosci.* **4,** 3–24.

Scott, B.H., Skinner, E.M.W. 1979. The Premier kimberlite pipe Transvaal, South Africa, Kimberlite Symposium II, Cambridge England (Extended Abstracts).

Scott Smith, B.H., Danchin, R.V., Harris, J.W., Stracke, K.J. 1983a. Kimberlites near Orroroo, South Australia: Appendix. Kimberlites III: Documents, *Annales Scientifiques de L'Universite de Clermont-Ferrand II,* No. 74, 123–128.

Scott Smith, B.H., Danchin, R.V., Harris, J.W., Stracke, K.J. 1984. Kimberlites near Orroroo, South Australia, *TIKC* **1,** 121–142.

Scott Smith, B.H., Skinner, E.M.W. 1983. Kimberlite and American Mines, near Prairie Creek, Arkansas. Kimberlites III: Documents. *Annales Scientifiques de L'Universite de Clermont-Ferrand II,* No. 74, 27–36.

Scott Smith, B.H., Skinner, E.M.W. 1984(a). A new look at Prairie Creek Arkansas, *TIKC* **1,** 255–283.

Scott Smith, B.H., Skinner, E.M.W. 1984(b). Diamondiferous lamproites, *J. Geol.* **92,** 433–438.

Scott Smith, B.H., Skinner, E.M.W., Clement, C.R. 1983b. Further data on the occurrence of pectolite in kimberlite, *Mineral. Mag.* **47,** 75–78.

Seifert, F., Von Schreyer, W. 1966. Fluide phasen im system K_2O–MgO–SiO_2–H_2O und ihre mögliche Bedeutung fur die Entstehung ultrabasischer Gestein, *Ber. Bunsengesell.* **70,** 1045–1050.

Sengor, A.M., Burke, K. 1978. Relative timing of rifting and volcanism on earth and its tectonic implication, *Geol. Res. Lett.* **5,** 419–421.

Shand, S.J. 1934. The heavy minerals of kimberlite, *Geol. Soc. S. Africa Trans.* **7,** 57–68.

Shand, S.J. 1947. *Eruptive Rocks,* 3rd ed. John Wiley & Sons, New York.

Sharp, W.E. 1974. A plate tectonic origin for diamond-bearing kimberlite, *Earth Planet. Sci. Letts.* **21,** 351–354.

Shaw, D.M. 1970. Trace element fractionation during anatexis, *Geochim. Cosmochim. Acta* **34,** 237–243.

Shchelkova, S.G., Brovkin, A.A. 1969. Titan-olivine from Siberian kimberlites, *Zap. Vses. Mineral. Obshch.* **98,** 246–247 (Russian).

Shee, S.R. 1978. The mineral chemistry of xenoliths from the Orapa kimberlite pipe, Botswana, M.Sc. thesis, Univ. Cape Town. R.S.A.

Shee, S.R. 1979. The opaque oxides of the Wesselton Mine. Kimberlite Symposium II, Cambridge (Extended Abstracts).

Shee, S.R. 1984. The oxide minerals of the Wesselton Mine kimberlite, Kimberley, South Africa, *TIKC* **1,** 59–73.

Shee, S.R., Gurney, J.J. 1979. The mineralogy of xenoliths from Orapa, Botswana, *SIKC* **2,** 37–49.

Shee, S.R., Gurney, J.J. Robinson, D.N. 1982. Two diamond-bearing peridotite xenoliths from the Finsch kimberlite, South Africa, *Contrib. Mineral. Petrol.* **81,** 79–87.

Sheppard, S.M.F., Dawson, J.B. 1975. Hydrogen, carbon and oxygen isotope studies of megacryst and matrix minerals from Lesothan and South African kimberlites, *Phys. Chem. Earth* **9,** 747–763.

Sheppard, S.M.F., Epstein, S. 1970. D/H and $^{18}O/^{16}O$ ratios of minerals of possible mantle or lower crustal origin, *Earth Planet. Sci. Lett.* **9,** 232–239.

Sheridan, M.F., Wohletz, K.H. 1983. Hydrovolcanism: Basic considerations and review, *J. Volcanol. Geotherm. Res.* **17,** 1–29.

Shoemaker, E.M., Moore, H.J. 1956. Diatremes of the Navajo and Hopi reservations, *U.S. Geol. Surv. Trace Elements Inv. Rpt.* **640,** 197–203.

Shoemaker, E.M., Roach, C.H., Byers, F.M. Jr. 1962. Diatremes and uranium deposits in the Hopi Buttes, Arizona, *Geol. Soc. Am.,* Buddington Vol., 327–355.

Sigurdsson, H., Schilling, J.G. 1976. Spinels in Mid-Atlantic Ridge basalts: Chemistry and occurrence, *Earth Planet. Sci. Lett.* **29,** 7–20.

Sillitoe, R.H., Sawkins, F.J. 1971. Geologic, mineralogic and fluid inclusion studies relating to the origin of copper-bearing tourmaline breccia pipes, *Econ. Geol.* **66,** 1028–1041.

Simakov, S.K. 1983. Free-carbon segregation in mantle fluid upon reaction of nitrogen with methane, *Dokl. Akad. Nauk SSSR* **268,** 182–186.

Singewald, J.T., Milton, C. 1930. An alnöite pipe, its contact phenomena and ore deposition near Avon, Missouri, *J. Geol.* **38,** 54–66.

Skinner, E.M.W., Clement, C.R. 1979. Mineralogical classification of Southern African kimberlites, *SIKC* **1,** 129–139.

Skinner, E.M.W., Scott, B.H. 1979. Petrography, mineralogy and geochemistry of kimberlites and associated lamprophyre dykes near Swartruggens, Western Transvaal, R.S.A., Kimberlite Symposium II, Cambridge (Extended Abstracts).

Smirnov, G.I. 1959. Mineralogy of Siberian kimberlites, *Int. Geol. Rev.* **1,** 21–39.

Smith, A.L. 1970. Sphene, perovskite and co-existing Fe–Ti oxide minerals, *Am. Mineral.* **55,** 264–269.

Smith, C.B. 1977. Kimberlite and mantle-derived xenoliths at Iron Mountain, Wyoming, M.Sc. thesis, Colorado State Univ. Fort Collins.

Smith, C.B. 1983. Pb, Sr, and Nd isotopic evidence for sources of African Cretaceous kimberlite, *Nature* **304,** 51–54.

Smith, C.B., McCallum, M.E., Coopersmith, H.G., Eggler, D.H. 1979(a). Petrochemistry and structure of kimberlites in the Front Range and Laramie Range, Colorado Wyoming, *SIKC* **1,** 186–189.

Smith, J.V. 1974. *Feldspar Minerals Volume 2: Chemical and Textural Properties,* Springer Verlag, New York, 690 pp.

Smith, J.V., Brennesholtz, R., Dawson, J.B. 1978. Chemistry of micas from kimberlites and xenoliths, I. Micaceous kimberlites, *Geochim. Cosmochim. Acta* **42,** 959–971.

Smith, J.V., Hervig, R.L., Ackermand, D., Dawson, J.B. 1979(b). K, Rb and Ba in micas from kimberlite and peridotite xenoliths and implication for the origin of basaltic rocks, *SIKC* **1,** 241–251.

Snowden, D.V. 1981. Mineralogy and petrology of two kimberlites at Dutoitspan mine, Kimberley, M.Sc. thesis, Rhodes Univ. Grahamstown, South Africa.

Sobolev, N.V. 1977. *Deep-Seated Inclusions in Kimberlites and the Problem of the Composition of the Upper Mantle,* American Geophys. Union, Washington D.C.

Sobolev, N.V. 1985. Kimberlites of the Siberian Platform: Their geological and mineralogical features, in *Kimberlite, Occurrence and Origin: A Basis for Conceptual Models,* J. E. Glover and P.G. Harris, eds. *Geol. Dept. Univ. Western Australia Pub.,* No. 8, 275–287.

Sobolev, S.F., Lapin, A.V., Nazerenko, I.I., Kislova, I.V., Ilupin, I.P. 1975. Selenium in the kimberlites and plutonic peridotite xenoliths of Yakutia, *Geochem. Int.* **12,** 40–46.

Soloman, S.C. 1976. Geophysical constraints on radial and lateral temperative variations in the upper mantle, *Am. Mineral.* **61,** 788–803.

Sorensen, H. 1974. *The Alkaline Rocks.* John Wiley & Sons, New York.

Spencer, A.B. 1969. Alkali igneous rock of the Balcones Province, Texas, *J. Petrol.* **10,** 272–307.

Spera, F.J. 1984. Carbon dioxide in petrogenesis III: Role of volatiles in the ascent of alkaline magma with special reference to xenolith-bearing mafic lavas, *Contrib. Mineral. Petrol.* **88,** 217–232.

Stacey, J.S., Kramers, J.D. 1975. Approximation of terrestrial lead isotope evolution by a two stage model, *Earth Planet. Sci. Lett.* **26,** 207–221.

Staritski, Y.G. 1963. Some features of magmatism and metallogeny of platform regions, *Int. Geol. Rev.* **5,** 402–415.

Staudigel, H., Zindler, A., Hart, S.R., Leslie, T., Chen, C.Y., Clague, D. 1984. The isotope systematics of a juvenile intraplate volcano: Pb, Nd and Sr isotopes ratios of basalts from Loihi Seamount, Hawaii, *Earth Planet. Sci. Lett.* **69,** 13–29.

Stearns, H.T., MacDonald, S.A. 1946. Geology and groundwater resources of the island of Hawaii, *Hawaii Div. Hydrol. Bull.* **67,** 13–49.

Stephens, W.E., Dawson, J.B. 1977. Statistical comparison between pyroxenes from kimberlites and their associated xenoliths, *J. Geol.* **85,** 433–449.

Steuber, A.M., Goles, G.G. 1967. Abundance of Na, Mn, Cr, Sc, and Co in ultramafic rocks, *Geochim. Cosmochim. Acta* **31,** 75–93.

Stracke, N.J., Ferguson, J., Black, L.P. 1979. Structural setting of kimberlites in South Eastern Australia, *SIKC* **1,** 71–91.

Sutherland, F.L., Hollis, J.D., Barron, L.M. 1984. Garnet lherzolite and other inclusions from a basalt flow, Bow Hill, Tasmania, *TIKC* **2,** 145–160.

Suwa, K., Oana, S., Wada, H., Osaki, S. 1975. Isotope geochemistry and petrology of African carbonatites, *Phys. Chem. Earth* **9,** 735–745.

Svisero, D.P., Meyer, H.O.A., Tsai, H. 1979. Kimberlite minerals from Vargem (Minas Gerais) and Redondao (Piaui) diatremes, Brazil, and garnet lherzolite xenolith from Redondao diatreme, *Rev. Brasil. Geosci.* **7,** 1–13.

Svisero, D., Meyer, H.O.A., Haralyi, N.L.E., Hasui, Y. 1984. A note on the geology of some Brazilian kimberlites, *J. Geol.* **92,** 331–338.

Switzer, G.S. 1977. Composition of garnet xenocrysts from three kimberlite pipes in Arizona and New Mexico, in *Mineral Sciences Investigations,* B. Mason, ed., Smithsonian Institution No. 19, 1–21.

Sykes, L.R. 1978. Intraplate seismicity, reactivation of pre-existing zones of weakness, alkaline magmatism and other tectonism post-dating continental fragmentation, *Rev. Geophys. Space Phys.* **16,** 621–688.

Taljaard, M.S. 1936. South African melilite basalts and their relations, *Trans. Geol. Soc. S. Africa* **39,** 281–316.

Tatarintsev, V.I., Tsymbal, S.N., Garanin, V.K., Kudriavtseva, G.P., Marshintsev, V.K. 1983. Chilled particles from Yakutian kimberlites, *Dokl. Akad. Nauk SSSR* **270,** 1199–1203 (Russian).

Taylor, L.A. 1984. Kimberlitic magmatism in the Eastern United States: Relationships to mid-Atlantic tectonism, *TIKC* **1,** 417–424.

Taylor, L.A., Shervais, J.W., Hunter, R.H. 1983. Major and trace element geochemistry of garnets and ilmenites from Eastern U.S.A. kimberlites, Geol. Soc. Amer. Ann. Mtg. Indianapolis (Abstract).

Thiessen, R., Burke, K., Kidd, W.S.F. 1979. African hotspots and their relation to the underlying mantle, *Geology* **7,** 263–266.

Thompsom, R.N. 1974. Some high-pressure pyroxenes, *Mineral. Mag.* **39,** 768–787.

Tollo, R.P. 1982. Petrology and mineral chemistry of ultramafic and related inclusions from the Orapa A/K-1 kimberlite pipe, Botswana, M.Sc. thesis, Univ. Mass. at Amherst.

Tomanovskaya, V.I. 1974. Geochemical features of kimberlites of the Siberian Platform, in *Mineralogy, Geochemistry and Occurrence of Diamond Deposits,* V.A. Milashev, ed. Pub. Instit. Arctic Geol., Leningrad, pp. 32–44 (Russian).

Tompkins, L.A., Bailey, S.W., Haggerty, S.E., 1984. Kimberlitic chlorites from Sierra Leone, West Africa: Unusual chemistries and structural polytypes, *Am. Mineral.* **69,** 237–249.

Tompkins, L.A., Haggerty, S.E. 1984. The Koidu kimberlite complex, Sierra Leone: Geological setting, petrology and mineral chemistry, *TIKC* **1,** 81–105.

Tompkins, L.A., Haggerty, S.E. 1985. Groundmass oxide minerals in the Koidu kimberlite dikes, Sierra Leone, West Africa, *Contrib. Mineral. Petrol.* **91,** 245–263.

Treiman, A.H., Schedl, A. 1983. Properties of carbonatite magma and processes in carbonatite magma chambers, *J. Geol.* **91,** 437–447.

Tremblay, M. 1956. Geology of the Williamson Diamond Mine. Mwadui, Tanganyika, Ph.D. thesis, McGill Univ., Montreal.

Trofimov, V.S. 1967. *Distribution and Genesis of Diamond Deposits,* Izdatelstvo Nedra, Moscow (Russian).

Trofimov, V.S. 1971. On the origin of diamantiferous diatremes, *Bull. Volcanol* **24,** 767–776.

Trofimov, V.S. 1980. Role of intermediate magma chambers in the formation of kimberlites and diamonds, *Int. Geol. Rev.* **22,** 490–496.

Tsai, H., Shieh, Y., Meyer, H.O.A. 1979. Mineralogy and S^{34}/S^{32} ratios of sulfides associated with kimberlite, xenoliths and diamonds, *SIKC* **2,** 87–103.

Turcotte, D.L. 1983. Mechanisms of crustal deformation, *J. Geol. Soc. London* **140,** 701–724.

Turcotte, D.L., Oxburgh, E.R. 1978. Intra-plate volcanism, *R. Soc. London Philos. Trans.* **288A,** 561–579.

Ukhanov, A.V. 1963. Olivine melilitite from the diamond-bearing diatremes on Anabar, *Dokl. Akad. Nauk SSSR* **153,** 176–178.

Ukhanov, A.V., Borodaeva, T.Y., Borodaev, Y.S. 1982. Composition and zonality of olivines from the Udachnaya pipe as a reflection of the path of kimberlite magma evolution, *Geokhimiya* **1982,** 664–676 (Russian).

Ukhanov, A.V., De Virts, A.L. 1983. Meteoric origin of water serpentinizing Yakutian kimberlites, *Dokl. Akad. Nauk SSSR* **268,** 706–709 (Russian).

Ulmer, G.C., Rosenhauer, M., Woermann, E., Ginder, T., Drory-Wolff, A., Wasilewski, P. 1976. Applicability of electrochemical-oxygen fugacity measurement to geothermometry, *Am. Mineral.* **61,** 653–660.

Vaganov, V.I. 1978. Petrological inter-relations of kimberlite with alkaline-ultrabasic and alkaline-basaltic rocks and with carbonatites, *Dokl. Akad. Nauk SSSR* **241,** 143–145.

Vanuxem, L. 1837. Mafic dike at East Canada Creek, in Ann. Rept. New York Geol. Surv. 3rd. District 2, p. 265.

Vasilyev, V.G., Kovalskii, V.V., Tcherskii, N.V. 1961. *Problem of the Origin of Diamonds,* Yakutizdat, Yakutsk (Russian).

Vasilyev, V.G., Kovalskii, V.V., Tcherskii, N.V. 1968. *Origin of Diamonds,* Izdatelstvo Nedra, Moscow.

Velde, D. 1975. Armalcolite-Ti-phlogopite-diopside-analcite-bearing lamproites from Smoky Butte, Garfield County, Montana, *Am. Mineral.* **60,** 566–573.

Verhoogen, J. 1938. Les pipes de kimberlites de Katanga, *Ann. Serv. Mines Katanga Spec. Pub.* **9,** 1–50.

Verwoerd, W.J. 1966. South African carbonatites and their probable mode of origin, *Ann. Univ. Van Stellenbosch, 41, SerA,* **2,** 116–233.

Verwoerd, W.J. 1970. Economic geology and genesis of kimberlite, in Ann. 24th. Cong. Brasil. Geol. Soc. Brasilia, pp. 51–70.

Vinogradov, A.P., Kropotova, O.I. 1967. The isotopic fractionation of carbon in geological processes, *Int. Geol. Rev.* **10,** 497–506.

Vinogradov, A.P., Kropotova, O.I., Ustinov, V.I. 1965. Possible sources of diamonds as indicated by $^{12}C/^{13}C$ ratios, *Geochem. Int.* **2,** 495–503.

Vinogradov, V.I., Ilupin, I.P. 1972. Isotopic composition of sulfur in kimberlite of the Siberian Platform, *Dokl. Akad. Nauk SSSR* **207,** 221–223.

Vlasov, K.A. 1966. Loparite. Geochemistry and Mineralogy of rare elements and genetic types of their deposits II: Mineralogy of rare elements, in Israel Program for Scientific Translations, Jerusalem, pp. 418–424.

Vollmer, R., Norry, M.J. 1983. Possible origin of K-rich volcanic rocks from Virunga East Africa, by metasomatism of continental crustal material, Pb, Nd, and Sr isotopic evidence, *Earth Planet. Sci. Lett.* **64,** 374–386.

Von Eckermann, H. 1948. The alkaline district of Alnö Island, Sveriges Geologiska Undersokning Series Ca. No. 36.

Von Eckermann, H. 1961. The petrogenesis of the Alnö alkaline rocks, *Bull. Geol. Instit. Univ. Uppsala* **40,** 25–36.

Von Eckermann, H. 1967. A comparison of Swedish, African and Russian kimberlites, in *Ultramafic and Related Rocks,* P.J. Wyllie, ed. John Wiley & Sons, New York, pp. 302–312.

Voskrensenskaya, V.B., Kovalskii, V.V., Nikishov, K.N., Parinova, Z.F. 1965. Discovery of titan olivine in Siberian kimberlites, *Zap. Vses. Mineral. Obshch.* **94,** 600–603 (Russian).

Vyshemirskii, V.S., Doilnitsin, Y.F., Krymova, V.N., Pertseva, A.P., Ryzhkova, S.M. 1971. Organic origin of bitumens in the Vilyuy kimberlite pipes, *Dokl. Akad. Nauk SSSR* **197,** 215–216.

Wagner, P.A. 1914. *The Diamond Fields of Southern Africa,* Transvaal Leader, Johannesburg.

Wagner, P.A. 1929. *Handbuck der Regionale Geologie,* The Union of South Africa 7,(7a), pp. 148–158 and 161–222.

Warner, R.D., Luth, W.C. 1973. Two-phase data for the join monticellite ($CaMgSiO_4$)–forsterite (Mg_2SiO_4): Experimental results and numerical analysis, *Am. Mineral* **58,** 998–1008.

Wass, S.Y. 1979. Multiple origins of clinopyroxenes in alkali basaltic rocks, *Lithos* **12,** 115–132.

Watkinson, D.H., Chao, Y. 1973. Shortite in kimberlite from the Upper Canada Gold Mine, Ontario, *J. Geology* **87,** 229–233, *J. Geol.* **81,** 229–233.

Watkinson, D.H., Wyllie, P.J. 1971. Experimental study of the compositional join $NaAlSiO_4$–$CaCO_3$–H_2O and the genesis of alkalic rock–carbonatite complexes, *J. Petrol.* **12,** 357–378.

Watson, K.D. 1955. Kimberlite at Bachelor Lake, Quebec, *Am. Mineral.* **40,** 565–579.

Watson, K.D., Bruce, G.S.W., Holiday, L.B. 1978. Kimberlitic dike in Keith Township, Ontario, *Can. Mineral.* **16,** 97–102.

Wedephohl, K.H., Muramatsu, Y. 1979. The chemical composition of kimberlites compared with the average composition of three basaltic magma types, *SIKC* **1,** 300–312.

Welke, H.J., Allsopp, H.L., Harris, J.W. 1974. Measurements of K, Rb, U, Sr and Pb in diamonds containing inclusions, *Nature* **252,** 35–37.

Wells, P.R.A. 1977. Pyroxene thermometry in simple and complex systems, *Contrib. Mineral. Petrol.* **62,** 129–139.

Wendlandt, R.F. 1977. Barium phlogopite from Haystack Butte, Highwood Mountain, Montana, *Carnegie Inst. Washington Yearb.* **76,** 534–539.

Wendlandt, R.F. 1984. An experimental and theoretical analysis of partial melting in the system $KAlSiO_4$–CaO–MgO–SiO_2–CO_2 and applications to the genesis of potassic magmas, carbonatites and kimberlites, *TIKC* **1,** 359–369.

Wendlandt, R.F., Eggler, D.H. 1980(a). The origins of potassic magmas, 1. Melting relations in the systems $KAlSiO_4$–SiO_2 and $KAlSiO_4$–MgO–SiO_2–CO_2 to 30 kb, *Am. J. Sci.* **280,** 385–420.

Wendlandt, R.F., Eggler, D.H. 1980(b). The origins of potassic magmas: Stability of phlogopite in natural spinel lherzolite and in the system $KAlSiO_4$–MgO–SiO_2–H_2O–CO_2 at high pressures and high temperatures, *Am. J. Sci.* **280,** 421–458.

Whitelock, T.K. 1973. The Monastery Mine kimberlite pipe, *Lesotho Kimberlites,* 214–230.

Wicks, F.J., Plant, A.G. 1979. Electron microprobe and X-ray microbeam studies of serpentine textures, *Can. Mineral.* **17,** 785–830.

Wicks, F.J., Zussman, J. 1975. Microbeam X-ray diffraction patterns of the serpentine minerals, *Can. Mineral.* **13,** 244–258.

Wilkinson, J.F.G. 1975. An Al-spinel ultramafic inclusion suite and high pressure megacrysts in an analcimite and their bearing on basaltic magma fractionation at elevated pressures, *Contrib. Mineral. Petrol.* **53,** 71–104.

Williams, A.F. 1932. *The Genesis of Diamond.* Ernest Benn Ltd., London (2 volumes).

Williams, G.F. 1939. The kimberlite province and associated diamond deposits of Tanganyika Territory, *Geol. Surv. Tanganyika Bull.* **12.**

Williams, G.H. 1887. On the serpentine and peridotite occurring in the Onondago Salt group at Syracuse, New York, *Am. J. Sci.* **34** (Ser. 3), 137–145.

Williams, H., McBirney, A.R. 1979. *Volcanology.* Freeman, Cooper & Co. San Francisco.

Williams, H.R., Williams, R.A. 1977. Kimberlites and plate tectonics in West Africa, *Nature* **270,** 507–508.

Wilson, A.N. 1982. *Diamonds from Birth to Eternity,* Gem. Inst. Amer., Santa Monica, Calif.

Wilson, C.J.N. 1980. The role of fluidization in the emplacement of pyroclastic flows: An experimental approach, *J. Volcanol. Geotherm. Res.* **8,** 231–249.

Wilson, C.J.N. 1984. The role of fluidization in the emplacement of pyroclastic flows, 2: Experimental results and their interpretation, *J. Volcanol. Geotherm. Res.* **20,** 55–84.

Wilson, J.T. 1963. A possible origin of the Hawaiian Islands, *Can. J. Phys.* **41,** 863–870.

Wilson, J.T. 1965. A new class of faults and their bearing on continental drift, *Nature* **207,** 343–347.

Wishart, D. 1969. Fortran II programmes for 8 methods of cluster analysis: Clustan I, Kansas State Geol. Surv/Univ. Kansas Computer analysis Contrib, 38.

Woermann, E., Hirschberg, A. Lamprecht, A. 1970. Das system Hematit-ilmenit-geikielith unter hohen temperaturen und hohen drucken, *Fortsch. Mineral.* **47,** 1–86.

Wohletz, K.H., Sheridan, M.F. 1979. A model of pyroclastic surge, in *Ash-Flow Tuffs*, C.E. Chapin and W.E. Elston, eds. *Geol. Soc. Amer. Spec. Paper* **180**, 177–193.

Wohletz, K.H., Sheridan, M.F. 1981. Rampart crater ejecta: Experiments and analysis of melt/water interaction. NASA Tech. Mem. 82385, 134–136.

Wohletz, K.H., Sheridan, M.F. 1982. Melt/water interactions: Series II experimental design, NASA Tech. Mem. 84211, 169–171.

Wohletz, K.H., Sheridan, M.F. 1983. Hydrovolcanic explosions II. Evolution of basaltic tuff rings and tuff cones, *Am. J. Sci.* **283**, 385–413.

Wohletz, K.H., Smyth, J.R. 1984. Origin of a Roberts Victor sanidine-coesite grospydite: Thermodynamic considerations, *TIKC* **2**, 33–42.

Wolfe, J.A. 1980. Fluidization versus phreatomagmatic explosions in breccia pipes, *Econ. Geol.* **75**, 1105–1111.

Wood, B.J. 1974. Solubility of alumina in orthopyroxene coexisting with garnet, *Contrib. Mineral. Petrol.* **46**, 1–15.

Wood, D.A. 1979. A variably veined sub-oceanic upper mantle–Genetic significance for mid-ocean ridge basalts from geochemical evidence, *Geology* **7**, 499–503.

Woolsey, T.S., McCallum, M.E., Schumm, S.A. 1975. Modeling of diatreme emplacement by fluidization, *Phys. Chem. Earth* **9**, 29–42.

Wright, A.E., Bowes, D.R. 1968. Formation of explosion breccias, *Bull. Volcanol.* **32**, 15–32.

Wright, J.V., Smith, A.L., Self, S. 1980. A working terminology of pyroclastic deposits, *J. Volcan. Geothermal Res.* **8**, 315–336.

Wyatt, B.A. 1977. The melting and crystallization behaviour of a natural clinopyroxene–ilmenite intergrowth, *Contrib. Mineral. Petrol.* **61**, 1–9.

Wyatt, B.A. 1979(a). Manganoan ilmenite from the Premier kimberlite. Kimberlite Symposium II, Cambridge (Extended Abstracts).

Wyatt, B.A. 1979(b). Kimberlite chromium picro-ilmenites with intergrowths of titanian chromite and rutile, *SIKC* **2**, 257–264.

Wyatt, B.A., McCallister, R.H., Boyd, F.R., Ohashi, Y. 1975. An experimentally produced clinopyroxene-ilmenite intergrowth, *Carnegie Instit. Washington Yr. Book* **74**, 536–539.

Wyllie, P.J. 1965. Melting relationships in the system CaO–MgO–CO_2–H_2O with petrological applications, *J. Petrol.* **6**, 101–123.

Wyllie, P.J. 1966. Experimental studies of carbonatite problems: The origin and differentiation of carbonatite magmas, in *Carbonatites*, O.F. Tuttle and J. Gittins, eds. John Wiley & Sons, New York, pp. 311–352.

Wyllie, P.J. 1977. Mantle fluid compositions buffered by carbonates in peridotite–CO_2–H_2O, *J. Geol.* **85**, 187–208.

Wyllie, P.J. 1978. Mantle fluid compositions buffered in peridotite–CO_2–H_2O by carbonates, amphiboles and phlogopite, *J. Geol.* **86**, 687–713.

Wyllie, P.J. 1979(a). Magmas and volatile components, *Am. Mineral.* **64**, 469–500.

Wyllie, P.J. 1979(b). Kimberlite magmas from the system peridotite–CO_2–H_2O, *SIKC* **1**, 319–329.

Wyllie, P.J. 1980. The origin of kimberlite, *J. Geophys. Res.* **85**, 6902–6910.

Wyllie, P.J., Biggar, G.M. 1966. Fractional crystallization in the "carbonatite systems" CaO–MgO–CO_2–H_2O and CaO–CaF_2–P_2O_5–CO_2–H_2O, in Mineral. Soc. India. Internat. Mineral. Assoc. 4th Gen Mtg., pp. 92–105.

Wyllie, P.J., Cox, K.G., Biggar, G.M. 1962. The habit of apatite in synthetic and igneous systems, *J. Petrol.* **3**, 238–243.

Wyllie, P.J., Haas, J.L. 1965. The system CaO–SiO_2–CO_2–H_2O: 1. Melting relationships with excess vapour at 1 kilobar pressure, *Geochim. Cosmochim. Acta* **29**, 871–892.

Wyllie, P.J., Huang, W.L. 1975(a). Influence of mantle CO_2 in the generation of carbonatites and kimberlites, *Nature* **257**, 297–299.

Wyllie, P.J., Huang, W.L. 1975(b). Peridotite, kimberlite and carbonatite explained in the system $CaO–MgO–SiO_2–CO_2$, *Geology* **3,** 621–624.

Wyllie, P.J., Huang, W.L. 1976. Carbonation and melting reactions in the system $CaO–MgO–SiO_2–CO_2$ at mantle pressures with geophysical and petrological applications, *Contrib. Mineral. Petrol.* **54,** 79–107.

Wyllie, P.J., Tuttle, O.F. 1960. The system $CaO–CO_2–H_2O$ and the origin of carbonatites, *J. Petrol.* **1,** 1–46.

Xu, T., 1982. Zircons in the kimberlites from Maping, Guizhou Province and Pengjiabang, Hubei Province, China, *Zhongguo Dizhi Kexueyuan Yichang Dizhi Kuangchan Yanjiuso Sokan* **5,** 28–39 (Chinese).

Yevdokimov, A.N., Bagdasarov, E.A. 1982. Compositions and typical chemical features of pyrope garnets from kimberlites in the Middle and Lower Kuonam fields in Yukutia, *Int. Geol. Rev.* **24,** 548–558.

Yoder, H.S. 1975. Relationship of melilite-bearing rocks to kimberlite: A preliminary report on the system akermanite–CO_2, *Phys. Chem. Earth* **9,** 883–894.

Yoder, H.S., Kushiro, I. 1968. Melting of a hydrous phase: Phlogopite, *Carnegie Inst. Washington Yearb.* **67,** 161–167.

Young, R.S., Benfield, D.A., Strachan, K.G.A. 1954. Cobalt in kimberlites, *Am. Mineral.* **39,** 143–144.

Zartman, R.E. 1977. Geochronology of some alkalic rock provinces in Eastern and central United States, *Ann. Rev. Earth Planet. Sci.* **5,** 257–286.

Zartman, R.E., Brock, M.R., Heyl, A.V., Thomas, H.H. 1967. K–Ar and Rb–Sr ages of some alkalic intrusive rocks from the central and Eastern United States, *Am. J. Sci.* **265,** 848–870.

Zenz, F.A. 1971. Regimes of fluidization behaviour, in *Fluidization,* J.F. Davidson and D. Harrison, eds. Academic Press, London, pp. 1–23.

Zhabin, A.G. 1967. Carbonatite-kimberlite from Arbarastakh, Yakutia SSSR, *Dokl. Akad. Nauk SSSR* **177,** 167–170.

Zhang, R., Liu, B. 1983. Kimberlites from North China, *Geochem. J.* **17,** 209–221.

Zhou, J. 1980. Microanalysis techniques of minerals and their geological application, *Geol. Rev.* **6,** 547–551 (Chinese).

Zhou, J., Zhou, K., Fang, Y., Yang, G. 1982. Electron probe study of ilmenites from kimberlites, *Zhongguo Dizhi Kexeuyuan Kuangchan Dizhi Yanjiuso Sokan* **5,** 103–114 (Chinese).

Zinchuk, N.N., Kharkiv, A.D. 1978. Comparative characteristics of chlorite from kimberlites of the Mir Pipe and country rocks, *Int. Geol. Rev.* **20,** 428–434.

Zinchuk, N.N., Melnik, Y.M., Kharkiv, A.D. 1983. Characteristics of the composition and origin of brucite in kimberlites of Yakutia, *Dokl. Akad. Nauk SSSR* **269,** 449–454.

Zinchuk, N.N., Melnik, Y.M., Kharkiv, A.D. 1984. Pyroaurite in kimberlitic rocks of Yakutia and its genesis, *Dokl. Akad. Nauk SSSR* **267,** 157–162.

Zverev, V.L., Kravtsov, A.I., Ilupin, I.P. Pryakhina, Y.V., Voytov, G.I., Demin, N.V., Titayeva, N.A., Chesko, A.L., Semenov, G.S. 1979. Uranium isotopes in kimberlites of Eastern Siberia, *Dokl. Akad. Nauk SSSR* **245,** 210–213.

Zverev, V.L., Semenov, G.S., Spiridonov, A.I., Chesko, A.L. 1976. Uranium isotope separation in kimberlite magmatism, *Geochem. Int.* **12,** 174–176.

INDEX